



ADVANCES IN ENGINEERING SCIENCES

**EDITOR
PROF. BIROL KILIC, PH.D.**

Advances in Engineering Sciences

EDITOR

Prof., Birol Kilic, Ph.D.

Publisher

Platanus Publishing®

Editor in Chief

Prof. Birol Kilic, Ph.D.

Cover & Interior Design

Platanus Publishing®

Editorial Coordinator

Arzu Betül Çuhacioğlu

The First Edition

December, 2024

Publisher's Certificate No

45813

ISBN

978-625-6216-23-2

©copyright

All rights reserved. No part of this publication may be reproduced or transmitted in any form or by any means, electronic or mechanical, including photocopy, or any information storage or retrieval system, without permission from the publisher.

Platanus Publishing®

Address: Natoyolu Cad. Fahri Korutürk Mah. 157/B, 06480, Mamak,
Ankara, Turkey.

Phone: +90 312 390 1 118

web: www.platanuskitap.com

e-mail: platanuskitap@gmail.com



PLATANUS PUBLISHING®

İÇİNDEKİLER

CHAPTER 1	9
A Folding Wind Turbine System Mounted on an Recreational Vehicle	
Ümran Özge Şebik & Sıtkı Kocaoğlu	
CHAPTER 2	23
The Role of Bioplastics in Sustainable Living	
H. Duygu Bilgen	
CHAPTER 3	33
An Example of an Applicaton Based on Cloud-IoT	
Batın Demircan	
CHAPTER 4	49
Electronic monitoring for unwanted catches and further considerations for Turkish Fishery	
Ozan Soykan & F. Ozan Düzbastılar	
CHAPTER 5	61
Alternative Energy Approaches in Fishing Vessels	
F. Ozan Düzbastılar & Ozan Soykan	
CHAPTER 6	95
The Evaluation of Photovoltaic Power Systems With Different Simulation Softwares for Bozcaada	
Ersin Akyüz	
CHAPTER 7	111
Production of Alumina-Copper Hybrid Composites by Hot Pressing Technique: Investigation of Mechanical, Structural, and Tribological Properties	
Cevher Kürşat Macit & Merve Horlu & Burak Tanyeri & Bünyamin Aksakal	
CHAPTER 8	129
Long-Term Consistency Analysis of Global Precipitation Datasets: A Case Study in Konya	
Omer Faruk Atiz & Savas Durduran	

CHAPTER 9	141
Exploring the Influence of Pb Doping on CdPbS Thin Films: From Grain Size to Photocatalytic Performance	
Sabit Horoz	
CHAPTER 10.....	155
Investigation of Structural and Optical Properties of Mo Doped PbZnS Nanoparticles	
Kübra Köşe Kaya	
CHAPTER 11.....	169
Investigating LaTiO₃ as a Photocatalyst for the Effective Degradation of Reactive Black 5	
Kübra Köşe Kaya	
CHAPTER 12.....	181
Current Studies on Dye Removal With Metal Oxide Based Nano Adsorbents	
Hasan Kıvanç Yeşiltaş & Behzat Balcı	
CHAPTER 13.....	193
A General Overview of Recovery of Precious Metals From Electronic Waste	
Mirac Nur Ciner & Emine Elmaslar Ozbas & H. Kurtulus Ozcan	
CHAPTER 14.....	205
Theoretical Perspective on the Production and Biocompatibility of Metal-Reinforced PLA Composites	
İbrahim Baki Şahin & İhsan Korkut	
CHAPTER 15.....	233
Innovative Technology Applications Nano and Micro Encapsulation Applications for Ensuring Food Safety Roles	
Nuray Gamze Yörük	
CHAPTER 16.....	247
Plastic Waste Management: Recycling and Disposal	
Mazlum Cengiz	

CHAPTER 17261

Comparison of Biodiesel Production Methods and Innovative Approaches
Zehra Gülsen Yalçın & Mustafa Dağ & Muhammed Bora Akın

CHAPTER 18289

Optimization Analysis of Autonomous Mobile Robots
Engin Ünal & Faruk Karaca

CHAPTER 19307

Optimization of Additive Manufacturing for the Aerospace and Defense Industry
Engin Ünal & Faruk Karaca

CHAPTER 20335

Implementing Smart Disaster Management Systems in Smart Cities
Mesut Samastı & Ceren Altan

CHAPTER 21353

Evaluation of Biomass Potential Based on Animal Waste in Turkey
Yağmur Arıkan Yıldız

CHAPTER 22365

Optimal Sizing of Pv-Wind-Battery Hybrid System Using Genetic Algorithm
Özge Pınar Akkaş

CHAPTER 23383

Prediction of Surface Leakage Currents in High-Voltage Insulators By Machine Learning Approaches
Serhat Berat Efe

CHAPTER 24395

XRD and XRF Characterizations of Electrospun Nanofibers
Atike İnce Yardımcı & Yaser Açıkbaş

CHAPTER 25405

Chemometric Evaluation of Physicochemical Properties and Bioactive Compounds of Hot Air and Microwave Dried Potatoes by FTIR Spectroscopy
Katibe Sinem Coruk & Hande Baltacıoğlu

CHAPTER 26.....	423
Biofilm Synthesis for Active Food Packaging	
Mukaddes Karataş	
CHAPTER 27.....	451
Carbon Capture and Sequestration Via Torrefied Biomass	
Zuhal Akyürek	
CHAPTER 28.....	463
Review of AI-Powered Digital Twin Technology for Real-Time Mechanical System Simulation and Optimization	
Hamid Zamanlou & Filiz Karabudak	
CHAPTER 29.....	471
Developing a Monitoring and Warning System for Cold Storage of Hotels for Sustainable Tourism	
Ahmet Coşgun	
CHAPTER 30.....	491
Applications of Hybrid Laser Welding in Titanium Materials	
Ferit Artkin	
CHAPTER 31.....	503
The Effect of Hybrid Laser Welding Technology on Aluminum Alloys	
Ferit Artkin	
CHAPTER 32.....	513
Biomechanical Workload Analysis of Aircraft Technicians	
Haşim Kafalı & İbrahim Güçlü	
CHAPTER 33.....	527
Production Methods of Fiber Reinforced Composites	
Sümeyye Erdem Korkmaz	
CHAPTER 34.....	553
Applications and Developments of Vacuum Infusion Method in Mechanical Engineering	
Sümeyye Erdem Korkmaz	

CHAPTER 35579

Negative Effects of Salt Stress On Plants

Gözde Hafize Yıldırım

CHAPTER 36589

Smart Agriculture Systems

Gözde Hafize Yıldırım

CHAPTER 37597

Load Frequency Control in A Two-Area Power System With Renewable Energy Integration Using Sliding Mode Controller

Asaf Sayıl & Yağmur Arıkan Yıldız



CHAPTER 1

A Folding Wind Turbine System Mounted on an Recreational Vehicle

Ümran Özge Şebik¹ & Sıtkı Kocaoğlu²

¹ Res. Asst, Ankara Yıldırım Beyazıt University, 0009-0005-9604-1310

² Asst. Prof., Ankara Yıldırım Beyazıt University, 0000-0003-1048-9623

1. INTRODUCTION

1.1. Description of the Project

Wind energy is a clean and renewable energy source, which is created by using the speed of the wind. By turning the blades of a wind turbine, an electrical generator produces electricity. As a strategy to lessen our reliance on fossil fuels and mitigate the effects of climate change, wind energy has gained popularity in recent years. It can be used in both urban and rural areas and is a cheap, dependable source of electricity. Technology for producing wind energy is advancing quickly, making it an increasingly appealing option for supplying our energy requirements. Electricity, water pumping, and grain grinding are all produced using wind energy. In addition to these more conventional applications, wind energy is increasingly used to power residences, commercial buildings, and to refuel electric vehicles.

Along with the emergence of COVID the daily life that is known changed and it is still changing over the years. The effect of the pandemic on people also forced people to stay in quarantine. As the people are not accustomed to living within their homes indefinitely, many of the population have asked to go outside and get rid of this effect of limitation. The common desire to live freely lead many of the families to buy a RV (Recreational Vehicle). Like the many of the countries, the quarantine rules of Turkey also let the RV owners to stay inside their RVs and travel with their vehicles during the COVID. The owners of RVs have significantly increased, and it is still increasing. Although energy demand of RVs is much lesser than the houses, many of the people wants to get cheaper and renewable energy to get both clean and economically sustainable. Wind turbines have become increasingly used as a source of renewable energy for RVs. These small, portable wind turbines can be mounted on the roof or exterior of an RV, providing a reliable source of electricity while on the road. Living off-grid is one of the main advantages of installing a wind turbine in an RV.

A wind turbine can offer a reliable source of power without the need for these external connections that campground hookups or generators typically provide for RVs. Travelers who want to spend a lot of time in remote areas or who want to lessen their impact on the environment while traveling will find this to be especially helpful. The wind power in RVs has mostly used with the solar power to get higher energy production capacity by using hybrid systems. By using the wind energy when the RV is parked or the weather conditions are not comfortable for the solar energy, the vehicle can close the energy gap. The opposite situation can be occurred when there are no winds. Although the problem can be solved by

switching the energy sources, the installation stages of wind turbines creates another problem for the RV owner since it takes a lot of time and energy to finish the setup.

1.2. Main Objective of the Project

In this project, our goal is to fix the problem of installation of wind turbines in RVs and make it usable while the vehicle is on the road or in a parking state. The main idea is designing a folding wind turbine placed on the RV which can be operated by a remote controller. Having an automatic folding wind turbine will increase the energy efficiency by using the aerodynamics of the RV.

1.3. Expected Benefits/Outcomes of the Project

Providing continuous and off-grid energy source for a fully equipped RV will lower the cost of energy and since the component that we aim to achieve will be controlled remotely, it will also eliminate the turbine installation step. This will create a more efficient, practical and eco-friendly energy source for a RV.

2. MATERIAL AND METHOD

2.1. Review of the Current State of the Art

The use of wind turbines on RVs is a relatively recent development. First attempts to use a wind turbine on RVs started on early 2000s. These early wind turbines were small, portable units that were designed to be mounted on the roof of an RV or to the ground. They were typically used to charge the batteries of the RV, allowing the occupants to use electrical devices while off the grid. Over time, wind turbines for RVs have become more sophisticated and efficient.

Today, it is possible to find wind turbines that are specifically designed for use on RVs, with features such as foldable blades for easy storage and transport. These wind turbines are often used in conjunction with solar panels to provide a reliable source of power for RVs, particularly for those who enjoy boondocking (camping without hookups). Wind turbines for RVs are typically small, with blade diameters ranging from 1 meter to about 2 meters. They are generally not as powerful as larger wind turbines used for utility-scale electricity generation, but they are well-suited for the smaller energy needs of an RV. In addition to charging batteries, wind turbines for RVs can also be used to power small appliances and electronic devices.

2.2. Relevance of the Project with the Current State of the Art

The current wind turbine systems that are used for RVs are heavy, hard-to-install and can not be used while the vehicle is moving. Our approach and solution for this subject is to create a folding wind turbine system which can be used for both on the road and parking state.



Fig 1.1: A conventional wind turbine system which is installed near a RV.[9]

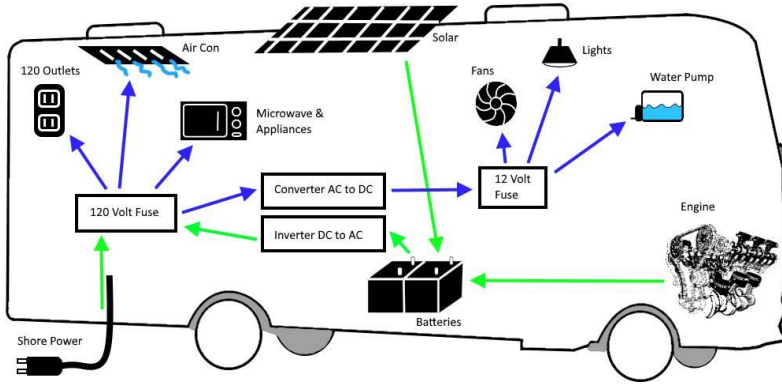
2.3. Method

2.3.1 Electrical System and Components of a RV

RVs have two major electrical systems; one is DC and the other one is AC. The working principle of an AC system is much more similar of a house when the DC system is similar to a car. Since the RV is a combination of a living place and vehicle at the same time, the system must also use and mix these two principles.

The appliances like air conditioning, microwave etc. are using AC power system because of their big energy need, while the things like lights, fans, TV are using DC power system. The two RV electrical systems are connected so that if you have AC power, it will charge the batteries for the DC system by using a device called inverter. The utilization of an inverter is very common in the energy industry since we deal with the AC and DC power systems in order to get electrical output.

Fig 1.2: An illustration of an RV system with basic components and appliances.[8]



2.3.2 Solar and Wind Systems on RV

Since the solar panels create a DC energy, it can be constantly used to charge the RVs' batteries. Although, the wind turbine creates AC energy that needs to be converted to DC to use it on RVs' batteries. Instead of using it for charging the batteries, we can use it as an AC power source for powering the appliances which need more electrical energy.



Fig 1.3: A RV powered by the solar panels on the roof and a wind turbine that is installed on the ground.[12]

2.3.3 Basic Electricity Components of RVs

RVs, or recreational vehicles, typically have several electrical components that allow them to function properly and provide electrical power for various devices and appliances. Some of the basic electrical components found in RVs include:

2.3.3.1 Batteries

RVs often have one or more batteries to store electrical energy and provide power when the RV is not connected to an external power source.



Fig 1.4: Batteries which are installed in a RV in Başkent Caravan.

2.3.3.2 Inverters

Inverters convert direct current (DC) electricity from the batteries into alternating current (AC) electricity, which is used to power most appliances and devices found in an RV.



Fig 1.5: An inverter that is used for RVs in Başkent Karavan

2.3.3.3 Electrical Panel

The electrical panel, also known as a breaker panel, is a central location where the RV's electrical system is managed and controlled. It contains circuit breakers that protect the RV's electrical system from overloading and fuses that protect individual circuits.



Fig 1.6: An inside of an electrical panel.[11]

2.3.3.4 Shore Power Cords

RVs often have a shore power cord that allows them to be connected to an external power source, such as an electrical outlet or a generator, to recharge the batteries and power appliances and devices.



Fig 1.7: Shore power cord which is connected to a RV.[10]

2.3.3.5 MPPT Charge Controller

A maximum power point tracker (MPPT) is a device that is used to optimize the power output of a photovoltaic (PV) system by adjusting the electrical load on the PV array to match the maximum power point of the system. It achieves this by continuously monitoring the PV array's voltage and current output and changing the load to draw the most power possible. By enabling the PV system to function at its maximum power output, which can lead to increased energy production and possibly lower overall costs, this can boost the system's efficiency. Both on-grid systems with battery backup and off-grid PV systems frequently employ MPPTs.



Fig 1.8: A solar regulator model which is commonly used in Başkent Caravan.

2.3.4 Solar Power System Components

2.3.4.1 Solar Panels

A solar panel is a device that uses solar energy to create electricity. It is constructed of photovoltaic (PV) cells, which are built of silicon-based semiconductors. The PV cells' exposure to sunlight excites the semiconductor's electrons, which then produce a current. After passing through a number of electrical parts, including a solar charge controller or an inverter, this current is transformed into a form that may be used to power electrical appliances.

Solar power can be produced via on-grid or off-grid systems, and is frequently utilized to power residences, companies, and other buildings. A solar panel is a device that uses solar energy to create electricity. It is constructed of photovoltaic (PV) cells, which are built of silicon-based semiconductors. The PV cells' exposure to sunlight excites the semiconductor's electrons, which then produce a current. After passing through a number of electrical parts, including a solar charge controller or an inverter, this current is transformed into a form that may be used to power electrical appliances. Solar power can be produced via on-grid or off-grid systems, and is frequently utilized to power residences, companies, and other buildings.

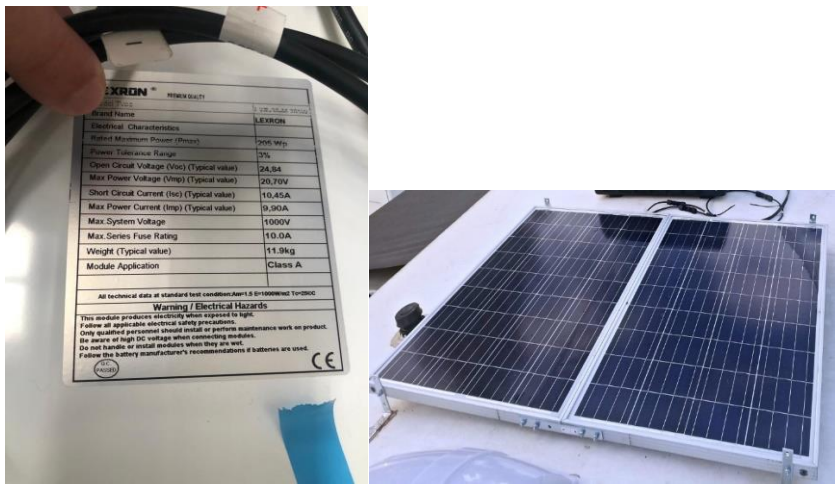


Fig 1.9: Two solar panels from Başkent Caravan. The values are from Lexron LXR-205w

2.3.4.2 Solar Cable

A solar cable is a type of electrical cable that is specifically designed for use in solar power systems. It is used to connect the various components of a solar power system, such as the solar panels, inverters, and storage batteries.

Solar cables are typically made from high-quality materials that can withstand the harsh conditions found in solar power systems, such as exposure to sunlight and extreme temperatures. They are also designed to be highly resistant to corrosion, which is important in outdoor environments. Solar cables are an important component of any solar power system, as they are responsible for transmitting electricity from the solar panels to the other components of the system.



Fig 2.0: Solar cable that is used in Başkent Caravan.

2.3.5 Wind Power System Components

A wind turbine is a device that transforms the kinetic energy of the wind into electrical energy. A rotor with blades and a generator are the components of a wind turbine, which is mounted on a tower. When the blades of the generator are blown by the wind, a shaft attached to it rotates. The generator converts the rotating shaft's mechanical energy into electrical energy that can be used to power structures like homes and businesses.

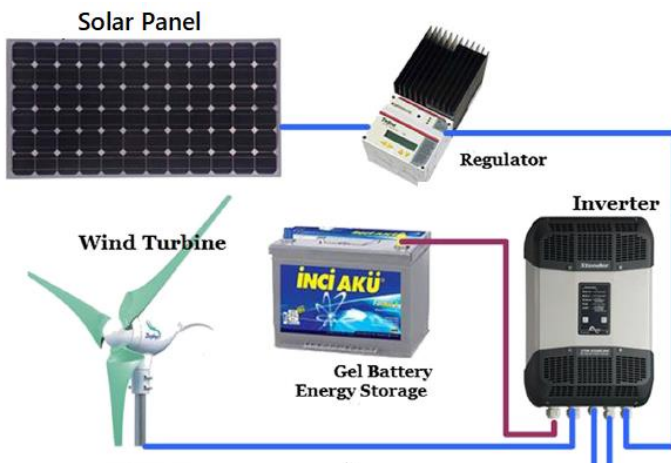


Fig 2.1: Installed system components. [9]

2.3.6 Energy Need of a RV

Use of wind and solar energy is important for boondocking RV owners. Boondocking is a phenomenon of camping outside on an undesignated campground without hookups to electricity on shore power. For simulation purposes, total daily consumption is assumed to be 4.5 kWh, and an energy consumption value is assigned to each hour. The most energy-consuming device, the air conditioner, is assumed to run 8 hours per day, resulting in a daily energy consumption of 4 kWh.

Calculated energy consumption			
Appliance	Power (W)	# of hours used/day [h]	Energy used/day [Wh]
Air conditioner	560	5 ^a	2800
Refrigerator	70	8 ^a	560
LCD TV	65	2 ^a	130
Electrolyser	400	0.5	200
Lighting	100	2 ^a	200
Water heater	1500	0.22	330
Total			4220
a Discreted time.			

Table-1 Calculated energy consumption for a RV with following items above.[9]

The values and types of solar panels and wind turbine is not clear yet. The assumptions below will change in the future.

The following components are assumed to be installed in the vehicle: six units of 285 W monocrystalline photovoltaic panels, a 1 kW permanent magnet synchronous wind generator with a 12.5 m/s wind speed, two 60 An MPPT's (Regulators) with control panels, a 4 kW inverter with a control panel, and six units of 240 Ah, 12 V gel type batteries. Although turbines with permanent magnet synchronous generators are more expensive, their compact and light structure makes them better suited for mobile applications. Deep discharge, overcharge, and a high number of cycles are more tolerable in sealed lead acid mono-block gelled electrolyte batteries.

The system has two main energy production sources, and one energy storage unit. The measurements of an energy storage unit are calculated to provide 1.5-2

days of autonomy, so that storage units can provide power for 2 days even if there is no sun or wind energy available. This is based on a daily load profile.

2.3.7 Yearly Wind and Solar Data

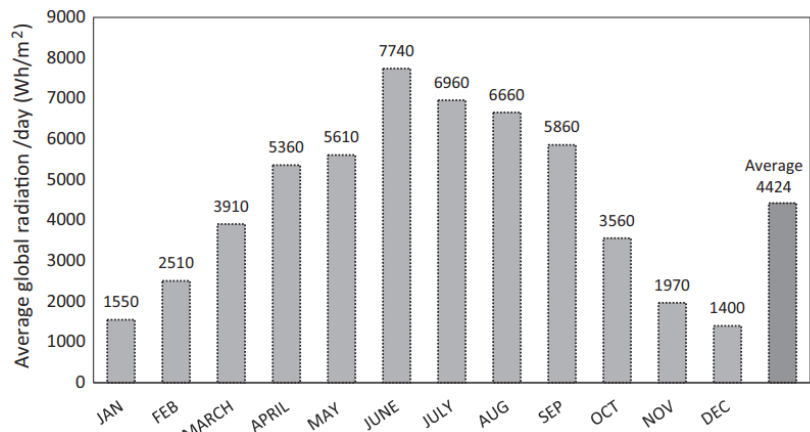


Table-2 Monthly average daily radiation on a unit surface for Ankara, Turkey.[13]

The system is intended for Ankara, Turkey's capital city. In photovoltaic power generation calculations, solar radiation values on a unit surface in Ankara were taken from and illustrated in the figure below. Similarly, wind speed values collected from a Davis instrument measurement station at 30 meters height were used in wind turbine power generation estimates. [13]

Month	Best weibull parameters at turbine hub height	
	k	c (m/s)
January	1.8697	3.9634
February	2.1186	4.1863
March	2.3002	4.1363
April	1.6414	2.9319
May	1.4042	2.6242
June	1.2652	2.4302
July	1.3761	3.7725
August	1.5686	4.2050
September	1.3678	3.7420
October	1.5640	4.4809
November	1.6895	3.6636
December	1.5861	3.0165

Table-3 Best monthly Weibull parameters for Ankara, Turkey.[13]

REFERENCES

1. AZoCleantech. (n.d.). *Advantages and disadvantages of wind energy*. Retrieved October 31, 2024, from <https://www.azocleantech.com/article.aspx?ArticleID=71>
2. Power & Beyond. (n.d.). *What is wind energy? Definition, types, and more*. Retrieved October 31, 2024, from <https://www.power-and-beyond.com/what-is-wind-energy-definition-types-and-more-a-e95f3c16c898e889f0757f62ee91038d/>
3. U.S. Department of Energy. (n.d.). *How a wind turbine works (text version)*. Retrieved October 31, 2024, from <https://www.energy.gov/eere/wind/how-wind-turbine-works-text-version>
4. CleanTechnica. (2022, December 29). *The RV industry started to move in a good direction for EVs in 2022*. Retrieved October 31, 2024, from <https://cleantecnica.com/2022/12/29/the-rv-industry-started-to-move-in-a-good-direction-for-evs-in-2022/>
5. Renewable Energy World. (n.d.). *History of wind turbines*. Retrieved October 31, 2024, from <https://www.renewableenergyworld.com/storage/history-of-wind-turbines/#gref>
6. The RV Geeks. (n.d.). *RV wind turbine*. Retrieved October 31, 2024, from <https://www.thervgeeks.com/rv-wind-turbine/>
7. Out and About Live. (n.d.). *Living off the grid: Wind-powered caravanning*. Retrieved October 31, 2024, from <https://www.outandaboutlive.co.uk/caravans/articles/practical-advice/living-off-the-grid-wind-powered-caravanning>
8. Outdoorsy. (n.d.). *RV electricity basics*. Retrieved October 31, 2024, from <https://www.outdoorsy.com/blog/rv-electricity-basics9-> Yazici, M. S., Yavasoglu, H. A., & Eroglu, M. (2013). A mobile off-grid platform powered with photovoltaic/wind/battery/fuel cell hybrid power systems. *International Journal of Hydrogen Energy*, 38(26), 11639–11645. <https://doi.org/10.1016/j.ijhydene.2013.04.025>
- 10- Leisure Travel Vans. (n.d.). The magic of an RV's electrical system. Retrieved October 31, 2024, from <https://leisurevans.com/blog/magic-rvs-electrical-system/>
- 11- Getaway Couple. (n.d.). Understanding your RV electrical panel. Retrieved October 31, 2024, from <https://www.getawaycouple.com/rv-electrical-panel/>
- 12- Battle Born Batteries. (n.d.). RV wind turbine: What you need to know. Retrieved October 31, 2024, from <https://battlebornbatteries.com/rv-wind-turbine/>
- 13- Devrim, Y., & Bilir, L. (2016). Performance investigation of a wind turbine–solar photovoltaic panels–fuel cell hybrid system installed at İncek region – Ankara, Turkey. *Energy Conversion and Management, 126*, 759–766. <https://doi.org/10.1016/j.enconman.2016.08.062>



CHAPTER 2

The Role of Bioplastics in Sustainable Living

H. Duygu Bilgen¹

¹ Prof. Dr., Mersin University, Dept. Of Environmental Engineering, Mersin, Turkiye.
ORCID ID 0000-0002-9510-8131

Introduction

Sustainable living is a lifestyle considers environmental, economic, and social factors together, aiming to make decisions that address the needs of future generations. Sustainability means meeting today's needs while also taking into account the needs of future generations. This concept has emerged as one of the most targeted ideas on a global scale in recent years. Major environmental issues, such as climate change, depletion of natural resources, biodiversity loss, and pollution caused by petroleum-based plastics, reveal the urgency of the transition to sustainable living.

Since the mid-twentieth century, the term "plastic age" has been used to describe the period marked by the widespread use of petroleum-based plastics, which began in the 1940s. During this time, the production and use of plastic materials rapidly increased, with plastics replacing other materials in many industries (Thompson et al., 2009). Particularly from the 1950s onward, the proliferation of single-use plastic products and packaging has made plastics an inseparable part of daily life (Jambeck et al., 2015). However, the increasing presence and usage of plastics in every aspect of life have led to the issue of plastic pollution (Rochman et al., 2016). Today, there is even a "seventh continent," formed solely from the accumulation of plastic waste (Lebreton et al., 2017). It is known that the main reason why these materials create increasing waste over time is that petroleum-based plastics can remain in nature for thousands of years without biodegrading (Andrady, 2011; Zhang et al., 2020; Xu et al., 2024).

Currently, over 300 million tons of petroleum-based plastics are produced each year (Plastics Europe, 2021). This figure shows an increasing trend, as plastic demand continues to rise in both industrial and consumer sectors (Geyer et al., 2017). If this trend continues, total plastic production is expected to exceed 9 billion tons by 2024 (Jambeck et al., 2015). Recent studies have demonstrated that the breakdown of plastics in the environment releases harmful chemicals, which accumulate in food chains, affecting biodiversity and ecosystem services (Lebreton et al., 2017). Research reports have confirmed that the degradation of petroleum-based plastics has resulted in micro- and nano-sized plastics reaching human blood, and even being detected in breast milk, which is supposed to be the cleanest (Liu et al., 2021; Zbinden et al., 2022). This situation has led to an increased awareness of the negative impacts of plastics on humans and the environment (Rochman et al., 2016). Addressing plastic pollution requires growing public awareness to promote comprehensive policy interventions,

innovative waste management solutions, and sustainable consumption and production practices (Jambeck et al., 2015).

In this context, bioplastics are emerging as a significant alternative to traditional plastics and play a crucial role in achieving sustainable living.

The Concept of Bioplastics

Bioplastics are materials derived from natural resources, typically produced from renewable raw materials, and are largely biodegradable. These materials are obtained from biological sources such as starch, cellulose, chitin, and fatty acids. Bioplastics have the potential to revolutionize the plastic industry and have numerous applications. However, it is also important to note that not all plastics labeled as bioplastics are 100% biodegradable.

Differences Between Biologically Originated and Biodegradable Plastics

Bioplastics can generally be categorized into two main groups: biologically originated and biodegradable plastics.

Biologically originated plastics are produced from biological sources, such as plants or microorganisms. However, not all of these materials have the ability to decompose biologically under natural conditions (Kumar et al., 2020). For instance, the most well-known bioplastic type, PLA (Polylactic Acid), has gained popularity particularly in the form of filaments for 3D printing, entering homes and everyday use (Khan et al., 2021). PLA is termed a bioplastic because it is biologically originated, but it can not degrade in nature for many years and only exhibits biodegradable properties under industrial composting conditions (Dussault et al., 2018). Similarly, Bio-PE (Biological Polyethylene), derived from sugarcane, has characteristics similar to traditional polyethylene, despite being produced from biological sources (Reddy et al., 2013). Polyamide 11 (PA11) is produced from fatty acids derived from trees and is widely used in many industrial applications, but it is not biodegradable (Saini et al., 2018). Bio-PP (Biological Polypropylene) is also derived from biological sources but does not possess biodegradable properties (Pereira et al., 2020).

Biodegradable plastics, on the other hand, are materials that can be decomposed by microorganisms through natural processes. These types of plastics can rapidly biodegrade under suitable conditions (e.g., compost environments) (Thompson et al., 2009). Biodegradable plastics, such as PHA (Polyhydroxyalkanoates), are produced by bacteria and can decompose in natural environments within a few months (Khatami et al., 2019). Similarly, PBAT (Polybutylene Adipate Terephthalate) is categorized as a biodegradable plastic

and is commonly used in film and packaging applications (Wang et al., 2018). PBS (Polybutylene Succinate) is a biodegradable polymer utilized in various applications (Zhang et al., 2021). Starch-based plastics, derived from foods such as sugarcane, potatoes, and corn, are commonly used in food packaging and single-use products, decomposing significantly faster than traditional plastics (Bashir et al., 2020). Plastics made from cellulose are often used in films and coatings, while chitosan-based plastics, derived from the shells of crustaceans, possess biodegradable characteristics (Raghavan et al., 2021).

The fundamental difference between these two types of plastics is that being biologically originated does not guarantee biodegradability. A plastic can be made from biological sources but may not decompose biologically depending on environmental conditions. Biodegradable plastics, however, have direct potential to provide environmental benefits.

Environmental Impacts

The positive environmental impacts of bioplastics, emerging as alternatives to traditional petroleum-based plastics, are critical for achieving sustainable living. The reliance on fossil fuels in the production of traditional plastics is a significant issue, as these are non-renewable resources and produce substantial greenhouse gas emissions that contribute to climate change (Friedrich & Wenzel, 2020). Since bioplastics are produced from renewable resources, they reduce this dependency (Duflou et al., 2012). This transition not only significantly reduces total energy consumption but also leads to greenhouse gas emissions during bioplastic production being 85% lower than those from traditional plastics (Huang et al., 2018). While traditional plastics can persist in nature for hundreds of years, bioplastics are characterized by their ability to decompose biologically within a few months under specialized composting conditions (Hakkarainen & Kautto, 2020). This facilitates waste management and minimizes environmental impacts (Aguado et al., 2019). The ability of bioplastics to decompose helps reduce soil and water pollution, as they can break down rapidly before reaching aquatic environments (Bacelar et al., 2020).

Economic Benefits

The economic advantages of bioplastics significantly impact the adoption of sustainable living. The initiation of bioplastic production and the transition to industrial-scale bioplastic manufacturing create new job opportunities in agriculture and industry (Nizami et al., 2017). The cultivation of bioplastic raw materials provides farmers with new income sources, while utilizing industrial

waste as raw material contributes to waste management (López et al., 2020). Bioplastics can be easily integrated into a circular economy model (Geissdoerfer et al., 2018). Recycling or composting bioplastics after use allows waste to transform into valuable resources (Pivnenko et al., 2016). As technology advances, the production costs of bioplastics are also decreasing (Duflou et al., 2012). By using waste materials instead of food as raw materials, production costs are reduced, enhancing sustainability (Rujnić-Sokele & Pilipović, 2017). This situation is causing the market share of bioplastics to increase steadily (Khan et al., 2021).

Social Awareness

The use of bioplastics has begun to raise awareness of sustainable lifestyles among individuals and communities (Zhou et al., 2020). This process contributes to the development of environmental sustainability consciousness within society (Pérez et al., 2021). Educational programs, workshops, and campaigns are methods used to create awareness about the benefits of bioplastics (López-Rodríguez et al., 2020). Additionally, especially in today's context where the impacts of climate change are starkly visible, it has been observed that consumers are shifting toward environmentally friendly alternatives, leading to increased demand for these products in the market (Coyle, 2021).

Future Directions

Advancements in bioplastic technology will enhance the performance of these materials, allowing for a broader range of applications. Research is progressing towards reducing costs and increasing durability. In improving the mechanical and thermal properties of bioplastics, the inclusion of 100% biodegradable additives is becoming increasingly important. Utilizing organic waste as raw material and ongoing studies on the recycling and reuse of bioplastics will contribute to the establishment of a sustainable economic model.

General Framework for Current and Future Regulations

The European Climate Law, published in 2021, outlines the EU's goal to reduce carbon emissions by 55% by 2030 compared to the pre-industrial era and to become the world's first carbon-neutral continent by 2050 as part of the Green Deal (European Commission, 2021). In line with these objectives, the EU has introduced the Carbon Border Adjustment Mechanism (CBAM) within the Fit For 55 package, which imposes carbon pricing on imports for certain sectors (Zhang et al., 2021). The upcoming CBAM regulation, expected to cover multiple sectors, has prompted businesses to prepare accordingly (Böhringer et al., 2021).

To maintain future competitiveness, many organizations are already calculating their corporate carbon footprints and implementing carbon reduction projects (Köhler et al., 2021). Additionally, efforts related to the plastic sector will commence by 2026. The effectiveness of bioplastics in reducing carbon footprints compared to petroleum-based plastics will facilitate compliance with these regulations (Müller et al., 2020).

The global impacts of waste from single-use plastic products, which are often used once or for a short duration, are significant for both the environment and human health (Jambeck et al., 2015). The likelihood of single-use plastics entering our oceans is considerably higher than that of reusable alternatives (Rochman et al., 2013). The ten most commonly found single-use plastic products on European beaches represent 70% of all marine litter in the EU (European Commission, 2020). The EU aims to be a leader in the global fight against marine litter and plastic pollution (European Parliament, 2019). EU regulations seek to reduce the volume and environmental impact of specific plastic products (European Commission, 2018-a).

Through its Directive on Single-Use Plastics, the EU applies different measures to various products. These measures are tailored to achieve the most effective outcomes and consider the availability of more sustainable alternatives. The Directive addresses ten items: cotton swabs, cutlery, plates, straws and stirrers, balloons and balloon sticks, food containers, beverage cups, beverage containers, cigarette butts, plastic bags, packaging, and hygiene products. According to the Directive, single-use plastic products may not be placed on the market in EU Member States where sustainable alternatives are readily available and affordable. This ban applies to cotton swabs, cutlery, plates, straws, stirrers, and balloon sticks. Additionally, it will apply to cups, food and beverage containers made from expanded polystyrene, and all products made from oxo-degradable plastics (European Commission, 2018-b).

For other single-use plastic products, the EU focuses on limiting their use through:

- Awareness-raising measures to reduce consumption
- Design requirements such as attaching caps to bottles
- Labeling requirements to inform consumers about the plastic content of products, disposal options to avoid, and the environmental harm caused if products are discarded in nature

- Waste management and cleanup obligations for producers, including Extended Producer Responsibility (EPR) plans

Specific targets include a separate collection target of 77% for plastic bottles by 2025, increasing to 90% by 2029. From 2025, it is aimed to use 25% recycled plastic in PET beverage bottles, and from 2030, all plastic beverage bottles are to contain 30% recycled plastic (European Commission, 2018-b).

Furthermore, the EU's overarching policy aims to gradually reduce the use of non-recyclable plastics and encourage the adoption of biodegradable and recyclable packaging materials. Greater restrictions on the use of non-recyclable plastics are expected in line with the EU's strategy for sustainable packaging solutions. The European Green Deal and circular economy plans promote the use of bioplastics and recyclable materials, with stricter regulations anticipated in these areas. Notably, under the EU's Single-Use Plastics Directive (2019/904),

Germany banned many single-use plastic products in 2021, including food packaging and food containers made from polystyrene foam. Additionally, Germany's "Einwegkunststofffondsgesetz," effective in 2024, will impose extended responsibilities on producers of single-use plastic products, aiming to increase their environmental accountability and promote the use of biodegradable alternatives.

Conclusion

Biodegradable bioplastics are a crucial component of sustainable living. These materials offer environmentally friendly alternatives, playing a critical role in decreasing plastic pollution and fostering a healthier future. The adoption of biodegradable bioplastics can significantly impact a wide range of stakeholders, from individuals to industries, establishing them as a foundational material for a sustainable future. However, the development and regulation of non-harmful alternatives like bioplastics must be prioritized through legal frameworks. To achieve this, education, innovation, and collaboration should be encouraged to promote the widespread use of bioplastics, thereby delivering environmental, economic, and social benefits.

References

- Aguado, R., et al. (2019). "Life cycle assessment of biodegradable plastics." *Waste Management*, 85, 348-355.
- Andrady, A. L. (2011). "Microplastics in the marine environment", *Marine Pollution Bulletin*, 62(8), 1596-1605.
- Bacelar, E., et al. (2020). "The potential of biodegradable plastics in reducing plastic pollution." *Science of The Total Environment*, 736, 139301.
- Bashir, S., et al. (2020). "Starch-based bioplastics: Properties, applications, and challenges." *Journal of Applied Polymer Science*, 137(31), 48929.
- Böhringer, C., et al. (2021). "The EU's carbon border adjustment mechanism: Design and impacts." *Climate Policy*, 21(7), 896-908.
- Coyle, K. (2021). "Consumer trends towards sustainable products: Implications for marketing." *Marketing Intelligence & Planning*, 39(6), 711-723.
- Duflou, J. R., et al. (2012). "Bio-based plastics: A review of the current status and future perspectives." *Journal of Cleaner Production*, 23(1), 1-13.
- Dussault, L., et al. (2018). "Polylactic Acid (PLA): A Comprehensive Review on the Role of Processing Conditions on Its Properties." *Materials*, 11(11), 2342.
- European Commission. (2018-a). "Proposal for a Directive of the European Parliament and of the Council on the reduction of the impact of certain plastic products on the environment."
- European Commission. (2018-b). "Directive (EU) 2019/904 of the European Parliament and of the Council on the reduction of the impact of certain plastic products on the environment." *Official Journal of the European Union*.
- European Commission. (2020). "EU Strategy for Plastics in a Circular Economy."
- European Commission. (2021). "Fit for 55: Delivering the EU's 2030 Climate Target on the way to climate neutrality."
- European Parliament. (2019). "Resolution on the EU strategy for plastics in a circular economy."
- Friedrich, J., & Wenzel, H. (2020). "The role of bio-based plastics in the transition towards a circular economy." *Resources, Conservation and Recycling*, 162, 105042.
- Geissdoerfer, M., et al. (2018). "The Circular Economy – A new sustainability paradigm?" *Journal of Cleaner Production*, 143, 757-768.
- Geyer, R., Wilcox, C., & Lavender Law, K. (2017). "Production, use, and fate of all plastics ever made", *Science Advances*, 3(7), e1700782.
- Hakkarainen, M., & Kautto, P. (2020). "Biodegradable plastics: a review of the current state of research." *Frontiers in Materials*, 7, 12.

- Huang, J., et al. (2018). "Life cycle assessment of biodegradable and conventional plastics: A comparative study." *Journal of Cleaner Production*, 196, 743-751.
- Jambeck, J. R., Geyer, R., & Wilcox, C. (2015). "Plastic waste inputs from land into the ocean", *Science*, 347(6223), 768-771.
- Khan, M. I., et al. (2021). "3D Printing of Polylactic Acid (PLA) for Industrial Applications: A Review." *Materials Today: Proceedings*, 46, 123-128.
- Khan, M. I., et al. (2021). "Recent advances in biodegradable polymers and their applications." *Materials Today: Proceedings*, 46, 1250-1255.
- Khatami, A., et al. (2019). "Production of polyhydroxyalkanoates from renewable resources: A review." *Frontiers in Bioengineering and Biotechnology*, 7, 303.
- Köhler, A., et al. (2021). "Corporate climate strategies: Carbon footprint accounting and management." *Journal of Cleaner Production*, 284, 124731.
- Kumar, V., et al. (2020). "Bioplastics: A Sustainable Alternative to Conventional Plastics." *Environmental Science & Technology*, 54(14), 9000-9014.
- Lebreton, L., Greer, S. D., & Borrero, J. C. (2012). "Numerical modeling of floating debris in the world's oceans.", *Marine Pollution Bulletin*, 64:653-661, doi:10.1016/j.marpolbul.2011.10.027.
- Lebreton, L., Greer, S. D., & Borrero, J. C. (2017). "Numerical modeling of floating debris in the world's oceans", *PLOS ONE*, 12(6), e0171970.
- Liu, Y., et al. (2021). "Microplastics in human body: A review." *Environmental Science & Technology*, 55(8), 5130-5140.
- López, A., et al. (2020). "Bioeconomy: A new opportunity for rural development." *Sustainability*, 12(14), 5731.
- López-Rodríguez, A., et al. (2020). "Raising awareness of bioplastics: Educational initiatives and their impact on consumer behavior." *Journal of Environmental Education*, 51(1), 24-34.
- Müller, C., et al. (2020). "Assessing the potential of bioplastics in reducing greenhouse gas emissions." *Sustainable Production and Consumption*, 22, 158-170.
- Nizami, A. S., et al. (2017). "Bioplastics: A review of the current state and future perspectives." *Renewable and Sustainable Energy Reviews*, 81, 168-181.
- Pereira, J. A., et al. (2020). "Biobased Polypropylene: Synthesis, Properties, and Applications." *Polymer International*, 69(10), 1213-1221.
- Pivnenko, K., et al. (2016). "Biodegradable plastics: A review." *Waste Management*, 55, 132-145.
- Raghavan, P., et al. (2021). "Chitosan-based bioplastics: A review." *Carbohydrate Polymers*, 264, 118042.

- Rujnić-Sokele, M., & Pilipović, A. (2017). "Bioplastics and their use in food packaging: A review." *Sustainability*, 9(10), 1667.
- Saini, R., et al. (2018). "The Properties and Applications of Polyamide 11." *Journal of Materials Chemistry A*, 6(20), 9168-9180.
- Shen, L., et al. (2020). "Bio-based plastics: A review." *Environmental Science & Technology*, 54(2), 1271-1281.
- Thompson, R.C.; Swan, S.H.; Moore, C.J.; vom Saal, F.S. (2009). "Our plastic age". *Phil. Trans. R. Soc. B*. 2009, 364, 1973–1976.
- Wang, Y., et al. (2018). "Biodegradable poly(butylene adipate-co-terephthalate) for the development of sustainable packaging." *Journal of Cleaner Production*, 172, 1376-1385.
- Zhang, Y., et al. (2020). "Microplastics in the environment: A review of the effects on human health." *Environmental Science and Pollution Research*, 27(8), 8462-8480.
- Zhang, Y., et al. (2021). "Polybusiness: the science behind poly(butylene succinate)." *Green Chemistry*, 23(4), 1305-1321.
- Zhang, X., et al. (2021). "The implications of the EU Carbon Border Adjustment Mechanism." *Environmental Economics and Policy Studies*, 23(1), 1-25.
- Zhou, Y., et al. (2020). "Sustainability awareness and its influence on green consumption behavior: A case study of Chinese consumers." *Journal of Cleaner Production*, 267, 122103.



CHAPTER 3

An Example of an Application Based on Cloud-IoT

Batın Demircan¹

¹Lect., Balıkesir University, Balıkesir Vocational School, Department of Electronic and Automation, Balıkesir, Turkey, ORCID: 0000-0002-0765-458X

1. Introduction

The Internet of Things (IoT) smart applications have gained popularity in recent years and are increasingly being adopted across various sectors such as cities, agriculture, healthcare, and industry (Oliveira, Di Felice, & Kamienski, 2024). IoT enables the transfer of information between a range of equipment by integrating different technologies with communication solutions. In terms of remote data monitoring, IoT is directly applied to the real-time acquisition and transmission of large volumes of data (Rahman, Selvaraj, Rahim, & Hasanuzzaman, 2018; Ramakrishna Madeti & Singh, 2016). In this context, the use of cloud computing becomes a flexible and cost-effective platform for processing and storing such data (Swathi & Guruprasad, 2014). Additionally, IoT now refers to billions of physical devices connected to the internet worldwide, used for collecting and sharing data (Hussain, Osman, Moin, & Memon, 2021; Kumar, Tiwari, & Zymbler, 2019; Yusri & Nashiruddin, 2020).

The International Telecommunication Union's Telecommunication Standardization Sector (ITU-T) defines the Internet of Things (IoT) as "a global infrastructure for society that provides advanced services by connecting physical and virtual objects based on existing and evolving interoperable information and communication technologies" (Zmud et al., 2018). The integration of IoT with cloud computing is referred to as CloudIoT (Ramakrishna Madeti & Singh, 2016). IoT encompasses various techniques, including smart sensors, wireless communication, networks, data analytics technologies, and cloud computing (Asghar, Negi, & Mohammadzadeh, 2015; Nemer, Sheltami, Shakshuki, Elkhail, & Adam, 2021; Nižetić, Šolić, López-de-Ipiña González-de-Artaza, & Patrono, 2020).

In this study, measurement data from a temperature sensor was transferred to an Arduino Uno control board and used in a Cloud-IoT-based application supported by LabVIEW software. An LM35 temperature sensor was employed to measure ambient temperature. Data from this sensor was processed by a program developed in the LabVIEW environment, allowing for both local visualization and storage on a computer for the user. Additionally, the data was sent to the ThingSpeak Internet of Things (IoT) and cloud computing platform, where it was further visualized and displayed on the platform.

2. Hardware and Software System Architecture

Arduino Uno was used to capture data from the external environment via analog sensor measurements. The Arduino Uno board is equipped with an ATmega328P microcontroller, operating at 16 MHz. It features 16 digital input/output pins and 6 analog input pins. Communication with a computer is established through a USB connection (Arduino, 2024). The appearance of the Arduino Uno control board is shown in Figure 1 (Peter, 2024).

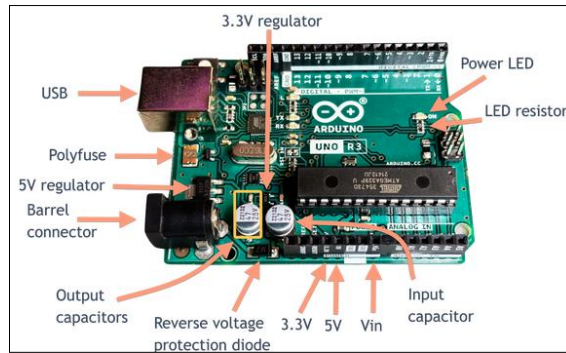


Figure 1. Aruino Uno R3

The LM35 temperature sensor was used to measure ambient temperature. This sensor produces a voltage of 10 mV per 1°C (Daumemo, 2021). It is connected to the “A0” analog channel of the Arduino Uno control board, as shown in Figure 2.

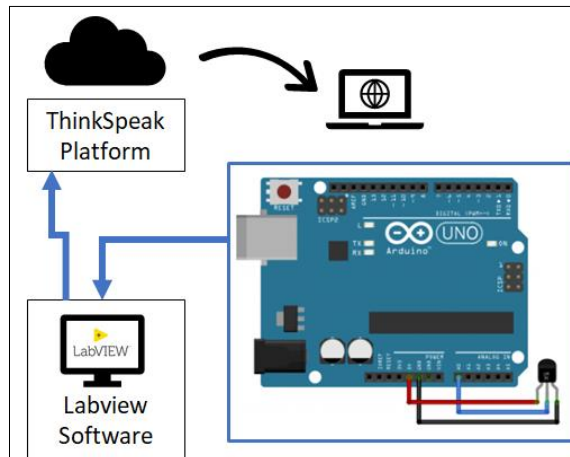


Figure 2. Hardware and software arthitecture

The hardware structure used in the study is shown in Figure 3. Arduino Uno board communicates with the LabVIEW software through a USB interface.

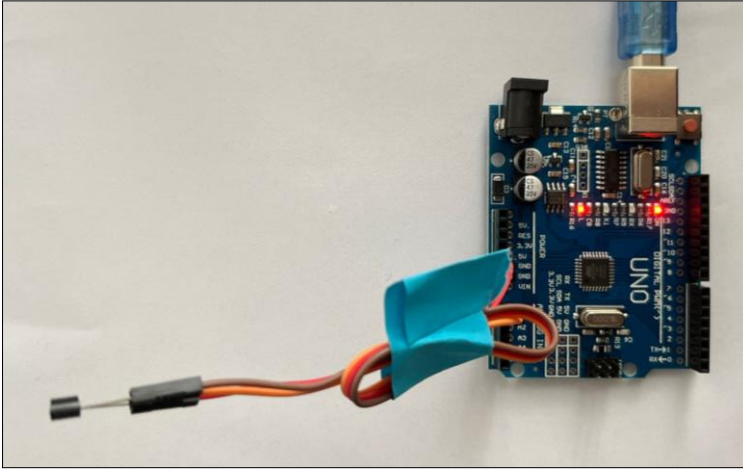


Figure 3. Experimental setup

In this study, LabVIEW software was used to log the data measured from the hardware on the computer and transmit it to the ThingSpeak online platform. LabVIEW is a paid software, but a student version is available.

The download screen of the LabVIEW software from the National Instruments website as shown in Figure 4 (National Instruments Corp., 2024).

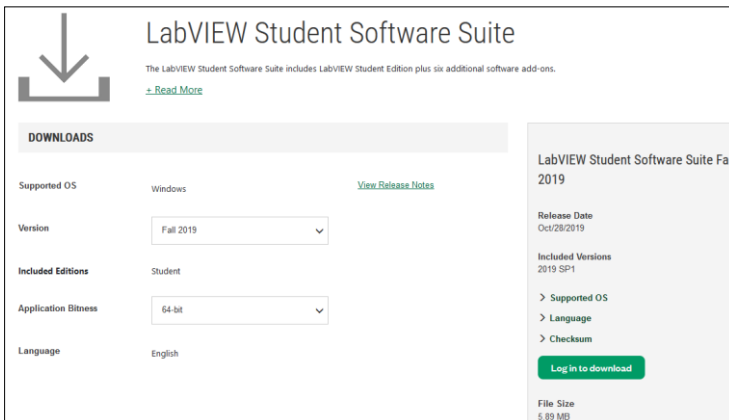
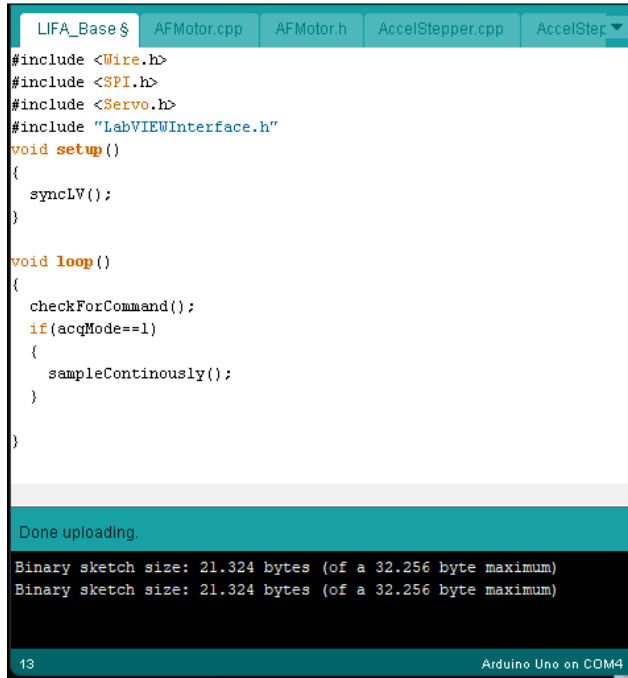


Figure 4. LabVIEW software download screen

For the communication between LabVIEW software and Arduino, the program intended for upload to the Arduino Uno can be found in the installation directory of LabVIEW. Specifically, the Arduino software with the "*.ino" extension, located at the path "C:\Program Files (x86)\National Instruments\LabVIEW 2019\vi.lib\LabVIEW Interface for Arduino\Firmware\LIFA_Base," must be directly uploaded to the Arduino Uno.

It is crucial to note the version of the compiler used for this upload. Higher versions of the IDE software have resulted in errors in the communication section with LabVIEW; hence, "Arduino IDE 1.0.1" was selected for this purpose. The software and library information uploaded to the Arduino is presented in Figure 5.



```
#include <Wire.h>
#include <SPI.h>
#include <Servo.h>
#include "LabVIEWInterface.h"

void setup()
{
    syncLV();
}

void loop()
{
    checkForCommand();
    if(acqMode==1)
    {
        sampleContinuously();
    }
}
```

Done uploading.

Binary sketch size: 21.324 bytes (of a 32.256 byte maximum)
Binary sketch size: 21.324 bytes (of a 32.256 byte maximum)

13 Arduino Uno on COM4

Figure 5. Arduino IDE software and Arduino program

In LabVIEW, the software loop is executed on this graphical interface through visual programming. The "Timed Loop" menu, located under the "Functions" palette in LabVIEW, should be selected and placed in the programming area. The program loop continuously operates within this structure, based on the specified software loop duration.

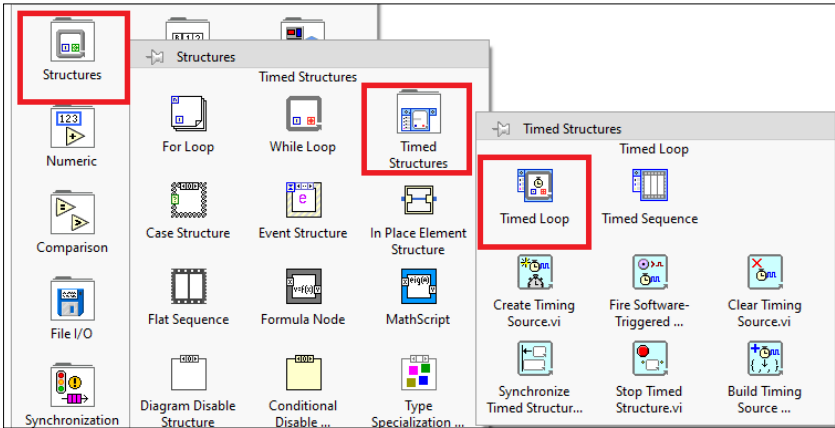


Figure 6. Labview structures menu

To establish a connection between the LabVIEW software and the Arduino Uno control board, the Arduino software libraries must be utilized. Since the version of LabVIEW being used is 2019, the "Arduino" software module should be installed via the "VI Package Manager (VIPM)."

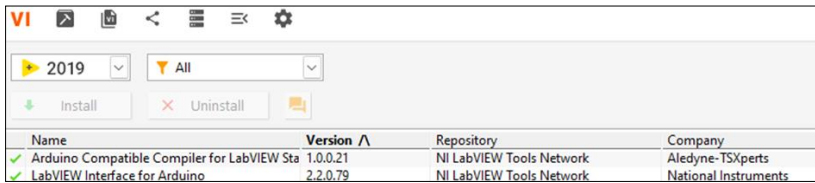


Figure 7. Labview VI package manager

Following the installation of the software modules, the 'Init' and 'Close' menus, as shown in Figure 8, are used for communication with the Arduino Uno controller board.

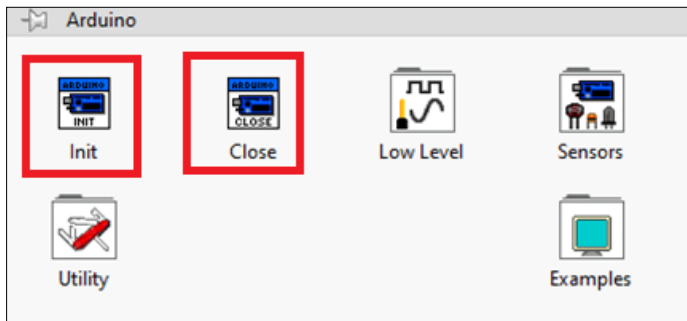


Figure 8. Labview Arduino menu-1

The 'Analog Read Pin' menu, shown in Figure 9, is used for measuring the analog voltage from the LM35 temperature sensor by the controller board.

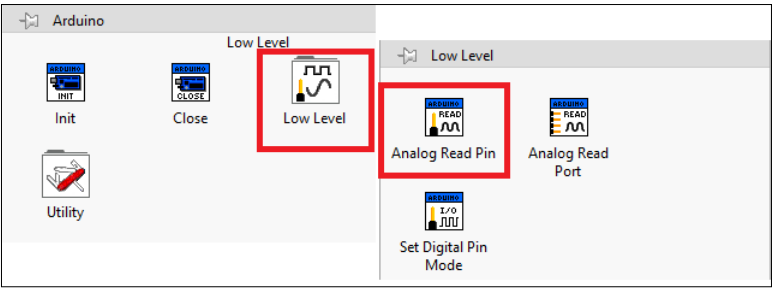


Figure 9. Labview Arduino menu-2

The menus located in the 'Data Communication' tab, shown in Figure 10, are used for sending the obtained measurement data to the ThingSpeak platform.

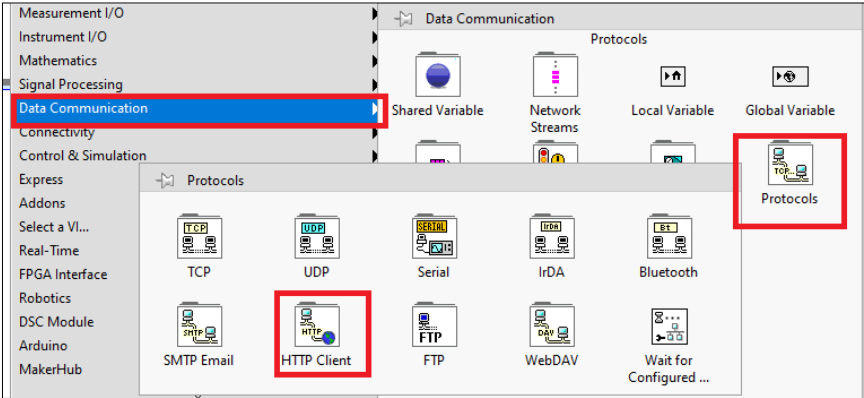


Figure 10. Labview data communication menu

The 'Http Client' menu, shown in Figure 10, includes the 'Open Handle,' 'Get,' and 'Close Handle' menus, shown in Figure 11.

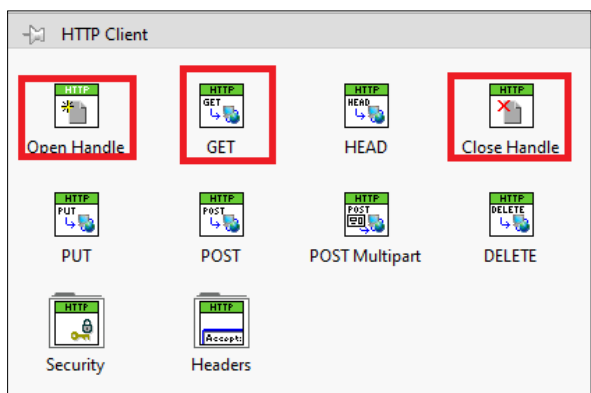


Figure 11. Labview HTTP menu

The registration of a free account on the ThingSpeak platform for sending the temperature measurements transferred to LabVIEW software is shown in Figure 12.

ThingSpeak Usage Intent

How are you using ThingSpeak?*

☐ Commercial work (including research)
☐ Government work (including research)
☐ Personal, non-commercial projects
☒ Student use, Teaching, or Research in academia

What is the name of your University?*

Balikesir University

What best describes your current role?*

☐ Student
 ☒ Professor
 ☐ Researcher

What is the name of your Course or Project?*

iot_labview

Figure 12. ThinkSpeak platform menu-1

A channel structure, as shown in Figure 13, has been created within the Cloud-IoT platform on the ThingSpeak website for data acquisition.

New Channel

Name Labview_Thing

Description Data received from Labview software

Field 1 Data 1 ☒

Figure 13. ThinkSpeak platform menu-2

To send data to a channel within the IoT structure, an object definition must be created. The 'API' associated with this object is generated by the Cloud platform, as shown in Figure 14.

Private View Public View Channel Settings Sharing API Keys Data Import / Export

Write API Key

Key QNUREPO5V2NO75VM

Generate New Write API Key

Help

API keys en generated v

API Ke

• Write

Figure 14. ThinkSpeak platform menu-3

The 'API' created on the cloud platform is shown in Figure 15.

API Requests

Write a Channel Feed

GET https://api.thingspeak.com/update?api_key=QNUREPO5V2NO75VM&field1=0

Figure 15. ThinkSpeak platform menu-4

After the program structure was created for reading analog data and sending the measurement data to the cloud environment, the 'string' data type, as shown in Figure 16, was utilized for transmitting the temperature measurement data to the controller board.

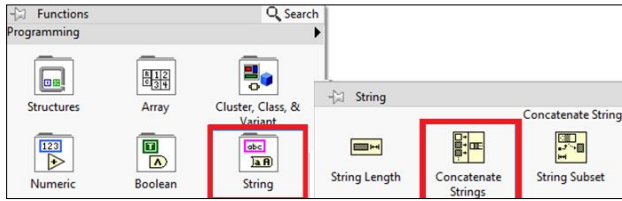


Figure 16. Labview software string menu-1

The second 'string' structure used for data transmission to the cloud platform is shown in Figure 17.

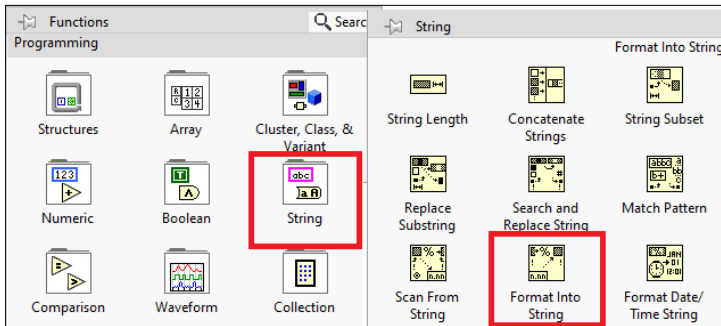


Figure 17. Labview software string menu-2

The 'API' file on the cloud platform was configured as shown in Figure 18 when transferred to the LabVIEW software.

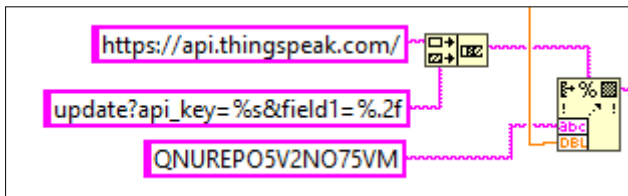


Figure 18. Aciklama.

To enable simultaneous recording after real-time transmission of measurement data to the cloud, the 'For Loop' structure from the 'Functions' menu was used.

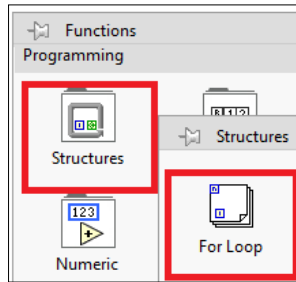


Figure 19. Labview software structures menu

The selection of the 'Set Attributes' module, operating within the For loop, is shown in Figure 20.

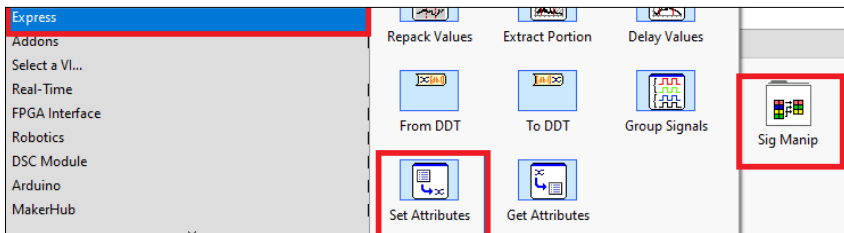


Figure 20. Labview software express menu

The 'File I/O' menu, shown in Figure 21, was used to write the measurement results to the computer.

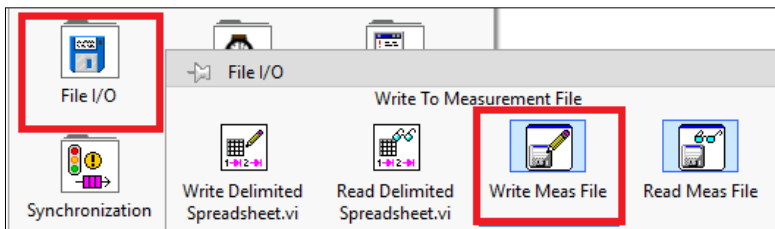


Figure 21. Labview software file I/O menu

The program structure developed in the LabVIEW software created for the study is shown in Figure 22.

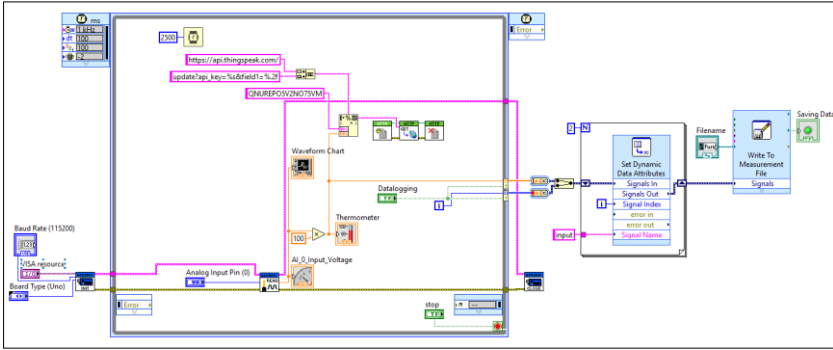


Figure 22. The developed Labview program

3. Experimental Results

As a result of the application implemented based on Cloud-IoT, real-time temperature data was measured in the user program developed in LabVIEW software. The developed software also facilitated the recording of data in a computer environment. Developed LabVIEW program as shown in Figure 23.

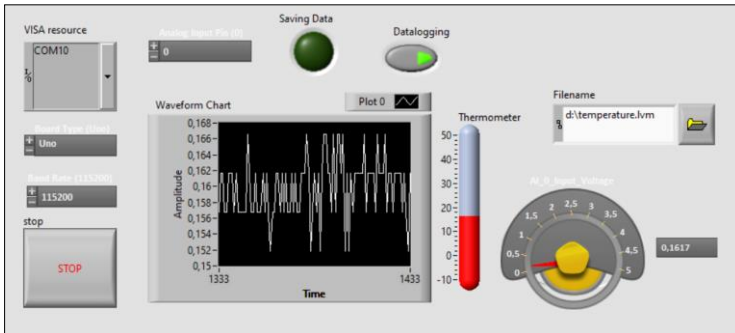


Figure 23. The front panel of the developed LabVIEW program

The temperature data measured in real-time has been sent to the ThingSpeak platform. The temperature data measured in real-time has been sent to the ThingSpeak platform, as shown in Figure 24.

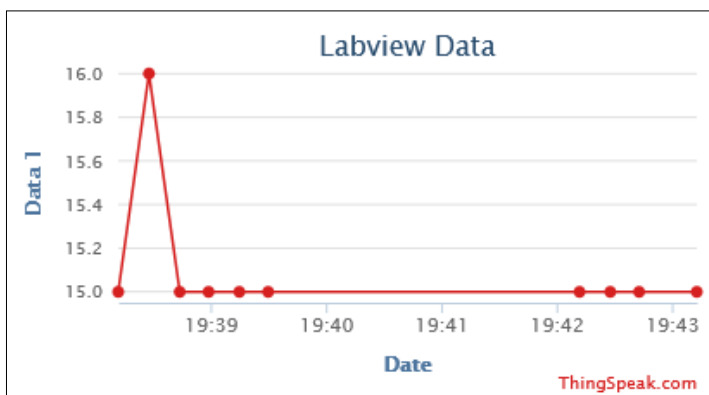


Figure 24. The data graph sent to the ThingSpeak platform

Data obtained from the LM35 sensor has been recorded in a computer environment in “.lvm” format. A screenshot of the file on the computer is shown in Figure 25.

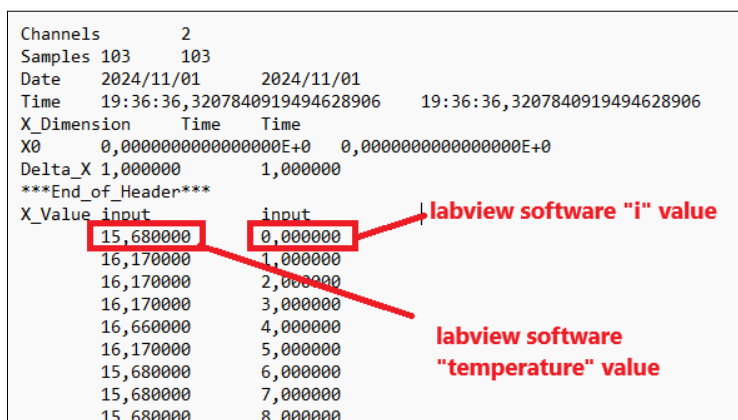


Figure 25. The temperature log file

An examination of the recorded real-time temperature measurement data shows that the interval between each measurement point is 2.5 seconds. The temperature change, starting from 15 °C within a specified time period, is shown in Figure 26.

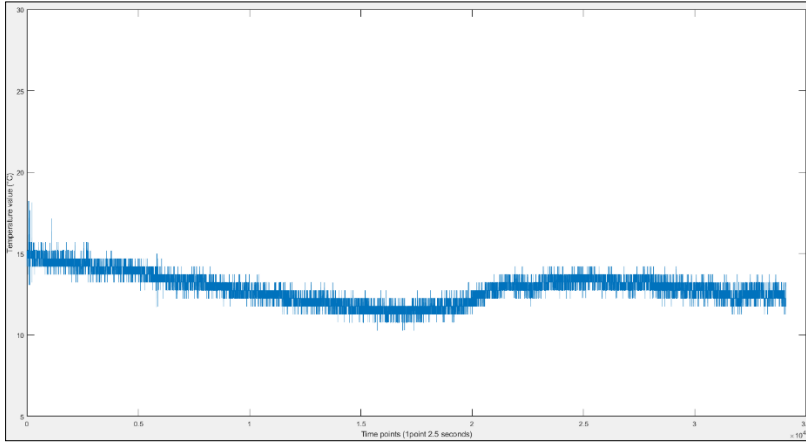


Figure 26. Graph of measured temperature

4. Conclusion

In this study, a cloud-based application for real-time temperature measurement and recording was implemented within the rapidly advancing field of Cloud-IoT technology. The system employed an LM35 temperature sensor for temperature measurement and an Arduino Uno controller for data transmission and measurement acquisition. ThinkSpeak was used as the cloud computing platform, while a program developed in LabVIEW software handled data reading, recording, and transmission to the cloud platform.

5. References

- Arduino. (2024). UNO R3 | Arduino Documentation. Retrieved October 17, 2024, from <https://docs.arduino.cc/hardware/uno-rev3/>
- Asghar, M. H., Negi, A., & Mohammadzadeh, N. (2015). Principle application and vision in Internet of Things (IoT). *International Conference on Computing, Communication and Automation, ICCCA 2015*, 427–431. <https://doi.org/10.1109/CCAA.2015.7148413>
- Daumemo. (2021). How to measure temperature with Arduino and LM35 sensor - Daumemo. Retrieved October 27, 2024, from <https://daumemo.com/how-to-measure-temperature-with-arduino-and-a-cheap-lm35-sensor/>
- Hussain, S. Z. R., Osman, A., Moin, M. A., & Memon, J. A. (2021). IoT enabled real-time energy monitoring and control system. *9th International Conference on Smart Grid, IcSmartGrid 2021*, 97–102. <https://doi.org/10.1109/ICSMARTGRID52357.2021.9551208>
- Kumar, S., Tiwari, P., & Zymbler, M. (2019). Internet of Things is a revolutionary approach for future technology enhancement: a review. *Journal of Big Data*, 6(1), 1–21. <https://doi.org/10.1186/S40537-019-0268-2/FIGURES/9>
- National Instruments Corp. (2024). LabVIEW Student Software Suite. Retrieved October 17, 2024, from https://www.ni.com/en/support/downloads/software-products/download.labview-student-software-suite.html?srltid=AfmBOopsUqVBsoC2QPyYmpGRM7D2T-C5_VnFbhaPIfgHncEF0zuEvDzr#352823
- Nemer, I., Sheltami, T., Shakshuki, E., Elkhail, A. A., & Adam, M. (2021). Performance evaluation of range-free localization algorithms for wireless sensor networks. *Personal and Ubiquitous Computing*, 25(1), 177–203. <https://doi.org/10.1007/S00779-020-01370-X>
- Nižetić, S., Šolić, P., López-de-Ipiña González-de-Artaza, D., & Patrono, L. (2020). Internet of Things (IoT): Opportunities, issues and challenges towards a smart and sustainable future. *Journal of Cleaner Production*, 274, 122877. <https://doi.org/10.1016/J.JCLEPRO.2020.122877>
- Oliveira, F. B., Di Felice, M., & Kamienski, C. (2024). IoTDeploy: Deployment of IoT Smart Applications over the Computing Continuum. *Internet of Things*, 28, 101348. <https://doi.org/10.1016/J.IOT.2024.101348>
- Peter. (2024). The Ultimate Guide to Powering Your Arduino Uno Board . Retrieved October 17, 2024, from <https://techexplorations.com/blog/arduino/guide-to-arduino-uno-r3-power/>
- Rahman, M. M., Selvaraj, J., Rahim, N. A., & Hasanuzzaman, M. (2018). Global modern monitoring systems for PV based power generation: A review.

- Renewable and Sustainable Energy Reviews, 82, 4142–4158.
<https://doi.org/10.1016/J.RSER.2017.10.111>
- Ramakrishna Madeti, S., & Singh, S. N. (2016). Monitoring system for photovoltaic plants: A review. <https://doi.org/10.1016/j.rser.2016.09.088>
- Swathi, B. S., & Guruprasad, H. S. (2014). Integration of Wireless Sensor Networks and Cloud Computing. Retrieved from <http://www.ipasj.org/IJCS/IJCS.htm>
- Yusri, A., & Nashiruddin, M. I. (2020). LORAWAN Internet of Things Network Planning for Smart Metering Services. 2020 8th International Conference on Information and Communication Technology, ICoICT 2020. <https://doi.org/10.1109/ICOICT49345.2020.9166455>
- Zmud, J., Miller, M., Moran, M., Tooley, M., Borowiec, J., Brydia, B., ... Gunnels, A. (2018). A Primer to Prepare for the Connected Airport and the Internet of Things. A Primer to Prepare for the Connected Airport and the Internet of Things. <https://doi.org/10.17226/25299>



CHAPTER 4

Electronic monitoring for unwanted catches and further considerations for Turkish Fishery

Ozan Soykan¹ & F. Ozan Düzbastılar²

¹Assoc. Prof. Dr., Ozan SOYKAN Ege University, Faculty of Fisheries, Fishing and Processing Department, 35100, Bornova, İzmir/TÜRKİYE, Orcid: 0000-0002-2227-1245

² Prof. Dr., Faik Ozan DÜZBASTILAR Ege University, Faculty of Fisheries, Fishing and Processing Department, 35100, Bornova, İzmir/TÜRKİYE, Orcid: 0000-0002-5376-7198,

Introduction

Commercial fishing is one of the world's growing industries and, due to the nature of the activity, is very difficult to manage and regulate compared to other industries. Globally, increased gear selectivity, effort restrictions, quota limitations, temporal and spatial restrictions, transferable quotas, and discard bans are the technical measures in force within fisheries management (Plet-Hensen et al., 2017). One of the most important regulations in EU fisheries in recent times is the landing obligation, which in the concept of the Common Fisheries Policy focuses in particular on unwanted or, in other words, “discarded” catches (CFP). Discard is generally identified as “the catch is that portion of the total organic material of animal origin in the catch, which is thrown away, or dumped at sea for whatever reason. It does not include plant materials and post-harvest waste such as offal. The discards may be dead, or alive.” (FAO, 2018). The degree of discarding is shaped by various factors, including species composition, the condition of the catch, fishing techniques, equipment used, regulatory policies, and market demand (Tsagarakis et al., 2014). Additionally, the discard rate was estimated at 10.8% between 2010 and 2014, resulting in an annual total of 9.1 million metric tons of discards (Roda et al., 2019). In the Mediterranean, around 240,000 metric tons of discards were reported annually (Roda et al., 2019).

Discard practices are influenced by numerous factors, making it challenging to evaluate the effectiveness of any specific measure or action. Furthermore, bycatch and discard reduction measures are often implemented in conjunction with other management strategies, making assessment of their effectiveness even more difficult. The most common bodies to regulate discarding are gear restrictions, seasonal and regional closures, species prohibitions, and length limitations. Many regulations are enforced inconsistently, and their implementation is often less restrictive than intended (Suuronen and Gilman, 2020). In addition, discard data, which is very limited and scarce for many areas and fishery types, is crucially important to assess the magnitude of discarding. Therefore, a simpler, more flexible, and more inclusive approach is required to monitor and document not only target species but also unwanted catches to fully control the fisheries. In addition, such an approach must represent a high proportion of the total fishing effort, since the coverage of other monitoring, control, and surveillance (MCS) measures is around 1% globally (James et al., 2019).

Electronic monitoring (EM) in the fishing industry

The exploitation of marine resources requires a sustainable and measurable management strategy. Although the term “sustainability” has been pronounced by a massive community, measurability has been generally highlighted by the scientific community. Measuring the fisheries or a type of fishery requires reliable fisheries-dependent data basically on (a) the number and length of fish that are caught, (b) the total weight of each species in the catch composition, (c) fishing effort (e.g., the number of hours or days spent fishing), and (d) by-catch species with their number, length, and weight including protected species. This type of dataset establishes the concept of fully documented fisheries (FDF), which is essential for assessing fish stocks and monitoring and managing the environmental impacts of fishing. The most common measures to provide FDF include self-sampling, reference fleets, on-board observers, and electronic monitoring (EM), and three of them (self-sampling, on-board observers, and electronic monitoring) are also prevalent tools for MCS (James et al., 2019). Among these measures, EM appears to be innovative, practical, applicable, highly representative, and therefore a promising solution for catch monitoring. Recently, the use of EM systems has become widespread worldwide in many types of fisheries such as purse seining, bottom trawling, longline fishing, etc (Figure 1a, 1b).

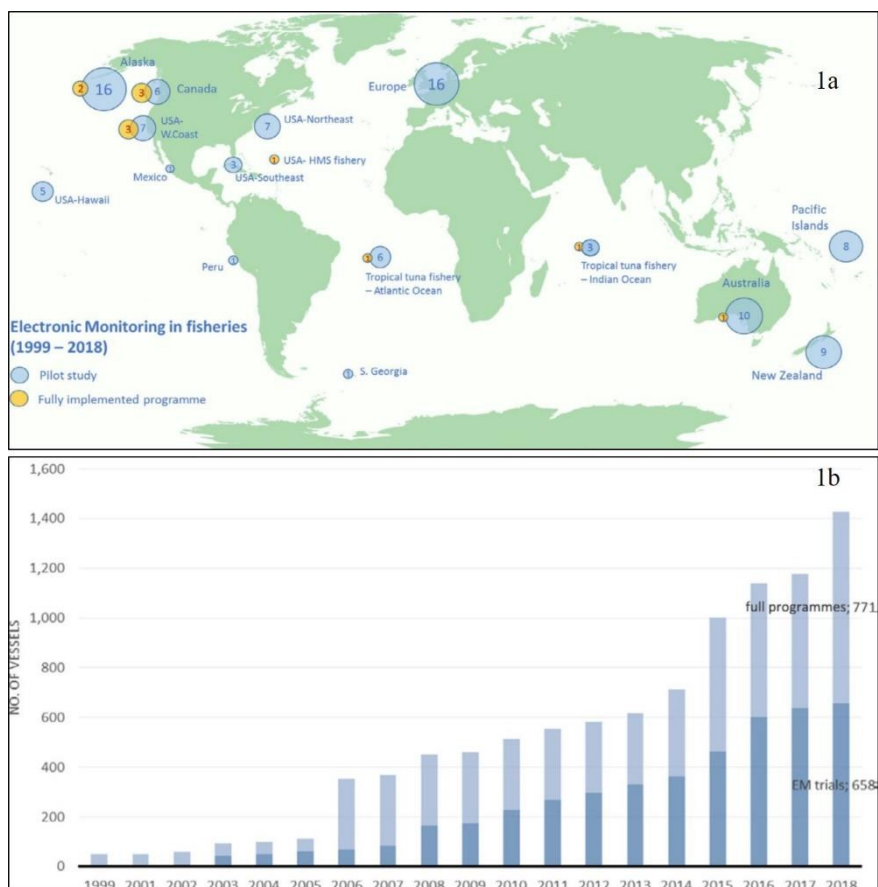
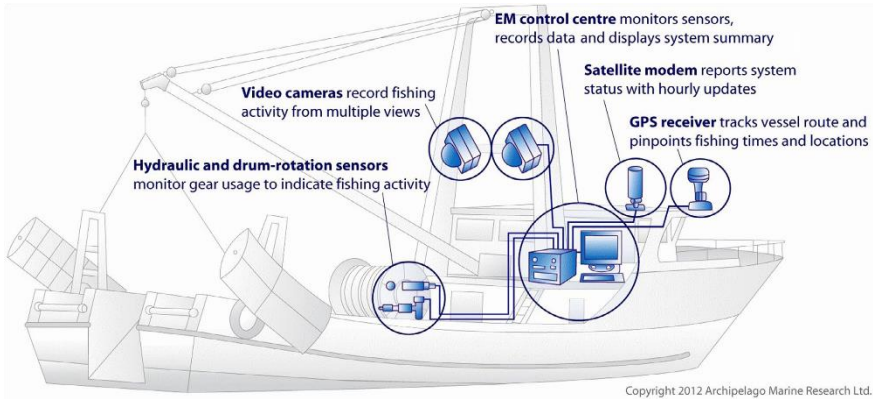


Figure 1. EM implemented to fishery based on world oceans and seas (1a) and the trend in the world fishing fleet (1b)

Source: van Helmond et al., 2019

Electronic monitoring plays a crucial role, particularly in preventing illegal fishing. Traditional monitoring methods do not allow for continuous oversight of every vessel, but with these systems, monitoring processes become more effective and efficient. Additionally, the accuracy of species and quantities caught by fishermen is recorded through these systems, leading to better data management. An EM system typically consists of three primary components: (a) a GPS recorder that provides data on the vessel's location, (b) cameras that capture visual information on fishing activities and catches, and (c) hydraulic and drum-rotation sensors that track the deployment and retrieval of gear (van Helmond et al., 2019) (Figure 2).

Figure 2. Main elements of the EM system deployed on a vessel



Source: van Helmond et al., 2019

Detailed and visualized documentation of the catch (Figure 3) allows us to obtain accurate results on by-catch species in terms of number, length, and weight compared to other monitoring options once the machine learning technology is very well adapted to the system. To achieve this goal, computer vision machine learning may also be applied to EM systems with the expected following benefits:

- Automated species detection, identification, count, and length estimation of fish and other invertebrates as they are taken on board and placed on the conveyor belt.
- Species identification of fish images collected in controlled environments. This can also be referred as preparing an image databank for by-catch species including their metric and meristic characters covering protected, endangered, and threatened species (PETS).

Rapid and reliable data implementation to fishery management plans in a short time, which is very crucial due to dynamism and fluctuations in seasonal fishing effort and fish populations, can lead to a simpler and rapid management framework while ensuring the environmental and economic performance of fisheries are improved.

EM-based data, such as catch composition and length frequencies, can then be utilized for quota management or to control unwanted catches. For instance, fishing grounds may be closed, or the fishing season adjusted if catches are found to contain a high percentage of spawners, juveniles, vulnerable species, or other non-target species. It is also possible to use EM-based morphometric data during gear modifications such as mesh size and shape for mitigating unwanted catches.

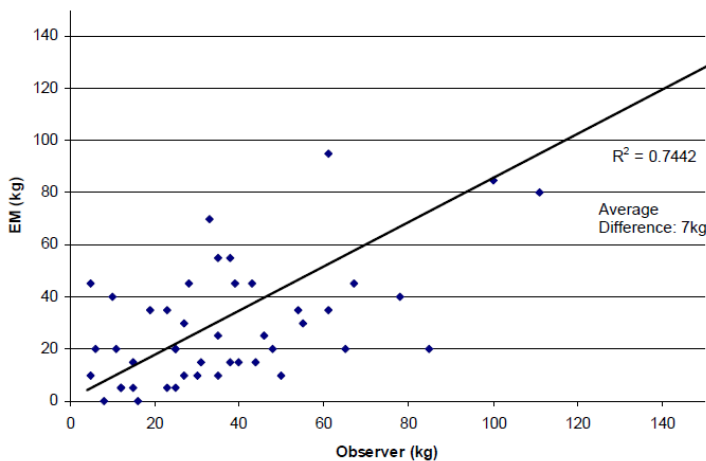
It is also reported that EM and observer data for discard amount estimation have a good correlation (McElderry et al., 2010) (Figure 4).

Figure 3. Some image samples taken form EM system in the New Zealand in-shore trawl fishery



Source: McElderry et al., 2010

Figure 4. Relation between discard estimations of EM and observer based data



Source: McElderry et al., 2010

In expanding the use of EM systems among fishermen and the fishing industry, several concerns need to be addressed. First, reviewers are still the key elements of EM-based data, as video footages are still required to be manually analyzed, which makes the procedure tedious and expensive. Another one is the fishers' consideration of EM as an intrusion into their work life, a threatening situation to their privacy. The latter is the deployment costs of EM systems which may be a challenging financial issue for the fishers. Regarding the first concern, face masking by computer vision technology integrated into the EM system may be a possible solution. Second, some incentives such as additional quota scoring and direct payment could attract fishers' attention and provide their participation to EM supported catch monitoring. Instead of being unusual and unpopular to fishers, the use of EM systems among fishers can also be promoted by a "win & win" approach. This can be explained as while the decision makers obtain the required scientific data to manage fishery resources via EM on the quality and quantity of unwanted catches, on the other hand, fishers, who are mostly blamed for the impact they create on the marine environment, may use EM records as a way to prove the reliability of their documentation, in the spirit of the "black boxes" used in airplanes (van Helmond et al., 2019). This approach may also meet additional market expectations, as consumers increasingly want to know the origin or sustainability of the products they purchase. Michelin et al (2018) reported the future demand of seafood retailers on EM, who are willing to create and/or increase the traceability and transparency of their products in compliance with the "net-to-plate" strategy. This case shows that EM implementation in commercial fishery may directly affect the seafood industry as well. Therefore, seafood companies can be involved during the promotion and dissemination of EM in fisheries, more than that, they may be asked to cover some of the initial expenses (sponsorship) such as purchase and deployment that are accounted to be high costs for fishers, to strength the image of the fishing industry as a whole. In conclusion, although there are still some points to address such as data ownership, data storage, and data misuse, EM, from many perspectives, seems to be a powerful and promising tool in fisheries monitoring especially for unwanted catches.

The case of Türkiye

Türkiye, surrounded by seas on three sides, holds significant potential in the fishing industry. However, ensuring sustainable fishing practices and conserving marine resources requires the implementation of modern monitoring methods. In this context, electronic monitoring (EM) systems have already become a promising technology for Turkish fisheries. By 2022, total fisheries production

had risen to nearly 800,000 metric tons, with capture fisheries contributing 328,000 (41%) metric tons and the Turkish fishing fleet comprises 14064 vessels across all length classes and types (Turkstat, 2024). Among the fleet, purse seiners (n=396) and trawlers (n=759) which are generally known as industrial vessels due to their high catch capacity, comprise around 6% of the fleet. Although deck equipment such as navigational systems, echo-sounders, and sonars are inevitable for such vessels, none of them were equipped with EM systems. Electronic monitoring systems continuously track maritime activities through cameras, sensors, and other data collection devices installed on fishing vessels. These systems aim to enhance compliance with fishing regulations, prevent illegal, unreported, and unregulated (IUU) fishing, and protect the marine ecosystem. Given the size of Türkiye's fishing sector and the challenges in monitoring, these systems are supported by both commercial fishers and environmental protection organizations.

Application fields of Electronic Monitoring Systems in Türkiye

1. **Prevention of Illegal and Unreported Fishing:** Electronic monitoring systems are an effective tool for preventing illegal and unreported fishing, especially on Türkiye's large and offshore fishing vessels. Traditional inspection methods require the physical presence of coast guards and inspection teams, whereas electronic monitoring automates and continuously monitors these processes.
2. **Catch Reporting and Data Accuracy:** Electronic monitoring ensures the accuracy of the types and quantities of fish caught by fishers, contributing to more reliable fisheries data. This leads to more trustworthy assessments of catch amounts and stock evaluations, which are critical for fisheries management. This will enable getting reliable data, especially for discards which is very controversial in terms of quality and quantity in Türkiye
3. **Prevention of Illegal Fishing Gear Use:** It can be challenging to detect illegal fishing gear and methods used in Türkiye. However, with electronic monitoring systems, identifying and prohibiting the use of such equipment has become more feasible.

Advantages of Electronic Monitoring

- **Sustainability:** To protect fish stocks in the seas and ensure the continuity of the ecosystem, electronic monitoring systems encourage

fishers to comply with fishing regulations. This helps prevent overfishing and improper fishing practices.

- **Reducing Monitoring Costs:** Electronic monitoring replaces human-dependent inspections, saving both time and costs. The use of technology digitalizes inspection processes, making it a more economical solution for both the government and fishers. These methods seem to be beneficial for Türkiye when the huge fishing areas around the Türkiye are considered.
- **Data Collection and Analysis:** The electronic recording of collected data accelerates data analysis, a crucial step in fisheries management. Having more reliable and real-time data is of great importance in monitoring the health of marine ecosystems. This is again very required for discard analyze and amount estimation.

Challenges Encountered

- **High Installation and Operating Costs:** Installing electronic monitoring systems on fishing vessels can initially incur high costs. These expenses may present a significant barrier, especially for small-scale fishers. However, the long-term benefits of these systems balance out the costs. The traditional approach of Turkish fishers may be the other challenging obstruction to integration. At this point incentives from the state, fishery authority, in this case it is the Ministry of Agriculture and Rural Affairs, and non-governmental organizations (NGOs) supports may encourage the fishery sector.
- **Technology Adaptation and Training:** To use electronic monitoring systems effectively, fishers must receive the necessary training. This can extend the process of adapting to the technology.

Nevertheless, in the long run, the benefits of these systems are critical for promoting sustainable fishing. Furthermore, with the growth of international trade, electronic monitoring is seen as a necessary step for Turkish fisheries to remain competitive in global markets. Turkish fishing fleet, especially trawlers and purse seiners, shall be prepared for adopting to EM.

Future outlook and conclusion

Türkiye aims to expand the implementation of electronic monitoring systems to achieve its sustainable fishing goals. Particularly in the export of fish products to international markets, the use of such technologies is crucial for compliance

with environmental standards. Markets like the European Union have strict regulations on sustainable fishing practices, and for Türkiye to integrate into these markets, the widespread use of electronic monitoring systems in the fisheries sector is essential.

Consequently, the adoption of electronic monitoring systems in Turkish fisheries is a crucial tool for both preserving the marine ecosystem and ensuring the sustainability of the fishing industry. With the right policies and incentives, expanding the use of this technology can contribute to more efficient utilization of Türkiye's maritime resources. To establish an effective discard management strategy, adopting a fully documented fisheries approach is crucial.

This approach not only includes the implementation of technical measures but also the integration of innovative tools and technologies like electronic monitoring. It's vital to carefully consider the discard characteristics (such as species composition, DPUE values, discard ratios, etc.) of fishery in Türkiye decision-making. Management actions could involve implementing spatial and temporal closures, shutting down fisheries in regions, and during periods where high discard ratios are observed. The findings from future studies on discards will be essential in promoting the sustainable management of biological resources.

In conclusion, electronic monitoring is a critical technology for the protection of marine ecosystems and the sustainability of fishing. With legal regulations, financial support, and policies that facilitate fishers' adaptation to these technologies, Türkiye can move towards a more efficient and environmentally friendly future in the capture fishery sector.

References

- James, K. M., Campbell, N., Viðarsson, J. R., Vilas, C., Plet-Hansen, K. S., Borges, L., ... & Ulrich, C. (2019). Tools and technologies for the monitoring, control and surveillance of unwanted catches. *The European Landing Obligation*, 363-382.
- Plet-Hansen, K. S., Eliassen, S. Q., Mortensen, L. O., Bergsson, H., Olesen, H. J., & Ulrich, C. (2017). Remote electronic monitoring and the landing obligation—some insights into fishers' and fishery inspectors' opinions. *Marine Policy*, 76, 98-106.
- Suuronen, P., & Gilman, E. (2020). Monitoring and managing fisheries discards: new technologies and approaches. *Marine policy*, 116, 103554.
- van Helmond, A. T., Mortensen, L. O., Plet-Hansen, K. S., Ulrich, C., Needle, C. L., Oesterwind, D., ... & Poos, J. J. (2020). Electronic monitoring in fisheries: lessons from global experiences and future opportunities. *Fish and Fisheries*, 21(1), 162-189.
- Turkstat. 2024. Fishery Statistics (access 15.08.2024). Available: <https://bi-runi.tuik.gov.tr/medas/?kn=97&locale=en>
- McElderry, H., Beck, M., Pria, M. J., & Anderson, S. (2011). Electronic monitoring in the New Zealand inshore trawl fishery: A pilot study. *DOC Marine Conservation Services Series*, 9, 44.



CHAPTER 5

Alternative Energy Approaches in Fishing Vessels

F. Ozan Düzbastılar¹ & Ozan Soykan²

¹ Prof. Dr., Faik Ozan DÜZBASTILAR Ege University, Faculty of Fisheries, Fishing and Processing Department, 35100, Bornova, İzmir/TÜRKİYE, Orcid: 0000-0002-5376-7198,

² Assoc. Prof. Dr., Ozan SOYKAN Ege University, Faculty of Fisheries, Fishing and Processing Department, 35100, Bornova, İzmir/TÜRKİYE, Orcid: 0000-0002-2227-1245

Introduction

Due to safety concerns stemming from environmental factors such as weather, sea conditions, and visibility (Jaremin & Kotulak, 2004), as well as specific characteristics such as age and length of fishing vessels, the fishing industry frequently operates in high-risk work environments (Atacan & Düzbastılar, 2023). This sector strives to meet global demand, which³ in 2020 amounted to 214 million tons of aquatic animals and algae from aquaculture and fisheries combined (FAO, 2022). In response to this significant demand and to promote sustainability, the fisheries sector is currently facing challenges such as maritime regulations (IMO, 2024), strict fishing quotas (Kindt-Larsen, Kirkegaard, & Dalskov, 2011), as well as national and international regulatory frameworks and scientific fisheries management initiatives (Gavaris, 2009). In addition, factors such as increasing fishing pressure (Jennings & Kaiser, 1998), environmental degradation (Brown, et al., 2021), fish farming, wild-capture fisheries, local and international regulatory measures, extended stays at sea, and technological advances have all played a role together in the growing complexity and contributed to the growing challenges in the fishing industry (FAO, 2014). Activities such as aquaculture production (Folk & Kautsky, 1992) and fisheries-related demands (such as economic growth, increased energy consumption, and transportation) contribute significantly to widespread ecological degradation. They are emerging as a major cause of environmental decline (Brown, et al., 2021).

In 2020, despite a decrease in the total number of vessels, the global number of fishing vessels stood at 4.1 million, while the number of motorised vessels worldwide remained stable at 2.5 million (FAO, 2022). China, Indonesia, Peru, India, the Russian Federation, the United States of America, and Vietnam collectively contributed to global catch production, accounting for nearly 49% of the world's total production (FAO, 2022). According to the FAO statistics, China has the largest fishing fleet in the world with around 564,000 fishing vessels (FAO, 2022). The global fishing fleet is estimated to consume approximately 30 to 40 million tons of fuel annually, accounting for more than 1% of global shipping fuel demand (Chassot, et al., 2021; Parker, et al., 2018). Tyedmers, Watson, & Pauly (2005) reported that the distribution and intensity of fuel consumption by marine fisheries totalled 50 billion litres of fuel (approximately

41.6 billion tons) in 2000, most of which was consumed in coastal fishing grounds in the Northern Hemisphere. In 2011, fishing consumed 40 billion litres (approximately 32 billion tons) of fuel and was estimated to produce a total of 179 million tons of CO₂ (Parker, et al., 2018). According to data from the same year, five countries with large fishing fleets - China, Indonesia, Vietnam, the United States, and Japan - account for more than a third of global fisheries and half of total emissions from global fisheries (Parker, et al., 2018).

The increasing energy requirements of fishing fleets are leading to a rise in pollutant emissions. Typically, four-stroke compression ignition diesel engines used in fishing vessels (Szczepanek, 2015) are responsible for exhaust emissions consisting of oxygen (O₂), nitrogen (N₂), hydrocarbons (HC), water vapour, and carbon monoxide (CO), carbon dioxide (CO₂), sulphur oxides (SO_x), nitrogen oxides (NO_x), and particulate matter (PM). Hydrocarbon fuels are considered the main source of greenhouse gases (GHGs) such as CO₂ and pollutant emissions (CO, HC, NO_x, SO₂) and PM in the atmosphere (Korican, Vladimir, & Fan, 2023). Burning fossil fuels in fisheries releases GHGs directly into the atmosphere, with CO₂ making up the highest proportion of all GHGs (Xu, Lin, Yin, Martens, & Krafft, 2023); (Korican, Vladimir, & Fan, 2023).

Both fishing and aquaculture production require a variety of fishing boats with different fuels (Gabrielii & Jafarzadeh, 2020), engines, and propulsion systems (Son, Lee, & Sul, 2018), varying depending on needs. Fuel saving (Korican, Vladimir, & Fan, 2023) and increasing fuel efficiency (Szczepanek, 2015) in various applications in fishing boats have become critical issues worldwide. Many factors affect the fuel consumption of fishing boats in terms of structural and operational aspects (Szczepanek, 2015), such as the performance of the engine, on-board auxiliary systems, age, shape and design of fishing vessels, fishing equipment, and activity, as well as the speed of the boat, and weather conditions (Tyedmers, Watson, & Pauly, 2005).

One reason for the fluctuating fuel consumption is that fishing boats, particularly trawlers and purse seiners, perform activities that require varying amounts of energy, such as navigating, searching for fish, and setting and hauling the net (Korican, Vladimir, & Fan, 2023).

Types of fishing vessels

It is known that fishing vessels are designed according to fishing methods and gear, and the equipment and technologies on board are developed according to these criteria (He, Chopin, Suuronen, Ferro, & Lansley, 2021). Humans have been captured for thousands of years (Thermes, van Anrooy, & Gudmundsson,

2023). Although there are different views on the definition (Smith & Basurto, 2019), small-scale fishing has been practiced for thousands of years and is mostly carried out along the coast using passive fishing gear (Thermes, van Anrooy, & Gudmundsson, 2023; He, Chopin, Suuronen, Ferro, & Lansley, 2021).

The design of fishing vessels is based on the fishing methods and gear used. Therefore, the equipment and technologies on board are developed according to these two main criteria (He, Chopin, Suuronen, Ferro, & Lansley, 2021). Fishermen used various fishing tools and methods in their fishing activities ranging from primitive to sophisticated. Despite varying definitions (Smith & Basurto, 2019), include artisanal fisheries (traditional fishing practices, non-mechanized equipment, and methods, fishing activities carried out by individuals, families, or small communities, etc.) and small-scale fisheries (includes artisanal fishing, ranging from simple, traditional equipment to more advanced and mechanized equipment, targeting local and sometimes regional markets, etc.) have a long history and are carried out predominantly along the coasts using passive fishing equipment (He, Chopin, Suuronen, Ferro, & Lansley, 2021; Thermes, van Anrooy, & Gudmundsson, 2023; FAO, 2022; FAO, 2014).

The development of technology, the increasing need for food, and the process of enabling fishing vessels to stay at sea longer have led to the emergence of semi-industrial/industrial fishing. Industrial fishing refers to large-scale, highly mechanized, and capital-intensive fishing activities. In contrast, semi-industrial fishing, which falls between artisanal and industrial fishing, has more advanced technology and larger vessels than artisanal fishing but is carried out on a smaller scale than industrial fishing. Semi-industrial fishing essentially refers to small-scale commercial fishing using a semi-industrial fishing vessel (Belhabib, et al., 2020; Thermes, van Anrooy, & Gudmundsson, 2023). The characteristics and operation of semi-industrial and industrial fishing vessels have evolved significantly in recent decades due to advances in vessel systems and equipment technology, innovations in vessel design, propulsion systems, on-board equipment, and fishing methods (Thermes, van Anrooy, & Gudmundsson, 2023). Industrial fishing, which was the first significant activity of the Japanese in the 1920s, refers to the use of large vessels, typically longer than 15 meters, primarily for offshore fishing operations (Gillett, 2007).

A technical document published by FAO provides definitions and classifications of the main types of semi-industrial and industrial fishing vessels: trawlers, purse seiners, seiners, dredgers, gillnetters, trap setters, longliners, pole and line vessels, trollers and multipurpose vessels (Thermes, van Anrooy, & Gudmundsson, 2023). These fishing vessels are equipped with special tools that

vary depending on the fishing method and gear used, such as deck equipment (Hoşsucu, Düzbastılar, Ceyhan, & Ayaz, 1999), fish detection devices (GPS, Sonar, etc.) and catch handling and processing equipment (net drum, trawl winch, machines for filleting and cutting, etc.) which have high energy requirements during both navigation and fishing (Thermes, van Anrooy, & Gudmundsson, 2023). Unlike fishing vessels used in industrial fishing, small fishing boats are designed to travel shorter distances to fishing grounds using generally passive fishing gear, smaller crews, and some minimum equipment (Guyader, et al., 2013). According to the European Commission, fishing boats under 12 m are considered small fishing vessels (Commission, 2006).

With designs ranging from simple trawlers to factory trawlers, they are among the world's most important industrial fishing vessels fishing in very shallow waters up to 2,000 m. Trawlers are categorized as beam trawlers, side trawlers, stern trawlers, freezer trawlers, and factory trawlers (Thermes, van Anrooy, & Gudmundsson, 2023). They use a variety of techniques and gears (bottom and midwater trawls), trawl nets of varying sizes and designs (single boat otter trawl, bottom pair trawl etc.), and special equipment to set and haul the net and, where appropriate process seafood of high commercial value (He, Chopin, Suuronen, Ferro, & Lansley, 2021; Thermes, van Anrooy, & Gudmundsson, 2023). Many trawlers on deck have various-sized trawl winches for the releasing, pulling, and storing of warp wires, and net drums for deployment, retrieval, and storage of the sweeps and net. The vessels have fish detection devices such as sonar, net sounders, various types of echo-sounders, and trawl control and monitoring equipment. After being caught, the fish are kept fresh in ice or chilled seawater or frozen in containers. In some cases, trawlers can slaughter, sort, and cool the fish, which requires more energy (Thermes, van Anrooy, & Gudmundsson, 2023).

Purse seiners vary greatly in size, from small fishing boats used in coastal waters to fully mechanized, large industrial vessels employed on the high seas. The vessels are categorized as American and European types of purse seiners (Thermes, van Anrooy, & Gudmundsson, 2023). Typical equipment on purse seiners includes a power block or triple roller (triplex) and storage systems for hauling and stowing the net (Düzbastılar & Hoşsucu, 1997). The fish is pumped on board on large purse seine vessels, while on smaller vessels, a brailer (large scoop net) is usually used. The net drums, purse seine, and other winches, rollers, as well as the fish pumps, are mechanically driven by the main or auxiliary engine, as well as by electrical, hydraulic, or electro-hydraulic systems. Some

purse seiners have sieve systems on deck for sorting and grading fish by size and species, allowing the release of undersized individuals (Düzbastılar, et al., 2022).

Other fishing vessels include dredgers, lift netters, gillnetters, trap setters, longliners, line vessels, multipurpose vessels, and recreational fishing vessels. The size and design of fishing boats and their equipment vary from country to country depending on fishing habits and the magnitude of the fishery economy. The energy consumption of fishing vessels is also related to the fishing techniques and characteristics of fishing gear (Kaykaç, Düzbastılar, Zengin, Sürer, & Rüzgar, 2017; Davie, Minto, Officer, Lordan, & Jackson, 2015), the type of fishing vessels with a variety of main and auxiliary engines and their navigation and fishing equipment (Korican, Vladimir, & Fan, 2023). Fishing techniques and characteristics of fishing gear and the fishing site are related to the fuel consumption of fishing vessels. Kaykaç et al. (2017) conducted a study to measure the fuel consumption and towing resistance of beam trawl in sea snail fishing in the Black Sea. They compared three different sledges for differences in fuel consumption and towing resistance on two sea ground types (sandy and sandy muddy) during the fishing operation.

Researchers found that the energy consumption of fishing vessels depends on the structure, design, and size of the boat (Szelangiewicz, Abramowski, Zelazny, & Sugalski, 2021; Gulbrandsen, 1986), the engine conditions, and usage patterns; fishing gears, fishing and navigating patterns, distance to the fishing area, target species and fish migration patterns and the traditions on board (Basurko, Gabiña, & Uriondo, 2013; Gulbrandsen, 1986).

Energy conversion in the propulsion system of fishing boat

A diesel-powered main engine usually generates the power required for the propulsion system on fishing vessels and the boat is thrust by a propeller at the end of the system (Figure 1). The propulsion system consists of the diesel engine (as the prime mover), flywheels, reduction gear and shaft, intermediate shaft, stuffing box, stuffing box bulkhead, stern tube (as the transmission system), and the propeller (as the propulsor) (Shi, Stapersma, & Grimmelius, 2009; Notti & Sala, 2012).

The propulsion systems on board fishing vessels power the vessel by converting rotational motion into translational motion. Engine power (HP_e) and motion are transmitted from the main drive to the propeller (THP-thrust horsepower; propeller-generated power) via a rotating rod called propulsion shafting. 80 to 90% of the total power generated by the main engine from fuel energy is used in the propulsion systems (Gulbrandsen, 1986).

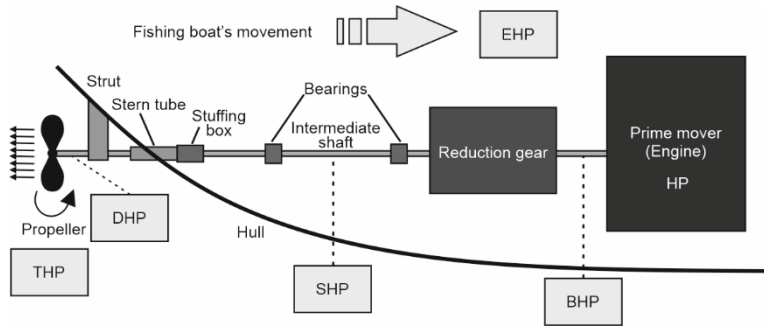


Figure 1. The drive system and the power output

As shown in Fig. 1, brake horsepower (BHP) is the power delivered to the engine output shaft of a piston engine that is between 0.8 and 0.9 times the horsepower (HP) (Gudmundsson, 2014). Shaft horsepower (SHP) is equal to BHP minus any mechanical losses in the reduction gear, typically between 0.95 and 0.99 times BHP. A series of model tests and calculations can be used to determine the shaft power required to move a ship at a given speed (Rawson & Tupper, 2001). Delivered horsepower (DHP) is the power transported to the propeller, which takes into account losses through the gearbox, bearings, and stern tube seal and is typically between 0.97 and 0.99 times the SHP. Thrust horsepower (THP) represents the remaining power after the propeller compensates all losses along the drive train, generally between 0.65 and 0.75 times the DHP. In addition, the thrust delivered by the propeller is intended to overcome the vessel's resistance, which depends largely on the shape of the vessel's hull (Shi, Stapersma, & Grimmelius, 2009). Finally, effective horsepower (EHP) refers to the power required to move the ship's hull at a given speed without propeller action, typically between 0.70 and 0.75 times the THP (Gudmundsson, 2014). Internal combustion engines are generally not very efficient, with even the best engines struggling to reach 50% efficiency. Only about 40% of the energy in the fuel is converted into power at the flywheel, while the rest is lost through exhaust gasses or released into the water. Due to thermal and mechanical losses in diesel engines, only about 25% of the fuel energy can be used as net thrusting energy (Figure 2).

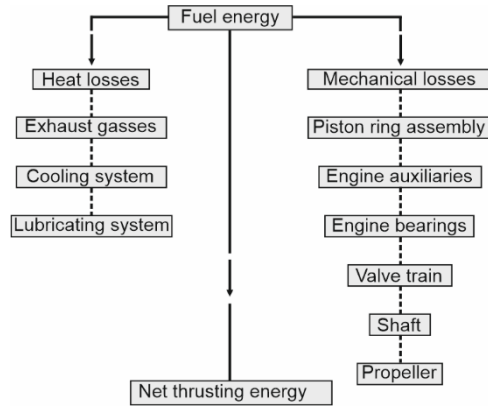


Figure 2. Energy losses of internal combustion diesel engine

While artisanal and small-scale fishing typically uses motorized boats powered by low-power, air-cooled diesel engines, industrial fishing operates large vessels equipped with high-capacity, water-cooled diesel engines to meet the energy needs of various equipment. Traditionally, these internal combustion engines used diesel fuel to provide sufficient mechanical power, electricity, and thermal energy to fishing vessels (Szczepanek, 2015; Behrendt, 2014). Fishing vessels have one or more main engines for propulsion depending on boat size and fishing method, additionally, auxiliary engines are used to meet energy requirements for electricity, heating/cooling, handling, and hauling systems (cranes, net drum, trawl winch, etc.) and other operating systems (water pumps, wastewater disposal, etc.) (Korican, Vladimir, & Fan, 2023). For example, in a study (Düzbastılar, Tosunoğlu, & Kaykaç, 2003), the power requirement of a trawl winch was estimated at 32 hp according to Koyama's formula (Koyama, 1971), while BHP for a trawler was estimated at 400 hp. It is recommended that the power requirement of a trawl winch should be at least half of EHP or equal to EHP (Düzbastılar, Tosunoğlu, & Kaykaç, 2003).

In the propulsion system propellers are one of the main components of fishing vessels. Ideally, the propeller should be designed for optimal performance under all relevant operating conditions. The vessel's speed is achieved by its propulsion system, typically a screw propeller, which converts engine torque into thrust to move the surrounding water. The screw propeller, mounted on a shaft at the stern, creates a flow velocity that resembles the shape of a screw. Depending on the boat size and fishing method, there are many types of propellers used in fishing vessels. There are two types of screw propulsion: fixed pitch propeller and controllable pitch propeller (Breslin & Andersen, 1996). Generally, small fishing vessels have fixed pitch propellers, while large fishing boats equipped with

certain high-tech tools (marine deck equipment, sonar systems for fishing, joystick steering, generator, etc.) use controllable pitch propellers in industrial fishing.

Marine diesel engines are the most effective energy sources for fishing fleets worldwide; however, they are responsible for high exhaust emissions from fishing and navigation. Depending on the fishing area, fishing vessels range from small boats with engines under 10 horsepower to large tonnage vessels with thousands of horsepower and higher fuel consumption. This also leads to higher NO_x emissions, contributing to various health and environmental problems. It is estimated that GHGs from fishing vessels could be reduced by 10-30% through more efficient engines, larger propellers, better boat design and hull modifications, and speed reductions (Thermes, van Anrooy, & Gudmundsson, 2023).

Energy efficiency and fuel savings in fishing vessels

The path to successful energy conservation, particularly through energy efficiency and fuel-saving practices, lies through a detailed inspection of fishing gear and methods, fishing vessel technology, characteristics of engines, propulsion systems including reduction gears, propellers, and nozzles, and sail-assisted propulsion or other complementary energy approaches, introduction advanced technology and finally conservation and improvement of natural resources (Boopendranath, 2002; Gulbrandsen, 1986). For example, fuel consumption varies depending on fishing gear and fishing methods for target species with different vessel designs and sizes (Gulbrandsen, 1986).

The International Maritime Organization (IMO) has created a mandatory plan for all ships, the Ship Energy Efficiency Management Plan (SEEMP) (IMO, 2022a), which is designed to continuously plan, monitor, and track the fuel efficiency and safety of ship operations, thereby increasing fuel efficiency through four steps (planning, implementation, monitoring, and self-evaluate) (Hussein, Elsayed, & Yehia, 2021). The SSEMP applies to all vessels of 400 GT and above, including fishing vessels. The IMO has introduced the requirement that newly built ships comply with the developed Energy Efficiency Design Indexes (EEDI) (IMO, 2022b), Energy Efficiency eXisting ships Index for existing ships (EEXI) (IMO, 2022c), and Energy Efficiency Operational Indicator (EEOI) (IMO, 2009) to reduce CO₂ emissions from ships. The EEDI and EEXI regulations apply to ships of 400 GT and above operating in international trade, but not to the fishing sector. Díaz-Secades (2024) argues that the indices in the IMO standards can also be used for fishing vessels, particularly

given the role of fishing vessels larger than 400 GT in CO₂ emissions. For fishing vessels, EEOI factors link the amount of CO₂ emitted into the atmosphere with the mass of fuel consumed, fish caught, and the distance travelled. To calculate the EEOI for fishing vessels, the following factors are taken into account: the amount of fuel consumed in grams, the type of fuel, the conversion factor expressed in the mass (tons) of CO₂ produced by the combustion of one ton of fuel, the mass of transported catch (tons), and distance in nautical miles corresponding to the operational task carried out (Hussein, Elsayed, & Yehia, 2021; IMO, 2016). Between 1990 and 2011, emissions from the global fishing industry increased by about one-third (Hussein, Elsayed, & Yehia, 2021). Similarly, work has been carried out to formulate the Enhanced Emissions Index (EEI) for fishing vessels, which is formulated as the ratio of emissions generated by the vessel power system and the amount of catch considered as a benefit to society (BS). The addition of SO_x and NO_x emissions to the commonly calculated amounts of CO₂ emissions represents an extension of existing approaches to formulating energy efficiency indices for ships while adapting the presentation of societal benefits to the fisheries sector through the assessment of diesel, LNG and methanol (Koričan, Vladimir, Haramina, Alujević, & Vučković, 2023).

Increasing fishing vessels' fuel efficiency will reduce GHGs and increase fishing income. Therefore, reducing ship emissions has become one of the most important and current research topics in maritime sciences (Korican, Vladimir, & Fan, 2023; Sarica, Gökçe, Dalgıç, & Özbilgin, 2018; Behrendt, 2014; Szczepanek, 2015; Moon, Ruy, & Park, 2024). The two main components of fishing vessel fuel consumption are operational activities and structural factors (Szczepanek, 2015). For example, the speed of fishing vessels is the most important factor affecting fuel consumption for operational activities (Boopendranath, 2002), while the selection of an appropriate propeller is an element of structural factors (Gulbrandsen, 1986) (Figure 3).

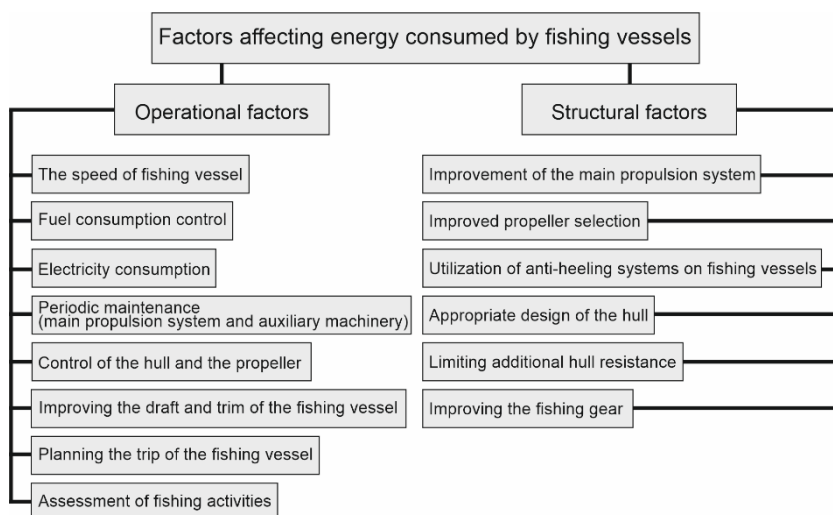


Figure 3. Factors affecting the energy consumption of fishing vessels are classified according to several criteria (Adopted from Szczepanek, 2015)

Behrendt (2014) summarised reducing energy consumption and increasing energy efficiency for fishing vessels as technological/structural activities, operational activities, and added logistical activities in addition to Szczepanek's (2015) definition. One of the technological activities is the optimization of the hull's shape to reduce resistance. The decrease in hull resistance is evidenced by the need for propulsion power in the range of 10 to 25% (Behrendt, 2014). For example, a fishing vessel should have a bulbous bow to reduce drag around the hull at cruising speed. By changing the way water flows around the hull, the bulbous bow increases speed, range, fuel efficiency, and stability by reducing drag. According to a project report, the bulbous bow can reduce fuel consumption by 5% while navigating; however, if the skipper decides to move 0.3 knots faster, the overall fuel consumption increases despite the improved fuel efficiency (Kemp, 2018). The installation of the submerged parts (sacrificial anodes, stern and rudder systems, propeller structures, bow thrusters, etc.) of the fishing vessel causes additional hydrodynamic resistance.

The force required to propel a boat primarily depends on the speed of the vessel, the waterline length (LWL), which is the length of the boat at the waterline level, and the displacement, which includes the weight of the boat along with the crew, fishing gear, fish, and ice. In many cases, fuel consumption could be estimated depending on the engine characteristics (power, specific fuel consumption, rpm, etc.) dimensions (LWL, tonnage, etc.), and speed of the vessel (cruising, fishing, etc.) (Figure 4). In small-scale fishing with fishing vessels

shorter than 12 m, the energy saving rate is about 37% when the vessel's speed is reduced by 6 knots from 7 knots (Gulbrandsen, 1986).

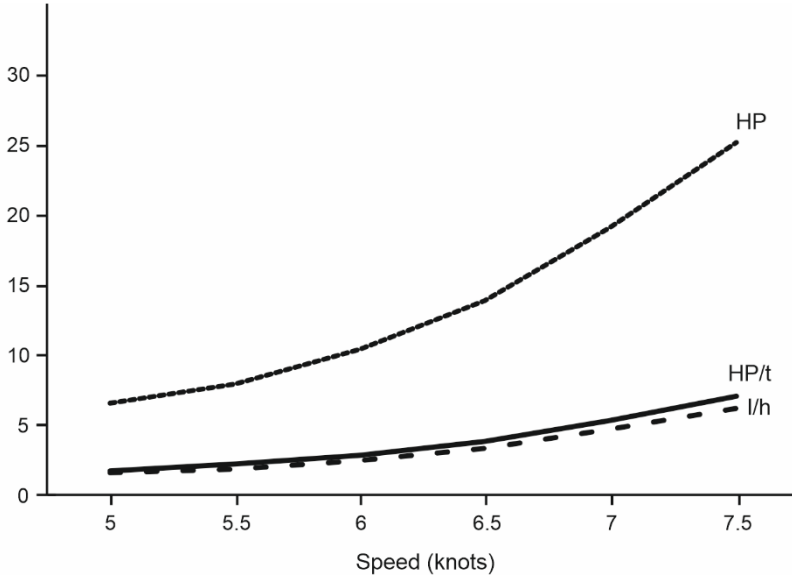


Figure 4. A fishing boat has a waterline length of 8.0 m (LWL) and a displacement in service condition (in waves and with some fouling organisms on the hull) of 3.5 t. HP: Power requirement HP/t: The value for the HP per tonne displacement, and l/h: The fuel consumption in litres (l) per hour (h) (Adopted and derived from Gulbrandsen (1986)).

The other factor related to technological/structural issues is an improvement in the effectiveness of the propulsion system such as the selection of the type of propeller (fixed pitch propeller and controllable pitch propeller, kort nozzle) and its characteristics (i.e. rotation speed of the propeller), fin stabilizers, and selection of reduction gear and main engine (Behrendt, 2014; Szczepanek, 2015). For small fishing boats, an energy saving of 14% can be achieved by increasing the engine gear ratio from 2 to 4 (Gulbrandsen, 1986). In addition to the design and engine characteristics of the fishing vessel, other structural and operational elements, such as cooling and keeping fish in a cold medium, also play an important role in increasing energy efficiency. A study analysing existing refrigeration systems on board fishing vessels indicated that the electrical energy requirement of the refrigeration system accounted for half of the total energy produced (Ruiz, 2012). Ruiz (2012) suggested improving insulation and compressor systems, researching new and environmentally friendly refrigerants, using alternative cooling systems (liquid ice, pre-cooling, etc.), and using waste heat systems to increase energy efficiency.

The second activity is the operational issue of energy saving for fishing vessels, as described by Behrendt (2014) and Szczepanek (2015). This includes maintaining the hull and propeller to prevent fouling organisms, polishing the propeller blades and rudder system, performing routine maintenance on the main engine (improves energy efficiency by up to 30%) and auxiliary equipment, maintaining the proper draft and trim by loading the vessel appropriately and planning efficient cruising. For example, up to 40% of energy can be saved by removing fouling organisms (barnacles, calcareous tubeworms, mussels, etc.) attached to the ship's hull (Gulbrandsen, 1986). Gulbrandsen (1986) observed that the fuel consumption of small fishing vessels increased by 7% after one month, by 44% after six months and by 88% after one year, which was due to the formation of fouling on the hull.

The last factor described by Behrendt (2015) is the logistic activity related to reducing travel time as cargo and increasing the qualifications of the crew. For example, a fishing location should be chosen that is closest to the vessel, or the catch should be landed at the nearest fishing port (Szczepanek, 2015). Crew training is another important factor in increasing energy efficiency, as the crew can be trained in energy-saving management and the coordination of various energy system devices.

Energy efficiency and fuel saving have become a much-studied topic in recent years. A four-dimensional model to assess fishing vessel fuel consumption was developed by Kemp (2018) using data from 50 fishing vessels. There are (1) all engines in the vessel (starboard propulsion engine, port propulsion engine, and an auxiliary generator, etc.), (2) this mode is the fishing activity of the fishing vessel depending on the fishing method (e.g. trawling, long-lining, etc.), (3) the third dimension is defined loads depending on propulsion, cooling, hydraulics, AC, DC, and engine overhead, and (4) the final dimension is propulsion modes including cruising, fishing, and anchoring. Kemp (2018) used a model called the Vessel Energy Analysis Tool (VEAT) to calculate the fuel a vessel will consume over a range of loads. Additionally, it was noted that various technological features of the vessel, such as the presence of a turbocharger, the type of diesel engine cycle (two-stroke or four-stroke), hull design, trim, bulbous bow, and keel cooler, are closely related to fuel consumption and energy efficiency (Kemp, 2018). Korican, Vladimir & Fan (2023) aimed the study at assessing, through the development of a mathematical model, the energy efficiency of fishing vessels in the Adriatic against the background of new decarbonisation targets, lack of environmental regulations and the aging diesel-powered fleet, proposing improvement measures. One of the study's results related to exhaust gases showed

that the emission indices of the purse seiner part of the fleet ranged between 0.32 and 2.01 kg CO₂ equivalent per kg of catch. In comparison, the emission indices of the trawler part of the fleet ranged between 2.08 and 14.11 kg CO₂ equivalent per kg catch. They found that trawlers had a higher emission index (13-15%) than purse seiners and the index was influenced by factors such as engine power, gross tonnage, and age of the fishing vessel (Korican, Vladimir, & Fan, 2023). For example, for small fishing boats less than 12 m long, a reduction of half a ton by using lighter materials results in an energy saving of around 19% (Gulbrandsen, 1986).

Fuel consumption depends on many factors including fishing techniques, the technology, size and speed of the vessel, equipment on deck, etc. For example; the fuel consumption of the Polish fleet was distributed 60-75% for the primary propulsion system that powers the vessel, 10-15% for axillary equipment for fishing (hydraulic drive), and 2-15% for electrical equipment for fishing and traveling (Behrendt, 2014). In Scandinavia, the amount of diesel fuel needed to catch 1 kg of fish was 0.94 litres for trawling, 0.18 to 0.30 litres for longline and gillnet fishing, and 0.08 litres for purse seining (Gulbrandsen, 1986).

Sala et al. (2011), introduced a new fuel consumption monitoring system to evaluate the energy performance of fishing vessels under different operating conditions. It was tested on two semi-pelagic trawlers in the Adriatic, each with an engine power of around 900 kW and an overall length (LOA) of around 30 meters. Although the fishing vessels were made of different materials and equipped with different types of propellers, they used fishing gear of the same design and size. Their total and instantaneous fuel consumption was calculated for various activities, such as trawling and navigating at different speeds. The highest fuel consumption was recorded during trawling (130 l/h at 4.4 knots) and traveling (100-130 l/h at 11 knots). Another result indicated a 15% fuel saving when traveling half a nautical mile per hour slower. In both fishing and cruising, reducing the speed of fishing vessels reduces fuel consumption (Abernethy, Trebilcock, Kebede, Allison, & Dulvy, 2010).

Sala et al. (2022) conducted energy audits on ten vessels from three typical Mediterranean trawl fisheries: midwater pair trawl, bottom otter trawl, and Rapido beam trawl. These fisheries use approximately 2.9 litres of fuel per kilogram of landed fish, varying consumption rates by gear type and vessel size. Normally, this fuel consumption produces 7.6 kg of CO₂ per kilogram of fish. They established benchmarks for monitoring progress to minimize energy consumption throughout the supply chain for reducing the environmental impact of fishing (Sala, et al., 2022).

When fishing, higher speeds result in increased fuel consumption due to the resistance between the fishing gear, fluid, and seafloor. Düzbastılar, Tosunoğlu & Kaykaç (2023) theoretically calculated the resistance of conventional, tailored trawls and their gears (doors, warp wires, cables) at different towing speeds (v). The relationships between trawl size and energy demand have been studied. The drag forces (F_D) of trawls were calculated as a function of towing speed ($F_D=323.07v^2$ for conventional trawl net, $F_D=282.14v^2$ for tailored trawl net), water depth, and warp length. Both resistances increase 1.8 times when the towing speed increases from 1.5 to 2 knots. At towing speeds of 2.5, 3, and 3.5 knots, the trawl resistance forces increase by 2.8, 4, and 5.5 times, respectively, compared to the resistance at the initial towing speed (Düzbastılar, Tosunoğlu, & Kaykaç, 2003). These results suggest that the fuel consumption of fishing vessels is strongly influenced by fishing activity at higher speeds, due to the drag forces of the fishing equipment and hull. In addition, it has been reported that the different fuel consumption in the cruise phase could also depend on different hull designs, types of propellers, installed power engines, surface currents, and sea conditions (Sala, De Carlo, Buglioni, & Lucchetti, 2011; Gulbrandsen, 1986).

Additional devices have been used in fishing vessels to reduce the fuel consumption of diesel engines. One of these was a magnetic device for saving fuel in fishing vessels. Three different devices were used in both laboratory and real fishing conditions. In all cases, fuel savings reached around 2%, and exhaust emissions around 0.6% (Gabiña, et al., 2016).

Significant gains can be achieved if the above suggestions for reducing fuel consumption by increasing energy efficiency are applied to fishing vessels. For example, reductions in fuel consumption through modifications of internal combustion engines have been estimated at 2-6%, through optimization of hull design at 8-10%, through selection of appropriate propellers at 3-6%, and through the application of antifouling paint at 1-2% to reduce friction force, 2-5% through applications (grinding, polishing) to minimize friction of submerged vessel surfaces and 1-2% through optimization of trim (Behrendt, 2014).

Alternative fuels and energy sources in fishing vessels

The differences between studies suggest a possible range of between 279 and 400 tonnes/year in global shipping fuel consumption (McGill, Remley, & Winther, 2013). Today's fishing methods rely heavily on diesel and recent study results show that 70% of the total cost is spent on travel alone (Anand, 2018). In recent years, fluctuations in oil prices and the resulting environmental pollution have led to the experimentation with different fuel technologies in maritime

transport. According to the IMO, approximately 77% of the total marine fuels used worldwide are residual fuels (McGill, Remley, & Winther, 2013). The fishing industry can benefit greatly from using alternative fuels such as natural gas (NG) or perhaps hydrogen. Liquid fuels, such as ethanol, methanol, liquefied biogas (LBG), and biodiesel (fatty acid methyl ester), and gaseous fuels, such as propane, hydrogen, and natural gas, are the two main types of alternative marine fuels in maritime transport (Banawan, El Gohary, & Sadek, 2010).

For coastal fishing ships, hydrogen fuel cells are a viable option, while biodiesel, LNG (liquefied natural gas), and LBG are suitable for all types of fishing vessels (Gabrielii & Jafarzadeh, 2020). The trawler fleet in Italian waters has a high energy consumption, accounting for about 40% of total costs, with an increase in recent years due to rising fuel prices (Altosole, Buglioni, & Figari, 2014; Gabiña, et al., 2016). Although the proportion of GHGs from fishing is quite small compared to sea transport, it has reached a level that must be reduced quantitatively.

Alternative fuels to reduce the fuel costs and emissions from internal combustion engines in fishing vessels have ranged from methanol to propane (Yaakob & Husain, 2015). Banawan, El Gohary & Sadek (2010) compared seven different fuels (ethanol, methanol, LBG, biodiesel, hydrogen, propane, and NG) in terms of availability, renewability, safety, adaptability, IMO compliance, performance, and cost and showed that they have acceptable values with the matrix they used.

Diesel-electric, hybrid, battery-electric, and alternative fuel vessels are technologies currently used in cruise ships, ships, ferries, and sport fishing boats (Kemp & Atshan, 2021). The adoption of alternative energy and propulsion systems depends on key factors such as efficiency, cost, and the suitability of existing ships for conversion. Technological advancements in reducing emissions from conventional diesel engines, particularly the reduction in battery costs, increased capacities, and the rise of hybrid systems, are creating promising conditions for reducing environmental pollutants

Dual fuel

The fuel price is a dominant cost factor in the operation of fishing vessels, regardless of the size and type of boats. For this reason, fuel efficiency and using alternative fuels instead of conventional diesel fuel in fishing vessels have become increasingly important in recent years. Fisherman usually uses high-quality diesel oil called high-speed diesel oil (HSD) (Santoso, Semin, Cahyono, & Sampurno, 2021).

The significant difference in efficiency between gasoline and diesel engines has led engine designers to look for a way to achieve the efficiency of a diesel engine in natural gas-powered gasoline engines, called dual-fuel or multi-fuel engines (Breeze, 2014). A dual-fuel engine is a diesel engine that runs on both gaseous and liquid fuels. In gas operation, the engine works according to the Otto process, in which the lean air-fuel mixture is supplied to cylinders during the suction stroke. In diesel mode, the engine operates according to the diesel process, in which diesel fuel is supplied to the cylinders at the end of the compression stroke. Dual-fuel engines feature flexibility, a higher compression ratio, lower emissions, and better efficiency, and are designed to operate on gaseous fuels, with diesel serving as a backup fuel source.

Natural gas (NG) is now used much more frequently to power ships (gas ships) as environmental aspects have become more important in the maritime sector. The fishing industry does not use NG very often due to bunkering and storage problems (Yaakob & Husain, 2015). The specific cost of gases is lower than that of all types of diesel fuel. Although these pure and low-emission gases are expensive to manage, store, and distribute, they are still cheaper than diesel fuel (Santoso, Semin, Cahyono, & Sampurno, 2021). While NG theoretically produces fewer emissions than diesel fuel, dual-fuel diesel engines that can run on either fuel often involve significant upfront costs. One study found that a modified dual-fuel diesel engine (50% NG + 50% diesel) producing about 10 horsepower reduced NO_x emissions by a third and even found that emissions decreased as the gas ratio increased (Santoso, Semin, Cahyono, & Sampurno, 2021). In another study, a dual-fuel overhaul was performed on a diesel engine, and diesel fuel was used only to trigger ignition. In this way, fuel costs should be reduced (Ismail, Zulkifli, Fawzi, & Osman, 2016). In addition, NG, one of the alternative fuels, performs better than other fuels such as ethanol, biodiesel, and hydrogen in terms of cost, safety, performance, adaptability, and IMO compliance (Banawan, El Gohary, & Sadek, 2010).

Heavy fuel

Heavy oil, also known as residual fuel, consists of the remains from the bottom of the barrel that is produced during oil refining. It is extremely viscous, so it needs to be heated to around 130°C to flow. HFO contains heavy metal contaminants and is typically high in sulphur, with an average content of about 2.5% by weight, equivalent to 25,000 parts per million (ppm). Consuming HFO releases large amounts of air pollutants (i.e. sulphur oxides (SO_x), nitrogen oxides (NO_x) and particulate matter (PM) – as well as climate pollutants such as carbon dioxide (CO₂), nitrous oxide (N₂O), and black carbon (Comer, Olmer, Mao, Roy,

& Rutherford, 2017). HFO is also used in fishing vessels, particularly in the commercial maritime transport sector. In 2015, fishing vessels were responsible for 9.4% of Arctic HFO consumption. The use of HFO contributes to the production of greenhouse gases, including black carbon (Comer, 2018). Comer (2018) found that 159 of the 755 fishing vessels, or 21%, in the IMO Arctic in 2015 were fuelled by HFO. In particular, across the 17 countries, it was observed that Russian-flagged fishing vessels were responsible for 64% of HFO consumption and 21% of black carbon emissions from fishing vessels (all fuels) in the IMO Arctic in 2015 (Comer, 2018).

Low-sulphur residual fuel oil

Fuel can be obtained from low-sulphur oil or produced through desulfurization, but the high cost and complexity of this process increase the final fuel price. In addition, the complex chemical composition of ultra-low sulphur fuel oil can pose operational risks to ships (HELCOM, 2019).

LNG/LPG

LNG currently represents the first and most likely alternative fuel to be considered a true replacement for HFO for ships (HELCOM, 2019). It is assumed that the global use of LNG will increase significantly, particularly in coastal shipping. Typically, CO₂ emissions are reduced by 20% compared to diesel or gas oil; however, methane slip from some engines may partially offset this reduction (Gabrielii & Jafarzadeh, 2020). However, a study on the use of LNG instead of MGO in fishing vessels found that the energy consumption of the vessel using LNG as fuel would be higher, which would be responsible for the resulting methane emissions and thus increase the global warming potential almost the same as MGO. Additionally, LNG's acidification and eutrophication potential is 85% lower than that of MGO, meaning it has less impact on terrestrial and freshwater ecosystems. However, it was noted that it was easy to conclude that LNG was more environmentally friendly than MGO (Leira, 2018).

To date, only LPG carriers have used LPG as fuel. In 2019, seven such ships were ordered, and four LPG tankers were converted to operate on LPG. Compared to diesel, LPG combustion results in approximately 15% lower CO₂ emissions. Additionally, there is a significant reduction or complete elimination of SO_x and PM emissions, with the extent of NO_x reduction depending on the engine technology (Gabrielii & Jafarzadeh, 2020).

Biodiesel

Various biodiesel fuels, including hydrogenated vegetable oil (HVO), can be used in ships with minimal adjustments. Although supply and demand remain limited, CO₂ emissions are reduced by around 50% compared to diesel oil, considering emissions from HVO production (Gabrielii & Jafarzadeh, 2020).

Ferry line in Denmark uses soybean oil, while fish and chicken oils have also been tested. Although oils and fats have been used in the automotive industry for years, their remaining potential is uncertain (McGill, Remley, & Winther, 2013). Blending biodiesel with conventional diesel is critical for the UK government to meet its commitment to reduce CO₂ emissions by 20% by 2010. Currently, both pure vegetable oil (SVO), i.e. oil obtained from plant material (rapeseed, oil palm, etc.), and biodiesel are produced in the UK (Rossiter, 2007).

These fuels face challenges such as limited miscibility with intermediate fuel oil (IFO), freezing sensitivity, and preservation issues. Biodiesel, algae fuel, methanol, hydrogenation-derived renewable diesel (HDRD), and pyrolysis oil are almost sulphur-free. Algae and HDRD fuels are compatible with diesel engines, but biodiesel (fatty acid methyl ester) requires engine modifications due to incompatibility with some materials. While pyrolysis oil is also sulphur-free, it is high in acidity, and low cetane levels, and is naturally immiscible with diesel, requiring modification for marine use (McGill, Remley, & Winther, 2013).

Liquefied biogas

Biogas is a renewable energy source produced from organic wastes (fisheries and forestry, food waste and wastewater, etc.). No significant modifications are required for ships that already use LNG, as LBG produces similar emissions. While the production of LBG is currently limited, expanding production facilities could promote its wider use in the future. Although there is potential for using a mixture of LNG and LBG in maritime transport, improvements are needed in the production, storage, and transport stages for its use in fishing vessels.

Methanol

Due to its chemical structure, methanol is the simplest form of alcohol and is often used in the chemical industry. It can be made from many different fossil and renewable raw materials, with the majority being made from natural gas (HELCOM, 2019). To achieve the same energy content, a methanol fuel tank requires 2-2.5 times the volume of diesel fuel (Gabrielii & Jafarzadeh, 2020; HELCOM, 2019). In addition to the needed additional space, fuel costs remain the biggest challenge. The use of methanol virtually eliminates SO_x emissions

and significantly reduces PM emissions compared to diesel, although the extent of NO_x reduction depends on the engine technology (Gabrielii & Jafarzadeh, 2020). However, methanol increases the risk of corrosion, which must be addressed by adequately modernizing the fuel tanks and fuel system (McGill, Remley, & Winther, 2013).

Electric

Recent advances in ship electrification offer the potential for greater energy efficiency, improved energy management, and fuel savings for larger vessels. Benefits also include power redundancy and reduction in noise and vibration, which is particularly important for passenger ferries. Battery-powered propulsion systems, the most popular energy storage technology, are already being developed for smaller ships (HELCOM, 2019). Electric drive systems are based on an electric motor that provides all the power for the propeller. The electrical energy required to drive the ship's propeller can come from various sources, such as a generator with a diesel engine, a battery, or a fuel cell. Diesel-electric systems are common on passenger ships and military vessels, which have large electrical loads in addition to propulsion loads (Kemp & Atshan, 2021).

Researchers in Indonesia investigated converting a 10 GT purse-seine vessel to electric propulsion. The fishing and navigation phases required a total battery capacity of 6000 Ah. Technical and economic analysis showed that a battery-powered fishing vessel generates higher revenues and lower costs compared to a diesel-powered vessel (Prananda, Koenhardono, & Tjoa, 2019). Unlike on-board charging from fossil fuel generators, batteries charged from shore power are typically classified as an alternative fuel. An all-electric gillnet fishing vessel has also been demonstrated in Norway, using batteries that can be charged on land or via an on-board diesel generator (Kemp & Atshan, 2021). While using shore power eliminates local emissions, the emissions from shore power generation must still be considered. These systems can achieve an emissions reduction of nearly 90% (Gabrielii & Jafarzadeh, 2020). Lithium-ion batteries are the most widely used. However, they are both heavy and more suitable for short distances. However, some fishing boats are equipped with this type of battery. The cost of a diesel engine is higher than the cost of the tank that stores the diesel fuel used as energy, while an electric battery is more expensive and heavier than the electric motor that drives the propeller (Kemp & Atshan, 2021).

Ammonia

Ammonia can be used as fuel in both internal combustion engines and fuel cells. Compared to hydrogen, it has a higher energy density and is easier to store,

allowing longer operating distances. Although ammonia is available worldwide, the main challenges are its toxicity and corrosiveness. The only emissions from an ammonia fuel cell are water and pure nitrogen. Therefore, when produced regeneratively, ammonia can be considered a carbon-neutral fuel (Gabrielii & Jafarzadeh, 2020).

Hydrogen

Hydrogen can be used as a marine fuel and converted into electricity through fuel cells or internal combustion engines. Fuel cells enable converting energy sources (e.g., hydrogen, methanol, ammonia, natural gas, biogas) with greater efficiency than conventional combustion engines. Water is the only emission produced by a hydrogen-powered fuel cell, making it a zero-emission technology (Gabrielii & Jafarzadeh, 2020). However, the hydrogen production method is important for reducing GHGs. A hydrogen fuel cell with an electric motor produces around 75% fewer emissions than a simple diesel engine (Gabrielii & Jafarzadeh, 2020). While hydrogen is extremely attractive in terms of emissions reduction, its main challenge in maritime applications is its high cost and limited bunkering infrastructure. Due to the high cost of tanks, and fuel cells, and range limitations due to low density, current technology is limited to the use of hydrogen in short-sea shipping. Therefore, this alternative can only be viewed as a long-term perspective. Particular attention should be paid to the storage of hydrogen on board ships to ensure safe operation (HELCOM, 2019).

Hybrid system

The hybrid drive system combines the advantages of mechanical and electric drives through the use of a gearbox. However, this integration also leads to increased weight and volume. Fishing vessels often operate under low or no load during fishing operations. In such cases, both electric and mechanical propulsions can be a solution when additional power is required (Hwang, Kim, Jeon, & Kim, 2022). The first hybrid trawler powered by batteries and LNG was scheduled for delivery in 2020. The fishing boat's main engine is capable of dual-fuel, with 95% of its energy derived from LNG. In addition, when switching from diesel to LNG, an auxiliary engine can support the primary engine. To further reduce fuel consumption in the conventional diesel cycle by fifteen percent, a 500 kWh battery is used. In addition, the energy capacity of this battery is about 10 hours. In addition, CO₂ emissions are reduced by 20-25%, NO_x emissions are reduced by 80%, and SO_x and particulate matter emissions are negligible in this hybrid system (Gabrielii & Jafarzadeh, 2020).

A simulation based on the technical specifications of South Korean fishing vessels (7.99-ton class) determined that hybrid systems can reduce fuel consumption by approximately 10%, significantly reducing CO₂ emissions (Hwang, Kim, Jeon, & Kim, 2022). In a study, the project was developed into an alternative electromechanical energy supply system for a 12-meter coastal fishing vessel. The proposed system combined a hydrogen fuel cell, lithium battery, and diesel generator for propulsion (Gutiérrez & Meana, 2012).

A study was conducted to develop a hybrid propulsion system for a catamaran fishing boat that integrates a conventional diesel engine, sails, and solar panels. The models were tested at speeds consistent with real conditions, starting at approximately 10 knots. The results showed that a hybrid ratio of 40:60, combining diesel engine and solar sail, provided the optimal benefit. This configuration reduced fuel consumption by 6 litres per hour and reduced emissions of toxic gases into the atmosphere. In addition, the ship maintained good stability and seaworthiness (Santosa, et al., 2014).

The study discussed the potential and barriers to the development of hybrid and fully electric propulsion systems on fishing vessels generally less than 10 meters in length. In particular, they assessed the availability and conversion or implementation costs of electric and hybrid systems to reduce fuel costs for small vessels using trawls and dredges (Johnson, Waldman, Rybchenko, Bell, & Ready, 2022). Another study compares the current propulsion system of a longline fishing vessel with alternative designs such as hybrid and diesel-electric propulsion, focusing on efficiency and fuel consumption. The comparisons are based on simulation models using electricity demand estimates. In addition, an economic evaluation of the proposed alternatives is carried out. The results, taking into account market trends, operating patterns, and cost analysis, highlight the potential for hybrid propulsion in future longline fishing vessels (Andersson & Logason, 2015).

Different power systems can be combined so that hybrid systems used in fishing boat navigation can also meet the power needs of various devices on board. The plan is to generate the necessary energy from solar and wind energy to keep the fish caught in Indonesia in a cold chain (2-4 C°). Two 100W solar panels and a 300W wind turbine were combined to generate the required daily energy (720Wh) (Banjarnahor, Hanifan, & Budi, 2017).

Wind

Wind energy could reduce ships' consumption of conventional power. Wind propulsion can be divided into soft sail, fixed sail, rotor, kite, and turbine

technologies (HELCOM, 2019). A study investigated the implementation of wind turbine-assisted propulsion for propulsion power generation on a modern Scottish seiner/trawler. Typical operating costs and conditions for such vessels are presented. The wind turbine performance is evaluated in all operating modes, including steam and fishing, and the corresponding fuel savings are calculated. The results show that the annual fuel savings achieved by using the wind turbine on this vessel are between 20% and 25% (Bos & MacGregor, 1987). A study presented field measurement results of a 400W commercial wind turbine generator (WTG) installed on a prototype fishing boat to obtain a preliminary survey of the energy saving of the diesel engine in the fishing boat (Wang, et al., 2009).

Solar energy

Solar energy applications use electricity generated by photovoltaic (PV) cells. The biggest limitation of this evolving technology is the limited space for both solar cells and energy storage. While advancing technology enables the deployment of next-generation energy storage systems, further technical developments are required to fully power ships with this energy. The effectiveness of solar power depends on the location and is therefore particularly suitable as a supplement to auxiliary energy. However, PV systems have low efficiency and require a lot of decks or installation space for cell installation (HELCOM, 2019).

Nevertheless, the possibility of operating a fishing boat (10 GT, total length: 14 m, 54 HP) with solar energy was investigated in Indonesia. They calculated the number of solar panels and batteries that would provide the necessary electrical energy by considering all factors such as the dimensions of the boat, power requirements, auxiliary, fishing, and navigating equipment. Therefore, 2 solar panels and 3 batteries should be installed on the fishing boat in the system, which will reduce fuel consumption. The electrical energy obtained from the solar cell is used to charge the batteries and devices powered by alternating current such as navigation lights, televisions, radios, communication devices, etc. are operated with the help of an inverter (Sudjasta, Prayitno, & Hatuwe, 2021). A study conducted in Indonesia aimed to cover at least half of electricity needs by installing solar panels on fishing boats. It was also stated that the system would pay for itself in approximately 9 years (Nugraha, Luthfiani, Sotyaramadhani, Widagdo, & Desnanjaya, 2022).

In Sri Lanka, a study was planned to develop an alternative propulsion mechanism using solar panels for fishing boats that fish at sea for a few days and

transmit power to the propulsion system using the electricity provided by the charged batteries. The study assumes a 60-ft fishing vessel has a speed of 6 knots and calculates a navigating time of 1 hour with 11 hours of charging time. The payback period of the system is estimated at around 8 years (Gamage, Wimalasooriya, Boteju, & Wimal Siri, 2021). A study was conducted on the process of using solar energy for lighting, communications, and other on-board requirements to save fuel for a private fishing fleet of small-scale fishermen who target pelagic species and undertake long voyages of 30 to 45 days in much of the Indian Ocean (Babu & Jain, 2013). In South Korea, fishing vessels are switching to battery-powered systems to reduce fuel costs and engine noise while powering essential equipment. However, the problem arises when the batteries are discharged and the equipment fails. To prevent this, they examined the feasibility of installing a solar auxiliary power system on fishing vessels weighing 9 to 10 tons (Yoon, Jeon, Hwang, & Kim, 2021).

Diesel-electric

A diesel-electric powertrain consists of power sources, electrical panels, electrical control units, and a main electric drive motor (Figure 5). Diesel-electric propulsion is particularly fuel-efficient on ships where auxiliary loads, such as cruise ships and ships with highly fluctuating operating profiles, make up a significant portion of the propulsion requirement. The potential of this system for fishing vessels is also being investigated (Bastos, Branco, & Arouca, 2021; Notti & Sala, 2012). An energy management system optimizes fuel efficiency by matching the number of engines in operation to the combined propulsion and auxiliary loads, keeping engines near their design point and rated speed, which reduces emissions, particularly NO_x. However, the system's additional energy conversion stages increase conversion losses, producing higher specific fuel oil consumption at top speeds (Gabrielii & Jafarzadeh, 2020).

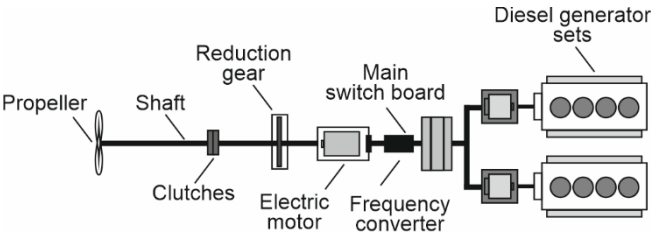


Figure 5. Structure of a diesel-electric powertrain

Conclusion

The IMO has set a goal of reducing GHGs by at least 50% by 2050. To achieve the objectives of the Paris Agreement, greenhouse gas emissions from ships must be reduced by 75-85% per ton-mile, taking into account the expected growth in shipping volumes by 2050 (Wang & Wright, 2021). The use of carbon-containing fuels (LNG, LPG, etc.), carbon-neutral fuels (biofuels, synthetic methane, etc.), and non-carbon fuels (hydrogen, ammonia, etc.) will therefore be widespread soon. When evaluating alternative fuels and increasing the energy efficiency of fishing vessels, it is important to consider a range of technical, financial, and environmental factors related to fuel consumption. Particular attention should be paid to the engine, fuel system, maintenance costs, and any retrofit investments required to modify the ships' energy systems. It is also important to assess the risk of long-term financial losses, despite possible price increases of the alternative fuel. In addition, technical measures, such as the installation of scrubbers, and management strategies, including control of vessel speed and distance management from fishing areas, can help reduce the environmental impact of fishing vessels.

References

- Abernethy, K. E., Trebilcock, P., Kebede, B., Allison, E. H., & Dulvy, N. K. (2010). Fuelling the decline in UK fishing communities? *ICES Journal of Marine Science*, 67(5), 1076–1085. doi:<https://doi.org/10.1093/icesjms/fsp289>
- Altosole, M., Buglioni, G., & Figari, M. (2014). Alternative propulsion technologies for fishing vessels: a case study. *International Review of Mechanical Engineering (I.R.E.M.E.)*, 8(2), 1-7. Retrieved from <https://www.praiseworthyprize.org/jsm/index.php?journal=ireme&page=article&op=view&path%5B%5D=14667>
- Anand, R. M. (2018). Renewable energy solutions for sustainable fishing practices and improved Livelihoods of the fisherfolk in the South West Coast of India. In E. &. The European Conference on Sustainability (Ed.), (pp. 1-8).
- Andersson, A., & Logason, K. (2015). Feasibility study of hybrid propulsion systems for long-liner fishing vessels. *Master's Thesis in the International Master's Programme Naval Architecture and Ocean Engineering*, 1-81. Sweden: Department of Shipping and Marine Technology Division of Marine Technology CHALMERS UNIVERSITY OF TECHNOLOGY.
- Atacan, C., & Düzbastılar, F. (2023). Determination of risk perception in small-scale fishing and navigation. *Ege Journal of Fisheries and Aquatic Sciences*, 40(1), 1-14. doi:DOI: 10.12714/egejfas.40.1.01
- Babu, S., & Jain, J. V. (2013). On-board solar power for small-scale distant-water fishing vessels. *IEEE Global Humanitarian Technology Conference (GHTC)*, (pp. 1-4). San Jose, CA. doi:10.1109/GHTC.2013.6713644
- Banawan, A. A., El Gohary, M. M., & Sadek, I. S. (2010). Environmental and economical benefits of changing from marine diesel oil to natural-gas fuel for short-voyage high-power passenger ships. *Proceedings of the Institution of Mechanical Engineers, Part M: Journal of Engineering for the Maritime Environment*, 224(2), 103-113. doi:DOI: 10.1243/14750902JEME181
- Banjarnahor, D. A., Hanifan, M., & Budi, E. M. (2017). Design of hybrid solar and wind energy harvester for fishing boat. *International Conference on Green and Renewable Energy Resources (ICGRER 2016)*. 75, pp. 1-8. IOP Conf. Series: Earth and Environmental Science, IOP Publishing. doi:10.1088/1755-1315/75/1/012007
- Bastos, R. F., Branco, D. A., & Arouca, M. C. (2021). Potential of diesel electric system for fuel saving in fishing vessels: a case study on a bottom longline fleet of Brazil. *Journal of Marine Engineering & Technology*, 20(1), 1-16. doi:0.1080/20464177.2018.1507445
- Basurko, O. C., Gabiña, G., & Uriondo, Z. (2013). Energy performance of fishing vessels and potential savings. *Journal of Cleaner Production*, 54, 30-40. doi:<https://doi.org/10.1016/j.jclepro.2013.05.024>

- Behrendt, C. (2014). Energy saving technologies for fishing vessels. *Scientific Journals*, 39(111), 11-15.
- Belhabib, D., Cheung, W., Kroodsmas, D., Lam, V., Underwood, P., & Virdin, J. (2020). Catching industrial fishing incursions into inshore waters of Africa from space. *Fish and Fisheries*, 21, 379-392. doi:DOI: 10.1111/faf.12436
- Boopendranath, M. R. (2002). Energy Optimization in Fishing. In B. Meenakumari, M. R. Boopendranath, & P. Pravin, *ICAR Winter School Manual: Advances in Harvest Technology* (pp. 230-237). , Cochin: Central Institute of Fisheries Technology.
- Bos, N., & MacGregor, J. R. (1987). The use of a wind turbine for propulsive power generation aboard a Scottish Seiner/Trawler. *Wind Engineering*, 11(1), 38-50. Retrieved 12, 2024, from <https://www.jstor.org/stable/43749297>
- Breeze, P. (2014). Chapter 5-Piston Engine–Based Power Plants. In P. Breeze, *Power Generation Technologies (Second Edition)* (pp. 93-110). Elsevier. doi:doi.org/10.1016/B978-0-08-098330-1.00005-3
- Breslin, J. P., & Andersen, P. (1996). *Hydrodynamics of Ship Propellers (Cambridge Ocean Technology Series, Series Number 3)*. Cambridge University Press.
- Brown, D., Boyd, D. S., Brickell, K., Ives, C. D., Natarajan, N., & Parsons, L. (2021). Modern slavery, environmental degradation and climate change: Fisheries, field, forests and factories. *Environment and Planning E: Nature and Space*, 4(2), 191-207. doi:<https://doi.org/10.1177/2514848619887156>
- Buhaug, Ø., Corbett, J. J., Endresen, Ø., Eyring, V., Faber, J., Hanayama, S., . . . Yoshida, K. (2009). *Second IMO GHG Study*. International Maritime Organization (IMO). Retrieved from <https://wwwcdn.imo.org/localresources/en/OurWork/Environment/Documents/SecondIMOGHGStudy2009.pdf>
- Chassot, E., Antoine, S., Guillotreau, P., Lucas, J., Assan, C., Marguerite, M., & Bodin, N. (2021). Fuel consumption and air emissions in one of the world's largest commercial fisheries. *Environmental Pollution*, 273, 1-11. doi:<https://doi.org/10.1016/j.envpol.2021.116454>
- Comer, B. (2018). *Heavy Fuel Oil use by Fishing Vessels in the IMO Polar Code Arctic, 2015*. European Climate Foundation.
- Comer, M., Olmer, N., Mao, X., Roy, B., & Rutherford, D. (2017). *Prevalence of heavy fuel oil and black carbon in Arctic shipping, 2015 to 2025*. Washington DC: International Council on Clean Transportation.
- Commission, E. (2006). Council Regulation (EC) No. 1198/2006 of 27 July 2006 on the European Fisheries Fund.
- Davie, S., Minto, C., Officer, R., Lordan, C., & Jackson, E. (2015). Modelling fuel consumption of fishing vessels for predictive use. *ICES Journal of Marine Science*, 72(2), 708-719. doi:doi:10.1093/icesjms/fsu084

- Díaz-Secades, L. A. (2024). Enhancement of maritime sector decarbonization through the integration of fishing vessels into IMO energy efficiency measures. *Journal of Marine Science and Engineering*, 12(663), 1-16. doi:10.3390/jmse12040663
- Düzbastılar, O. F., & Hoşsucu, H. (1997). The mechanical systems of purse seine vessel. *Mediterranean Fisheries Congress*, (pp. 119-126). İzmir.
- Düzbastılar, O. F., Tosunoğlu, Z., & Kaykaç, H. M. (2003). Geleneksel ve kesimli dip trol ağları ile donam dirençlerinin teorik olarak hesaplanması. *Ege Journal of Fisheries and Aquatic Sciences*, 20(1-2), 15-25. Retrieved from <http://www.egejfas.org/tr/download/article-file/57933>
- Düzbastılar, O. F., Tosunoğlu, Z., Ceyhan, T., Kaykaç, H. M., Aydın, C., Güleş, Ö., & Metin, G. (2022). European pilchard after sieving and discarding from a purse seine fishery in the Eastern Mediterranean. *Turkish Journal of Fisheries & Aquatic Sciences*, 23(1), 1-13. doi:<https://doi.org/10.4194/TRJFAS21516>
- FAO. (2014). *The State of World Fisheries and Aquaculture: Opportunities and challenges*. Rome: FAO. <https://www.fao.org/3/i3720e/i3720e.pdf> adresinden alındı
- FAO. (2022). *The State of World Fisheries and Aquaculture 2022. Towards Blue Transformation*. Rome: FAO.
- Folk, C., & Kautsky, N. (1992). Aquaculture with its environment: Prospects for sustainability. 17(1), 5-24. doi:[https://doi.org/10.1016/0964-5691\(92\)90059-T](https://doi.org/10.1016/0964-5691(92)90059-T)
- Gabiña, G., Basurko, O. C., Notti, E., Sala, A., Aldekoa, S., Clemente, M., & Uriondo, Z. (2016). Energy efficiency in fishing: Are magnetic devices useful for use in fishing vessels? *Applied Thermal Engineering*, 670–678. doi:<https://doi.org/10.1016/j.applthermaleng.2015.10.161>
- Gabrielii, C., & Jafarzadeh, S. (2020). *Alternative fuels and propulsion systems*. Norway: SINTEF Energy Research. Retrieved from https://www.sintef.no/contentassets/f18e738f011347999884e200f817b956/coolfish-report-propulsion_and_fuels-signed.pdf
- Gamage, O., Wimalasooriya, C., Boteju, C., & Wimalasiri, W. K. (2021). Feasibility on introducing an alternative solar powered propelling system for multi-day fishing boats in Sri Lanka . In O. (. AIP Conference Proceedings 2403 (Ed.). doi:10.1063/5.0070707
- Gavaris, S. (2009). Fisheries management planning and support for strategic and tactical decisions in an ecosystem approach context. *Fisheries Research*, 100(1), 6-14. doi:<https://doi.org/10.1016/j.fishres.2008.12.001>
- Gillett, R. (2007). *A Short History of Industrial Fishing in the Pacific Islands*. Bangkok: FAO. Retrieved 7 2, 2024, from <https://openknowledge.fao.org/server/api/core/bitstreams/85897812-2dc6-4ebc-8a69-56c67572f6e6/content>

- Gudmundsson, S. (2014). Chapter 7-Selecting the Power Plant. In S. Gudmundsson, *General Aviation Aircraft Design: Applied Methods and Procedures* (pp. 181-234). Butterworth-Heinemann, Elsevier Inc. doi:<https://doi.org/10.1016/C2011-0-06824-2>
- Gulbrandsen, O. (1986). *Bay of Bengal Programme - Development of Small-Scale Fisheries*. Reducing Fuel Cost of Small Fishing Boats. FAO.
- Gulbrandsen, O. (2012). *Fuel savings for small fishing vessels*. Rome: FAO.
- Gutiérrez, C., & Meana, D. (2012). Application of hybrid-electric power supply system in fishing vessels. *EPJ Web of Conferences*. 33, pp. 1-8. EDP Sciences. doi:10.1051/epjconf/20123304009
- Guyader, O., Berthou, P., Koutsikopoulos, C., Alban, F., Demanèche, S., Gaspar, M., . . . Maynou, F. (2013). Small scale fisheries in Europe: A comparative analysis based on a selection of case studies. *Fisheries Research*, 140, 1-13. doi:<https://doi.org/10.1016/j.fishres.2012.11.008>
- He, P., Chopin, F., Suuronen, P., Ferro, R., & Lansley, J. (2021). *Classification and illustrated definition of fishing gears*. FAO Fisheries and Aquaculture Technical Paper. 672. Rome: FAO. doi:<https://doi.org/10.4060/cb4966en>
- HELCOM. (2019). *Alternative fuels for shipping in the Baltic Sea Region*. HELCOM - Helsinki Commission Katajanokanlaituri 6 B FI-00160 Helsinki, Finland. Retrieved from chrome-extension://efaidnbmnnnibpcajpcgclefindmkaj/<https://helcom.fi/wp-content/uploads/2019/10/HELCOM-EnviSUM-Alternative-fuels-for-shipping.pdf>
- Hoşsucu, H., Düzbastılar, O. F., Ceyhan, T., & Ayaz, A. (1999). Ortasu trolü avcılığında güverte ekipmanları. *Ege Journal of Fisheries and Aquatic Sciences*, 15(1-2), 139-149.
- Hussein, A. W., Elsayed, A., & Yehia, W. (2021). Fishing vessels energy efficiency operational and technological measures. *SYLWAN*, 165(1), 197-211.
- Hwang, J., Kim, J., Jeon, H., & Kim, S. (2022). A study on the application of hybrid propulsion system of small size fishing vessels in South Korea. *Journal of International Maritime Safety, Eenvironmental Affairs, and Shipping*, 6(4), 206–215. doi:10.1080/25725084.2022.2149176
- IMO. (2009). GUIDANCE FOR THE DEVELOPMENT OF A SHIP ENERGY EFFICIENCY MANAGEMENT PLAN (SEEMP). (MEPC.1/Circ.683). London. Retrieved from <https://www.register-iri.com/wp-content/uploads/MEPC.1-Circ.683.pdf>
- IMO. (2009). Guidelines for voluntary use of the ship energy efficiency operational indicator (EEOI). (MEPC.1/Circ.684).
- IMO. (2016). IMO Train the Trainer (TTT) Course on Energy Efficient Ship Operation. *Module 2 – Ship Energy Efficiency Regulations and Related Guidelines*, 1-45.

- London. Retrieved from <https://wwwcdn.imo.org/localresources/en/OurWork/Environment/Documents/Air%20pollution/M2%20EE%20regulations%20and%20guidelines%20final.pdf>
- IMO. (2022a). Resolution MEPC.346 (78) 2022 Guidelines for the Development of a Ship Energy Efficiency Management Plan (SEEMP); Annex 8; International Maritime Organization (IMO): London, UK, 2022; pp. 1–36.
- IMO. (2022b). Guidelines on the method of calculation of the attained Energy Efficiency Design Index (EEDI) for new ships. (*s (resolution MEPC.364(79))*).
- IMO. (2022c). 2022 Guidelines on the method of calculation of the attained Energy Efficiency Existing Ship Index (EEXI). (*resolution MEPC.350(78)*).
- IMO. (2024). International Regulations for the Safety of Fishing Vessels. 1-186. Retrieved June 26, 2024, from <https://wwwcdn.imo.org/localresources/en/About/Conventions/Documents/Consolidated%20text%20of%20the%20Agreement.pdf>
- Ismail, M. M., Zulkifli, F. H., Fawzi, M., & Osman, S. A. (2016). Conversion method of a diesel engine to a CNG-diesel dual fuel engine and its financial saving. *ARPN Journal of Engineering and Applied Sciences*, 11(8), 5078-5083.
- Jaremin, B., & Kotulak, E. (2004). Mortality in the Polish small-scale fishing industry. *Occupational Medicine*, 54(4), 258-260. doi:<https://doi.org/10.1093/occmed/kqh054>
- Jennings, S., & Kaiser, M. J. (1998). The effects of fishing on marine ecosystems. *Advances in Marine Biology*, 34, 201-352. doi:[https://doi.org/10.1016/S0065-2881\(08\)60212-6](https://doi.org/10.1016/S0065-2881(08)60212-6)
- Johnson, M., Waldman, S., Rybchenko, S., Bell, M., & Ready, S. (2022). *Electrifying the fleet - More sustainable propulsion options for the small-scale fishing fleet*. National Federation of Fisherman's Organisations (NFFO), Future Fisheries Alliance (RSPB, MCS, WWF), North Sea Wildlife Trusts.
- Kaykaç, M. H., Düzbastılar, O. F., Zengin, M., Süer, S., & Rüzgar, M. (2017). Measurements of fuel consumption of beam trawler and towing resistance of beam trawl used for veined rapa whelk (*Rapana venosa Valenciennes, 1846*) and underwater observations: Preliminary results. *Turkish Journal of Fisheries and Aquatic Sciences*, 17, 901-909. doi:DOI: 10.4194/1303-2712-v17_5_06
- Kemp, C. (2018). *Vessel Energy Analysis Tool (Model Documentation) - Fishing Vessel Energy Efficiency Project*. Nunatak Energetics.
- Kemp, C., & Atshan, S. (2021). *Electric power systems for fishing vessels: Feasibility, fuel savings and costs*. Alaska Longline Fishermen's Association.
- Kindt-Larsen, L., Kirkegaard, E., & Dalskov, J. (2011). Fully documented fishery: a tool to support a catch quota management system. *ICES Journal of Marine Science*, 68(8), 1606–1610. doi:<https://doi.org/10.1093/icesjms/fsr065>

- Korican, M., Vladimir, N., & Fan, A. (2023). Investigation of the energy efficiency of fishing vessels: Case study of the fishing fleet in the Adriatic Sea. *Ocean Engineering*, 1-12.
- Koričan, M., Vladimir, N., Haramina, T., Alujević, N., & Vučković, K. (2023). Extended emission index for fishing vessels: Assessment of the environmental friendliness of a purse seiner with an alternative power system. *WIT Transactions on Ecology and the Environment*, 261, 225-232. doi:doi:10.2495/ESUS230191
- Koyama, T. (1971). A calculation method for matching trawl gear to towing power of trawlers. H. Kristjonsson içinde, *Modern fishing gear of the world* (s. 352-358). FAO.
- Leira, B. (2018). LNG as fuel on fishing vessels. 111. Norway: MSc Thesis, Norwegian University of Science and Technology.
- McGill, R., Remley, W., & Winther, K. (2013). *Alternative Fuels for Marine Applications*. IEA Advanced Motor Fuels Implementing Agreement.
- Moon, S. W., Ruy, W. S., & Park, K. P. (2024). A study on fishing vessel energy system optimization using bond graphs. *Journal of Marine Science and Engineering*, 12(6, 903), 1-23. doi:https://doi.org/10.3390/jmse12060903
- Notti, E., & Sala, A. (2012). On the opportunity of improving propulsion system efficiency for italian fishing vessels. *Second International Symposium on Fishing Vessel Energy Efficiency*, (s. 2-6). Vigo.
- Nugraha, M. A., Luthfiani, F., Sotyaramadhani, G., Widagdo, A., & Desnanjaya, G. N. (2022). Technical-economical assessment of solar PV systems on small-scale fishing vessels. *International Journal of Power Electronics and Drive Systems (IJPEDS)*, 13(2), 1150-1157. doi:10.11591/ijpeds.v13.i2.pp1150-1157
- Parker, R. W., Blanchard, J. L., Gardner, C., Green, B. S., Hartmann, K., Tyedmers, P. H., & Watson, R. A. (2018). Fuel use and greenhouse gas emissions of world fisheries. *Nature Climate Change*, 8, 333-339. doi:https://doi.org/10.1038/s41558-018-0117-x
- Prananda, J., Koenhardono, E. S., & Tjoa, R. C. (2019). Design of an optimum battery electric fishing vessel for Natuna Sea. *International Journal of Marine Engineering Innovation and Research*, 4(2), 111-121.
- Rawson, K. J., & Tupper, E. C. (2001). Powering of ships: general principles. In K. J. Rawson, & E. C. Tupper, *Basic Ship Theory (Fifth Edition)* (pp. 365-410). Butterworth-Heinemann. doi:https://doi.org/10.1016/B978-075065398-5/50013-3
- Rossiter, T. (2007). Biofuels for the fishing industry . *ICES CM 2007/M:01*, (pp. 1-9).
- Ruiz, V. (2012). Analysis of existing refrigeration plants onboard fishing vessels and improvement possibilities. *Second International Symposium on Fishing Vessel Energy Efficiency*, (pp. 1-8). Vigo.

- Sala, A., Damalas, D., Labanchi, L., Martinsohn, J., Moro, F., Sabatella, R., & Notti, E. (2022). Energy audit and carbon footprint in trawl fisheries. *scientific data*, 9(428), 1-20. doi:doi.org/10.1038/s41597-022-01478-0
- Sala, A., De Carlo, F., Buglioni, G., & Lucchetti, A. (2011). Energy performance evaluation of fishing vessels by fuel mass flow measuring system. *Ocean Engineering*, 38, 804-809. doi:doi:10.1016/j.oceaneng.2011.02.004
- Santosa, P. I., Utama, I. K., Aryawan, W. D., Purwanto, D. B., Chao, R.-M., & Nasirudin, A. (2014). An investigation into hybrid catamaran fishing vessel: Combination of diesel engine, sails and solar panels. *IPTEK, Journal of Proceeding Series*, 1, pp. 36-41.
- Santoso, A., Semin, Cahyono, B., & Sampurno, B. (2021). Developing small dual-fuel diesel engine to control marine pollution by reducing NOx emission for application in fishing vessels. *IOP Conf. Series: Earth and Environmental Science*, (pp. 1-5). doi:doi:10.1088/1755-1315/698/1/012001
- Sarıca, A., Gökçe, G., Dalgıç, G., & Özbilgin, H. (2018). Detection and reduction of fuel consumption in fishing vessels. *Turkish Journal of Maritime and Marine Sciences*, 4(1), 8-19. Retrieved from <https://dergipark.org.tr/tr/pub/trjmms/issue/40088/476923>
- Shi, W., Stapersma, D., & Grimmelius, H. T. (2009). Analysis of energy conversion in ship propulsion system in off-design operation conditions. In A. A. Mammoli, & C. A. Brebbia, *WIT Transactions on Ecology and the Environment: Energy and Sustainability II* (Vol. 121, pp. 449-460). WIT Press. doi:doi:10.2495/ESU090411
- Smith, H., & Basurto, X. (2019). Defining small-scale fisheries and examining the role of science in shaping perceptions of who and what counts: A systematic review. *Frointers in Marine Science*, 6(236), 1-19. doi:doi: 10.3389/fmars.2019.00236
- Son, Y.-k., Lee, S.-Y., & Sul, S.-K. (2018). DC Power System for Fishing Boat. *2018 IEEE International Conference on Power Electronics, Drives and Energy Systems (PEDES)* (pp. 1-6). Chennai, India: IEEE. doi:doi: 10.1109/PEDES.2018.8707631
- Sudjasta, B., Prayitno, S., & Hatuwe, M. R. (2021). Utilization of solar energy on 10 GT fishing vessels as alternative electricity facilities at PPI Cituis Tangerang Regency. 328, pp. 1-6. E3S Web of Conferences, ICST. doi:10.1051/e3sconf/202132809001
- Szczepanek, M. (2015). Factors affecting the energy efficiency of fishing vessels. *Scientific Journals of the Maritime University of Szczecin*, 42(114), 38-42. Retrieved from <https://repository.am.szczecin.pl/handle/123456789/762>
- Szelangiewicz, T., Abramowski, T., Zelazny, K., & Sugalski, K. (2021). Reduction of resistance, fuel consumption and GHG emission of a small fishing vessel by adding a bulbous bow. *Energies*, 14(7), 1-17. doi: <https://doi.org/10.3390/en14071837>

- Thermes, S., van Anrooy, R., & Gudmundsson, A. (2023). *Classification and definition of fishing vessel types. Second edition.* 267. Rome: FAO. doi:<https://doi.org/10.4060/cc7468en>
- Tyedmers, P. H., Watson, R., & Pauly, D. (2005). Fueling global fishing fleets. *Ambio*, 34(8), 635–638. Retrieved from <http://www.jstor.org/stable/4315668>
- Wang, L., Chen, S.-S., Wei, C.-Y., Wang, K.-H., Lee, J.-D., Huang, C.-C., & Lee, W.-J. (2009). Energy saving of a prototype fishing boat using a small wind turbine generator: Practical installation and measured results. *IEEE Xplore, Power & Energy Society General Meeting*, 1-6. doi:10.1109/PES.2009.5275927
- Wang, Y., & Wright, L. A. (2021). A comparative review of alternative fuels for the maritime sector: Economic, technology, and policy challenges for clean energy implementation. *World*, 2(4), 456-481. doi:10.3390/world2040029
- Xu, Y., Lin, J., Yin, B., Martens, P., & Krafft, T. (2023). Marine fishing and climate change: A China's perspective on fisheries economic development and greenhouse gas emissions. *Ocean and Coastal Management*, 245(106861), 1-11. doi:<https://doi.org/10.1016/j.ocecoaman.2023.106861>
- Yaakob, O., & Husain, A. S. (2015). Dual fuel powered fishing boats using natural gas. *Jurnal Mekanikal*, 38, 1-7.
- Yoon, K., Jeon, H., Hwang, J., & Kim, J. (2021). A study on the feasibility of installing solar auxiliary power for small fishing boats. *Journal of the Korean Society of Marine Environment & Safety*, 27(6), 883-889. doi:doi.org/10.7837/kosomes.2021.27.6.883



CHAPTER 6

The Evaluation of Photovoltaic Power Systems With Different Simulation Softwares for Bozcaada

Ersin Akyüz¹

¹ Assoc. Prof. Dr., Balıkesir University, Faculty of Engineering, Department of Electrical and Electronics Engineering, Balıkesir, Turkey , ORCID: 0000-0001-9786-3221

Introduction

Energy, serving as the primary component for the survival of life forms, plays a crucial role in various aspects, ranging from fulfilling basic life needs to shaping the economic development structures of nations [1]. Fossil fuels, which are the main resources used to obtain energy, have limited reserves in the world. Due to the scarcity of fossil fuels, a sustainable method should be followed, especially in the field of energy, when the issues of the danger of depletion of these fuels, the import of these energy resources by countries, and the destruction of nature are considered (Karaca & Bingul, 2019). Energy sources are basically divided into fossil fuels, known as non-renewable energy, and renewable energy sources. Non-renewable energy sources have general characteristics such as being fossil-based, not needing to be stored, not being able to be produced in any quantity, and not being sustainable (Konyali, 2019). Non-renewable energy sources are divided into two groups: nuclear and fossil. Nuclear sources are uranium and thorium, which are used to produce nuclear energy. Fossil sources are oil, natural gas and coal (Demirbas, 2022). Renewable energy sources are obtained from sources such as solar, wind, biomass, geothermal, wave energy. These energy sources are called renewable energy because they do not run out and exist continuously. Renewable energy sources are energies used in the form of direct or indirect conversion of the sun, air and water into electrical energy or heat energy.

Renewable energies are obtained from sources that exist in nature such as water power, solar, wind, biomass, geothermal, wave energy. They are energies in the form of converting air, water, sun directly or indirectly into electricity or heat, and are called renewable because they are inexhaustible and continuous. As an alternative to non-renewable fossil-based energies, it has started to be developed and widespread in parallel with the increase in technological possibilities. Solar energy, which is the first alternative energy source among renewable energy sources, is an energy that is intensively utilized worldwide due to its suitability in terms of capacity and efficiency, its applicability as a renewable resource, its simple technology in this field, and most importantly, its sustainability and environmental friendliness (Habibullah, 2016; Ozkoca, 2019). Solar energy is the radiant energy generated by fusion reactions in which hydrogen is continuously converted into helium, and the mass change that takes place is transformed into heat energy and dissipated into the vacuum of space. The radiation intensity of solar energy is approximately 1370 W/m^2 , but the amount that reaches the earth can vary between $0\text{-}1100 \text{ W/m}^2$ due to losses in the atmosphere. Even a small portion of solar energy that can reach the earth is much

more than the current energy consumption of humanity. Solar energy is used by converting it into electrical energy through photovoltaic (PV) panels called photovoltaic systems (Akcna, Kuncan, & Minaz, 2020).

The distribution of Turkey's installed capacity by resources as of the end of August 2024 is as follows: 28.3% hydraulic energy, 21.7% natural gas, 19.2% coal, 10.8% wind, 16.2% solar, 1.5% geothermal and 2.4% other resources (T.C. Enerji ve Tabii Kaynaklar Bakanlığı, 2024). On the other hand, Figure 1 shows the solar energy potential map of Turkey (GEPA, 2024). According to this map, the average annual amount of solar radiation per 1m2 of surface area increases as you go south.

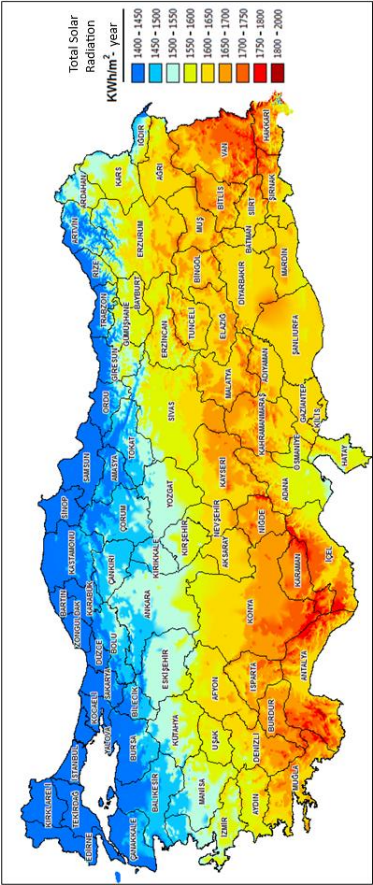


Figure 1. Solar radiation map of Turkey (GEPA, 2024)

Turkey's installed solar electricity capacity is 8,479 MW by the end of June 2022. The share of solar energy in total installed capacity is 8.35% and the change in installed capacity over the years is shown in Figure 2. Photovoltaic (PV) systems used in electricity generation from solar energy are basically divided into two. These systems are grid-connected (on grid) and off grid (off grid). Off-grid systems are used to meet the electricity demand in places where grid electricity is not available or not suitable for use. Batteries are charged with direct current obtained from solar energy through panels. The stored energy is converted into alternative energy through an inverter (Brian, 2023). Power systems using solar and wind energy can be simulated in computer simulation environment. At this point, PVsyst and HOMER software can be shown as example platforms.

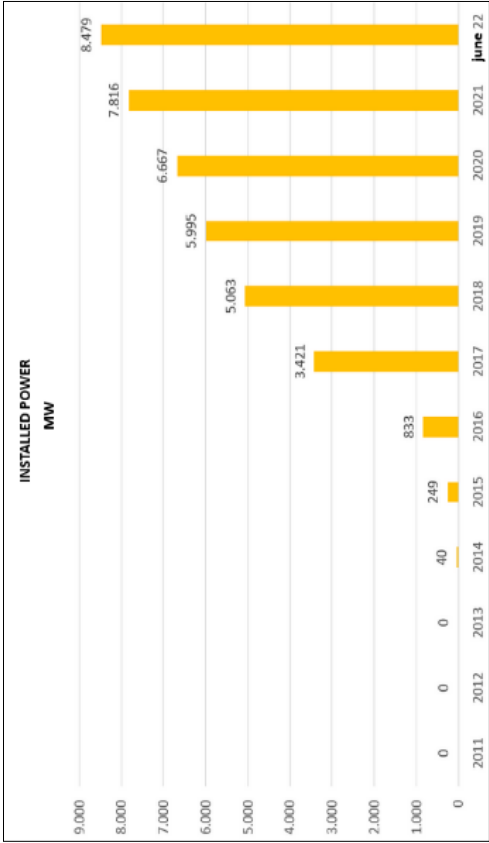


Figure 2. Total installed capacity of PV (T.C. Enerji ve Tabii Kaynaklar Bakanlığı, 2022).

HOMER software was developed by the US National Renewable Energy Laboratory. It helps in the design and implementation of small-scale grids and distributed power systems. The software can calculate technology costs, electricity load and energy resource utilization for systems built in different ways. Simulation, optimization and sensitivity analysis of energy systems are performed with HOMER software (HOMER, 2021). PVSyst software is a simulation software developed by the University of Geneva, Switzerland, which is used to design and analyze the results of photovoltaic systems such as grid-connected or off-grid PV systems, PV irrigation systems and DC grids (PVSyst, 2024). In another study using PVSyst software, an ideal region for solar power generation and utilization was first identified and the feasibility and design considerations of a 500 KWp grid-tidal micro solar photovoltaic plant were discussed (Nallamotheu, Janga, & Pendem, 2024).

The technical and economic analysis of a stand-alone hybrid solar-wind energy system with battery storage for an island campus has been carried out using HOMER software (Ma, Yang, & Lu, 2014). In another study, a 1kWp photovoltaic system was designed for Hamirpur, Himachal Pradesh, India using PVSyst software and a system simulation study was performed (Yadav, Kumar, & Chandel, 2015). Feasibility and sensitivity analysis of renewable energy-based off-grid and grid-connected microgrids by investigating wind and solar energy potentials were conducted using HOMER software (Nurunnabi, Roy, Hossain, & Pota, 2019). HOMER software was used in the study on the techno-economic feasibility and optimum design of a hybrid micro-hydro-photovoltaic-diesel-battery-wind power system designed to electrify a typical remote village located in the southern part of Nigeria (Oladigbolu, Ramli, & Al-Turki, 2020). In another study on meeting the power needs of an autonomous desalination system in the Canary Islands from renewable energy systems, the hybrid energy system models created were analyzed technically and economically through HOMER software (Padrón, Avila, Marichal, & Rodríguez, 2019). In another study using HOMER software, an optimal hybrid microgrid design was proposed for a district in Lahore, Pakistan, which provides continuous and cost-effective energy supply by utilizing reliable energy sources (Khaled, Zahid, Zahid, & Ilahi, 2024).

Solar energy has emerged as a promising solution with advancements in technology and the development of various solar-powered devices. For these systems, which can be installed either grid-connected or off-grid, sizing and cost analyses are essential. The cost of the generated energy also depends on the location of the system. Therefore, the energy demand

of the load should be determined, and the system should be modeled to complete performance and cost analyses. In this study, sizing and cost analyses for a photovoltaic system with a 3 kWh/d load in Bozcada were completed using computer software such as PVsyst and HOMER. Through these analyses, the energy generated by both grid-connected and off-grid systems was calculated, and an economic evaluation was conducted.

Analysis and Simulation

The simulation software HOMER (Homerenergy, 2024) and PVSYST (PVsyst, 2024) were used to evaluate the techno-economic feasibility and sizing of remote homes in Bozcada, Turkey. HOMER was developed by the National Renewable Energy Laboratory (NREL) as a potential simulation and optimization tool for renewable energy systems. Optimal economic designs for PV can be achieved with energy storage in batteries. Typically, the optimal design is realized by minimizing the Net Present Cost (NPC), where NPC represents the sum of investment costs plus the discounted present value of all future operational costs over the system's lifetime.

Economic Analysis

In HOMER software, cost of energy (COE) is minimized using a cost optimization approach, which also determines the sizing of system components accordingly. In renewable energy investments, the levelized economic analysis (LEC) method enables comparison across multiple renewable energy systems. Rather than merely comparing initial capital or operating costs, this analysis aims to calculate the cost of delivering a service over the project's lifespan (Ding, Fu, & Lisa Hsieh, 2024). This approach considers the total net present cost over the system's operational lifetime, including projected expenses such as capital cost (CC), operation and maintenance costs (OMC), and repair and replacement costs (RRC). By evaluating the financial impacts over time, it effectively incorporates the temporal aspect of costs (Kashefi Kaviani, Riahy, & Kouhsari, 2009; Yang, Zhou, Lu, & Fang, 2008).

$$ACS(\$) = \sum_{i=1}^n N_i x [(CC_i + RC_i x F_i(ir, L_i, y_i)) x CRF(ir, R) + OMC_i]$$

Here, “n” represents the number of hybrid system components, such as PV panels and wind turbines, while “N” denotes the unit count for each “i” system component. The capital cost (\$/kW) refers to the difference between the total renewal costs of component “i” over the system's lifetime and the residual component cost at the end of that lifetime, which is calculated as the present single-payment value. Additionally, “i” represents the annual operation and maintenance cost of the component. The real interest rate (ir), denoted as the real discount rate (RDR), is a function of the nominal interest (discount) rate (ir_{nominal}) and the annual inflation rate (fr) (Gül & Akyüz, 2023).

$$ir = \frac{ir_{nominal} - fr}{1 + fr}$$

The capital recovery factor (CRF) is the ratio of a fixed annuity over a specific period to the present value of that annuity. Here, CRF is calculated using the interest rate as follows (Gül & Akyüz, 2023).

$$CRF = \frac{(1 + R)^N \cdot R}{(1 + R)^N - 1}$$

Here, “R” represents the given discount rate, and “N” is the useful system lifetime (in years).

System Description

The design of a solar energy system is site-specific and depends on available resources and the load profile. The simulation location, Çanakkale/Bozcaada, is shown in Figure 3.



Figure 3. Bozcaada location

The schematic of the planned system in HOMER software is shown in Figure 4. Accordingly, the system consists of AC load, AC/DC converter, battery, and PV panel components. The size of each system element has been optimized according to the load determined by HOMER.

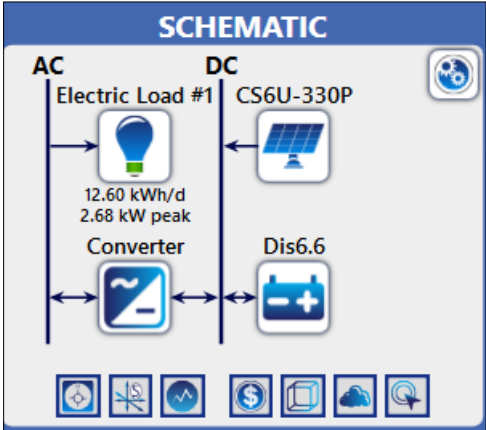


Figure 4. System schematic (HOMER)

The load profile for the designated farmhouse, with an annual average load of 12.6 kWh/day, an average of 0.53 kW, and a peak load value of 2.68 kW, is shown in Figure 5. The same load values were selected in the PVsyst software. In PVsyst, the configuration includes 10 LED lamps, 1 PC, 1 TV (5 hours/day), 1 dishwasher and washing machine (2 hours/day), 1 air conditioner, and 1 fan, totaling 12.642 Wh/day and averaging 379.3 kWh/month.

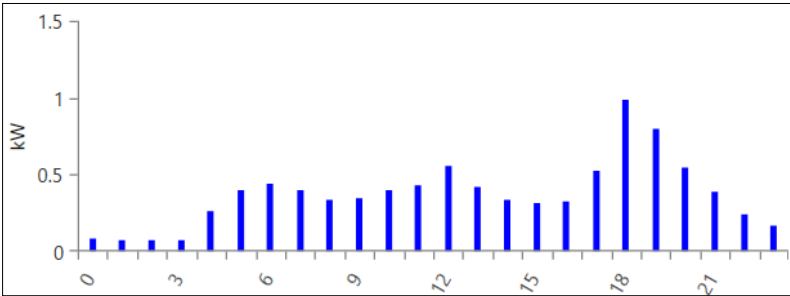


Figure 5. Peak load values

Figure 6 shows that solar radiation levels are higher during the summer months. Between January and December, the monthly solar global radiation values range from 1.65 to 6.792 kWh/m²/day. The annual average daily solar global radiation level is found to be 4.01 kWh/m²/day. Ambient temperatures vary between 7.82 and 25.8 °C.

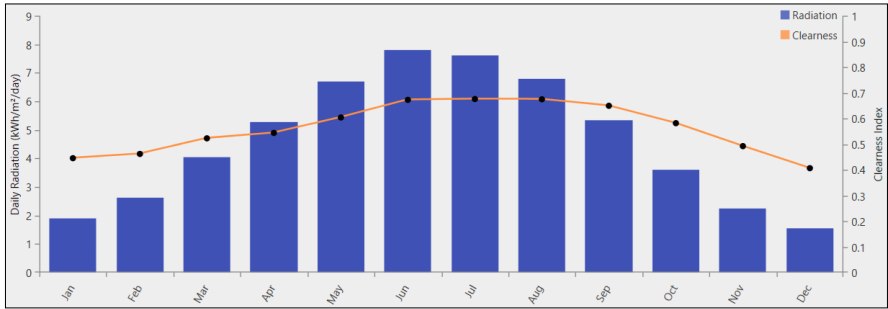


Figure 6. Solar daily radiation (kWh/m²/day)

The Global Horizontal Irradiation graph used by the PVsyst software is shown in Figure 7. Accordingly, the annual horizontal irradiation value produced is 1,753 kWh/m², reaching its highest level in June and its lowest level in December.

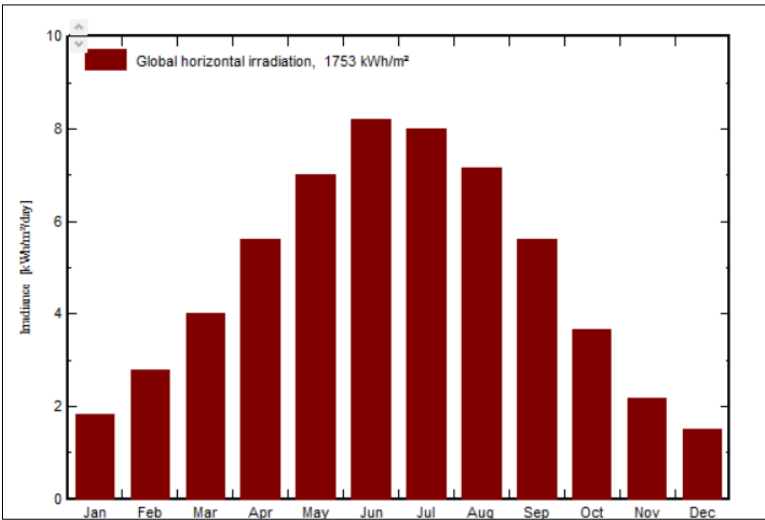


Figure 7. Global horizontal irradiation

The monthly temperature variation provided in the HOMER software is shown in Figure 8. According to this graph, the highest average daily temperatures are 25.08°C in July and August, while the lowest temperature is 7.8°C in January.

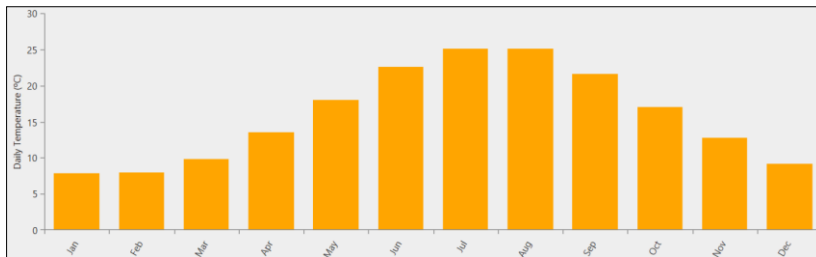


Figure 8. Daily temperature graph

Results and Discussions

The size of each system component corresponding to the specified load in the analysis conducted with HOMER is shown in Figure 9. For this load, the HOMER software calculated 6.36 kW for the PV, 33 kWh for the battery, and 2.51 kW for the converter. Based on these values, the levelized cost of energy was calculated as \$0.0736 per kWh in the economic analysis.




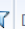
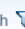



Architecture						
			CS6U-330P (kW)		Converter (kW)	
			6.36	5	2.51	CC

Figure 9. HOMER size optimization results

The sizing analysis results conducted with PVsyst software for approximately the same load are presented in Figure 10. Accordingly, for this load, the PVsyst software calculated 6.05 kW for the PV, 44.2 kWh for the battery, and 1 kW for the converter. Based on these values, the levelized cost of energy was calculated as \$0.0104 per kWh in the economic analysis.

PV Array			
PV modules	CWT550 - 108PM12 - V	Battery:	RI-ENERGYPACK-7.16kWh
Nominal power	6.05 kWp	Battery voltage	51 V
MPP voltage	31.4 V	Total capacity	868 Ah
MPP current	17.5 A		
Main results			
System Production	10069 kWh/yr	Normalized prod.	1.81 kWh/kWp/day
Specific prod.	1664 kWh/kWp/yr	Array losses	3.56 kWh/kWp/day
Performance Ratio	0.326	System losses	0.18 kWh/kWp/day

Figure 10. PVsyst size optimization results

According to the analysis results conducted with both software, the HOMER software calculated the PV panel size as 5% larger, while the PVsyst software did not calculate the battery size as 33% larger.

In the comparison graphs of software results shown in Figure 11, the annual energy production in the PVsyst simulation was 12,526 kWh/year under standard test conditions, while the energy produced in the operating environment was 10,043 kWh/year. According to the HOMER simulation results, the annual energy production was 10,200 kWh/year, with the highest energy production occurring in June and July, and the lowest in November.

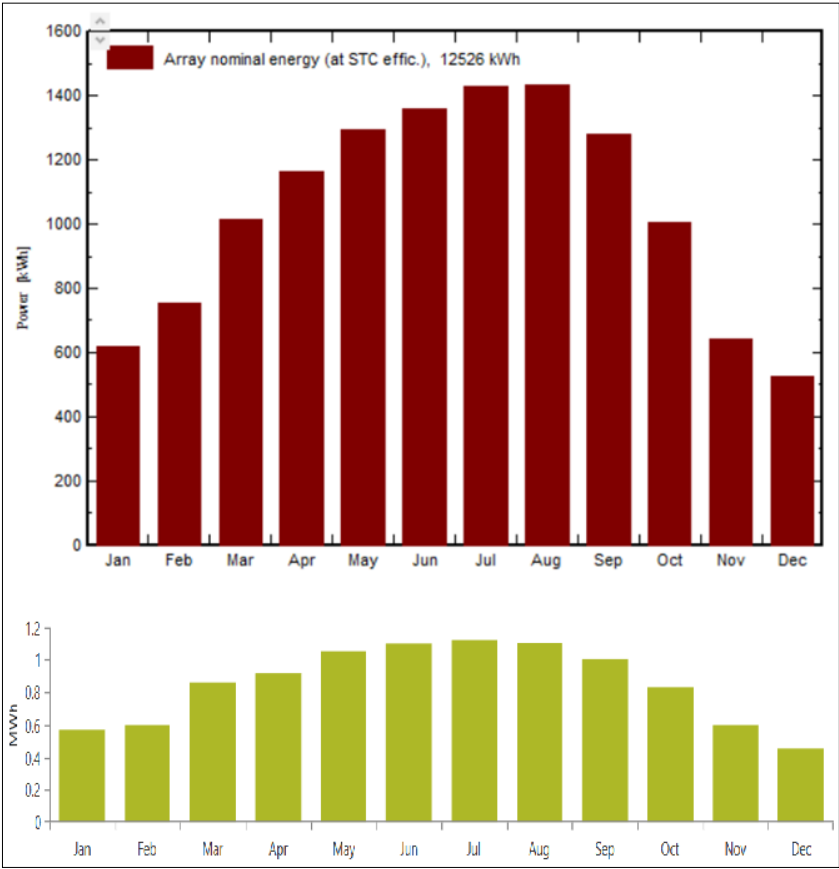


Figure 11. Pvsyst software vs Homer software

Both graphs shown in Figure 11 contain values approximately 20% higher because they are provided under standard test conditions in the PVsyst software. Under operating conditions, this value approaches the results obtained from the HOMER software. According to Table 1, the excess energy amount in the PVsyst

software is 6122 kWh/year, while in the HOMER software, this value is 5255 kWh/year.

Table 1. Simulation eletrical results

	PVsyst – 6.05kW/1kW	HOMER – 6.36kW/1kW
Annual Energy Prod. (kWh/yr)	10043/1660	10200/1612
Excess Energy	6122/1012	5255/944

Conclusion

In this study, PVsyst and HOMER software were compared to conduct sizing and techno-economic analysis of a photovoltaic (PV) system designed to meet a specific load profile in Bozcada, Turkey. Both software tools effectively demonstrated their capability to simulate and optimize PV-based energy systems. However, distinct differences emerged in the sizing and cost analysis results due to each software’s internal calculation methods. The results indicated that HOMER suggested a slightly larger PV system size (6.36 kW) compared to PVsyst, while PVsyst calculated a battery capacity (44.2 kWh) that was 33% larger than that proposed by HOMER. Consequently, HOMER estimated the levelized cost of energy as \$0.0736 per kWh, whereas PVsyst provided an estimate of \$0.0104 per kWh. These differences highlight the importance of accounting for cost discrepancies in project feasibility assessments.

The energy production simulations showed that PVsyst projected an annual energy output of 12,526 kWh under Standard Test Conditions (STC); however, this output decreased to 10,043 kWh/year in practical operational conditions. In contrast, HOMER provided an output closer to real-world conditions, with an annual production of 10,200 kWh. This suggests that while PVsyst is useful for performance estimates under standard conditions, it may predict higher outputs under ideal conditions compared to HOMER. Additionally, the excess energy estimate in PVsyst (6,122 kWh/year) was higher than in HOMER (5,255 kWh/year), reflecting different assumptions in energy usage and system efficiency calculations. The PVsyst model aligns with standard output data but may overestimate excess energy, potentially impacting decisions on energy storage and overall system design.

In conclusion, while both PVsyst and HOMER provide valuable insights for designing grid-connected and off-grid systems, the choice between them should

be made based on the specific requirements of the project. For systems that demand precise operational performance in local conditions, HOMER may better reflect real-world scenarios. For performance predictions under standard conditions, PVsyst's features are advantageous. Ultimately, using both tools together offers a balanced approach, combining PVsyst's design parameters and HOMER's practical optimization capabilities to maximize the efficiency and economic feasibility of renewable energy projects.

References

- Akcan, E., Kuncan, M., & Minaz, M. R. (2020). PVsyst Yazılımı ile 30 kW Şebekeye Bağlı Fotovoltaik Sistemin Modellenmesi ve Simülasyonu. *Avrupa Bilim ve Teknoloji Dergisi*, (18), 248–261. <https://doi.org/10.31590/EJO-SAT.685909>
- Brian, B. (2023). On-Grid Solar System Vs. Off-Grid Solar System - Professional Distributed PV Module Manufacturer. Retrieved September 21, 2024, from <https://www.maysunsolar.com/blog-on-grid-solar-system-vs-off-grid-solar-system/>
- Demirbas, B. (2022). Türkiye’de yenilenebilir enerjinin durumu, ekonomiye ve çevreye etkilerinin değerlendirilmesi (Niğde Ömer Halisdemir Üniversitesi / Sosyal Bilimler Enstitüsü / İşletme Ana Bilim Dalı / Üretim Yönetimi ve Pazarlama Bilim Dalı). Niğde Ömer Halisdemir Üniversitesi / Sosyal Bilimler Enstitüsü / İşletme Ana Bilim Dalı / Üretim Yönetimi ve Pazarlama Bilim Dalı, Niğde. Retrieved from <https://tez.yok.gov.tr/UlusalTezMerkezi/tezSorguSonucYeni.jsp>
- Ding, J.-W., Fu, Y.-S., & Lisa Hsieh, I.-Y. (2024). The cost of green: Analyzing the economic feasibility of hydrogen production from offshore wind power. *Energy Conversion and Management*: X, 100770. <https://doi.org/10.1016/J.ECMX.2024.100770>
- GEPA. (2024). GEPA. Retrieved September 21, 2024, from <https://gepa.enerji.gov.tr/>
- Gül, M., & Akyüz, E. (2023). Techno-economic viability and future price projections of photovoltaic-powered green hydrogen production in strategic regions of Turkey. *Journal of Cleaner Production*, 430, 139627. <https://doi.org/10.1016/J.JCLEPRO.2023.139627>
- Habibullah, M. (2016). Rüzgar-fotovoltaik- biyogaz hibrit güç sistemlerinin akıllı mikro şebekelerde kullanımının kontrol ve dizaynı. Retrieved September 20, 2024, from <https://tez.yok.gov.tr/UlusalTezMerkezi/tezSorguSonucYeni.jsp>
- HOMER. (2021). HOMER - Hybrid Renewable and Distributed Generation System Design Software. Retrieved September 20, 2024, from <https://home-renergy.com/>
- Homerenergy. (2024). HOMER - Hybrid Renewable and Distributed Generation System Design Software. Retrieved November 3, 2024, from <https://homerenergy.com/>
- Karaca, C., & Bingul, A. (2019). TÜRKİYE’DE FOSİL ENERJİ BAĞIMLILIĞININ NEDEN OLDUĞU EKONOMİK VE ÇEVRESEL MALİYETLER 99. Retrieved September 20, 2024, from TÜRKİYE’DE FOSİL ENERJİ BAĞIMLILIĞININ NEDEN OLDUĞU EKONOMİK VE ÇEVRESEL

- Kashefi Kaviani, A., Riahy, G. H., & Kouhsari, S. M. (2009). Optimal design of a reliable hydrogen-based stand-alone wind/PV generating system, considering component outages. *Renewable Energy*, 34(11), 2380–2390. <https://doi.org/10.1016/J.RENENE.2009.03.020>
- Khaled, O., Zahid, M., Zahid, T., & Ilahi, T. (2024). Techno-Economic Feasibility of Hybrid Energy Systems Installation in Pakistan. *IEEE Access*, 12, 41643–41658. <https://doi.org/10.1109/ACCESS.2024.3376409>
- Konyali, I. (2019). Türkiye İçin Mevcut Enerji Üretimine Alternatif Yenilenebilir ve Sürdürülebilir Enerji Kaynaklarının Seçimi. Retrieved September 20, 2024, from Türkiye İçin Mevcut Enerji Üretimine Alternatif Yenilenebilir ve Sürdürülebilir Enerji Kaynaklarının Seçimi website: <https://openaccess.hacettepe.edu.tr/xmlui/handle/11655/8966>
- Ma, T., Yang, H., & Lu, L. (2014). A feasibility study of a stand-alone hybrid solar–wind–battery system for a remote island. *Applied Energy*, 121, 149–158. <https://doi.org/10.1016/J.APENERGY.2014.01.090>
- Nallamothu, B. K., Janga, R., & Pendem, S. R. (2024). Design and Analysis of Grid Connected Solar PV System Using PVsyst Software. 2024 IEEE Students Conference on Engineering and Systems: Interdisciplinary Technologies for Sustainable Future, SCES 2024. <https://doi.org/10.1109/SCES61914.2024.10652298>
- Nurunnabi, M., Roy, N. K., Hossain, E., & Pota, H. R. (2019). Size optimization and sensitivity analysis of hybrid wind/PV micro-grids- A case study for Bangladesh. *IEEE Access*, 7, 150120–150140. <https://doi.org/10.1109/ACCESS.2019.2945937>
- Oladigbolu, J. O., Ramli, M. A. M., & Al-Turki, Y. A. (2020). Feasibility study and comparative analysis of hybrid renewable power system for off-grid rural electrification in a typical remote village located in Nigeria. *IEEE Access*, 8, 171643–171663. <https://doi.org/10.1109/ACCESS.2020.3024676>
- Ozkoca, M. I. (2019, September 12). Kojenerasyon Ve Güneş Enerjisinin Bütünleştirildiği Hibrit Sistemin Ekonomik Ve Emisyon Analizi. Retrieved September 20, 2024, from Kojenerasyon Ve Güneş Enerjisinin Bütünleştirildiği Hibrit Sistemin Ekonomik Ve Emisyon Analizi website: <https://polen.itu.edu.tr/items/0db032c0-2cc9-4201-95ae-bf360337fc97>
- Padrón, I., Avila, D., Marichal, G. N., & Rodríguez, J. A. (2019). Assessment of Hybrid Renewable Energy Systems to supplied energy to Autonomous Desalination Systems in two islands of the Canary Archipelago. *Renewable and Sustainable Energy Reviews*, 101, 221–230. <https://doi.org/10.1016/J.RSER.2018.11.009>

- PVsyst. (2024). PVsyst – Photovoltaic software. Retrieved September 21, 2024, from <https://www.pvsyst.com/>
- T.C. Enerji ve Tabii Kaynaklar Bakanlığı. (2022). Güneş - T.C. Enerji ve Tabii Kaynaklar Bakanlığı. Retrieved September 21, 2024, from <https://enerji.gov.tr/bilgi-merkezi-enerji-gunes>
- T.C. Enerji ve Tabii Kaynaklar Bakanlığı. (2024). Elektrik - T.C. Enerji ve Tabii Kaynaklar Bakanlığı. Retrieved September 21, 2024, from <https://enerji.gov.tr/bilgi-merkezi-enerji-elektrik#:~:text=>
- Yadav, P., Kumar, N., & Chandel, S. S. (2015). Simulation and performance analysis of a 1kWp photovoltaic system using PVsyst. 4th IEEE Sponsored International Conference on Computation of Power, Energy, Information and Communication, ICCPEIC 2015, 358–363. <https://doi.org/10.1109/ICCPEIC.2015.7259481>
- Yang, H., Zhou, W., Lu, L., & Fang, Z. (2008). Optimal sizing method for stand-alone hybrid solar–wind system with LPSP technology by using genetic algorithm. *Solar Energy*, 82(4), 354–367. <https://doi.org/10.1016/J.SOLENER.2007.08.005>



CHAPTER 7

Production of Alumina-Copper Hybrid Composites by Hot Pressing Technique: Investigation of Mechanical, Structural, and Tribological Properties

Cevher Kürşat Macit¹ & Merve Horlu² & Burak Tanyeri³ & Bünyamin Aksaka⁴

¹ Arş. Gör., Firat University, School of Aviation, Aircraft Airframe-Engine Main-tenance, 0000-0003-0466-7788

² Aisin Automotive Industry Trade Inc, 0000-0003-0775-2849

³ Doc. Dr., Firat University, School of Aviation, Aircraft Airframe-Engine Main-tenance, 0000-0002-3517-9755

⁴ Prof. Dr., Firat University, School of Aviation, Aircraft Airframe-Engine Main-tenance, 0000-0003-4844-9387

1. Introduction

There is a growing demand for dynamic electrical contact materials, which is expected to continue increasing as the electronics, aerospace, and electric vehicle industries expand. Electrical contact materials are substances utilized in switches and connections to establish electrical circuits [1][2]. An ideal contact material should possess relatively good mechanical qualities such as high bending strength, hardness, and beneficial resistance to corrosion, along with favorable electrical, thermal, and tribological characteristics [2]. These requirements ensure that the material will not corrode in an environment with high levels of oxygen or at high temperatures. Due to their exceptional electrical and thermal properties, copper, gold, and silver have been the primary materials selected for these applications [2][3]. However, it is widely acknowledged that the limited tribological and mechanical qualities of these materials restrict their range of applications [4][5]. Copper (Cu) is widely utilized in various electrical and electronic devices, such as electric brushes, pantograph sliders, and overhead current collection systems in trains, due to its exceptional electrical and thermal conductivity as well as its ductility [6][7].

Copper and its alloys are anticipated to persist in utilization and exploration in the field of study. However, Cu's relatively poor mechanical properties limit its wide potential applications [1]. The substance Cu is expected to have enhanced mechanical properties as research on it progresses. Introducing a further process can enhance the mechanical and machinability characteristics of Cu [6][7]. Extensive efforts have been made to enhance the mechanical qualities of copper (Cu), often resulting in a compromise on its physical attributes. Zirconium dioxide (ZrO_2), silicon carbide (SiC), molybdenum disulfide (MoS_2), and graphite are types of solid lubricants that have demonstrated favorable outcomes in enhancing the tribological characteristics of copper matrix composites [6][7].

By establishing a friction pair surface, the occurrence of direct contact between the material interface is significantly reduced, resulting in a substantial decrease in both friction and wear. [8][9]. Solid lubricating films with improved friction-reduction and anti-wear performance have recently been developed and widely used in a variety of sectors [8][9]. Composites benefit from such lubricating films' excellent strength, tribological behavior, and thermal stability [8][9]. Upon evaluating the literature studies, it becomes evident that the subject in question is now a topic of controversy, and there is a growing body of research on it [8][9].

In order to enhance the mechanical and tribological characteristics of the composite while preserving its ductile nature, nano-sized ceramic particles are employed as a means of reinforcement [10].

Alumina (Al_2O_3) is a highly beneficial alternative for improving the properties of metal matrix composites. Both alumina and metal components are easily obtainable and affordable, making them economically competitive and suitable for potential industrial applications. Al_2O_3 offers several additional advantages, such as its remarkable hardness and high melting point, as well as its strong thermal stability and coefficient of thermal expansion. Additionally, it demonstrates exceptional chemical inertness and notable wear resistance, rendering it very compatible with metal matrices [11][12]. It is also a commonly employed ceramic reinforcement that remains unreactive with the matrix at elevated temperatures and does not produce unwanted phases.

In this study, hybrid powders produced using powder metallurgy production parameters are used to test samples by hot pressing and then prepared for testing using metallography. The microstructures of the samples were investigated using X-ray diffraction (XRD), Fourier transform infrared spectroscopy (FT-IR), scanning electron microscope (SEM), and energy dispersive X-ray spectroscopy (EDX). The mechanical and tribological parameters of the samples were evaluated by hardness and wear tests.

2. MATERIALS and METHOD

2.1. Preparation of Hybrid Composites

Table 1 shows the particle sizes, names, and contents of the powders used in the study, and the amount of samples used by weight. In order to obtain a homogeneous distribution, the particle size of the reinforcement elements was chosen to be smaller than the matrix material. The powders were mixed in a ball mixer at 350 rpm for 3 hours with the addition of ethyl alcohol and citric acid. The resulting solution was then dried in an oven at 80 °C in a controlled atmosphere for 18 hours. The dried mixture was lubricated with zinc stearate ($\text{Zn}(\text{C}_{18}\text{H}_{35}\text{O}_2)_2$) and placed in a graphite mold preloaded with 10 MPa in one direction using a hydraulic press. The samples were preloaded in a cold press before being pressed in a hot press at 700 °C in an argon (99.9% purity) environment for 90 minutes under a pressure of 350 MPa. Figure 1 shows the sample preparation scheme. After the hot pressing process in a fluid Argon atmosphere, the samples were allowed to cool in the oven. The samples were heat-pressed and cooled, then sintered, and then examined for microstructure, mechanical properties, and tribology. The Bakelite combination was made with

Fiber Polyester Resin and hardener and the samples were placed in molds. Then the combination was poured onto the prepared mixture and left to harden for 24 hours. Finally, sanding and polishing were done and then cleaned with alcohol.

Table 1. Particle sizes of powders and nomenclature of powders and amount of additives by wt. %

Sample Name	Cu	Al ₂ O ₃
Particle size	44μm	5μm
Nomenclature	Cu (%)	Al ₂ O ₃ (%)
Cu	100	-
Cu-1Al ₂ O ₃	99	1
Cu-5Al ₂ O ₃	95	5

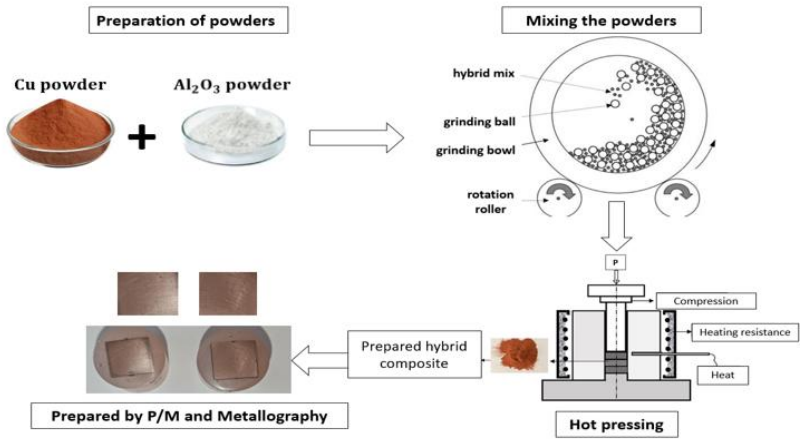


Figure 1. Sample preparation scheme

2.2. Characterization of Hybrid Composites

The hybrid composites were characterized using X-ray diffraction (XRD) on a Rigaku RINT-2000 X apparatus. The scan range was $2\theta = 20$ to 80° and the voltage was 40 kV/40 mA. The functional groups of pure and Al_2O_3 doped Copper samples generated via powder metallurgy were characterized using FT-IR measurements. The Thermo Scientific Nicolet IS5 FT-IR spectrometer with a scan range of $3000\text{--}500\text{ cm}^{-1}$ was utilized for the analysis. SEM and EDX analyses were done on the samples' structure using a Zeiss EVO MA10 SEM equipment in the Cu matrix structure, as well as to investigate the wear surfaces.

2.3. Hardness and Tribology

The hardness values were determined by averaging the values obtained from 3 various locations at HV_{30} for a duration of 15 seconds under a load of 100 grams. Upon examination of the literature studies, it was found that the crucial test criteria for wear tests conducted in dry conditions are the quantity of reinforcement, applied load, sliding speed, and sliding distance [13][14]. The abrasion tests conducted in this study utilized a pin-disc abrasion tester to examine the effects of dry abrasion. Steel wear pins were subjected to a load of 15 N, a sliding speed of 50 mm/sec, and a sliding distance of 1000 meters. The weight loss of the specimens was measured at intervals of 100 meters across a total sliding distance of 1000 meters. A weight laboratory instrument balance with a precision value of 10^{-4} was used to assess the weight loss. The observed values were recorded and weight loss graphs were created for each specimen based on the distance [15][16][17].

3. RESULTS and DISCUSSION

3.1. Characterization

3.3.1. XRD

XRD analysis spectra of the produced hybrid composites are shown in Figure 2. The hybrid composites' diffraction patterns show distinct peaks that are associated with the face-centered cubic phase of copper. Diffraction peaks at 43.2 , 50.3 , and 74.1° were observed, corresponding to the (111), (200), and (220) reflections of Cu, respectively. Following a duration of five hours of ball milling, the diffraction patterns revealed that the $\alpha\text{-Al}_2\text{O}_3$, $\beta\text{-Al}_2\text{O}_3$, and $\delta\text{-Al}_2\text{O}_3$ phases exhibited remarkable stability and did not undergo any phase transformation. The most stable phase of alumina is $\alpha\text{-Al}_2\text{O}_3$, and milled powders show an increase in lattice tension and a decrease in crystallite size through line broadening [18][19].

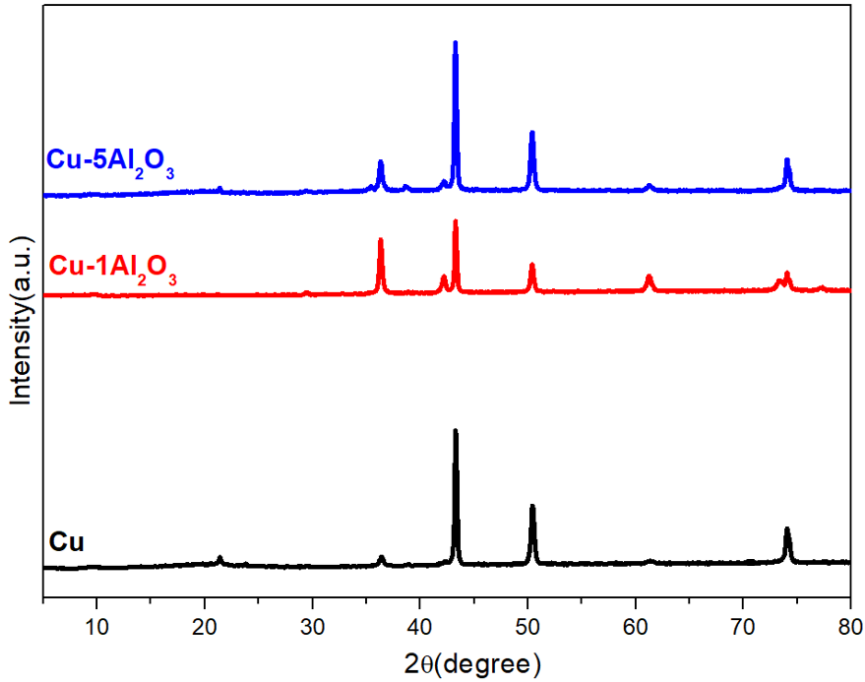
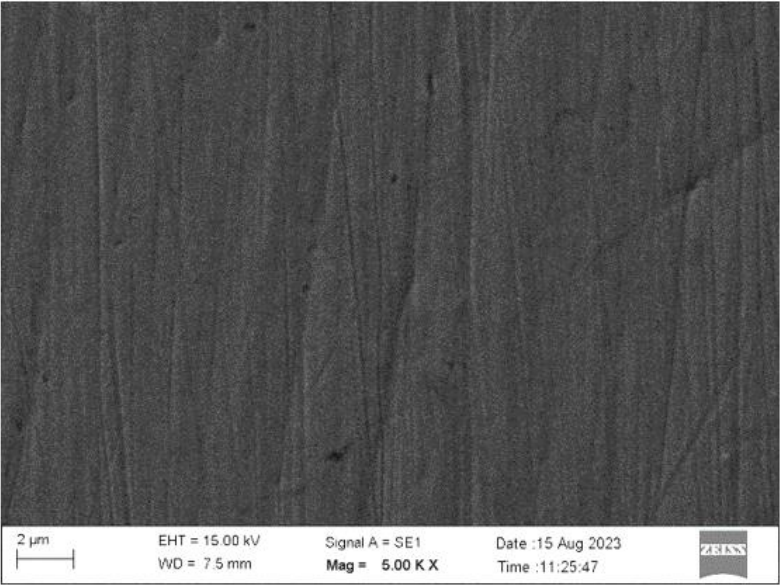


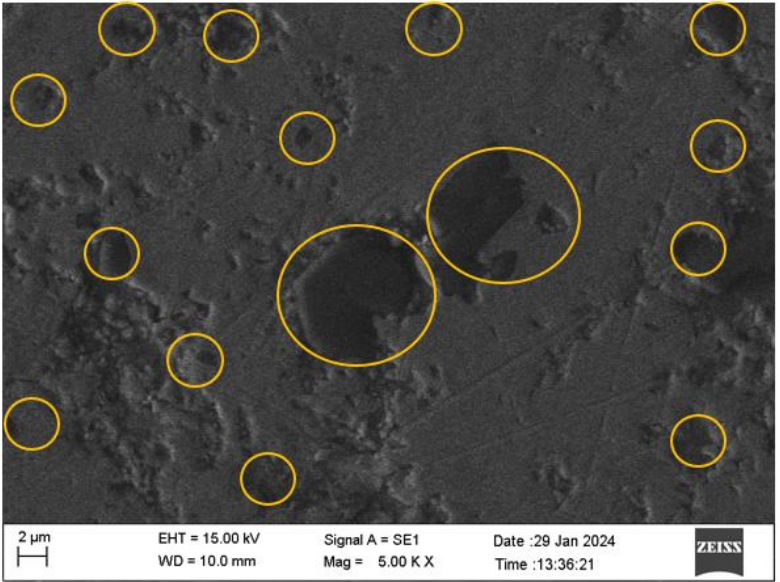
Figure 2. XRD diffraction patterns

3.3.3. SEM

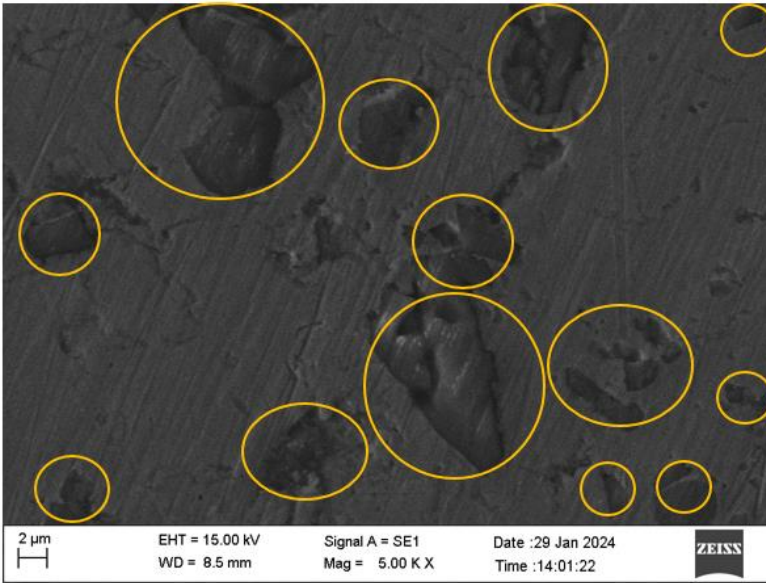
The qualitative information regarding the particle size distribution and morphology of the hybrid composite samples following ball milling and hot pressing processes was obtained using SEM analysis. SEM images and EDX analysis results of Cu/Al₂O₃ hybrid composite samples are shown in Figure 4 and Figure 5. By subjecting the material to a grinding process for 5 hours, the size of the particles is decreased, leading to a significantly more even dispersion of the strengthening elements and reducing the formation of clumps [20][21]. By introducing hard alumina particles, the weldability of the copper powder particles was reduced, resulting in the formation of small irregular particles instead of large flake-shaped particles [22][23]. Crushing and cold welding of the powder particles occurs as a result of contact between the grinding balls and the walls of the grinding flasks during the grinding operation [22][24]. The effect of the amount of alumina reinforcement on the microstructure is shown in Figure 4 b-c. The microstructure exhibited finer particles as the amount of reinforcement increased.



a)

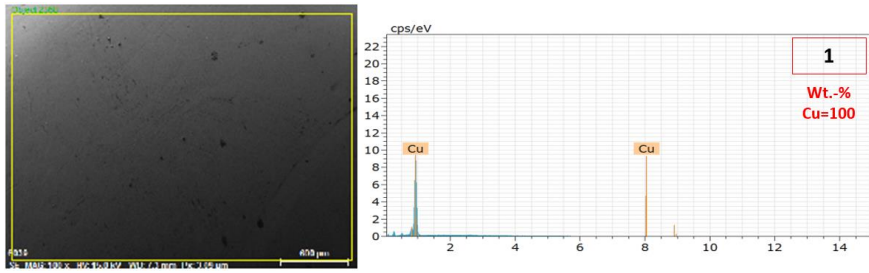


b)

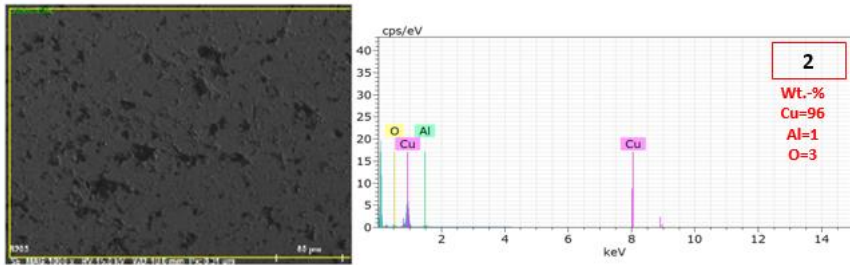


c)

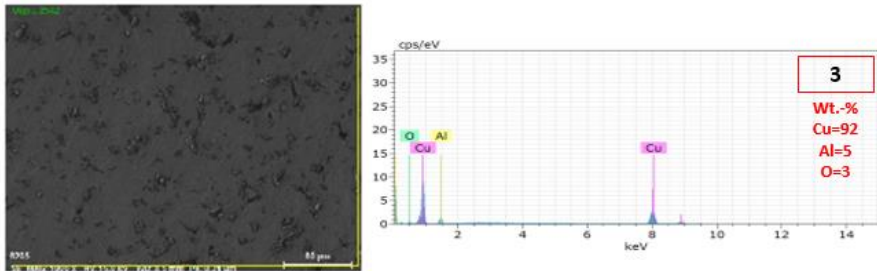
Figure 4. SEM images of the produced hybrid composite groups: a) Cu, b) Cu-
1Al₂O₃,
c) Cu-5Al₂O₃



a)



b)



c)

Figure 5. EDS analysis results of the produced hybrid composite groups: a) Cu, b) Cu-1Al₂O₃, c) Cu-5Al₂O₃

3.3. Hardness and Tribology

Figure 7 displays the mean hardness measurements acquired from 3 different regions on the specimens. Compared to the pure Cu sample, all reinforcements exhibited a significant enhancement in hardness values. The incorporation of high-strength into a copper matrix, together with the addition of hard ceramic Al₂O₃, significantly enhanced the hardness of the material. The hardness of the

Cu-5Al₂O₃ hybrid composite was measured to be 213 HV, which was the highest value observed. The maximum level of hardness emerged when these enhancements were evenly distributed within the Cu matrix, resulting in a homogeneous increase in hardness throughout the composite. Due to the relationship between finer grain structures and higher hardness values, both regular hard Al₂O₃ can prevent grain growth in the copper matrix by adhering to the grain boundaries. As a result, they contribute to the formation of a superior grain structure compared to pure copper [12]. The presence of Al₂O₃ particles in the matrix alloy acts as a shield for the softer Cu matrix, preventing deformation and providing protection against cutting and penetration of the slides on the surface of the composites.

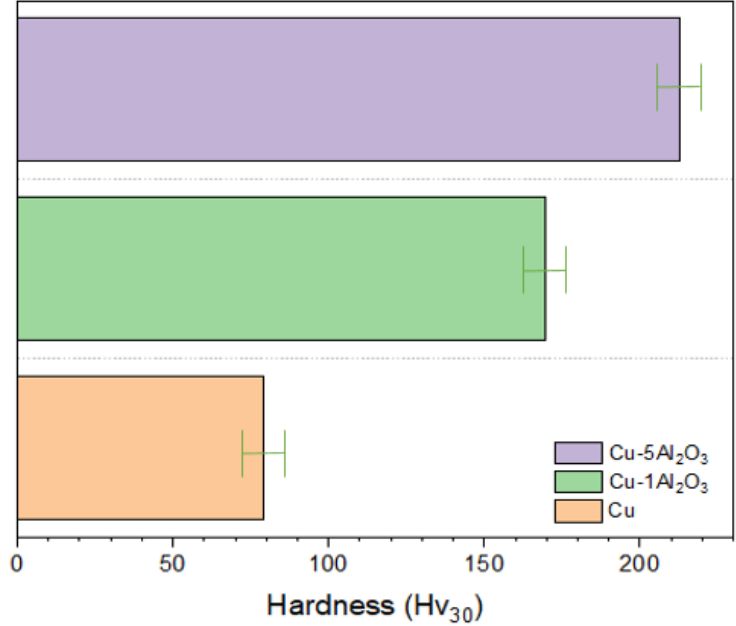
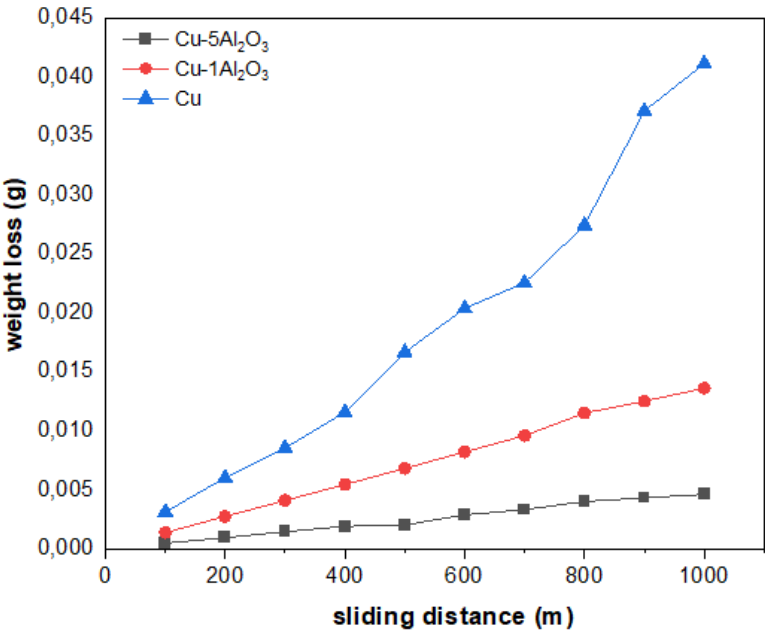


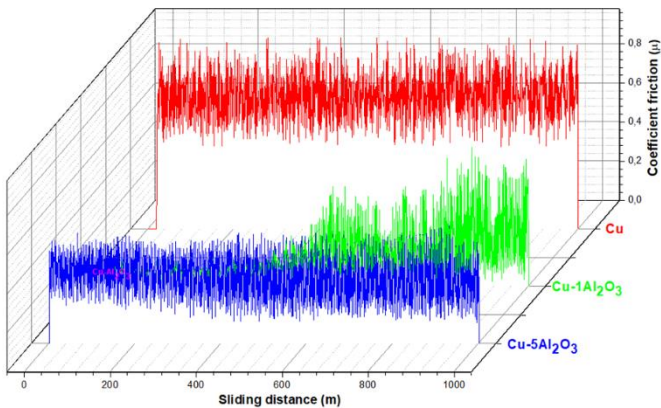
Figure 7. Variation in Hardness values of the produced composites

The wear weight loss graphs of Al₂O₃ reinforced composites under a single load are shown in Figure 8-a. The wear tests revealed that Al₂O₃ reinforcements reduced weight loss after wear. In comparison to the pure Cu sample, the Cu-5Al₂O₃ sample with the lowest weight loss was 9 times lower. The addition of reinforcement is thought of to improve composite strength by reducing agglomeration and filling pores and gaps in the matrix structure. This method creates a thin lubricating layer between the matte surfaces, significantly reducing

mass loss [25]. The use of Al_2O_3 as a reinforcing element in Cu matrix composites leads to a rise in hardness that can be attributed to the Orowan process [16].



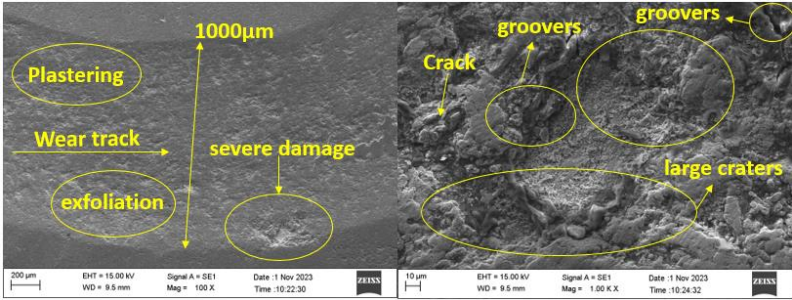
a)



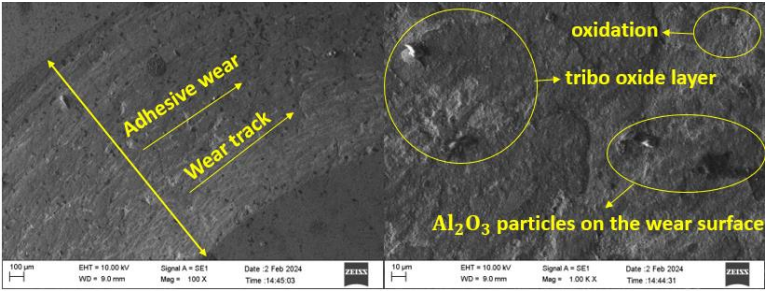
b)

Figure 8. a) Weight losses after wear tests and b) variation of Friction coefficients for the produced hybrid composites

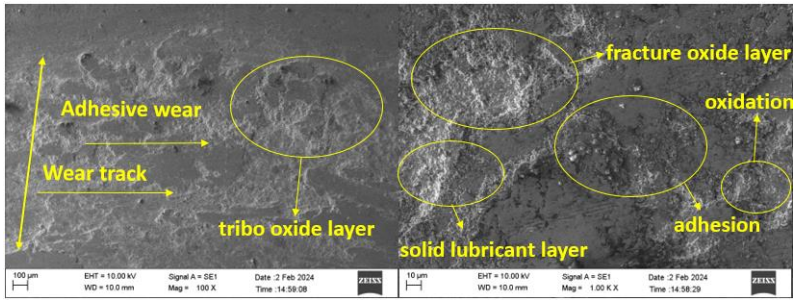
Figure 9-b depicts the decrease in the coefficient of friction in hybrid composites during 1000-meter sliding distance wear testing. Al_2O_3 -reinforced hybrid composites showed a considerable drop in coefficient of friction values. SEM images shown in Figure 9 confirm that the wear scar surfaces during the wear process depend on the material type, microstructure, hardness, and manufacturing parameters. The significant depression caused by the steel abrasive pin in the Cu sample without reinforcement is mostly attributed to the extensive plastic deformation caused by the comparatively lower hardness of copper. This resulted in more severe wear than the newly manufactured reinforced hybrid composites. In contrast, the greater hardness of the hybrid composites permitted only micro-inclusions and scratches to produce shallow grooves on the specimen surfaces, as shown in the images of the wear scars [26].



a)



b)



c)

Figure 9. SEM images after wear tests for different composite groups: a) Cu, b) Cu-1Al₂O₃, c) Cu-5Al₂O₃

Cracks were visible in pure Cu samples, but not on the wear surfaces of Al₂O₃ reinforced samples, which had less distortion and a lower wear depth. An increase in the weight % of Al₂O₃ results in a decrease in the rate at which wear occurs (an increase in wear resistance). This is due to the formation of bonds at the interfaces between the reinforcing particles and Cu particles, which in turn causes thermal stresses at these interfaces [27][28]. Reduced friction leads to the formation of parallel grooves and scratches in the direction of sliding, with a lower number of scratches on the composite surface. The oxide layer on the surface acts as a protective barrier for the composite and generates strong cohesion forces on the contact surfaces, resulting in adhesion wear when there are higher sliding speeds and shorter sliding distances. The presence of robust adhesive forces on the worn contact surfaces is the cause of the oxide layer that safeguards the composite material [26][29].

4. CONCLUSIONS

The matrix material Cu was combined with reinforcements of Al₂O₃. The powders, which were thoroughly mixed to achieve homogeneity, underwent a cold pressing process followed by a hot pressing process in an environment filled with argon gas. The following outcomes were acquired as a consequence of the experiments:

The scanning electron microscope (SEM) pictures and energy-dispersive X-ray (EDX) analysis revealed a uniform distribution of the reinforcing powders throughout the copper (Cu) matrix structure. XRD analysis results showed the formation of characteristic peaks of Al and C on the Cu matrix structure, albeit at low intensity.

- The density values of the hybrid composites decreased with Al_2O_3 reinforcement.
- The measured hardness values demonstrated that the incorporation of Al_2O_3 additions led to a significant enhancement in hardness. Moreover, the hardness values exhibited a direct correlation with the quantity of Al_2O_3 reinforcement. The hybrid composite comprising 5wt% Al_2O_3 yielded the highest hardness result.
- As a result of 1000 m sliding distance wear tests, a 295% lower coefficient of friction result was obtained for the hybrid composite with 5wt% Al_2O_3 doping compared to the pure Cu sample.
- The wear tests showed comparable findings, however the addition of Al_2O_3 reinforcements significantly improved the wear resistance of Cu matrix composites. The incorporation of Al_2O_3 reinforcement minimized the emergence of significant cracks and voids in the wear scars depicted in the post-wear (SEM) images.
- The findings of this study are expected to enable the use of more durable machine parts in high-wear areas, resulting in reduced maintenance costs in industries such as electronics, aerospace, and electric vehicles.

REFERENCES

- [1] G. Xie, M. Forslund, J. Pan, Direct electrochemical synthesis of reduced graphene oxide (rGO)/copper composite films and their electrical/electroactive properties, *ACS Appl. Mater. Interfaces*. 6 (2014) 7444–7455.
- [2] Z. Yang, D.J. Lichtenwalner, A.S. Morris, J. Krim, A.I. Kingon, Comparison of Au and Au–Ni alloys as contact materials for MEMS switches, *J. Microelectromechanical Syst.* 18 (2009) 287–295.
- [3] J. Wang, L. Guo, W. Lin, J. Chen, S. Zhang, T. Zhen, Y. Zhang, The effects of graphene content on the corrosion resistance, and electrical, thermal and mechanical properties of graphene/copper composites, *New Carbon Mater.* 34 (2019) 161–169.
- [4] P.B. Joshi, N.S.S. Murti, V.L. Gadgil, V.K. Kaushik, P. Ramakrishnan, Preparation and characterization of Ag–ZnO powders for applications in electrical contact materials, *J. Mater. Sci. Lett.* 14 (1995) 1099–1101.
- [5] X. Gao, H. Yue, E. Guo, S. Zhang, L. Yao, X. Lin, B. Wang, E. Guan, Tribological properties of copper matrix composites reinforced with homogeneously dispersed graphene nanosheets, *J. Mater. Sci. Technol.* 34 (2018) 1925–1931.
- [6] J. Li, L. Zhang, J. Xiao, K. Zhou, Sliding wear behavior of copper-based composites reinforced with graphene nanosheets and graphite, *Trans. Nonferrous Met. Soc. China*. 25 (2015) 3354–3362.
- [7] M. Rashad, F. Pan, H. Hu, M. Asif, S. Hussain, J. She, Enhanced tensile properties of magnesium composites reinforced with graphene nanoplatelets, *Mater. Sci. Eng. A*. 630 (2015) 36–44.
- [8] H. Liang, Y. Bu, J. Zhang, Z. Cao, A. Liang, Graphene oxide film as solid lubricant, *ACS Appl. Mater. Interfaces*. 5 (2013) 6369–6375.
- [9] L. Fathyunes, J. Khalil-Allafi, Characterization and corrosion behavior of graphene oxide-hydroxyapatite composite coating applied by ultrasound-assisted pulse electrodeposition, *Ceram. Int.* 43 (2017) 13885–13894.
- [10] M.S. Abd-Elwahed, A.F. Meselhy, Experimental investigation on the mechanical, structural and thermal properties of Cu–ZrO₂ nanocomposites hybridized by graphene nanoplatelets, *Ceram. Int.* 46 (2020) 9198–9206.
- [11] J. Leng, G. Wu, Q. Zhou, Z. Dou, X. Huang, Mechanical properties of SiC/Gr/Al composites fabricated by squeeze casting technology, *Scr. Mater.* 59 (2008) 619–622.
- [12] N. Kumar, A. Bharti, M. Dixit, A. Nigam, Effect of powder metallurgy process and its parameters on the mechanical and electrical properties of copper-based materials: Literature review, *Powder Metall. Met. Ceram.* 59 (2020) 401–410.

- [13] S. Pradeep Devaneyan, R. Ganesh, T. Senthilvelan, On the mechanical properties of hybrid aluminium 7075 matrix composite material reinforced with SiC and TiC produced by powder metallurgy method, *Indian J. Mater. Sci.* 2017 (2017) 3067257.
- [14] M.H. Rahman, H.M.M. Al Rashed, Characterization of silicon carbide reinforced aluminum matrix composites, *Procedia Eng.* 90 (2014) 103–109.
- [15] G. Abouelmagd, Hot deformation and wear resistance of P/M aluminium metal matrix composites, *J. Mater. Process. Technol.* 155 (2004) 1395–1401.
- [16] M. Rahimian, N. Parvin, N. Ehsani, Investigation of particle size and amount of alumina on microstructure and mechanical properties of Al matrix composite made by powder metallurgy, *Mater. Sci. Eng. A.* 527 (2010) 1031–1038.
- [17] F. Hasan, R. Jaiswal, A. Kumar, A. Yadav, Effect of TiC and graphite reinforcement on hardness and wear behaviour of copper alloy B-RG10 composites fabricated through powder metallurgy, *JMST Adv.* 4 (2022) 1–11.
- [18] G. Iacob, V.G. Ghica, M. Buzatu, T. Buzatu, M.I. Petrescu, Studies on wear rate and micro-hardness of the Al/Al₂O₃/Gr hybrid composites produced via powder metallurgy, *Compos. Part B Eng.* 69 (2015) 603–611.
- [19] S. Cava, S.M. Tebcherani, I.A. Souza, S.A. Pianaro, C.A. Paskocimas, E. Longo, J.A. Varela, Structural characterization of phase transition of Al₂O₃ nanopowders obtained by polymeric precursor method, *Mater. Chem. Phys.* 103 (2007) 394–399.
- [20] T. Varol, A. Canakci, Microstructure, electrical conductivity and hardness of multilayer graphene/copper nanocomposites synthesized by flake powder metallurgy, *Met. Mater. Int.* 21 (2015) 704–712.
- [21] Z. Zhang, X. Lu, J. Xu, H. Luo, Characterization and tribological properties of graphene/copper composites fabricated by electroless plating and powder metallurgy, *Acta Metall. Sin. (English Lett.)* 33 (2020) 903–912.
- [22] M.S. Belardja, H. Djelad, M. Lafjah, F. Chouli, A. Benyoucef, The influence of the addition of tungsten trioxide nanoparticle size on structure, thermal, and electroactivity properties of hybrid material–reinforced PANI, *Colloid Polym. Sci.* 298 (2020) 1455–1463.
- [23] M.C. Şenel, M. Gürbüz, E. Koç, Fabrication and characterization of aluminum hybrid composites reinforced with silicon nitride/graphene nanoplatelet binary particles, *J. Compos. Mater.* 53 (2019) 4043–4054.
- [24] H. Asgharzadeh, M. Sedigh, Synthesis and mechanical properties of Al matrix composites reinforced with few-layer graphene and graphene oxide, *J. Alloys Compd.* 728 (2017) 47–62.
- [25] Y. Şahin, Abrasive wear behaviour of SiC/2014 aluminium composite, *Tribol. Int.* 43 (2010) 939–943.

- [26] H. Saito, A. Iwabuchi, T. Shimizu, Effects of Co content and WC grain size on wear of WC cemented carbide, *Wear*. 261 (2006) 126–132.
- [27] F. Nouh, T. El-Bitar, H.M. Yehia, O. El-Kady, Preparation and Characterization of Al-Cu-Al₂O₃/Gr Nano Compound by Metallic Powder Method and Study of the Effect of the Rolling Process on Physical Properties as Suitable Materials for Heat Sink, (n.d.).
- [28] O. El-Kady, H.M. Yehia, F. Nouh, Preparation and characterization of Cu/(WC-TiC-Co)/graphene nano-composites as a suitable material for heat sink by powder metallurgy method, *Int. J. Refract. Met. Hard Mater.* 79 (2019) 108–114.
- [29] Z. Zhang, D.L. Chen, Consideration of Orowan strengthening effect in particulate-reinforced metal matrix nanocomposites: A model for predicting their yield strength, *Scr. Mater.* 54 (2006) 1321–1326.



CHAPTER 8

Long-Term Consistency Analysis of Global Precipitation Datasets: A Case Study in Konya

Omer Faruk Atiz¹ & Savas Durduran²

¹ Necmettin Erbakan University, ORCID:0000-0001-6180-7121

² Prof. Dr., Necmettin Erbakan University, ORCID: 0000-0003-0509-4037

1. Introduction

Precipitation data is essential to monitor climate change on both regional and global scales, as well as to manage water resources, and sustainable agricultural activities. The historic precipitation time series plays a critical role in trend analysis, climate modelling, crop yield estimation and hydrological modeling studies (Sarker et al., 2012; Ding et al., 2023). The accurate precipitation time series are essential in arid and semi-arid regions because high agricultural productivity depends on the limited surface water and groundwater (Kartal and Nones 2024). In the past years, several studies reported that meteorological droughts and extreme weather events occurred in Konya (Yilmaz 2017; Koycegiz and Buyukyildiz 2019; Saris and Gedik 2021). Therefore, accurate and consistent precipitation datasets are essential for sustainable water resource management and agricultural planning, especially considering climate variability.

In-situ precipitation measurements are conducted by various public agencies, such as Türkiye's General Directorate of Meteorology (MGM). However, in-situ measurements are often not cost-effective, especially across large provinces. In addition, it is difficult to conduct spatial analysis because the small number of meteorological stations does not extensively represent the study area. Even if the data interpolation methods can expand the spatial coverage in specific study areas, they cannot expand the temporal resolution. Advancements in remote sensing and computational capabilities have led to the development of several global meteorological datasets. Datasets such as CHIRPS (Climate Hazards Group InfraRed Precipitation with Station data), ERA5-Land (European Centre for Medium-Range Weather Forecasts), GPM (Global Precipitation Measurement mission), PERSIANN-CDR (Precipitation Estimation from Remotely Sensed Information using Artificial Neural Networks-Climate Data Record), and TerraClimate provide global precipitation data with varying spatial and temporal resolutions.

Despite the advantages of global open-access precipitation datasets, their consistency can vary worldwide because of differing data acquisition and computational methods (Wu et al., 2023). Several studies have been conducted on the analysis of global and regional consistencies of global datasets (Sun et al., 2018; Pradhan et al., 2022). However, they still need to be locally validated in climate analysis of smaller regions. Thus, the objective of this study is to assess the accuracy and consistency of global precipitation datasets in Konya Province, Türkiye. The flow of this chapter is as follows: First, the global datasets and study area are introduced, along with the statistical methods used for consistency

analysis. Next, the results are presented and discussed, and finally, conclusions are drawn.

2. Data and methods

Konya Province is a metropolitan region in Türkiye, with a population of over 2 million as of 2024. Known as Türkiye’s primary grain-producing area, Konya has extensive plains and a predominantly arid and continental climate. The average annual temperature is approximately 12 °C and average annual total precipitation is 325 mm. The meteorological station at Konya Public Airport was selected as the reference point for consistency analysis. The geographical location of Konya and the in-situ measurement test point are shown in Figure 1.

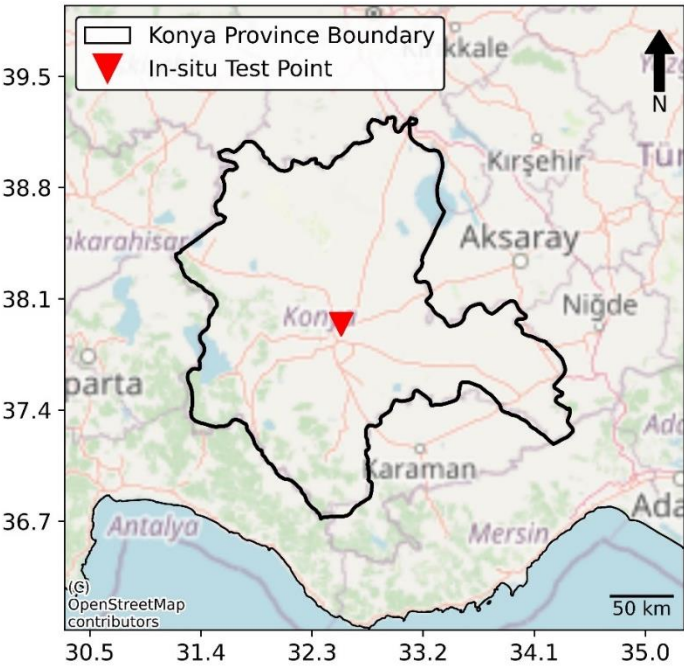


Figure 1. Konya province and test point

Global precipitation datasets are produced in several ways such as gauge-based, satellite-based or reanalysis of measurements based on precipitation process modelling (Sun et al. 2018). In this study, CHIRPS, ERA5-Land, GPM, and PERSIAN-CDR datasets were investigated. The details of the global and reference datasets are given in Table 1. The global precipitation data were retrieved from Climate Engine platform which is a cloud-based climate and remote sensing data processing platform (Huntington et. al., 2017).

First daily data were aggregated to monthly scale since the reference data was on monthly basis. After matching the data spans, temporal alignment was performed.

Table 1. Details of global and reference datasets

Dataset Name	Spatial Resolution	Temporal Resolution	Start time	Reference
CHIRPS	0.05°	Daily	1981	Funk et. al., 2014
ERA5-Land	0.125°	Daily	1950	Muñoz Sabater, 2019
GPM	0.1°	Daily	2000	Skofronick-Jackson et. al., 2018
PERSIAN-CDR	0.25°	Daily	1981	Ashouri et. al., 2015
TerraClimate	~0.04°	Monthly	1958	Abatzoglou et. al, 2018
MGM	N/A	Monthly	1926	General Directory of Meteorology, 2024

The Root Mean Square Error (RMSE), Mean Bias Error (MBE), Correlation Coefficient (CC), and Coefficient of Determination (R^2) metrics were selected to analyze long-term consistency and their effectiveness in comparison of precipitation datasets. The formulas of selected statistical metrics are given in Equations 1-4.

$$RMSE = \sqrt{\frac{1}{n} \sum_i^n (P_i^{global} - P_i^{reference})^2} \quad (1)$$

$$MBE = \frac{1}{n} \sum_i^n P_i^{global} - P_i^{reference} \quad (2)$$

$$CC = \frac{Cov(p^{global}, p^{reference})}{\sigma_{global} \times \sigma_{reference}} \quad (3)$$

$$R^2 = CC^2 \quad (4)$$

p^{global} and $p^{reference}$ indicate monthly aggregated precipitations, σ_{global} and $\sigma_{reference}$ show their variances, respectively. The overall and seasonal statistics were computed using the above metrics. While RMSE shows accuracy,

MBE shows the average bias or tendency. CC and R^2 metrics indicate how well global precipitation data agrees with reference.

3. Results

Annual total precipitations from different datasets are illustrated in Figure 2 to understand general variations.

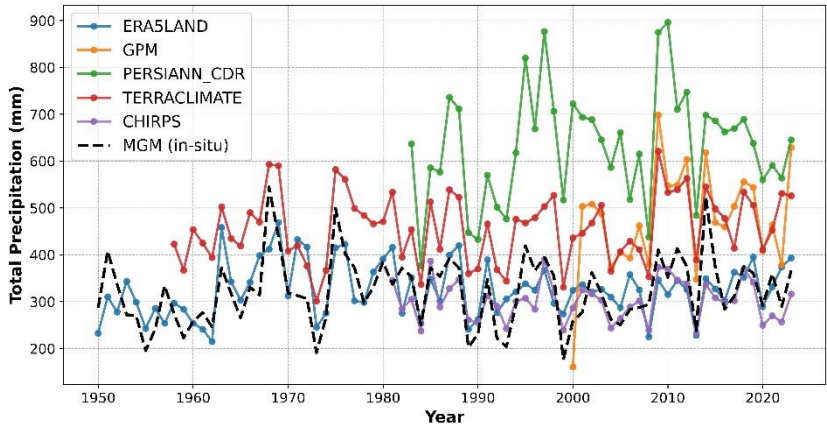


Figure 2. Annual total precipitations

As seen in Figure 2, ERA5-Land and CHIRPS datasets show a similar and more consistent variations compared to in-situ measurements. TerraClimate time series slightly overestimates the precipitation, but GPM and PERSIAN-CDR clearly not inline with reference. The summary of overall statistics using monthly aggregated precipitation measurements is shown in Table 2. According to Table 2, CHIRPS was found to be best in terms of accuracy with an RMSE of 13.4 mm, followed by ERA5-Land, TerraClimate and GPM. PERSIAN-CDR is found to be not adequate in representing actual measurements. In terms of consistency, CHIRPS has the highest correlation with 0.84, followed by GPM and TerraClimate. While this level of correlation can be accepted as very strong, other data sources can be classified as strong. From R^2 values, none of the global datasets has a strong linear fit to reference data, but moderate fit. To summarize, it can be said that CHIRPS is the most accurate dataset overall, while PERSIANN-CDR has the least reliability. ERA5-Land performs moderately well with minimal bias. GPM and TerraClimate show good correlation but notable overestimation.

Table 2. Summary of overall statistics

Dataset	RMSE (mm)	MBE (mm)	CC	R²
CHIRPS	13.4	-1.8	0.84	0.70
ERA5-Land	15.4	0.4	0.77	0.60
GPM	23.8	13.0	0.83	0.69
PERSIAN-CDR	39.4	25.9	0.71	0.51
TerraClimate	20.4	11.1	0.83	0.68

The overall statistics do not consider seasonal variabilities. Table 3 provides insight into seasonal variations, capturing how each dataset performs across winter, spring, summer, and fall. Seasonal performance reveals that datasets often vary significantly in their accuracy and biases depending on the time of year. CHIRPS performs consistently well across all seasons, with minimal bias and strong correlation, making it the most reliable dataset overall. TerraClimate shows good performance in summer and fall, with low errors and minimal biases, though it tends to overestimate in winter. ERA5-Land also performs well in summer and fall but has moderate biases in other seasons. GPM shows acceptable accuracy in summer but has high RMSE and overestimation in winter, making it less reliable in the colder months. PERSIANN-CDR consistently shows high RMSE and strong overestimation across all seasons, making it the least reliable dataset for capturing precipitation patterns in Konya Province.

Table 3. Summary of seasonal statistics

Season	Dataset	RMSE (mm)	MBE (mm)	CC	R ²
Winter	CHIRPS	15.4	-3.7	0.85	0.73
	ERA5-Land	16.5	3.1	0.75	0.56
	GPM	32.2	23.2	0.85	0.72
	PERSIAN-CDR	63.5	51.7	0.64	0.41
	TerraClimate	30.9	26.7	0.88	0.77
Spring	CHIRPS	13.3	-1.4	0.76	0.57
	ERA5-Land	16.9	5.7	0.69	0.47
	GPM	25.8	11.4	0.67	0.45
	PERSIAN-CDR	31.2	23.8	0.64	0.41
	TerraClimate	21.0	14.4	0.75	0.56
Summer	CHIRPS	9.6	-1.8	0.86	0.75
	ERA5-Land	11.0	-2.3	0.79	0.62
	GPM	12.7	5.0	0.86	0.74
	PERSIAN-CDR	20.3	9.8	0.70	0.49
	TerraClimate	9.4	-1.3	0.84	0.71
Fall	CHIRPS	14.8	-0.4	0.81	0.65
	ERA5-Land	16.3	-5.0	0.75	0.56
	GPM	20.4	12.6	0.83	0.69
	PERSIAN-CDR	28.2	18.1	0.81	0.66
	TerraClimate	13.6	4.5	0.85	0.72

In addition to seasonal statistics, annual change of RMSE is illustrated in Figure 3. As seen in Figure 3, CHIRPS is the most accurate and stable dataset, with low RMSE values, suggesting it is well-suited for long-term precipitation analysis in this region. ERA5-Land and TerraClimate show moderate accuracy with occasional fluctuations, making them reasonable alternatives. GPM has higher variability, indicating potential reliability issues in certain years while PERSIAN-CDR is less reliable.

The accuracy and consistency of various precipitation datasets can vary at different time periods. Above analysis were conducted between all available precipitation products and in-situ measurements.

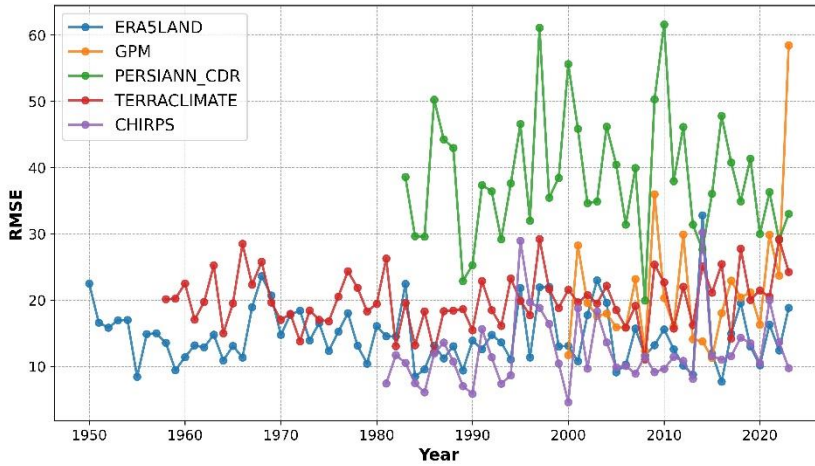


Figure 3. Annual variation of RMSE

Therefore, the data spans were aligned to between 2001-2023. The overall statistics considering only data between 2001-2023 is presented in Table 4.

Table 4. Summary of overall statistics between 2001-2023

Dataset	RMSE (mm)	MBE (mm)	CC	R ²
CHIRPS	13.7	-2.4	0.84	0.71
ERA5-Land	15.6	-0.5	0.78	0.61
GPM	24.0	13.1	0.83	0.69
PERSIAN-CDR	39.1	26.5	0.74	0.55
TerraClimate	21.2	11.8	0.83	0.69

Table 4 suggests that CHIRPS is still the most accurate and consistent. The statistics for all global datasets did not significantly change.

Figure 4 shows scatter plots comparing precipitation values from global datasets with in-situ data (MGM). Each plot includes a regression line with the regression equation and a 1:1 line, which represents perfect agreement between dataset and in-situ values. TerraClimate has a slope closest to 1, suggesting that it aligns reasonably well with in-situ data, although it still shows slight overestimation. GPM and PERSIANN-CDR have slopes greater than 1, indicating that they tend to overestimate precipitation, especially at higher values. CHIRPS and ERA5-Land have slopes less than 1, with CHIRPS showing the most significant underestimation.

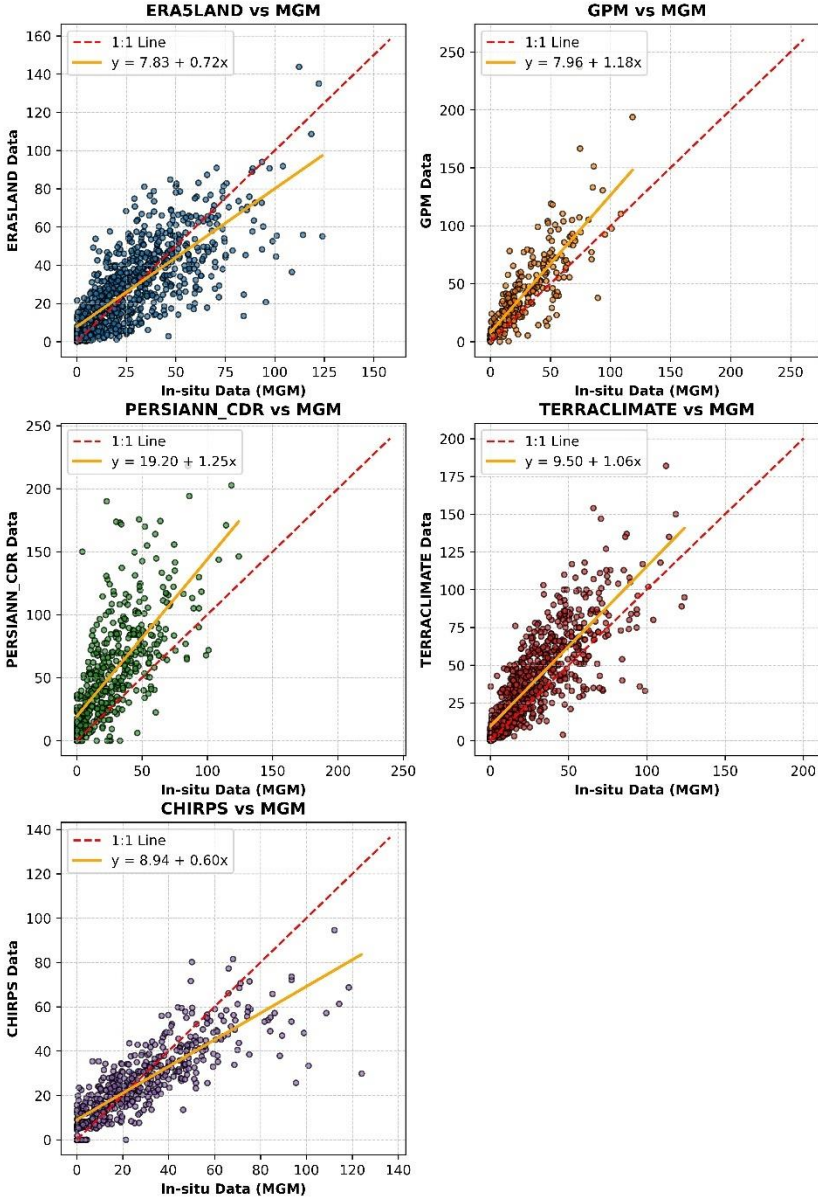


Figure 4. Scatter plots and regression lines

4. Conclusion

This study assessed the long-term consistency and reliability of five open-access precipitation datasets (CHIRPS, ERA5-Land, GPM, PERSIANN-CDR, and TerraClimate) in representing precipitation patterns in Konya Province, Turkey. By comparing each dataset against in-situ measurements from the Turkish General Directorate of Meteorology, we evaluated accuracy, systematic

bias, and seasonal variability using key statistical metrics: RMSE, MBE, CC, and R^2 .

In conclusion, CHIRPS emerged as the preferred dataset for accurate precipitation analysis in Konya Province, followed by ERA5-Land for its stable long-term performance. GPM, PERSIANN-CDR, and TerraClimate may be useful for broader trend analysis but require caution due to their tendency to overestimate precipitation. Seasonal analysis revealed that each dataset's performance varies by season, TerraClimate generally performing well in summer, showed greater variability in other seasons. This study underscores the importance of ongoing evaluation of open-access precipitation datasets to ensure data quality and reliability, especially in regions with variable climates.

Future research should investigate the impact of these datasets on hydrological and agricultural models specific to Konya, to develop sustainable policies that enhance climate resilience and support water resource management in the region.

Acknowledgements

The authors are grateful to the Turkish General Directorate of Meteorology (MGM) and Climate Engine platform for providing data used in this study.

References

- Abatzoglou, J. T., Dobrowski, S. Z., Parks, S. A., & Hegewisch, K. C. (2018). TerraClimate, a high-resolution global dataset of monthly climate and climatic water balance from 1958–2015. *Scientific Data*, 5, 170191.
- Ashouri, H., Hsu, K., Sorooshian, S., Braithwaite, D. K., Knapp, K. R., Cecil, L. D., ... & Prat, O. P. (2015). PERSIANN-CDR: Daily precipitation climate data record from multi-satellite observations for hydrological and climate studies. *Bulletin of the American Meteorological Society*, 96, 69–83.
- Ding, Y., Jiang, C., Zhou, Z., Gao, T., Wang, S., Zhang, X., ... & Shi, H. (2023). Evaluation of precipitation and its time series components in CMIP6 over the Yellow River Basin. *Climate Dynamics*, 60(3), 1203–1223.
- Funk, C. C., Peterson, P. J., Landsfeld, M. F., Pedreros, D. H., Verdin, J. P., Rowland, J. D., ... & Verdin, A. P. (2014). A quasi-global precipitation time series for drought monitoring (Data Series 832, 4 p.). U.S. Geological Survey.
- General Directory of Meteorology. (2024). Precipitation data. Retrieved from <https://www.mgm.gov.tr/>
- Huntington, J., Hegewisch, K., Daudert, B., Morton, C., Abatzoglou, J., McEvoy, D., & Erickson, T. (2017). Climate Engine: Cloud computing of climate and remote sensing data for advanced natural resource monitoring and process understanding. *Bulletin of the American Meteorological Society*, 98, 2397–2410.
- Kartal, V., & Nones, M. (2024). Assessment of meteorological, hydrological and groundwater drought in the Konya closed basin, Türkiye. *Environmental Earth Sciences*, 83(9), 1–27.
- Koycegiz, C., & Buyukyildiz, M. (2019). Temporal trend analysis of extreme precipitation: A case study of Konya Closed Basin [In Turkish]. *Pamukkale University Journal of Engineering Sciences*, 25(8), 956–961
- Muñoz Sabater, J. (2019). ERA5-Land monthly averaged data from 1950 to present. Copernicus Climate Change Service (C3S) Climate Data Store (CDS). <https://doi.org/10.24381/cds.68d2bb30>
- Pradhan, R. K., Markonis, Y., Godoy, M. R. V., Villalba-Pradas, A., Andreadis, K. M., Nikolopoulos, E. I., ... & Hanel, M. (2022). Review of GPM IMERG performance: A global perspective. *Remote Sensing of Environment*, 268, 112754.
- Saris, F., & Gedik, F. (2021). Meteorological drought analysis in Konya Closed Basin [In Turkish]. *Journal of Geography*, (42), 295–308.
- Sarker, M. A. R., Alam, K., & Gow, J. (2012). Exploring the relationship between climate change and rice yield in Bangladesh: An analysis of time series data. *Agricultural Systems*, 112, 11–16.
- Skofronick-Jackson, G., Huffman, G. J., Petersen, W. A., & Bolvin, D. T. (2018). Global Precipitation Measurement (GPM): Unified precipitation estimation from

space. In C. Andronache (Ed.), *Remote Sensing of Clouds and Precipitation* (pp. 131-152). Springer.

Sun, Q., Miao, C., Duan, Q., Ashouri, H., Sorooshian, S., & Hsu, K. L. (2018). A review of global precipitation data sets: Data sources, estimation, and intercomparisons. *Reviews of Geophysics*, 56(1), 79-107.

Wu, X., Feng, X., Wang, Z., Chen, Y., & Deng, Z. (2023). Multi-source precipitation products assessment on drought monitoring across global major river basins. *Atmospheric Research*, 295, 106982.

Yilmaz, M. (2017). Drought analysis of Konya Closed Basin with the use of TMPA satellite-based precipitation data [In Turkish]. *Journal of the Faculty of Engineering and Architecture of Gazi University*, 32(2), 541-549.



CHAPTER 9

Exploring the Influence of Pb Doping on CdPbS Thin Films: From Grain Size to Photocatalytic Performance

Sabit Horoz^{1,2}

¹ Sivas University of Science and Technology, Department of Fundamental Engineering Sciences, ORCID: 0000-0002-3238-8789

² Nanophotonics Research and Application Center, Sivas Cumhuriyet University, 58140 Sivas, Turkey

1. Introduction

Semiconductor thin films have become central to advancements in a wide range of technological fields, including photovoltaics, optoelectronics, and environmental remediation. Their unique properties, such as tunable energy band gaps, high surface area-to-volume ratios, and efficient charge transport, make them ideal for these applications. Among semiconductor materials, cadmium sulfide (CdS) thin films have garnered significant interest due to their favorable optical and electronic characteristics, including a direct band gap (~ 2.42 eV) that facilitates visible light absorption [1, 2].

However, pure CdS thin films are often limited in performance for applications requiring higher photocatalytic efficiency or specific electronic properties. To overcome these limitations, doping CdS with various elements has been widely studied as a strategy to tune the material's physical properties. Among the possible dopants, lead (Pb) has shown potential to significantly enhance the structural and functional performance of CdS, resulting in the formation of CdPbS thin films with modified grain size, band gap, and photocatalytic activity [3, 4]. Pb doping introduces additional energy levels within the band structure, which can reduce the energy band gap and improve the material's ability to absorb a broader spectrum of light, making it more suitable for applications like photocatalysis and solar cells [5].

The chemical bath deposition (CBD) technique has been a favored method for growing CdPbS thin films due to its simplicity, cost-effectiveness, and ability to produce uniform and adherent films at relatively low temperatures. CBD allows for fine control over film thickness and composition, making it ideal for the deposition of doped thin films where precise control over doping concentration is critical [6, 7]. Previous studies have demonstrated that increasing Pb concentration in CdPbS thin films can result in enhanced photocatalytic efficiency by promoting electron-hole separation and improving light absorption [8]. However, beyond a certain concentration, Pb doping can negatively affect the crystal structure, leading to defects that reduce material performance [9].

In this context, the present study focuses on investigating the effects of varying Pb concentrations (%0, %5, %10, %15, and %20) on the structural, optical, and photocatalytic properties of CdPbS thin films synthesized via CBD. The grain size, which plays a crucial role in the surface area and defect density of thin films, is expected to increase with moderate Pb doping, leading to improved charge transport properties. Simultaneously, we hypothesize that Pb

doping will reduce the energy band gap, allowing for more efficient utilization of visible light in photocatalytic reactions.

The photocatalytic activity of semiconductors is closely linked to their ability to generate and sustain electron-hole pairs under light irradiation. Pb doping in CdS has been shown to facilitate this process by lowering the recombination rate of electron-hole pairs, thus enhancing photocatalytic efficiency. By systematically varying the Pb concentration in this study, we aim to identify the optimal doping level that maximizes photocatalytic performance while maintaining desirable structural and optical properties. The broader goal of this research is to contribute to the development of advanced semiconductor materials for environmental applications, such as wastewater treatment and air purification, where efficient photocatalysis is essential.

This work seeks to establish the relationship between Pb doping concentration and the key material properties of CdPbS thin films, including grain size, energy band gap, and photocatalytic efficiency. The insights gained from this study are expected to provide a pathway for the development of more efficient and cost-effective photocatalysts, with potential applications extending to clean energy production and environmental remediation technologies.

2. Experimental Part

In this study, CdPbS thin films with varying Pb concentrations (%0, %5, %10, %15, and %20) were synthesized using the chemical bath deposition (CBD) technique. This method was chosen due to its simplicity, cost-effectiveness, and ability to produce high-quality thin films with controlled thickness and composition.

2.1. Materials and Reagents

The precursor solutions for the CBD process were prepared using cadmium acetate dihydrate ($\text{Cd}(\text{CH}_3\text{CO}_2)_2 \cdot 2\text{H}_2\text{O}$), lead acetate trihydrate ($\text{Pb}(\text{CH}_3\text{CO}_2)_2 \cdot 3\text{H}_2\text{O}$), and thiourea ($\text{CH}_4\text{N}_2\text{S}$) as the sulfur source. Ammonium hydroxide (NH_4OH) was used to adjust the pH of the solution to a desired level for optimal film growth. Deionized water was used as the solvent. Glass substrates were cleaned ultrasonically in acetone, ethanol, and deionized water for 15 minutes each, followed by drying in a nitrogen stream before deposition.

2.2. Chemical Bath Deposition (CBD) Process

The CBD process was carried out in a thermostated water bath maintained at 80°C. The cleaned glass substrates were vertically immersed in the precursor solution containing cadmium acetate (0.1 M), thiourea (0.1 M), and varying concentrations of lead acetate (0 M, 0.05 M, 0.1 M, 0.15 M, and 0.2 M to achieve Pb concentrations of %0, %5, %10, %15, and %20, respectively). The pH of the solution was adjusted to 10 using ammonium hydroxide to ensure the formation of a stable CdPbS film. The deposition process was carried out for 60 minutes to allow for the uniform growth of the thin films.

After deposition, the films were removed from the solution, thoroughly rinsed with deionized water, and dried in air at room temperature. The as-deposited films were further annealed at 200°C for 1 hour in a vacuum furnace to improve crystallinity and ensure homogeneity of Pb distribution.

3. Results and Discussion

In this section, the effects of varying Pb concentrations (%0, %5, %10, %15, and %20) on the structural, optical, and photocatalytic properties of CdPbS thin films are discussed. The films were characterized using XRD, UV-Vis spectroscopy, and photocatalytic degradation tests. The results obtained from these techniques provide insights into how Pb doping influences the behavior of CdPbS films.

3.1. Structural Analysis: Grain Size

X-ray diffraction (XRD) patterns revealed that all synthesized CdPbS thin films exhibited a polycrystalline nature with a cubic crystal structure. The grain size was calculated using the Scherrer equation from the broadening of the XRD peaks. As shown in Figure 1, the grain size increased with increasing Pb concentration, reaching a maximum of approximately 50 nm at %15 Pb. This increase in grain size can be scientifically explained by the substitution of Pb^{2+} ions for Cd^{2+} ions in the CdS lattice. Pb^{2+} has a larger ionic radius (1.19 Å) compared to Cd^{2+} (0.97 Å), and its incorporation into the CdS structure leads to lattice expansion. The larger ions reduce the lattice strain by occupying substitutional sites, which decreases the overall defect density and allows grains to grow more freely without significant internal stress.

Furthermore, Pb doping introduces additional energy levels in the material's electronic structure, which can facilitate the migration of grain boundaries. This,

in turn, promotes coalescence of smaller grains into larger grains. As the grains grow, the film achieves a more energetically favorable state with fewer grain boundaries, leading to enhanced crystallinity and a reduction in boundary-related scattering. Additionally, Pb doping is known to act as a catalyst for grain growth by reducing activation energy barriers for atom migration during the film deposition process, which further explains the observed increase in grain size with moderate Pb concentrations.

However, beyond %15 Pb, the grain size decreased slightly, dropping to around 45 nm at %20 Pb. This reduction can be attributed to excessive Pb doping, which introduces lattice distortions and defects due to the oversaturation of Pb atoms in the crystal structure. When the dopant concentration exceeds the solubility limit in the CdS lattice, Pb atoms no longer substitute for Cd but instead occupy interstitial sites or form secondary phases (such as PbS) that are not well integrated into the host lattice. These secondary phases can act as scattering centers and impede the growth of well-ordered grains.

The introduction of such defects causes local strain in the crystal lattice, which can disrupt the movement of grain boundaries, leading to grain size reduction. Moreover, excessive doping tends to increase the formation of dislocations and other crystallographic defects that prevent atoms from migrating across grain boundaries efficiently, thus inhibiting further grain growth. These defects can also limit the mobility of adatoms during the thin film deposition process, further restricting the coalescence of grains. The presence of amorphous regions or secondary phases at higher doping concentrations can also act as barriers to grain boundary movement, thereby resulting in smaller grains.

While moderate Pb doping facilitates grain growth by reducing lattice strain and promoting crystal cohesion, excessive Pb incorporation leads to lattice distortions and defect formation that hinder further growth, thus causing a decrease in grain size. The optimal Pb concentration for maximizing grain size without inducing detrimental structural effects is %15.

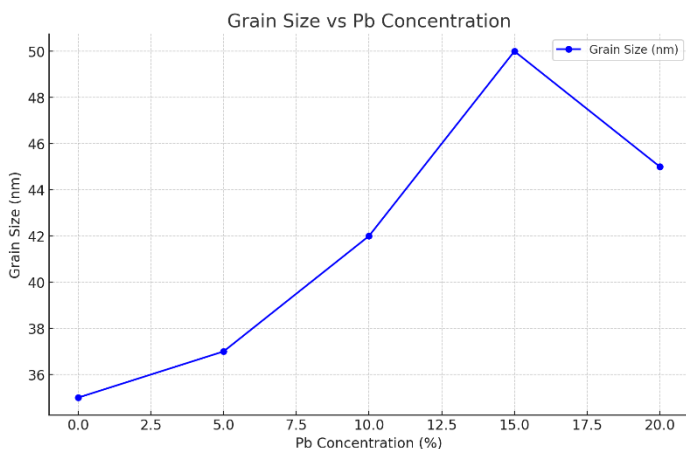


Figure 1. The grain sizes for CdPbS thin films.

3.2. Optical Properties: Energy Band Gap

The optical absorption spectra of the CdPbS thin films were measured using UV-Vis spectroscopy, and the energy band gaps were calculated from Tauc plots. As illustrated in Figure 2, the band gap decreased consistently with increasing Pb concentration up to %15, where the minimum band gap value of 2.00 eV was recorded. This reduction in band gap is primarily due to the introduction of additional electronic states within the band structure, a phenomenon commonly observed in heavily doped semiconductors. When Pb^{2+} ions substitute for Cd^{2+} ions in the CdS lattice, they introduce impurity levels within the forbidden energy gap, effectively narrowing the band gap by enabling electronic transitions at lower energy levels.

This band gap narrowing can be attributed to two main factors: first, the perturbation of the crystal potential due to the presence of larger Pb^{2+} ions alters the electronic band structure, reducing the energy required for valence band electrons to transition to the conduction band. Second, the doped Pb atoms introduce localized states near the conduction and valence band edges, which act as intermediate energy levels. These localized states facilitate sub-band gap absorption processes, where lower energy photons can excite electrons into the conduction band through these intermediate states, effectively reducing the optical band gap.

At Pb concentrations beyond %15, the band gap increased slightly, reaching approximately 2.10 eV at %20 Pb. This reversal in the band gap trend suggests

that excessive Pb doping introduces defects or impurity states that not only disrupt the crystal structure but also counteract the beneficial effects of moderate doping. When the concentration of Pb exceeds the solubility limit in the CdS lattice, it can lead to the formation of secondary phases, such as PbS or amorphous regions, which do not contribute to band gap narrowing but instead introduce additional scattering centers and defects.

These defect states, often located near grain boundaries or within disordered regions, can trap charge carriers and act as recombination centers, reducing the effective number of free carriers available for photocatalytic processes. Moreover, these defects increase the potential for non-radiative recombination, where electron-hole pairs are annihilated before contributing to photocatalytic activity or light absorption, leading to a reduction in the material's overall efficiency. This increased recombination rate at high doping levels effectively reduces the optical absorption efficiency and results in an observed increase in the band gap.

Furthermore, it is possible that excessive Pb doping induces a Burstein-Moss shift, where the Fermi level moves into the conduction band due to an increase in carrier concentration. As the conduction band becomes populated with free carriers, the energy required to excite additional electrons from the valence band increases, causing an apparent widening of the band gap. This mechanism is commonly observed in degenerate semiconductors with high carrier concentrations and can explain the slight increase in the band gap observed at %20 Pb doping.

In conclusion, while moderate Pb doping introduces beneficial electronic states that reduce the band gap and enhance optical absorption, excessive doping introduces structural defects and impurity states that disrupt the crystal lattice and increase recombination rates, resulting in a slight widening of the band gap. Optimizing the Pb concentration is thus critical for maximizing the optical performance of CdPbS thin films.

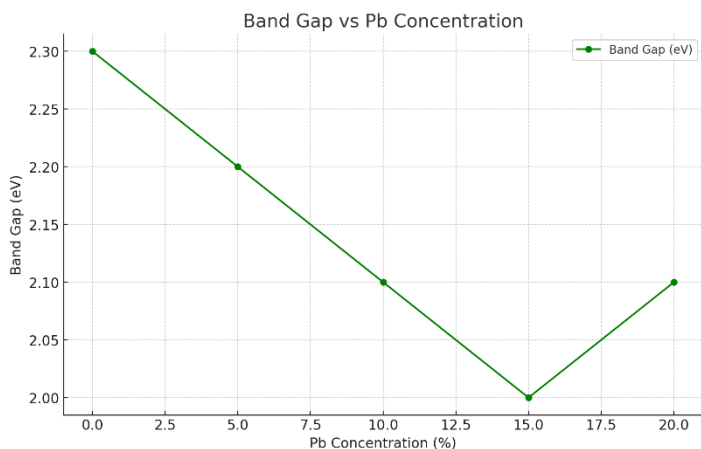


Figure 2. The energy band gaps for CdPbS thin films.

3.3. Photocatalytic Activity

The photocatalytic activity of the CdPbS thin films was evaluated by monitoring the degradation of methylene blue under visible light irradiation, a well-established method for assessing the performance of semiconductor photocatalysts. As depicted in Figure 3, the photocatalytic efficiency increased with Pb concentration, reaching a maximum degradation efficiency of 85% at %15 Pb. This enhancement in photocatalytic performance can be explained by the synergistic effects of both structural and optical improvements in the material as a result of Pb doping.

One of the key contributors to this enhanced performance is the increase in grain size observed with moderate Pb doping. Larger grains typically present fewer grain boundaries, which are known to act as recombination sites for photogenerated electron-hole pairs. By reducing the density of grain boundaries, the probability of non-radiative recombination decreases, allowing for a longer lifetime of charge carriers and thereby improving the overall photocatalytic efficiency. Larger grains also provide a more favorable surface for catalytic reactions, as they tend to reduce surface defects that might otherwise trap charge carriers.

Additionally, the reduction in the energy band gap with increasing Pb concentration up to %15 further enhances photocatalytic activity. A narrower band gap allows the material to absorb a broader spectrum of visible light, increasing the number of photons that can generate electron-hole pairs under

illumination. This increased light absorption improves the overall photocatalytic performance by ensuring more efficient utilization of the available light energy for initiating photocatalytic reactions. Furthermore, a reduced band gap facilitates charge carrier excitation at lower energy levels, which is crucial for generating the reactive species (such as hydroxyl radicals) responsible for the degradation of methylene blue.

However, similar to the trends observed in grain size and band gap, the photocatalytic activity decreased slightly at %20 Pb, with efficiency dropping to 80%. This decrease is primarily attributed to the higher defect density introduced by excessive Pb doping. When the Pb concentration exceeds the solubility limit within the CdS lattice, the formation of defects such as vacancies, dislocations, and interstitials becomes more pronounced. These defects act as recombination centers for the photogenerated electron-hole pairs, thereby reducing their lifetime. As a result, fewer charge carriers remain available for participation in the photocatalytic reaction, leading to a decrease in degradation efficiency.

Moreover, the excessive Pb doping at %20 may also lead to the formation of secondary phases, such as PbS, or the introduction of amorphous regions, both of which can interfere with the crystalline structure of the CdPbS thin films. These secondary phases are often less active or completely inactive in photocatalytic processes, and their presence reduces the effective surface area available for catalytic reactions. This reduction in active surface area limits the number of adsorption sites for methylene blue molecules and impedes the reaction kinetics, further contributing to the observed decrease in photocatalytic efficiency.

In addition, at higher doping levels, the excessive Pb content can lead to increased carrier recombination rates due to enhanced scattering effects caused by structural imperfections. These imperfections act as traps for charge carriers, which reduces the probability of their participation in redox reactions at the surface of the material. Consequently, while moderate Pb doping enhances photocatalytic efficiency by optimizing charge carrier generation and migration, excessive doping introduces detrimental effects that reduce the overall effectiveness of the material.

While moderate Pb doping (up to %15) significantly improves the photocatalytic activity of CdPbS thin films by increasing grain size, reducing the band gap, and enhancing light absorption, excessive Pb doping results in defect formation and surface area reduction, which negatively affect the photocatalytic performance. These findings underscore the importance of optimizing dopant

concentrations to maximize the efficiency of semiconductor photocatalysts for practical applications in environmental remediation and energy conversion.

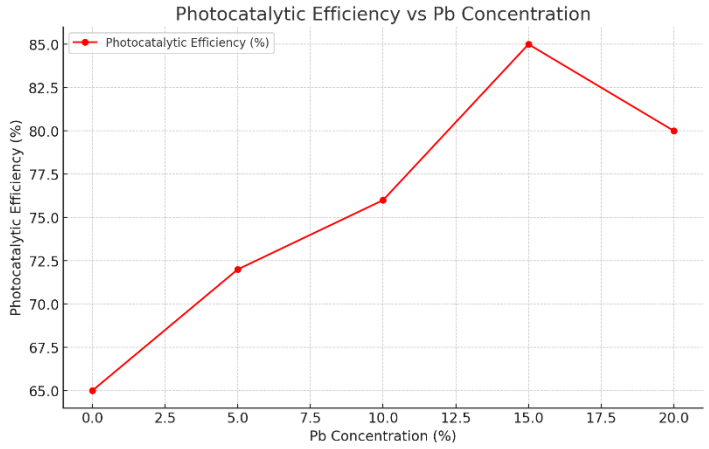


Figure 3. The photocatalytic activity of CdPbS thin films.

3.4. Discussion and Mechanism

The observed trends in structural, optical, and photocatalytic properties indicate that Pb doping plays a critical role in determining the performance of CdPbS thin films. At lower doping levels, Pb^{2+} ions effectively substitute Cd^{2+} in the CdS lattice, enhancing grain growth and reducing the band gap, which in turn leads to improved photocatalytic activity. This enhancement can be attributed to the increased generation of electron-hole pairs, as well as the lower energy required to initiate photocatalytic reactions.

However, beyond a critical Pb concentration (% 15), the benefits of Pb doping are outweighed by the negative effects of excessive doping, such as defect formation and grain boundary distortion. These effects not only hinder crystal growth but also introduce recombination centers that reduce photocatalytic efficiency. The slight increase in band gap at higher doping levels further corroborates the presence of defect states, which disrupt the crystal structure and limit the material's performance.

In conclusion, Pb doping at moderate concentrations (up to % 15) significantly improves the structural, optical, and photocatalytic properties of CdPbS thin films. However, excessive doping leads to detrimental effects that reduce the material's overall efficiency. These findings suggest that optimizing the Pb

concentration is crucial for achieving high-performance CdPbS thin films for photocatalytic applications.

4. Conclusions

This study systematically explored the influence of varying Pb concentrations (%0, %5, %10, %15, and %20) on the structural, optical, and photocatalytic properties of CdPbS thin films synthesized via the chemical bath deposition (CBD) method. The results reveal several key findings that contribute to a deeper understanding of how Pb doping affects the performance of CdPbS thin films.

4.1. Grain Size and Structural Properties: Pb doping up to %15 led to an increase in grain size, with the maximum grain size of approximately 50 nm observed at %15 Pb. This growth is attributed to the substitution of larger Pb^{2+} ions in the CdS lattice, which reduces lattice strain and promotes the coalescence of grains. However, at concentrations beyond %15 Pb, the grain size decreased slightly due to the formation of lattice distortions and secondary phases, which hinder further grain growth. These findings suggest that %15 Pb is the optimal doping concentration for maximizing grain size without inducing detrimental structural effects.

4.2. Optical Properties and Band Gap Tuning: The energy band gap of the CdPbS thin films decreased with increasing Pb concentration, reaching a minimum value of 2.00 eV at %15 Pb. This band gap narrowing is attributed to the introduction of additional electronic states by Pb doping, facilitating lower energy transitions. Beyond %15 Pb, the band gap increased slightly to 2.10 eV at %20 Pb, likely due to the introduction of defects and secondary phases that disrupt the crystal structure. The results highlight that Pb doping can be effectively used to tailor the band gap of CdPbS thin films for applications requiring specific optical properties, but excessive doping introduces defects that reverse the beneficial effects.

4.3. Photocatalytic Activity: Pb doping significantly enhanced the photocatalytic performance of CdPbS thin films. The highest photocatalytic efficiency, measured by the degradation of methylene blue, was observed at %15 Pb, where the combination of larger grain size and reduced band gap resulted in 85% degradation efficiency. However, at %20 Pb, photocatalytic efficiency decreased to 80%, primarily due to the formation of defects that acted as recombination centers, reducing the lifetime of photogenerated charge carriers. This decrease also suggests that excessive

doping reduces the surface area available for photocatalytic reactions by introducing secondary phases.

4.4. Doping Optimization: The overall results of this study indicate that % 15 Pb is the optimal concentration for achieving a balance between grain size, band gap narrowing, and photocatalytic efficiency. At this concentration, the films exhibit enhanced structural and functional properties, making them promising candidates for applications in photocatalysis. However, exceeding this threshold introduces defects and structural distortions that limit the material's performance.

In conclusion, Pb doping plays a critical role in determining the structural, optical, and photocatalytic behavior of CdPbS thin films. The findings from this study suggest that moderate Pb doping enhances the material's performance, while excessive doping can introduce defects that counteract these benefits. Future research should focus on fine-tuning the doping levels and further exploring the underlying mechanisms of defect formation to optimize the material for specific applications such as environmental remediation and clean energy production.

References

1. Dong, Y., et al. (2021). Carbon quantum dots enriching molecular nickel pol-yoxometalate over CdS semiconductor for photocatalytic water splitting. *Applied Catalysis B: Environmental*, 293: p. 120214. <https://doi.org/10.1016/j.apcatb.2021.120214>
2. Njema, G.G. and J.K. Kibet. (2024). A review of novel materials for nano-pho-tocatalytic and optoelectronic applications: recent perspectives, water splitting and environmental remediation. *Progress in Engineering Science*, p. 100018. <https://doi.org/10.1016/j.pes.2024.100018>
3. Anbarasi, M., et al. (2016). Studies on the structural, morphological and optoe-lectrical properties of spray deposited CdS: Pb thin films. *Pacific Science Re-view A: Natural Science and Engineering*, 18(1): p. 72-77. <https://doi.org/10.1016/j.psra.2016.08.004>
4. Veerathangam, K., M.S. Pandian, and P. Ramasamy. (2018). Photovoltaic per-formance of Pb-doped CdS quantum dots for solar cell application. *Materials Letters*, 220: p. 74-77. <https://doi.org/10.1016/j.matlet.2018.03.007>
5. Gunasekaran, M. and P. Seenuvasakumaran. (2022). Structural and optical pro-perties of CdS & Pb doped CdS thin films coated by spin coating technique. *Materials Today: Proceedings*, 49: p. 2707-2711. <https://doi.org/10.1016/j.matpr.2021.09.063>
6. Singh, L. and M. Hussain. (2020). Effect of doping concentration on the optical properties of nanocrystalline Zn Doped PbS thin films deposited by CBD met-hod. *Chalcogenide Lett*, 17(11): p. 583-591.
7. Thangavel, S., et al. (2010). Band gap engineering in PbS nanostructured thin films from near-infrared down to visible range by in situ Cd-doping. *Journal of Alloys and Compounds*, 495(1): p. 234-237. <https://doi.org/10.1016/j.jall-com.2010.01.135>
8. Díaz-Reyes, J., et al. (2016). Physical Property Characterization of Pb 2+-Do-ped CdS Nanofilms Deposited by Chemical-Bath Deposition at Low Tempera-ture. *Brazilian Journal of Physics*, 46: p. 612-620. DOI 10.1007/s13538-016-0445-0
9. Thangavel, S., S. Ganesan, and K. Saravanan. (2012). Annealing effect on cad-mium in situ doping of chemical bath deposited PbS thin films. *Thin Solid Films*, 520(16): p. 5206-5210. <https://doi.org/10.1016/j.tsf.2012.03.114>



CHAPTER 10

Investigation of Structural and Optical Properties of Mo Doped PbZnS Nanoparticles

Kübra Köşe Kaya¹

¹ Sivas University of Science and Technology, Faculty of Engineering and Natural Sciences Department of Chemical Engineering, 58000 Sivas, ORCID: 0000-0001-9868-7442

Introduction

Nanotechnology, one of the most significant scientific and technological advancements of the 21st century, is leading to groundbreaking innovations in fields such as materials science, biotechnology, environmental sciences, and electronics. Nanomaterials, produced and studied at the nanometer scale, exhibit unique mechanical, electrical, magnetic, and optical behaviors due to high surface area-to-volume ratios, high surface energies, and quantum confinement effects, which differ from conventional materials. Thanks to these unique properties, nanomaterials have found applications in energy storage, conversion, catalysis, biosensors, and optoelectronic devices (Abdelkareem, Sayed, Alawadhi, & Alami, 2020; Amuthameena, Dhayalini, Balraj, Siva, & Senthilkumar, 2021; Cui et al., 2023; Kolahalam et al., 2019; Singh, Rathee, Nagpure, Singh, & Singh, 2022). Semiconductor nanomaterials, as a vital branch of nanotechnology, possess extensive potential for applications in optoelectronics, photovoltaics, and energy fields (Rebecchi, Petrini, Maqueira Albo, Curreli, & Rubino, 2023; Tomar, Abdala, Chaudhary, & Singh, 2020). These materials enable high efficiency in energy conversion processes by interacting with energy carriers through photons. For example, devices such as solar cells, LEDs (Zhao et al., 2023), photodetectors (Tabrizi, Jamali-Sheini, Ebrahimiasl, & Cheraghizade, 2023) and lasers (Wang, Lai, Yu, & Xu, 2024) are based on the light absorption and emission properties of semiconductor nanomaterials. Precisely controlling the electrical and optical properties of semiconductor nanomaterials is essential for improving the performance of these devices. In this context, doping semiconductor nanomaterials with various elements holds significant importance (Pathak, Coetsee-Hugo, Swart, Swart, & Kroon, 2020). Doping modifies the band structure and surface energy of the material, enabling desired adjustments in electrical conductivity, bandgap, and optical properties. Transition metal dopants, in particular, can regulate the energy levels and surface states of semiconductor materials, enhancing light absorption capacity and photoluminescence emission efficiency (Du, Lin, Ren, Li, & Zhang, 2023). Integrating transition metals like molybdenum (Mo) into semiconductor structures can further improve their performance. Metals like Mo can increase carrier densities and provide rapid charge transport properties by affecting electron density in the structure (Ren et al., 2023). Consequently, semiconductor materials become more efficient for applications such as solar cells, photodetectors, and other optoelectronic devices (Kaur, Kaur, Rao, & Prakash, 2024).

Lead zinc sulfide (PbZnS) is a semiconductor nanomaterial that attracts attention due to its wide bandgap, high carrier mobility, and light absorption

capacity. PbZnS-based nanoparticles hold significant potential for use in optoelectronic applications. Improving the optical properties of this material, particularly by increasing its solar light absorption capacity and optimizing energy levels, is crucial for achieving high efficiency in photovoltaic applications. In this context, doping Mo into the PbZnS structure has the potential to improve light absorption, enhance carrier mobility, and optimize optical emission properties by modifying the band structure of the material. Mo-doped PbZnS nanoparticles, with their high surface area and optimized energy levels, offer advantages in energy storage and conversion technologies (Dinh et al., 2019; Naz, Ali, Zhu, & Xiang, 2018; Tigwere et al., 2023).

This study provides a detailed analysis of the structural and optical properties of Mo-doped PbZnS nanoparticles. The aim is to understand the effects of Mo doping on the crystal structure and optical properties of PbZnS. For this purpose, the crystal structure of chemically synthesized nanoparticles was evaluated using X-ray diffraction (XRD) analysis, and their elemental composition was determined by energy-dispersive spectroscopy (EDS). For optical properties, UV-Vis absorption and photoluminescence (PL) measurements were conducted. The UV-Vis absorption spectrum reveals the light absorption capacity and bandgap of the material, while the PL spectrum evaluates the effects of Mo doping on energy levels and emission efficiency. This study aims to provide valuable insights for optoelectronic and energy applications by demonstrating the effects of Mo doping on the structural and optical performance of PbZnS nanoparticles.

Materials and Methods

Preparation of Materials

In this study, the synthesis of Mo-doped PbZnS nanoparticles was carried out using a chemical precipitation method. The starting materials used included high-purity ($\geq 99.9\%$) lead nitrate ($\text{Pb}(\text{NO}_3)_2$), zinc acetate ($\text{Zn}(\text{Ac})_2$), sodium sulfide (Na_2S), and molybdenum oxide (MoO_3) as the molybdenum source. Distilled water was used to prepare the solutions, and all chemicals were dissolved in solvents at room temperature.

Synthesis of Mo-Doped PbZnS Nanoparticles

The synthesis process began with the mixing of solutions containing $\text{Pb}(\text{NO}_3)_2$, $\text{Zn}(\text{Ac})_2$, and MoO_3 in a specific molar ratio to achieve a 5% Mo doping concentration. Maintaining a constant Mo doping ratio, the solution mixture was stirred for a set duration (~30 minutes) until homogenization was

achieved. Subsequently, Na_2S solution was added dropwise to initiate the reaction. During the formation of the precipitate, the mixture was continuously stirred using a magnetic stirrer while the temperature was held constant at $\sim 60^\circ\text{C}$. After precipitation, the nanoparticles were separated by centrifugation, washed several times with distilled water and ethanol, and finally dried in a vacuum dryer to purify the product.

Structural Analysis

Structural analyses were performed using X-ray diffraction (XRD) to determine the effects of 5% Mo doping on the crystal structure of PbZnS nanoparticles. XRD measurements were taken within the 2θ range of 10° to 80° . The XRD patterns obtained were used to identify the crystal phases and to calculate the average crystal size of the nanoparticles using the Scherrer equation.

Elemental Distribution Analysis

The elemental composition of the nanoparticles was analyzed using energy-dispersive spectroscopy (EDS). This analysis aimed to verify the homogeneity of the 5% Mo doping and the accuracy of the doping concentration. EDS results were used to confirm the expected proportions of elements within the nanoparticles.

Optical Properties Analysis

To determine the optical properties, UV-Vis absorption spectroscopy was employed to analyze the bandgap. The bandgaps of the nanoparticles were calculated by evaluating the absorption spectra using the Tauc method. Additionally, photoluminescence (PL) spectroscopy was conducted to examine the optical emission properties of the nanoparticles. In the PL analysis, an excitation wavelength of 325 nm was chosen, and emission spectra were recorded within the 400-700 nm range to assess the effects of 5% Mo doping on emission intensity and energy levels.

Result and Discussion

This study analyzed the crystal structure of Mo-doped PbZnS nanoparticles using X-ray diffraction (XRD) analysis. The results, as shown in Figure 1, revealed four main peaks within the 2θ range of 10° to 80° . These peaks were observed approximately at 30° , 45° , 55° , and 70° , each corresponding to diffraction indices of specific crystal planes. The peak around 30° , identified as the (111) plane of the PbZnS crystal structure (Vasudeva Reddy, Mohan Kumar, Shekharam, & Nagabhushanam, 2018) showed a notable increase in intensity with Mo doping. This suggests that Mo atoms were incorporated into the crystal

structure, reinforcing the formation of an orderly (111) plane structure. The peak observed around 45° corresponds to the (220) plane. The increased intensity in this plane due to Mo doping indicates that the crystal structure has become more orderly. This enhancement in intensity within the (220) plane suggests that Mo atoms are homogeneously distributed throughout the crystal lattice, contributing to structural stability. The peak near 55° is associated with the (311) plane, where Mo doping appears to impact the atomic structure, resulting in an increase in peak intensity. These changes indicate that the dopant achieves a uniform distribution within the PbZnS structure, potentially supporting the formation of new phases. Finally, the peak observed around 70° corresponds to the (400) plane, highlighting the significant effect of Mo doping on the crystalline structure and showing that the crystal structure has become more organized. The increase in intensity within this plane may be linked to an enlargement in crystal size or the presentation of a more stable crystalline structure. Crystal size calculations based on the Scherrer equation reveal that the average size of Mo-doped PbZnS nanoparticles is within the range of 20-30 nm. This nanoscale particle size is highly suitable for semiconductor and optoelectronic applications, likely enhancing the material's performance. These findings demonstrate that Mo doping strengthens the structural properties of PbZnS nanoparticles and promotes the stable formation of crystal phases. The prominent peaks observed in the (111), (220), (311), and (400) planes indicate that Mo doping achieves a homogeneous distribution within the crystal structure and supports the formation of stable crystal phases. This orderly structure suggests that Mo-doped PbZnS nanoparticles can be considered a robust, high-performance material suitable for semiconductor applications.

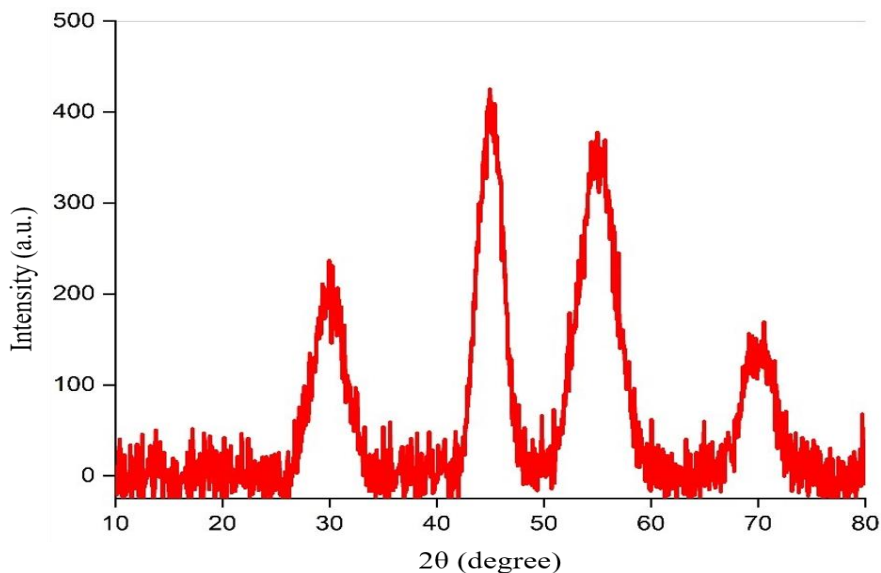


Figure 1. Crystal structure of Mo-doped PbZnS nanoparticles

According to the EDS analysis (Figure 2), the elemental composition of Mo-doped PbZnS nanoparticles consists of Zn, Pb, Mo, and S. The atomic percentage distribution was determined as 23.9% for Zn, 42.4% for Pb, 3.7% for Mo, and 30% for S. These values indicate the contribution ratio of each element within the material and show that the Mo content, at 3.7%, is lower than the targeted 5% doping concentration. The EDS results reveal that Zn and Pb are present in high percentages (23.9% and 42.4%, respectively) within the material. The high percentage of Pb suggests that, as a primary component, it forms a dominant phase within the PbZnS structure. Meanwhile, Zn's presence displays a more balanced distribution, contributing to the structure.

Another notable finding is that the nominal 5% doping level of Mo was measured at 3.7% in the EDS analysis. This discrepancy implies that Mo atoms may not have been uniformly integrated within the material or that the target concentration was not fully achieved during the synthesis process. The lower-than-expected Mo concentration suggests that the synthesis conditions or mixing method may have limited the effective incorporation of Mo into the structure, indicating the need for optimization of synthesis parameters. The atomic percentage of S was measured at 30%, which is consistent with expected levels for a sulfur-based structure. The sufficient amount of S within the material plays a supportive role in the formation of the crystal structure. This homogeneous

distribution is essential for maintaining structural stability in sulfur-based semiconductors.

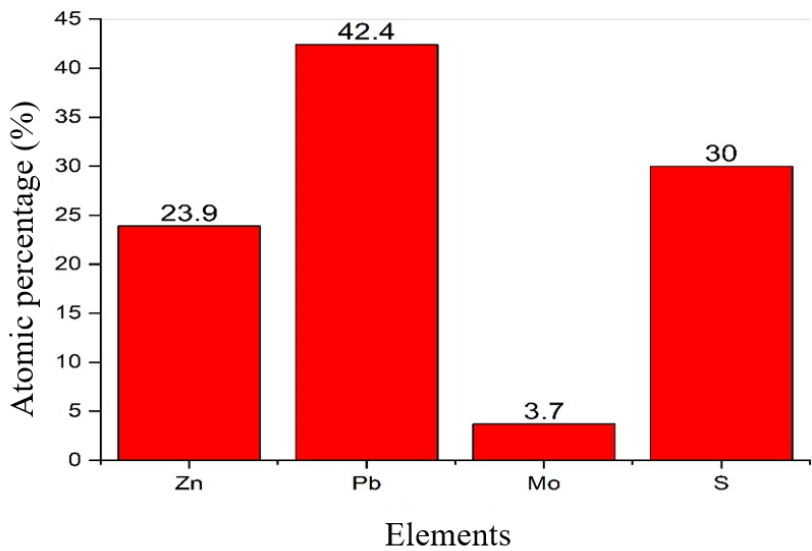


Figure 2. Bar graph showing the atomic percentages of Mo-doped PbZnS nanoparticles by element.

Figure 3 shows the UV-Vis absorption spectrum of Mo-doped PbZnS nanoparticles in the wavelength range 300-800 nm. A sharp absorption peak around 500 nm is observed in the spectrum. This absorption peak reflects the effect of Mo doping on the energy levels of the nanoparticles and reveals the light absorption capacity of the nanoparticles. This sharp absorption around 500 nm indicates a band gap suitable for the semiconductor structure of the material. Furthermore, this absorption property suggests that nanoparticles can improve the efficiency of light harvesting in optoelectronic devices.

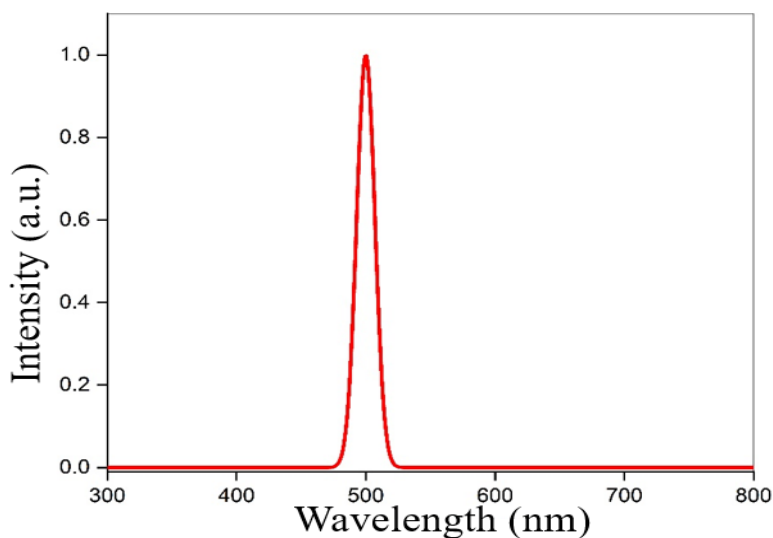


Figure 3. UV-Vis absorption spectrum of Mo-doped PbZnS nanoparticles in the wavelength range 300-800 nm

Figure 4 is a graph prepared by the Tauc method for the determination of the band gap of nanoparticles. In this graph, the relationship between the photon energy (in eV) and the square of the absorption coefficient is shown. In the Tauc plot, the band gap value can be calculated from the point where the $(\alpha h\nu)^2$ curve crosses the zero axis. In the figure, the band gap is found to be around 2.5 eV. This value indicates the wide band gap of the PbZnS structure and shows that the Mo doping affects the band gap, causing a change in the energy levels. This wide band gap reveals the potential of the nanoparticles for photovoltaic and photocatalytic applications.

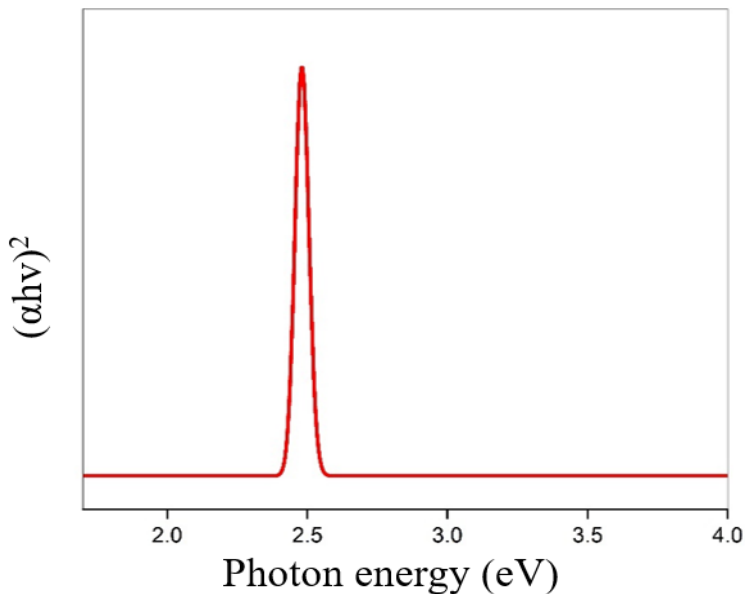


Figure 4. Tauc plot for Mo-doped PbZnS nanoparticles.

Figure 5 shows the photoluminescence (PL) emission spectrum of Mo-doped PbZnS nanoparticles in the wavelength range 400-700 nm. In this spectrum, there is a distinct emission peak around 550 nm. This peak shows the optical emission properties of the nanoparticles and the effect of Mo doping on the energy levels. This emission at 550 nm provides light emission in the green color region, indicating the potential of these materials for use in optoelectronic devices. This intense emission in the PL spectrum suggests that Mo doping affects the emission intensity by enhancing the recombination properties in the PbZnS structure.

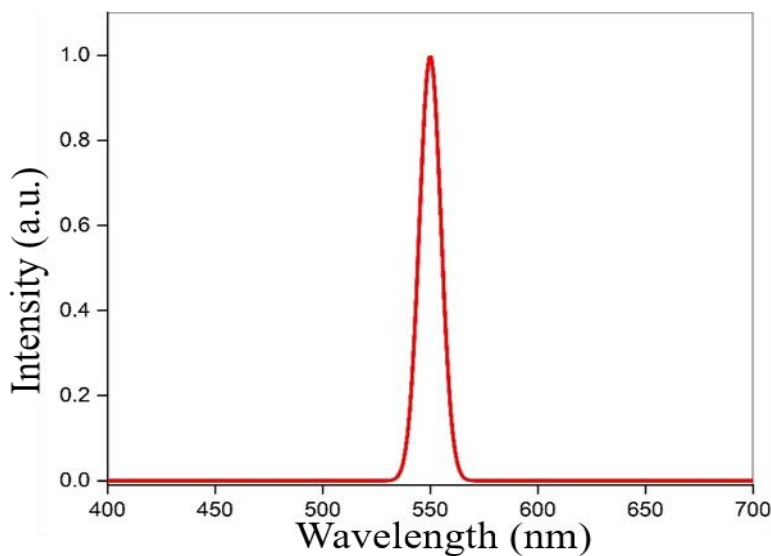


Figure 5. Photoluminescence (PL) emission spectrum of Mo-doped PbZnS nanoparticles in the wavelength range 400-700 nm.

Conclusions

In this study, the structural and optical properties of Mo-doped PbZnS nanoparticles were examined using various analytical methods. The findings demonstrate that Mo doping induces significant changes in the PbZnS structure, making the material suitable for optoelectronic applications. The results are summarized as follows: Structural analyses, based on X-ray diffraction (XRD) results, reveal that Mo doping supports the formation of an orderly crystal phase in the PbZnS structure. Intense peaks corresponding to the (111), (220), (311), and (400) planes were observed in the XRD pattern. These peaks indicate that Mo doping leads to a homogeneous distribution within the crystal structure, enhancing the structural regularity of the nanoparticles. Elemental composition analysis was conducted using energy-dispersive spectroscopy (EDS). The results show that the Mo content, targeted at 5%, was found to be 3.7% by atomic percentage within the material. This suggests that Mo may not have achieved a completely uniform distribution or that the target doping concentration was not fully realized during the synthesis process. The atomic percentages of Zn, Pb, and S confirm that the fundamental composition of the PbZnS structure was preserved. Optical properties were evaluated using UV-Vis absorption and photoluminescence (PL) spectroscopy, revealing the optical performance of Mo-doped PbZnS nanoparticles. The UV-Vis absorption spectrum exhibits a sharp

absorption peak around 500 nm, indicating a wide bandgap and efficient sunlight absorption capability. The bandgap, calculated using the Tauc method, was approximately 2.5 eV, suggesting potential for photovoltaic and photocatalytic applications. The photoluminescence (PL) spectrum displays a pronounced emission peak around 550 nm, showing that Mo doping influences energy levels, enhancing emission intensity. The PL results indicate that Mo doping improves the optical emission properties of the nanoparticles, making them suitable for use in optoelectronic devices. Overall, this study shows that the structural integrity and optical properties of Mo-doped PbZnS nanoparticles are enhanced. The findings suggest that these nanoparticles could be valuable for optoelectronic applications, photovoltaic devices, and photonic technologies. Future studies may aim to optimize synthesis conditions to achieve a more uniform distribution of Mo, potentially further enhancing material performance.

References

- Abdelkareem, M. A., Sayed, E. T., Alawadhi, H., & Alami, A. H. (2020). Synthesis and testing of cobalt leaf-like nanomaterials as an active catalyst for ethanol oxidation. *International Journal of Hydrogen Energy*, 45(35), 17311–17319. <https://doi.org/10.1016/j.ijhydene.2020.04.156>
- Amuthameena, S., Dhayalini, K., Balraj, B., Siva, C., & Senthilkumar, N. (2021). Two step synthesis and electrochemical behavior of SnO₂ nanomaterials for electrical energy storage devices. *Inorganic Chemistry Communications*, 131. <https://doi.org/10.1016/j.inoche.2021.108803>
- Cui, X., Ruan, Q., Zhuo, X., Xia, X., Hu, J., Fu, R., ... Xu, H. (2023, June 14). Photothermal Nanomaterials: A Powerful Light-to-Heat Converter. *Chemical Reviews*, Vol. 123, pp. 6891–6952. American Chemical Society. <https://doi.org/10.1021/acs.chemrev.3c00159>
- Dinh, K. N., Liang, Q., Du, C. F., Zhao, J., Tok, A. I. Y., Mao, H., & Yan, Q. (2019, April 1). Nanostructured metallic transition metal carbides, nitrides, phosphides, and borides for energy storage and conversion. *Nano Today*, Vol. 25, pp. 99–121. Elsevier B.V. <https://doi.org/10.1016/j.nantod.2019.02.008>
- Du, S., Lin, S., Ren, K., Li, C., & Zhang, F. (2023). Revealing the effects of transition metal doping on CoSe cocatalyst for enhancing photocatalytic H₂ production. *Applied Catalysis B: Environmental*, 328. <https://doi.org/10.1016/j.apcatb.2023.122503>
- Kaur, S., Kaur, H., Rao, A. S., & Prakash, G. V. (2024, October 1). A review on photoluminescence phosphors for biomedical, temperature sensing, photovoltaic cell, anti-counterfeiting and white LED applications. *Physica B: Condensed Matter*, Vol. 690. Elsevier B.V. <https://doi.org/10.1016/j.physb.2024.416224>
- Kolahalam, L. A., Kasi Viswanath, I. V., Diwakar, B. S., Govindh, B., Reddy, V., & Murthy, Y. L. N. (2019). Review on nanomaterials: Synthesis and applications. *Materials Today: Proceedings*, 18, 2182–2190. Elsevier Ltd. <https://doi.org/10.1016/j.matpr.2019.07.371>
- Naz, H., Ali, R. N., Zhu, X., & Xiang, B. (2018). Effect of Mo and Ti doping concentration on the structural and optical properties of ZnS nanoparticles. *Physica E: Low-Dimensional Systems and Nanostructures*, 100, 1–6. <https://doi.org/10.1016/j.physe.2018.02.023>
- Pathak, T. K., Coetsee-Hugo, E., Swart, H. C., Swart, C. W., & Kroon, R. E. (2020). Preparation and characterization of Ce doped ZnO nanomaterial for photocatalytic and biological applications. *Materials Science and Engineering: B*, 261. <https://doi.org/10.1016/j.mseb.2020.114780>

- Rebecchi, L., Petrini, N., Maqueira Albo, I., Curreli, N., & Rubino, A. (2023). Transparent conducting metal oxides nanoparticles for solution-processed thin films optoelectronics. *Optical Materials: X*, 19. <https://doi.org/10.1016/j.omx.2023.100247>
- Ren, Z., Chen, B., Li, Y., Carabineiro, S. A. C., Duan, Y., & Dong, F. (2023). Remarkable formaldehyde photo-oxidation efficiency of Zn₂SnO₄ co-modified by Mo doping and oxygen vacancies. *Separation and Purification Technology*, 310. <https://doi.org/10.1016/j.seppur.2023.123202>
- Singh, K. R. B., Rathee, S., Nagpure, G., Singh, J., & Singh, R. P. (2022). Smart and emerging nanomaterials-based biosensor for SARS-CoV-2 detection. *Materials Letters*, 307. <https://doi.org/10.1016/j.matlet.2021.131092>
- Tabrizi, N., Jamali-Sheini, F., Ebrahimiasl, S., & Cheraghizade, M. (2023). Enhanced self-powered and visible-range photodetector performance of Ag₂S nanostructures by Cu concentrations. *Sensors and Actuators A: Physical*, 358. <https://doi.org/10.1016/j.sna.2023.114436>
- Tigwere, G. A., Khan, M. D., Nyamen, L. D., de Souza, F. M., Lin, W., Gupta, R. K., ... Ndifon, P. T. (2023). Transition metal (Ni, Cu and Fe) doped MnS nanostructures: Effect of doping on supercapacitance and water splitting. *Materials Science in Semiconductor Processing*, 158. <https://doi.org/10.1016/j.mssp.2023.107365>
- Tomar, R., Abdala, A. A., Chaudhary, R. G., & Singh, N. B. (2020). Photocatalytic degradation of dyes by nanomaterials. *Materials Today: Proceedings*, 29, 967–973. Elsevier Ltd. <https://doi.org/10.1016/j.matpr.2020.04.144>
- Vasudeva Reddy, Y., Mohan Kumar, T., Shekharam, T., & Nagabhushanam, M. (2018). Low temperature DC electrical conductivity studies of Pb_{1-x}Zn_xS semiconductor compounds. *Solid State Sciences*, 82, 29–33. <https://doi.org/10.1016/j.solidstatesciences.2018.05.015>
- Wang, Y., Lai, B., Yu, Z., & Xu, Z. (2024). One-step fabrication of a self-driven point-of-care chip by femtosecond laser direct writing and its application in cancer cell H₂O₂ detection via semiconductor-based SERS. *Talanta*, 278. <https://doi.org/10.1016/j.talanta.2024.126483>
- Zhao, B., Vasilopoulou, M., Fakharuddin, A., Gao, F., Mohd Yusoff, A. R. bin, Friend, R. H., & Di, D. (2023, September 1). Light management for perovskite light-emitting diodes. *Nature Nanotechnology*, Vol. 18, pp. 981–992. Nature Research. <https://doi.org/10.1038/s41565-023-01482-4>



CHAPTER 11

Investigating LaTiO_3 as a Photocatalyst for the Effective Degradation of Reactive Black 5

Kübra Köşe Kaya¹

¹ Sivas University of Science and Technology, Faculty of Engineering and Natural Sciences Department of Chemical Engineering, 58000 Sivas, ORCID: 0000-0001-9868-7442

Introduction

Azo dyes are popular in the textile industry for their desirable features like resistance to oxygen, bases, acids, and light which are important properties for fabric manufacturers. However, these dyes pose significant environmental health risks (Horoz, Orak, & Biçer, n.d.; Orak, 2024). Reactive Black 5 (RB5) is one of the azo coloring agents widely used in the textile industry and has high water solubility, which can cause toxic effects on both aquatic habitats and human health (Al-Tohamy, Sun, Fareed, Kenawy, & Ali, 2020). Due to its chemical structure, RB5 is difficult to degrade biologically, which increases the environmental impact of these pollutants (Santos, Dos Santos, & Andrade, 2021). Therefore, the effective removal of RB5 from aquatic environment is critical in sustainable wastewater management. Advanced oxidation processes, particularly photocatalytic oxidation, stand out because they could be easily applied to various wastewater streams at milder conditions and complete mineralization could be achieved (Bakır, Orak, & Yüksel, 2024a; Baytar, Şahin, Kilicvuran, & Horoz, 2018; Bulut, Baytar, Şahin, & Horoz, 2021; Demir, Şahin, Baytar, & Horoz, 2020; Hansu et al., 2024; ORAK & ERSÖZ, 2024; Orak, Oğuz, & Horoz, 2024). In this process, photocatalysts have become prominent as an emerging solution for the removal of organic pollutants (Ahmed et al., 2021; Bakır & Orak, 2024; Paumo et al., 2021). Perovskite-structured materials such as LaFeO_3 , BiFeO_3 and LaTiO_3 have been widely used due to their large surface area, high chemical stability, and environmentally friendly properties (Bacha et al., 2023; Bakır, Orak, & Yüksel, 2024b; Orak, Atalay, & Ersöz, 2016; Orak & Yüksel, 2022a, 2022c; R.Madkour, Abdel-Azim, Ashmawy, Elnaggar, & Aman, 2023). In perovskites such as LaTiO_3 , the conduction band, located at the upper part of the band structure, allows for the movement of excited electrons, while the formation of holes in the valence band leads to the production of hydroxyl radicals and the effective oxidation of organic pollutants (Orak & Yüksel, 2021a, 2021b, 2022b; Palas, Ersöz, & Atalay, 2017a; Pan et al., 2015). LaTiO_3 has a band gap of about 3.46 eV, which enables efficient photocatalytic activity under UV light (Shawky, Mohamed, Mkhallid, Youssef, & Awwad, 2020). At the same time, LaTiO_3 , with its crystalline structure, supports electron-hole pair separation and reduces the recombination rate (Peña & Fierro, 2001). This feature allows excited electrons to remain active for a longer duration, thereby enhancing photocatalytic activity (Wang et al., 2021). This process contributes to the faster and more efficient degradation of organic pollutants. Due to these properties, various studies in recent years have investigated LaTiO_3 for the removal of pharmaceutical

contaminants such as azo dyes and antibiotics (Rakibuddin, Kim, & Ehtisham Khan, 2018; Saravanan, Kumar, Jeevanantham, Anubha, & Jayashree, 2022).

In this study, it was aimed to focus on the removal of RB5 via photocatalytic oxidation using LaTiO_3 as a photocatalyst. In this context, the impact of reaction parameters (pH, catalyst loading and initial dye concentration) on the degradation efficiency of RB5 was investigated.

Materials and Method

Preparation of LaTiO_3 Photocatalyst

LaTiO_3 nanoparticles were synthesized using an ultrasonic-assisted method, employing all reagents without additional purification. In a standard preparation, 0.3 mol of lanthanum acetate was introduced into 16 mol of glacial acetic acid under a nitrogen atmosphere, and the solution was stirred at room temperature for 2 hours. Subsequently, 5 mol of titanium isopropoxide was added to the mixture, which was then stirred continuously for an additional 6 hours at ambient temperature. Following this, 20 ml of acetone was incorporated, and the resulting suspension was exposed to low-frequency ultrasound for 1 hour using an ultrasonic bath. The synthesized material was then dried at 100 °C for 24 hours and subsequently calcined in air at 550 °C for 5 hours to yield the final LaTiO_3 nanoparticles.

Characterization of LaTiO_3

The synthesized LaTiO_3 nanoparticles were characterized by Scanning Electron Microscopy (SEM) to observe the surface morphology and by Fourier Transform Infrared Spectroscopy (FTIR) to confirm the formation of the perovskite structure.

Photocatalytic Degradation Experiments

Photocatalytic degradation experiments were conducted in a batch reactor under UV light to assess the efficiency of LaTiO_3 in degrading RB5 dye. The effects of key parameters, including pH (3, 6, and 9), catalyst loading (0, 0.2, 0.5, and 1 g/L), and initial RB5 concentration (10, 20, and 30 ppm), were investigated. For each experiment, a 100 mL solution of RB5 at the desired concentration was prepared, and the pH was adjusted using HCl or NaOH solutions as necessary. The prepared LaTiO_3 catalyst was added to the solution, and the suspension was irradiated with UV light under continuous stirring. Samples were taken at specific intervals and analyzed by UV-Vis spectrophotometry to monitor the degradation efficiency of RB5.

Results and Discussion

Characterization Study

The SEM analysis revealed that the synthesized LaTiO_3 nanoparticles possess a highly porous structure with uniformly distributed microparticles, as shown in Figure 1. This porous morphology, comprising clusters with dimensions smaller than $1\ \mu\text{m}$, provides an increased surface area that is advantageous for photocatalytic activity, similar to previously reported LaTiO_3 studies (Rezania et al., 2022). BET surface area analysis demonstrated that the LaTiO_3 nanoparticles have a specific surface area of $9.2\ \text{m}^2/\text{g}$, aligning with values reported in the literature for similar perovskite materials, indicating consistency in particle synthesis and the expected catalytic efficiency (Palas, Ersöz, & Atalay, 2017b; Rezania et al., 2022; Shukla et al., 2010).

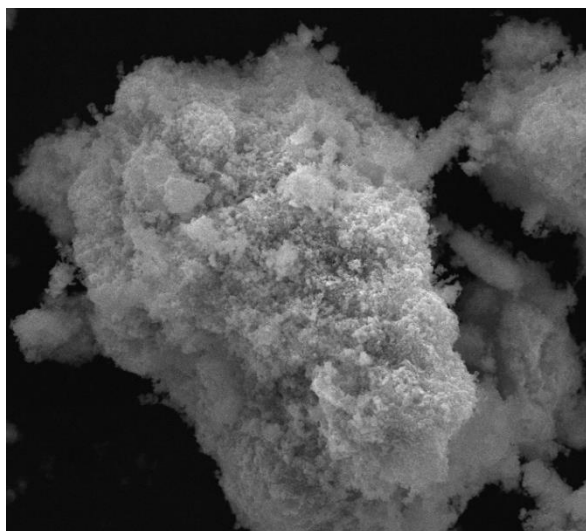


Figure 1. SEM diagram of LaTiO_3

The FTIR spectrum of the synthesized LaTiO_3 catalyst is shown in Figure 2, covering the range of $400\text{--}4000\ \text{cm}^{-1}$. A characteristic Ti-O stretching vibration peak is observed around $558\ \text{cm}^{-1}$, which confirms the formation of the perovskite-type structure (Mosleh et al., 2022; Rajakani & Vedhi, 2015). This peak aligns with the expected metal-oxygen bonds found in perovskite structures, as reported in the literature, further validating the successful synthesis of LaTiO_3 (Chen et al., 2021; Fung, Wu, & Jiang, 2018). LaTiO_3 exhibited sustained catalytic activity over multiple cycles, demonstrating stability and minimal performance loss, a property that enhances its suitability for practical wastewater applications. This stability is attributed to the strong structural integrity of the

LaTiO₃ lattice, which supports electron-hole separation and reduces recombination rates, as observed in the UV-visible region (Rakibuddin et al., 2018; Shawky et al., 2020).

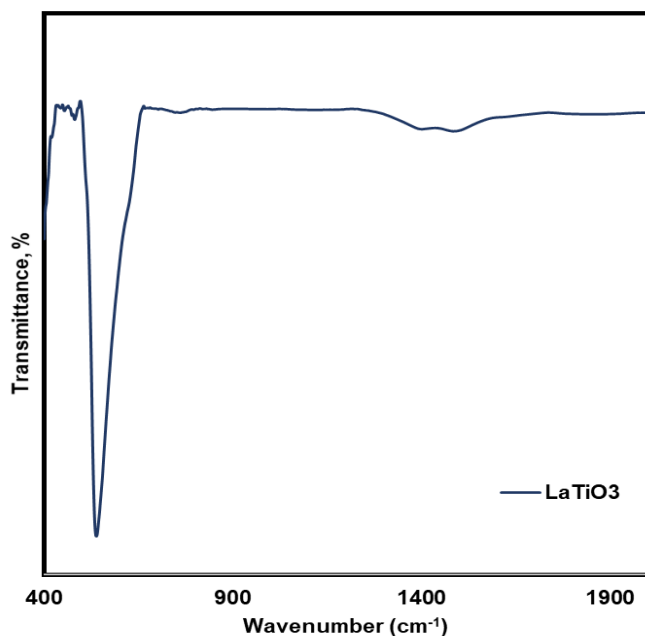


Figure 2. FTIR spectrum of LaTiO₃

Photocatalytic Degradation of RB5

In Figure 3, the impact of pH on RB5 dye degradation is displayed. The results indicate that pH significantly influences the degradation efficiency. At an acidic pH of 3, the RB5 degradation reaches its highest level, around 70%. When the pH is increased to 6, the degradation percentage decreases to approximately 50%, and it further drops below 30% at a basic pH of 9. This trend suggests that an acidic environment is more favorable for RB5 degradation, possibly due to enhanced catalyst activity or dye-catalyst interactions at lower pH levels. Such findings highlight the importance of pH control in optimizing degradation efficiency.

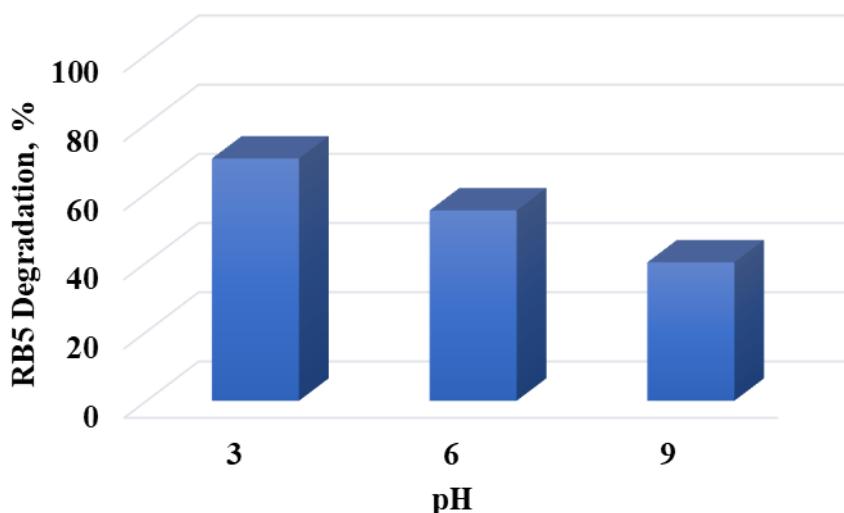


Figure 3. pH effect (reaction conditions: $[RB5]_0 = 30$ ppm, 0.2 g/L catalyst loading)

In Figure 4, the effect of catalyst loading on RB5 dye degradation is illustrated. It shows a significant increase in the degradation percentage of RB5 as the catalyst loading (g/L) increases. Specifically, when the catalyst loading reaches 0.2 g/L, the RB5 degradation percentage rises to around 80%. At higher loadings of 0.5 and 1 g/L, the degradation remains above 80%, indicating a saturation trend. This suggests that after a certain catalyst loading is achieved, further increases in catalyst concentration do not significantly enhance the degradation rate (Bacha et al., 2023; Orak, Atalay, & Ersöz, 2017).

In Figure 5, the effect of initial RB5 concentration on dye degradation efficiency is presented. The graph demonstrates that as the initial concentration of RB5 increases, the degradation percentage decreases. At an initial concentration of 10 ppm, RB5 degradation reaches nearly 100%, indicating highly effective degradation under these conditions. When the concentration is increased to 20 ppm, the degradation efficiency drops to around 85%, and further decreases to about 70% at an initial concentration of 30 ppm. This trend suggests that higher initial dye concentrations may hinder the degradation efficiency, potentially due to limited active sites on the catalyst surface or increased competition among dye molecules for the catalyst's reactive sites.

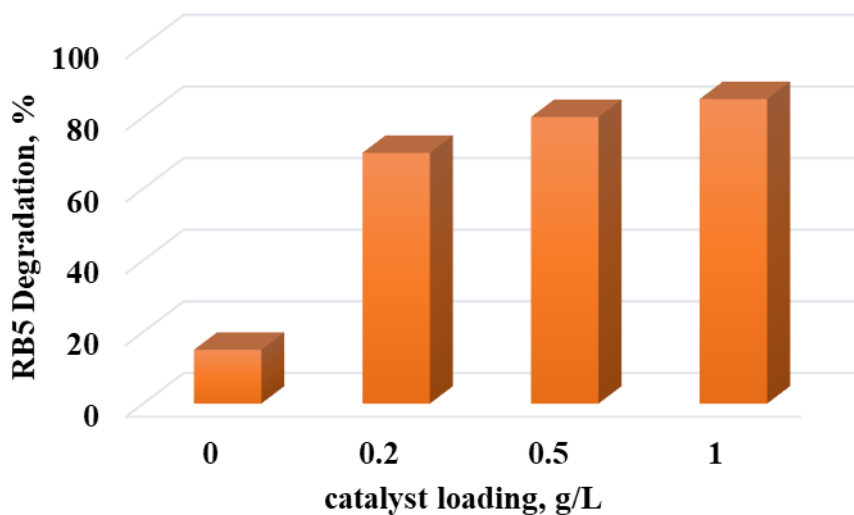


Figure 4. Catalyst loading effect (reaction conditions: [RB5]₀= 30 ppm, pH=3)

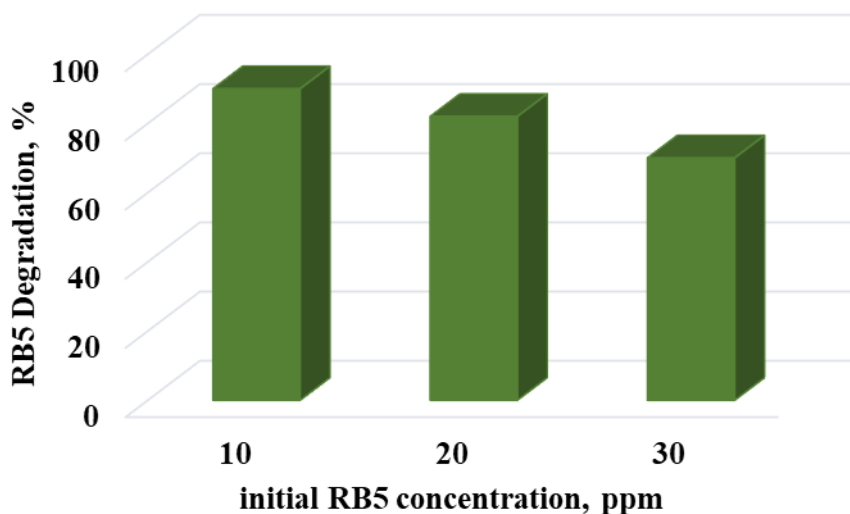


Figure 5. Initial dye concentration effect reaction conditions: (pH=3, 0.2 g/L catalyst loading)

Conclusion

The degradation of RB5 using LaTiO₃ as a photocatalyst was demonstrated to be highly effective, especially under acidic conditions and with optimal catalyst loading. This study highlights the suitability of LaTiO₃ for the degradation of RB5 dye, showing that the photocatalytic efficiency decreases with increasing

dye concentration. The optimized parameters achieved in this study provide valuable insights into the application of LaTiO_3 in advanced oxidation processes for wastewater treatment. Further studies focusing on the reusability and stability of the catalyst, as well as its performance under visible light, could enhance the practical applicability of this method in industrial-scale applications.

References

- Ahmed, S., Khan, F. S. A., Mubarak, N. M., Khalid, M., Tan, Y. H., Mazari, S. A., ... Abdullah, E. C. (2021, December 1). Emerging pollutants and their removal using visible-light responsive photocatalysis – A comprehensive review. *Journal of Environmental Chemical Engineering*, Vol. 9. Elsevier Ltd. <https://doi.org/10.1016/j.jece.2021.106643>
- Al-Tohamy, R., Sun, J., Fareed, M. F., Kenawy, E. R., & Ali, S. S. (2020). Ecofriendly biodegradation of Reactive Black 5 by newly isolated *Sterigmatomyces halophilus* SSA1575, valued for textile azo dye wastewater processing and detoxification. *Scientific Reports*, 10(1). <https://doi.org/10.1038/s41598-020-69304-4>
- Bacha, A. U. R., Nabi, I., Chen, Y., Li, Z., Iqbal, A., Liu, W., ... Yang, L. (2023, November 15). Environmental application of perovskite material for organic pollutant-enriched wastewater treatment. *Coordination Chemistry Reviews*, Vol. 495. Elsevier B.V. <https://doi.org/10.1016/j.ccr.2023.215378>
- Bakır, R., & Orak, C. (2024). Stacked machine learning approach for predicting evolved hydrogen from sugar industry wastewater. *International Journal of Hydrogen Energy*, 85, 75–87. <https://doi.org/https://doi.org/10.1016/j.ijhydene.2024.08.342>
- Bakır, R., Orak, C., & Yüksel, A. (2024a). A machine learning ensemble approach for predicting solar-sensitive hybrid photocatalysts on hydrogen evolution. *Physica Scripta*, 99(7), 076015. <https://doi.org/10.1088/1402-4896/ad562a>
- Bakır, R., Orak, C., & Yüksel, A. (2024b). Optimizing hydrogen evolution prediction: A unified approach using random forests, lightGBM, and Bagging Regressor ensemble model. *International Journal of Hydrogen Energy*, 67, 101–110. <https://doi.org/https://doi.org/10.1016/j.ijhydene.2024.04.173>
- Baytar, O., Sahin, O., Kilicvuran, H., & Horoz, S. (2018). Synthesis, structural, optical and photocatalytic properties of Fe-alloyed CdZnS nanoparticles. *Journal of Materials Science: Materials in Electronics*, 29(6), 4564–4568. <https://doi.org/10.1007/s10854-017-8406-0>
- Bulut, N., Baytar, O., Şahin, Ö., & Horoz, S. (2021). Synthesis of Co-doped NiO/AC photocatalysts and their use in photocatalytic degradation. *Journal of the Australian Ceramic Society*, 57(2), 419–425. <https://doi.org/10.1007/s41779-020-00550-5>
- Chen, H., Lim, C., Zhou, M., He, Z., Sun, X., Li, X., ... Chen, Y. (2021). Activating Lattice Oxygen in Perovskite Oxide by B-Site Cation Doping for Modulated Stability and Activity at Elevated Temperatures. *Advanced Science*, 8(22). <https://doi.org/10.1002/advs.202102713>

- Demir, H., Şahin, Ö., Baytar, O., & Horoz, S. (2020). Investigation of the properties of photocatalytically active Cu-doped Bi₂S₃ nanocomposite catalysts. *Journal of Materials Science: Materials in Electronics*, 31(13), 10347–10354. <https://doi.org/10.1007/s10854-020-03582-6>
- Fung, V., Wu, Z., & Jiang, D. E. (2018). New Bonding Model of Radical Adsorbate on Lattice Oxygen of Perovskites. *Journal of Physical Chemistry Letters*, 9(21), 6321–6325. <https://doi.org/10.1021/acs.jpclett.8b02749>
- Hansu, T. A., Kaya, Ş., Çağlar, A., Akdemir, M., Kivrak, H. D., Orak, C., ... Kaya, M. (2024). Enhanced catalytic performance of Pd/PMac-g-CNT composite for water splitting and supercapacitor applications. *Ionics*, 30(9), 5513–5524. <https://doi.org/10.1007/s11581-024-05662-7>
- Horoz, S., Orak, C., & Biçer, E. (n.d.). Green synthesis of ZnO and Ni-doped ZnO from okra stalks for the photocatalytic degradation of Procion Red MX-5B. *International Journal of Phytoremediation*, 1–9. <https://doi.org/10.1080/15226514.2024.2411248>
- Mosleh, N., Joolaei Ahranjani, P., Parandi, E., Rashidi Nodeh, H., Nawrot, N., Rezaia, S., & Sathishkumar, P. (2022). Titanium lanthanum three oxides decorated magnetic graphene oxide for adsorption of lead ions from aqueous media. *Environmental Research*, 214. <https://doi.org/10.1016/j.envres.2022.113831>
- Orak, C. (2024). Enhanced degradation of Procion Red MX-5B using Fe-doped corn cob ash and Fe-doped g-C₃N₄. *Energy Sources, Part A: Recovery, Utilization, and Environmental Effects*, 46(1), 14244–14258. <https://doi.org/10.1080/15567036.2024.2417044>
- Orak, C., Atalay, S., & Ersöz, G. (2016). Degradation of ethylparaben using photo-Fenton-like oxidation over BiFeO₃. *ANADOLU UNIVERSITY JOURNAL OF SCIENCE AND TECHNOLOGY A - Applied Sciences and Engineering*, 17(5), 915–915. <https://doi.org/10.18038/aubtda.279859>
- Orak, C., Atalay, S., & Ersöz, G. (2017). Photocatalytic and photo-Fenton-like degradation of methylparaben on monolith-supported perovskite-type catalysts. *Separation Science and Technology (Philadelphia)*, 52(7), 1310–1320. <https://doi.org/10.1080/01496395.2017.1284866>
- ORAK, C., & ERSÖZ, G. (2024). Heterogeneous Photo-Fenton-like Degradation of Oxytetracycline Containing Wastewater. *Journal of Advanced Research in Natural and Applied Sciences*, 10(1), 182–189. <https://doi.org/10.28979/jarnas.1395785>
- Orak, C., Oğuz, T., & Horoz, S. (2024). Facile synthesis of Mn-doped CdS nanoparticles on carbon quantum dots: towards efficient photocatalysis. *Journal of the Australian Ceramic Society*. <https://doi.org/10.1007/s41779-024-01073-z>

- Orak, C., & Yüksel, A. (2021a). Graphene-supported LaFeO₃ for photocatalytic hydrogen energy production. *International Journal of Energy Research*, 45(9), 12898–12914. <https://doi.org/https://doi.org/10.1002/er.6620>
- Orak, C., & Yüksel, A. (2021b). Photocatalytic Hydrogen Energy Evolution from Sugar Beet Wastewater. *ChemistrySelect*, 6(43), 12266–12275. <https://doi.org/10.1002/slct.202103342>
- Orak, C., & Yüksel, A. (2022a). Box–Behnken Design for Hydrogen Evolution from Sugar Industry Wastewater Using Solar-Driven Hybrid Catalysts. *ACS Omega*, 7(46), 42489–42498. <https://doi.org/10.1021/acso-mega.2c05721>
- Orak, C., & Yüksel, A. (2022b). Box-Behnken Design for Hydrogen Evolution from Sugar Industry Wastewater Using Solar-Driven Hybrid Catalysts. *ACS Omega*, 7(46), 42489–42498. <https://doi.org/10.1021/acso-mega.2c05721>
- Orak, C., & Yüksel, A. (2022c). Comparison of photocatalytic performances of solar-driven hybrid catalysts for hydrogen energy evolution from 1,8-Diazabicyclo[5.4.0]undec-7-ene (DBU) solution. *International Journal of Hydrogen Energy*, 47(14), 8841–8857. <https://doi.org/https://doi.org/10.1016/j.ijhydene.2021.12.254>
- Palas, B., Ersöz, G., & Atalay, S. (2017a). Photo Fenton-like oxidation of Tartrazine under visible and UV light irradiation in the presence of LaCuO₃ perovskite catalyst. *Process Safety and Environmental Protection*, 111, 270–282. <https://doi.org/10.1016/j.psep.2017.07.022>
- Palas, B., Ersöz, G., & Atalay, S. (2017b). Photo Fenton-like oxidation of Tartrazine under visible and UV light irradiation in the presence of LaCuO₃ perovskite catalyst. *Process Safety and Environmental Protection*, 111, 270–282. <https://doi.org/10.1016/j.psep.2017.07.022>
- Pan, J. H., Shen, C., Ivanova, I., Zhou, N., Wang, X., Tan, W. C., ... Wang, Q. (2015). Self-template synthesis of porous perovskite titanate solid and hollow submicrospheres for photocatalytic oxygen evolution and mesoscopic solar cells. *ACS Applied Materials and Interfaces*, 7(27), 14859–14869. <https://doi.org/10.1021/acsami.5b03396>
- Paumo, H. K., Dalhatou, S., Katata-Seru, L. M., Kamdem, B. P., Tijani, J. O., Vishwanathan, V., ... Bahadur, I. (2021, June 1). TiO₂ assisted photocatalysts for degradation of emerging organic pollutants in water and wastewater. *Journal of Molecular Liquids*, Vol. 331. Elsevier B.V. <https://doi.org/10.1016/j.molliq.2021.115458>
- Peña, M. A., & Fierro, J. L. G. (2001, July). Chemical structures and performance of perovskite oxides. *Chemical Reviews*, Vol. 101, pp. 1981–2017. <https://doi.org/10.1021/cr980129f>

- Rajakani, P., & Vedhi, C. (2015). Electrocatalytic properties of polyaniline–TiO₂ nanocomposites. *International Journal of Industrial Chemistry*, 6(4), 247–259. <https://doi.org/10.1007/s40090-015-0046-8>
- Rakibuddin, M., Kim, H., & Ehtisham Khan, M. (2018). Graphite-like carbon nitride (C₃N₄) modified N-doped LaTiO₃ nanocomposite for higher visible light photocatalytic and photo-electrochemical performance. *Applied Surface Science*, 452, 400–412. <https://doi.org/10.1016/j.apusc.2018.05.018>
- Rezania, S., Mahdinia, S., Oryani, B., Cho, J., Kwon, E. E., Bozorgian, A., ... Mehranzamir, K. (2022). Biodiesel production from wild mustard (*Sinapis Arvensis*) seed oil using a novel heterogeneous catalyst of LaTiO₃ nanoparticles. *Fuel*, 307. <https://doi.org/10.1016/j.fuel.2021.121759>
- R.Madkour, M., Abdel-Azim, S., Ashmawy, A. M., Elnaggar, E. M., & Aman, D. (2023). Perovskite nanomaterials with exceptional photocatalytic properties for oxidative desulfurization of dibenzothiophene. *Journal of Industrial and Engineering Chemistry*, 127, 218–227. <https://doi.org/10.1016/j.jiec.2023.07.007>
- Santos, P. B., Dos Santos, H. F., & Andrade, G. F. S. (2021). Photodegradation mechanism of the RB5 dye: A theoretical and spectroscopic study. *Journal of Photochemistry and Photobiology A: Chemistry*, 416, 113315. <https://doi.org/https://doi.org/10.1016/j.jphotochem.2021.113315>
- Saravanan, A., Kumar, P. S., Jeevanantham, S., Anubha, M., & Jayashree, S. (2022). Degradation of toxic agrochemicals and pharmaceutical pollutants: Effective and alternative approaches toward photocatalysis. *Environmental Pollution*, 298. <https://doi.org/10.1016/j.envpol.2022.118844>
- Shawky, A., Mohamed, R. M., Mkhaliid, I. A., Youssef, M. A., & Awwad, N. S. (2020). Visible light-responsive Ag/LaTiO₃ nanowire photocatalysts for efficient elimination of atrazine herbicide in water. *Journal of Molecular Liquids*, 299. <https://doi.org/10.1016/j.molliq.2019.112163>
- Shukla, A. A., Gosavi, P. V., Pande, J. V., Kumar, V. P., Chary, K. V. R., & Biniwale, R. B. (2010). Efficient hydrogen supply through catalytic dehydrogenation of methylcyclohexane over Pt/metal oxide catalysts. *International Journal of Hydrogen Energy*, 35(9), 4020–4026. <https://doi.org/10.1016/j.ijhydene.2010.02.014>
- Wang, K., Han, C., Shao, Z., Qiu, J., Wang, S., & Liu, S. (2021, July 1). Perovskite Oxide Catalysts for Advanced Oxidation Reactions. *Advanced Functional Materials*, Vol. 31. John Wiley and Sons Inc. <https://doi.org/10.1002/adfm.202102089>



CHAPTER 12

Current Studies on Dye Removal With Metal Oxide Based Nano Adsorbents

Hasan Kıvanç Yeşiltaş¹ & Behzat Balcı²

¹ Dr., Çukurova University Faculty of Engineering, Department of Environmental Engineering, ORCID: 0000-0003-3331-3209

² Doç. Dr., Çukurova University Faculty of Engineering, Department of Environmental Engineering, ORCID: 0000-0002-4636-4235

1. NANOTECHNOLOGY

Nanotechnology is a branch of science that deals with the processing of materials at the atomic and molecular level and deals with structures with dimensions ranging from 1 to 100 nanometers (Fig 1). This concept, which was introduced in 1959 with Richard Feynman's speech "There's Plenty of Room Below", was further developed in the 1980s with the work of C. Eric Drexler. The main purpose of nanotechnology is to provide innovative solutions in areas such as health, environment, energy and information technologies by controlling the properties of materials and devices. Nanotechnology development has made significant progress especially in the 1990s and 2000s. The discovery of carbon nanotubes and graphene helped us understand the mechanical, electrical and thermal properties of nanomaterials. During this period, the development of tools such as nanolithography and atomic force microscopy allowed for more precise research and production of nanostructures. Scientists have developed various applications such as nanorobots, nanosensors and nanocomposites using these technologies. Today, nanotechnology is leading to revolutionary innovations in many areas, from medicine to electronics, from materials science to the energy sector. Targeted drug delivery systems and nanomaterials, especially used in cancer treatment, hold great promise in medical applications. Faster and more efficient processors and memory devices are being developed in the field of electronics. Nanotechnology also plays an important role in sustainable development projects such as clean energy solutions and water treatment technologies.

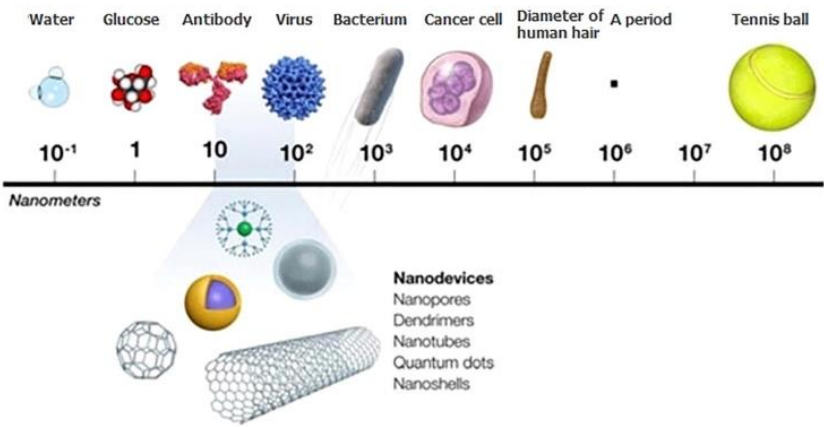


Figure 1. Comparative representation of the nanometer unit with other materials

2. NANOMATERIAL

Nanomaterials are defined as materials with dimensions in the nanometer scale (1 nanometer = 1 meter in 1 billion meters). Nanoparticles can be synthesized by various methods and the relevant methods are shown in Figure 2. These materials have unique physical, chemical and biological properties and exhibit different properties from traditional materials. These materials, which can be controlled at the atomic level, have advantages such as large surface area, increased reactivity and stability in certain environments. The main types of nanomaterials include nanoparticles, nanofibers, nanosheets and nanotubes.

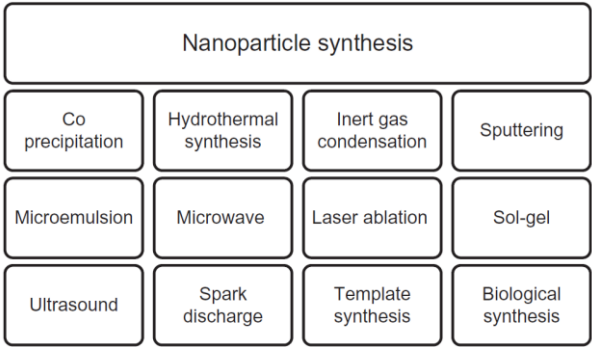


Figure 2. Nanoparticle synthesis methods

Nanomaterials have a wide range of applications in various fields such as medicine, electronics, energy, environment and materials science. In medicine, targeted drug delivery systems and nanomaterials used in cancer treatment are revolutionizing the diagnosis and treatment of diseases. The electronics sector is developing faster and more efficient processors and storage devices. Nanomaterials also play an important role in energy and environmental technologies such as solar panels, batteries and water purification systems. The development of nanomaterials continues rapidly in parallel with the developments in nanotechnology. Scientists are developing new methods and technologies to process materials at the atomic and molecular level. Considering the potential risks of nanomaterials, research is being conducted to ensure safe and sustainable use. In this way, the innovative solutions offered by nanotechnology guide the technologies of the future while trying to minimize the negative effects on the environment and human health.

2.1. Metal Oxide Based Nanomaterials

Metal oxides are crystalline solids containing metal cations and oxide anions. They usually react with water to form bases or with acids to form salts. Most oxides occur in soil, and these oxide minerals typically consist of oxides, hydroxides, oxyhydroxides, and hydrated oxides. Metal oxides are a widely used class of compounds with properties that span various aspects of materials science, physics, and chemistry.

Metals can form a wide variety of oxide compounds. These elements can be synthesized with a variety of structural geometries and a different electronic structure that can exhibit metallic, semiconductor, or insulator properties. Metal oxides have important applications in the electronics, biomedical, and energy sectors due to their physical, chemical, and optical properties. Metal oxides have high adsorption capacities due to their high adsorption capacities and large surface areas. They also have significant advantages in adsorption processes due to their low solubility and small grain diameters.

3. DYESTUFFS AND DYESTUFFS REMOVAL METHODS

Substances that provide a colorful image by chemically bonding to the material to which they are applied are called dyes. There are many different dyes that can be naturally found in nature and synthesized artificially. Dyes that have been used by mankind for many years have come to the present day by being synthesized into more insoluble and complex structures under the influence of the Industrial Revolution. Although they were used specifically in the past in the status or commercial sector, today dyes are used according to people's wishes without any meaning. The use and production of dyes has progressed until today with a focus on consumption and aesthetics, and has been produced using a wide variety of natural and inorganic materials and various synthesis methods until today.

With the Industrial Revolution, dyes obtained from natural materials gave way to special dyes of synthetic origin, and while the variety of colors increased, more durable dyes began to be produced. As this process progressed, the types of dyes produced increased day by day as textiles and other industries developed. However, depending on the development of consumption and dyes, substances that are difficult to process and less decomposable in nature began to be produced. When the use of dyes and the presence of dye waters are evaluated today, it is seen that production and process waters that can disrupt the ecosystem are formed, and that there is a consumption far from the philosophy of sustainability due to consumption. Due to these negativities noticed by consumers and

manufacturers, research on less toxic and biodegradable dyes continues, and the dye sector and the sectors using the sector's products are trying to continue more environmentally friendly activities.

The use of dyes is widespread in various industrial activities such as leather, cosmetics, food, pharmaceutical, paper and textile industries. Since dyes vary from process to process and their usage patterns differ even in facilities performing the same job, laboratory studies should be conducted according to source and process changes in the event of dye wastewater formation and treatment methods should be tested in detail. Dyestuff sources, percentages and types formed according to industrial activities are given in Figure 3.

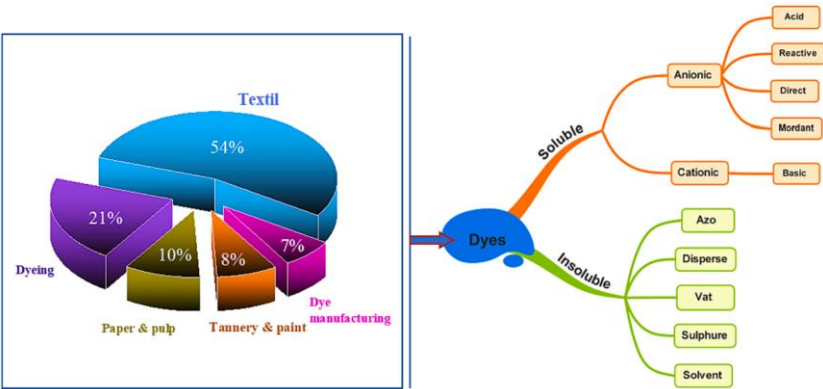


Figure 3. Dyestuff sources, percentages and types by industry

Wastewater containing dyes contains toxic components, color, high organic load and undesirable ions and can cause an ugly appearance and odor in the water environment if released directly to the receiving environment. This wastewater damages water ecosystems, reduces light and oxygen transmission and can lead to the death of living things (Fig 4). For this reason, the discharge of dye-containing wastewater into the receiving environment without treatment is controlled in accordance with legal regulations.

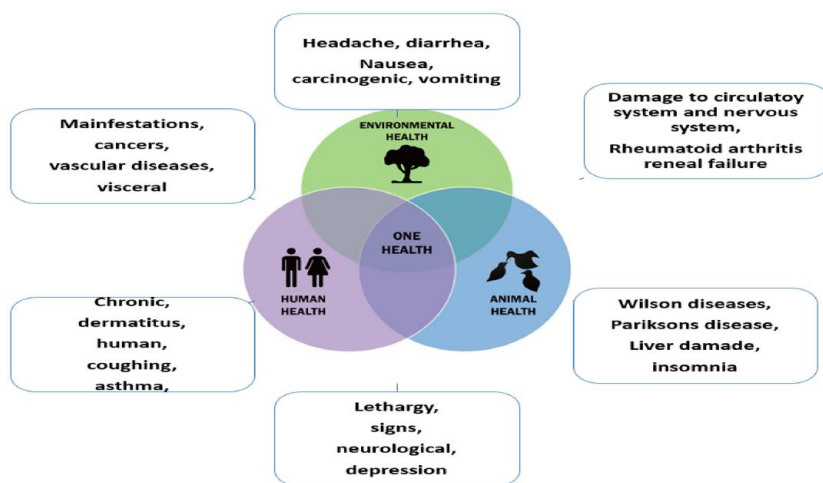


Figure 4. Harmful effects of dyes on living things

Wastewater containing dyes can be treated using physical, chemical and biological methods. Although biological methods are used in the treatment of industrial wastewater, they are not always preferred due to the variability, toxicity and high organic load caused by production. In addition, the need for qualified personnel and energy consumption are disadvantages of biological processes. While pure quality effluent is obtained with filtration techniques, chemical oxidation processes are used to remove colorants. One of the physical-chemical treatment methods, the coagulation-flocculation and sedimentation method, is widely used in industrial water treatment and is effective in the treatment of wastewater containing dyes. In addition, more than one treatment method can be used to produce suitable wastewater depending on the composition of industrial water and discharge standards.

In the treatment of wastewater containing dyes, various advantages and disadvantages of each method vary depending on the process and composition of the wastewater. Research on the treatment of wastewater containing dyes using alternative methods or materials is still ongoing.

4. NANO ADSORBENTS IN DYE REMOVAL

There are more than 100 metals in the periodic table. Metal oxides are formed as a result of the reaction of the relevant metals with oxides. When the literature is examined on dye removal, there are various studies that are widely synthesized

with nickel (Ni), manganese (Mn), copper (Cu), iron (Fe) and zinc (Zn) metals. It has been seen that nano adsorbent synthesis can be carried out by researchers only with metal salts, as well as organic-based materials and cellulose etc.

Ngoc et al. (2022) studied the removal of Congo red dye with Cobalt chromate (CoCr_2O_4) adsorbent, which they synthesized by solvothermal method, and the retention capacity of the adsorbent was determined as 59.4 mg.g^{-1} . Mustafa et al. (2016) studied the removal of Erythrosine with Copper oxide (CuO) adsorbent, which they synthesized by sonochemical method, and a removal value of 93.68% was determined. Yogesh Kumar et al. (2017) studied the removal of Methyl orange with Copper oxide (CuO), which they synthesized by hydrothermal method, and the researchers obtained 93.2% dye removal. Ullah et al. (2017) synthesized nanoadsorbent using Copper oxide (CuO) and cauliflower waste, potato and peas peels waste materials by the precipitation method. Researchers who studied the removal of methyl blue obtained 93.20%, 96.23% and 79.11% removal efficiency with the adsorbents they synthesized separately with cauliflower waste, potato and peas peels waste, respectively.

Yakar et al. (2020) studied the removal of Maxilon Blue GRL dye with Iron oxide (Fe_3O_4) particles synthesized by the precipitation method and determined the adsorption capacity of the synthesized material as 0.23 mg.g^{-1} . Khosravi et al. (2014) studied the removal of reactive yellow dye with Iron oxide (Fe_3O_4) adsorbent synthesized by the hydrothermal method and reached the adsorbent capacity value of 32.5 mg.g^{-1} . Ding et al. (2021) studied the removal of Methyl blue by synthesizing cellulose-added Iron oxide (Fe_3O_4) material by the precipitation method. The researchers determined the adsorption capacity of the synthesized material as 285.71 mg.g^{-1} . AAoh et al. (2018) studied the removal of Bromophenol Blue with Nickel oxide (NiO) nanomaterial by microwave method and reported that the retention capacity of the material was 93.46 mg.g^{-1} .

Cheng et al. (2012) investigated the removal of Congo red dye with Nickel oxide (NiO) material synthesized by precipitation method. As a result of the study, the researchers determined the adsorption capacity of the material they synthesized as 39.7 mg.g^{-1} . Chakrabati et al. (2009) studied the removal of Congo Red with Manganese (III) oxide (Mn_2O_3) nanomaterial synthesized by hydrothermal method and reported that the retention capacity of the material was 38.6 mg.g^{-1} . Qin et al. (2017) studied the removal of Methylene Blue dye with Manganese dioxide (MnO_2) nanomaterial. They determined the adsorbent capacity of the material they synthesized by precipitation method as 627.1 mg.g^{-1} . Noreen et al. (2021) studied the removal of golden yellow with the nanoadsorbent they synthesized by treating Cassia fistula leaf material with Zinc

oxide (ZnO) and the researchers reported the retention capacity of the synthesized material as 57.11 mg.g⁻¹. Badawi et al., 2022 synthesized Zinc oxide (ZnO) nanoparticles by the precipitation method and investigated the removal of azo dyes. Data from relevant studies are given in Table 1.

Table 1. Studies and details investigating dye removal with nano adsorbents

Material	SM*	Dyesuff	AC or RR*	Reference
Cobalt chromate (CoCr ₂ O ₄)	Solvothermal	Congo red	59.4 mg.g ⁻¹	Ngoc et al., 2022
Copper oxide (CuO)	Sonochemical	Erythrosine	93.68%	Mustafa et al., 2016
Copper oxide (CuO)	Hydrothermal	Methyl orange	93.20%	Yogesw Kumar et al., 2017
Copper oxide (CuO) + cauliflower waste	Precipitation	Methyl blue	96.23%	Ullah et al., 2017
Copper oxide (CuO) + potatoes	Precipitation	Methyl blue	87.37%	Ullah et al., 2017
Copper oxide (CuO) + peas peels waste	Precipitation	Methyl blue	79.11%	Ullah et al., 2017
Iron oxide (Fe ₃ O ₄)	Precipitation	Maxilon Blue GRL	0.23 mg.g ⁻¹	Yakar et al., 2020
Iron oxide (Fe ₃ O ₄)	Hydrothermal	Reactive Yellow	32.5 mg.g ⁻¹	Khosravi et al., 2014
Iron oxide (Fe ₃ O ₄) + cellulose beads	Precipitation	Methyl blue	285.71 mg.g ⁻¹	Ding et al., 2021
Nickel oxide (NiO)	Microwave	Bromophenol Blue	93.46 mg.g ⁻¹	AAoh et al., 2018
Nickel oxide (NiO)	Precipitation	Congo Red	39.7 mg.g ⁻¹	Cheng et al., 2012
Manganese (III) oxide (Mn ₂ O ₃)	Hydrothermal	Congo Red	38.6 mg.g ⁻¹	Chakrabati et al., 2009
Manganese dioxide (MnO ₂)	Precipitation	Methylene Blue	627.1 mg.g ⁻¹	Qin et al., 2017
Zinc oxide (ZnO)	Cassia fistula leaf	Golden Yellow	57.11 mg.g ⁻¹	Noreen et al., 2021
Zinc oxide (ZnO)	Precipitation	Azo dyes	-	Badawi et al., 2022

* SM: Synthesis Method, AC: Adsorption Capacity, RR:Removal Ratio

When Table 1 is examined, it is understood that removal is investigated using metal oxides from various dye solutions. In addition, it is seen that precipitation-based methods are more commonly preferred in case of metal oxide synthesis. In addition to the mentioned method, it is observed that microwave-assisted production, hydrothermal and sonochemical methods are also used and synthesis can be carried out with organic-based materials. In addition, when the synthesized materials are evaluated in terms of retention capacities, it is understood that Methylene Blue removal is quite high compared to other studies when

Manganese dioxide (MnO_2) is used with the precipitation method and retention capacities are lower than 100 mg.g^{-1} in the table.

5. RESULTS

Metal oxides are among the widely used adsorbents in recent years. Due to the magnetic properties they contain, they can be separated from the solution by magnets after the removal processes, thus creating a significant usage advantage among active carbon and other used adsorbents. In addition to the related processes, they are important in terms of sustainability due to their usability in adsorbent synthesis together with organic materials and their re-evaluation in waste materials. In the case of evaluating metal oxides in terms of dye removal, there have been various studies carried out in recent years and it has been reported by researchers that removal results with high efficiency have been obtained.

It is thought that in the future, within the scope of green production applications, only materials with inorganic content will not be synthesized and new and improved materials that also include waste materials will be produced. At this stage, while the toxic and environmentally harmful metals in the nanomaterials are replaced by organic-based compounds, the amount of metal to be used in the synthesis of the nanomaterial will also decrease. When evaluated in this context, it is thought that more sustainable and innovative approaches will be realized in this field over time.

REFERENCES

- Ali Mansoori, G., Bastami, T. R., Ahmadpour, A., & Eshaghi, Z. (2008). Environmental application of nanotechnology. *Annual review of nano research*, 439-493.
- Al-Aoh, H. A. (2018). Adsorption performances of nickel oxide nanoparticles (NiO NPs) towards bromophenol blue dye (BB). *Desalin. Water Treat*, 110, 229-238.
- Al-Arjan, W. S. (2022). Zinc oxide nanoparticles and their application in adsorption of toxic dye from aqueous solution. *Polymers*, 14(15), 3086.
- Abbo, H. S., Gupta, K. C., Khaligh, N. G., & Titinchi, S. J. (2021). Carbon nanomaterials for wastewater treatment. *ChemBioEng reviews*, 8(5), 463-489.
- Bhagyaraj, S., Oluwafemi, O. S., Kalarikkal, N., & Thomas, S. (Eds.). (2018). *Synthesis of inorganic nanomaterials: advances and key technologies*.
- Cheng, B., Le, Y., Cai, W., & Yu, J. (2011). Synthesis of hierarchical Ni (OH) ₂ and NiO nanosheets and their adsorption kinetics and isotherms to Congo red in water. *Journal of hazardous materials*, 185(2-3), 889-897.
- Chakrabarti, S., Dutta, B. K., & Apak, R. (2009). Active manganese oxide: a novel adsorbent for treatment of wastewater containing azo dye. *Water Science and Technology*, 60(12), 3017-3024.
- Ding, F., Ren, P., Wang, G., Wu, S., Du, Y., & Zou, X. (2021). Hollow cellulose-carbon nanotubes composite beads with aligned porous structure for fast methylene blue adsorption. *International Journal of Biological Macromolecules*, 182, 750-759.
- Parker, C. (2016). Nanomedicine: How Much Are We Willing to. <https://www.thepipettepen.com/nanomedicine-how-much-are-we-willing-to-pay/>. Accessed: 12.11.2024.
- Hosny, N. M., Gomaa, I., & Elmahgary, M. G. (2023). Adsorption of polluted dyes from water by transition metal oxides: A review. *Applied Surface Science Advances*, 15, 100395.
- Hussain, C. M. (Ed.). (2018). *Handbook of nanomaterials for industrial applications*. Elsevier.
- Ibrahim, R. K., Hayyan, M., AlSaadi, M. A., Hayyan, A., & Ibrahim, S. (2016). Environmental application of nanotechnology: air, soil, and water. *Environmental Science and Pollution Research*, 23, 13754-13788.
- Kamarudin, N. S., Jusoh, R., Setiabudi, H. D., Sukor, N. F., & Shariffuddin, J. H. (2021). Potential nanomaterials application in wastewater treatment: Physical, chemical and biological approaches. *Materials Today: Proceedings*, 42, 107-114.

- Kasbaji, M., Ibrahim, I., Mennani, M., Mohamed, M. M., Salama, T. M., Moneam, I. A., Mbarki, M., Moubarik, A., & Oubenali, M. (2023). Future Trends in Dye Removal by Metal Oxides and Their Nano/Composites: A Comprehensive Review. *Inorganic Chemistry Communications*, 111546.
- Kumar, K. Y., Archana, S., Raj, T. V., Prasana, B. P., Raghu, M. S., & Muralidhara, H. B. (2017). Superb adsorption capacity of hydrothermally synthesized copper oxide and nickel oxide nanoflakes towards anionic and cationic dyes. *Journal of science: advanced materials and devices*, 2(2), 183-191.
- Khosravi, M., & Azizian, S. (2014). Adsorption of anionic dyes from aqueous solution by iron oxide nanospheres. *Journal of Industrial and Engineering Chemistry*, 20(4), 2561-2567.
- Mustafa, G., Tahir, H., Sultan, M., & Akhtar, N. (2013). Synthesis and characterization of cupric oxide (CuO) nanoparticles and their application for the removal of dyes. *African Journal of Biotechnology*, 12(47), 6650-6660.
- Ngoc, P. K., Mac, T. K., Nguyen, H. T., Thanh, T. D., Van Vinh, P., Phan, B. T., Duong, A.T., & Das, R. (2022). Superior organic dye removal by CoCr₂O₄ nanoparticles: adsorption kinetics and isotherm. *Journal of Science: Advanced Materials and Devices*, 7(2), 100438.
- Noreen, S., Ismail, S., Ibrahim, S. M., Kusuma, H. S., Nazir, A., Yaseen, M., ... & Iqbal, M. (2021). ZnO, CuO and Fe₂O₃ green synthesis for the adsorptive removal of direct golden yellow dye adsorption: kinetics, equilibrium and thermodynamics studies. *Zeitschrift Für Physikalische Chemie*, 235(8), 1055-1075.
- Reynolds, T. D., & PA, R. (2011). Çevre Mühendisliğinde Temel İşlemler ve Süreçler. 2. baskı. Çev: Öğütveren ÜB. Ankara: Efil Yayınevi.
- Sadegh, H., Ali, G. A., Gupta, V. K., Makhlouf, A. S. H., Shahryari-Ghoshekandi, R., Nadagouda, M. N., Sillanpää, M., & Megiel, E. (2017). The role of nanomaterials as effective adsorbents and their applications in wastewater treatment. *Journal of Nanostructure in Chemistry*, 7, 1-14.
- Saravanan, A., Kumar, P. S., Hemavathy, R. V., Jeevanantham, S., Jawahar, M. J., Neehaanthini, J. P., & Saravanan, R. (2022). A review on synthesis methods and recent applications of nanomaterial in wastewater treatment: Challenges and future perspectives. *Chemosphere*, 307, 135713.
- Osagie, C., Othmani, A., Ghosh, S., Malloum, A., Esfahani, Z. K., & Ahmadi, S. (2021). Dyes adsorption from aqueous media through the nanotechnology: A review. *Journal of Materials Research and Technology*, 14, 2195-2218.
- Qin, Q., Sun, T., Yin, W., & Xu, Y. (2017). Rapid and efficient removal of methylene blue by freshly prepared manganese dioxide. *Cogent Engineering*, 4(1), 1345289.

- Tan, K. B., Vakili, M., Horri, B. A., Poh, P. E., Abdullah, A. Z., & Salamatnia, B. (2015). Adsorption of dyes by nanomaterials: recent developments and adsorption mechanisms. *Separation and purification technology*, 150, 229-242.
- Tchobanoglous, G., Burton, F., & Stensel, H. D. (2003). *Wastewater engineering: treatment and reuse*. American Water Works Association. Journal, 95(5), 201.
- Thanigaivel, S., Priya, A. K., Gnanasekaran, L., Hoang, T. K., Rajendran, S., & Soto-Moscoso, M. (2022). Sustainable applicability and environmental impact of wastewater treatment by emerging nanobiotechnological approach: Future strategy for efficient removal of contaminants and water purification. *Sustainable Energy Technologies and Assessments*, 53, 102484.
- Ullah, H., Ullah, Z., Fazal, A., & Irfan, M. (2017). Use of vegetable waste extracts for controlling microstructure of CuO nanoparticles: green synthesis, characterization, and photocatalytic applications. *Journal of Chemistry*, 2017(1), 2721798.
- Yakar, A., Ünlü, A., Yeşilçayır, T., & Bıyık, İ. (2020). Kinetics and thermodynamics of textile dye removal by adsorption onto iron oxide nanoparticles. *Nanotechnology for Environmental Engineering*, 5, 1-12.



CHAPTER 13

A General Overview of Recovery of Precious Metals From Electronic Waste

Mirac Nur Ciner¹ & Emine Elmaslar Ozbas² & H. Kurtulus Ozcan³

¹ Res. Asst., Istanbul University-Cerrahpasa, Engineering Faculty, Environmental Engineering, ORCID: 0000-0002-9920-928X

² Prof. Dr., Istanbul University-Cerrahpasa, Engineering Faculty, Environmental Engineering, ORCID: 0000-0001-9065-6684

³ Prof. Dr., Istanbul University-Cerrahpasa, Engineering Faculty, Environmental Engineering, ORCID: 0000-0002-9810-3985

Introduction

In recent years, there has been a growing global awareness regarding environmental pollution and conservation. Societies' efforts to protect natural resources and leave future generations with a better environment have led to the questioning of existing economic and social structures and the development of new environmental protection policies. In this context, the creation of new policies to ensure sustainable and balanced economic and social development has become a necessity, especially in developing countries. As the world population grows, urbanization accelerates, and technological advancements progress, the consumption of electrical and electronic equipment has also rapidly increased. This, in turn, has led to a rise in the volume of waste electrical and electronic equipment (WEEE).

Electronic waste (e-waste) refers to a type of waste that has reached the end of its useful life. E-waste includes discarded devices with electronic systems from a wide range of fields, such as computers, mobile phones, DVDs, industrial electronics, automobiles, lighting, medical devices, and household appliances used in daily life (Marra et al. 2018).

The recyclable resources embedded in e-waste hold an immense economic value of 57 billion USD, surpassing the gross domestic product of numerous countries (Buechler et al. 2020).

In 2019, the global generation of e-waste reached approximately 53.6 million tons (MT), reflecting a 21% rise compared to five years earlier. However, only 17.4% of this e-waste by weight was collected and recycled, leaving valuable metals and high-value recyclable materials unprocessed and discarded (Chancerel & Rotter 2009; Cucchiella et al. 2015; Kiddee et al. 2013).

Over the past few decades, the increased production and usage of electronic devices, especially consumer electronics, have paralleled a rise in e-waste. Recycling e-waste to recover valuable metals and repurpose the waste holds tremendous potential for protecting the environment and fostering economic development by mitigating its harmful effects on nature.

Contracts and Regulations Regarding Electronic Waste

Table 1 provides a comparative view of e-waste laws in different countries.

Table 1. Different laws covering e-waste

Co- untry/Re- gion	Law Names	Year of Publica- tion/ Implemen- tation	Scope
Japan	Law for the Promotion of Resource Reutilization	1991/2001	Personal computers (including CRT or LCD screens, liquid crystal display), small secondary batteries (sealed nickel-cadmium batteries, sealed nickel-hydrogen batteries, lithium secondary batteries, and small sealed lead-acid batteries)
Japan	Home Appliance Recycling Law	1998/2001	Televisions (CRT or LCD), air conditioners, refrigerators and freezers, washing machines and dryers
Japan	Law for Recycling of Small Electrical and Electronic Products	2013	Wired and wireless communication devices, radio and television receivers, photo and audio devices, etc. Total of 28 categories
Republic of Korea	Act on the Promotion of Resources Saving and Recycling	1992/2003	Batteries (mercury, silver oxide, potassium, nickel-cadmium, manganese, and nickel rechargeable batteries), fluorescent lamps
Republic of Korea	Act on the Recycling of Electrical and Electronic Products and Automobiles	2007	TV, refrigerator, washing machine (household), air conditioners (except car air conditioners), personal computers (including monitors and keyboards), etc. Total of 27 categories
European Union	Waste Electrical and Electronic Equipment (WEEE) Directive	2003/2004	Large and small household appliances, IT and telecommunications equipment, consumer equipment, lighting equipment, electronic and electrical tools, toys, leisure and sports equipment, medical devices, monitoring and control instruments, vending machines

Co- untry/Re- gion	Law Names	Year of Publica- tion/ Implemen- tation	Scope
European Union	Restriction of Hazardous Substances (RoHS) Directive	2006	Large and small household appliances, IT and communication equipment, consumer products, lighting equipment, electrical and electronic tools, toys, leisure and sports equipment, medical equipment, test and control instruments, vending machines. Total of 11 categories
European Union	Eco-Design Directive (EuP)	2005/2007	Heating and hot water equipment, electric motor systems, lighting equipment for households and services sector, household appliances, office equipment for homes and services sector, fans, and air conditioners, etc.
European Union	Waste Electrical and Electronic Equipment (New WEEE)	2008/2012	All electrical and electronic products
European Union	WEEELABEX Standard	2011	Formulated ten types of e-waste such as CRT screens, tablet screens, temperature-changing equipment (compressors), and lamps
United States	R2 Certification	2009	Cathode ray tube and stripping, circuit board (batteries, mercury-containing parts, and lead must be removed in advance), batteries, mercury-containing materials, and PCB-containing materials
United States	e-Stewards Certification	2010	On-site disposal security for hazardous waste, electrical and electronic products, and other problematic parts and materials (such as mercury crushing)
China	Administrative Measures on the Prevention and Control of Environmental Pollution from E-Waste	2007	Lead-acid batteries, cadmium-nickel batteries, mercury switches, cathode ray tubes, and PCB capacitors, etc.
China	Regulation on the Recycling and Disposal of Waste Electrical and Electronic Products	2009/2016	TVs, refrigerators, air conditioners, washing machines, vacuum cleaners, computers, printers, fax machines, photocopiers, and telephones

Co- untry/Re- gion	Law Names	Year of Publica- tion/ Implemen- tation	Scope
Turkey	Regulation on the Control of Waste Electrical and Electronic Equipment	26-Dec-22	Covers electrical and electronic equipment designed specifically and assembled to form part of a product that is not within the scope of this Regulation, and which can only function as part of that product. Excludes equipment, weapons, ammunition, and war materials used for national security purposes, except for non-military products
Turkey	Regulation on the Restriction of the Use of Certain Hazardous Substances in Electrical and Electronic Equipment	26-Dec-22	Covers all electrical and electronic equipment except for military, special-purpose medical, renewable energy R&D, and large industrial electrical and electronic equipment

Recovery and Recycling of Electronic Waste

The current WEEE (Waste Electrical and Electronic Equipment) recycling chain consists of three main steps: (i) collection, (ii) pre-treatment, and (iii) recovery. The collection of WEEE is the initial stage of the recycling process and determines the amount of material entering the recovery chain. The successful implementation of a collection strategy requires a high level of consumer awareness (Marra et al. 2018).

WEEE undergoes pre-treatment, where larger valuable and hazardous materials are selectively separated, and its components, as well as material fragments, are processed before being directed to final refining stages. During pre-treatment, reusable parts and hazardous components are removed, which involves disassembly and manual separation. Following this, different material fractions, such as plastics and metals, are separated (Chancerel & Rotter 2009; Cucchiella et al. 2015; Kiddee et al. 2013).

Methods for Recovering Valuable Metals from Electronic Waste

Recovering metals and useful materials from electrical and electronic equipment generally involves chemical processes. Techniques such as ion exchange, solvent extraction, electrochemical methods, and leaching are employed to separate and extract valuable metals from leached solutions.

Hydrometallurgical Recovery Methods

Hydrometallurgical recovery has gained greater usage in recent years compared to pyrometallurgical methods due to its controllability, reliability of results, and predictability. In the hydrometallurgical process, valuable metals from e-waste are selectively separated using acid or caustic leaching. This process generally requires small particle sizes to increase metal yield (Akcil et al. 2015; Hageluken 2006). Certain reactive materials that alter pH are added during the process. Additionally, metals are recovered from their solutions through solvent extraction, which involves the use of organic diluents (Cui & Zhang 2008).

Compared to pyrometallurgical methods, hydrometallurgical techniques have lower initial investment costs, reduced environmental impact, higher metal recovery rates, and are more suitable for small-scale operations. Furthermore, metal losses during physical processes in hydrometallurgical systems are kept at low levels (around 10% to 35%). For these reasons, hydrometallurgical methods have significant potential for metal recovery from WEEE (Gulliani et al. 2023).

Ion Exchange

Ion exchange is a process in which ions from a solution are exchanged with ions of the same polarity on the inner surface of a solid. This occurs as a specialized form of sorption. The mechanism of ion exchange is based on replacing ions in the solution with those originally present in the solid.

Ion exchange shares many characteristics with adsorption and is often viewed as a specific type of sorption since it involves interactions between a solution and a solid surface. Similar models are used to analyze both processes. However, unlike adsorption, which typically involves a unidirectional transfer, ion exchange requires a bidirectional exchange of materials to maintain electroneutrality, making it distinct from adsorption (Raji et al. 2023; Nikonenko et al. 2020).

Electrochemical Methods

Electrochemical processes play a crucial role in refining metals to achieve high purity. Techniques such as electrowinning and electrorefining are commonly employed to separate and recover metals from wastewater. These methods are utilized not only for the primary extraction of metals from ores (electrowinning) but also for refining metals to achieve exceptional purity (electrorefining). Many metals are extracted from wastewater through electrochemical methods that rely on fundamental chemical and electrochemical principles, such as the cathodic

reduction of metal ions on the cathode of an electrolytic cell. Electrefining is typically conducted using aqueous electrolytes or molten salts (Rai et al. 2021).

Leaching Method

Leaching solvents mainly include substances like H_2SO_4 and H_2O_2 , HNO_3 , NaOH , and HCl (Chancerel et al. 2009; Cucchiella et al. 2015; Kiddee et al. 2013). Leaching involves the extraction of a soluble component from a solid using a solvent, often referred to as a lixiviant. The material to be leached must be finely ground to release the component. Additionally, a fine particle size increases the reaction rate during leaching. Some of the key factors to consider in the leaching process include:

1. The chemical and physical characteristics of the material to be leached.
2. The corrosive effects of the reagent on the construction materials of the leaching vessels.
3. The selectivity of the leaching for the desired component.
4. The feasibility of recycling the leaching reagent, which is crucial both economically and environmentally.

The selectivity of a leaching agent for a specific component in the waste material depends on several factors, such as the concentration of the leaching agent, temperature, and contact time (Koizhanova et al. 2023).

The Positive Environmental Impacts of Recovering Valuable Metals from Electronic Waste

One of the most prominent environmental impacts of mining activities is the alteration of natural landscapes. Mining operations require the removal of large areas of topsoil, leaving these lands barren for extended periods. Additionally, the storage of extracted soil and mining waste (often referred to as overburden) can lead to the formation of massive and unstable structures. These structures not only transform the natural landscape but also impose significant stress on the rock formations beneath, presenting various risks (Blanche et al. 2024).

Acid mine drainage (AMD) is another major environmental concern, as it contains high acidity and heavy metal concentrations. Once AMD begins, it is difficult to stop and control. The result is contamination of surface and groundwater, and the remediation of polluted water is highly costly (Acharya & Kharel 2020; U.S. EPA 2023; Rodríguez-Galán et al. 2019).

Mining, by its nature, is a process with inherent negative environmental impacts. Accidents at mining sites can result in significant disasters, affecting both the environment and human health. However, if efforts are focused on recovering valuable metals from e-waste and investments are directed toward this area, the negative effects of mining on the environment and human health can be substantially reduced. Recycling e-waste facilitates the sustainable recovery of valuable metals, contributing to the conservation of natural resources. This method helps mitigate environmental damages associated with mining, such as habitat destruction, water, and soil pollution, while also promoting energy savings. Extracting metals from e-waste requires significantly less energy compared to traditional mining operations.

In addition to environmental benefits, recycling e-waste also contributes to the economy. The recovery of valuable metals helps reduce mining costs and ensures that these metals originate from more sustainable and ethical sources. This approach not only addresses waste management challenges but also encourages the use of renewable resources.

In this context, it is essential for governments and the private sector to invest in e-waste recycling projects, support innovative technologies in this field, and raise public awareness. By doing so, the environmental impact of valuable metal recovery can be minimized, and the economic benefits maximized.

Conclusions

In conclusion, the effective management and recycling of e-waste represents a critical opportunity to advance both environmental sustainability and economic development. By leveraging advanced hydrometallurgical processes, the recovery of valuable metals from e-waste can be achieved with greater efficiency, thereby mitigating the environmental and ecological consequences associated with traditional mining methods. Conventional mining often leads to significant habitat destruction, pollution, and excessive energy consumption, highlighting the urgency of transitioning to e-waste recycling as a sustainable alternative. This shift not only conserves finite natural resources but also addresses broader concerns related to environmental degradation and energy inefficiency inherent in mining operations.

Furthermore, the promotion of e-waste recycling has the potential to stimulate economic growth by generating employment opportunities and fostering the development of industries focused on renewable and sustainable resource utilization. Realizing this significant transformation necessitates a collaborative effort involving governments, private enterprises, and academic institutions to

invest in cutting-edge recycling technologies, develop robust infrastructure, and enhance public understanding of the importance of e-waste management. A systemic approach that incorporates financial incentives, policy support, and public education is essential to drive widespread adoption.

By embracing sustainable practices in e-waste recycling, societies can reduce the environmental footprint of metal recovery processes while maximizing economic benefits. This transformative approach not only aligns with global sustainability goals but also ensures a resilient and resource-efficient future for subsequent generations. Such initiatives enable the harmonization of environmental responsibility and economic progress, laying the groundwork for a circular economy that emphasizes the sustainable use of resources and the preservation of ecological balance.

References

- Acharya, B. S., & Kharel, G. (2020). Acid mine drainage from coal mining in the United States—an overview. *Journal of Hydrology*, 588, 125061.
- Akcil, A., Erust, C., Gahan, C. S., Ozgun, M., Sahin, M., & Tuncuk, A. (2015). Precious metal recovery from waste printed circuit boards using cyanide and non-cyanide lixivants—a review. *Waste Management*, 45, 258-271.
- Blanche, M. F., Dairou, A. A., Juscar, N., Romarice, O. M. F., Arsene, M., Bernard, T. L., & Leroy, M. N. L. (2024). Assessment of land cover degradation due to mining activities using remote sensing and digital photogrammetry. *Environmental Systems Research*, 13(1), 41.
- Buechler, D. T., Zyaykina, N. N., Spencer, C. A., Lawson, E., Ploss, N. M., & Hua, I. (2020). Comprehensive elemental analysis of consumer electronic devices: Rare earth, precious, and critical elements. *Waste Management*, 103, 67-75.
- Chancerel, P., & Rotter, V. S. (2009, May). Assessing the management of small waste electrical and electronic equipment through substance flow analysis—the example of gold in Germany and the USA. In 2009 IEEE International Symposium on Sustainable Systems and Technology (pp. 1-6). IEEE.
- Cucchiella, F., D’Adamo, I., Koh, S. L., & Rosa, P. (2015). Recycling of WEEEs: An economic assessment of present and future e-waste streams. *Renewable and Sustainable Energy Reviews*, 51, 263-272.
- Cui, J., & Zhang, L. (2008). Metallurgical recovery of metals from electronic waste: A review. *Journal of Hazardous Materials*, 158(2-3), 228-256.
- Gulliani, S., Volpe, M., Messineo, A., & Volpe, R. (2023). Recovery of metals and valuable chemicals from waste electric and electronic materials: a critical review of existing technologies. *RSC Sustainability*, 1(5), 1085-1108.
- Hagelucken, C. (2006, May). Improving metal returns and eco-efficiency in electronics recycling—a holistic approach for interface optimisation between pre-processing and integrated metals smelting and refining. In *Proceedings of the 2006 IEEE International Symposium on Electronics and the Environment*, 2006. (pp. 218-223). IEEE.
- Kiddee, P., Naidu, R., & Wong, M. H. (2013). Electronic waste management approaches: An overview. *Waste management*, 33(5), 1237-1250.
- Koizhanova, A., Kenzhaliyev, B., Magomedov, D., Kamalov, E., Yerdenova, M., Bakrayeva, A., & Abdylidayev, N. (2023). Study of factors affecting the copper ore leaching process. *ChemEngineering*, 7(3), 54.
- Marra, A., Cesaro, A., & Belgiorno, V. (2018). The recovery of metals from WEEE: State of the art and future perspectives. *Global Nest Journal*, 20(4), 679-694.

- Nikonenko, V., Urtenov, M., Mareev, S., & Pourcelly, G. (2020). Mathematical modeling of the effect of water splitting on ion transfer in the depleted diffusion layer near an ion-exchange membrane. *Membranes*, 10(2), 22.
- Rai, V., Liu, D., Xia, D., Jayaraman, Y., & Gabriel, J.-C. P. (2021). Electrochemical approaches for the recovery of metals from electronic waste: A critical review. *Recycling*, 6(3), 53.
- Raji, Z., Karim, A., Karam, A., & Khalloufi, S. (2023). Adsorption of heavy metals: mechanisms, kinetics, and applications of various adsorbents in wastewater remediation—a review. *Waste*, 1(3), 775-805.
- Rodríguez-Galán, M., Baena-Moreno, F. M., Vázquez, S., Arroyo-Torralvo, F., Vilches, L. F., & Zhang, Z. (2019). Remediation of acid mine drainage. *Environmental Chemistry Letters*, 17, 1529-1538.
- U.S. Environmental Protection Agency (EPA). (2023). Abandoned Mine Drainage.



CHAPTER 14

Theoretical Perspective on the Production and Biocompatibility of Metal-Reinforced PLA Composites

İbrahim Baki Şahin⁴ & İhsan Korkut⁵

⁴Ahi Evran University, Faculty of Engineering and Architecture, Department of Mechanical Engineering, Kırşehir, Turkey. ORCID ID: 0000-0001-8090-9748

⁵Gazi University, Faculty of Technology, Department of Manufacturing Engineering, Ankara, Turkey. ORCID ID: 0000-0002-5001-4449

Introduction

The advancements in biomedical engineering have significantly highlighted the necessity for innovative materials and manufacturing techniques that enhance human health and quality of life. Among these materials, bioresorbable polymers, particularly polylactic acid (PLA), have gained prominence due to their environmentally friendly and biocompatible nature. PLA is widely utilized in various biomedical applications, including orthopedic implants and surgical sutures, owing to its favorable degradation properties in biological environments [1, 2]. However, the mechanical strength and thermal stability of PLA are often inadequate for certain applications, which can limit its performance [3].

To overcome these limitations, the development of metal-reinforced PLA composites has emerged as a promising solution. The incorporation of metal reinforcements into PLA significantly enhances its mechanical and thermal properties, thereby expanding its applicability in biomedical fields. Studies have shown that metal reinforcements can improve tensile and compressive strength, elastic modulus, and impact resistance, leading to composites that exhibit superior structural and functional performance [4, 5]. Furthermore, the biocompatibility and biodegradation behavior of these composites are critical factors that warrant thorough investigation. The interactions between metal particles and biological systems, as well as the effects of degradation products on biocompatibility, are essential for ensuring the safety and efficacy of these materials in medical applications [1, 6].

The production techniques for metal-reinforced PLA composites are varied and play a crucial role in determining the final properties of the material. Techniques such as extrusion and injection molding are commonly employed, and optimizing production parameters is vital for achieving desired mechanical and thermal characteristics [7, 8]. Additionally, microstructural characterization and mechanical performance analyses are integral to understanding how metal reinforcements can enhance the resilience and functionality of PLA composites. For instance, the incorporation of metal nanoparticles has been shown to improve the thermal stability of PLA composites, which is essential for maintaining performance under physiological conditions [5, 9].

A significant aspect of this study involves evaluating the biocompatibility of metal-reinforced PLA composites. Biocompatibility is defined by the material's acceptability by the human body and its non-toxicity to biological systems. Theoretical biocompatibility tests, cell culture experiments, and biodegradation analyses are essential to assess how these composites interact with biological

environments [1, 6]. The degradation of PLA and its composites can influence the pH of the surrounding medium, potentially affecting cell viability and function [7, 10]. Therefore, understanding the degradation mechanisms and the resultant biological interactions is crucial for the safe application of metal-reinforced PLA composites in clinical settings.

In conclusion, the exploration of metal-reinforced PLA composites presents a significant opportunity for advancements in biomedical applications. The theoretical foundations of production techniques, mechanical performance analyses, and biocompatibility evaluations provide a comprehensive framework for understanding the potential of these materials. Future research directions should focus on optimizing composite formulations and production methods to further enhance the properties of PLA composites, ensuring their viability in various biomedical applications such as orthopedic implants, dental materials, and tissue engineering [1, 3].

Chapter 1: Production Methods of Metal-Reinforced PLA Composites: Theoretical Approaches

1.1 Introduction and Overview

The exploration of metal-reinforced polylactic acid (PLA) composites has gained significant traction in biomedical applications due to their enhanced mechanical properties, which are crucial for the development of effective biomedical implants, tissue engineering scaffolds, and surgical sutures. The production methods for these composites are pivotal, as they directly influence the microstructure, mechanical properties, and biocompatibility of the final products.

Various production techniques are employed to fabricate metal-reinforced PLA composites, including melt blending, 3D printing, and extrusion methods. For instance, the incorporation of metal particles, such as stainless steel fibers, has been shown to significantly enhance the tensile strength and modulus of PLA composites, making them suitable for demanding biomedical applications [11]. The optimization of these production processes is essential to achieve the desired mechanical properties and ensure uniform distribution of metal reinforcements within the PLA matrix [12]. Additionally, the processing parameters, such as temperature and mixing time, play a crucial role in determining the interfacial bonding between the metal particles and the PLA matrix, which can affect the overall performance of the composite [13].

The theoretical foundations of these production methods involve understanding the interactions between the PLA matrix and the metal reinforcements at the molecular level. For example, studies have indicated that the mechanical properties of PLA composites can be significantly improved through the use of compatibilizers that enhance the interfacial adhesion between the PLA and metal particles [14]. Furthermore, the microstructural characterization of these composites, using techniques such as scanning electron microscopy (SEM) and X-ray diffraction (XRD), provides insights into the dispersion of metal particles and the crystallinity of the PLA matrix, which are critical for optimizing the mechanical performance [15].

Biocompatibility is another crucial aspect that must be addressed when developing metal-reinforced PLA composites for biomedical applications. The presence of metal particles can influence the degradation behavior of PLA, which in turn affects its biocompatibility. Theoretical studies suggest that the degradation products from PLA and the metal reinforcements can have varying effects on cell viability and proliferation, necessitating thorough biocompatibility assessments [16]. Moreover, the incorporation of biocompatible metal particles, such as hydroxyapatite, has been shown to enhance the interaction between the composite and biological tissues, promoting better integration and functionality in medical applications [17].

In conclusion, the production methods and theoretical foundations of metal-reinforced PLA composites are critical for enhancing their mechanical properties and biocompatibility, thereby expanding their potential applications in the biomedical field. Future research should focus on refining these production techniques and exploring new metal reinforcements to further improve the performance of PLA composites in various medical applications.

1.2 Materials Used in the Production of Metal-Reinforced PLA Composites

1.2.1 Polylactic Acid (PLA)

PLA is a biodegradable, biocompatible, and environmentally friendly polymer obtained from renewable sources such as corn starch, sugarcane, or potatoes. Its chemical structure and biodegradability make it widely applicable in biomedical fields. However, PLA's mechanical strength and thermal stability may be insufficient for certain applications, thereby necessitating reinforcement with metals [18].

1.2.2 Metal Reinforcements

Metal reinforcements are used to enhance the mechanical and thermal strength of PLA. Commonly used metals include biocompatible options such as gold, silver, titanium, and iron. The particle size, shape, and surface properties of these metals play a crucial role in determining the final properties of the composite [19]. Table 1, where the metals used in metal-reinforced PLA composites are provided.

Table 1. Metals Used in Metal-Reinforced PLA Composites [12].

Metal Type	Particle Size	Shape	Surface Properties	Pro-	Biocompati-
Gold	Nano	Spherical	Surface Functionalized	bility	High
Silver	Micro	Irregular	Surface Functionalized		Medium
Titanium	Nano	Spherical	Surface Functionalized		High
Iron	Micro	Irregular	Surface Functionalized		Medium

1.3 Production Methods

1.3.1 Extrusion Method

The extrusion method is widely used for producing metal-reinforced PLA composites. In this technique, PLA and metal particles are mixed in specific ratios and melted through an extruder at high temperatures, followed by a molding process. Theoretically, the homogeneous distribution of metal particles enhances the mechanical strength and thermal properties of the composite. Additionally, parameters such as the temperature and speed of the extruder affect the microstructure and physical properties of the final material [20]. Fig. 1 presents a schematic representation of metal-reinforced PLA composites produced by the extrusion method.

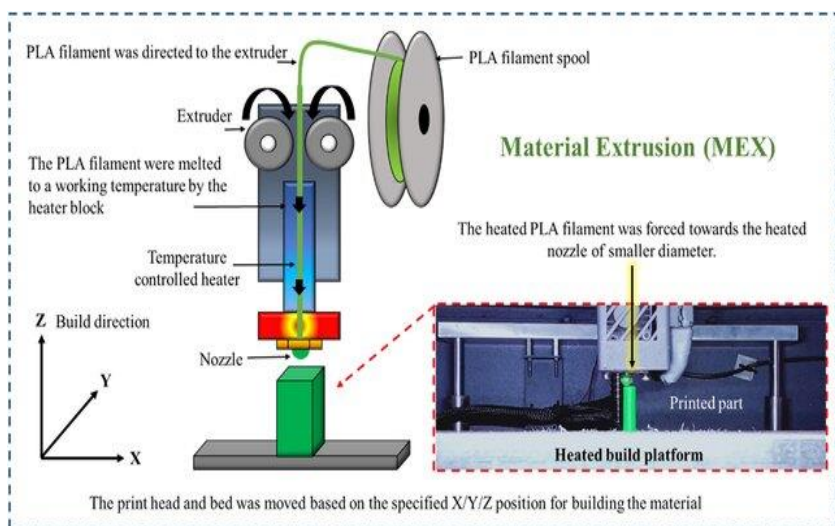


Fig.1. Schematic Representation of Metal-Reinforced PLA Composites Produced by Extrusion Method [20].

1.3.2 Solution Casting Method

The solution casting method is another important technique for producing metal-reinforced PLA composites. Here, PLA and metal particles are dissolved in a solvent, and thin films, fibers, or other shapes are obtained from this solution. Upon evaporation of the solvent, metal particles are homogeneously distributed within the PLA matrix. Theoretically, this method allows control over particle surface properties and distribution, improving the mechanical and biocompatibility attributes of the composite [21]. Fig. 2 illustrates the solvent casting method scheme.

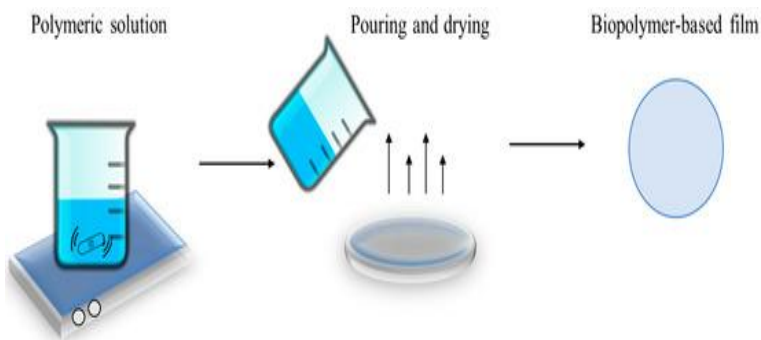


Fig.2. Solvent casting method scheme [22].

1.3.3 Electrospinning Method

The electrospinning method is used to produce nanofiber-based metal-reinforced PLA composites. In this process, the PLA and metal particle solution is drawn into thin nanofibers under high voltage. Electrospinning offers a significant advantage in controlling the structure and surface properties of PLA nanofibers. Theoretically, the uniform distribution of metal particles and the high surface area of nanofibers can enhance cell interactions and biocompatibility of the composite [23]. Fig. 3 shows an SEM image of nanofibers produced by the electrospinning method.

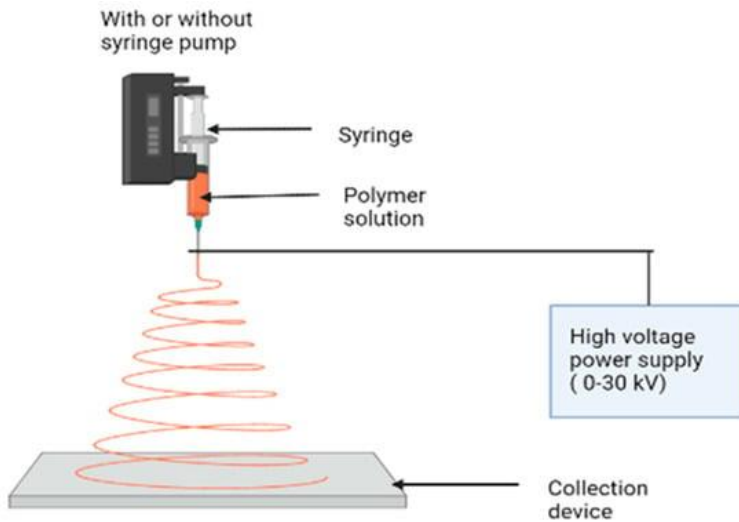


Fig.3. SEM Image of Nanofibers Produced by Electrospinning Method [23].

1.3.4 Compression Molding Method

Compression molding is another important method for producing metal-reinforced PLA composites. In this method, metal particles are mixed with PLA powder and then molded under high pressure and temperature. Theoretically, high-density composites obtained through compression molding exhibit superior mechanical strength and structural integrity [24]. Table 2 shows a comparison of production methods.

Table 2. Comparison of Production Methods [25].

Production Method	Mechanical Strength	Thermal Stability	Homogeneous Distribution	Production Method
Extrusion	High	Medium	Good	Extrusion
Solution Casting	Medium	High	Very Good	Solution Casting
Electrospinning	Very High	Medium	Excellent	Electrospinning
Compression Molding	High	High	Good	Compression Molding

1.4 Distribution of Metal Reinforcements at Micro and Nano Scales

The homogeneous distribution of metal particles within the PLA matrix directly affects the final properties of the composite. A uniform distribution ensures superior performance in terms of mechanical strength, thermal stability, and biocompatibility. Theoretically, critical parameters such as particle size, particle-matrix interface, and mixing techniques must be carefully controlled to achieve this goal [26, 27].

Particle Size and Shape	Particle-Matrix Interface	Mixing Techniques
<ul style="list-style-type: none">•The size and shape of the metal particles play a key role in determining the properties of the composite. Nano-scale metal particles offer a larger surface area, enabling more effective interaction with the PLA matrix.	<ul style="list-style-type: none">•The quality of the particle-matrix interface affects the mechanical integrity of the composite. Theoretically, improving the surface properties of metal particles is crucial for strengthening interfacial bonds	<ul style="list-style-type: none">•Effective mixing techniques are essential for achieving a uniform distribution of metal particles. Advanced mixing techniques, such as ultrasonic mixing and high-shear mixing, ensure the even distribution of particles and high-performance of the composite

1.5 Optimization of Production Parameters

In the production of metal-reinforced PLA composites, parameters like temperature, pressure, solution concentration, and mixing speeds are of great importance. Theoretically, optimizing these parameters can lead to significant improvements in the microstructural and mechanical properties of the composite [28].

- **Temperature and Pressure**
- Temperature and pressure are critical parameters concerning the melting of PLA and the distribution of metal particles.
- Appropriate temperature and pressure values ensure the homogeneous microstructure and mechanical strength of the composite.
- **Solution Concentration and Mixing Speed**
- Solution concentration and mixing speed are important for ensuring even particle distribution and good bonding with the PLA matrix.
- Optimum mixing speed and solution concentration result in high-performance metal-reinforced PLA composites.

Chapter 2: Theoretical Mechanical and Thermal Properties of Metal-Reinforced PLA Composites

2.1 Introduction

Metal-reinforced PLA (Polylactic Acid) composites play a significant role in biomedical engineering to provide robustness and durability. In this chapter, we will delve into the theoretical mechanical and thermal properties of these composites. The distribution of metal particles within the PLA matrix significantly impacts the final properties of these composites.

2.2 Mechanical Properties

Reinforcing PLA with metal particles is essential to enhance its brittleness and increase its durability, thereby making it more suitable for demanding biomedical applications. This reinforcement not only improves the mechanical properties of PLA, such as tensile strength and impact resistance, but also enhances its thermal stability and biocompatibility. By incorporating metal particles, the composite material can better withstand the mechanical stresses and environmental

conditions encountered in medical settings, ultimately extending the lifespan and performance of biomedical devices and implants [29].

2.2.1 Tensile Strength

Theoretically, homogeneous distribution of metal particles within the PLA matrix increases tensile strength. This results in higher values in stress and strain curves obtained from tensile tests. The binding strength of metal particles and interfacial forces are the main factors determining this tensile strength [29]. Fig. 4 illustrates the setup for tensile testing of metal-reinforced PLA composites and Table 3 details how different metal particle distributions affect the tensile strength in a PLA matrix.

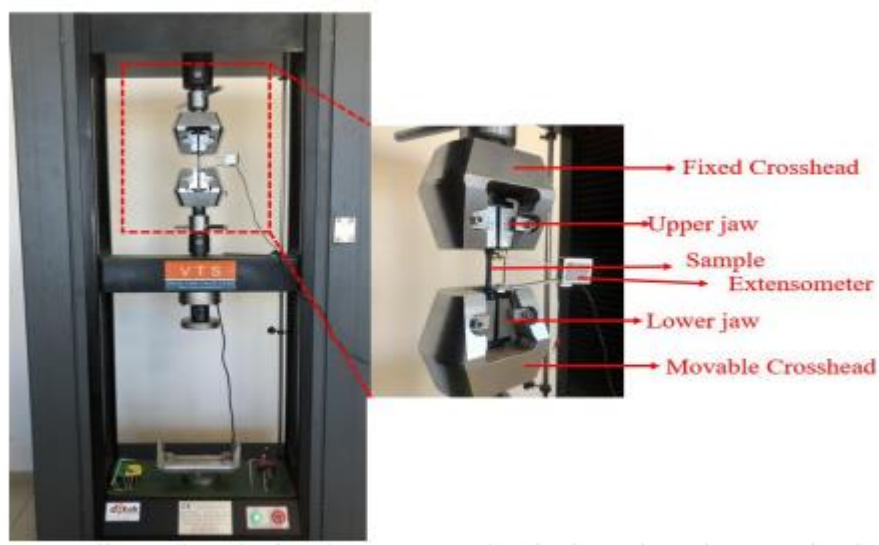


Fig.4.Schematic Representation of Tensile Testing of Metal-Reinforced PLA Composites

Table 3. Effect of Metal Particle Distribution on Tensile Strength in PLA Matrix[29]

Particle Size	Tensile Strength (MPa)
Nano	55
Micro	45

2.2.2 Impact Resistance

Metal-reinforced PLA composites also show significant improvements in impact resistance. Theoretically, metal particles absorb the impact energy, preventing the material from breaking. The increased energy distribution during impact provided by metal particles ensures the composite's structural integrity [30].

2.2.3 Hardness

The hardness values of metal-reinforced PLA composites are higher than that of pure PLA. Theoretically, integrating metal particles into the matrix enhances the elastic modulus of the material, thereby improving hardness performance [30].

2.2.4 Fatigue Resistance

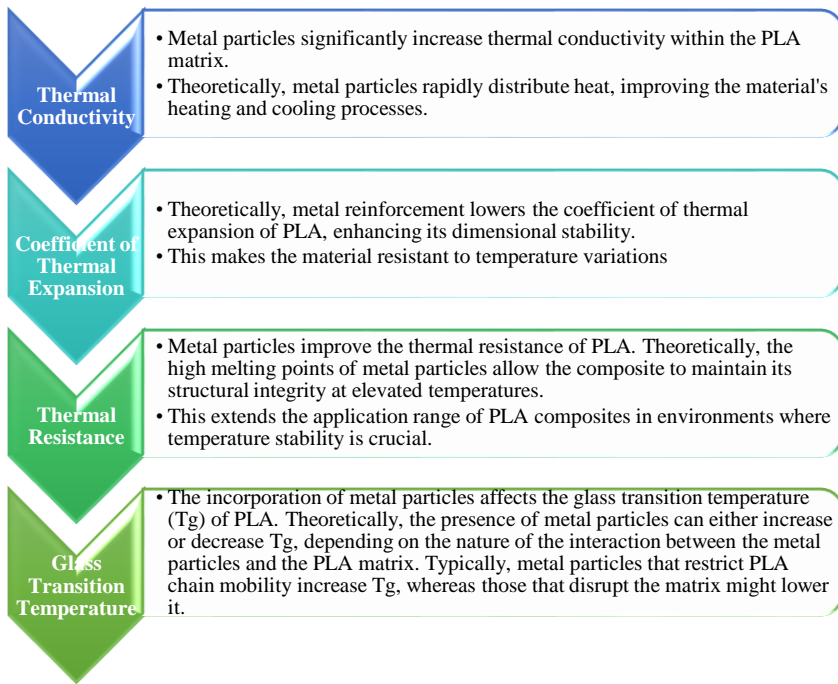
Under repeated loading, the fatigue resistance of metal-reinforced PLA composites demonstrates superior properties compared to pure PLA. Theoretically, metal particles prevent the formation of fatigue cracks, thereby extending the composite's lifespan [31].

Table 4. Mechanical Properties of Metal-Reinforced PLA Composites [31].

Metal Type	Tensile Strength (MPa)	Impact Resistance (kJ/m²)	Hardness (HV)	Fatigue Resistance (S-N Curve)
Gold	50	15	60	High
Silver	45	12	55	Medium
Titanium	55	18	65	High
Iron	48	14	58	Medium

2.3 Thermal Properties

The thermal properties of metal-reinforced PLA composites provide significant advantages over pure PLA. These composites exhibit high thermal conductivity, wide temperature resistance, and excellent thermal stability [32].



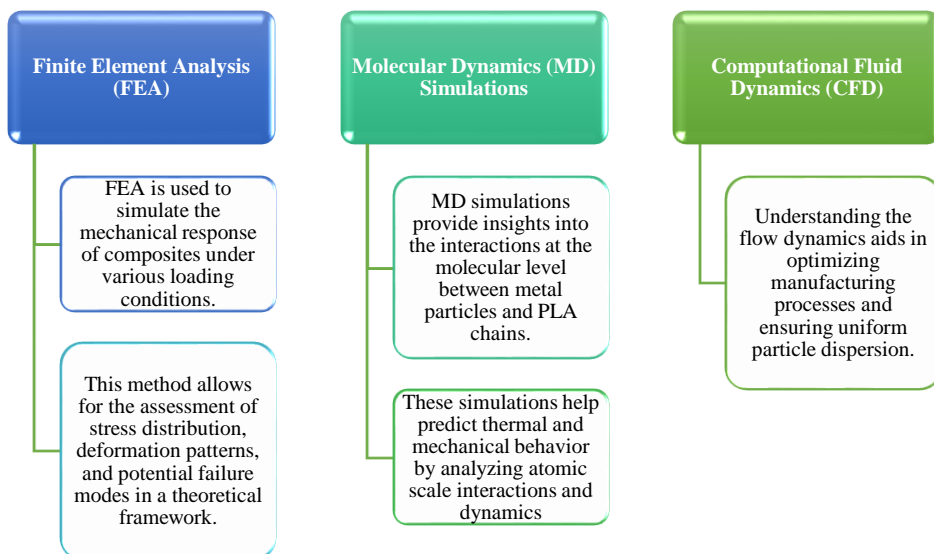
2.4 Theoretical Modeling and Simulation

Theoretical models and simulations play a pivotal role in understanding and predicting the properties of metal-reinforced PLA composites. Table 5 shows this properties

Table 5. the properties of metal-reinforced PLA composites

Factor	Description	Key References
Particle Size and Distribution	Smaller particles provide a larger surface area, improving bonding at the interface, thereby enhancing tensile strength and impact resistance. Uniform distribution ensures stress is evenly distributed, preventing localized failures and enhancing fatigue resistance.	[33, 34]
Interfacial Bonding	A strong interface between metal particles and the PLA matrix is crucial for effective load transfer during mechanical stress. Compatibilizers can enhance this bonding, improving overall composite performance.	[35, 36]
Thermal Conductivity	Metal particles increase the thermal conductivity of the composite, aiding in more effective heat dissipation, crucial for temperature-sensitive applications.	[37]
Crystallinity	Metal reinforcements can act as nucleating agents, affecting PLA's crystallization, enhancing thermal stability and mechanical strength.	[38, 39]

Table 6. Analytical Methods for PLA Analysis[40-42]



Chapter 4: Clinical Applications and Future Outlook: A Theoretical Perspective

Metal-reinforced PLA (Polylactic Acid) composites are promising materials in the biomedical engineering domain, offering a wide range of clinical applications. Their unique mechanical and biocompatibility properties make them ideal for use in medical devices, implants, and tissue engineering. In this chapter, we will explore the clinical applications of metal-reinforced PLA composites and future research directions from a theoretical perspective.

4.2 Clinical Applications

The clinical applications of metal-reinforced polylactic acid (PLA) composites are indeed diverse, owing to their mechanical durability, biocompatibility, and customizable properties. Theoretical analyses have evaluated the potential of these materials in various medical applications, highlighting their suitability for use in biodegradable surgical sutures, bone fixation devices, and stents. One significant application of metal-reinforced PLA composites is in the development of biodegradable surgical sutures. PLA is recognized for its favorable mechanical properties, including an elastic modulus of 3,000–4,000 MPa and tensile strength of 50–70 MPa, making it an excellent candidate for sutures that require both strength and biocompatibility [43]. The incorporation of metal particles can further enhance these properties, providing

additional strength and durability, which are critical for maintaining the integrity of sutures during the healing process. In the context of bone fixation devices, metal-reinforced PLA composites have shown promise due to their ability to support mechanical loads while being biocompatible and biodegradable. The addition of metal reinforcements can improve the mechanical strength of PLA, making it suitable for applications such as screws, plates, and pins used in orthopedic surgery [44]. The theoretical analyses suggest that these composites can effectively promote bone healing while gradually degrading in the body, thus eliminating the need for a second surgery to remove the implants.

Table 7. Clinical Applications of Metal-Reinforced PLA Composites [45]

Application Area	Metal Used	Mechanical Properties	Biocompatibility	Clinical Advantages
Orthopedic Implants	Titanium	High	High	Bone-Like Properties
Tissue Engineering	Gold	Medium	High	Cell Proliferation
Dental Implants	Silver	Medium	Medium	Gingival Compatibility
Cardiovascular Stents	Iron	High	Medium	Blood Circulation

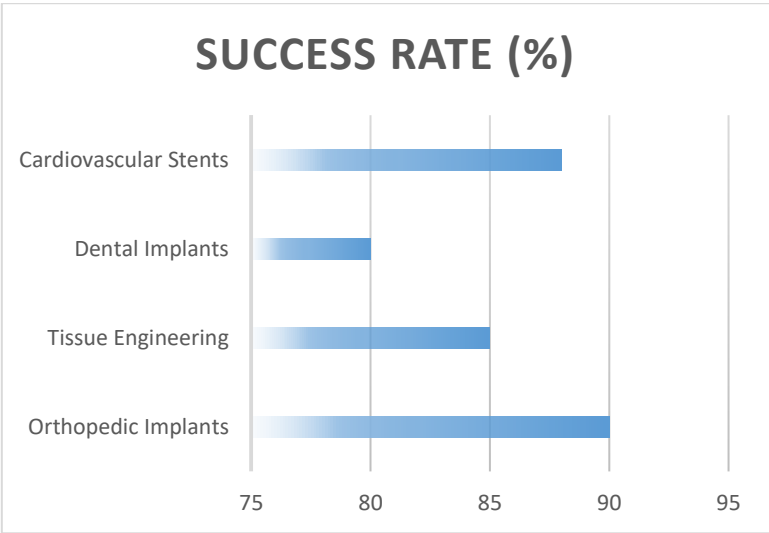


Fig.5. Success Rates of Metal-Reinforced PLA Composites in Different Clinical Applications [45].

4.2.1 Orthopedic Implants

Metal-reinforced PLA composites are used in orthopedic implants due to their bone-like mechanical properties and compatibility with bone tissue. Theoretical models analyze the load-bearing capacities of these implants and their interactions with surrounding tissues [46].

Table 8. Theoretical Models and Case Studies for Metal-Reinforced PLA Composite Orthopedic Implants [46].

Category	Description
Theoretical Model	Finite Element Analysis (FEA) can be used to analyze the load-bearing capacity and mechanical durability of orthopedic implants. This model simulates the stress and deformation behavior of the implant under various loads.
Parameters	Material properties of the implant (elastic modulus, Poisson's ratio), loading conditions (static and dynamic loads), and implant-bone interface properties are considered.
Example	Metal-reinforced PLA composites can be used in orthopedic implants such as knee prostheses, hip prostheses, and spinal fixation devices. For instance, in knee prostheses, metal-reinforced PLA composites enhance load-bearing capacity and extend the lifespan of the implant due to their bone-like mechanical properties.
Case Study	In a knee prosthesis surgery using metal-reinforced PLA composites, the post-operative recovery process and implant performance can be examined. This case study could evaluate the biocompatibility and mechanical durability between the patient's bone tissue and the implant.

4.2.2 Tissue Engineering

In tissue engineering applications, metal-reinforced PLA composites serve as scaffolding and biodegradable materials. Theoretical studies are used to evaluate the performance of these composites in cell proliferation and tissue regeneration processes [47].

Table 9. Theoretical Models and Case Studies for Metal-Reinforced PLA Composite Scaffolds in Tissue Engineering

Category	Description
Theoretical Model	Biomechanical models can be used to analyze cell proliferation and tissue regeneration processes in tissue engineering applications. These models simulate the behavior of cells on the scaffold and tissue formation.
Parameters	Biodegradation rate of the scaffold material, cell adhesion and proliferation rates, and biochemical factors necessary for tissue formation are considered.
Example	Metal-reinforced PLA composites can serve as scaffold materials in bone and cartilage tissue engineering. These scaffolds provide a suitable environment for cell adhesion, proliferation, and differentiation.
Case Study	In the treatment of a bone fracture using a metal-reinforced PLA composite scaffold, the processes of cell proliferation and tissue regeneration can be studied. This case study could assess the biodegradation rate of the scaffold material and the formation of new bone tissue.

4.2.3 Dental Implants

For dental implants, metal-reinforced PLA composites stand out due to their compatibility with gingival tissue and jawbone. Theoretical analyses assess their durability and biocompatibility, ensuring reliability in dental implants [48].

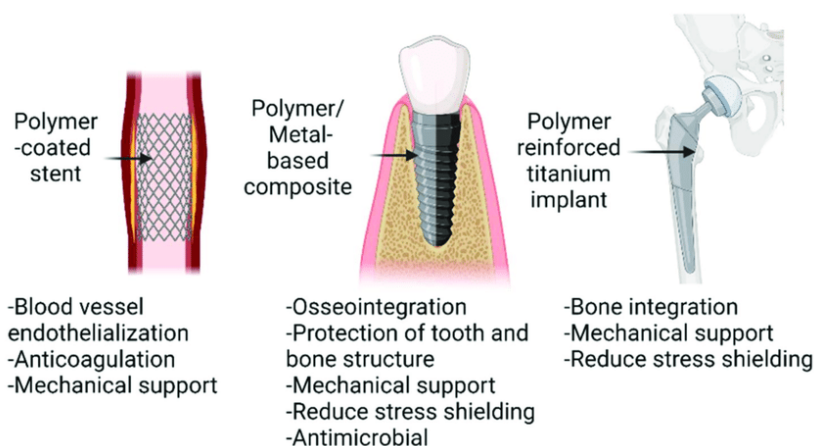


Fig.6. Use of Metal-Reinforced PLA Composites as Dental Implants

Table 10. Theoretical Models and Case Studies for Metal-Reinforced PLA Composite Dental Implants

Category	Description
Theoretical Model	Biomechanical and biomaterial models can be used to analyze the integration and biocompatibility of dental implants with the jawbone. These models simulate the interaction between the implant and bone tissue and biological responses.
Parameters	Material properties of the implant, properties of the jawbone, depth and angle of implant placement, and biological responses (inflammation, osseointegration) are considered.
Example	Metal-reinforced PLA composites can be used in dental applications such as dental root implants and dental prostheses. These composites are compatible with gingival tissue and jawbone, providing durable and long-lasting implants.

Case Study	In a dental root implant surgery using metal-reinforced PLA composites, the durability and biocompatibility of the implant can be evaluated. This case study could assess the integration of the implant with the jawbone and its compatibility with gingival tissue.
-------------------	---

4.2.4 Cardiovascular Stents

Metal-reinforced PLA composite stents are used to reopen and maintain the patency of blood vessels. Theoretical models examine the biomechanical behavior of these stents and their biocompatibility, evaluating their impact on blood circulation [49].

Table 11. Theoretical Models and Case Studies for Metal-Reinforced PLA Composite Cardiovascular Stents

Category	Description
Theoretical Model	Biomechanical models can be used to analyze the behavior and biocompatibility of cardiovascular stents. These models simulate the mechanical support provided by the stents to the vessel walls and their impact on blood flow.
Parameters	Material properties of the stent, blood flow dynamics, interaction with vascular tissues, and biocompatibility factors are considered.
Example	Metal-reinforced PLA composite stents are used to reopen and maintain the patency of blood vessels. These stents provide mechanical support to the vessel walls and ensure proper blood flow.

Case Study	In a cardiovascular procedure using metal-reinforced PLA composite stents, the biomechanical behavior and biocompatibility of the stents can be examined. This case study could evaluate the impact of the stents on blood circulation and their interaction with vascular tissues.
-------------------	---

4.3 Future Perspectives

Future research will focus on optimizing the clinical applications of metal-reinforced PLA composites and exploring new potential usage areas through both theoretical and experimental studies.

4.3.1 Smart Materials and Implants

Theoretical approaches can explore the design of smart metal-reinforced PLA composites with sensing and responsive capabilities. Such smart materials could create implants that react to environmental changes and optimize medical treatments.

Table 12. Future Research Directions for Smart Metal-Reinforced PLA Composites

Category	Description
Specific Features	Future research could focus on developing smart metal-reinforced PLA composites with features such as self-healing, shape memory, and real-time monitoring capabilities. These features could enhance the functionality and longevity of medical implants.
Technologies	Advanced technologies such as 3D printing, sensor integration, and responsive polymers could be employed to create these smart materials. For example, incorporating piezoelectric sensors into the composite matrix could enable real-time

	monitoring of stress and strain in orthopedic implants.
--	---

4.3.2 Nanotechnology Integration

Nanotechnology can be used to further enhance the properties of metal-reinforced PLA composites. Theoretical studies could investigate the integration of nanomaterials into the composite matrix and its impact on biocompatibility and mechanical properties.

Table 13. Integration of Nanotechnology into Metal-Reinforced PLA Composites

Category	Description
Technical Details	The integration of nanotechnology into metal-reinforced PLA composites can significantly enhance their mechanical, thermal, and biocompatibility properties. Techniques such as electrospinning, nanoparticle dispersion, and surface functionalization can be utilized to achieve this integration.
Specific Examples	
Electrospinning	This technique can be used to produce nanofiber-based composites with a high surface area, improving cell interactions and biocompatibility. For instance, incorporating silver nanoparticles into PLA nanofibers via electrospinning can enhance the antibacterial properties of wound healing materials.
Nanoparticle Dispersion	Uniform dispersion of nanoparticles such as gold, titanium, or iron within the PLA matrix can improve the composite's mechanical strength and thermal conductivity. For example, gold nanoparticles can be used to enhance the electrical conductivity and biocompatibility of cardiovascular stents.
Surface Functionalization	Functionalizing the surface of nanoparticles with biocompatible molecules can improve their interaction with the PLA matrix and biological tissues. For instance, coating titanium nanoparticles with hydroxyapatite can enhance the osteointegration of orthopedic implants.

4.3.3 Personalized Medical Solutions

The potential of metal-reinforced polylactic acid (PLA) composites in personalized medical device and implant designs is significant, as these materials can be tailored to meet the individual anatomical and physiological characteristics of patients. Theoretical models play a crucial role in exploring how these composites can be effectively utilized in such applications.

One of the key advantages of metal-reinforced PLA composites is their mechanical durability, which is essential for medical devices that must withstand various stresses during use. The incorporation of metal particles can enhance the mechanical properties of PLA, making it suitable for load-bearing applications such as orthopedic implants and surgical devices. However, specific studies directly linking metal reinforcement to improved mechanical properties in PLA composites were not identified in the references provided.

The advancements in additive manufacturing (AM) technology further expand the possibilities for personalized medical devices. AM allows for the precise fabrication of complex geometries that can conform to the specific anatomical features of a patient. This capability is particularly beneficial in surgical planning and pre-operative procedures, where customized implants can be created based on detailed imaging data. The reference provided Sudin et al. [50] discusses thermomechanical properties of PLA composites but does not specifically address AM technology or its applications in surgical planning.

Moreover, the biocompatibility of metal-reinforced PLA composites is a critical factor in their application in medical devices. While theoretical studies suggest that the incorporation of biocompatible materials can enhance the interaction between the implant and surrounding biological tissues, the reference Chen et al.[51] cited does not support this claim as it focuses on poly(ϵ -caprolactone) composites rather than PLA.

The customization of these composites can also extend to their degradation properties. Theoretical models can be employed to predict the degradation rates of metal-reinforced PLA composites, allowing for the design of implants that degrade at a controlled rate, matching the healing process of the patient. However, the reference Jiang et al. [52] discusses properties of L-lactide-grafted sisal fiber-reinforced PLA composites and does not specifically address degradation rates or controlled degradation in metal-reinforced PLA composites.

In conclusion, while the theoretical exploration of metal-reinforced PLA composites highlights their potential in the development of personalized medical

devices and implants, the claims made in this response require more specific supporting evidence from relevant studies. Further research is needed to substantiate the mechanical durability, biocompatibility, and degradation properties of these composites in medical applications.

5. Conclusion and Future Research Directions

The potential of metal-reinforced PLA composites in clinical applications is rapidly expanding due to their mechanical durability, biocompatibility, and customizable properties. Theoretical analyses provide critical insights for evaluating and optimizing their effectiveness in various medical fields.

Future research should focus on integrating theoretical approaches with experimental studies to further enhance the performance of metal-reinforced PLA composites in clinical applications. The discovery of new materials, integration of nanotechnology, development of personalized medical solutions, and creation of smart materials will mark significant advancements in biomedical engineering.

This theoretical perspective offers a foundational understanding of the clinical applications and future research directions of metal-reinforced PLA composites, aiming to broaden their potential usage in biomedical engineering. The following table presents a detailed overview of the theoretical models and case studies concerning metal-reinforced PLA composite orthopedic implants:

Table 14. Theoretical Models and Case Studies for Metal-Reinforced PLA Composite Orthopedic Implants

Theoretical Importance of Metal-Reinforced PLA Composites	
- Potential in Biome- dical Field	Metal-reinforced PLA composites hold significant potential in biomedical engineering due to their enhanced mechanical strength, biocompatibility, and customizable properties.
- Clinical Applicati- ons	These composites can be utilized in various critical clinical applications such as orthopedic implants, tissue engineering, dental implants, cardiovascular stents, and wound healing ma- terials.
Limitations of Current Theoretical Studies	
- Limited Data and Real-World Applica- tions	Current theoretical studies often rely on limited datasets and may not fully predict challenges encountered in real-world applications.

- Customization and Performance Optimization	Theoretical research on optimizing the performance of personalized medical devices and implants is relatively limited.
- Nanotechnology and Smart Materials	More theoretical studies are needed on the integration of nanotechnology and the development of smart materials.
Future Research Needs	
- Integration of Theoretical and Experimental Approaches	The integration of theoretical models and experimental studies will accelerate the material development process and enhance performance in clinical applications.
- Discovery of New Components	The discovery of new nanomaterials and components can further improve the biological functions of metal-reinforced PLA composites.
- Personalized Solutions	In-depth theoretical research is required to develop personalized medical devices and implant designs.
- Industrial Applications	Theoretical studies on the industrial-scale production and applications of metal-reinforced PLA composites will expedite their market introduction.
- Clinical Performance and Safety	Advanced theoretical analyses are essential to evaluate the clinical safety and performance of these materials, ensuring their impact on human health.

Acknowledgements: The authors would like to thank the Gazi University Scientific Research Projects Coordination Unit for their support. (Project code: FKA-2024-9628)

References

1. Silva, D.d., et al., Biocompatibility, Biodegradation and Excretion of Polylactic Acid (PLA) in Medical Implants and Theranostic Systems. *Chemical Engineering Journal*, 2018. **340**: p. 9-14.
2. Xu, B., et al., New Insights Into the Biodegradation of Polylactic Acid: From Degradation to Upcycling. *Environmental Reviews*, 2022. **30**(1): p. 30-38.
3. Wu, Y., et al., Biodegradable Polylactic Acid and Its Composites: Characteristics, Processing, and Sustainable Applications in Sports. *Polymers*, 2023. **15**(14): p. 3096.
4. Silva, M., et al., Engineering Ligament Scaffolds Based on PLA/Graphite Nanoplatelet Composites by 3D Printing or Braiding. *Journal of Composites Science*, 2023. **7**(3): p. 104.
5. Sobhan, A., et al., Development of a Biosensor With Electrically Conductive and Biodegradable Composite by Combinatory Use of Silver Nanoparticles, Novel Activated Biochar, and Polylactic Acid. *Journal of the Electrochemical Society*, 2021. **168**(10): p. 107501.
6. Momeni, S., Accelerating the Biodegradation of Poly(lactic Acid) Through the Inclusion of Plant Fibers: A Review of Recent Advances. *Acs Sustainable Chemistry & Engineering*, 2023. **11**(42): p. 15146-15170.
7. Brdlik, P.M., et al., Biodegradation of Poly(Lactic Acid) Biocomposites Under Controlled Composting Conditions and Freshwater Biotope. *Polymers*, 2021. **13**(4): p. 594.
8. Wang, Y., et al., Study of the Preparation and Properties of TPS/PBSA/PLA Biodegradable Composites. *Journal of Composites Science*, 2021. **5**(2): p. 48.
9. Grzabka-Zasadzińska, A., et al., Thermal and Mechanical Properties of Silica–Lignin/Polylactide Composites Subjected to Biodegradation. *Materials*, 2018. **11**(11): p. 2257.
10. Flynn, A., et al., Evaluation of Biodegradation of Polylactic Acid Mineral Composites in Composting Conditions. *Journal of Applied Polymer Science*, 2020. **137**(32).
11. Clarke, A.J., Fabrication and Performance of Continuous 316 Stainless Steel Fibre-Reinforced 3d-Printed PLA Composites. *Polymers*, 2023. **16**(1): p. 63.
12. Vakharia, V.S., et al., Additive manufacturing and characterization of metal particulate reinforced polylactic acid (PLA) polymer composites. *Polymers*, 2021. **13**(20): p. 3545.
13. Park, J.W., et al., Mechanical Strength Enhancement of Polylactic Acid Hybrid Composites. *Polymers*, 2019. **11**(2): p. 349.

14. Agüero, Á., et al., Effect of Different Compatibilizers on Environmentally Friendly Composites From Poly(lactic Acid) and Diatomaceous Earth. *Polymer International*, 2019. **68**(5): p. 893-903.
15. Lu, J., et al., Properties of Polylactic Acid Reinforced by Hydroxyapatite Modified Nanocellulose. *Polymers*, 2019. **11**(6): p. 1009.
16. Akindoyo, J.O., et al., Synergized Poly(lactic Acid)–hydroxyapatite Composites: Biocompatibility Study. *Journal of Applied Polymer Science*, 2018. **136**(15).
17. Abir, A.A. and B. Trindade, A Comparative Study of Different Poly (Lactic Acid) Bio-Composites Produced by Mechanical Alloying and Casting for Tribological Applications. *Materials*, 2023. **16**(4): p. 1608.
18. Taib, N.-A.A.B., et al., A review on poly lactic acid (PLA) as a biodegradable polymer. *Polymer Bulletin*, 2023. **80**(2): p. 1179-1213.
19. Vinay, D., R. Keshavamurthy, and V. Tambrallimath, Enhanced mechanical properties of metal filled 3D printed polymer composites. *Journal of The Institution of Engineers (India): Series D*, 2023. **104**(1): p. 181-195.
20. Thompson, C., C. González, and J. LLorca, Material extrusion fabrication of continuous metal wire-reinforced polymer–matrix composites. *Composites Communications*, 2024. **50**: p. 102024.
21. Bidadi, H., et al., Nonlinear properties of ZnO-polymer composites prepared by solution-casting method. *Vacuum*, 2013. **87**: p. 50-54.
22. Kuila, B.K. and A.K. Nandi, Physical, mechanical, and conductivity properties of poly (3-hexylthiophene)– montmorillonite clay nanocomposites produced by the solvent casting method. *Macromolecules*, 2004. **37**(23): p. 8577-8584.
23. Hosseini Ravandi, S.A., et al., Recently developed electrospinning methods: A review. *Textile Research Journal*, 2022. **92**(23-24): p. 5130-5145.
24. Jaafar, J., et al., A review of important considerations in the compression molding process of short natural fiber composites. *The International Journal of Advanced Manufacturing Technology*, 2019. **105**: p. 3437-3450.
25. Murariu, M. and P. Dubois, PLA composites: From production to properties. *Advanced drug delivery reviews*, 2016. **107**: p. 17-46.
26. Bright, B.M., et al., Feasibility study on thermo-mechanical performance of 3D printed and annealed coir fiber powder/polylactic acid eco-friendly biocomposites. *Polymer Composites*, 2024. **45**(7): p. 6512-6524.
27. Agüero, A., et al., Effect of different compatibilizers on environmentally friendly composites from poly (lactic acid) and diatomaceous earth. *Polymer International*, 2019. **68**(5): p. 893-903.
28. Adeniyi, A.G. and J.O. Ighalo, A systematic review of pure metals reinforced plastic composites. *Iranian Polymer Journal*, 2021. **30**(7): p. 751-768.

29. Farah, S., D.G. Anderson, and R. Langer, Physical and mechanical properties of PLA, and their functions in widespread applications—A comprehensive review. *Advanced drug delivery reviews*, 2016. **107**: p. 367-392.
30. Ranjan, N., et al., Innovative high-performance metal reinforced polymers composites for 3D printing applications: a review. *Advances in Materials and Processing Technologies*, 2024. **10**(3): p. 1800-1813.
31. Wang, Q., et al., Toughened poly (lactic acid)/BEP composites with good biodegradability and cytocompatibility. *Polymers*, 2019. **11**(9): p. 1413.
32. Ulkir, O., Investigation on the mechanical and thermal properties of metal-PLA composites fabricated by FDM. *Rapid Prototyping Journal*, 2024.
33. Begum, S.A., P.S.G. Krishnan, and K. Kanny, Properties of Poly (Lactic Acid)/Hydroxyapatite Biocomposites for 3D Printing Feedstock Material. *Journal of Thermoplastic Composite Materials*, 2023. **37**(2): p. 644-668.
34. Guo, R., et al., Electrical and Thermal Conductivity of Polylactic Acid (PLA)-Based Biocomposites by Incorporation of Nano-Graphite Fabricated With Fused Deposition Modeling. *Polymers*, 2019. **11**(3): p. 549.
35. Ho, M.-p., et al., Effect of Silk Fiber to the Mechanical and Thermal Properties of Its Biodegradable Composites. *Journal of Applied Polymer Science*, 2012. **127**(4): p. 2389-2396.
36. Liao, X., A.V. Nawaby, and H.E. Naguib, Porous Poly(lactic Acid) and PLA-nanocomposite Structures. *Journal of Applied Polymer Science*, 2011. **124**(1): p. 585-594.
37. Choudhary, N., V. Sharma, and P. Kumar, Reinforcement of Polylactic Acid With Bioceramics (Alumina and YSZ Composites) and Their Thermomechanical and Physical Properties for Biomedical Application. *Journal of Vinyl and Additive Technology*, 2021. **27**(3): p. 612-625.
38. Doungekaw, K., Printability and Mechanical Properties of PLA/Iron Composites for FDM 3D Printing. *Key Engineering Materials*, 2024. **978**: p. 47-51.
39. Gu, J. and J.M. Catchmark, Polylactic Acid Composites Incorporating Casein Functionalized Cellulose Nanowhiskers. *Journal of Biological Engineering*, 2013. **7**(1): p. 31.
40. Żur, P., A. Kołodziej, and A. Baier, Finite elements analysis of pla 3d-printed elements and shape optimization. *Eur J Eng Sci Technol*, 2019. **2**(1): p. 5964.
41. Zhou, S.Q., et al., Molecular dynamics simulation on interacting and mechanical properties of polylactic acid and attapulgite (100) surface. *Journal of applied polymer science*, 2013. **128**(5): p. 3043-3049.
42. Stewart, S.R., J.E. Wentz, and J.T. Allison. Experimental and computational fluid dynamic analysis of melt flow behavior in fused deposition modelling of

- poly (lactic) acid. in ASME international mechanical engineering congress and exposition. 2015. American Society of Mechanical Engineers.
43. Chen, Y., et al., Halloysite nanotube reinforced polylactic acid composite. *Polymer Composites*, 2017. **38**(10): p. 2166-2173.
 44. Wang, Z., et al., A comparative study on the in vivo degradation of poly (L-lactide) based composite implants for bone fracture fixation. *Scientific reports*, 2016. **6**(1): p. 20770.
 45. Buj-Corral, I., et al., Characterization of 3D printed metal-PLA composite scaffolds for biomedical applications. *Polymers*, 2022. **14**(13): p. 2754.
 46. Zhao, C., et al., Development of PLA/Mg composite for orthopedic implant: Tunable degradation and enhanced mineralization. *Composites Science and Technology*, 2017. **147**: p. 8-15.
 47. Liu, S., et al., Current applications of poly (lactic acid) composites in tissue engineering and drug delivery. *Composites Part B: Engineering*, 2020. **199**: p. 108238.
 48. Karacan, I., et al., Antibiotic containing poly lactic acid/hydroxyapatite biocomposite coatings for dental implant applications. *Key Engineering Materials*, 2017. **758**: p. 120-125.
 49. Hasanpur, E., et al., In vitro corrosion study of PLA/Mg composites for cardiovascular stent applications. *Journal of the Mechanical Behavior of Biomedical Materials*, 2021. **124**: p. 104768.
 50. Sudin, N.A.S., et al., Thermomechanical Properties and Thermal Behavior of Poly(Lactic Acid) Composites Reinforced With TiO_2 Nanofiller. *Solid State Phenomena*, 2021. **317**: p. 341-350.
 51. Chen, J., et al., Green Poly(ϵ -Caprolactone) Composites Reinforced With Electrospun Polylactide/Poly(ϵ -Caprolactone) Blend Fiber Mats. *Acs Sustainable Chemistry & Engineering*, 2014. **2**(9): p. 2102-2110.
 52. Jiang, A., X. Xu, and H. Wu, Preparation and Properties of L-lactide-grafted Sisal Fiber-reinforced Poly(lactic Acid) Composites. *Polymer Composites*, 2014. **37**(3): p. 802-809.



CHAPTER 15

Innovative Technology Applications Nano and Micro Encapsulation Applications for Ensuring Food Safety Roles

Nuray Gamze Yörük¹

¹ Assoc. Prof. Dr., Dokuz Eylül University, Faculty of Veterinary, Department of Food Hygiene and Technology, ORCID: 0000-0003-0867-4141

1. INTRODUCTION

Food and Agricultural Organization (FAO) reports that the world's population will increase by 34% by 2050, with developing countries accounting for a significant share of this increase. It has also been reported that there may be a 43% growth in urbanization and that feeding a larger population in the coming years will be possible by increasing current food production, especially annual meat (135%) and cereal (43%) production by more than 70% (FAO, 2009). For this reason, in recent years, there has been an increase in food diversity globally, both in order to prevent humanity from experiencing a shortage of access to food and due to the food consumption habits and demands of people due to population growth and developing technology. This situation makes controls increasingly difficult to ensure food safety. In various sectors of the food production chain, production facilities and agricultural environments, the presence of resistant bacteria has been observed, which can produce toxins and form biofilms during the production and processing of food, making it pathogenic to humans. For example, *Listeria monocytogenes* and *Staphylococcus aureus* (Gram-positive bacilli and cocci) are microorganisms that can contaminate a variety of foods even in refrigerated and freezing conditions, and are resistant to all adverse conditions and harmful due to their biofilm-forming capacity (Bland et al., 2022; Rodrigues et. al., 2024).

In this sense, global food loss due to microbial spoilage has been increasing year by year in recent years (Saka & Gülel, 2015). In addition, outbreaks of foodborne diseases associated with *Escherichia coli* O157:H7, *Salmonella* spp., *Listeria monocytogenes*, and the like indicate the need to pay attention to microbiological food safety, especially during food processing and storage (Kumar et al., 2020). Some antimicrobial agents are used to prevent and inhibit the growth of microorganisms in foods. They are usually used in combination with other preservation techniques to extend the shelf life of foods. The main preservatives frequently used in the food industry today are chemically synthesized ones (Nile et al., 2020). As a result, there is increasing consumer awareness and concern about the potential carcinogenic and mutagenic risks of chemical preservatives such as nitrites and parabens. The demand for "more natural", "fresher" and "minimally processed" food is increasing. In this sense, the development of alternative natural and low-toxic antimicrobial agents to replace traditional synthetic antimicrobial agents has attracted increasing attention (Taylor et al., 2008).

Natural bioactive compounds, although safe, sometimes present an unpleasant taste or odor and instability. These compounds are often difficult to incorporate

directly into foods, so nanocapsulation provides an alternative to solve this problem. The use of nano- or microcapsules in foods is a trend used in the cereal, bakery, dairy and beverage industries, (Martins et al., 2022). The idea of bioactive encapsulation using natural nanocarriers stems from the consideration of the nature-derived functionalities of these nanoparticles. As an example, casein micelles can naturally encapsulate and transport vital nutrients through milk; amylose chains can bind various flavor compounds developed during bread making and released during subsequent heating, and starch derivatives can form inclusion complexes with many nutraceuticals. *Caseins* are important proteins in cow's milk, accounting for 80% of the total protein content (Hoofman & Valvo, 2004). They also occur naturally in the form of spherical micelles whose nanoparticles are typically between 50 and 200 nm. Caseins have physical chemical properties similar to copolymers with well-balanced hydrophobic and hydrophilic regions and can self-assemble to form nano-sized carriers with excellent thermal stability, offering enormous potential for use as a natural carrier for bioactive food ingredients with hydrophobic or delicate properties. *Cyclodextrins* are hollow molecular nanocarriers with specific dimensions to encapsulate many different components by inserting the appropriate "guest" structure into their cavities. In *amylose nanocarriers*, different bioactive components, such as ligands, can be nanoencapsulated within amylose nanostructures. The presence of ligands can lead to a conformational change in amylose, i.e., to a unit strand (V-shaped amylose) with dense double helices and a central hydrophobic cavity, which can bind lipophilic molecules such as fatty acids through hydrophobic interactions (Assadpour & Jafari, 2019; Desmukh et al., 2022). Lactoferrin (Lf) is a recognized antibacterial agent found in fresh human milk (Sawale et al., 2022).

At the same time, nanocapsules are much easier to penetrate cells and membranes than microcapsules. Nanoscale food additives can be used to influence the flavor, texture, nutrient composition or shelf life of the food product and even offer functions such as detecting microbial pathogens and food quality indicators. In the case of food packaging, nanotechnologies are thought to greatly improve food quality and shelf life (Singh et al., 2017). Both the scientific communities of the developed and developing world concur that nanotechnology will be the subsequent advancement in technology (Malik et al., 2023).

2. ENCAPSULATION TECHNIQUES

The encapsulation technique, which incorporates a preferred substance (core) into another compound(s) as a wall material, helps us to protect bioactive components against harmful factors such as light, oxygen, heat, pH, water, shear or other degrading effects to improve the properties of bioactive components such as functionality, solubility, bioavailability and nutritional value, to mask bad odors/tastes and control their release, and ultimately to improve their functionality, solubility, bioavailability and nutritional value (Esfanjani et al., 2018; Akhavan et al., 2018). to enhance the properties of bioactive ingredients such as functionality, solubility, bioavailability and nutritional value, to mask unpleasant odors/tastes and control their release, and ultimately to maintain and enhance the unique capabilities of bioactive ingredients (Ray et al., 2016). Finding the appropriate wall material and determining the encapsulation procedure are the main issues to be addressed before starting the encapsulation process (Shishir et al., 2018). The choice of wall material has a significant impact on how the enclosed component is delivered. It should be selected based on various factors such as material cost, purpose of encapsulation, type of process, efficiency, release mechanism, and minimum chemical reactivity with the core. The selection of wall materials must also adhere to regulations set by official bodies like the European Food Safety Authority (EFSA) or USFDA (Wandrey et al., 2010). Since the molecular weight, polarity, solubility and other physicochemical properties of bioactive ingredients are variable, the best encapsulation yield and efficiency can be achieved with different procedures. This reveals the lack of a general procedure for encapsulation of bioactive substances (Ray et al., 2016). Proteins as wall material are the best choice due to the following advantages:

- (1) Their amphipathic nature, which makes them good emulsifiers that link both the core and the surrounding environment,
- (2) They are environmentally friendly and biodegradable in the environment;
- (3) Naturally occurring in food and
- (4) Accessible from many renewable sources (El-Salam et al., 2016; Mohammadi et al., 2016).

Several proteins, including phosphoproteins (such as caseins from milk), globular proteins (e.g. ovalbumin, whey proteins, soy proteins, and pea proteins), and prolamins (e.g. storage proteins from cereals), are suitable carriers that encapsulate bioactive compounds (Hosseini & Jafari, 2020). On the other hand,

the distinctive molecular structure and self-organization properties of polysaccharides, the second most used carriers of bioactive substances, are considered to be their most important benefits. The most common polysaccharides surrounding bioactive components can be divided into three groups depending on their surface charge, including neutral (e.g. guar gum and dextran), anionic (such as carrageenans, gum arabic, alginates, pectins and xanthan) and cationic (e.g. chitosan) (Abd El-Salam et al., 2016). Interestingly, it has been confirmed that a combination of different wall materials such as proteins & polysaccharides leads to better results compared to single cases (Aceituno-Medina et al., 2013; Belščak-Cvitanović et al., 2015). The techniques often used for encapsulation of bioactive compounds can be categorized as:

- a) Chemical procedures (e.g. molecular inclusion complexes, interfacial polymerization),
- b) Physicochemical approaches (e.g. complex coacervation, liposomal entrapment and ionic gelation),
- c) Physical systems (e.g. co-extrusion, freeze drying, spray drying, fluidized bed coating, spray bed drying, spray-freeze drying and systems based on supercritical fluids) and
- d) Emerging encapsulation procedures such as electrospinning/electrospraying (as electrohydrodynamic processes) (Table 1)(Zabot et al., 2022).

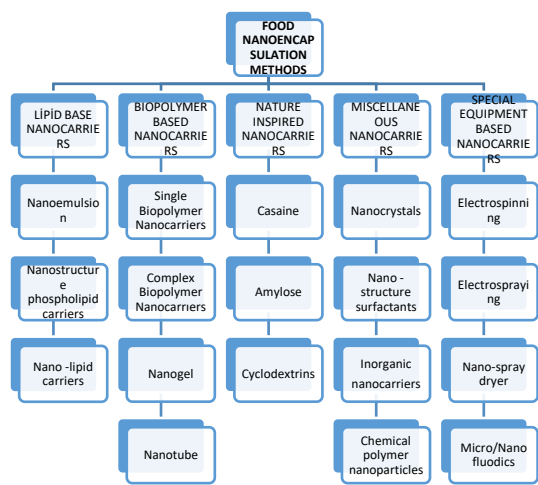


Table 1. Food Nanoencapsulation Methods

The antioxidant, anti-esterification and antimicrobial activities of bioactive components from plants and spices are attributed to the presence of essential bioactive components such as flavonoids, lignans, terpenoids, polyphenolics, carotenoids, sulfides, curcumin, saponins, coumarins, plant sterols, phthalides. Different bioactive compounds (e.g. Essential oils (EOs), Plant extracts, Polyphenolic compounds (Quercetin, Anthocyanins, Catechins, Vitamin E or α -tocopherol, Ascorbic acid, Carotenoids, Natural anti-browning agents) (Murcia et al; 2004; Hosseini & Jafari, 2020).

Nanoencapsulation is a technology that packages substances in miniature using techniques such as nanocomposites, nanoemulsification and nanostructures that provide final product functionality including controlled release (Paredes et al., 2016). Nanocapsules can be incorporated into food to provide any nutrient. Encapsulated compounds in foods include vitamins, essential fatty acids, minerals, flavors, antimicrobial agents, colorants, antioxidants and polyphenols (Martins et al., 2022). The absorption of these nutrients can be increased by adding nanoparticles to the food to be produced. Nanoparticle additives can be easily absorbed by the body and extend the shelf life of the product. Apart from all these, it is also aimed to bring different food and nutrition approaches such as improving the taste, reducing the amount of salt, sugar, fat and preservatives in the treatment of some diseases or in some food-related diseases (eg. obesity and diabetes) (Wandrey et al., 2010).

Nano-sized dispersions, emulsions and filled micelles do not precipitate, which gives the product a longer shelf life. Since the size of nano additives is much smaller than the wavelength of light, they do not cause color problems, so they can be added even to clear and transparent foods. Substances that are difficult to be dissolved by the body can be absorbed more easily at the nanoscale size due to their larger surface area. If any active substance needs to be protected during storage or during its passage through the intestines, nanotechnology can provide excellent protective layers. They can also protect against environmental factors, making the use of food flavors and antioxidants advantageous. The main objective is to improve the functionality of such ingredients while keeping their concentration to a minimum (Hosseini & Jafari, 2020). The types of nanoadditives available on the market are antioxidants, colorants, flavorings, vitamins, antioxidants, antimicrobials and preservatives. Silver, titanium dioxide, magnesium, iron, silica, calcium and selenium are used for these purposes in the food industry in nanoscale sizes (Alfadul an& Elneshwy, 2010; Palza, 2015). Nanosalt, nanopolysilicin, nanominerals, nanoparticles, nanofibers, nanosheets, etc. are examples of the types of nanoadditives used today to increase yield.

aluminosilicate materials are widely used as anti-solidifying agents in granulated or powdered processed foods, while titanium dioxide is a common food whitening and brightening additive used in confectionery, some cheeses and sauces. Nosalt is a nanoadditive in the form of salt, which has a great effect even when used in small quantities and is used to give better and more intense flavor to food. Nanopolysilicin is a nanoadditive added to oil that protects it from oxidation by closing the gap between phytoglycogen octenyl succinate nanoparticles. Nanominerals are nanoadditives with faster and higher absorption in the stomach, used as an alternative to large-sized minerals that are not easily digestible in the stomach. Nutraceuticals, on the other hand, are nanoadditives that are used to increase the nutritional value of food, such as bioactive proteins, and increase absorption in the GI tract (Shabnam et al., 2020).

The antimicrobial properties of nanomaterials are of great interest due to their ability to inhibit the growth of spoilage-causing microorganisms and their mechanical density, indicating their use in packaging films to inhibit the growth of microbes and antibiotic carriers (Suvarna et al., 2022). Through the technology used in nanocomposites, microbial control can be achieved by encapsulating essential oils and products of natural origin. It is also thought that this nanoencapsulation technique can provide an effect in the prevention and control of microorganisms with high antimicrobial resistance factor in the food industry. In addition, the use of common metals and transition metals, one of the new approaches applied in nanoencapsulation for the denaturation of pathogenic biofilms, is also discussed (Rodrigues et al., 2024).

In studies, various natural antimicrobial substances can be added to food packaging films as nanomaterials. For example, Pediocin from the *Pediococcus* strain of Lactic acid bacteria combines with polylactic acid biopolymers showing activity against *L. monocytogenes* when used in raw ham (Woraprayote et al., 2013). Nisin is a "generally recognized as safe" antimicrobial agent added to various food products. Nisin is combined with pectin and polylactic acid and is often incorporated into composite packaging film, where it reduces the proliferation of *L. monocytogenes* and *Alicyclobacillus acidoterrestris* in food products (Wu et al., 2018). The application of microencapsulation technique in maintaining the stability of food will also support increased bioavailability and help to ensure oxidation and hydrolysis under processing conditions. Active food packaging processes inhibit microbial growth and protect sensitive ingredients from adverse conditions such as oxygen, humidity and temperature in the external environment (Rodrigues et al., 2024).

Ghasami and Abbasi (2014), have demonstrated that an investigation was conducted to study the impact of alkaline pH and ultrasound treatment on the production, structure, encapsulation efficiency (EE), and protective qualities of natural casein micelles. By increasing the pH, the turbidity of skim milk decreased. Simultaneously, the size of casein micelle particles increased, along with their physical stability and ability to encapsulate substances.

Li et al., (2014) revealed that stabilized nanoemulsions with cheese juice protein isolation show good stability and potential for use as a water-insoluble curcumin distribution system, without requiring a second layer of polysaccharide.

Although some *in vivo* studies have been conducted on the bioavailability of encapsulated ingredients, there is a paucity of information on the utilisation of these ingredients to extend the shelf life of diverse food systems (Hosseini & Jafari, 2020). In general, chemical changes caused by light, along with microbial degradation and certain chemical reactions such as oxidation of proteins and lipids, biochemical and physical disorders such as enzymatic or non-enzymatic acidification, and mechanical damage and fluid transition, The transfer of moisture (both absorption and loss) within the food matrix (fluid) or between the matrix and the environment, gelatinisation and retrogradation in the molecule, freezing damage, increased crystallisation, and the formation of phases in the emulsion structures, affect the structure, appearance, aromatic properties and bioactive components of the food (Kong & Singh, 2016). In this context, the most significant factors influencing the quality and reliability of food are microbial contamination, lipid oxidation and acidification reactions. (Hosseini & Jafari, 2020).

Plant-based bioactive ingredients with antimicrobial, antioxidant, and anti-emulsion activities are among the best choices for blocking degradation factors in foodstuffs. However, their industrial applications also face some challenges, such as low water solubility, poor chemical stability, bad smell, dose-dependent activity, inactivation when complex with food components, etc. Capsulation, especially nanocapsulation, is a technology that protects against these barriers. (Hosseini & Jafari, 2020). The nanocapsulation of food ingredients and additives is thought to provide protective barriers, flavor and flavor masking, controlled release and better dispersibility for water-insoluble food components and ingredients. The production of nanoparticles is important in relation to the inclusion of a lipophilic component such as EOs in liquid products such as alcoholic beverages, which provides better dissemination and therefore a higher antimicrobial effect than other methods. Thus, nanocapsulation may also be useful in the prevention of diseases harmful to human health (Hosseini and Jafari,

2020; Rodrigues et al., 2024). Furthermore, a combination of proteins and polysaccharides as a wall material is used to better results from separate forms. Therefore, the encapsulation method and the type of encapsulants greatly influence the release mechanism of bioactive components and their physicochemical properties. These factors, along with the optimization of the encapsulation process conditions, lead to a cost-effective, well-encapsulated component that has higher efficiency than the free form to extend the shelf life of the food, as many studies have confirmed. Despite some *in vivo* studies on the bioavailability of encapsulated ingredients, there is limited information on the use of these ingredients to increase the shelf life of different food systems (Hosseini & Jafari, 2020).

3. RESULT

In conclusion, nanoencapsulation can be defined as the utilisation of film, layer, coating, or microdispersion at the nanometre scale for the purpose of encapsulation. It is evident that the encapsulation layer is on a nanometre scale and serves to provide protection for food or flavour molecules/contents. The active component is predominantly present in a molecular or nanoscale state. The most significant advantage is that it ensures homogeneity and superior microbial, physical, and chemical characteristics, while simultaneously enhancing the efficiency of encapsulation. The principal advantages of nanotechnology in food component micro/nanocapsulation are as follows (Khare & Vasisht, 2014). An increase in surface area may result in enhanced bioavailability of flavours and food components. This is particularly significant in the context of low-resolution and/or flavour components. This is particularly relevant for individuals with reduced taste and smell perception thresholds. To illustrate, consider the dissolution of omega-3 fish oil using a mixture-based system.

- Transparent to light (important in beverage applications): Nanoemulsions comprising oil droplets of less than 100 nm in diameter and microemulsions are optically transparent. Furthermore, spray drying allows for a higher content retention capacity during the drying process, which in turn reduces the amount of volatile organic carbon released.

- The solution is more closely aligned with the actual molecular structure (homogeneity in system properties such as density).

- The encapsulated compound exhibits heightened activity, as exemplified by antimicrobial agents in nanoemulsion/microemulsion forms (Paredes et al., 2016).

Nanoencapsulation with bioactive compounds from plant sources improves the organoleptic properties of foods such as structure, color, taste, prolongs shelf life by increasing nutrient bioavailability, and may be sustainable and economically innovative for a circular economy.

Despite some *in vivo* studies on the bioavailability of encapsulated ingredients, there is very limited information on the application of these substances to increase shelf-life in different foods. Nanoencapsulation techniques with natural antimicrobial, which some food and food product as one of the innovative technology alternatives in foods, will be more preferred globally in the future due to its advantageous features such as industry, sustainability, public health aspects and most importantly, appealing to the public's understanding of more natural food.

REFERENCES

- Abd El-Salam, M. H., El-Shibiny, S., Grumezescu, A. M. (2016). Natural biopolymers as nanocarriers for bioactive ingredients used in food industries. Ed: Grumezescu, A.M. Encapsulations, Academic Press, 793-829. <https://doi.org/10.1016/B978-0-12-804307-3.00019-3>
- Aceituno-Medina, M., Lopez-Rubio, A., Mendoza, S., Lagaron, J. M. (2013). Development and characterization of food-grade electrospun fibers from amaranth protein pullulan blends. *Food Res Int*, 54, 667-674. <http://dx.doi.org/10.1016/j.foodres.2013.07.055>
- Akhavan, S., Assadpour, E., Katouzian, I., Jafari, S.M. (2018). Lipid nano scale cargos for the protection and delivery of food bioactive ingredients and nutraceuticals. *Trends in Food Science & Technology*, 74, 132-146.
- Alfadul, S. M. and Elneshwy, A. A. (2010). Use of nanotechnology in food processing, packaging and safety review. *African Journal of Food Agriculture, Nutrition and Development*, 10(6), 2719-2739.
- Assadpour, E. and Jafari, S. M. (2019). Chapter 3 -Nanoencapsulation: Techniques and Developments for Food Applications. *Nanomaterials for Food Applications*, 35-61. <https://doi.org/10.1016/b978-0-12-814130-4.00003-8>.
- Belščak-Cvitanović, A., Levic, S., Kalušević, A., Špoljarić, I., Đorđević, V., Komes, D., ... (2015). Efficiency assessment of natural biopolymers as encapsulants of green tea (*Camellia sinensis* L.) bioactive compounds by spray drying. *Food Bioprocess Technology*, 8(12), 2444-2460. DOI 10.1007/s11947-015-1592-y
- Bland, R., Brown, S. R. B., Waite-Cusic, J., Kovacevic J. (2022). Probing antimicrobial resistance and sanitizer tolerance themes and their implications for the food industry through the *Listeria monocytogenes* lens. *Comprehensive Reviews In Food Science And Food Safety*, 21, 1777-1802. <https://doi.org/10.1111/1541-4337.12910>.
- Desmukh, S.P., Pawar, K. K., Dalavi, D.K. (2022). Incorporation of Nanocarriers as Antimicrobial Agents in Food Packaging. In book: *Nanotechnology in Intelligent Food Packaging*. Ed: Annu, Tanima Bhattacharya and Shakeel Ahmed, 203-234.
- Esfanjani, A. F., Assadpour, E., Jafari, S. M. (2018). Improving the bioavailability of phenolic compounds by loading them within lipid-based nanocarriers. *Trends in Food Science & Technology*, 76, 56-66.
- FAO. (2009). How to Feed the World in 2050. http://www.fao.org/fileadmin/templates/wsfs/docs/expert_paper/How_to_Feed_the_World_in_2050.pdf (2009).
- Ghasami, S. and Abbasi, S. (2014). Formation of natural casein micelle nanocapsule by means of pH changes and ultrasound. *Food Hydrocolloids*. 42(1), 42-47. doi: 10.1016/j.foodhyd.2013.10.028.

- Hoffman, J.R. and Falvo, M.J. (2004). Protein – Which is best?. *Journal of Sports Science & Medicine*, 3(3), 118-130.
- Hosseini, H. and Jafari, S. M. (2020). Introducing nano/microencapsulated bioactive ingredients for extending the shelf-life of food products. *Advances in Colloid and Interface Science*, 282, 102210.
- Khare, A.R. and Vasisht, N. 2014. *Nanoencapsulation in the Food Industry*, Elsevier Inc. Available at: <http://linkinghub.elsevier.com/retrieve/pii/B9780124045682000145>.
- Kong, F. and Singh, R. P. (2016). 2 - Chemical deterioration and physical instability of foods and beverages. Ed: Subramaniam, P. *The Stability and Shelf Life of Food* (2nd ed.), Woodhead Publishing, Cambridge, 43-76. <https://doi.org/10.1016/B978-0-08-100435-7.00002-2>
- Kumar, D. D., Bimlesh, M., Ramesh, P., Rajan, S., Rajesh, B., Minaxi (2016). Formulation and characterization of nanoencapsulated curcumin using sodium caseinate and its incorporation in ice cream. *Food and Function*, (7), 417-424. doi: 10.1039/c5fo00924c.
- Li, M., Ma, Y., Chi, J. (2014). Whey-protein-stabilized nano emulsions as a potential delivery system for water-insoluble Curcumin. *LWT- Food Science and Technology*, 59, 49-58. <https://doi.org/10.1016/j.lwt.2014.04.054>.
- Malik, S., Muhammed K, Waheed, Y. (2023). Nanotechnology: A Revolution in Modern Industry. *Molecules*, 28 (2), 661. doi: 10.3390/molecules28020661
- Martins, V. F. R., Pinatdo, M. E., Morais, R. M. S. C., Morais, A. M. M. B. (2022). Valorisation of Micro/Nanoencapsulated Bioactive Compounds from Plant Sources for Food Applications Towards Sustainability. *Foods*, 12(1), 32. <https://doi.org/10.3390/foods12010032>
- Mohammadi, A., Jafari, S. M., Esfanjani, A. F., Akhavan, S. (2016). Application of nanoencapsulated olive leaf extract in controlling the oxidative stability of soybean oil. *Food Chemistry*, 190, 513-519. <http://dx.doi.org/10.1016/j.foodchem.2015.05.115>.
- Murcia, M. A., Egea, I., Romojaro, F., Parras, P., Jimenez, A.M., Martinez-Tome, M. (2004). Antioxidant evaluation in dessert spices compared with common food additives”. Influence of irradiation procedure. *Journal of Agricultural and Food Chemistry*, 52(7), 1872-1881.
- Nile, S.H., Baskar, V., Selvaraj, D., Nile, A., Xiao, J., Kai, G. (2020). Nanotechnologies in Food Science: Applications, Recent Trends, and Future Perspectives. *Nano-Micro Letter*, 12, 45. <https://doi.org/10.1007/s40820-020-0383-9>.
- Paredes, A. J., Asencio, C. M., Manuel, L. J., Allemandi, D. A., Palma, S.D. (2016). Nanoencapsulation in the food industry: manufacture, applications and characterization. *Journal of Food Bioengineering and Nanoprocessing*, 1(1), 56-79.

- Palza, H. (2015). Antimicrobial polymers with metal nanoparticles. *International Journal of Molecular Sciences*, 16(1), 2099–116.
- Ray, S., Raychaudhuri, U., Chakraborty, R. (2016). An overview of encapsulation of active compounds used in food products by drying technology. *Food Bioscience*, 13, 76-83. <http://dx.doi.org/10.1016/j.fbio.2015.12.009>.
- Rodrigues, S. O., Silva, J. M. O., Banwo, K., Lima, C. M. G., Guiné, R. P. F., Verruck, S., Pagnossa, J. P. (2024). Nanoencapsulation of natural products and their role in the preservation and control of contaminations in the food industry. *Food Science and Technology*, 12, 14. 10.5327/fst.00222.
- Saka, E. and Gülel, G. T. (2015). Gıda Endüstrisinde Nanoteknoloji Uygulamaları. *Etlik Veteriner Mikrobiyoloji Dergisi*, 26 (2), 52-57.
- Sawale, M., Ozadali, F., Valentine, C. J., Benyathiar, P., Drolia, R., Dharmendra, K. M. (2022). Impact of bovine lactoferrin fortification on pathogenic organisms to attenuate the risk of infection for infants. *Food Control*, 139, 109078. <https://doi.org/10.1016/j.foodcont.2022.109078>.
- Shabnam, S., Meryam, P., Mazumder, J., Sardar, M. (2020). Chapter 12: Phytonanotechnology: A new horizon for the food industry. *Phytonanotechnology*, 221-244. <https://doi.org/10.1016/B978-0-12-822348-2.00012-7>.
- Shishir, M. R. I., Xie, L., Sun, C., Zheng, X., Chen, W. (2018). Advances in micro and nano-encapsulation of bioactive compounds using biopolymer and lipid-based transporters. *Trends in Food Science & Technology*, 78, 34-60. <https://doi.org/10.1016/j.tifs.2018.05.018>
- Singh, T., Shukla, S., Kumar, P., Wahla, V., Bajpai, V. K., Rather, İ. A. (2017). Application of Nanotechnology in Food Science: Perception and Overview. *Frontiers in Microbiology*, 8, 1501. <https://doi.org/10.3389/fmicb.2017.01501>.
- Suvarna, V., Nair, A., Mallya, R., Khan, T., Omri, A. (2022). Antimicrobial Nanomaterials for Food Packaging. *Antibiotics*, 11(6), 729. <https://doi.org/10.3390/antibiotics11060729>.
- Taylor, P., Vargas, M., Pastor, C., Chiralt, A. (2008). Recent advances in edible coatings for fresh and minimally processed fruits. *Critical Review of Food Science Nutrition*, 48, 496–511. <https://doi.org/10.1080/10408390701537344>.
- Wandrey, C., Bartkowiak, A., Harding, S. A. (2010). Materials for encapsulation. Ed: Zuidam, N. J. and Nedovic, V. *Encapsulation Technologies for Active Food Ingredients and Food Processing*, Springer, Dordrecht. 31-100.
- Woraprayote, W., Kingcha, Y., Amonphanpokin, P., Kruenate, J., Zendo, T., Sonomoto, K., Benjakul, S., Visessanguan, W. (2013). Anti-Listeria Activity of Poly (Lactic Acid)/Sawdust Particle Biocomposite Film Impregnated with Pe-diocin PA-1/AcH and Its Use in Raw Sliced Pork. *International Journal of Food Microbiology*, 167(2), 229-235. <https://doi.org/10.1016/j.ijfood-micro.2013.09.009>.

- Wu, H., Teng, C., Liu, B., Tian, H., Wang, J. (2018). Characterisation and Long Term Antimicrobial Activity of the Nisin Anchored Cellulose Films. *International Journal of Biological Macromolecules*, 113, 487-493. <https://doi.org/10.1016/j.ijbiomac.2018.01.194>.
- Zabot, G. L., Rodrigues, F.S., Ody, L. P., Tres, M.V., Herrera, E., Palacin, H., Córdova-Ramos, J. S., Best, I., Olivera-Montenegro, L. (2022). Encapsulation of Bioactive Compounds for Food and Agricultural Applications. *Polymers*, 14 (19), 4194.



CHAPTER 16

Plastic Waste Management: Recycling and Disposal

Mazlum Cengiz¹

¹ Şırnak University, Department of Machinery and Metal Technologies, Şırnak, Turkey, 73000, ORCID: 0000-0002-3724-6894

1. Introduction

Plastic has become a central material for various fields of industry, and it has replaced various materials like metal, glass, paper, and wood due to limited raw materials. It has become a fundamental part of the packaging, shipping, food, construction, healthcare, automotive, electronics, and textile industries because its great properties including being low weight, practicality, good stiffness, long-lasting nature, resistance to wear, ease of manufacturing, design versatility, effective insulation, resistance to corrosion, poor conductivity of electricity and heat and cost-effectiveness (Nayanathara Thathsarani Pilapitiya & Ratnayake, 2024; Tamizhdurai et al., 2024; Zhang et al., 2021). Especially, synthetic semi-aromatic plastics, such as polyethylene terephthalate and polybutylene terephthalate, exhibit outstanding physio-chemical properties, including high heat distortion temperatures, strong mechanical strength, great chemical resistance, and effective electrical insulation. These characteristics have positioned plastic products as an essential part of daily life for humans (Ali et al., 2021; Nayanathara Thathsarani Pilapitiya & Ratnayake, 2024). In 2018, the amount of plastic produced was 360 million metric tons and is anticipated to reach 500 million tons by 2025 and 670 million tons by 2040 (He et al., 2024; Zhang et al., 2021). Figure 1 displays global plastic production over the years.

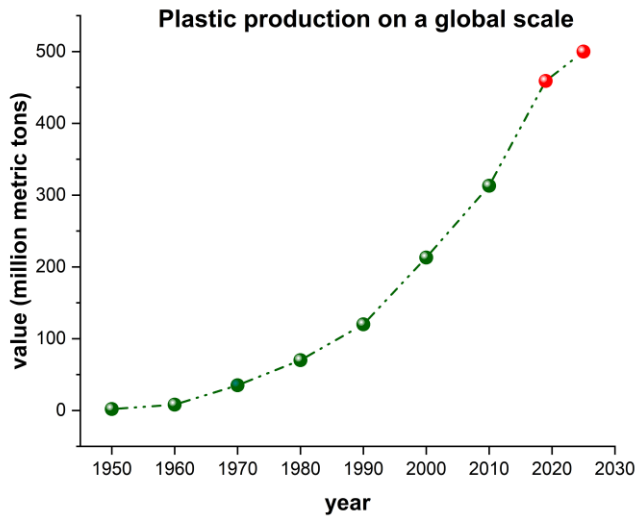


Figure 1: Worldwide plastic production through the years (Our World in Data, n.d.; Zhang et al., 2021).

Plastics are used across a wide range of sectors. For example, 85% of medical devices are made from plastics (Nayanathara Thathsarani Pilapitiya & Ratnayake, 2024). The utilization of plastics offers many advantages, as listed below:

- **Environmental advantages:** The use of polyethylene terephthalate for beverage containers, compared to metal and glass, reduces greenhouse gas emissions, as the production of metal and glass generates higher emissions. Additionally, utilization of plastic composites in aircraft and automobiles leads to lower fuel consumption since they are lighter than metals (Nayanathara Thathsarani Pilapitiya & Ratnayake, 2024).
- **Economic advantages:** Plastics are cheaper than metals and other composites, making them a more cost-effective alternative for replacing parts in automobiles, buses, and airplanes. It is a natural electrical insulator that addresses the essential needs of the quickly expanding electrical and electronic systems. It is also heat-resistant (Evode, Qamar, Bilal, Barceló, & Iqbal, 2021).
- **Social advantages:** Plastic tanks allow for storage of drinking water, and plastic food packaging stores and keeps food products fresh by regulating temperature and pressure (Nayanathara Thathsarani Pilapitiya & Ratnayake, 2024). Plastics has a key role in explaining a sustainable, effective, hygienic, cost-efficient, and environmentally-friendly packaging system (Evode et al., 2021) . Furthermore, they allow the production of affordable goods and are used in protective equipment such as helmets and medical gear, contributing to public safety and health.

Packaging is the primary industry for plastics, representing more than 40% of the total global plastic production. Globally, over 400 million metric tons of plastic waste are generated per year (Tamizhdurai et al., 2024). Single-use plastics such as cups, straws, and plates, accounts for approximately 70% of the total global plastic production (Hossain, Tajvidi, Bousfield, & Gardner, 2021). Furthermore, low-density plastics such as flexible films, plastic bags, and Styrofoam are commonly used due to their unique features, including versatility, lightweight, and durability(M. Cengiz, 2022).

On the other hand, the extensive use of various plastic products has led to a substantial accumulation of plastic waste (Evode et al., 2021). Almost 60% of plastic produced ends up in the natural environment as waste (Zhang et al., 2021). Around 6,300 million metric tons of plastic waste were made between 1950 and

2015 and it is predicted to be 12,000 million metric tons by 2050 (Hossain et al., 2021). The amount of plastic collected is 14% of total plastic waste, but only 2% of this waste is recycled into products of the same or similar value. This low recycling rate is primarily due to the requirement for high purity, the difficulties associated with collection and sorting, and the simple structure of the plastic (Mulakkal et al., 2021). Plastics decompose extremely slowly in the environment because of their stable chemical structure (Tamizhdurai et al., 2024). Therefore, plastic pollution threaten the ecosystem and earth will encounter a substantial and potentially insurmountable issue unless there is a significant reduction in consumption and an increase in recycling efforts (Hossain et al., 2021; Tamizhdurai et al., 2024).

Especially, low density plastics pose significant threats to the environment because they are difficult to recycle due to accumulation issues and their tendency to obstruct machinery in recycling facilities. As a result, they are often sent directly to landfills or incinerated. Improper landfilling of plastics leads to soil, water and air pollution, contributing to climate change, and it can take up to thousands of years for plastic to decompose in soil (M. Cengiz, 2022). Furthermore, plastic pollution physically, chemically, and economically affects the marine environment (Kibria, Masuk, Safayet, Nguyen, & Mourshed, 2023). It is estimated that approximately 10-20 million tons of plastic waste are disposed of into the oceans (Chang, 2023). Plastic waste released into the ocean per capita by countries is demonstrated in Figure 2. Moreover, plastic waste breaks down into smaller fragments, even microplastics when exposed to ultraviolet light. Microplastics is nearly impossible to recover and disrupt food chains while damaging ecosystem (Evide et al., 2021; Liang, Tan, Song, & Li, 2021). Additionally, marine species can consume ingested plastic, often leading to injury or even death (LI, TSE, & FOK, 2016). Microplastics have been found in sea salt, tap water, canned fish, bottled water, honey, and sugar, raising concerns about the possible effects of plastic waste on the environment, and human health (Evide et al., 2021).

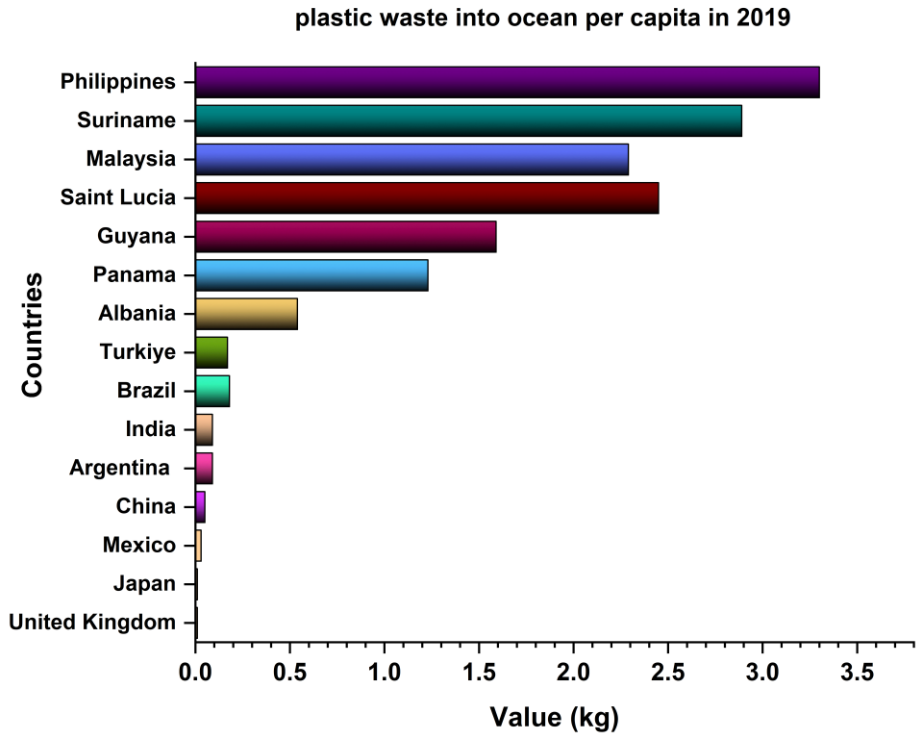


Figure 2. Plastic waste released into the ocean per capita by countries (Our World in Data, n.d.).

Reducing plastic consumption, recycling and reusing, and the adaptation of biodegradable or compostable plastics manufactured from sustainable materials and renewable biomass, such as corn starch, sugarcane, or potato starch, appear to be a feasible solution to address the demand for plastics while also minimizing the environmental impact of plastic materials made from fossil-based resources (Mazlum Cengiz & Gazal, 2023). Figure 3 shows plastic waste management approaches to reduce plastic waste.

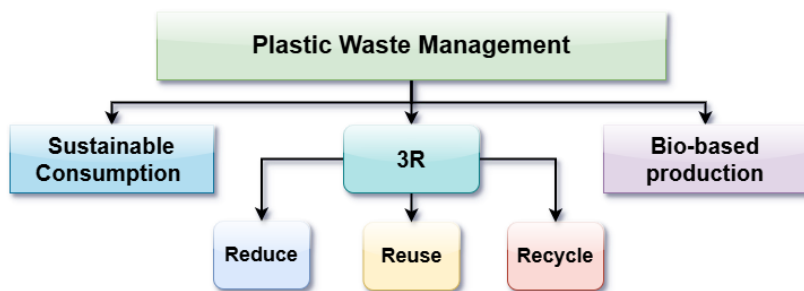


Figure 3. Schematic illustration of plastic waste management.

2. Disposal Methods for Plastic Waste

Synthetic plastics comprise of hydrocarbons derived from fossil fuels, and their natural degradation takes hundreds of years. They accumulate in aquatic and soil habitats and break down in small pieces over time, becoming microplastics and attaching the aquatic and terrestrial plants and animals, potentially transferring these particles to humans through the food web. The long-term ingestion of plastics by humans has been linked to obesity, and even chromosomal alterations and cancer. Consequently, the buildup of plastic waste poses a serious threat to both the natural ecosystem and human health (He et al., 2024).

Therefore, it is important to use suitable disposal methods; otherwise, plastic waste will threaten the ecosystem as one of the most significant contributors to global environmental pollution (Nayanathara Thathsarani Pilapitiya & Ratnayake, 2024). The disposal methods are landfilling, incineration, recycling, and biological degradation (Naderi Kalali et al., 2023).

2.1. Landfilling

Low-density plastics can easily contaminate the open environment through air and water. To avoid further contamination, a large quantity of plastic waste is primarily sent to landfills for disposal. Nevertheless, plastics degrade extremely slowly in soil and pollute the soil and groundwater with their chemical composition, including additives, flame retardants, plasticizers, and pigments (Lim & Thian, 2022; Nayanathara Thathsarani Pilapitiya & Ratnayake, 2024; Zhang et al., 2021). Furthermore, microplastics in soil can enter the aquatic environments.

2.2. Incineration

Plastic waste can be incinerated for energy recovery such as power generation and heat production, which can be preferable over landfilling (Nayanathara Thathsarani Pilapitiya & Ratnayake, 2024). Besides, incineration lowers the volume of plastic waste (Tiwari, Azad, Dutta, Yadav, & Kumar, 2023). Conversely, incineration of plastics demands a significant amount of energy and releases toxic gases, ash, and compounds, including greenhouse gases, furans, dioxins, polychlorinated biphenyls, and heavy metals like mercury (Evode et al., 2021; Lim & Thian, 2022). These can cause serious health issues such as respiratory problems, impaired lung function, and an increased risk of cancer (Tiwari et al., 2023; Zhang et al., 2021).

2.3. Recycling

Recycling plastic waste creates secondary materials that can be used to produce original products or new products with similar or improved functionality. The purpose of recycling is to reduce waste and recover raw materials, thus mitigating the harmful impacts of waste on the natural environment and society (Evode et al., 2021).

In these recycling methods, separation process is essential in the processing cycle. Separation processes include manual sorting (visual recognition according to shape, color, and plastic brand markings), automated dry sorting (X-ray sorting, infrared sorting, electrostatic sorting, air sorting, mechanical sorting), and automated wet sorting (sink float, hydrocyclone, selective dissolution, hydroglycolysis) (Nayanathara Thathsarani Pilapitiya & Ratnayake, 2024).

The diverse mix of material components in plastics, including plasticizers, additives, and colorants, makes recycling plastics challenging (Lim & Thian, 2022). Recycling methods for plastic waste can be categorized into three types: mechanical, chemical and thermal recycling. Plastic waste disposal techniques, along with plastic waste recycling methods are displayed in Figure 4.

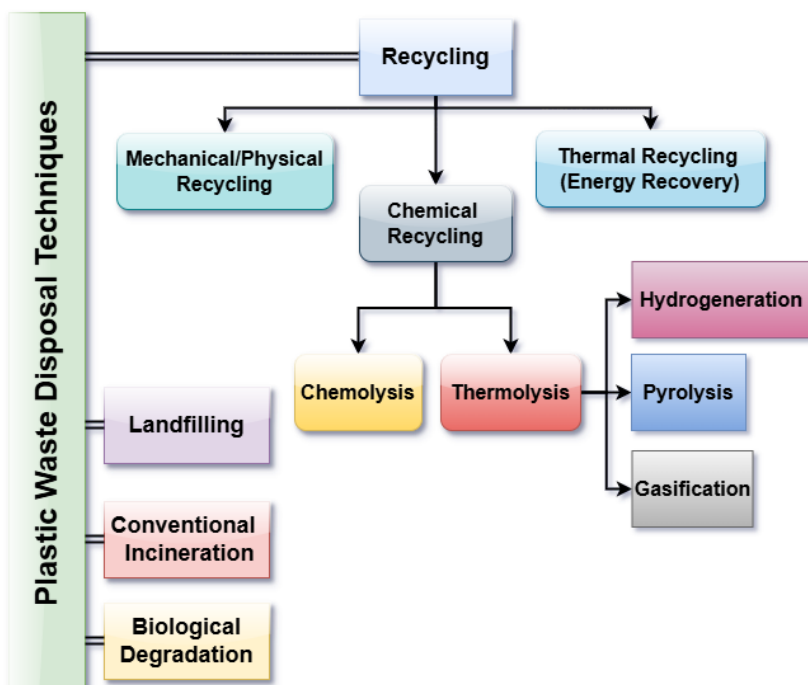


Figure 4. Plastic waste management approaches.

2.3.1. Mechanical Recycling

In mechanical recycling, physical steps, including cutting or shredding, contaminant removal, flotation, milling, washing and drying, agglomeration, extrusion, and quenching are employed to form pellets or flakes (Tejaswini, Pathak, Ramkrishna, & Ganesh, 2022). Mechanical recycling preserves the chemical structure of the materials without significant alteration and is a cost-effective technique. However, it is not suitable for multi-layer plastics or material containing different materials. The quality of recycled plastic often falls short of that of original plastic, which can restrict the range of applications for mechanically recycled plastics (Nayanathara Thathsarani Pilapitiya & Ratnayake, 2024).

2.3.2. Chemical Recycling

Chemical recycling converts plastic waste into smaller molecules by breaking down polymer bonds, producing raw materials for the manufacturing of plastics and petrochemicals. Also, chemical recycling generates different fuel fractions from plastic waste (Nayanathara Thathsarani Pilapitiya & Ratnayake, 2024; Thiounn & Smith, 2020).

Thermolysis is the primary method used in chemical recycling. Pyrolysis, gasification and hydrogenation are the main techniques for thermolysis. Pyrolysis employs various technologies to convert plastic waste into oils and high-calorific clean gas, which is utilized in gas engines to generate electricity (Dai et al., 2022). Gasification uses air to transform plastic waste into fuel or flammable gases, which are a blend of hydrogen (H_2), methane (CH_4), carbon dioxide (CO_2), and carbon monoxide (CO), and are also called syngas (Jiang et al., 2022). In addition, gasification produces ammonia (NH_3), hydrogen sulfide (H_2S), and nitrogen oxides (NO_x) along with syngas. Hydrogenation (also known as hydrocracking) is a chemical process involving the reaction of hydrogen (H_2) with plastic waste. hydrochloric acid (HCl), syncrude, hydrogenated solid residue, and off-gas are the primary products (Nayanathara Thathsarani Pilapitiya & Ratnayake, 2024; Zhang et al., 2021).

Additionally, chemolysis (also called as solvolysis or depolymerization) is another chemical method used to treat or depolymerize plastic waste into monomers. The main chemolysis reaction pathways consist of glycolysis, hydrolysis, methanolysis, and alcoholysis. The operating parameters for monomer recycling are heavily influenced by the type of plastic, making it challenging to efficiently recycle monomers from plastic mixtures containing different plastic types. As a result, the application of chemolysis is somewhat limited (Zhang et al., 2021).

2.3.3. Thermal Recycling

In thermal recycling (energy recovery), plastic waste is burned to generate heat, steam, and subsequently electricity. This process can be carried out using various technologies, including grate technology (which burns plastic waste to generate heat and then electricity), two-stage incineration (which ensures more complete combustion and fewer pollutants), and fluidized bed combustion (which burns plastic waste more efficiently and cleanly) (Nayanathara Thathsarani Pilapitiya & Ratnayake, 2024).

2.4. Biological Degradation

Biodegradable plastic waste can be broken down by microorganisms such as fungi, bacteria, and yeasts, which convert the physical and chemical attributes of plastic waste into polymer carbon while emitting biogas rich in methane, carbon dioxide, water, and heat (Ali et al., 2021; He et al., 2024).

However, synthetic plastic waste biodegrades extremely slowly due to its strong structure, consisting of long polymer chains. Therefore, the oxo-

biodegradation process, which is oxidization of carbon polymers, is crucial for non-biodegradable plastic waste prior to its direct degradation or biodegradation by natural organisms (Lim & Thian, 2022). Following the oxo-biodegradation process, invertebrates (such as mealworms and lesser waxworms), microorganisms, and compost treatment (which involves blending compost with a specific amount of plastics and treating it with present microorganisms at a controlled temperature, typically ranging from 40 to 60°C) are applied to decompose synthetic plastic (Nayanathara Thathsarani Pilapitiya & Ratnayake, 2024).

3. Conclusion

Although plastic usage offers several benefits, its waste poses a serious threat to natural habitats, particularly marine life, due to its chemical and physical properties. Poor waste management and waste disposal strategies causes soil, water and air pollution associated with plastic waste. Therefore, it is crucial to implement complete waste management strategies and adopt proper disposal methods. Sustainable consumption, recycling, reuse, repurposing of plastic materials and products, along with the production and use of biodegradable plastics from sustainable feedstocks, are essential to mitigating the environmental effects of plastic waste. Additionally, these approaches recover raw materials, contribute to the preservation of human and animal well-being, so provide economic and social benefits. For instance, plastic waste can be recovered and reused in different sectors or converted into fuel, which decreases the quantity of plastic waste sent to landfills.

Some pathways for repurposing plastic waste are as follows:

- Plastic oil (also known as pyrolysis oil) derived from plastic waste can be used for energy generation (Chang, 2023).
- Plastic waste can be efficiently and cleanly incinerated to generate heat and electricity.
- Plastic waste can be converted into fuel, used in household products, utilized as construction material, and repurposed in the textile industry (Lamba, Kaur, Raj, & Sorout, 2022).
- Plastic waste can be recycled and used in the production of new products, such as carpets or clothing fibers.
- Plastic waste contains a high concentration of carbon, so carbon materials derived from plastic waste can be used for the

manufacturing of energy storage systems such as supercapacitors, batteries, and pollutant adsorbents (Chen, Wei, Ni, & Chen, 2022).

- Certain types of plastic waste can be used in hot mixed asphalt for road construction (Abdy et al., 2022).

Conventional disposal methods, incineration and landfilling cause serious secondary pollutants, so not preferable to use for disposal of plastic waste. Mechanical recycling (physical recycling) is the most convenient method, but it has some limitations, such as being unsuitable for composite plastics and producing materials that are inferior to the original plastic. Pyrolysis, hydrogenation, and gasification are much better energy recovery methods since they recover valuable materials like oil and gas. Additionally, oxo-biodegradation is a promising disposal technique since it accelerates plastic biodegradation. Thermal recycling allows controlled incineration, improving efficiency and reducing harmful emissions. As a result, plastic waste recycling provides several benefits over conventional disposal techniques, including raw material conservation, energy recovery, and reduced greenhouse gas emissions.

References

- Abdy, C., Zhang, Y., Wang, J., Yang, Y., Artamendi, I., & Allen, B. (2022). Pyrolysis of polyolefin plastic waste and potential applications in asphalt road construction: A technical review. *Resources, Conservation and Recycling*, 180, 106213. <https://doi.org/10.1016/j.resconrec.2022.106213>
- Ali, S. S., Elsamahy, T., Al-Tohamy, R., Zhu, D., Mahmoud, Y. A.-G., Koutra, E., ... Sun, J. (2021). Plastic wastes biodegradation: Mechanisms, challenges and future prospects. *Science of The Total Environment*, 780, 146590. <https://doi.org/10.1016/j.scitotenv.2021.146590>
- Cengiz, M. (2022). A Mini-Review on Household Materials That Are Hard to Recycle. *SEMPOZYUMU*, 63.
- Cengiz, Mazlum, & Gazal, C. (2023). ATIKLARIN PAZARLANMASININ DÖNGÜSEL EKONOMİ AÇISINDAN ÖNEMİ: TÜRKİYE'DEKİ ÜNİVERSİTELER İÇİN BİR ATIK YÖNETİMİ MODELİ ÖNERİSİ. In *SÜRDÜRÜLEBİLİRLİK VE TOPLUMSAL DÖNÜŞÜM* (Vol. 1, pp. 13–53). NOBEL BİLİMSEL.
- Chang, S. H. (2023). Plastic waste as pyrolysis feedstock for plastic oil production: A review. *Science of The Total Environment*, 877, 162719. <https://doi.org/10.1016/j.scitotenv.2023.162719>
- Chen, Z., Wei, W., Ni, B.-J., & Chen, H. (2022). Plastic wastes derived carbon materials for green energy and sustainable environmental applications. *Environmental Functional Materials*, 1(1), 34–48. <https://doi.org/10.1016/j.efmat.2022.05.005>
- Dai, L., Zhou, N., Lv, Y., Cheng, Y., Wang, Y., Liu, Y., ... Ruan, R. (2022). Pyrolysis technology for plastic waste recycling: A state-of-the-art review. *Progress in Energy and Combustion Science*, 93, 101021. <https://doi.org/10.1016/j.pecs.2022.101021>
- Evode, N., Qamar, S. A., Bilal, M., Barceló, D., & Iqbal, H. M. N. (2021). Plastic waste and its management strategies for environmental sustainability. *Case Studies in Chemical and Environmental Engineering*, 4, 100142. <https://doi.org/10.1016/j.csee.2021.100142>
- He, Y., Deng, X., Jiang, L., Hao, L., Shi, Y., Lyu, M., ... Wang, S. (2024). Current advances, challenges and strategies for enhancing the biodegradation of plastic waste. *Science of The Total Environment*, 906, 167850. <https://doi.org/10.1016/j.scitotenv.2023.167850>
- Hossain, R., Tajvidi, M., Bousfield, D., & Gardner, D. J. (2021). Multi-layer oil-resistant food serving containers made using cellulose nanofiber coated wood flour composites. *Carbohydrate Polymers*, 267, 118221. <https://doi.org/10.1016/j.carbpol.2021.118221>
- Jiang, J., Shi, K., Zhang, X., Yu, K., Zhang, H., He, J., ... Liu, J. (2022). From plastic waste to wealth using chemical recycling: A review. *Journal of Environmental*

- Kibria, Md. G., Masuk, N. I., Safayet, R., Nguyen, H. Q., & Mourshed, M. (2023). Plastic Waste: Challenges and Opportunities to Mitigate Pollution and Effective Management. *International Journal of Environmental Research*, 17(1), 20. <https://doi.org/10.1007/s41742-023-00507-z>
- Lamba, P., Kaur, D. P., Raj, S., & Sorout, J. (2022). Recycling/reuse of plastic waste as construction material for sustainable development: A review. *Environmental Science and Pollution Research*, 29(57), 86156–86179. <https://doi.org/10.1007/s11356-021-16980-y>
- LI, W. C., TSE, H. F., & FOK, L. (2016). Plastic waste in the marine environment: A review of sources, occurrence and effects. *Science of The Total Environment*, 566–567, 333–349. <https://doi.org/10.1016/j.scitotenv.2016.05.084>
- Liang, Y., Tan, Q., Song, Q., & Li, J. (2021). An analysis of the plastic waste trade and management in Asia. *Waste Management*, 119, 242–253. <https://doi.org/10.1016/j.wasman.2020.09.049>
- Lim, B. K. H., & Thian, E. S. (2022). Biodegradation of polymers in managing plastic waste—A review. *Science of The Total Environment*, 813, 151880. <https://doi.org/10.1016/j.scitotenv.2021.151880>
- Mulakkal, M. C., Castillo Castillo, A., Taylor, A. C., Blackman, B. R. K., Balint, D. S., Pimenta, S., & Charalambides, M. N. (2021). Advancing mechanical recycling of multilayer plastics through finite element modelling and environmental policy. *Resources, Conservation and Recycling*, 166, 105371. <https://doi.org/10.1016/j.resconrec.2020.105371>
- Naderi Kalali, E., Lotfian, S., Entezar Shabestari, M., Khayatzaadeh, S., Zhao, C., & Yazdani Nezhad, H. (2023). A critical review of the current progress of plastic waste recycling technology in structural materials. *Current Opinion in Green and Sustainable Chemistry*, 40, 100763. <https://doi.org/10.1016/j.cogsc.2023.100763>
- Nayanathara Thathsarani Pilapitiya, P. G. C., & Ratnayake, A. S. (2024). The world of plastic waste: A review. *Cleaner Materials*, 11, 100220. <https://doi.org/10.1016/j.clema.2024.100220>
- Our World in Data. (n.d.). Plastic Pollution. Retrieved November 9, 2024, from <https://ourworldindata.org/plastic-pollution>
- Tamizhdurai, P., Mangesh, V. L., Santhosh, S., Vedavalli, R., Kavitha, C., Bhutto, J. K., ... Kumaran, R. (2024). A state-of-the-art review of multilayer packaging recycling: Challenges, alternatives, and outlook. *Journal of Cleaner Production*, 447, 141403. <https://doi.org/10.1016/j.jclepro.2024.141403>
- Tejaswini, M. S. S. R., Pathak, P., Ramkrishna, S., & Ganesh, P. S. (2022). A comprehensive review on integrative approach for sustainable management of plastic

waste and its associated externalities. *Science of The Total Environment*, 825, 153973. <https://doi.org/10.1016/j.scitotenv.2022.153973>

Thiounn, T., & Smith, R. C. (2020). Advances and approaches for chemical recycling of plastic waste. *Journal of Polymer Science*, 58(10), 1347–1364. <https://doi.org/10.1002/pol.20190261>

Tiwari, R., Azad, N., Dutta, D., Yadav, B. R., & Kumar, S. (2023). A critical review and future perspective of plastic waste recycling. *Science of The Total Environment*, 881, 163433. <https://doi.org/10.1016/j.scitotenv.2023.163433>

Zhang, F., Zhao, Y., Wang, D., Yan, M., Zhang, J., Zhang, P., ... Chen, C. (2021). Current technologies for plastic waste treatment: A review. *Journal of Cleaner Production*, 282, 124523. <https://doi.org/10.1016/j.jclepro.2020.124523>



CHAPTER 17

Comparison of Biodiesel Production Methods and Innovative Approaches

Zehra Gülten Yalçın¹ & Mustafa Dağ² & Muhammed Bora Akın³

¹ Asst. Prof. Dr., Çankırı Karatekin University, Faculty of Engineering, Department of Chemical Engineering, Uluayazı Campus, 18100, Çankırı, Turkey, ORCID: 0000-0001-5460-289X

² Res. Asst. Dr., Çankırı Karatekin University, Faculty of Engineering, Department of Chemical Engineering, Uluayazı Campus, 18100, Çankırı, Turkey, ORCID: 0000-0001-9540-3475

³ Asst. Prof. Dr., Çankırı Karatekin University, Faculty of Engineering, Department of Chemical Engineering, Uluayazı Campus, 18100, Çankırı, Turkey, ORCID: 0000-0003-3841-1633

INTRODUCTION

Increasing environmental concerns, limited fossil fuel reserves, and the need for sustainable energy sources have led to the exploration of alternative energy options. In this context, biofuels hold a significant place among renewable energy sources. Biodiesel, a prominent type of biofuel, is produced through the transesterification of vegetable oils, waste oils, or animal fats into methyl or ethyl esters. This method converts triglycerides into biodiesel and produces glycerin as a byproduct, which can be utilized in various industrial applications, such as biopolymer production (Lamichhane et al., 2020). The chemical structure of biodiesel, characterized by its fatty acid composition, enables its effective use in diesel engines, offering comparable properties to conventional diesel fuels (Mondal & Jana, 2019).

The environmental benefits of biodiesel are substantial; its combustion leads to lower emissions of harmful pollutants compared to petrodiesel. Studies have shown that biodiesel can significantly reduce emissions of carbon dioxide (CO₂), hydrocarbons (HC), and particulate matter (PM) (Krishnamurthy et al., 2013; Mehta et al., 2010). Notably, biodiesel blends have been reported to reduce CO, HC, and particulate emissions in varying degrees, contributing to improved air quality (Veillette et al., 2017). Moreover, the use of biodiesel can lead to a reduction in greenhouse gas emissions; some estimates suggest up to a 78% decrease in CO₂ emissions when biodiesel is used (Mondal & Jana, 2019; Peng, 2015).

The compatibility of biodiesel with existing diesel engines enhances its appeal as a sustainable alternative to fossil fuels. It can be blended with petrodiesel in various ratios, allowing for a smooth transition to renewable energy sources without requiring significant changes in current engine technologies (Song et al., 2013). The increasing use of biodiesel in many countries underscores its potential to play a critical role in achieving energy independence and reducing reliance on fossil fuels (Yuan et al., 2022).

Biodiesel holds a significant place among renewable energy sources. Global production reached 24 billion liters in 2016, followed by 45.4 billion liters in 2020 (Edeh, 2020). The International Energy Agency's (IEA) "Renewables 2023" report projects that global biofuel demand will grow by approximately 30% between 2023 and 2028, representing an increase of 38 billion liters. This growth is particularly supported by countries like Brazil, Indonesia, and India, where biofuel policies and rising transportation fuel demand drive increased biodiesel and ethanol consumption. By 2028, total global biofuel demand is

expected to reach 200 billion liters. Estimates indicate that two-thirds of this increase will come from renewable diesel and ethanol, with the remainder from biodiesel and bio-jet fuel (International Energy Agency, 2023). Additionally, the European Union (EU), under the Renewable Energy Directive III (RED III), plans to double its share of renewable energy by 2030. While blending rates for biodiesel are expected to remain relatively stable, renewable diesel is projected to reach a 3.5% level by 2028 (International Energy Agency, 2023).

The leading biodiesel-producing countries globally include the United States, Brazil, and EU member states. These countries are leaders in biodiesel production due to easy access to agricultural resources and environmentally friendly policies promoting biofuel production. The United States, producing approximately 7.5 billion liters of biodiesel annually, is considered a world leader, with production largely based on oilseed crops like soybeans. Brazil, with policies promoting biodiesel production from sugarcane and other vegetable oils and advantages in raw material access, holds a strong position with an annual production capacity of approximately 5.5 billion liters. The European Union also stands out as a global leader with a total production of around 12 billion liters of biodiesel, particularly high in countries like Germany, France, and Spain. The EU's environmental targets drive increased biodiesel production, reflecting trends in the biofuel economy's growth based on 2021 data (Mizik, 2021).

The growing demand for biodiesel is linked to its environmental benefits and the need for alternative energy sources amid rising fossil fuel prices (Živković & Veljković, 2017). By 2020, the EU implemented policies to promote biodiesel production, aiming for 10% of fuel to come from renewable sources (Frkova et al., 2020). This legal framework has allowed biodiesel to grow as a viable alternative to conventional diesel, particularly in transportation (Elgharbawy et al., 2021). Furthermore, using waste cooking oil and other non-food raw materials in biodiesel production is gaining interest as it addresses concerns over food security and environmental sustainability (Qamar et al., 2020). This trend towards biodiesel production reflects a shift in broader energy policies aimed at reducing greenhouse gas emissions and promoting a circular economy (Živković & Veljković, 2017; Petrescu et al., 2021).

In summary, the biodiesel sector shows strong growth, with increasing production capacities in key regions like the EU, the US, and Brazil. The environmental benefits of biodiesel, coupled with supportive policies and the use of diverse feedstocks, make it a critical component in the renewable energy field (Živković & Veljković, 2017; Kumar et al., 2023).

While biodiesel stands out for its environmental advantages, it can have adverse effects on certain engine components. Compared to conventional diesel, biodiesel has a higher viscosity and a lower calorific value, which can weaken fuel atomization and reduce combustion efficiency (Tutak et al., 2023; Nguyen et al., 2023). As a result, advanced injection timing and improved combustion conditions, which become necessary, lead to higher nitrogen oxide (NO_x) emissions (Bibin et al., 2022; Siddeg et al., 2022). Additionally, studies show that biodiesel's solvent properties may increase wear on fuel system components and injectors, as it can degrade rubber and plastic materials commonly used in these systems (Nguyen et al., 2023; Khan et al., 2021). Furthermore, literature indicates that the lower energy content of biodiesel can lead to increased fuel consumption, thereby accelerating wear and tear on engine parts (Niekerk et al., 2019).

Policy changes in biodiesel production also significantly impact the industry. Stricter emission regulations promote innovations in biodiesel technology, driving the development of more efficient production methods and cleaner-burning fuels (Khan et al., 2021; Ng et al., 2017). However, promoting first-generation biodiesel derived from food crops could exacerbate food security issues, potentially leading to public backlash and reduced subsidies or stricter regulations for biodiesel production (Khan et al., 2021; Jiang et al., 2017). In contrast, policies supporting a shift to second-generation biofuels that use non-food feedstocks could mitigate negative impacts associated with food competition and environmental degradation (Khan et al., 2021; Valente et al., 2011). The economic sustainability of the biodiesel industry is also highly responsive to policy changes. Renewable energy incentives help stabilize the market, whereas removing such incentives may lead to decreased investment and reduced R&D activities in biodiesel technologies (Ng et al., 2017; Valente et al., 2011).

BIODIESEL PRODUCTION

Transesterification, the foundation of biodiesel production, is a process in which triglyceride molecules react with an alcohol to produce fatty acid methyl or ethyl esters (biodiesel) and glycerin. This reaction involves a nucleophilic attack by the alcohol on the ester bonds of triglycerides, resulting in the formation of fatty acid esters, with glycerin produced as a byproduct. The breakdown of triglyceride ester bonds during this process leads to the formation of biodiesel (Ulukardeşler, 2023; Saad et al., 2019). The efficiency of the reaction is significantly influenced by specific process parameters such as the type of alcohol used, catalyst selection, temperature, and molar ratios (Elgharbawy et al., 2021; Yadav, 2017; Mohamed et al., 2023).

The choice of alcohol is particularly important; methanol and ethanol are the most commonly used alcohols in transesterification due to their availability and cost-effectiveness (Batan et al., 2010; Nnamani et al., 2020). In biodiesel production, methanol is often preferred due to its advantageous properties. Methanol's short-chain structure facilitates a high reaction rate, which is critical for an efficient transesterification process. This efficiency is further enhanced when the reaction occurs under alkaline conditions, significantly boosting biodiesel yield (Sánchez et al., 2015; Chamoumi et al., 2014). Methanol is not only cost-effective but also polar, allowing a high conversion rate of triglycerides to fatty acid methyl esters (FAME) (Sánchez et al., 2015; Chamoumi et al., 2014).

While ethanol is also used in biodiesel production, it is less favored due to its tendency to absorb water. This property can lead to the formation of undesirable byproducts during the transesterification process, reducing biodiesel yield (Buasri et al., 2012; Saadon et al., 2015). The presence of water in the reaction mixture can complicate the process, especially with oils high in free fatty acids (FFA), causing hydrolysis and saponification, which lowers yield (Saadon et al., 2015; Ferreira et al., 2017). In such cases, the use of acidic catalysts or the application of two-stage transesterification processes is often recommended to mitigate these issues and enhance biodiesel yield (Zhu et al., 2015; Sahu et al., 2021).

The use of ethanol in biodiesel production increases combustion efficiency due to its oxygen content (Hashemi-Nejhad, 2023). Furthermore, ethanol can be produced through fermentation processes using biomass sources like agricultural waste or energy crops, aligning it with sustainability goals (Rahimi et al., 2020; Sakdasri et al., 2017). This renewable aspect of ethanol not only provides a lower carbon footprint but also supports the circular economy by promoting the use of waste materials (Maranduba et al., 2015; Nježić et al., 2018). Despite the advantages of ethanol, challenges remain regarding its economic sustainability compared to methanol. Ethanol production costs can be higher, especially considering the agricultural inputs required for biomass cultivation (Harsono et al., 2011).

The type of catalyst also plays a critical role in the transesterification process. While homogeneous catalysts like sodium hydroxide are widely used, there is growing interest in heterogeneous catalysts due to their potential to facilitate glycerin separation from biodiesel and allow catalyst reuse (Semwal et al., 2011; Mohamed et al., 2023). Additionally, reaction conditions such as temperature and stirring speeds are important for optimizing biodiesel yield. Studies have shown that altering these parameters can significantly impact the conversion efficiency

of triglycerides to biodiesel (Gebremariam & Marchetti, 2019; Mishra et al., 2021; Harmawan et al., 2021; Sadaf et al., 2018).

The free fatty acid (FFA) content in oils used for biodiesel production is a crucial factor affecting reaction yield. Oils with high FFA levels tend to saponify when using alkaline catalysts, leading to soap formation, which further reduces biodiesel yield (Ferreira et al., 2017; Zhu et al., 2015). Therefore, in cases where feedstocks have high FFA content, it is often necessary to use acidic catalysts or implement a two-stage process where FFAs are first esterified before transesterification is conducted to achieve satisfactory yields (Zhu et al., 2015; Sahu et al., 2021). This approach optimizes the production process by effectively converting triglycerides and FFAs to biodiesel.

In the transesterification process, alkaline catalysts such as sodium hydroxide (NaOH) and potassium hydroxide (KOH) are commonly used due to their high efficiency in facilitating the reaction between triglycerides and alcohol. These catalysts significantly accelerate the conversion of triglycerides into FAME (fatty acid methyl esters), which are the main components of biodiesel. This efficiency is attributed to the catalysts' ability to promote the reaction under relatively mild conditions, making them preferred choices for commercial biodiesel production (Kittithammavong et al., 2014; Toldrá-Reig et al., 2020). However, the effectiveness of these catalysts can be influenced by various factors, such as the properties of the feedstocks and the water content in the reaction environment. High water content leads to soap formation, which complicates the separation of biodiesel from glycerin and reduces overall yield (Ferreira et al., 2017).

In situations where the feedstock has high levels of FFAs or water, acidic or enzymatic catalysts are explored as alternatives to mitigate the adverse effects associated with soap formation. Acidic catalysts like sulfuric acid effectively catalyze transesterification for oils with high FFA content, ensuring more complete conversion without the risk of soap production (Sahu et al., 2021). Furthermore, enzymatic catalysts hold promise due to their ability to operate under milder conditions and minimize byproduct formation, thereby potentially enhancing the overall efficiency of the biodiesel production process (Neag et al., 2023). Research continues to explore these alternative catalytic systems to optimize biodiesel yields and address challenges posed by conventional alkaline catalysts under specific feedstock conditions (Neag et al., 2023; Faruque et al., 2020).

After transesterification, the reaction products separate into two main phases: biodiesel and glycerin. In the transesterification process, where triglycerides (oils

and vegetable oils) react with alcohol in the presence of a catalyst, biodiesel production has been well-established as the primary method, yielding FAME (fatty acid methyl esters) as the main product and glycerin as a byproduct (Klaus et al., 2013; Ayoub et al., 2023; Elgharbawy et al., 2021). Glycerin, which is produced at about 10% of the biodiesel yield, can be separated from the biodiesel phase and used in various industrial applications, including pharmaceuticals, cosmetics, and food production (Chou & Su, 2019; Chilakamarthy et al., 2021).

On the other hand, biodiesel must undergo several purification steps to meet motor fuel standards in terms of viscosity, density, and flammability. These purification processes, which directly impact biodiesel quality, have a significant effect on combustion characteristics and engine performance (Díaz et al., 2024; Ampairojanawong et al., 2020; Singh et al., 2020). Purification typically involves removing residual methanol, catalyst residues, and glycerin impurities; if not sufficiently removed, these residues can negatively affect engine performance (Blinová et al., 2013; Sakkamas et al., 2020). The efficiency of these purification steps is crucial to ensure that biodiesel meets strict regulatory standards for use as a motor fuel (Postaue et al., 2022; Agustina et al., 2022).

Moreover, the purity level achieved through these processes has significant effects on the combustion characteristics of biodiesel. High-purity biodiesel provides better combustion efficiency, improving engine performance and reducing emissions (Asdrubali et al., 2015; Nila et al., 2021). Therefore, carefully managing both the transesterification process and subsequent purification steps is vital to producing effective fuel and ensuring environmental sustainability (Dieng et al., 2020; Kittithammavong et al., 2014).

While biodiesel production is commonly carried out through transesterification, other methods are also being explored to support biofuel production from various raw materials. These alternative methods are developed considering factors such as the properties of the raw material, environmental conditions, and the cost of the production process. Although less common than transesterification, these methods can offer significant advantages for enhancing sustainability in biodiesel production and addressing diverse industrial requirements. A summary of the classification of raw materials used in biodiesel production is presented in Table 1.

Table 1. Classification of biodiesel production feedstocks (Kalita et al., 2022)

Classification Name	Type of Feedstock
First Generation	Edible oils such as rapeseed, sunflower, palm, peanut, soy-bean, coconut, peanut, corn, and canola
Second Generation	Non-edible oils such as jatropha, karanja, castor oil, mahua, tobacco, rubber, polanga, and oleander
Third Generation	Feedstocks such as poultry fat, chicken fat, animal tallow, fish oil, algae, and waste cooking oil
Fourth Generation	Feedstocks including photobiological solar, synthetic cells, and electro-biofuels

Thermal Cracking (Pyrolysis)

Thermal cracking, also known as pyrolysis, is a significant process involving the thermal decomposition of organic compounds at high temperatures in an oxygen-free environment. This method typically operates within the 400-600°C range; vegetable oils and animal fats are subjected to heat, causing the long-chain triglycerides to break down into shorter-chain hydrocarbons. The products obtained through this process exhibit properties similar to biodiesel, positioning thermal cracking as an alternative to conventional biodiesel production methods such as transesterification. Unlike transesterification, thermal cracking can utilize a broader range of feedstocks, enhancing its applicability in biofuel production (Kareem & Al.Tameemi, 2022; Beims et al., 2017).

However, the thermal cracking process requires careful control of product quality and byproducts. High temperatures can lead to impurity formation, necessitating additional refining steps to ensure the purity and quality of the final biofuel product. Research shows that thermal conditions significantly impact the composition and quality of pyrolysis products, with higher temperatures increasing the yield of gas and liquid products but also raising impurity levels (Ronsse et al., 2012; Jiang et al., 2016). For example, as pyrolysis temperature rises, the distribution of bio-oil, biogas, and charcoal may vary, affecting the overall efficiency and quality of the produced biofuel (Ronsse et al., 2012).

Additionally, the thermal cracking process can produce various byproducts, such as tars and gases, which may complicate the refining process. The presence of these byproducts can create the need for further processing to remove unwanted components and enhance biofuel quality, potentially introducing operational challenges. Managing these byproducts is critical to optimizing the economic feasibility of thermal cracking as a biofuel production method (Beims et al., 2017). Therefore, while thermal cracking is promising for producing biodiesel-like fuels, careful evaluation of operational parameters and product

management is essential to mitigate possible disadvantages related to impurity levels and byproduct formation.

Supercritical Alcohol Method

The supercritical alcohol method is a technique used in biodiesel production to reduce the need for catalysts and accelerate the process. In this method, alcohol (usually methanol or ethanol) is brought to a supercritical state and then reacted with oils. Under supercritical conditions, the alcohol exhibits properties that enhance its solvent power, enabling more efficient reactions with oils. This method typically requires high temperatures (approximately 240-350°C) and high pressures (up to 35 MPa), and because no catalyst is used, side reactions such as soap formation are avoided (Deshpande et al., 2017; León et al., 2018; Gumba et al., 2016). Additionally, this technique allows biodiesel production with feedstocks high in free fatty acid content, a scenario that often poses challenges for conventional methods (Deshpande et al., 2017; Gumba et al., 2016).

However, the supercritical alcohol process can be costly due to its high energy requirements. The energy-intensive nature of maintaining supercritical conditions and the necessary infrastructure for high-pressure operations contribute to overall production costs (Deshpande et al., 2017; León et al., 2018). Despite these challenges, the supercritical alcohol method is seen as a promising alternative to conventional transesterification methods that use catalysts, as it achieves high conversion rates and purity in biodiesel production (Deshpande et al., 2017; Gumba et al., 2016). Furthermore, using waste oils and feedstocks with high free fatty acid content can help offset biodiesel production costs, making it a viable option for sustainable energy solutions (Deshpande et al., 2017; Gumba et al., 2016).

In conclusion, while the supercritical alcohol method presents certain economic challenges, its advantages in terms of efficiency and feedstock versatility make it a significant area of research and development in biodiesel production.

Microwave-Assisted Biodiesel Production

Microwave-assisted biodiesel production is an innovative technique that enhances the efficiency and speed of the transesterification process. In this method, a mixture of oil and alcohol is rapidly heated with microwave irradiation, increasing the frequency of molecular collisions and significantly accelerating the reaction rate (Peng et al., 2018; Sherbiny et al., 2010). Applying microwave

energy in biodiesel production improves energy efficiency and allows for faster biodiesel formation compared to traditional methods (Tiwari et al., 2022; Welter et al., 2023). Additionally, this method can be effectively combined with catalysts and integrated with supercritical alcohol methods, further optimizing the production process (Gumba et al., 2016; Sherbiny et al., 2010).

One of the primary advantages of microwave-assisted biodiesel production is its low energy costs and high yield. Studies have shown that microwave use significantly reduces both reaction time and energy consumption, making it a cost-effective alternative for biodiesel synthesis (Martinez-Guerra & Gude, 2017; Godwin et al., 2010). Furthermore, the ability to use waste cooking oil as a raw material not only reduces production costs but also contributes to sustainability by reducing waste (Nayebzadeh, 2017; Mitani, 2018). However, despite these benefits, there are technical challenges to address for the method's feasibility at an industrial scale. Issues such as reactor design and the uniform distribution of microwave energy can complicate the scalability of this technology (Davies et al., 2020; González et al., 2020).

In conclusion, microwave-assisted biodiesel production offers significant advantages in terms of efficiency and sustainability, yet overcoming technical challenges related to reactor design and energy distribution will be crucial for successful industrial applications (Silviana et al., 2022; Benaskar et al., 2012). Continued research and development in this field are necessary to fully realize the potential of microwave technology in biodiesel production.

Ultrasonication in Biodiesel Production

Ultrasonication is an advanced technique used to increase efficiency and accelerate the reaction rate in biodiesel production via transesterification. In this process, ultrasonic waves create cavitation effects, leading to the formation and collapse of small gas bubbles in the mixture, releasing intense localized energy. This energy facilitates the effective mixing of oil and alcohol molecules, resulting in higher biodiesel yield and a faster reaction within a shorter timeframe (Martín et al., 2015; Stebeleva & Minakov, 2021). The cavitation effect produced by ultrasonication increases the frequency of molecular collisions, potentially reducing the need for a catalyst and enabling the reaction to occur at lower temperatures and pressures (Tiwari et al., 2022; Goh et al., 2020). This method is particularly advantageous for achieving high yield levels that are difficult to attain with traditional mixing techniques (Silviana et al., 2022).

For example, when working with low-quality feedstocks or oils with high free fatty acid (FFA) content, ultrasonication minimizes the formation of byproducts

like soap, allowing for the production of purer biodiesel (Niculescu et al., 2019; Jiménez et al., 2023). Studies have shown that ultrasound-assisted transesterification can significantly reduce catalyst load, methanol-to-oil molar ratio, reaction time, and temperature compared to mechanical mixing processes (Onanuga & Coker, 2013; Sungnat & Wongwuttanasatian, 2018). Additionally, ultrasonication offers several benefits in biodiesel production, such as shorter reaction time, reduced catalyst consumption, increased yield, and lower energy requirements (Narwani et al., 2016; Mandal et al., 2022).

However, the industrial application of ultrasonication involves special equipment and cost requirements. The need for continuous high-energy ultrasonic waves and proper cooling of the system introduces technical challenges that impact scalability (Naveena et al., 2015; Barma et al., 2018). Despite these challenges, ultrasonication represents a promising approach for enhancing biodiesel production efficiency and reducing costs, and it remains an active area of research and development (Timyamprasert, 2015; Aboelazayem et al., 2018).

In a recent study, the effects of an ultrasonic bath on the characteristics of biodiesel derived from hazelnut oil were examined. The results indicated that ultrasonic bath application increased the conversion in biodiesel's chemical structure, promoting the formation of shorter-chain fatty acid methyl esters and enhancing biodiesel purity. While 1-2 hours of sonication positively affected biodiesel yield, extended sonication led to increased reversions and reduced yield. Additionally, FTIR analyses showed that shorter sonication times improved transesterification efficiency, but three hours of sonication provided values closer to biodiesel's original characteristics. Ultimately, ultrasonic bath application reduces the need for chemical additives in biodiesel production, offering environmental and economic benefits (Şimşek, 2024).

Enzymatic Conversion in Biodiesel Production

Enzymatic conversion is emerging as an environmentally friendly alternative in biodiesel production. In this method, enzymes, particularly lipases, are used as biocatalysts to facilitate the reaction between oils and alcohols under mild conditions. This approach allows enzymatic transesterification to operate at low temperatures and neutral pH, significantly reducing energy consumption and minimizing side reactions such as soap formation, which are common in traditional chemical processes (Amini et al., 2015; Alhanif, 2023). The selectivity of enzymes results in high-purity biodiesel, making this method especially advantageous compared to conventional base-catalyzed processes, which often produce lower-quality products and more waste (Alhanif, 2023).

The mechanism of enzyme-catalyzed biodiesel synthesis begins with the formation of an enzyme-substrate complex as the oil (substrate) molecule binds with the enzyme (Figure 1). The triglyceride structure in the oil interacts with the enzyme, leading to the hydrolysis of ester bonds, allowing the enzyme to attach to the substrate's first ester group. This initial enzyme-substrate complex enables the fatty acid chain to undergo transesterification with a methyl alcohol molecule through the action of the enzyme. In the subsequent stage, the enzyme separates from the structure to form biodiesel, a fatty acid alkyl ester, and a diglyceride molecule. At this stage, the enzyme becomes reactivated and ready to react with another substrate molecule. This cycle continues, completing the biodiesel production process (Figure 1). Throughout the mechanism, the enzyme is not consumed, serving a catalytic role that enhances reaction efficiency (Kalita et al., 2022).

In biodiesel production, enzymes widely used as biocatalysts are primarily lipases. In this process, *Candida antarctica* lipase stands out due to its high stability and effective activity in transesterification reactions, while *Mucor miehei* lipase contributes to biodiesel synthesis by esterifying various fatty acids. *Pseudomonas cepacia* lipase provides high yield in biodiesel production, and *Rhizopus oryzae* lipase is preferred for processing feedstocks with high free fatty acid content. Additionally, *Aspergillus niger* lipase is used for biodiesel production from waste oils, showing high stability in repeated use. *Thermomyces lanuginosus* lipase is also an efficient biocatalyst for biodiesel synthesis from various oils. These enzymes are chosen for their high activity, low byproduct formation, and environmentally friendly properties. Moreover, through various immobilization methods, these enzymes can be reused, aiming to reduce production costs (Kalita et al., 2022).

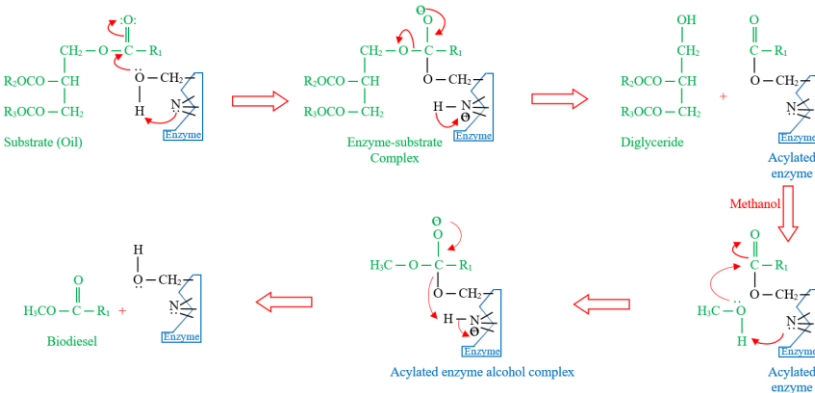


Figure 1. Mechanism of enzyme-catalyzed biodiesel synthesis (Kalita et al., 2022)

However, the economic feasibility of enzymatic biodiesel production is influenced by factors such as enzyme cost and reusability. The high cost of enzymes can be a barrier to widespread use, necessitating the development of various enzyme immobilization techniques to improve reusability and reduce overall process costs (Ramos et al., 2016; Escamilla-Alvarado et al., 2016). For example, studies on immobilizing lipases have shown that this approach can significantly enhance enzyme stability and activity, making the enzymatic process more economical (Ramos et al., 2016). Additionally, innovative strategies, such as the use of glycerin extraction columns (as shown in Figure 2), have been explored to reduce the inhibitory effects of byproducts, further improving the efficiency of the enzymatic process (Ramos et al., 2016).

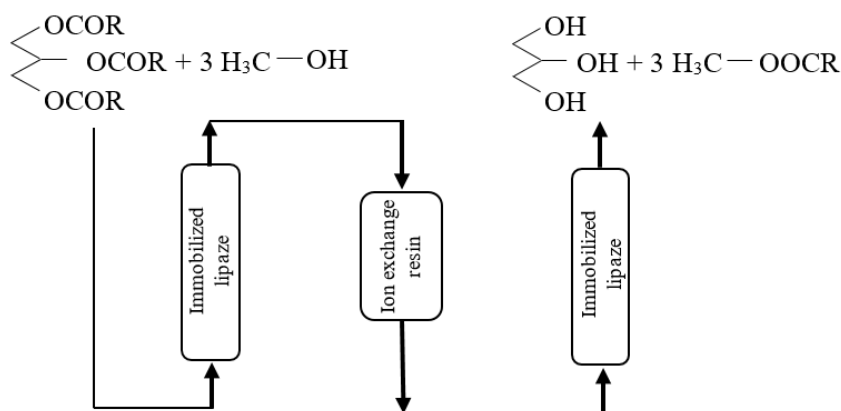


Figure 2. Schematic representation of the two-column method to reduce inhibitor effects (Ramos et al., 2016)

In summary, while enzymatic conversion offers a sustainable and efficient alternative in biodiesel production, addressing economic challenges related to enzyme costs and reusability is crucial for broader application of this method within the biofuel industry.

Electrochemical Method in Biodiesel Production

The electrochemical method offers an innovative approach to enhance the transesterification process in biodiesel production, aiming to improve reaction efficiency and reduce dependency on catalysts. In this method, a mixture of oil and alcohol is exposed to an electric current in an electrochemical cell, accelerating the reaction. The core principle of electrochemical transesterification is that the energy provided by the electric current can minimize or even eliminate the need for conventional chemical catalysts, enabling biodiesel production without acidic or basic catalysts. This method offers several advantages,

including reduced catalyst usage, shorter reaction times, improved energy efficiency, and the production of high-purity biodiesel (Ratanabuntha et al., 2018).

Typically, the oil and alcohol solution is brought into contact with electrodes, where the electric current activates ions in the solution to facilitate the transesterification reaction (Figure 3). The potential difference between the anode and cathode electrodes drives the reaction, although efficiency depends on factors such as electrode material, current density, and solution conditions. Additionally, while higher current densities can increase reaction rates, they may also elevate the risk of side reactions (Ratanabuntha et al., 2018).

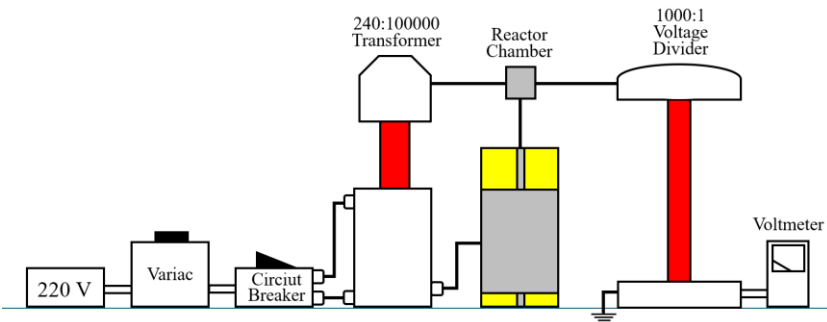


Figure 3. Equipment providing high voltage (Ratanabuntha et al., 2018)

Despite its potential, the electrochemical method in biodiesel production faces challenges, particularly on larger scales, such as equipment costs, optimization of current density, and electrode durability. While this approach promises a catalyst-free and energy-efficient alternative for biodiesel synthesis, further research is necessary to address these technical challenges and ensure its full industrial viability. Integrating electrochemical techniques with existing biodiesel production methods could provide a more sustainable and economically viable process, especially in regions with feedstocks high in free fatty acid levels (Ratanabuntha et al., 2018).

Biodiesel production methods offer various advantages and disadvantages, each with its unique strengths and limitations. While transesterification remains the most widely used method, newer techniques like supercritical fluid processing and ultrasound-assisted synthesis are also gaining attention. Each of these methods has its distinct advantages and disadvantages, as summarized in Table 2.

Table 2. Advantages and disadvantages of biodiesel production methods

Method	Advantages	Disadvantages
Transesterification	<ul style="list-style-type: none">- Widely used and well-researched method (Şahin & Aydın, 2018; Supriyanto et al., 2021).- High yield conversion of triglycerides to biodiesel (Blinová et al., 2013).- Can use various feedstocks, including waste oils (Souza et al., 2012; Asri & Sari, 2015).	<ul style="list-style-type: none">- Requires catalyst (typically alkaline), leading to soap formation that complicates purification (Postaue et al., 2022).- Produces a significant amount of wastewater (Postaue et al., 2022).
Supercritical Fluid Processing	<ul style="list-style-type: none">- Does not require a catalyst, simplifying the process (León et al., 2018; Gumba et al., 2016).- Higher reaction rates and yields due to high temperature and pressure (Gumba et al., 2016).- Can process feedstocks with high FFA content (Gumba et al., 2016).	<ul style="list-style-type: none">- High operating costs due to extreme conditions (Gumba et al., 2016).- Requires special equipment (Gumba et al., 2016).
Ultrasound-Assisted Synthesis	<ul style="list-style-type: none">- Enhances mass transfer and reaction rates (Silviana et al., 2022).- Can be conducted at lower temperatures compared to traditional methods (Silviana et al., 2022).- Significantly reduces reaction time (Silviana et al., 2022).	<ul style="list-style-type: none">- Equipment can be expensive (Silviana et al., 2022).- Limited scalability for industrial applications (Silviana et al., 2022).
Microwave-Assisted Synthesis	<ul style="list-style-type: none">- Provides shorter reaction times due to rapid heating (Silviana et al., 2022).- Improves biodiesel yield and quality (Silviana et al., 2022).- Can be more energy-efficient than conventional heating (Silviana et al., 2022).	<ul style="list-style-type: none">- Requires high initial investment for microwave reactors (Silviana et al., 2022).- Parameters need careful optimization (Silviana et al., 2022).
Pyrolysis (Thermal Cracking)	<ul style="list-style-type: none">- Can convert a wide range of biomass into biodiesel (Daud et al., 2015).- Produces biochar byproduct that can be used as a soil conditioner (Daud et al., 2015).	<ul style="list-style-type: none">- Complex process with various byproducts (Daud et al., 2015).- High energy consumption due to required high temperatures (Daud et al., 2015).
Electrochemical Methods	<ul style="list-style-type: none">- Can operate under mild conditions (Silviana et al., 2022).- Offers potential for continuous production (Silviana et al., 2022).- Reduces use of hazardous chemicals (Silviana et al., 2022).	<ul style="list-style-type: none">- Still in research phase with limited commercial applications (Silviana et al., 2022).- Requires further optimization for efficiency (Silviana et al., 2022).

Table 2 provides a detailed comparison of the advantages and disadvantages of different methods used in biodiesel production. Transesterification, a traditional method, stands out for its widespread use and high conversion efficiency of triglycerides to biodiesel. However, the need for catalysts and the formation of soap as a byproduct can limit the process’s efficiency. In contrast, alternative methods like supercritical fluid processing simplify the process by

eliminating the need for catalysts but increase operational costs due to the high temperature and pressure requirements.

Innovative techniques like ultrasound-assisted and microwave-assisted synthesis draw attention for reducing reaction times and enhancing energy efficiency. However, the industrial scalability of these methods is limited by the costs of specialized equipment and restricted scalability. Pyrolysis (thermal cracking) has the potential to convert a wide range of biomass into biofuel, but the high-temperature requirements and complex byproducts necessitate additional refining steps.

Electrochemical methods present a sustainable alternative with the advantages of operating under mild conditions and reducing the use of hazardous chemicals. However, this method is still in the research phase and has not achieved widespread commercial use.

In conclusion, transesterification remains a viable method in biodiesel production, supporting environmental sustainability and economic efficiency. Biodiesel's chemical structure, suitable for diesel engines, offers environmental benefits due to its low sulfur and nitrogen content. Research on biodiesel production continues, focusing on optimizing process parameters to increase its usability in a broader range of applications.

Overall, each method's contributions to the biodiesel production process have been evaluated in terms of environmental sustainability and economic feasibility, highlighting the advantages and limitations of various techniques. These comparisons will guide efforts to optimize the biodiesel production process and develop more efficient and sustainable solutions suited for industrial applications.

Conclusion

This study provides a detailed examination of the advantages and disadvantages of various alternative methods in biodiesel production, with a particular focus on transesterification. In addition to the widely used transesterification method, the study evaluates the potential of innovative techniques such as supercritical fluid processing, ultrasound-assisted synthesis, microwave-assisted synthesis, pyrolysis, and electrochemical methods. Each method's opportunities and challenges are compared in terms of efficiency, energy cost, and environmental impacts. Specifically, the compatibility of each method with different feedstock characteristics, environmental conditions, and cost factors contributes significantly to sustainable biofuel production. This study serves as an important resource for the development of more efficient and environmentally friendly biodiesel production processes in the biofuel industry.

References

- Aboelazayem, O., Gadalla, M., & Saha, B. (2018). Valorisation of high acid value waste cooking oil into biodiesel using supercritical methanolysis: experimental assessment and statistical optimisation on typical egyptian feedstock. *Energy*, 162, 408-420. <https://doi.org/10.1016/j.energy.2018.07.194>
- Agustina, T., Heraldy, E., Hadiah, F., Hasanudin, H., Arita, S., Prakoso, T., ... & Ramadhani, D. (2022). Biodiesel production of palm oil mill effluent by using hydrotalcite catalyst. *Journal of Ecological Engineering*, 23(6), 172-181. <https://doi.org/10.12911/22998993/148153>
- Alhanif, M. (2023). Biodiesel production: potential and future trends – a review. *Chemtag Journal of Chemical Engineering*, 4(1), 29. <https://doi.org/10.56444/cjce.v4i1.3944>
- Amini, Z., Mazaheri, H., & Chyuan, O. (2015). Partial purification of bacterial lipase to be further used in biofuel production as a renewable energy source. <https://doi.org/10.17758/urebe.u0115222>
- Ampairojanawong, R., Boripun, A., Ruankon, S., Suwanasri, T., & Kangsadan, T. (2020). Development of purification process using electrocoagulation technique for biodiesel produced via homogeneous catalyzed transesterification process of refined palm oil. *E3s Web of Conferences*, 141, 01010. <https://doi.org/10.1051/e3sconf/202014101010>
- Asdrubali, F., Cotana, F., Rossi, F., Presciutti, A., Rotili, A., & Guattari, C. (2015). Life cycle assessment of new oxy-fuels from biodiesel-derived glycerol. *Energies*, 8(3), 1628-1643. <https://doi.org/10.3390/en8031628>
- Asri, N. and Sari, D. (2015). Pre-treatment of waste frying oils for biodiesel production. *Modern Applied Science*, 9(7), 99. <https://doi.org/10.5539/mas.v9n7p99>
- Ayoub, M., Johari, S.A.M., Shamsuddin, M.R., Abdullah, B., Farukkh, S., Naqvi, S.R., Danish, M. Kinetic study for biodiesel production from dairy waste via catalytic microwave heating, *Sustainable Processes and Clean Energy Transition - ICSuPCET2022*, Materials Research Forum LLC, Materials Research Proceedings, vol. 29, pp. 307-314, 2023. <https://doi.org/10.21741/9781644902516-34>.
- Barma, S., Sathish, R., Baskey, P., & Biswal, S. (2018). Chemical beneficiation of high-ash indian noncoking coal by alkali leaching under low-frequency ultrasonication. *Energy & Fuels*, 32(2), 1309-1319. <https://doi.org/10.1021/acs.energyfuels.7b03291>
- Batan, L., Quinn, J., Willson, B., & Bradley, T. (2010). Net energy and greenhouse gas emission evaluation of biodiesel derived from microalgae. *Environmental Science & Technology*, 44(20), 7975-7980. <https://doi.org/10.1021/es102052y>
- Beims, R., Bertoli, S., Botton, V., Ender, L., Simionatto, E., Meier, H., ... & Wiggers, V. (2017). Co-processing of thermal cracking bio-oil at petroleum refineries.

- Brazilian Journal of Petroleum and Gas, 11(2), 99-113. <https://doi.org/10.5419/bjpg2017-0009>
- Benaskar, F., Patil, N., Engels, V., Rebrov, E., Meuldijk, J., Hulshof, L., ... & Schouten, J. (2012). Microwave-assisted Cu-catalyzed Ullmann ether synthesis in a continuous-flow milli-plant. *Chemical Engineering Journal*, 207-208, 426-439. <https://doi.org/10.1016/j.cej.2012.06.147>
- Bibin, C., Devan, P., Sheeja, R., & Madhu, S. (2022). Thermal and chemical exhaust gas recirculation potential of punnai oil biodiesel fuelled diesel engine for environmental sustainability.. <https://doi.org/10.21203/rs.3.rs-1266110/v1>
- Blinová, L., Fiala, J., & Balog, K. (2013). Biodiesel production from waste cooking oil in laboratory scale. *Applied Mechanics and Materials*, 448-453, 1656-1659. <https://doi.org/10.4028/www.scientific.net/amm.448-453.1656>
- Buasri, A., Chaiyut, N., Loryuenyong, V., Rodklum, C., Chaikwan, T., Kumphan, N., ... & Wittayarounayut, W. (2012). Transesterification of waste frying oil for synthesizing biodiesel by KOH supported on coconut shell activated carbon in packed bed reactor. *ScienceAsia*, 38(3), 283. <https://doi.org/10.2306/scienceasia1513-1874.2012.38.283>
- Chamoumi, M., Veillette, M., Fauchoux, N., & Heitz, M. (2014). Biodiesel Production From Used Frying Oil and Microalgae: A Preliminary Study. *WIT Transactions on Ecology and the Environment*, 180, 453-461. <https://doi.org/10.2495/WM140391>.
- Chilakamarri, C., Sakinah, A., Zularisam, A., & Pandey, A. (2021). Glycerol waste to value added products and its potential applications. *Systems Microbiology and Biomanufacturing*, 1(4), 378-396. <https://doi.org/10.1007/s43393-021-00036-w>
- Chou, Y. and Su, J. (2019). Biogas production by anaerobic co-digestion of dairy wastewater with the crude glycerol from slaughterhouse sludge cake transesterification. *Animals*, 9(9), 618. <https://doi.org/10.3390/ani9090618>
- Daud, N., Abdullah, S., Hasan, H., & Yaakob, Z. (2015). Production of biodiesel and its wastewater treatment technologies: a review. *Process Safety and Environmental Protection*, 94, 487-508. <https://doi.org/10.1016/j.psep.2014.10.009>
- Davies, E., Deutz, P., & Zein, S. (2020). Single-step extraction-esterification process to produce biodiesel from palm oil mill effluent (POME) using microwave heating: a circular economy approach to making use of a difficult waste product. *Biomass Conversion and Biorefinery*, 12(7), 2901-2911. <https://doi.org/10.1007/s13399-020-00856-1>
- Deshpande, S., Sunol, A., & Philippidis, G. (2017). Status and prospects of supercritical alcohol transesterification for biodiesel production. *Wiley Interdisciplinary Reviews Energy and Environment*, 6(5). <https://doi.org/10.1002/wene.252>

- Díaz, L., Borges, M., & Brito, A. (2024). Biodiesel production performance estimation from simple viscosity measurements. *Renewable Energy and Power Quality Journal*, 9(1). <https://doi.org/10.24084/repqj09.233>
- Dieng, M., Iwanaga, T., Yurie, N., & Torii, S. (2020). Evaluation of performance and emission characteristics of biodiesel fuel produced from rapeseed oil. *Journal of Energy and Power Engineering*, 14(3). <https://doi.org/10.17265/1934-8975/2020.03.001>
- Edeh, I. (2020). Biodiesel Production as a Renewable Resource for the Potential Displacement of the Petroleum Diesel. In V. Beschkov (Ed.), *Biorefinery Concepts, Energy and Products*. IntechOpen. <https://doi.org/10.5772/intechopen.93013>
- Elgharbawy, A., Sadik, W., Sadek, O., & Kasaby, M. (2021). A review on biodiesel feedstocks and production technologies. *Journal of the Chilean Chemical Society*, 66(1), 5098-5109. <https://doi.org/10.4067/s0717-97072021000105098>
- Escamilla-Alvarado, C., Perez-Pimienta, J., Ponce-Noyola, T., & Poggi-Varaldo, H. (2016). An overview of the enzyme potential in bioenergy-producing biorefineries. *Journal of Chemical Technology & Biotechnology*, 92(5), 906-924. <https://doi.org/10.1002/jctb.5088>
- Faruque, M., Razzak, S., & Hossain, M. (2020). Application of heterogeneous catalysts for biodiesel production from microalgal oil—a review. *Catalysts*, 10(9), 1025. <https://doi.org/10.3390/catal10091025>
- Ferreira, D., Torres, C., Lins, V., & Park, S. (2017). Computational fluid dynamics investigation for austenitic aisi 904l stainless steel corrosion in a biodiesel stream piping. *Materials and Corrosion*, 69(2), 266-279. <https://doi.org/10.1002/maco.201709727>
- Frkova, Z., Venditti, S., Herr, P., & Hansen, J. (2020). Assessment of the production of biodiesel from urban wastewater-derived lipids. *Resources Conservation and Recycling*, 162, 105044. <https://doi.org/10.1016/j.resconrec.2020.105044>
- Gebremariam, S. and Marchetti, J. (2019). Techno-economic performance of a bio-refinery for the production of fuel-grade biofuel using a green catalyst. *Biofuels Bioproducts and Biorefining*, 13(4), 936-949. <https://doi.org/10.1002/bbb.1985>
- Godwin, D., Lawton, S., Moseley, J., Welham, M., & Weston, N. (2010). Energy efficiency of conventionally-heated pilot plant reactors compared with microwave reactors. *Energy & Fuels*, 24(10), 5446-5453. <https://doi.org/10.1021/ef100972f>
- Goh, B., Chong, C., Ge, Y., Ong, H., Ng, J., Tian, B., ... & Józsa, V. (2020). Progress in utilisation of waste cooking oil for sustainable biodiesel and biojet fuel production. *Energy Conversion and Management*, 223, 113296. <https://doi.org/10.1016/j.enconman.2020.113296>

- González, J., Gutiérrez, P., Medina, M., López-Zapata, B., Guerrero, G., & Valdés, L. (2020). Effects on biodiesel production caused by feed oil changes in a continuous stirred-tank reactor. *Applied Sciences*, 10(3), 992. <https://doi.org/10.3390/app10030992>
- Gumba, R., Saallah, S., Misson, M., Ongkudon, C., & Anton, A. (2016). Green biodiesel production: a review on feedstock, catalyst, monolithic reactor, and supercritical fluid technology. *Biofuel Research Journal*, 3(3), 431-447. <https://doi.org/10.18331/brj2016.3.3.3>
- Harmawan, T., Ani, W., Andani, P., & Fadly, T. (2021). Production of biodiesel through transesterification of crude palm oil (cpo) using montmorillonite nanoparticles (nano-mmt) as heterogeneous solid catalyst.. <https://doi.org/10.2991/as-sehr.k.210909.017>
- Harsono, S., Prochnow, A., Grundmann, P., Hansen, A., & Hallmann, C. (2011). Energy balances and greenhouse gas emissions of palm oil biodiesel in indonesia. *GCB Bioenergy*, 4(2), 213-228. <https://doi.org/10.1111/j.1757-1707.2011.01118.x>
- Hashemi-Nejhad, A. (2023). The effect of biodiesel, ethanol, and water on the performance and emissions of a dual-fuel diesel engine with natural gas: sustainable energy production through a life cycle assessment approach. *International Journal of Energy Research*, 2023, 1-24. <https://doi.org/10.1155/2023/4630828>
- International Energy Agency, *Renewables 2023: Analysis and Forecast to 2028*. IEA Publications, 2023. [Erişim Adresi: <https://www.iea.org/reports/renewables-2023>]
- Jiang, D., Wang, J., Fu, J., & Huang, Y. (2017). Could biofuel development stress china's water resources?. *GCB Bioenergy*, 9(9), 1447-1460. <https://doi.org/10.1111/gcbb.12440>
- Jiang, L., Dong, G., Fang, C., & Wang, J. (2016). Research progress of oil making from sewage sludge. *Applied Mechanics and Materials*, 851, 232-236. <https://doi.org/10.4028/www.scientific.net/amm.851.232>
- Jiménez, J., Bucio, J., Blas, V., Gamboa, O., Ramírez, N., & Calva, G. (2023). Characterization of oil extracted from activated sludge of wastewater treatment plants in chetumal, quintana roo. *International Journal of Biological and Natural Sciences*, 3(3), 2-6. <https://doi.org/10.22533/at.ed.813332327038>
- Kalita, P., Basumatary, B., Saikia, P., Das, B., & Basumatary, S. (2022). Biodiesel as renewable biofuel produced via enzyme-based catalyzed transesterification. *Energy Nexus*, 6, 100087. <https://doi.org/10.1016/j.nexus.2022.100087>
- Kareem, H. and Al.Tameemi, H. (2022). Upgrading the atmospheric distillation residue of al- samawah refinery utilizing thermal cracking process. *Al-Qadisiyah Journal for Engineering Sciences*, 15(4), 244-249. <https://doi.org/10.30772/qjes.v15i4.879>

- Khan, M., Bonifacio, S., Clowes, J., Foulds, A., Holland, R., Matthews, J., ... & Shallcross, D. (2021). Investigation of biofuel as a potential renewable energy source. *Atmosphere*, 12(10), 1289. <https://doi.org/10.3390/atmos12101289>
- Kittithammavong, V., Arpornpong, N., Charoensaeng, A., & Khaodhiar, S. (2014). Environmental life cycle assessment of palm oil- based biofuel production from transesterification: greenhouse gas, energy and water balances. *International Conference on Advances in Engineering and Technology (ICAET'2014)*. March 29-30, 2014 Singapore 615-621. <https://doi.org/10.15242/iee.e0314052>
- Klaus, O., Villetti, L., Siqueira, J., Souza, S., Santos, R., Nogueira, C., ... & Rosseto, C. (2013). Efficiency and fuel specific consumption of an engine running on fish biodiesel. *Scientific Research and Essays*, 8(42), 2120-2122. <https://doi.org/10.5897/sre2013.5550>
- Krishnamurthy, S., Gopinath, A., & Velraj, R. (2013). A comparative study on environmental emissions and per-formance of a stationary type diesel engine fuelled with biodiesels derived from two different feedstocks. *Environment Protection Engineering*, 39(4). <https://doi.org/10.37190/epe130410>
- Kumar, V., Dixit, S., Gautam, S., Tiwari, S., & Yadav, A. (2023). Biodiesel production: agricultural and economical aspect in india. *Applied Functional Materials*, 3(1), 11-24. <https://doi.org/10.35745/afm2023v03.01.0002>
- Lamichhane, G., Khadka, S., Adhikari, S., Koirala, N., & Poudyal, D. (2020). Biofuel production from waste cooking oils and its physicochemical properties in comparison to petrodiesel. *Nepal Journal of Biotechnology*, 8(3), 87-94. <https://doi.org/10.3126/njb.v8i3.33661>
- León, J., Montero, G., Coronado, M., García, C., Campbell, H., Ayala, J., ... & Sagaste, C. (2018). Renewable energy integration: economic assessment of solar energy to produce biodiesel at supercritical conditions. *International Journal of Photo-energy*, 2018, 1-9. <https://doi.org/10.1155/2018/8769582>
- Mandal, A., Cho, H., & Chauhan, B. (2022). Experimental investigation of multiple fry waste soya bean oil in an agricultural ci engine. *Energies*, 15(9), 3209. <https://doi.org/10.3390/en15093209>
- Maranduba, H., Robra, S., Nascimento, I., Cruz, R., Rodrigues, L., & Neto, J. (2015). Reducing the life cycle ghg emissions of microalgal biodiesel through integration with ethanol production system. *Bioresource Technology*, 194, 21-27. <https://doi.org/10.1016/j.biortech.2015.06.113>
- Martín, J., Martínez, G., González, J., Sánchez, N., & Álvarez, D. (2015). Biodiesel from soybean oil transesterification assisted by ultrasonic irradiation. *International Journal of Environmental Science and Development*, 6(1), 48-53. <https://doi.org/10.7763/ijesd.2015.v6.560>
- Martinez-Guerra, E. and Gude, V. (2017). Assessment of sustainability indicators for biodiesel production. *Applied Sciences*, 7(9), 869. <https://doi.org/10.3390/app7090869>

- Mehta, R., Chakraborty, M., Mahanta, P., & Parikh, P. (2010). Evaluation of fuel properties of butanol–biodiesel–diesel blends and their impact on engine performance and emissions. *Industrial & Engineering Chemistry Research*, 49(16), 7660–7665. <https://doi.org/10.1021/ie1006257>
- Mishra, A., R, A., & Mehta, P. (2021). Farm-to-fire analysis of karanja biodiesel. *Biofuels Bioproducts and Biorefining*, 15(6), 1737–1752. <https://doi.org/10.1002/bbb.2271>
- Mitani, T. (2018). Recent progress on microwave processing of biomass for bioenergy production. *Journal of the Japan Petroleum Institute*, 61(2), 113–120. <https://doi.org/10.1627/jpi.61.113>
- Mizik, T. (2021). Biofuel Economy. In *Renewable Energy Sources and Their Applications* (pp. 37). Taylor & Francis. <https://doi.org/10.1201/9781003350606-37>
- Mohamed, A. M., Yalcin, Z.G., & Dag, M. (2023). Experimental investigation of the production of biolubricant from waste frying oil. *Biomass Conversion and Biorefinery*, 13(7), 6395–6407. <https://doi.org/10.1007/s13399-023-03869-8>
- Mondal, B. and Jana, A. (2019). Techno-economic feasibility of reactive distillation for biodiesel production from algal oil: comparing with a conventional multiunit system. *Industrial & Engineering Chemistry Research*, 58(27), 12028–12040. <https://doi.org/10.1021/acs.iecr.9b00347>
- Narwani, A., Lashaway, A., Hietala, D., Savage, P., & Cardinale, B. (2016). Power of plankton: effects of algal biodiversity on biocrude production and stability. *Environmental Science & Technology*, 50(23), 13142–13150. <https://doi.org/10.1021/acs.est.6b03256>
- Naveena, B., Armshaw, P., & Pembroke, J. (2015). Ultrasonic intensification as a tool for enhanced microbial biofuel yields. *Biotechnology for Biofuels*, 8(1). <https://doi.org/10.1186/s13068-015-0321-0>
- Nayebzadeh, H. (2017). Temperature assessment and process optimization of alkali catalyzed transesterification of waste cooking oil using microwave flow system. *Research & Development in Material Science*, 1(3). <https://doi.org/10.31031/rdms.2017.01.000515>
- Neag, E., Stupar, Z., Măicăneanu, A., & Roman, C. (2023). Advances in biodiesel production from microalgae. *Energies*, 16(3), 1129. <https://doi.org/10.3390/en16031129>
- Ng, J., Teh, J., Wong, K., Wu, K., & Chong, C. (2017). A techno-economical and automotive emissions impact study of global biodiesel usage in diesel engines. *Journal of the Society of Automotive Engineers Malaysia*, 1(2), 124–136. <https://doi.org/10.56381/jsaem.v1i2.14>

- Nguyen, V., Pham, M., Le, N., Le, H., Truong, T., & Cao, D. (2023). A comprehensive review on the use of biodiesel for diesel engines. *International Journal of Renewable Energy Development*, 12(4), 720-740. <https://doi.org/10.14710/ijred.2023.54612>
- Niculescu, R., Clenci, A., & Iorga-Simăn, V. (2019). Review on the use of diesel–biodiesel–alcohol blends in compression ignition engines. *Energies*, 12(7), 1194. <https://doi.org/10.3390/en12071194>
- Niekerk, A., Drew, B., Larsen, N., & Kay, P. (2019). Influence of blends of diesel and renewable fuels on compression ignition engine emissions over transient engine conditions. *Applied Energy*, 255, 113890. <https://doi.org/10.1016/j.apenergy.2019.113890>
- Nila, I., Sari, N., Putra, R., & Fadlly, T. (2021). Conversion of palm oil to biodiesel using tio2/monmorillorite (mnt) composite catalyst from aceh tamiang bentonite.. <https://doi.org/10.2991/assehr.k.210909.007>
- Nježić, Z., Banković-Ilić, I., Stamenković, O., & Veljković, V. (2018). Environmental aspects of the production and use of corn oil biodiesel., 8(2). <https://doi.org/10.7562/se2018.8.02.02>
- Nnamani, R., Okwu, P., John, B., & Abayeh, O. (2020). Preliminary investigation of transesterified waste cooking oil (wco) as a biodiesel. *Journal of Chemical Society of Nigeria*, 45(5). <https://doi.org/10.46602/jcsn.v45i5.515>
- Onanuga, O. and Coker, J. (2013). Ultrasonic method of biodiesel production from palm kernel. *Journal of Applied and Natural Science*, 5(1), 1-4. <https://doi.org/10.31018/jans.v5i1.271>
- Peng, D. (2015). Exhaust emission characteristics of various types of biofuels. *Advances in Mechanical Engineering*, 7(7). <https://doi.org/10.1177/1687814015593036>
- Peng, Y., Amesho, K., Chen, C., Jhang, S., Chou, F., & Lin, Y. (2018). Optimization of biodiesel production from waste cooking oil using waste eggshell as a base catalyst under a microwave heating system. *Catalysts*, 8(2), 81. <https://doi.org/10.3390/catal8020081>
- Petrescu, A., McGrath, M., Andrew, R., Peylin, P., Peters, G., Ciais, P., ... & Dolman, A. (2021). The consolidated european synthesis of co2 emissions and removals for the european union and united kingdom: 1990–2018. *Earth System Science Data*, 13(5), 2363-2406. <https://doi.org/10.5194/essd-13-2363-2021>
- Postaue, N., Fonseca, J., Bergamasco, R., & Silva, C. (2022). Impact of biodiesel production on wastewater generation. *Engenharia Sanitaria E Ambiental*, 27(2), 235-244. <https://doi.org/10.1590/s1413-415220210086>
- Qamar, M., Liaquat, R., Jamil, U., Mansoor, R., & Azam, S. (2020). Techno-spatial assessment of waste cooking oil for biodiesel production in pakistan. *Sn Applied Sciences*, 2(5). <https://doi.org/10.1007/s42452-020-2716-1>

- Rahimi, V., Shafiei, M., & Karimi, K. (2020). Techno-economic study of castor oil crop biorefinery: production of biodiesel without fossil-based methanol and ligno-ethanol improved by alkali pretreatment. *Agronomy*, 10(10), 1538. <https://doi.org/10.3390/agronomy10101538>
- Ramos, L., Martin, L., Santos, J., & Castro, H. (2016). Combined use of a two-stage packed bed reactor with a glycerol extraction column for enzymatic biodiesel synthesis from macaw palm oil. *Industrial & Engineering Chemistry Research*, 56(1), 1-7. <https://doi.org/10.1021/acs.iecr.6b03811>
- Ratanabuntha, T., Tonmitr, K., & Suksri, A. (2018). Acceleration in biodiesel production from palm oil process by high voltage electric field. *International Journal of Smart Grid and Clean Energy*, 225-230. <https://doi.org/10.12720/sgce.7.3.225-230>
- Ronsse, F., Hecke, S., Dickinson, D., & Prins, W. (2012). Production and characterization of slow pyrolysis biochar: influence of feedstock type and pyrolysis conditions. *GCB Bioenergy*, 5(2), 104-115. <https://doi.org/10.1111/gcbb.12018>
- Saad, M., Dosoky, N., Zoromba, M., & Shafik, H. (2019). Algal biofuels: current status and key challenges. *Energies*, 12(10), 1920. <https://doi.org/10.3390/en12101920>
- Saadon, N., Yusof, N., Razali, N., Yashim, M., & Roslan, A. (2015). Fatty acid methyl ester (fame) production from waste cooking oil. *Advanced Materials Research*, 1113, 322-327. <https://doi.org/10.4028/www.scientific.net/amr.1113.322>
- Sadaf, S., Iqbal, J., Ullah, I., Bhatti, H., Nouren, S., Habib-ur-Rehman, _, ... & Iqbal, M. (2018). Biodiesel production from waste cooking oil: an efficient technique to convert waste into biodiesel. *Sustainable Cities and Society*, 41, 220-226. <https://doi.org/10.1016/j.scs.2018.05.037>
- Sahu, G., Saha, S., Datta, S., Chavan, P., Chauhan, V., & Gupta, P. (2021). Production of biodiesel from high free fatty acids content jatropha curcas oil using environment affable k-mg composite catalyst. *Asia-Pacific Journal of Chemical Engineering*, 16(3). <https://doi.org/10.1002/apj.2620>
- Sakdasri, W., Sawangkeaw, R., & Ngamprasertsith, S. (2017). An entirely renewable biofuel production from used palm oil with supercritical ethanol at low molar ratio. *Brazilian Journal of Chemical Engineering*, 34(4), 1023-1034. <https://doi.org/10.1590/0104-6632.20170344s20150660>
- Sakkamas, W., Boripun, A., Ampairojanawong, R., Ruankon, S., Suwanasri, T., & Kangsadan, T. (2020). Electrocoagulation with ac electrical current at low voltage for separation of crude glycerol from biodiesel product mixture. *E3s Web of Conferences*, 141, 01011. <https://doi.org/10.1051/e3sconf/202014101011>
- Sánchez, N., Martín, J., Martínez, G., & González, J. (2015). Biodiesel production from castor oil under subcritical methanol conditions. *International Journal of Environmental Science and Development*, 6(1), 61-66. <https://doi.org/10.7763/ijesd.2015.v6.562>

- Semwal, S., Arora, A., Badoni, R., & Tuli, D. (2011). Biodiesel production using heterogeneous catalysts. *Bioresource Technology*, 102(3), 2151-2161. <https://doi.org/10.1016/j.biortech.2010.10.080>
- Sherbiny, S., Refaat, A., & Sheltawy, S. (2010). Production of biodiesel using the microwave technique. *Journal of Advanced Research*, 1(4), 309-314. <https://doi.org/10.1016/j.jare.2010.07.003>
- Siddeg, A., Adam, U., Jaat, N., Khalid, A., Sapit, A., Mohd, S., ... & Jalal, M. (2022). Analysis of the influences of biodiesel on performance and emissions of a diesel engine. *Journal of Automotive Powertrain and Transportation Technology*, 2(2). <https://doi.org/10.30880/japtt.2022.02.02.001>
- Silviana, S., Anggoro, D., Hadiyanto, H., Salsabila, C., Aprilio, K., Utami, A., ... & Dalanta, F. (2022). A review on the recent breakthrough methods and influential parameters in the biodiesel synthesis and purification. *International Journal of Renewable Energy Development*, 11(4), 1012-1036. <https://doi.org/10.14710/ijred.2022.43147>
- Singh, S., Sachdeva, H., & Shan, V. (2020). Biodiesel, an alternative fossil fuel for present and future generation: a review. *International Journal of Advanced Research*, 8(4), 959-969. <https://doi.org/10.21474/ijar01/10865>
- Song, J., Yao, J., & Zhu, C. (2013). Exhaust emissions of a diesel engine fueled with soybean-oil-methyl-ester-diesel blends and their fuel properties. *Applied Mechanics and Materials*, 310, 129-132. <https://doi.org/10.4028/www.scientific.net/amm.310.129>
- Souza, D., Mendonça, F., Nunes, K., & Valle, R. (2012). Environmental and socioeconomic analysis of producing biodiesel from used cooking oil in rio de janeiro. *Journal of Industrial Ecology*, 16(4), 655-664. <https://doi.org/10.1111/j.1530-9290.2012.00517.x>
- Stebeleva, O. and Минаков, А. (2021). Application of cavitation in oil processing: an overview of mechanisms and results of treatment. *Acs Omega*, 6(47), 31411-31420. <https://doi.org/10.1021/acsomega.1c05858>
- Sungnat, C. and Wongwuttanasatian, T. (2018). Esterification of crude palm oil with low ultrasonic intensity. *Destech Transactions on Environment Energy and Earth Science*, (epe). <https://doi.org/10.12783/dteees/epe2018/23762>
- Supriyanto, E., Sentanuhady, J., Dwiputra, A., Permana, A., & Muflikhun, M. (2021). The recent progress of natural source and manufacturing process of biodiesel: a review.. <https://doi.org/10.20944/preprints202103.0719.v1>
- Şahin, T. and Aydın, F. (2018). Investigation of fuel properties of canola oil biodiesel, bioethanol and diesel fuel mixture. *International Journal of Automotive Engineering and Technologies*, 7(4), 158-163. <https://doi.org/10.18245/ijaet.477637>

- Şimşek, F. (2024). Investigation of the effects of ultrasonic bath application on the characteristic properties of biodiesel obtained from hazelnut oil. *Journal of the Faculty of Engineering and Architecture of Gazi University*, 39(3), 1583-1595. <https://doi.org/10.17341/gazimmfd.1230079>
- Timyamprasert, A. (2015). Optimization for community biodiesel production from waste palm oil via two-step catalyzed process. *Journal of Materials Science and Engineering A*, 5(6). <https://doi.org/10.17265/2161-6213/2015.5-6.008>
- Tiwari, T., Gangwar, S., Tripathi, K., Sharma, A., Mishra, V., & Awasthi, A. (2022). Conventional and intensified transesterification process of biodiesel production: a review. *International Journal of Engineering Research in Mechanical and Civil Engineering (Ijermce)*, 9(7), 17-24. <https://doi.org/10.36647/ijermce/09.07.a005>
- Toldrá-Reig, F., Mora, L., & Toldrá, F. (2020). Trends in biodiesel production from animal fat waste. *Applied Sciences*, 10(10), 3644. <https://doi.org/10.3390/app10103644>
- Tutak, W., Jamrozik, A., & Grab-Rogaliński, K. (2023). Co-combustion of hydrogen with diesel and biodiesel (rme) in a dual-fuel compression-ignition engine. *Energies*, 16(13), 4892. <https://doi.org/10.3390/en16134892>
- Ulukardeşler, A. (2023). Biodiesel production from waste cooking oil using different types of catalysts. *Processes*, 11(7), 2035. <https://doi.org/10.3390/pr11072035>
- Valente, O., Silva, M., Ávila, R., Vianna, J., & Sodré, J. (2011). Further developments on biodiesel production and applications in brazil. *International Journal of Sustainable Development and Planning*, 6(2), 119-134. <https://doi.org/10.2495/sdp-v6-n2-119-134>
- Veillette, M., Giroir-Fendler, A., Fauchoux, N., & Heitz, M. (2017). Biodiesel from microalgae lipids: from inorganic carbon to energy production. *Biofuels*, 9(2), 175-202. <https://doi.org/10.1080/17597269.2017.1289667>
- Welter, R., Santana, H., Torre, L., Barnes, M., Taranto, O., & Oelgemöller, M. (2023). Biodiesel production by heterogeneous catalysis and eco-friendly routes. *Chem-bioeng Reviews*, 10(2), 86-111. <https://doi.org/10.1002/cben.202200062>
- Xiang, L. and Zhang, Z. (2017). Experimental investigation of particulate matter emissions from a single cylinder diesel engine fuelled with waste cooking oil biodiesel..
- Yadav, A.K. (2017). Optimum production of biodiesel from an underutilized and potential feed stock, kusum seed oil. *Iranica Journal of Energy and Environment*, 8(1): 6-10.
- Yaqoob, H., Teoh, Y., Sher, F., Farooq, M., Jamil, M., Kausar, Z., ... & Rehman, A. (2021). Potential of waste cooking oil biodiesel as renewable fuel in combustion engines: a review. *Energies*, 14(9), 2565. <https://doi.org/10.3390/en14092565>

- Yuan, M., Chen, Y., Peng, S., Chen, L., Chang, C., Santikunaporn, M., ... & Lee, Y. (2022). Depression effect of the cold filter plugging point by blending of palm oil, palm stearin, and palm olein biodiesels in petrodiesels. *Frontiers in Energy Research*, 10. <https://doi.org/10.3389/fenrg.2022.956443>
- Zhu, F., Qi, J., Xiang, W., Zhao, L., & Xiong, Y. (2015). *<i>in situ&/i>* trans-esterification of sewage sludge for biodiesel production. *Applied Mechanics and Materials*, 768, 520-525.
- Živković, S. and Veljković, M. (2017). Environmental impacts the of production and use of biodiesel. *Environmental Science and Pollution Research*, 25(1), 191-199.



CHAPTER 18

Optimization Analysis of Autonomous Mobile Robots

Engin Ünal¹ & Faruk Karaca²

¹ Associat. Prof. Dr., Firat University Faculty of Technology, Department of Mechanical Engineering, ORCID: 0000-0002-0501-3690

² Prof. Dr., Firat University Faculty of Technology, Department of Mechanical Engineering, ORCID: 0000-0003-1874-9274

1. INTRODUCTION

Robotics is one of the branches of modern technology that combines several different engineering fields. Robotics is a science-based technology that deals with the theory and application of systems (Tzafestas, 2014). When the development of the application areas of robotic systems is examined, it is seen that their usage and application areas are increasing every day. Robotic systems are used primarily in military fields, in the healthcare sector, in rehabilitation studies, in industrial and industrial applications, in our homes, etc. It is used safely in many areas (Quaglia, Oderio, Bruzzone, & Razzoli, 2013). Mobile robots are robots that can move from one place to another without the help of operators. Unlike most industrial robots that can only be moved to a specific work area, they have the ability to roam freely to accomplish their desired goals in a predefined work area. This mobility enables them to be used in a wide range of applications in structured or unstructured environments (Tantawi, Sokolov, & Tantawi, 2019). Mobile ground robots are divided into two groups: wheeled mobile robots (WMR) and legged mobile robots (LMR). Wheeled robots are more widely used than other mobile robots (Sosa-Cervantes, Silva-Ortigoza, Marquez-Sanchez, Taud, & Saldana-Gonzalez, 2014). The reason why these robots are attractive is that they have advantages such as having lower mechanical complexity in application and less energy consumption (Savant, 2018).

Nowadays, industrial examples of robot and human interaction are quite common. In this direction, systems that require human needs have begun to be replaced by robots. Developments in the industry have led to the acceleration of the Industry 4.0 revolution. With the influence of technological developments, the internet of objects and services and cyber-physical system applications have begun to be used in production; This situation caused the start of the Industry 4.0 revolution (Wang, Ramik, Sabourin, & Madani, 2012). In the light of this information, the internet of things, the internet of services, and cyber-physical systems constitute the main elements of industry 4.0. With the integration of these elements, smart factories were born (Schluse, Priggemeyer, & Roßmann, 2020).

The concept of smart factory, which is also called the factory of objects, multi-space factory, simultaneous factory and is frequently used by academics as well as industrial practitioners, does not actually have a clear definition. However, by integrating all existing definitions, the concept of smart factory; With production processes that can adapt and reconfigure to technological developments such as automation, software combinations, hardware and mechanical infrastructure; It is possible to define it as a factory that can solve manufacturing-related problems

in a dynamic, flexible and agile way (Leal Filho, Azul, Brandli, Özuyar, & Wall, 2020).

As a result of these technological developments, the integration of robotics with industry has accelerated. Common types of robots used for industrial purposes:

- Robots used for production,
- Assistive robotic systems used for maintenance and repair,
- Robotic systems for packaging purposes,
- Multi-purpose autonomous assistant robots.

Autonomous robots, sensors, cameras, artificial intelligence applications, etc. Robots are robots that act according to the information they obtain from the environment and perform assigned tasks on their own, thanks to systems (Jalled & Voronkov, 2016). One type of such robots is autonomous mobile robots designed for cargo purposes. Autonomous mobile robots for industrial purposes are used in all kinds of industrial facilities and many sectors for logistics purposes (Cupek et al., 2020). There are academic and commercial studies in this direction.

Cargo robots, like tractors and forklifts used for cargo transportation, have different designs depending on their lifting and carrying methods. The most important parameters in the design of the system intended to be designed for this purpose are the weight and dimensions of the load intended to be carried. Experimental tests of prototypes in this field provide great convenience for the design process, cost and optimization through simulation programs, since the errors found can have negative consequences in terms of cost.

ANSYS; It is a computer-aided engineering program where analysis and simulations can be made in computer-aided engineering studies. ANSYS program enables effective studies in different disciplines such as mechanics, structural analysis, computational fluid dynamics and heat transfer. ANSYS program, one of the most used CAE (computer aided engineering) programs in the world, uses the finite element method. With the finite element method, objects of complex geometry, which are very difficult to analyze as a single piece, are analyzed separately by dividing them into small and numerous pieces. The results obtained from the analysis of a finite number of elements are combined to obtain a single and consistent analysis result (Cao, Li, & Yu, 2009; Özek & Süer, 2023).

In robots and vehicles, shafts are very important and fundamental components of mechanical engineering (Hou et al., 2022). They are used in many areas such

as automotive, mining, energy systems and structures and are of great importance in these areas (Asiri, 2021; T. Li, Chen, Zhang, Wang, & Huang, 2022; Popenda, Lis, Nowak, & Blecharz, 2020). They have different features in their machine structures; For example, in these machine systems, they perform rotary motion, transmit power, and help support loads (Hou et al., 2022). The design, construction and analysis of shafts is important and requires an in-depth understanding of their mechanical behavior, failure mechanisms and appropriate support structures (Kondratenko, Sedykh, & Surkova, 2020). In mining engineering, shafts play many roles, such as safety transport and underground access. Vertical shafts are used in mining engineering. The strength and stability of vertical shafts are critical to safety, sustainability and efficiency in mining systems and operations (Sun, Ma, Guo, Li, & Feng, 2020). In mechanical engineering, shafts are used for many purposes in mechanical systems such as engines, turbines and pumps (Özek, Bal, & Demir, 2019). They ensure the correct operation of systems by transmitting rotary motion and power between different parts. Mechanical properties of shafts, such as bending-torsion resistance and vibration properties, are important criteria for the reliability and performance of shafts (Xiaozhan Li, Wang, & Liang, 2022; Savaş & Özek, 2005; Serrano, Guardiola, Dolz, López, & Bouffaud, 2015). Shafts used in energy systems are used in wind turbines and compressed air energy storage systems. Miller converts wind energy into electrical energy and transfers the rotating movement in the turbines to the generator (Meng, Wang, Olumayegun, Luo, & Liu, 2019). In automotive engineering, shafts are found in different types such as crankshafts, camshafts and balance shafts. Again, they ensure the correct operation of the vehicle by taking the rotary motion of the engine and transferring it to various automotive structures (Sonone & Chaudhari, 2015). Additionally, shafts are frequently used in different fields and systems such as civil engineering, materials science and manufacturing. The importance of shafts lies in their ability to provide structural support, rotary motion and power transmission, enhance safety, increase efficiency and ensure the correct functioning of various systems and processes. Thus, the design, analysis and optimization of the mechanical behavior of shafts are vital to improve their performance and efficiency. Topology optimizations can be applied to shaft design to increase efficiency and reduce weight (Xiaozhan Li et al., 2022).

Static analysis and topology optimization are crucial in the design and improvement of mechanical components. Static analysis evaluates elements such as moments, forces and thermal effects, ignoring the dynamic responses of a structure. By applying structural static analysis on shafts, stresses, deformations

and displacements of shaft models subjected to different loads can be found. Thus, as a result of the analysis, it is ensured that the shafts can withstand the applied loads without excessive deflection or error. Additionally, as a result of these analyses, the structural integrity of the shafts is improved by detecting areas with excessive stress or weak points in the model (Chikelu, Nwigbo, Obot, Okolie, & Chukwuneke, 2023; Koçak & Bayraklılar, 2023). Topology optimization is a design tool that optimizes the material distribution of the design while attempting to minimize the weight of the part or maximize stiffness using specific parameters (Hu & Vambol, 2020; Lu & Chen, 2012; Pagac et al., 2021). Topology optimization creates a structure or model that meets specified criteria by removing unnecessary material from the part or model (Chen & Ye, 2021; Mesicek et al., 2019). Thus, topology optimization is used to improve the efficiency and performance of shafts and other mechanical parts while maintaining structural integrity and functionality (Chen & Ye, 2021; Hu, Vambol, Sun, & Zeng, 2021). Combining static analysis and topology optimization allows engineers to design lighter, stronger parts that are better suited to load conditions (Feng, Li, & Wu, 2017; Ji et al., 2020).

The desired result is to analyze the structural behavior of the specified mechanical shaft model and then improve the model using topology optimization. In this research, static analysis is performed on the specified shaft model by analyzing its mechanical response under applied boundary conditions. After this basic analysis, a design model is obtained that is resistant to previously applied load conditions with optimum use of weight and materials with reference to static analysis. To see the accuracy and effectiveness of the optimization, the optimized model is structurally analyzed again to verify the results.

This comparative analysis aims to check the structural analysis of the optimized model and the previous model. This research aims to contribute to sustainable engineering practices that enable more efficient resource use. The purpose of this research is to set an example for more conscious and optimal resource use by recognizing the world's limited resources. Structural durability, material usage efficiency and weight optimization requirements were examined in this study. The findings of this study allow for more effective use of materials in mechanical part design, promoting more environmentally friendly and energy-efficient systems.

In a study conducted by (Demir, Sucuoğlu, Böğrekci, & Demircioğlu, 2021), it was aimed to reduce the weight of a mobile transport robot by using topology optimization and structural analysis. The main goal was to reduce the weight of the robot by increasing its payload capacity and minimizing energy consumption.

First, the researchers created a CAD model. analysis was performed using CAE software. Based on the analysis results, topology optimization was used to reduce the weight of the robot. Topology optimization is a technique that reduces weight without compromising load capacity. By minimizing the design's material usage, this method successfully reduced the robot's weight by 25%. As a result, this led to an increase in load capacity and a decrease in energy consumption. In conclusion, this study shows that topology optimization can effectively improve the efficiency of mobile handling robots. In this research work, Çelebi and Tosun (Çelebi & Tosun, 2021) conducted a study to analyze the application of topology optimization in manufacturing and processing methods. Topology optimization aims to reduce manufacturing costs by making lighter parts by improving part performance and reducing material waste. The study compared the performance of parts for manufacturing and machining designed using topology optimization techniques. As a result of the optimizations made in this study, the desired mass reduction was achieved. After the optimization round, the design achieved approximately 63% mass reduction compared to the initial state. The piece, which initially weighed 300 grams, was successfully reduced to 100 grams while maintaining its structural integrity. There was also a decrease in volume. In conclusion, this research confirms that topology optimization can improve part performance through increased performance while effectively reducing manufacturing costs.

Orhan et al (Gülcan, Sokollu, Temel Yiğitbaşı, & Konukseven, 2022) conducted a study examining the electron beam melting method for the production of aircraft parts. The aim was to reduce the weight of the parts by 30% and obtain designs with geometry. The study used the method allowing design and topology optimization, thus optimizing the shapes of the parts and reducing their weight. Additionally, deflections of structures made of maraging steel material were analyzed. As a result, the weight of aircraft parts produced using electron beam melting was successfully reduced by 30%. Additionally, topology optimization led to designs with geometry. These findings hold promise for the aviation industry to produce more durable aircraft components.

Yeswanth and Abraham (Andrews, 2018) conducted a study using ANSYS Workbench 14.0 to analyze the parametric optimization of conventional steel driveshafts used in automobiles. The aim of this study was to replace the drive shaft with different composite materials. Different composite materials such as high modulus carbon/epoxy or E-glass polyester were selected and the drive shaft was modeled using CATIAV5R20. Then an analysis was made on the subject. As a result of the study, it was stated that the optimization of composite drive

shafts provides high strength and reliability, as well as a reduction in weight. In this way, they aim to reduce the weight of vehicles with composite shafts and, as a result, increase fuel consumption and the overall performance of the vehicle.

Shahane and Pawar (Shahane & Pawar, 2017) carried out the optimization of the connecting rod design of an internal combustion engine using finite element analysis. First, using ANSYS software, finite element analysis was performed to optimize the connecting rod shaft in static and dynamic conditions. Later, as a result of these analyses, connecting rod shaft optimization was carried out. The weight of the optimized connecting rod shaft was reduced by 4.37%. Additionally, it was declared that the optimized connecting rod was safe under previously applied static and dynamic boundary conditions. Thus, it has been stated that weight reduction after optimization can provide a positive increase in engine performance and efficiency. Finally, validation of the optimization based on different boundary conditions, such as fatigue analysis, is proposed.

Li Xue et al (Xue-ping Li, Zhao, & Liu, 2017) conducted a study investigating the application of topology optimization in determining the shape of crane mounting brackets. An analysis of the topology of the bracket was performed using ANSYS software. Research findings showed that the optimized design was both successful and safe. It was also emphasized that topology optimization plays an important role in ensuring strength and durability under specified conditions, as well as increasing efficiency and cost effectiveness through weight reduction.

Lei et al (Lei, Yunan, & Tianmin, 2019) conducted a study in which they used topology optimization to improve the mechanical performance of the transmission and extend its service life. In the study, a three-dimensional CAD model of the transmission was created using CREO 3.0 software. Then, optimization simulation of the transmission was carried out using ANSYS software. As a result, it was announced that there was a decrease in stress intensity as a result of the optimization. Jayanaidu et al (Jayanaidu, 2013) used ANSYS software to optimize driveshaft for automobile applications. It was intended to use and analyze titanium alloy instead of structural steel material.

In this study, the results of the design will be observed by performing stress and deformation analysis according to different carrying capacities of an autonomous load robot without the need for prototype production through the ANSYS simulation program, and it is aimed to shed light on the studies to be carried out in this field.

2. Material and Method

The sample load robot used in this study was conceived and designed to increase load carrying capacity and mobility, similar to modern robotic designs. The dimensions and design of the robot were chosen to ensure optimal performance under different load conditions. As seen in Figure 1, the sample load robot designed for analysis was prepared in a 3D environment via the Solidworks software.

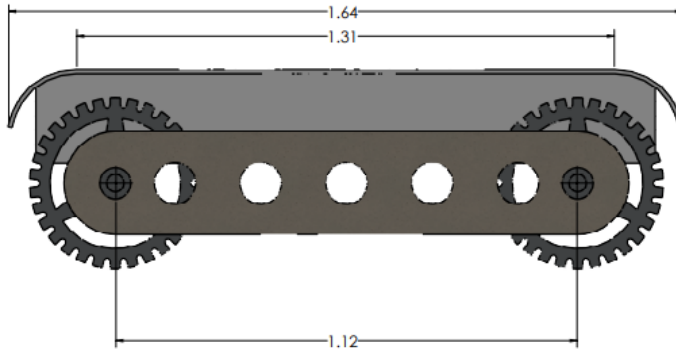


Figure 1. Designed mobile robot platform

The designed robot platform has dimensions of approximately 1.6 x 1.35 x 0.40 m and has a structure with 4 wheels. In addition to the weight of the robot, which is 330 kg, the diameter of the driving wheels used was determined as 0.21 m. These wheels are optimized to increase load carrying capacity and ensure mobility. Robot movements are provided with 2 motor vehicles used on the wheels. ANSYS is a software widely used in solving engineering problems and was used in this study to analyze the structural durability and performance of the robot. ANSYS solves the equations by approximation using the finite difference method (Hou et al., 2022). The use of this method has an important role in determining how the robot will behave under various load conditions.

Newton's second law of motion, one of the equations discussed in the motion of the robot, is as given in Equation 1:

$$F = m \cdot a \quad (1)$$

Here, F is force (N), m is mass (kg) and a is acceleration (m/s^2). It defines the relationship between the robot's total mass m and the force acting on it F and its acceleration a .

The set of equations used for torque and rotational motion is given in Equation 2:

$$\tau = I . \alpha \quad (2)$$

Here, τ is torque (Nm), I is moment of inertia (kg.m^2) and α is angular acceleration (rad/s^2). It defines the torque produced in the wheels and its effect on the rotational movement of the robot.

The kinetic energy of the system is:

$$E_k = \frac{1}{2} . m . v^2 \quad (3)$$

Here, E_k represents the kinetic energy (J), m represents the mass of the system (kg) and v represents the velocity (m/s).

The power equation of the system is given in Equation 4:

$$P = F . v \quad (4)$$

Here, P represents power (W), F represents force (N) and v represents speed (m/s). It defines the power consumed by the robot at a certain force and speed.

Static structural analysis of the robot is given in Equation 5:

$$F_y = m . g \quad (5)$$

Here, F_y represents the vertical load force (N) and g represents the gravitational acceleration (9.81 m/s^2). With this equation, the vertical load force is calculated by taking into account the robot's mass and gravitational acceleration.

The acceleration and speed equations of the robot are given in Equation 6 and Equation 7, respectively.

$$\vec{a} = \frac{F}{m} \quad (6)$$

$$v = u + \vec{a} . t \quad (7)$$

Here, a represents acceleration (m/s^2), F is force (N), m is mass (kg), v is final velocity (m/s), u is initial velocity (m/s) and t is time (s). With these equations,

the acceleration of the robot under a certain force and the speed that the robot will reach after a certain acceleration and time can be calculated.

Hooke's law, which defines the relationship between stress (σ) and strain (ϵ) for elastic materials, is given in Equation 8.

$$\sigma = E \cdot \epsilon \quad (8)$$

Here, σ is the stress (Pa), E is the elastic modulus (Pa) and ϵ is the strain.

The static equilibrium equations of the system can be written as in Equation 9.

$$\sum F = 0; \sum M = 0 \quad (9)$$

Static equilibrium equations state that the total forces and moments on a structure are zero.

Analyzes were made in the Static Structural module of the ANSYS program. ANSYS solves equations by convergence using the finite difference method. The network structure and analysis boundary conditions are seen in Figure 2.

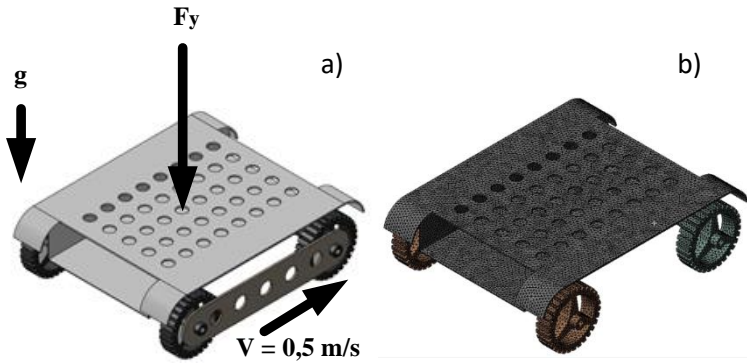


Figure 2. 3D model of the designed mobile robot platform a) physical model b) mesh structure

Figure 2a shows the forces acting on the robot. The gravity force (g), vertical load force (F_y) and movement of the robot at a certain speed ($V=0.5 \text{ m/s}$) are specified. These forces and motion conditions were used to simulate situations the robot might encounter in a real working environment. The mesh structure of the geometry is given in Figure 2b. For the mesh, the number of elements is 103250, the number of nodes is 198172, and the minimum and maximum element

quality values are 5.9×10^{-2} and 0.99; The average skewness value was used in the solution as 0.23.

Gravity was defined on the -y axis as well as the own load weight (330 kg) of this system prepared for analysis. The applied load was applied to the robot parallel to the ground. 7.5 kN, 10 kN, 12.5 kN were determined as load parameters. As a result of the applied load, the robot body, the shaft that provides connection to the wheels, and the force on the wheels, as well as the analysis of the stress and deformations caused by the force, were examined. During the analysis, the robot moves at a speed of 0.5 m/s while examining the data caused by the force. In the robot model used for analysis, the body was made of stainless steel (AISI 304) and the axles and wheels were made of aluminum alloy (7075-T6). The properties of the materials are given in Table 1.

Table 1. Materials used and their properties

	Unit	Stainless steel	Aluminum Alloy
Intensity	kg/m ³	7750	2770
Young's Modulus	MPa	1,93x10 ⁵	71000
Poisson's Ratio		0,31	0,33
Bulk Module	MPa	1,693x10 ⁵	69608
Shear Module	MPa	73664	26692
Yield Strength	MPa	207	280
Tensile Strength	MPa	586	310

In all analyses, the materials used for axles and wheels are constant. In modular robot simulations, the forward speed and gravitational acceleration were kept constant.

3. Results and discussion

The deformation that occurs on all parts of the robot in the unloaded state, caused only by the weight of the robot itself and the movement of the system, is shown in Figure 3.

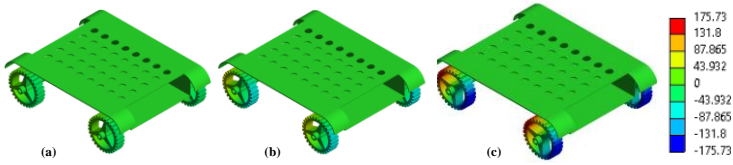


Figure 3. Total deformation in the time-dependent motion of the robot a) 0.2 s, b) 0.4 s, c) 0.7 s

Here, it can be seen that the most deformation occurs on the wheels when moving the load depending on time. As a result of the simulation, it is seen that there is an increase in deformation on the wheels from 0.4 seconds to 0.7 seconds. It can be understood from the relevant figure that the maximum value is approximately 175×10^{-3} mm in 0.7 seconds. It can be said that the change in deformation in the body is negligible.

As a result of the analysis, the stress and deformation results on the robot under three different load effects were calculated. The stress and deformation data of the robot for a 7.5 kN load are shown in Figure 4.

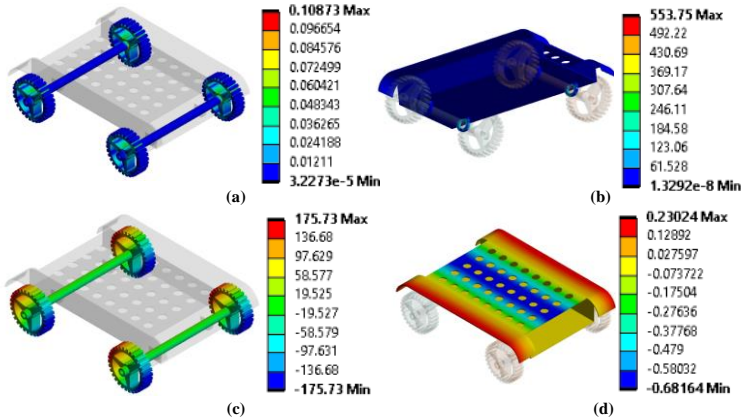


Figure 4. Stress and deformation results in robot parts under 7.5 kN load a) axle and wheel stress (MPa) b) body stress (MPa) c) axle and wheel deformation (mm) d) body deformation (mm)

In Figure 4a, the maximum value of the stress on the axle and wheels is seen as approximately 0.11 MPa. Since the load effect from the body is transmitted to the wheels during the rotation of the axles, greater stress was observed in these parts. Figure 4c shows the deformation on the axle and wheels. The maximum value of deformation occurred at the part of the wheels away from the ground,

approximately 175×10^{-3} mm. The stress and deformation on the body caused by load and movement are given in Figure 4b and Figure 4d, respectively. It has been observed that it remains at low levels as a result of the tension occurring in the body. It was observed that the stress value in the junction area of the axle and the body, which is a single piece with the body, remained in the range of 553 MPa - 1.3292×10^{-8} MPa. The reason for this is that the load on the body affects this joint area during the movement of the robot. The maximum value of the total deformation occurring in the body is approximately 0.2 mm, and this value occurred at the side ends of the body. The parameters selected in Figure 4 are also valid for Figure 5 and Figure 6 for stress and deformation.

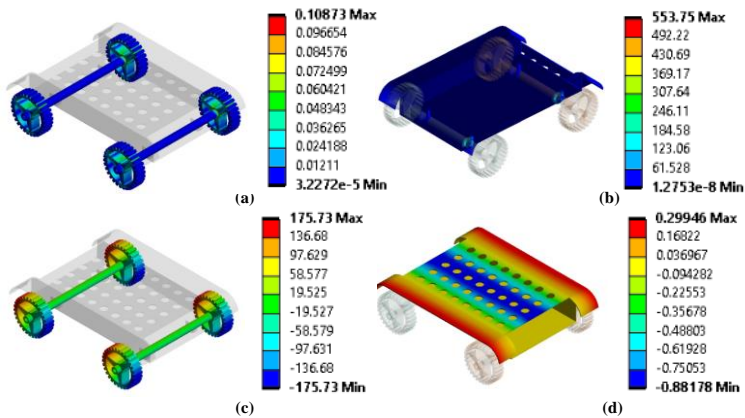


Figure 5. Stress and deformation results in robot parts under 10 kN load (a) axle and wheel stress (MPa) (b) body stress (MPa) (c) axle and wheel deformation (mm) (d) body deformation (mm)

The results obtained for $F_y = 10$ kN are shown in Figure 5. There was no significant difference in the stress and deformation analysis performed on the axle and wheel parts. Apart from this, an increase in the range of 0.29 mm - 0.88 mm was observed in the body deformation analysis.

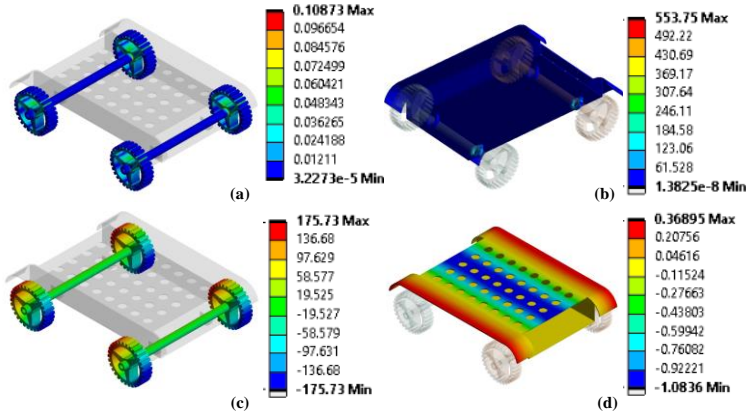


Figure 6. Stress and deformation results in robot parts under 12.5 kN load a) axle and wheel stress (MPa) b) body stress (MPa) c) axle and wheel deformation (mm) d) body deformation (mm)

In Figure 6, the results are observed under $F_y = 12.5$ kN load. As in Figure 4 and Figure 5, the stresses and deformations of the body, axle and wheels were examined. According to the results obtained, while no change in stress and deformation was observed on the axles and wheels, an increase in deformation was observed in the stress analysis of the robot body, while a very small increase was observed.

4. Conclusion

In the study, analysis was carried out for the modeled load robot while traveling at a speed of 0.5 m/s under 3 different loads: 7.5kN, 10kN and 12.5kN. For the analysis results, stress and deformation analysis results were examined in 3 different force parameters.

When the stress and deformation results were examined, it was seen that the changes were at such a low level that they could be neglected. In order to improve the results obtained, it is thought that the deformation occurring at the edges of the body can be reduced to lower levels with the support parts that can be added between the wheels and the body. At the same time, it is estimated that different material choices can achieve more successful results in stress and deformation analysis.

References

- Andrews, A. A. E. (2018). *Composite Drive Shaft Using Ansys*. 9–23.
- Asiri, S. (2021). Modeling and Analysis of Novel Spring Made of Composite With and Without Material Property Grading. *Sci. Int.(Lahore)*, 33, 371–378.
- Cao, Y., Li, Q., & Yu, L. (2009). A Software for Design and Analysis of PMSM Based on ANSYS. *2009 First International Conference on Information Science and Engineering*, 78–81. IEEE.
- Çelebi, A., & Tosun, H. (2021). Comparison of Optimization Methods For Additive Manufacturing And Machining Methods. *International Journal of 3D Printing Technologies and Digital Industry*, 5, 676–691.
- Chen, Y., & Ye, L. (2021). Topological design for 3D-printing of carbon fibre reinforced composite structural parts. *Composites Science and Technology*, 204, 108644.
- Chikelu, P. O., Nwigbo, S. C., Obot, O. W., Okolie, P. C., & Chukwuneke, J. L. (2023). Modeling and simulation of belt bucket elevator head shaft for safe life operation. *Scientific Reports*, 13, 1083.
- Cupek, R., Drewniak, M., Fojcik, M., Kyrkjebø, E., Lin, J. C.-W., Mrozek, D., ... Ziebinski, A. (2020). Autonomous guided vehicles for smart industries—the state-of-the-art and research challenges. *Computational Science–ICCS 2020: 20th International Conference, Amsterdam, The Netherlands, June 3–5, 2020, Proceedings, Part V* 20, 330–343. Springer.
- Demir, N., Sucuoğlu, H. S., Böğrekci, İ., & Demircioğlu, P. (2021). Topology Optimization of Mobile Transportation Robot. *International Journal of 3D Printing Technologies and Digital Industry*, 5, 210–219.
- Feng, J., Li, C., & Wu, Z. (2017). Analysis of static and dynamic characteristic of spindle system and its structure optimization in camshaft grinding machine. *AIP Conference Proceedings*, 020190.
- Gülcan, O., Sokollu, B., Temel Yiğitbaşı, S., & Konukseven, E. İ. (2022). Ağırlık Azaltma Amacıyla Elektron Işını İle Ergitme Yöntemiyle Üretilen Bir Uçak Parçasının Tasarımı, Topoloji Optimizasyonu Ve Testi. *International Journal of 3D Printing Technologies and Digital Industry*, 6, 207–217.
- Hou, N., Ding, N., Qu, S., Guo, W., Liu, L., Xu, N., ... Zäiri, F. (2022). Failure modes, mechanisms and causes of shafts in mechanical equipment. *Engineering Failure Analysis*, 136, 106216.
- Hu, Z., & Vambol, O. (2020). Topological Designing And Analysis of The Composite Wing Rib. *Aerospace Technic and Technology*, 4–14.
- Hu, Z., Vambol, O., Sun, S., & Zeng, Q. (2021). Development of a topology optimization method for the design of composite lattice ring structures. *Eastern-European Journal of Enterprise Technologies*, 4, 6–13.

- Jalled, F., & Voronkov, I. (2016). Object detection using image processing. *ArXiv Preprint ArXiv:1611.07791*, 1–6.
- Jayanaidu, P. (2013). Analysis of a Drive Shaft for Automobile Applications. *IOSR Journal of Mechanical and Civil Engineering*, 10, 43–46.
- Ji, Q., Li, C., Zhu, D., Jin, Y., Lv, Y., & He, J. (2020). Structural design optimization of moving component in CNC machine tool for energy saving. *Journal of Cleaner Production*, 246, 118976.
- Koçak, M. T., & Bayraklılar, M. S. (2023). Mechanical Shaft Optimization: A Study On Static Structural Analysis And Topological Optimization In Ansys. *International Journal of 3D Printing Technologies and Digital Industry*, 7, 541–549.
- Kondratenko, V. E., Sedykh, L. V., & Surkova, R. Y. (2020). Effective design features of rotor shafts. *IOP Conference Series: Materials Science and Engineering*, 971, 042010.
- Leal Filho, W., Azul, A. M., Brandli, L., Özuyar, P. G., & Wall, T. (2020). *Responsible consumption and production*. Springer.
- Lei, L., Yunan, S., & Tianmin, G. (2019). Topology optimization of Workbench gearbox Box reinforced bar based on ANSYS. *IOP Conference Series: Materials Science and Engineering*, 569, 022040.
- Li, T., Chen, Z., Zhang, K., Wang, J., & Huang, Z. (2022). Analysis of the influence of piston–cylinder friction on the torsional vibration characteristics of compressor crankshaft system. *Nonlinear Dynamics*, 110, 1323–1338.
- Li, Xiaozhan, Wang, S., & Liang, M. (2022). Modeling and Simulation of Combined Bending-torsion Experiment Based on ABAQUS. *Journal of Physics: Conference Series*, 2403, 012045.
- Li, Xue-ping, Zhao, L., & Liu, Z. (2017). Topological Optimization of Continuum Structure based on ANSYS. *MATEC Web of Conferences*, 95, 07020.
- Lu, J., & Chen, Y. (2012). Manufacturable mechanical part design with constrained topology optimization. *Proceedings of the Institution of Mechanical Engineers, Part B: Journal of Engineering Manufacture*, 226, 1727–1735.
- Meng, H., Wang, M., Olumayegun, O., Luo, X., & Liu, X. (2019). Process design, operation and economic evaluation of compressed air energy storage (CAES) for wind power through modelling and simulation. *Renewable Energy*, 136, 923–936.
- Mesicek, J., Pagac, M., Petru, J., Novak, P., Hajnys, J., & Kutiova, K. (2019). Topological Optimization of The Formula Student Bell Crank. *MM Science Journal*, 2019, 2964–2968.

- Özek, C., Bal, M., & Demir, Z. (2019). Bir Dalgıç Pompa Milinin Sonlu Elemanlar Metodu İle Gerilme Analizinin Modellenmesi. *Siirt Üniversitesi Uluslararası Bilim ve Mühendislik Sempozyumu (IESS 2019)*. Siirt.
- Özek, C., & Süer, E. (2023). Analysis of Stress Distribution Occurring in Guide Rails for Different Positions of Elevator Car by Finite Element Method. *Fırat Üniversitesi Mühendislik Bilimleri Dergisi*, 35, 923–935.
- Pagac, M., Hajnys, J., Halama, R., Aldabash, T., Mesicek, J., Jancar, L., & Jansa, J. (2021). Prediction of Model Distortion by FEM in 3D Printing via the Selective Laser Melting of Stainless Steel AISI 316L. *Applied Sciences*, 11, 1656.
- Popenda, A., Lis, M., Nowak, M., & Blecharz, K. (2020). Mathematical Modelling of Drive System with an Elastic Coupling Based on Formal Analogy between the Transmission Shaft and the Electric Transmission Line. *Energies*, 13, 1181.
- Quaglia, G., Oderio, R., Bruzzone, L., & Razzoli, R. (2013). A Modular Approach for a Family of Ground Mobile Robots. *International Journal of Advanced Robotic Systems*, 10. <https://doi.org/10.5772/56086>
- Savant, C. (2018). *Design of Driveline for Mobile Robot Platform*.
- Savaş, V., & Özek, C. (2005). Şehim Oranına Bağlı Olarak Bir Mil Üzerinde Oluşan Sıcaklık Dağılımının Araştırılması. *Makina Teknolojileri Elektronik Dergisi*, 1, 33–38.
- Schluse, M., Priggemeyer, M., & Roßmann, J. (2020). The virtual robotics lab in education: Hands-on experiments with virtual robotic systems in the industry 4.0 era. In *ISR 2020* (pp. 191–198). Berlin.
- Serrano, J. R., Guardiola, C., Dolz, V., López, M. A., & Bouffaud, F. (2015). Study of the turbocharger shaft motion by means of infrared sensors. *Mechanical Systems and Signal Processing*, 56–57, 246–258.
- Shahane, V. C., & Pawar, R. S. (2017). Optimization of the crankshaft using finite element analysis approach. *Automotive and Engine Technology*, 2, 1–23.
- Sonone, S., & Chaudhari, A. (2015). Design and Analysis of Balancer Shaft for a Four Stroke Single Cylinder Diesel Engine. *International Journal of Engineering Research & Technology (IJERT)*, 4.
- Sosa-Cervantes, C. Y., Silva-Ortigoza, R., Marquez-Sanchez, C., Taud, H., & Saldana-Gonzalez, G. (2014). Trajectory Tracking Task in Wheeled Mobile Robots: A Review. *2014 International Conference on Mechatronics, Electronics and Automotive Engineering*, 110–115. IEEE.
- Sun, Q., Ma, F., Guo, J., Li, G., & Feng, X. (2020). Deformation Failure Mechanism of Deep Vertical Shaft in Jinchuan Mining Area. *Sustainability*, 12, 2226.
- Tantawi, K. H., Sokolov, A., & Tantawi, O. (2019). Advances in Industrial Robotics: From Industry 3.0 Automation to Industry 4.0 Collaboration. *2019 4th*

Technology Innovation Management and Engineering Science International Conference (TIMES-ICON), 1–4. IEEE.

Tzafestas, S. G. (2014). Mobile Robot Control V. In *Introduction to Mobile Robot Control* (pp. 319–384). Elsevier.

Wang, T., Ramik, D. M., Sabourin, C., & Madani, K. (2012). Intelligent systems for industrial robotics: application in logistic field. *Industrial Robot: An International Journal*, 39, 251–259.



CHAPTER 19

Optimization of Additive Manufacturing for the Aerospace and Defense Industry

Engin Ünal¹ & Faruk Karaca²

¹ Associat. Prof. Dr., Firat University Faculty of Technology, Department of Mechanical Engineering, ORCID: 0000-0002-0501-3690

² Prof. Dr., Firat University Faculty of Technology, Department of Mechanical Engineering, ORCID: 0000-0003-1874-9274

1. INTRODUCTION

The topology optimization method has been recognized as a powerful tool for lighter part design in recent years. Topology optimization, whose theoretical background was determined by Bendsoe and Kikuchi in 1988, has now come to the fore again with the additive manufacturing method (Bendsøe & Kikuchi, 1988). The topology optimization method allows finding the material distribution that provides sufficient stiffness of a specific design space, taking into account critical loads and constraints. Material distribution is obtained by separating the design space into finite elements and determining the elements containing material and space using the optimization method. The biggest difficulty of the topology optimization method is that high calculation times occur when finding the solution by separating the design space into finite elements. As a result of topology optimization, the material distribution in the design space generally appears as complex and difficult to manufacture shapes. Additive manufacturing, one of the unconventional manufacturing methods, is a suitable method in the manufacturing of complex structures with the mechanical development of topology optimized parts. Unlike limited topology optimization methods based on traditional manufacturing method tolerances, topology optimization according to additive manufacturing allows the emergence of the optimal design without any compromises. The points to be considered in topology optimization suitable for the additive manufacturing method are that the construction direction of the design and the support material placements must be well determined (Liu et al., 2024). Additive manufacturing (AM) is a group of new manufacturing technologies that have been developed since the late 1980s. This technology is based on the automatic production of physical parts, layer by layer. AM, also known as 3D printing or rapid prototyping, is rapidly changing the perspective on how medical devices should be designed and what can be manufactured and prototyped. With AM technology, the computer aided design (CAD) model produces and transforms directly into a 3D object in a relatively short time and at low cost, avoiding the long processes of traditional production methods. ASTM and ISO standardization organizations divide the AM process into seven different categories: Powder Bed Fusion (PBF), Material Extrusion (ME), Inkjet Photopolymerization (IP), material spraying (MJ), Binder Spraying (BJ), Laminated Object Manufacturing (LOM) and Directed Energy Deposition (DED). Types of PBF processes are selective laser sintering (SLS), Selective Laser Melting (SLM), Direct Metal Laser Sintering (DMLS) and Electron Beam Melting (EBM). IP includes stereolithography (SLA) and Direct Light Processing (DLP) techniques. The most common ME process is melt deposition modeling

(MDM). Multi-jet modeling is available in the MJ process; these are multijet polyjet 3D printing (Özdemir & Özek, 2006; Sıvacı, Özgüvenç, & Bozkurt, 2022).

AM technologies have applications in various medical specialties. AM technologies providing comprehensive customization for medical practices based on individual patient data and requirements. Individual patient models are 3D designs developed with customized software. The new era of AM enables the designer to simulate the implant design before manufacturing, designing and manufacturing prosthetic implants qualified according to the patient's specific requirements such as the shape, size and mechanical properties of the implant, reducing the cost and time of implant production (Sıvacı et al., 2022).

With 3D printing, new product samples can be produced in accordance with the desired parameters without the need for new mold designs. Although fast mass production is not expected from him, fast production is achieved if he shares the design files with the entire production network (Ahangar, Cooke, Weber, & Rosenzweig, 2019).

ASTM F42 Technical Committee defines “Additive Manufacturing” as combining materials to manufacture parts layer by layer from 3D CAD design data, as opposed to subtractive manufacturing technology. It is also called additive manufacturing, direct digital manufacturing, rapid prototyping, rapid manufacturing, additive manufacturing and free-form manufacturing. The studies carried out so far in the metal parts manufacturing sector have been carried out within the constraints of manufacturability, improvement, development and innovation. The most important development in this field is the work to eliminate the manufacturability constraint. In studies on eliminating the manufacturability constraint, the most positive results are obtained in manufacturing studies using the additive manufacturing method. Additive manufacturing is one of the modern (unconventional) manufacturing methods. The basis of the method is based on adding layers of materials on top of each other. The purpose of this method is; It is to eliminate the manufacturability limitation by manufacturing parts that cannot be manufactured with traditional manufacturing methods due to their geometric complexity. It is seen that studies on this subject are given importance in recent literature sources (Ahangar et al., 2019).

Although additive manufacturing methods vary depending on the raw material used and the principle of combining layers, the basic manufacturing techniques are the same. In this regard, there are many additive manufacturing methods that manufacture using different manufacturing technologies. As examples of these;

Three Dimensional Printing (3DP), Melt Deposition Modeling (MDM), Laser Light Curing (LLC), Layer by Layer Object Manufacturing (LLOM), Selective Laser Sintering (SLS)/Selective Laser Melting (SLM) can be given.

In 1989 Nyrhilä invented and patented a new concept for pressure-free sintering of powder mixture with very low shrinkage. EOS GmbH, which was founded in 1989 and sold its first commercial machine STEREO 400 with Stereolithography technology in 1990, released the Laser sintering device in 1994. While it was the biggest rival of 3D Systems in Europe, it later (1997) lost the case filed by 3D Systems due to a patent dispute and stopped the production of its devices working on the light cure (stereolithography) principle. EOS now produces EOSINT devices based on the powder binding principle only by heating. In 1990, Selective Laser Melting (SLE-SLM) technology was originally developed by the Fraunhofer Institute in Germany and was commercialized by Fockele&Schwarze(F&S) GmbH. With an agreement made in June 2002, sales, marketing and technical support of all SLE devices started to be provided by MCP-HEK GmbH (Sun, Ng, Yang, & Zhang, 2024; Sürmen, 2019).

SLM, a metal melting-based process, which is a parallel process to the SLS process, was patented by Meiners in 1996 as a method of applying heat with a laser beam to completely melt metal powder in a protective gas atmosphere (K. Çelik & Özkan, 2017; Özer, 2020).

The first studies on Electron Beam Melting started in 1993 with the patent received by Ralf Larson on the melting and fusing of electrically conductive powders with electron beam. Later, in 1995, he continued with joint studies at Chalmers University of Technology in Gothenburg. Larson then founded Arcam AB in 1997 to commercialize this technology. The history of commercial enterprises in the field of additive manufacturing so far is also summarized in Figure 1.

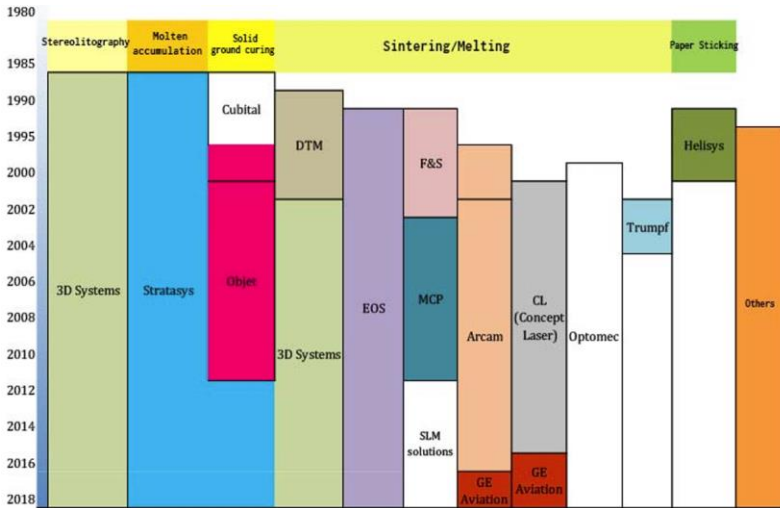


Figure 1. Commercial organizations in the field of additive manufacturing from past to present (Özsoy, Duman, & Gültekin, 2020).

In IDTechEx's "Additive Manufacturing of Metals 2015-2025" report, the market share of installation-based metal additive manufacturing companies is shown in Figure 2 (Özsoy et al., 2020).

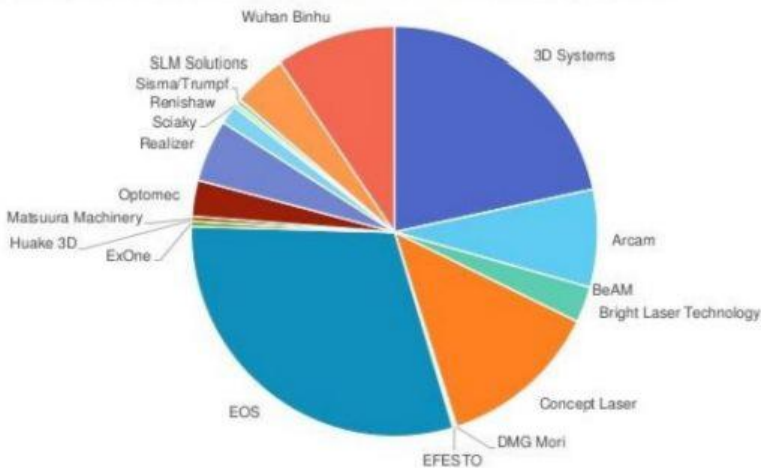


Figure 2. Market share of assembly-based metal additive manufacturing companies (Özsoy et al., 2020).

Recent technological developments and the discovery of new materials in additive manufacturing have made it an important application in the aerospace and defense industry. In general, powders of metals such as steel, aluminum and titanium, and various plastics and composites are used in aerospace and defense applications because they are materials that must withstand high temperatures. Challenging requirements such as lightweight components and precision designs of aircraft parts are the major factors driving the growth of the additive manufacturing market for the aerospace industry. In the aerospace industry, additive manufacturing is mainly used to produce critical parts of aircraft or for low-scale production associated with high performance and quality. The unique capabilities of additive manufacturing technology to produce complex parts such as jet wings, engine parts, space telescope, metal weapons, and rocket parts have increased its adoption in the aerospace and defense industry (Karakılınç, Yalçın, & Ergene, 2019).

2. ADDITIONAL MANUFACTURING

Additive manufacturing is a production process in which three-dimensional objects are created in layers using digital design data, and a whole can be obtained from parts with inductive logic, unlike traditional manufacturing methods.

2.1. Differences Between Traditional Production Methods and Additive Manufacturing

Manufacturing Process: Traditional manufacturing methods are based on the process of shaping and processing materials. These methods include casting, forging, turning, milling, welding and similar processes. Often, excess material may need to be cut or processed. Additive manufacturing is a process that creates an object by adding material in layers or by sintering. No excess is created when adding material and waste is minimal (Akgümüş Gök, Kılıçtek, Gök, & Yakut, 2023).

Material Usage: In traditional methods, large blocks or pieces are usually used. This can sometimes result in wastage of material, as excess may be cut off and thrown away. Additive manufacturing uses only the amount of material required. This minimizes waste and encourages economical use (Akgümüş Gök et al., 2023).

Freedom of Design: Traditional methods have some limitations in design, especially difficulties in the production of complex geometries. Additive manufacturing provides designers with great freedom. Complex structures,

hollow objects and greater design flexibility are possible (Akgümüş Gök et al., 2023).

Prototyping Speed: Traditional manufacturing methods can make prototyping a new product time-consuming. Additive manufacturing is ideal for rapid prototyping. Designs can be created digitally and quickly turned into physical prototypes (Akgümüş Gök et al., 2023).

Material Variety: Traditional methods are limited to certain materials and combining different materials can be difficult. Additive manufacturing offers the flexibility to use a wide range of materials, making it ideal for a variety of applications (Akgümüş Gök et al., 2023).

Customizability: Production of customized products using traditional methods is difficult and costly. Additive manufacturing enables the economical and efficient production of customized and personalized products (Akgümüş Gök et al., 2023).

2.2. Industries Where Additive Manufacturing is Widely Used

Additive manufacturing is a versatile manufacturing method used in a wide variety of industries and sectors. Here are some of the main sectors where additive manufacturing is widely used and application examples in these sectors:

Aerospace: Aerospace industries widely use Additive manufacturing for the production of lightweight and complex parts. For example, aircraft engine parts, air intakes and prototypes can be produced with 3D printers (Nichita, 2007).

Automotive: The automotive industry uses Additive Manufacturing for prototyping, production of personalized parts, and rapid production. Vehicle prototypes, customized auto parts and weight-saving components are prominent in this industry (Nichita, 2007).

Medicine and Health: In the medical and healthcare field, Additive Manufacturing is used to produce customized prosthetics, implants, anatomical models, and dental prosthetics for patients. This provides an important tool for surgical planning and training (Nichita, 2007).

Education: The education sector uses 3D printers to provide students with 3D design and manufacturing skills. Students can use 3D printing technologies to embody concepts and work on design projects (Nichita, 2007).

Jewelry Design: Jewelry design is a creative application of Additive Manufacturing. Designers can use 3D printing to produce complex jewelry pieces. This allows the creation of special and unique jewelry (Nichita, 2007).

Defense and Military: In the defense and military sectors, it is used for Additive manufacturing, rapid prototyping, parts production and vehicle maintenance. Rapid production of complex parts supports operations in the field (Nichita, 2007).

Energy and Maritime: Power generation and marine industries use Additive Manufacturing to optimize spare parts production and maintenance processes. The production of large and complex parts is especially important in these sectors (Nichita, 2007).

Engineering and Research: Engineering and research organizations use Additive manufacturing for prototyping, prototype testing, and modeling. It is an important tool for developing new products and optimizing designs (Nichita, 2007).

Food Industry: In the food industry, 3D printing is used to create creative designs, especially in cake decorating and food presentations. Specialty kitchen appliances and food items can also be produced (Nichita, 2007).

Architecture and Construction: Additive manufacturing is used in the construction industry, especially in the modeling and prototyping stages. It can work with concrete, ceramics and other construction materials. The application areas of additive manufacturing in these sectors are increasing and the technology is constantly developing. This is leading to more industries adopting Additive manufacturing while creating new opportunities (Nichita, 2007).

2.3. Advantages and Disadvantages of Additive Manufacturing

Advantages:

a) Customizability: Additive manufacturing makes it easier to customize the design. It is possible for every object to be customized and unique.

b) Production of Complex Geometries: Additive manufacturing can use complex and interlocking geometries to produce shapes that would be difficult or impossible with traditional methods.

c) Rapid Prototyping: Product prototypes can be produced quickly and economically, which speeds up the design process and facilitates the development of products.

d) Low Waste Production: Additive manufacturing keeps waste production to a minimum as it involves the direct use of material.

e) Local Manufacturing: Additive manufacturing offers the ability to produce products locally, which can reduce logistics costs and increase sustainability.

f) Freedom of Design: It provides great freedom to designers, which provides creative design opportunities.

g) Lighter and Efficient Parts: Additive manufacturing enables material savings and parts to be lighter and more efficient (Tezel, Topal, & Kovan, 2018).

Disadvantages:

a) High Initial Cost: Additive manufacturing systems and materials require investment, which increases initial costs.

b) Slow Production Speed: Some Additive manufacturing processes are slower than traditional production methods. Large and complex parts may take more time to produce.

c) Material Limitations: Additive manufacturing is limited to materials that are not suitable for some industrial applications. Durability, temperature tolerance and other properties of materials may be subject to limitations.

d) Surface Quality Issues: Additive manufacturing processes can result in rough surfaces or other quality issues. This may affect the surface quality of the final product and require finishing.

e) Limited Large Production Capacity: Additive manufacturing is less suitable for production in large quantities. It is not suitable for industries requiring mass production.

f) Inspection and Quality Control: Additive manufacturing processes can be difficult to monitor and control quality. It is important to ensure consistency of materials and processes.

g) Licensing and Intellectual Property Issues: Intellectual property and copyright issues related to 3D printing can be complex. Issues such as unauthorized copying and copyright infringement may arise. The advantages and disadvantages of additive manufacturing may vary depending on the industry, processes and applications used. Therefore, an evaluation must be made based on the project's requirements, cost factors and specific conditions (Tezel et al., 2018).

2.4. 3D Printer Concept in Additive Manufacturing

In the years when additive manufacturing became widespread, they were called 3D printers based on the logic of creating objects in layers. Additive

Manufacturing; While describing the production method, the concept of 3D printer is used more when describing the equipment with which these works are carried out (Bozkurt, Gülsoy, & Karayel, 2021).

2.5. Materials Usable in Additive Manufacturing

Materials used in additive manufacturing processes can be classified into two main categories: polymers (or plastics) and metallic materials. Information about the materials used in the industry belonging to these two categories is as follows. In addition to these, there are also newly developed alloys and composite materials studied at academic level:

2.5.1. Polymer (plastic) materials

Polylactic Acid: PLA is a biodegradable material and is commonly used in 3D printing. It is usually available in colored, transparent or matte coating. PLA is suitable for the production of simple parts, prototypes and models for educational purposes.

Acrylonitrile Butadiene Styrene: ABS is durable and impact resistant. It is heat resistant, so it is widely used in automotive parts and industrial applications. However, ABS prints tend to yellow over time.

Polyethylene Terephthalate Glycol: PETG has high strength and chemical resistance. It is used in applications such as food storage containers, medical devices and mechanical parts.

Nylon (Polyamide): Nylon offers durability and lubricity properties. It is used for the production of dental prosthetics, bearings and parts requiring high strength.

Thermoplastic Elastomer: TPE is an elastic and flexible material. It is widely used in engineering and is suitable for the production of soft elastic parts.

Polycarbonate: Polycarbonate offers high impact resistance and glass-like transparency. Therefore, it is used in the production of safety glasses, lenses and industrial protective equipment.

Polymer with a stable structure that maintains its strength at high temperatures, similar to PEEK/PEKK/PEI. They are mostly preferred in the aviation industry.

2.5.2. Metallic materials

Stainless Steel: Stainless steel is frequently used for the production of kitchen equipment, medical devices and industrial parts due to its durability and corrosion resistance. (AISI316 etc.)

Aluminum: Lightweight and durable, aluminum is used in many sectors such as aviation, automotive and space industries. (AlSi10Mg, ScalmAlloy etc.)

Titanium (Ti-6Al-4V): Titanium has high strength, low density and biocompatible properties. It is used for implants in the medical field and for engine parts in aviation (Y. H. Çelik, Yildiz, & Özek, 2016).

Cobalt Chrome: This material is used for medical implants and aerospace applications due to its durability and corrosion resistance.

Nickel Alloys: Nickel-based alloys are widely used in the aerospace, power generation and space industries due to their ability to withstand high temperatures.

Iron and Steels: Used in automotive, construction and industrial applications due to high strength and durability. In additive manufacturing, it is mostly used in mold manufacturing. The most commonly used method is powder bed systems. Each type of material has different advantages, disadvantages and application areas. Material selection is made based on printing needs, end product characteristics and cost factors. Additionally, each material's printing temperatures and process requirements may be different. Many different materials can be used in additive manufacturing, such as plastic, metal, ceramics, wood, food materials and biological tissues(Özek, Hasçalik, Çaydaş, Karaca, & Ünal, 2006).

2.6. Future Potential of Additive Manufacturing

The future potential of additive manufacturing is enormous and has the potential to create transformational impacts across many industries and applications. Here are some key points about the future potential of Additive Manufacturing:

Broader Industrial Applications: The use of additive manufacturing will spread to more industries. It will become more common in automotive, aerospace, energy, construction and many other industries. There will be greater use in large-scale production and more opportunities to produce customizable products.

Sustainability: Additive manufacturing offers the potential to reduce waste and use less materials. More sustainable production processes and local production opportunities can reduce environmental impact.

Further Material Developments: Additive manufacturing materials are constantly being developed and offer features such as greater durability, strength and heat tolerance. New materials allow for a wider range of applications.

3D Bioprinting: In the field of medicine and healthcare, 3D bioprinting has great potential in the production of human tissues and organs. This could enable the production of specialized organoids for organ transplants and drug testing.

Networked Manufacturing: 3D printing technologies enable the concept of digital sharing of files and remote production of products. This can increase the availability of products worldwide.

Design and Simulation Collaboration: In the future, designers and engineers will use 3D printing technologies to collaborate more effectively. Digital prototyping can speed up and perfect the design process.

Education and Learning Tools: 3D printing offers students and teachers the opportunity to better understand and visualize complex concepts. Students can use 3D printers to better understand real-world applications.

Production in Space: The development of 3D printers and raw materials for use in long-term missions in space can enable astronauts to produce spare parts and supplies locally for their needs.

Coordinated Production: Large-scale objects and structures can be produced more effectively thanks to the collaboration of multiple 3D printers and robots.

The future potential of additive manufacturing will further increase with continuous technological advancements and adoption of this technology by different industries. This will offer many advantages such as more original designs, rapid prototyping and customizable products (Garcia-Dominguez, Claver, Camacho, & Sebastian, 2020).

2.7. Additive Manufacturing Technologies Terminologies

ASTM F2792 standard is a standard that defines additive manufacturing processes called "Standard Terminology of 3D Printing and Additive Manufacturing Processes." The scope of this standard includes terms and definitions that classify additive manufacturing technologies in detail.

Additive Manufacturing (AM): It is used as the general term of additive manufacturing and covers many different processes.

Layered Manufacturing (LM): It is a synonym for the term layered manufacturing and again describes the processes of depositing materials in layers.

Binder Jetting: It involves combining the powder material in layers using a binding agent.

Directed Energy Deposition (DED): The material is melted by an energy source (usually a laser or electron beam) and combined into layers.

Fused Deposition Modeling (FDM): It involves heating, melting and combining plastic filaments into layers.

Material Jetting: It involves spraying liquid material into various layers in the form of droplets.

Powder Bed Fusion (PBF): It involves combining powder materials in layers by melting them with an energy source (usually laser). This term also includes SLS and DMLS processes.

Sheet Lamination: It refers to the processes in which sheets are used to combine material layers.

Vat Photopolymerization: It involves curing the liquid resin in layers with UV light or laser. Stereolithography (SLA) and Digital Light Processing (DLP) fall into this category.

Binder Jet Additive Manufacturing (BJAM): It involves combining the powder material with a binding agent.

Direct Write: It refers to writing the material directly on a surface with the energy source.

Material Extrusion: It involves adding material from one layer to another with a nozzle or similar tool. FDM falls into this category. The ASTM F2792 standard clearly defines additive manufacturing terms and provides standardization of the language used in the industry. In this way, additive manufacturing processes and technologies are better understood and agreement is achieved between users (Garcia-Dominguez et al., 2020).

2.8. General Standards Used in Additive Manufacturing

ISO/ASTM 52900:2015 - Additive manufacturing - General principles - Terminology: This standard defines the basic terms and concepts related to Additive manufacturing.

ISO 9001:2015 - Quality Management Systems: It is a general standard that regulates the quality management of additive manufacturing processes.

ISO 17296-1:2014 - Additive manufacturing - General principles - Part 1: Terminology: It is another international standard that defines the terms and concepts of additive manufacturing.

ASTM F2792-12(2017) - Standard Terminology for Additive Manufacturing Technologies: This ASTM standard provides terms and concepts for Additive manufacturing technologies.

ASTM F2923-14(2019) - Standard Specification for Additive Manufacturing Titanium6 Aluminum-4 Vanadium ELI (Extra Low Interstitial) with Powder Bed Fusion: This standard defines specific requirements for a particular Additive manufacturing process and material type.

ASTM F3091-14(2019) - Standard Specification for Powder Bed Fusion of Plastic Materials: Specifies the requirements for the use of plastic materials in Additive Manufacturing.

ASTM F2924-14(2019) - Standard Specification for Additive Manufacturing Titanium6 Aluminum-4 Vanadium with Powder Bed Fusion: Contains specific requirements for the use of Titanium alloys in Additive Manufacturing.

ISO 17296-2:2021 - Additive manufacturing - General principles - Part 2: Overview of process categories and feedstock: It is another ISO standard that addresses additive manufacturing process categories and material feeding methods.

3. TOPOLOGY OPTIMIZATION

When the part to be designed is required to fit into a limited space, be light in weight and have a long operating life, only a rough idea about the new design comes to mind. Parts are often designed by improving upon an existing design or concept. In such cases, dimensions or other design inputs are defined with the help of parameters. In cases where there is no existing design to work with, one or two conceptual designs can be created. These designs can be defined parametrically and then standard optimization methods can be applied. As an alternative method, optimization studies by starting with a simple material block

and allowing the optimization software to determine each design feature, shape and size are known as topology optimization (Figure 3).



Figure 3. Topology optimization (Recrosio, 2017)

Using topology optimization, the best distribution of the material within the part is found in the problem given with an optimization target and a constraint set. For optimization analysis, a set of constraints such as maximum stress/strain, displacement or natural frequency can be defined by the user. By obeying these constraints, the software creates voids in the material block in the model to minimize or maximize an optimization parameter such as mass, volume, or displacement. For example, the natural frequencies of a test platform can be optimized to minimize its mass, keeping it out of a designated objectionable range. As you can imagine, such optimization efforts can result in very new and complex shapes. Although it used to be impractical to manufacture complex shapes due to the limitations of traditional manufacturing methods, today, newer manufacturing methods allow the mass production of extremely complex designs.

Another example of topology optimization is a control arm shown in Figure 4. The mass of this part can be minimized without exceeding the displacement limits set by the user. The rough geometry defining the allowable dimensional limits of the control arm is as follows. All connection regions are shown on the model. In this example, the lower port (A) is loaded with a force of 33,000 N, indicated by the red arrows, in both horizontal and vertical directions. The top two attachment points (B and C) are fully constrained (built-in bracket) (Figure 4).

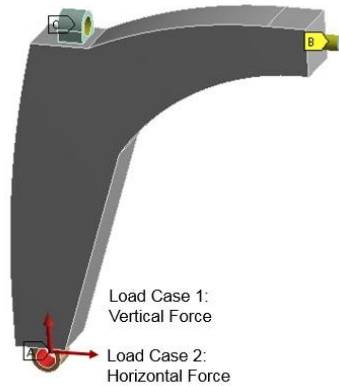


Figure 4. Topology optimization loading status (Hale, 2018)

Topology optimization was run to minimize the mass while limiting the maximum horizontal displacement at the point where the force was applied to 10.7 mm and the maximum vertical displacement to 1.2 mm. In this way, the optimized structure shown in Figure 5 was obtained.



Figure 5. Topology optimization design (Hale, 2018)

Shapes produced with topology optimization software can be exported as STL files for use with 3D printer software. As mentioned before, these shapes can be so complex that they are very difficult to manufacture. Some topology optimization software, such as ANSYS Topology Optimization, also allows defining manufacturing constraints such as symmetry regarding a plane, extrusion direction, and max/min allowable element size. These constraints help

prevent the emergence of optimized shapes that would be too difficult or costly to manufacture. Additionally, tools such as ANSYS SpaceClaim can be used to reverse engineer from exported STL files. In Figure 5, the control arm was manufactured using this process, the final dimension of which is shown in Figure 6.

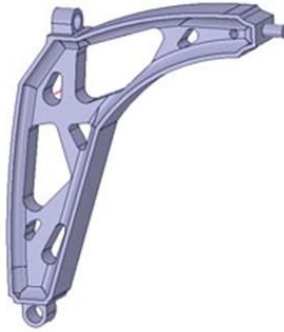


Figure 6. Topology optimization dimensioning (Hale, 2018)

Although there are other optimization tools that perform different tasks, topology optimization remains the most general and powerful tool for developing new shapes and concept designs (Tezel et al., 2018).

Advantages:

Lightweight and production-ready product designs can be prepared.

Reduces time to market, physical testing and prototype manufacturing time.

Optimized designs created should be based on FEA simulations including:

Available design space

Realistic load scenarios and boundary conditions

Design and manufacturing limitations (Martínez-García, Monzón, & Paz, 2021).

4. CURRENT STATUS OF ADDITIVE MANUFACTURING TECHNOLOGY IN THE AEROSPACE INDUSTRY

Additive manufacturing technology has great potential in the Aerospace industry. General Electric (GE) Aviation, Lockheed Martin, Airbus and BAE System, MTU Aero-Engine, Rolls-Royce plc. Pratt & Whitney, GE Avio Aero et al. Companies such as are international companies that use this technology widely. Boeing, the world's largest civilian and military aircraft and helicopter manufacturer, has announced that it plans to replace many of the parts in aircraft with those produced by additive manufacturing. Boeing company plans to make many parts of the aircraft producible through additive manufacturing in order to stock aircraft parts in different centers, deliver the parts to the required places and avoid possible delays. Boeing spokesman Nathan Hulings stated that 150 different parts in the F/A-18 Super Hornet aircraft were manufactured with Additive Manufacturing (Bozkurt et al., 2021). GE has spent 1.5 billion dollars on R&D studies on additive manufacturing since 2010. By purchasing ARCAM and CONCEPT LASER in 2016, the company has become a complement to its existing additive technologies. In 2015, GE started test flights of the new generation LEAP aircraft engine, which was manufactured with additive manufacturing machines for the first time and has 19 fuel injectors.

FAA (Federal Aviation Administration) manufactured and certified the T25 engine sensor protection unit used on GE90-94B engines with additive manufacturing in 2015. Providing pressure and temperature measurements for engine control systems, the T25 has been installed on more than 400 GE90-94B engines. It has been noted that the T25 sensor protection unit is just the beginning for additive manufacturing at GE aerospace (Figure 7a). Additionally, it is stated that the fuel injector produced by GE is 5 times more durable and 25% lighter (Figure 7b) (Bamberg, Dusel, & Satzger, 2015).

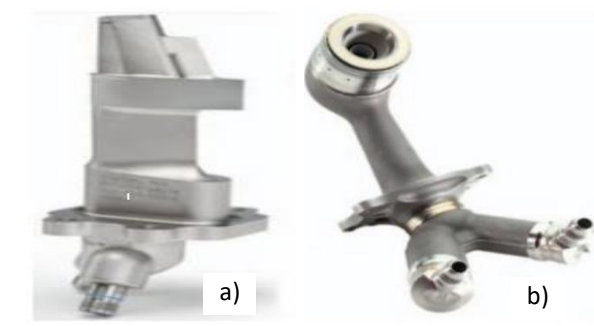


Figure 7. Manufactured by additive manufacturing a) FAA approved T25 pressure temperature sensor b) LEAP aircraft engine fuel nozzle for CFM (Bamberg et al., 2015).

Lockheed Martin Space Systems produced titanium shipping tanks in 2009 with Direct Electron Beam Melting (EBDM), one of the additive manufacturing methods initiated by Sciaky company. The EBDM method is preferred by aviation companies such as Airbus, General Electric and Lockheed Martin. Because Inconel is ideal for producing large-scale parts made of tantalum, titanium and other high-value metals. A lightweight "Nacelle hinge bracket" part was manufactured for Airbus A320 aircraft using additive manufacturing and selective laser melting method. In the study, a total mass saving of 64% was achieved with both topology and material selection (Figure 8).



Figure 8. Airbus hinge holder part (Getachew, Shiferaw, & Ayele, 2023).

He works on quality assurance and standards in the process chain for the production of engine parts with additive manufacturing at MTU Aero Engine, the largest subsystem supplier for aircraft engines.

Borescope eye production was carried out for the PW1100G-JM engine powering the Airbus A320neo with the Additive manufacturing device using EOS M280 (Figure 9).



Figure 9. Borescope eye and tensile sample manufactured (Bamberg et al., 2015).

The Rolls-Royce Trent XWB-97 is the largest aerospace/engine part manufactured by ARCAM Electron beam melting from the additive manufacturing method. As shown in Figure 10, the Titanium front roller bearing, which is located on the engine and has 48 aero foils, is approximately 1.5m in diameter and 0.5m thick, was produced by the additive manufacturing method. Here, with additive manufacturing, manufacturing time was reduced by 30% and cost and production speed were optimized during the design process (Bamberg et al., 2015).

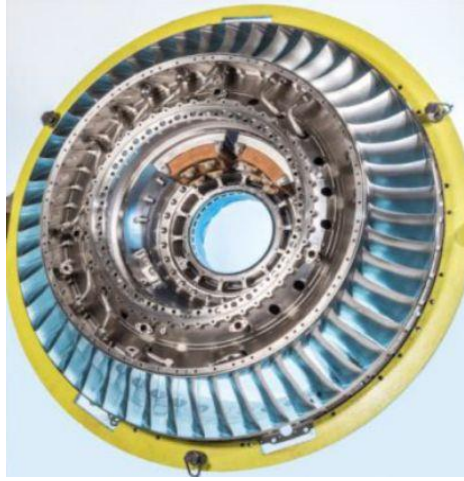


Figure 10. Rolls Royce Trent XWB engine front bearing housing (Bamberg et al., 2015).

Approximately twelve parts of the Pratt&Whitney Bombardier aircraft engine were fabricated using the additive manufacturing methods electron beam melting (EBM) and direct metal laser sintering (DMLS) (Figure 11). These parts are nickel and titanium material fasteners, fuel collectors and injection nozzles. Pratt&Whitney achieved a 50% reduction in the weight of the parts through design optimization.



Figure 11. Stator to be used in Pratt Whitney jet engine bombardiers manufactured by additive manufacturing (Özsoy et al., 2020).

Additive manufacturing today performs better than traditional manufacturing methods in the manufacturing of large parts. Companies that produce additive

manufacturing machines are conducting research and development to make improvements regarding the limitations of device dimensions. In this context, Lockheed Martin is working on additive manufacturing technology with large manufacturing volumes at Oak Ridge National Laboratory (ORNL). One of the problems encountered in the space and aviation industry is the limitation of construction volume and product size. The fuselage metal panel reinforced with metal wire and arc additive manufacturing was manufactured by Stelia Fusegela Aerospace, a company that has improved itself step by step in product size limitation (Figure 12) (Bamberg et al., 2015).



Figure 12. Body panel manufactured by additive manufacturing (Özsoy et al., 2020).

The sector in which additive manufacturing technologies are most widely used in the aviation field in Turkey is undoubtedly the defense industry. TEİ, TUSAŞ-TAİ, Kalegrup, Aselsan, FNSS, ROKETSAN, which are in the aviation and space sector, manufacture parts using additive manufacturing technology. Some of the devices in these sectors were purchased with the R&D incentives provided by the government. For the first time in our country, in 1993, Arçelik company purchased 1 SLA-250 and formed the rapid prototype part of the R&D department (Bamberg et al., 2015).

4.1. Advantages of Additive Manufacturing Technologies for the Aerospace Industry

There are many advantages for the space and aviation industry with the additive manufacturing method. These advantages are listed below.

Additive manufacturing technologies have many advantages, such as labor and cost savings from mold design and production activities, since they do not require special jigs/mold-like equipment during the production stage.

With the additive manufacturing method, it is possible to manufacture critical space and aviation parts with complex geometry using metal powder materials.

Within the framework of our country's 2023 vision, the use of additive manufacturing technologies in the production of national regional aircraft, engines and unique helicopters in the field of civil aviation will perhaps be inevitable.

The most important criterion in the aviation industry is that the parts are light. It is difficult to manufacture porous lightweight parts using any method other than additive manufacturing. The additive manufacturing method facilitates the fabrication of such lightweight porous parts.

Rapid spare parts manufacturing is possible by using additive manufacturing technologies in repair, maintenance and overhaul activities in the Aerospace industry.

The ease of design resulting from biomimetics (imitation of nature) will open horizons for very advanced technologies, especially for the aviation and space industry.

It has been calculated that additive manufacturing will provide an annual reduction in carbon dioxide released into the atmosphere for commercial aviation businesses (Chang & Moser, 2016; Liu et al., 2024; Sıvacı et al., 2022).

It is expected that additive manufacturing technologies will contribute to the reduction of residual materials. Additionally, there will be reductions in fuel consumption. Figure 13 shows the percentage benefits of additive manufacturing technology until 2026.

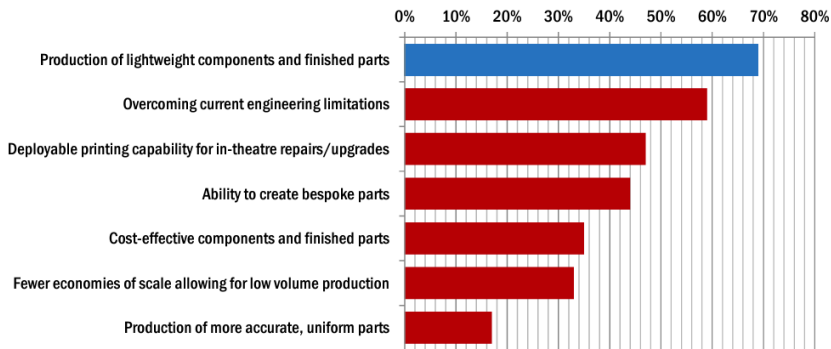


Figure 13. The key benefits of additive manufacturing over the next 10 years (Getachew et al., 2023).

4.2. Disadvantages of Additive Manufacturing Technologies for the Aerospace Industry

There are disadvantages for the space and aviation industry with the additive manufacturing method. These disadvantages are listed below.

The cost of materials used in additive manufacturing is high. In addition, the mechanical properties of the part manufactured by the additive manufacturing method may differ from those of the material used.

It creates a disadvantage due to high consumable (gas, powder material, fuel, etc.) expenses.

Additive manufacturing machines are acquired with high investment costs.

It is not very suitable for mass production because the process is slow and the build volume is low.

Compared to similar Computerized Numerical Control machines, the manufacturing cost (raw material, tools, gas, etc.) is higher.

In the additive manufacturing process, micropores and hairline cracks occur in cases where there is welding.

There may be a need for post-processing (heat treatment, polishing, etc.) on the manufactured parts (Malakizadi, Mallipeddi, Dadbakhsh, M'Saoubi, & Krajnik, 2022; Özsoy et al., 2020). In Figure 14, the challenges to the development of additive manufacturing technology until 2026 are shown as a percentage (Getachew et al., 2023).

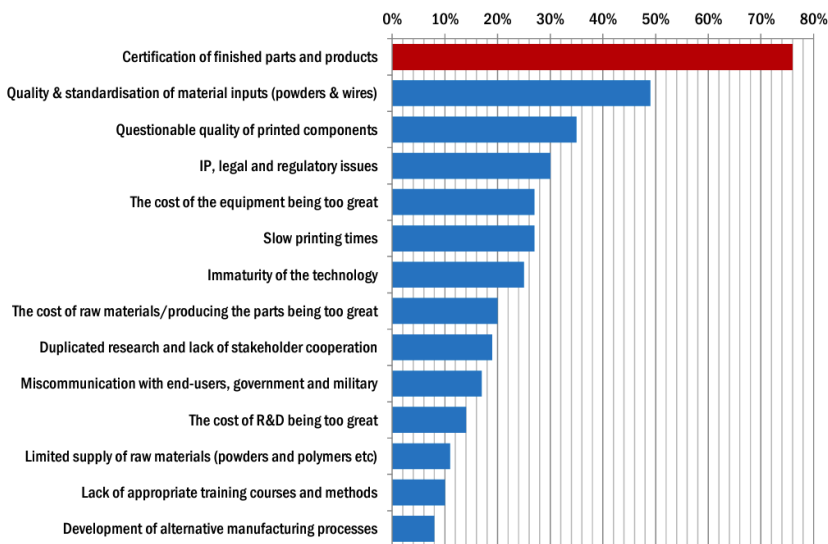


Figure 14. The key challenges hindering advancement of AM over the next ten years (Getachew et al., 2023).

5. CONCLUSIONS and RECOMMENDATIONS

It was prepared by examining international studies on additive manufacturing methods and materials used. Additive manufacturing methods and terms used in the literature are included. Metal materials and application examples commonly used in this manufacturing method were examined. Some of the following results were reached with this research:

Additive manufacturing method is a manufacturing method that enables flexibility in design and the manufacture of parts consisting of multiple materials.

Additive manufacturing technologies are mainly used in the production of parts for important industrial areas such as aerospace, automotive, biomedical, defense industry and energy sector.

Additive Manufacturing methods differ in terms of accumulating materials and forming layers, creating parts, and working principles.

The properties of the materials used in Additive Manufacturing methods affect the properties of the final part.

Since layers in AM methods are formed by melting the material locally with a heat source, the thermo-physical properties of the materials preferred by researchers are often important (Malakizadi et al., 2022; Sıvacı et al., 2022).

The current status of additive manufacturing technology in the aerospace sector is examined. Additionally, the advantages and disadvantages of the AM method for the aviation, space and defense sectors are presented. The results found in this study are summarized as follows:

Recent technological developments and the discovery of new materials in additive manufacturing have made it an important application in the aerospace and defense industry.

Challenging requirements such as lightweight components and precision designs of aircraft parts are the major factors driving the growth of the additive manufacturing market for the aerospace industry.

In the aerospace industry, additive manufacturing is predominantly used to produce critical parts of aircraft or for low-scale production associated with high performance and quality.

In studies on eliminating the manufacturability constraint, the most positive results are obtained in manufacturing studies with the additive manufacturing method.

Additive manufacturing technology's unique capabilities to produce complex parts such as jet wings, engine parts, space telescope, metal weapons, and rocket parts have increased its adoption in the aerospace and defense industry.

The material market used in additive manufacturing technology includes polymers and metals. Sectors include space, automotive, consumption, health, security, industrial machinery and education and research sectors.

REFERENCES

- Ahangar, P., Cooke, M. E., Weber, M. H., & Rosenzweig, D. H. (2019). Current Biomedical Applications of 3D Printing and Additive Manufacturing. *Applied Sciences*, 9, 1713.
- Akgümüř Gök, D., Kılıçtek, S., Gök, S., & Yakut, N. (2023). Katmanlı imalat teknolojilerinin karşılaştırılmasına yönelik bir araştırma. *Gümüşhane Üniversitesi Fen Bilimleri Enstitüsü Dergisi*, 13, 517–537.
- Bamberg, J., Dusel, K.-H., & Satzger, W. (2015). *Overview of additive manufacturing activities at MTU aero engines*. 156–163.
- Bendsøe, M. P., & Kikuchi, N. (1988). Generating optimal topologies in structural design using a homogenization method. *Computer Methods in Applied Mechanics and Engineering*, 71, 197–224.
- Bozkurt, Y., Gülsoy, H., & Karayel, E. (2021). Eklemeli İmalat Teknolojilerinin Tıbbi Ekipmanların Üretiminde Kullanımı. *El-Cezeri Fen ve Mühendislik Dergisi*, 8, 962–980.
- Çelik, K., & Özkan, A. (2017). Eklemeli İmalat Yöntemleri İle Üretim ve Onarım Uygulamaları. *Düzce Üniversitesi Bilim ve Teknoloji Dergisi*, 5, 107–121.
- Çelik, Y. H., Yıldız, H., & Özek, C. (2016). Effect of cutting parameters on workpiece and tool properties during drilling of Ti-6Al-4V. *Materials Testing*, 58, 519–525.
- Chang, S. H., & Moser, B. R. (2016). 3D printing technology insertion: Sociotechnical barriers to adoption. *Solid Freeform Fabrication 2016: Proceedings of the 27th Annual International Solid Freeform Fabrication Symposium - An Additive Manufacturing Conference, SFF 2016*, 1960–1975.
- Garcia-Dominguez, A., Claver, J., Camacho, A. M., & Sebastian, M. A. (2020). Analysis of General and Specific Standardization Developments in Additive Manufacturing From a Materials and Technological Approach. *IEEE Access*, 8, 125056–125075.
- Getachew, M. T., Shiferaw, M. Z., & Ayele, B. S. (2023). The Current State of the Art and Advancements, Challenges, and Future of Additive Manufacturing in Aerospace Applications. *Advances in Materials Science and Engineering*, 2023, 1–13.
- Hale, S. (2018). Topology Optimization: What is it for?
- Karakılınç, U., Yalçın, B., & Ergene, B. (2019). Toz Yataklı/Beslemeli Eklemeli İmalatta Kullanılan Partiküllerin Uygunluk Araştırması ve Partikül İmalat Yöntemleri. *Politeknik Dergisi*, 22, 801–810.
- Liu, S., Li, Q., Hu, J., Chen, W., Zhang, Y., Luo, Y., & Wang, Q. (2024). A Survey of Topology Optimization Methods Considering Manufacturable Structural

- Feature Constraints for Additive Manufacturing Structures. *Additive Manufacturing Frontiers*, 3, 200143.
- Malakizadi, A., Mallipeddi, D., Dadbakhsh, S., M'Saoubi, R., & Krajnik, P. (2022). Post-processing of additively manufactured metallic alloys – A review. *International Journal of Machine Tools and Manufacture*, 179, 103908.
- Martínez-García, A., Monzón, M., & Paz, R. (2021). Standards for additive manufacturing technologies. In *Additive Manufacturing* (pp. 395–408). Elsevier.
- Nichita, G. G. (2007). An Review About Rapid Manufacturing. *ANNALS of the ORADEA UNIVERSITY. Fascicle of Management and Technological Engineering*, 6, 1417–1422.
- Özdemir, N., & Özek, C. (2006). An investigation on machinability of nodular cast iron by WEDM. *The International Journal of Advanced Manufacturing Technology*, 28, 869–872.
- Özek, C., Haşçalık, A., Çaydaş, U., Karaca, F., & Ünal, E. (2006). Turning OF AISI 304 Austenitic Stainless Steel. *Journal of Engineering and Natural Sciences*, 2006, 117–121.
- Özer, G. (2020). Eklemeli Üretim Teknolojileri Üzerine Bir Derleme. *Ömer Halisdemir Üniversitesi Mühendislik Bilimleri Dergisi*, 9, 606–621.
- Özsoy, K., Duman, B., & Gültekin, D. İ. (2020). Metal Part Production with Additive Manufacturing for Aerospace and Defense Industry Metal Part Production with Additive Manufacturing for Aerospace and Defense Industry. *International Journal of Technological Sciences*, 11, 201–211.
- Recrosio, E. (2017). Topology Optimization: Control the Shape of your 3D Printed Model. Retrieved from <https://www.sculpteo.com/blog/2017/04/26/topology-optimization-controlthe-%0Ashape-of-your-3d-printed-model/%0A>
- Sıvacı, K., Özgüvenç, E. E., & Bozkurt, Y. (2022). Biyomedikal Uygulamalarında Eklemeli İmalat Teknolojileri. *Uludağ University Journal of The Faculty of Engineering*, 503–522.
- Sun, M., Ng, C. T., Yang, L., & Zhang, T. (2024). Optimal after-sales service offering strategy: Additive manufacturing, traditional manufacturing, or hybrid? *International Journal of Production Economics*, 268, 109116.
- Sürmen, H. K. (2019). Eklemeli İmalat (3b Baskı): Teknolojiler ve Uygulamalar. *Uludağ University Journal of The Faculty of Engineering*, 24, 373–392.
- Tezel, T., Topal, S., & Kovan, V. (2018). Hybrid Manufacturing: Investigation of The Usability of Additive Manufacturing with Machining. *3rd International Congress on 3D Printing Technologies and Digital Industry, Antalya, Türkiye*, 2, 60–65.



CHAPTER 20

Implementing Smart Disaster Management Systems in Smart Cities

Mesut Samastı¹ & Ceren Altan²

¹ Dr., Tübitak Tüside, Orcid: 0000-0002-4900-8279

² ORCID: 0009-0001-3178-8238

1 Introduction

With the advancement of technology in recent years, the increase in various production and energy needs has led to a surge in interventions into nature and ecological systems. Consequently, disasters that were already being encountered are escalating in severity, resulting in much larger economic, social, and ecological damages. In recent years, disasters such as major wildfires, earthquakes, floods, hurricanes, and droughts have inflicted harm upon numerous structures, living beings, and large-scale urban systems.

The earlier action is taken to rescue individuals affected by a disaster, the more lives can be saved. Therefore, disaster management aims to be as organized as possible to mitigate any potential damage, covering the pre-disaster, during-disaster, and post-disaster processes. The integration of these stages with technological advancements and innovations will enhance the outcomes. Research conducted on the Internet of Things (IoT) and artificial intelligence (AI) is emerging in the field of disaster management, with these technologies being utilized in smart city initiatives to enhance urban resilience. However, systems based on IoT may be susceptible to issues such as miscalculations or faulty sensing, which can adversely affect system operations and even endanger lives (Dugdale, Moghaddam, & Muccini, 2021). Additionally, it is crucial for IoT-based systems to be efficient in performance and energy consumption. Ray et al. (2017) categorized IoT-based disaster management applications into four groups: (i) service-oriented, (ii) natural, (iii) man-made, and (iv) post-disaster management (Ray, Mukherjee, & Shu, 2017). The group referred to as natural disaster management encompasses the management of disasters whose severity is increasing due to climate change, as mentioned above.

Prior to engaging in disaster management studies, it would be beneficial to examine and define examples of disasters to better understand the subject. Among disasters, floods are the first to be addressed. Floods are one of the most destructive and dangerous natural disasters. They typically occur as a result of heavy rainfall, excessive snowmelt, or sudden flash floods. All these effects are intensified due to climate change, resulting in river overflows, dam collapses, or the inability of impermeable surfaces to absorb accumulated water due to excessive rainfall (Al-Hussein, ve diğerleri, 2023). The sudden flow of water caused by floods destroys homes, agricultural lands, and infrastructure. Moreover, floods lead to health issues due to contamination and mud in floodwaters, rendering living spaces unusable.

Throughout history, numerous flood disasters with devastating effects have been encountered. Many floods have resulted in the loss of millions of lives and left millions of people homeless. As an example, the 2004 Indian Ocean Tsunami, accompanied by massive waves, caused the deaths of hundreds of thousands of people and widespread destruction. In this natural disaster, initially, a 9.1 magnitude earthquake occurred, followed by a tsunami with waves reaching heights of 20-30 meters. In total, these disasters led to approximately 200,000 fatalities (Satake, 2014). Additionally, it is estimated that the floods encountered in Germany, Belgium, the Netherlands, Austria, and Switzerland in 2021 caused 30 billion euros in damage in Europe (Guardian, 2022). The severe monsoon rains experienced in Nepal and India in 2019 also caused damage to the region's population, particularly impoverishing vulnerable communities further and resulting in homelessness and damage to agricultural lands (News, 2019). These examples demonstrate how destructive and life-threatening floods can be, highlighting the need for ongoing efforts to control floods and mitigate their impacts.

On the other hand, earthquakes occur as a result of the released energy caused by the movement and compression of tectonic plates on the Earth's surface (Survey, What is an earthquake and what causes them to happen? | U.S. Geological Survey, 2013). Depending on their magnitude and duration, earthquakes can lead to significant damage and loss of life. A destructive earthquake can cause buildings to collapse, infrastructure to be damaged, and communities to be disrupted. The impact of earthquakes is particularly severe in areas with structurally weak buildings. Additionally, earthquakes often trigger tsunamis, landslides, and fires.

There have been many destructive earthquakes throughout history. In 2010, a magnitude 7.0 earthquake struck Haiti, resulting in approximately 316,000 deaths or missing persons and 300,000 injuries. This disaster left approximately more than 1.3 million people homeless and caused critical damage to about 80% to 90% of the urban housing stock (DesRoches, Comerio, Eberhard, Mooney, & Rix, 2011). The earthquake with a magnitude of 9.1 that occurred in the Indian Ocean in 2004, followed by the ensuing tsunami, is considered one of the most damaging earthquakes by the U.S. National Science Foundation (2005), resulting in approximately 228,000 deaths (Foundation, 2005). Countries located on various earthquake belts around the world are more frequently exposed to earthquakes (Survey, Where do earthquakes occur?, 2012). Turkey, one of these countries, has faced earthquakes that have caused significant damage over the years. Moreover, earthquakes often leave irreversible material and psychological

damage lasts for years. In the earthquakes centered in Kahramanmaraş, Pazarcık, and Elbistan in 2023, approximately at least 51,000 people lost their lives in Turkey, and 8.500 people lost their lives in Syria, with more than 122.000 people injured. The earthquake zone was declared a level 4 alarm zone after these earthquakes. According to a report prepared by the Turkish Presidency of Strategy and Budget (2023) after the earthquake, this earthquake caused a loss of 103,6 billion dollars to the Turkish economy (Mussa, 2023) (Başkanlığı, 2023). Considering all these damages, it is evident that effective preparation and structural measures are vital in regions at risk of earthquakes.

Wildfires are another natural disaster that spreads rapidly and causes extensive damage. They are fatal disasters due to their long-lasting containment efforts and the harm they cause to both living beings and systems in the affected area, as well as the harmful gases and particles they release into the atmosphere, affecting future generations and the world as a whole. In Australia, a large-scale wildfire occurred in 2009, known as Black Saturday, which affected not only Australia but also the USA, Russia, Canada, and some European and Asian countries. In this wildfire, 173 people lost their lives, 414 people were injured, and approximately 4.5 billion dollars in damage was incurred (Shhahparvari, Abbasi, Chhetri, & Abareshi, 2019). Similarly, during the 2019-2020 bushfire season in Australia, wildfires continued for an extended period due to extreme heatwaves, resulting in hundreds of people being displaced and endangering the lives of around 3 billion animals in the region. This disaster, which caused significant social, economic, and ecological damage and nearly destroyed 19 million hectares of land, led to a shift in focus for climate action and wildfire management systems (Australia, 2020).

1.1 Disaster Management in Smart Cities

Considering the continuous exposure to various disasters worldwide and the anticipation of future occurrences, planning and finding solutions for disasters should not be merely a choice but a necessity to minimize the damage they cause.

The impacts of floods encountered in urban or rural areas are further exacerbated due to climate change or inadequate planning in harmony with nature. Additionally, the insufficient presence of permeable surfaces in cities or the lack of green infrastructure designs further amplify the damage caused by floods.

Given that regions more prone to earthquakes are situated along seismic belts, not being prepared for earthquakes and facing the resulting destruction is often a

consequence dependent on policymakers' priorities and choices. However, it is essential to reinforce structures to make them earthquake-resistant.

In summary, proactive planning and implementation of solutions for disasters are imperative considering the inevitability of their occurrence and the potential magnitude of their impacts. This involves developing strategies to address the specific vulnerabilities of different regions, whether urban or rural, and investing in resilient infrastructure and preparedness measures to minimize the damage and ensure the safety and well-being of communities.

Wildfires occur due to neglect or drought and can cause severe and challenging-to-repair damage in a very short period. Extra care should be taken in forested or high-risk fire areas, and various restrictions should be implemented. Necessary resources for facilitating disaster response in these areas should be consistently maintained in case of potential fire situations.

In cases where all mentioned practices are lacking, the implementation of smart city solutions in urban areas aims to create early warning systems for disasters, providing alerts before disasters occur to minimize damage. Early warning systems are established for earthquakes, floods, fires, and frost to prevent the destructive effects of these disasters. Pre-prepared emergency evacuation plans for disasters will prevent wrong actions during disasters due to stress and fear.

Acoustic location detection systems allow for the identification of the locations of casualties during disasters. Similarly, post-disaster communication systems aim to provide effective infrastructure for communication during disasters and emergencies, facilitating information exchange and coordinating rescue operations. These systems enable disaster victims to request assistance and ensure that rescue teams are in communication with each other and with management centers.

Disaster sensitivity maps and simulations analyze disaster risks in smart cities, determining cities' sensitivity to disasters and predicting possible impacts in advance. These tools assist local governments in developing disaster response and rescue plans, while also encouraging community awareness and preparedness for disasters. All the applications discussed in this study contribute significantly to strategic decision-making processes in disaster management.

1.2 Organization of The Paper/Study

This study aims to provide a detailed examination of the systems used in smart cities for disaster management. The initial stage of the study focuses on analyzing disasters that cause loss of life and property. Subsequently, academic research related to these disasters is reviewed. Following a literature review, smart systems designed to prevent or mitigate the impact of these disasters during emergencies are examined. A conceptual framework is developed for the integrated operation of these systems. Within the scope of the study, the benefits of integrating these applications in a specific-scale settlement area are analyzed.

The following applications are analyzed in the study, and the resulting economic, social, environmental, and health benefits are examined:

- Frost and Flood Warning Systems
- Advanced Earthquake Warning
- Advanced Flood Warning
- Fire Detection and Alert Systems
- Acoustic Detection and Location Tracking
- Emergency Evacuation Plans
- Post-Disaster Communication Systems
- Disaster Coordination Centers

2 Related Work/Studies

Today's technology is utilized to minimize the impact of all these disasters on individuals and systems in any city, appearing in smart city applications. One such application is the use of Internet of Things (IoT) technologies for disaster management in smart cities. IoT devices work by sending alerts about potential hazards of disasters for early detection. For instance, during events like earthquakes or tsunamis, sensor systems can detect abnormal vibrations and send this information to specialized cloud services. These services analyze the data and send instant notifications to users if a threat is detected. These notifications can be sent via Short Message Service (SMS), visualizations on websites, or through voice notifications (Ashok Kumar, Girish, & Rajesh, 2015).

IoT devices are used to monitor the situation in disaster areas in real-time. This allows continuous monitoring of factors such as water levels, air quality, and other environmental factors so that authorities can take necessary measures

promptly. Ashok Kumar et al. (2015) evaluated IoT technologies in disaster planning with their "Integrated Weather and Flood Alerting System," designed to reduce the damage caused by the recurring flood problem in India. By utilizing parameters such as rainfall level over the river, water flow, and water level in the river detected through sensors, various alerts are issued to alert the public about any anomalies (Ray, Mukherjee, & Shu, 2017) (Ashok Kumar, Girish, & Rajesh, 2015). Similarly, with another system based on Netdunio, the water level in rivers, lakes, and similar water bodies can be measured using sensors, enabling the detection of critical danger levels before they escalate (Ray, Mukherjee, & Shu, 2017) (Hernandez-Nolasco, Ovando, Acosta, & Pancardo, 2016).

Although satellite imaging and remote camera-based sensors are commonly used for wildfire management, these tools have some drawbacks. One of the main challenges is the delayed or late detection of fires by these devices and their low reliability, which can lead to critical damage in combating rapidly spreading fires (Bushnaq, Chaaban, & Al-Naffouri, 2021). In their study, Bushnaq et al. (2021) proposed the use of unmanned aerial vehicles (UAVs) based on IoT networks in the detection system, suggesting that, given the appropriate system cost, they could provide a faster and more accurate wildfire detection method compared to various satellite imagery techniques (Bushnaq, Chaaban, & Al-Naffouri, 2021).

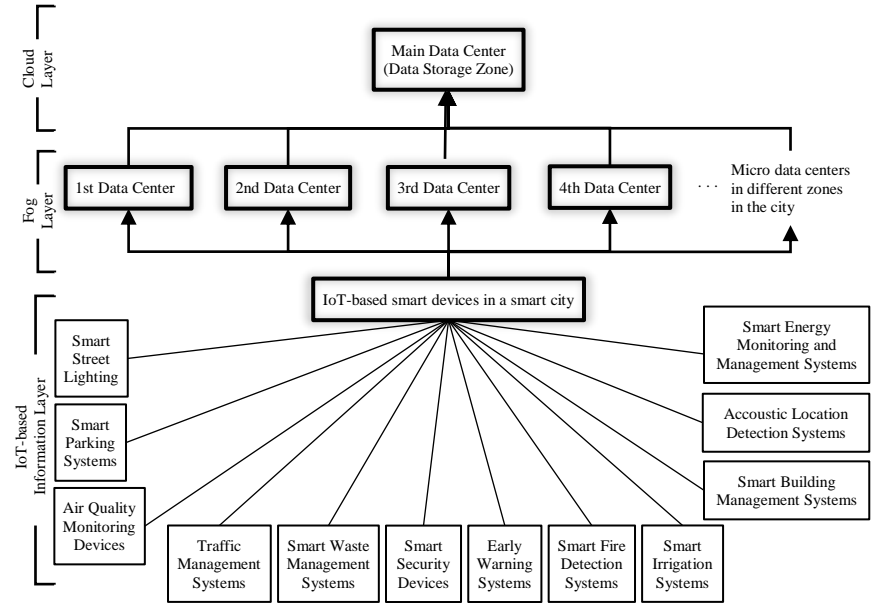


Fig. 1. The relationship of IoT, fog and cloud computing in the smart city emergency management systems

There is no disagreement in collecting necessary information for fire detection from sensors, measurement devices, etc., using the Internet of Things (IoT) technology. However, there are alternative approaches in monitoring and generating alarms based on this data. Srividhya and Sankaranarayanan (2020) have noted various challenges regarding energy utilization and data transfer durability (Srividhya & Sankaranarayanan, 2020). In the event of any forest fire, there will be intense data traffic when the data obtained via WSN (sensors) is transmitted to Cloud computing. In the proposed system, the information collected from IoT sensors is transferred to a fog layer between the Cloud, distributing the load caused by the data, thereby ensuring smoother system operation. Similarly, Kaur et al. (2019) have emphasized the importance of fog computing for both energy efficiency and early detection of wildfires, asserting that fog computing is the most suitable system for processing and analyzing critical data with minimum bandwidth, reduced latency, and time-sensitive data processing (Kaur, Sood, & Bhatia, Cloud-assisted green IoT-enabled comprehensive framework for wildfire monitoring, 2019) (Kaur & Sood, A smart disaster management framework for wildfire detection and prediction, 2020).

With the acceleration of research in artificial intelligence and Internet of Things (IoT) technologies today, these technologies have been integrated into earthquake management and early warning systems. Systems utilizing machine learning technologies for the analysis of earthquake waves enable the detection of the onset of primary waves before the seismic and largest waves, the separation of waves causing noise from earthquake waves, distinguishing between noise and microearthquakes, or discerning earthquakes from quarry explosions (Abdalzaher, Elsayed, Fouda, & Salim, 2023).

Early warning systems for earthquakes primarily involve positioning sensors around the settlement area to cover distances of approximately 10 km from each other. There is an earthquake alarm center between the sensors and the settlement area, where data obtained through sensors is transmitted. The speed of the data collected through sensors is greater than the speed of the waves that generate earthquakes. Thus, the transfer of vibration data collected during an earthquake to the earthquake alarm system and subsequently warning the inhabitants of the settlement area is ensured. Even if the earthquake is predicted seconds or a minute in advance, it is believed that potential loss of life and property can be prevented (Strauss & Allen, 2016). On a larger scale, measures such as evacuating people from unsafe buildings, halting the operation of nuclear power plants, shutting down gas pipeline transmission, or slowing down or halting transportation lines

can be taken to prevent larger losses (Wu, Hsiao, Teng, & Shin, 2002) (Kumar, Mittal, Arora, & Sharma, 2022).

3 Proposed Smart City Model

In this study, a conceptual framework has been established for systems within smart city applications that contribute to preventive or mitigating effects during disasters.

Fig. 2 outlines the general principle of operation for these systems.

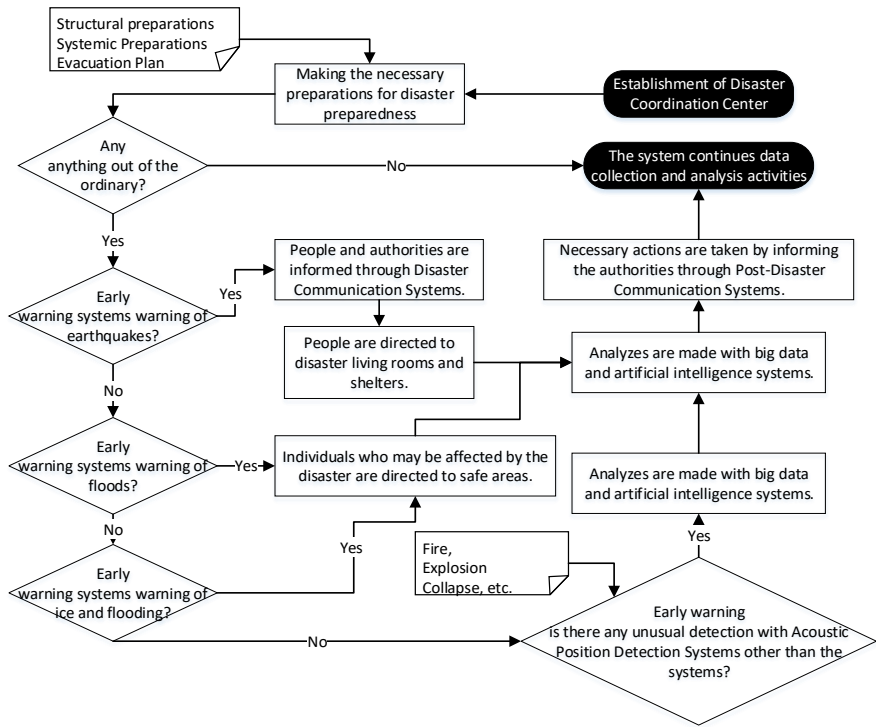


Fig. 2. Disaster management with smart city applications

The smart applications involved in this process provide advantages in minimizing economic, social, environmental, and health-related losses that may occur during or after a disaster. Since there are common gains among these applications, examinations have been generally conducted regarding these gains.

Economic Gains:

When implementing smart systems in disaster management, there are direct or indirect economic gains to be found. When examining the economic aspects of smart systems in disaster management, it is generally observed that the

following gains can be achieved (MEUCC, Icing and flood warning systems application, 2023) (MEUCC, Advanced earthquake warning application, 2023) (MEUCC, Advanced Flood Warning, 2023) (MEUCC, Fire Detection and Warning Systems, 2023) (MEUCC, Acoustic Detection and Location Determination, 2023) (MEUCC, Emergency Evacuation Plans, 2023) (MEUCC, Post-disaster communication systems, 2023) (MEUCC, Disaster coordination centers, 2023):

- Enhances coordination in disaster services.
- Ensures effective intervention in disasters by keeping communication channels open.
- Contributes to the acceleration of crisis management processes.
- Increases the effectiveness and efficiency of emergency response.
- Optimizes human resources and resource utilization.
- Enables the effective and efficient use of public resources.
- Reduces human and material losses in disaster areas.
- Reduces potential health expenditures and rehabilitation costs after disasters.
- Helps reduce traffic accidents by increasing road safety.
- Reduces fuel and time losses due to traffic.
- Lowers insurance costs.
- Increases the resilience of cities to disasters and ensures confidence in tourism and commercial activities.
- Minimizes workforce losses.
- Assists in maintaining the sustainability of businesses and minimizing financial losses.
- Contributes to reducing economic losses by reducing infrastructure damages and related public expenditures.
- Maintains economic stability and positively contributes to the national economy.

3.1 Governance and Social Gains

Apart from the economic gains achieved through the use of smart systems in disaster management, there are also social benefits for both communities and governments. These gains have positive effects on improving the quality of life for individuals in disaster-prone areas. It has been observed that smart systems in disaster management generally yield the following gains in terms of social and governance aspects (MEUCC, Icing and flood warning systems application, 2023) (MEUCC, Advanced earthquake warning application, 2023) (MEUCC, Advanced Flood Warning, 2023) (MEUCC, Fire Detection and Warning Systems, 2023) (MEUCC, Acoustic Detection and Location Determination, 2023) (MEUCC, Emergency Evacuation Plans, 2023) (MEUCC, Post-disaster communication systems, 2023) (MEUCC, Disaster coordination centers, 2023):

- It enhances transparency in disaster management and fosters a sense of solidarity within society.
- The governance capacity of public institutions increases.
- Collaboration among stakeholder organizations strengthens, leading to the development of common policies.
- It aids in raising awareness and consciousness within society regarding disaster management.
- It improves the efficiency of pre-disaster preparedness drills.
- It helps society to be better prepared for disasters.
- It increases the sense of security within the community.
- It ensures the continuity of communication and information flow.
- It prevents the formation of adverse psychological effects following disasters.
- It accelerates the return of society to normalcy after a disaster.
- Service quality improves thanks to information and communication technologies.
- It enables faster dissemination of information to the community during and after disasters.
- Social satisfaction with disaster management increases.
- Prompt intervention in emergencies minimizes loss of life.

- Swift and accurate intervention reduces injuries and property losses to a minimum

3.2Environmental Gains

Implementation of smart systems in disaster management can lead to environmental gains. Through the utilization of smart systems in disaster management, the following environmental benefits can generally be achieved (MEUCC, Icing and flood warning systems application, 2023) (MEUCC, Advanced earthquake warning application, 2023) (MEUCC, Advanced Flood Warning, 2023) (MEUCC, Fire Detection and Warning Systems, 2023) (MEUCC, Acoustic Detection and Location Determination, 2023) (MEUCC, Emergency Evacuation Plans, 2023) (MEUCC, Post-disaster communication systems, 2023) (MEUCC, Disaster coordination centers, 2023) :

- Prevention of environmental pollution resulting from the collapse of structures during disasters.
- Minimization of environmental damage through effective post-disaster waste management processes.
- Preservation of the natural environment through the efficient and effective use of resources required after disasters.
- Reduction of environmental impacts of disasters to preserve natural habitats.
- Contribution to the conservation of biodiversity by implementing protective measures for natural habitats and water sources.
- Preservation of the environment and natural habitats by taking necessary precautions in areas at risk of disasters through early warning systems.
- Facilitation of environmental risk monitoring.
- Minimization of environmental impacts using environmentally friendly communication technologies.
- Promotion of energy efficiency.
- Reduction of environmental impacts by minimizing energy and resource usage.
- Decrease in emission levels resulting from traffic post-fire or disaster.

- Assistance in environmentally friendly planning of areas prone to disaster risk.
- Contribution to the conservation of water sources.

3.3Health Gains

The implementation of smart systems in disaster management also brings direct or indirect gains in the health sector. These gains are outlined below (MEUCC, Icing and flood warning systems application, 2023) (MEUCC, Advanced earthquake warning application, 2023) (MEUCC, Advanced Flood Warning, 2023) (MEUCC, Fire Detection and Warning Systems, 2023) (MEUCC, Acoustic Detection and Location Determination, 2023) (MEUCC, Emergency Evacuation Plans, 2023) (MEUCC, Post-disaster communication systems, 2023) (MEUCC, Disaster coordination centers, 2023):

- Facilitates the rapid and efficient transmission of emergency calls.
- Enables the coordination of post-disaster health services.
- Facilitates the collection and analysis of data related to post-disaster health conditions.
- Assists in informing the public about post-disaster health risks.
- Facilitates the arrival of health teams to the disaster area and the provision of emergency medical interventions.
- Preserves human life by reducing casualties and property loss.
- Prevents damage to healthcare facilities and ensures uninterrupted provision of emergency medical services.
- Assists in the rapid delivery of drugs and medical supplies to the disaster area.
- Reduces panic and stress levels resulting from disasters, thereby positively impacting psychological health.
- Improves the quality of life for the community.
- Reduces the risk of spreading infectious diseases following a disaster.
- Helps mitigate the adverse effects of noise pollution.
- Assists in reducing the adverse effects of air pollution.

- Contributes to the improvement of service quality in the healthcare system by reducing healthcare expenditures and treatment costs.

4 Results/Conclusion

This study provides a detailed examination of eight smart systems deployed within the scope of smart cities and related to disaster management. Financially, the direct temporal returns on investments made in these systems are generally limited. However, the integration of smart system applications in disaster management holds the potential for multifaceted benefits across various domains. For instance, economically, these systems enhance coordination and optimize the effective and efficient use of resources, thereby reducing losses. From a social perspective, they facilitate collaboration among stakeholders by improving communication, thus enhancing community resilience to disasters. When examined from an environmental standpoint, smart systems contribute to pollution prevention, resource conservation, and sustainable urban planning. In terms of public health, they enable swift responses to emergencies, streamline healthcare services, and minimize health risks associated with disasters.

Overall, the adoption of smart systems in disaster management not only enhances preparedness and response efforts but also contributes to the general welfare and safety of communities. This study presents a pioneering effort in evaluating various smart systems that can be utilized in disaster management.

5. References

- Abdalzاهر, M., Elsayed, H., Fouda, M., & Salim, M. (2023). Employing Machine Learning and IoT for Earthquake Early Warning System in Smart Cities. *Energies*, 16(495), 1-22. doi:10.3390/en16010495
- Al-Hussein, A., Hamed, Y., Bouri, S., Hajji, S., Aljuaid, A. M., & Hachicha, W. (2023, December 13). The Socio-Economic effects of floods and ways to prevent them: a case study of the Khazir River Basin, northern Iraq. *Water*, 15(24), 4271. doi:10.3390/w15244271
- Ashok Kumar, V., Girish, B., & Rajesh, K. R. (2015, June). Integrated Weather and Flood Alerting System. *International Advanced Research Journal in Science, Engineering and Technology*, 2(6), 21-24. doi:10.17148/IARJSET.2015.2606
- Australia, W. (tarih yok). *In-depth: Australian bushfires*. March 13, 2024 tarihinde WWF Australia Web site: <https://wwf.org.au/what-we-do/australian-bushfires/in-depth-australian-bushfires/> adresinden alındı
- Başkanlığı, T. C. (2023). *2023 Kahramanmaraş and Hatay Earthquakes Report*. <https://www.sbb.gov.tr/wp-content/uploads/2023/03/2023-Kahramanmaraş-and-Hatay-Earthquakes-Report.pdf> adresinden alındı
- Bushnaq, O. M., Chaaban, A., & Al-Naffouri, T. Y. (2021). The role of UAV-IoT networks in future wildfire detection. *IEEE Internet of Things Journal*, 8(23), 16984-16999. doi:10.1109/jiot.2021.3077593
- DesRoches, R., Comerio, M. C., Eberhard, M. O., Mooney, W. D., & Rix, G. J. (2011, October 1). Overview of the 2010 Haiti earthquake. *Earthquake Spectra*, 27(1_suppl1), 1-21. doi:10.1193/1.3630129
- Dugdale, J., Moghaddam, M. T., & Muccini, H. (2021). IoT4Emergency. *ACM Sigsoft Software Engineering Notes*, 46(1), 33-36. doi:<https://doi.org/10.1145/3437479.3437489>
- Foundation, N. -N. (2005, May 19). *Analysis of the Sumatra-Andaman earthquake reveals longest fault rupture ever*. March 13, 2004 tarihinde NSF - National Science Foundation Web site: https://www.nsf.gov/news/news_summ.jsp?cntn_id=104179 adresinden alındı
- Guardian. (2022, July 13). *After the floods: Germany's Ahr valley then and now – in pictures*. March 13, 2024 tarihinde The Guardian website: <https://www.theguardian.com/world/2022/jul/13/floods-then-and-now-photographs-germany-ahr-valley-flooding-disaster-july-2021#:~:text=The%20dramatic%20floods%20of,worst%20hit%20by%20the%20flooding.> adresinden alındı
- Hernandez-Nolasco, J. A., Ovando, M. A., Acosta, F., & Pancardo, P. (2016, March 1). Water level meter for alerting population about floods. *2016 IEEE 30th International Conference on Advanced Information Networking and Applications*, 879-884. doi:10.1109/aina.2016.76

- Kaur, H., & Sood, S. K. (2020, January 6). A smart disaster management framework for wildfire detection and prediction. *The Computer Journal*, 63(11), 1644-1657. doi:10.1093/comjnl/bxz091
- Kaur, H., Sood, S. K., & Bhatia, M. (2019). Cloud-assisted green IoT-enabled comprehensive framework for wildfire monitoring. *Cluster Computing*, 23(2), 1149-1162. doi:10.1007/s10586-019-02981-7
- Kumar, R., Mittal, H., Arora, S., & Sharma, B. (2022, August). Earthquake Genesis and Earthquake Early Warning Systems: Challenges and a Way Forward. *Surveys in Geophysics*, 43(2), 1143-1168. doi:10.1007/s10712-022-09710-7
- MEUCC. (2023). Acoustic Detection and Location Determination. Ankara: Ministry of Environment, Urbanization and Climate Change, General Directorate of GIS. 2023 tarihinde <https://www.akillisehirler.gov.tr/wp-content/uploads/fizibilite-rapor/8-Akustik%20Alg%C4%B1lama%20ve%20Konum%20Tespiti.pdf> adresinden alındı
- MEUCC. (2023). Advanced earthquake warning application. Ankara: Ministry of Environment, Urbanization and Climate Change, General Directorate of GIS. <https://www.akillisehirler.gov.tr/wp-content/uploads/fizibilite-rapor/13-%C4%B0leri%20Deprem%20Uyar%C4%B1s%C4%B1.pdf> adresinden alındı
- MEUCC. (2023). Advanced Flood Warning. Ankara: Ministry of Environment, Urbanization and Climate Change, General Directorate of GIS. <https://www.akillisehirler.gov.tr/wp-content/uploads/fizibilite-rapor/13-%C4%B0leri%20Deprem%20Uyar%C4%B1s%C4%B1.pdf> adresinden alındı
- MEUCC. (2023). Disaster coordination centers. Ankara: Ministry of Environment, Urbanization and Climate Change, General Directorate of GIS. doi:<https://www.akillisehirler.gov.tr/wp-content/uploads/fizibilite-rapor/2-Afet%20Koordinasyon%20Merkezi.pdf>
- MEUCC. (2023). Emergency Evacuation Plans. Ankara: Ministry of Environment, Urbanization and Climate Change, General Directorate of GIS. <https://www.akillisehirler.gov.tr/wp-content/uploads/fizibilite-rapor/1-%20Acil%20Durum%20Tahliye%20Planlar%C4%B1.pdf> adresinden alındı
- MEUCC. (2023). Fire Detection and Warning Systems. Ankara: Ministry of Environment, Urbanization and Climate Change, General Directorate of GIS. <https://www.akillisehirler.gov.tr/wp-content/uploads/fizibilite-rapor/17-Yang%C4%B1n%20Alg%C4%B1lama%20ve%20Uyarma%20Sistemleri.pdf> adresinden alındı
- MEUCC. (2023). Icing and flood warning systems application. Ankara: Ministry of Environment, Urbanization and Climate Change, General Directorate of GIS. <https://www.akillisehirler.gov.tr/wp-content/uploads/fizibilite-rapor/9-Buzlanma%20ve%20Ta%C5%9Fk%C4%B1n%20Uyar%C4%B1%20Sistemleri.pdf> adresinden alındı

- MEUCC. (2023). Post-disaster communication systems. Ankara: Ministry of Environment, Urbanization and Climate Change, General Directorate of GIS. <https://www.akillisehirler.gov.tr/wp-content/uploads/fizibilite-rapor/1-%20Acil%20Durum%20Tahliye%20Planlar%C4%B1.pdf> adresinden alındı
- MEUCC. (2023). Post-disaster communication systems. Ankara: Ministry of Environment, Urbanization and Climate Change, General Directorate of GIS. <https://www.akillisehirler.gov.tr/wp-content/uploads/fizibilite-rapor/3-Afet%20Sonras%C4%B1%20%C4%B0leti%C5%9Fim%20Sistemleri.pdf> adresinden alındı
- Mussa, M. (2023, August 22). *Deprem bölgesinde fatura borçlarının silinmesi için süre uzatıldı*. March 13, 2024 tarihinde Milat Gazetesi Web site: <https://www.milatgazetesi.com/haber/deprem-bolgesinde-fatura-borclarinin-silinmesi-icin-sure-uzatildi-4201/> adresinden alındı
- News, C. (2019, July 16). *Monsoon season 2019: Floods in India, Nepal, Pakistan and Bangladesh leave death toll over 150 today*. March 13, 2024 tarihinde CBS News: <https://www.cbsnews.com/news/monsoon-season-2019-floods-india-nepal-pakistan-bangladesh-death-toll-rhinos-today-2019-07-16/> adresinden alındı
- Ray, P. P., Mukherjee, M., & Shu, L. (2017, January 1). Internet of Things for Disaster Management: State-of-the-Art and Prospects. *IEEE Access*, 5, 18818-18835. doi:10.1109/access.2017.2752174
- Satake, K. (2014, November 13). Advances in earthquake and tsunami sciences and disaster risk reduction since the 2004 Indian ocean tsunami. *Geoscience Letters*, 1(1). doi:10.1186/s40562-014-0015-7
- Shahparvari, S., Abbasi, B., Chhetri, P., & Abareshi, A. (2019). Fleet routing and scheduling in bushfire emergency evacuation: A regional case study of the Black Saturday bushfires in Australia. *Transportation Research Part D: Transport and Environment*, 67, 703-722. doi:10.1016/j.trd.2016.11.015
- Srividhya, S., & Sankaranarayanan, S. (2020). IOT–FOG enabled framework for Forest Fire Management System. *2020 Fourth World Conference on Smart Trends in Systems, Security and Sustainability (WorldS4)*. doi:10.1109/worlds450073.2020.9210328
- Strauss, J., & Allen, R. (2016). Benefits and costs of earthquake early warning. *Seismological Research Letters*, 87(3), 765-772. doi:10.1785/0220150149
- Survey, U. G. (2012, December 13). *Where do earthquakes occur?* March 13, 2024 tarihinde U.S. Geological Survey Web Site: <https://www.usgs.gov/faqs/where-do-earthquakes-occur#:~:text=The%20world's%20greatest%20earthquake%20belt,our%20planet's%20largest%20earthquakes%20occur.> adresinden alındı
- Survey, U. G. (2013, September 26). *What is an earthquake and what causes them to happen?* / U.S. Geological Survey. March 12, 2024 tarihinde

<https://www.usgs.gov/faqs/what-earthquake-and-what-causes-them-happen#:~:text=The%20tectonic%20plates%20are%20always,the%20shaking%20that%20we%20feel>. adresinden alındı

Wu, Y. M., Hsiao, N. C., Teng, T. L., & Shin, T. C. (2002). Near Real-Time Seismic Damage Assessment of the Rapid Reporting System. *Terrestrial, Atmospheric and Oceanic Sciences Journal*, 13(3), 313-324.
doi:10.3319/TAO.2002.13.3.313(CCE)



CHAPTER 21

Evaluation of Biomass Potential Based on Animal Waste in Turkey

Yağmur Arıkan Yıldız¹

¹ Assistant Prof., Sivas Science and Technology University, <https://orcid.org/0000-0003-0947-2832>

Introduction

Energy is one of the most important parameters that determines the standard of living, directs country policies and ensures progress in the level of development of the country when viewed from an economic and social perspective. The world population growth, industrial and technological developments are the most important reasons for the increase in energy demand. According to the report prepared by the International Energy Agency, world energy consumption increased by 2.5% in 2023 and reached 620 exajoules (EJ), and this demand is expected to increase by 4% in 2025. In addition, this demand is expected to increase by 8% in India, 6% in China, 3% in the USA and 1.7% in the European Union countries IEA (2024).

When we look at the energy situation in terms of Turkey, in 2023, electric energy consumption increased by 1.2% compared to the previous year and totaled 335.2 TWh, while electricity generation increased by 0.8% compared to the previous year and totaled 331.1 TWh. As of the end of October 2024, the installed capacity of our country reached 114,599 MW. In 2023, the distribution of our electricity generation by sources is shown in Figure 1. In 2023, 36.2% of our electricity generation was obtained from coal, 21.2% from natural gas, 19.3% from hydraulic energy, 10.3% from wind energy, 6.7% from solar energy, 3.4% from geothermal energy and the rest from other sources(Republic of Turkey Ministry of Foreign Affairs, 2024)

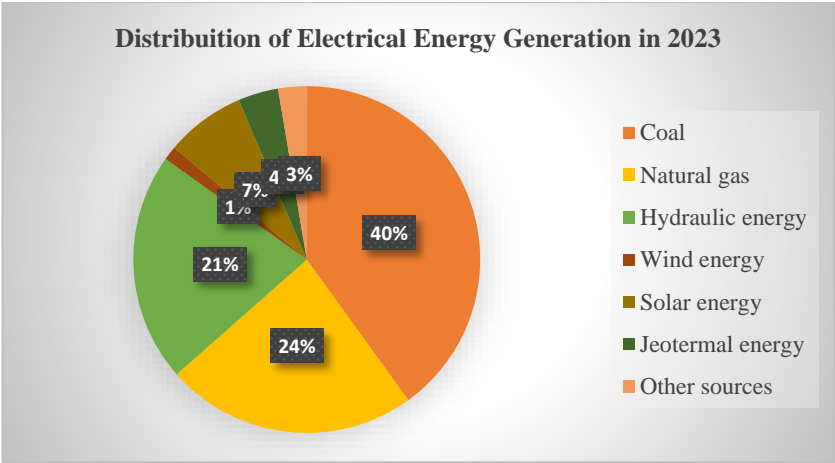


Figure 1. Distribution of electricity generation by sources in Turkey in 2023

The share of biomass energy in electricity production is among other sources and is quite low. The installed power potential of biomass and wastewater from 2011 to 2022 is given in Figure 2 and the potential has been increasing in recent

years. However, considering that Turkey is a country rich in agriculture and animal husbandry and has an abundant forest structure, it is known that this potential has not yet been used (Republic of Turkey Energy Ministry and Natural Sciences, 2023)

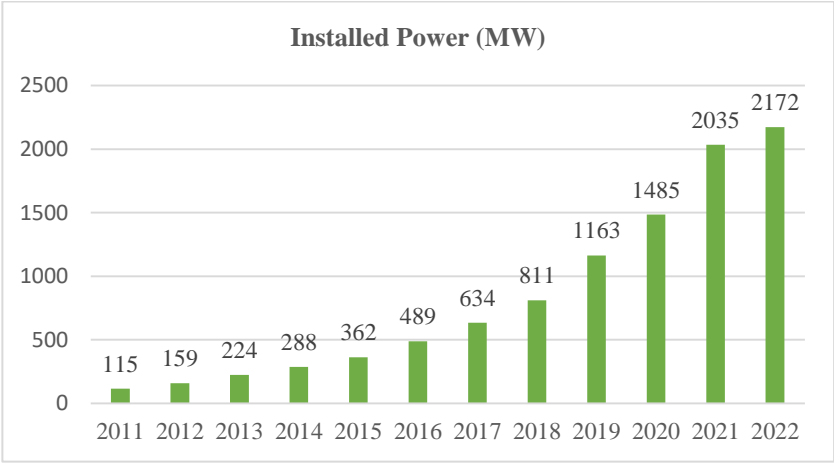


Figure 2. Biomass installed capacity in turkey by years

Biomass energy needs to be developed both in the world and in Turkey, and it is the focus of attention of researchers and investors because its potential is not fully utilized. Some examples of studies conducted on this subject are given.

Lauri et al. (2014) investigated the potential of wood in the world and some regions and stated that biomass obtained from this potential could meet 2-18% of the world's primary energy consumption in 2050. Toklu(2017) investigated different biomass resources that can be used in Turkey and their biomass energy potential. The total biomass energy potential in Turkey was stated as approximately 33 million tons of oil equivalent (Mtoe). Avcioğlu et al. (2019)investigated the biomass potential that can be obtained from agricultural residues in Turkey and reported an energy potential of 298.955 TJ from field crops and 65.491 TJ from horticultural crops. Irfan et al.(2020) investigated the use of agricultural waste, animal waste and municipal solid waste as biomass energy for Pakistan and stated that the percentage of use of this energy will increase in the coming years in line with the country's targets. Jekayinfa et al. (2020)emphasized the continuously increasing energy demand in Nigeria, one of the developing countries, and stated that the country does not have sufficient supply to meet this demand. In order to meet this supply, they found that the biomass energy potential that can be obtained from agricultural residues and animal residues in the region is 2.33 EJ. Benti et al.(2021) mentioned the

difficulty of access to sustainable energy sources in Ethiopia and stated that only 0.58% of the biomass potential in the country is utilized. They investigated the utilizable biomass resource potential and utilization methods. Antar et al. (2021) carried out a general review of biomass production and utilization in the world. They also presented possible approaches to increase biomass production. Júnior et al. (2023) calculated the biomass potential that could be obtained from forest residues, agricultural residues and residues from urban processes in North-eastern Brazil and stated that this potential could cover 4% of the energy demand of the region. Nehra et al. (2023) investigated the biomass potential from animal manure for rural Haryana, India and found that if this potential is utilized, an estimated saving of 1707.08 to 3583.73 million kg/year can be achieved.

In this paper, in order to investigate the biomass potential that Turkey can obtain from animal manure, the number of animals has been investigated and the amount of fertilizer that can be obtained from them has been found. The biomass energy potential to be obtained from these fertilizers and the installed power values of the facilities to use this potential have been calculated. The necessary economic analyses have been carried out for the establishment of these facilities and the positive contributions of the biomass energy to the environment have been emphasized.

Biomass Energy

The fuel obtained from biological sources is called biogas, and the type of renewable energy obtained is called biomass. Biogas which is colourless, odourless and lighter than air gas, contains high concentrations of methane (CH₄), carbon dioxide (CO₂) and low concentrations of hydrogen, nitrogen, and water vapor. When biogas gas is compared to other energy sources, 1 m³ biogas is equivalent to 0.60 m³ natural gas, 0.70 litres of gasoline, 0.65 litres of diesel fuel and 0.80 kg of coke (Yılmaz et al. 2017).

Biomass energy is any organic material that stores sunlight in the form of chemical energy. Biomass sources vary and can include agricultural waste, animal waste, industrial waste, municipal waste and garbage waste. Electricity, heat and fuel production can be achieved with biomass resources, and this can be achieved through different technological means. The resources selected for energy production can be converted into a desired energy form and then into electricity through thermo-chemical or bio-chemical conversion methods. The different processes used to obtain energy from biomass sources are summarized in Figure 3. (Bridgwater, 2006)

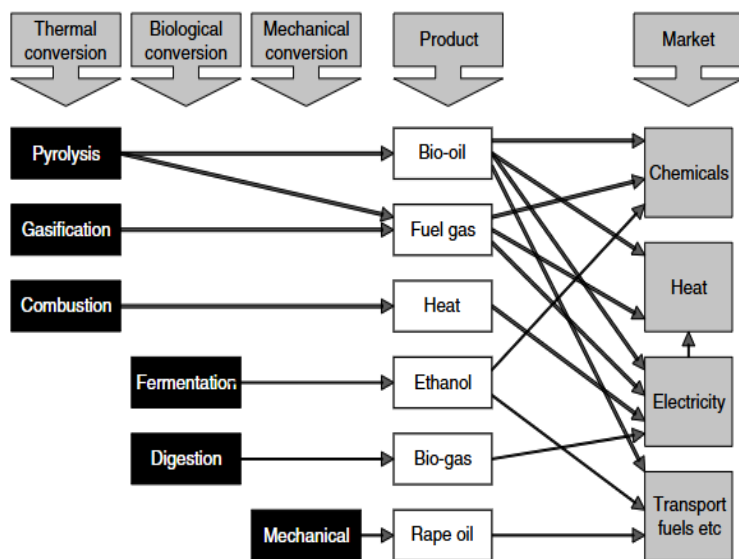


Figure 3. Different process for obtain biomass energy

In biomass energy obtained from animals, methane gas in animal manure is released during the anaerobic decay of organic matter. The more animal manure, the more organic matter it contains, and therefore the more methane emissions, and therefore the more biomass that can be obtained.

The formation stages of biomass obtained from animals are given in Figure 4 and explained below (Mignogna et al., 2023)

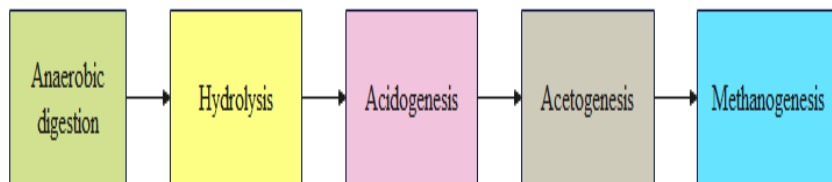


Figure 4. The formation process of biogas

Anaerobic Digestion and Hydrolysis: Organic wastes such as cellulose, starch, oil, protein, etc. are converted into simple organic substances such as sugars, amino acids, fatty acids.

Acidogenesis: Molecules formed as a result of hydrolysis are converted into volatile fatty acids such as acetic acid and butyric acid.

Acetogenesis: Acetonic bacterial groups convert free fatty acids into acetate, CO₂ and hydrogen.

Methanogenesis: Methane-forming bacteria use acetic acid, carbon dioxide, and hydrogen to create methane and carbon dioxide.

Material and Method

One of the biggest biogas production potentials in the world is animal waste. Turkey has a suitable environment and potential for all kinds of animal husbandry due to its geographical features. Cattle and sheep breeding has been continued from past to present, and there has been a significant increase in the number of facilities since the 2000s. The number of animals in Turkey for 2022 is given in Table 1 according to different categories (Gülaç, n.d.; TIGEM, 2023)

Table 1. Number of animals in Turkey for 2022

Cattle	16852000
Sheep	44688000
Goat	11578000
Laying hens chicken	109806000
Broiler chicken	251290000
Goose	1386000
Turkey	3670000
Duck	433000

The amount of manure obtained from cattle, sheep, goat and laying hens is given in Equation 1. The amount of energy production obtained from laying hens, geese, turkeys and ducks can be found from Equations 2-5, respectively(Yağlı et al., 2019).

$$T_{AWM\ (1)} = \frac{\sum_{i=1}^N q*365}{1000} \tag{1}$$

$$T_{AWM\ (2)} = \frac{\sum_{i=1}^N q*42}{1000} \tag{2}$$

$$T_{AWM\ (3)} = \frac{\sum_{i=1}^N q*98}{1000} \tag{3}$$

$$T_{AWM\ (4)} = \frac{\sum_{i=1}^N q*110}{1000} \tag{4}$$

$$T_{AWM\ (5)} = \frac{\sum_{i=1}^N q*65}{1000} \tag{5}$$

where N , T_{AWM} and q represent the number of animals, total amount of annual wet manure, the average amount of manure per animal, respectively. The amount of wet manure varies as the animals stay in the shelter. Accordingly, the amount of usable wet manure obtained from the animals is calculated with Equation 6 (Yağlı et al., 2019)

$$T_{AUWM} = T_{AWM} * r_f \quad (6)$$

where T_{AUWM} is the total amount of usable wet manure and r_f is the rate of usable. The solid matter ratio in the usable wet manure and the volatile solid matter ratio within this ratio are calculated with Equations 7 and 8, respectively. The amount of methane gas that can be obtained from the volatile solid matter ratio is found with Equation 9 (Yağlı et al., 2019) .

$$T_{sm} = T_{AUWM} * r_{sm} \quad (7)$$

$$T_{vsm} = T_{sm} * r_{vsm} \quad (8)$$

$$T_{CH_4} = T_{vsm} * \mu \quad (9)$$

The energy value of biogas with 60% methane content is taken as 22.7 MJ/Nm³ and accordingly the energy value of methane gas is taken as 36 MJ/Nm³, and the total annual energy amount of biogas produced from animals can be calculated. The energy that can be produced from methane gas can be found with the help of Equation 10. The electrical energy to be obtained as a result of burning methane gas in an electric motor can be found with the help of Equation 11 (Yağlı et al., 2019).

$$Q = T_{CH_4} * h_{CH_4} \quad (10)$$

$$E_g = T_{CH_4} * e_{CH_4} * \eta_c \quad (11)$$

where Q is the amount of energy that can be produced from methane, h is the value of methane gas. e_{CH_4} is the energy equivalent of 1 m³ methane and is equal to 10 kWh. η_c is the electricity conversion coefficient. η_c value varies between 25% and 40% depending on the power generation plant. The coefficients used for the above equations are given in Table 2 (Yağlı et al., 2019)

Table 2. Coefficients used in calculating energy from animal manure

Animal type	q (kg)	rf (%)	r_{rsm} (%)	r_{vsm} (%)	μ (Nm ³)
Cattle	29	100	12.41	84.65	0.33
Sheep	2.40	13	23.00	83.63	0.30
Goat	2.05	13	23.17	73.06	0.30
Laying hens chicken	0.13	99	18.75	75.00	0.35
Broiler chicken	0.19	66	20	77.278	0.35
Goose	0.33	68	17.27	61.28	0.35
Turkey	0.38	68	19.36	75.83	0.35
Duck	0.33	68	17.27	61.28	0.35

After calculating the amount of biomass energy, the calculation of the installed power facility that can be established, the cost value of this facility and the payback period required for the investment that can be made can be calculated with Equations 12-14, respectively(Masala et al., 2022)

$$P_{ins} = \frac{E_g}{t} \tag{12}$$

$$C_T = P_{ins} * u_p \tag{13}$$

$$n = \frac{C_T}{netcash} \tag{14}$$

where P_{ins} , E_g and t are the installed power of biomass, the amount of biomass energy and time, respectively. C_T and u_p represent the total cost of biomass plant unit price of biomass plant. n is the payback period and net cash is annual net cash inflow.

Finally, in order to show the positive contribution of the biomass energy obtained in the study to the environment, it will be shown how much carbon dioxide gas emissions will be reduced by the generated biomass energy. This is found with the help of Equation 15(World Bank, 2024)

$$T_{ghg-r} = E_g * \eta_{ghg} \tag{15}$$

where T_{ghg-r} the total amount of greenhouse gas reduction (GHG), η_{ghg} is the greenhouse gas conversion coefficient.

Results and Discussion

The methane gas value and the electrical energy that can be produced depending on the number of animals in Turkey and the amount of manure obtained from them are given in Table 3. In the calculations, the efficiency of the power plant engine has been accepted as 0.35.

Table 3. The amount of CH₄, energy generation results for 2022

Animal type	CH ₄ (km ³)	Eg (GWh)
Cattle	6183793.8	21643.28
Sheep	293663.3	1027.8
Goat	57194.0	200.179
Laying hens chicken	253879.8	888.58
Broiler chicken	71593.89	250.58
Goose	1128.99	3.95
Turkey	5360.0	18.76
Duck	234.0	0.819

According to Table 3, the amount of biomass energy that can be obtained from animal waste for 2022 is 24033.948 GWh. Considering that Turkey's electricity consumption was 335.2 TWh that year, approximately 7% of the energy need can be met from animal waste.

For the biomass energy that can be obtained from animal manure in Turkey, considering that the facilities operate for an average of 8000 hours a year, the facilities should have an installed capacity of 3GW. The cost value of a 1 kW plant is 3600 Euro in current figures, and the Euro-TL exchange rate is taken as 36 TL in the calculations (Eastern Mediterranean Development Agency, 2020) In addition, in 2024, the sales price of 1 kWh biomass energy has been taken as 3.00 TL considering the night support. Finally, the net greenhouse gas reduction amount has been calculated to determine the contribution of the generated energy to the environment. In 2024, the greenhouse gas reduction value of 1 MWh biomass energy is taken as 0.689 tCO₂ (World Bank, 2024) Accordingly, the installed power value, cost value, net-cash, payback period and net greenhouse gas reduction amount of the system to be installed are given in Table 4.

Table 4. The results of economic analysis

Installed power	3 GW
Total cost	388800 million TL
Net cash in a year	72101.844 million TL
Payback period	5.4 year
the total amount of greenhouse gas reduction	16 MtonCO ₂

Conclusion

In this study, the potential of biomass energy that can be obtained from animal manure in Turkey has been investigated and its economic and environmental evaluation has been made. In the study conducted using the number of animals in Turkey in 2022, 24033.948 GWh of electricity can be produced annually. In order to achieve this production, facilities with an installed capacity of approximately 3 GW need to be established and an investment of 388800 million TL is required. The annual profit amount of the biomass energy obtained is 72101.844 TL and the total investment can amortize itself in 5.4 years. In addition, thanks to the biomass energy obtained, a 16 MtonCO₂ reduction is achieved, making a great contribution to the sustainable environment.

References

- Antar, M., Lyu, D., Nazari, M., Shah, A., Zhou, X., & Smith, D. L. (2021). Biomass for a sustainable bioeconomy: An overview of world biomass production and utilization. In *Renewable and Sustainable Energy Reviews* (Vol. 139). Elsevier Ltd. <https://doi.org/10.1016/j.rser.2020.110691>
- Avcıoğlu, A. O., Dayıoğlu, M. A., & Türker, U. (2019). Assessment of the energy potential of agricultural biomass residues in Turkey. *Renewable Energy*, 138, 610–619. <https://doi.org/10.1016/j.renene.2019.01.053>
- Benti, N. E., Gurmesa, G. S., Argaw, T., Aneseyee, A. B., Gunta, S., Kassahun, G. B., Aga, G. S., & Asfaw, A. A. (2021). The current status, challenges and prospects of using biomass energy in Ethiopia. In *Biotechnology for Biofuels* (Vol. 14, Issue 1). BioMed Central Ltd. <https://doi.org/10.1186/s13068-021-02060-3>
- Bridgwater, T. (2006). Biomass for energy. In *Journal of the Science of Food and Agriculture* (Vol. 86, Issue 12, pp. 1755–1768). <https://doi.org/10.1002/jsfa.2605>
- Eastern Mediterranean Development Agency. (2020). *Feasibility report for establishing biogas facilities in Kahramanmaraş province*. <https://www.dogaka.gov.tr/assets/upload/dosyalar/19-4-kahramanmaras-ilinde-biyogaz-tesisleri-kurulmasina-yonelik-fizibilite-raporu.pdf>
- Gülaç, Z. N. (n.d.). *Status and Forecast Poultry 023*. Retrieved December 6, 2024, from <https://arastirma.tarimorman.gov.tr/tepge/Belgeler/PDF%20Durum-Tahmin%20Raporlar%C4%B1/2023%20Durum-Tahmin%20Raporlar%C4%B1/K%C3%BCmes%20Hayvanc%C4%B1%C4%B1%C4%9F%C4%B1%20Durum%20Tahmin%20Raporu%202023-381%20TEPGE.pdf>
- IEA. (2024). *World Energy Outlook 2023*. <https://www.iea.org/reports/world-energy-outlook-2023>.
- Irfan, M., Zhao, Z. Y., Panjwani, M. K., Mangi, F. H., Li, H., Jan, A., Ahmad, M., & Rehman, A. (2020). Assessing the energy dynamics of Pakistan: Prospects of biomass energy. *Energy Reports*, 6, 80–93. <https://doi.org/10.1016/j.egyr.2019.11.161>
- Jekayinfa, S. O., Orisaleye, J. I., & Pecenka, R. (2020). An assessment of potential resources for biomass energy in Nigeria. In *Resources* (Vol. 9, Issue 8). MDPI AG. <https://doi.org/10.3390/resources9080092>
- Lauri, P., Havlík, P., Kindermann, G., Forsell, N., Böttcher, H., & Obersteiner, M. (2014). Woody biomass energy potential in 2050. *Energy Policy*, 66, 19–31. <https://doi.org/10.1016/j.enpol.2013.11.033>

- Masala, F., Groppi, D., Nastasi, B., Piras, G., & Astiaso Garcia, D. (2022). Techno-economic analysis of biogas production and use scenarios in a small island energy system. *Energy*, 258. <https://doi.org/10.1016/j.energy.2022.124831>
- Mignogna, D., Ceci, P., Cafaro, C., Corazzi, G., & Avino, P. (2023). Production of Biogas and Biomethane as Renewable Energy Sources: A Review. In *Applied Sciences (Switzerland)* (Vol. 13, Issue 18). Multidisciplinary Digital Publishing Institute (MDPI). <https://doi.org/10.3390/app131810219>
- Nehra, M., & Jain, S. (2023). Estimation of renewable biogas energy potential from livestock manure: A case study of India. *Bioresource Technology Reports*, 22. <https://doi.org/10.1016/j.biteb.2023.101432>
- Republic of Turkey Ministry of Foreign Affairs. (2024). *Türkiye's International Energy Strategy*. <https://www.mfa.gov.tr/turkeys-energy-strategy.en.mfa>
- Santos Júnior, E. P., Silva, E. G. M., Sousa, M. H. de, Dutra, E. D., Silva, A. S. A. da, Sales, A. T., Sampaio, E. V. de S. B., Coelho Junior, L. M., & Menezes, R. S. C. (2023). Potentialities and Impacts of Biomass Energy in the Brazilian Northeast Region. *Energies*, 16(9). <https://doi.org/10.3390/en16093903>
- TIGEM. (2023). *Livestock sector in 2023*. <https://www.tigem.gov.tr/Folder/CarouselDosyasi/d722366d-7a4d-4929-ab06-10bc2614778e.pdf>
- Toklu, E. (2017). Biomass energy potential and utilization in Turkey. *Renewable Energy*, 107, 235–244. <https://doi.org/10.1016/j.renene.2017.02.008>
- World Bank. (2024). *State and Trends of Carbon Pricing 2024*. <http://hdl.handle.net/10986/41544>
- Yağlı, H., Koç, Y., Üniversitesi, İ. T., Ve Doğa, M., Fakültesi, B., & Bölümü, M. M. (2019). Hayvan Gübresinden Biyogaz Üretim Potansiyelinin Belirlenmesi: Adana İli Örnek Hesaplama. In *Eylül 2019 Çukurova University Journal of the Faculty of Engineering and Architecture* (Vol. 34, Issue 3).
- Yılmaz, A., Ünvar, S., Koca, T., & Koçer, A. (2017). Türkiye’de Biyogaz Üretimi ve Biyogaz Üretimi İstatistik Bilgileri. *NWSA Academic Journals*, 12(4), 218–232. <https://doi.org/10.12739/nwsa.2017.12.4.2a0129>



CHAPTER 22

Optimal Sizing of Pv-Wind-Battery Hybrid System Using Genetic Algorithm

Özge Pınar Akkaş¹

¹ Asst. Prof. Dr. , Kırıkkale University, Faculty of Engineering and Natural, Sciences, <https://orcid.org/0000-0001-5704-4678>

1. INTRODUCTION

Growing concerns regarding the depletion of fossil fuels, the acceleration of climate change, and the environmental damage caused by conventional energy sources have heightened the demand for clean, sustainable, and renewable energy solutions. Hybrid Renewable Energy Systems (HRES) offer a promising solution to address these concerns faced by developing countries. Research on HRES primarily focuses on overcoming the issues related to optimal sizing of system components in line with load demand. To achieve feasibility and minimize capital costs, capacity determination must be carried out using effective design methods before the system's installation (Moghaddam et al., 2019; Khan, Pal, & Saeed, 2018; Rajabi-Ghahnavieh & Nowdeh, 2014). Optimum sizing is the process of defining the number of system components necessary to meet load requirements while minimizing the overall system cost, with optimization techniques playing a crucial role in this process (Maleki & Pourfayaz, 2015).

In recent years, there has been a growing focus on the optimal design of hybrid systems utilizing sustainable energy resources, with multiple techniques being employed to identify the most efficient system configuration. Koholè, Y. W., Fohagui, F. C. V., Ngouleu, C. A. W., and Tchuen, G. (2024) have designed and optimized a HRES (Photovoltaic(PV)/Wind/Battery/Diesel) for a household, multimedia, and healthcare center in Kaele, Cameroon, using four meta-heuristic algorithms: Colliding Bodies Optimization, Charged System Search, Teaching-Learning-Based Optimization, and Water Evaporation Optimization to determine the optimal configuration. Maleki, A., and Askarzadeh, A. (2014) have conducted a comparative study on the optimal sizing of a hydrogen-based stand-alone photovoltaic/wind hybrid system. The study employs four heuristic algorithms: Particle Swarm Optimization (PSO), Tabu Search (TS), Simulated Annealing (SA), and Harmony Search (HS) to minimize total annual cost and ensure continuous load demand satisfaction. Rodríguez-Gallegos, C. D., Yang, D., Gandhi, O., Bieri, M., Reindl, T., and Panda, S. K. (2018) have proposed a multi-objective optimization approach for the sizing and placement of PV panels and batteries in off-grid systems powered by diesel generators. The study aims to minimize the levelized cost of electricity (LCOE), emissions and total grid voltage deviations using the Non-Dominated Sorting Genetic Algorithm III (NSGA-III). The approach incorporates robust design to account for worst-case weather scenarios, offering a comprehensive solution for sustainable energy system design. Al Afif, R., Ayed, Y., and Maaitah, O. N. (2023) have conducted a feasibility and optimal sizing analysis of hybrid renewable energy systems for Al-Karak, Jordan. The

study evaluates the performance of a hybrid PV/Wind/Battery system using HOMER software to minimize cost and ensure energy reliability under varying load conditions. Wankouo Ngouleu, C. A., Koholé, Y. W., Fohagui, F. C. V., and Tchuen, G. (2023) have performed a techno-economic analysis and optimal sizing of a standalone photovoltaic/wind hybrid system for rural electrification in Cameroon. The study employs meta-heuristic techniques to compare battery-based and hydrogen-based storage systems, aiming to minimize costs and maximize system efficiency. Montoya, O. D., Grisales-Noreña, L. F., Gil-González, W., Alcalá, G., and Hernandez-Escobedo, Q. (2020) have developed a mixed-integer nonlinear programming (MINLP) model to optimize the location and sizing of PV sources in DC networks. The study aims to minimize greenhouse gas emissions from diesel generators, using an artificial neural network (ANN) for solar power forecasting and the GAMS package with the CONOPT solver to achieve optimal system configuration. Zhang, G., Shi, Y., Maleki, A., and Rosen, M. A. (2020) have proposed an efficient heuristic approach to determine the optimal location and size of a grid-independent solar/hydrogen system for rural areas. The study focuses on minimizing system costs and ensuring energy reliability, utilizing a hybrid optimization algorithm to achieve optimal system configuration. Konchou, F. A. T., Temene, H. D., Tchinda, R., and Njomo, D. (2021) have designed and optimized a hybrid renewable energy system for a community multimedia center in Makenene, Cameroon. The study employs a multi-objective Particle Swarm Optimization (PSO) algorithm to determine the optimal configuration of a PV/Wind/Battery/Diesel system, focusing on minimizing the LPSP, Cost of Electricity (COE), NPC, and total greenhouse gas emissions (TGE). Marsa, N., Houcine, L., Zaafour, A., and Chaari, A. (2021) have proposed an optimal sizing methodology for a stand-alone PV/wind hybrid system using the BAT algorithm. The study aims to minimize the annualized cost of the system (ACS) while ensuring power balance, comparing the BAT algorithm's performance with Homer and PSO methods.

In this study, three distinct hybrid energy system configurations—PV-Battery, Wind-Battery, and PV-Wind-Battery—have been developed and the optimal sizing of components for each configuration has been determined while considering the NPS and LPSP constraints. To achieve this, the GA optimization approach has been implemented using MATLAB. The performance and outcomes of the three systems have been analyzed and compared based on the obtained results

1. Modeling of Hybrid Energy System

The model of the hybrid energy system comprises PV panels, wind turbines, and battery banks. The schematic representation of the system is illustrated in Figure 1.

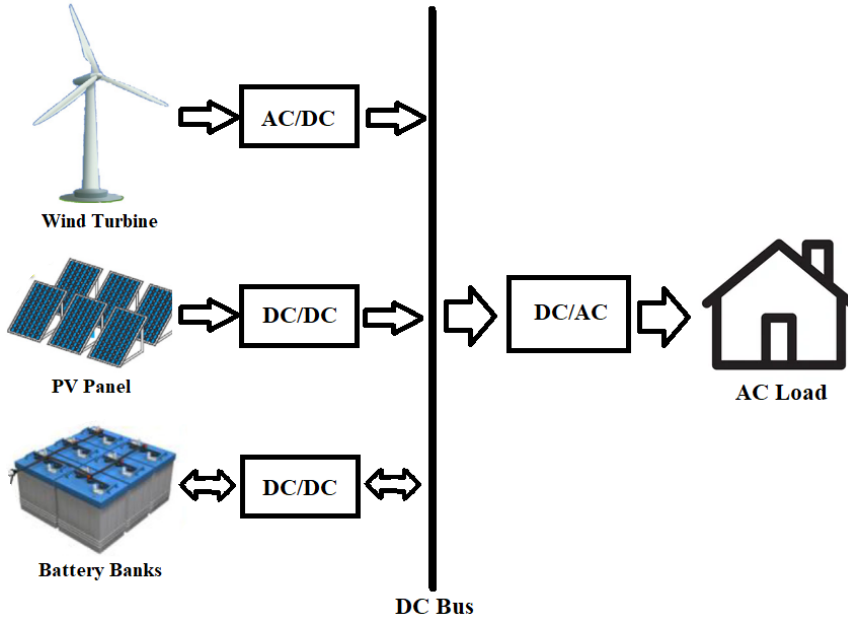


Figure 1. Schematic representation of the PV-Wind-Battery Hybrid System

1.1. Mathematical Models of System Components

The mathematical modeling of the components in the hybrid system is explained below.

1.1.1. Photovoltaic System (PVS)

PV solar panels utilize the photovoltaic effect to convert solar energy into electrical power. The output power of the PV system is expressed by Equation 1 (Wankou Ngouleu et al. (2023)).

$$P_{PVS}(t) = N_{PVS} \times P_{rt,PV} \times \eta_{PVS} \times \left(\frac{G_{SR}(t)}{G_{ref,SR}} \right) \times [1 + \beta(T_{cell}(t) - T_{ref,temp})] \quad (1)$$

In Equation 1, $P_{PVS}(t)$ (kW) represents the total power output generated by the solar panels at hour t , N_{PVS} denotes the number of solar panels, $P_{rt,PV}$ (kW) refers to the rated power of a single solar panel under standard reference conditions,

η_{PVS} indicates the efficiency of the PV panel, $G_{SR}(t)$ (W/m^2) represents the solar radiation at hour t , $G_{ref,SR}$ is the reference solar radiation (typically $G_{ref,SR}=1000$ W/m^2), $T_{ref,temp}$ corresponds to the reference temperature ($T_{ref,temp}=25^\circ C$), β is the temperature coefficient of the PV module at maximum power (for polycrystalline and monocrystalline silicon panels, $\beta=-3.7 \times 10^{-3}^\circ C$), $T_{cell}(t)$ ($^\circ C$) denotes the temperature of the PV cell at hour t , as described in Equation 2.

$$T_{cell}(t) = T_{at}(t) + \left(\frac{NOCT-20}{1000} \right) \times G_{SR}(t) \quad (2)$$

where $T_{at}(t)$ represents the ambient temperature at hour t ($^\circ C$), NOCT is assumed to be $45^\circ C$ under standard operating conditions.

1.1.2. Wind Turbine System (WTS)

The output power of the WTS is determined based on the wind speed relative to the turbine's operational limits. If the wind speed is below the cut-in speed or above the cut-out speed, the turbine produces no power. For wind speeds between the cut-in speed and the rated speed, the power output increases proportionally to the cube of the wind speed. Once the wind speed reaches the rated speed and up to the cut-out speed, the turbine operates at its maximum rated power. This approach ensures safe and efficient turbine operation under varying wind conditions. The output power produced by the WTS is described by Equation 3 (Hermann, D. T., Donatien, N., Armel, T. K. F., & René, T., 2022).

$$P_{WTS}(t) = N_{WTS} \times \begin{cases} 0 & \text{if } V(t) < V_{in} \text{ or } V(t) \geq V_{out} \\ V(t)^3 \times \left(\frac{P_{rt,WTS}}{V_{rt}^3 - V_{in}^3} \right) - P_{rt,WS} \times \left(\frac{V_{in}^3}{V_{rt}^3 - V_{in}^3} \right) & \text{if } V_{in} \leq V(t) < V_{rt} \\ P_{rt,WS} & \text{if } V_{rt} \leq V(t) < V_{out} \end{cases} \quad (3)$$

where, $P_{WTS}(t)$ (kW) represents the output power generated by the WTS at hour t , N_{WTS} denotes the number of wind turbines, $V(t)$ (m/s) is the wind speed at hour t , the parameters V_{in} , V_{rt} , V_{out} (all in m/s) correspond to the cut-in speed, rated speed, and cut-out speed of the wind turbine, respectively, finally, $P_{rt,WS}$ (kW) represents the rated power capacity of the wind turbine generator.

1.1.3. Battery System (BS)

The battery system functions as an energy reservoir, storing excess energy from PVS and WTS and releasing it to meet load demands when renewable generation is insufficient. The formulation of the BS model is detailed below (Maleki & Pourfayaz (2015); Wankouo Ngouleu et al. (2023)).

If the combined output of the PVS and WTS is higher than the load demand at hour t , the battery bank stores the surplus energy and enters a charging mode. The amount of energy available in the battery at this time is calculated using **Equation 4**.

$$E_{BS}(t) = E_{BS}(t-1)(1 - \sigma) + (P_{PVS}(t) + P_{WTS}(t) - P_{LD}(t) / \eta_{inv}) \times \eta_{chr} \times \Delta t \quad (4)$$

where $E_{BS}(t)$ and $E_{BS}(t-1)$ indicate the available energy (kWh) in the battery bank at hour t and the previous hour step $t-1$, respectively, the battery's hourly self-discharge rate is denoted by σ , η_{inv} and η_{chr} stand for the inverter efficiency and battery charging efficiency, respectively, Δt represents the time interval, $P_{LD}(t)$ signifies the load energy (kW) demand at hour t .

When the total energy supplied by the PVS and WTS does not meet the load demand, the battery bank discharges to cover the energy deficit. The available energy in the battery bank at hour t is calculated according to Equation 5.

$$E_{BS}(t) = E_{BS}(t-1)(1 - \sigma) - (P_{LD}(t) / \eta_{inv} - (P_{PVS}(t) + P_{WTS}(t))) \times \Delta t \quad (5)$$

The model assumes that the discharging efficiency of the battery is unity and excludes the influence of temperature on the battery bank's performance.

In this study, the initial state of charge for the battery system has been set to 50%.

The constraints outlined in Equation 6 regulate the energy level in the battery bank to ensure the extended operational life of the batteries.

$$E_{BS}^{Min} \leq E_{BS}(t) \leq E_{BS}^{Max} \quad (6)$$

where E_{BS}^{Min} refers to the minimum allowable energy in the battery bank and E_{BS}^{Max} represents its maximum storage capacity.

E_{BS}^{Max} corresponds to the nominal capacity of the battery bank, indicated as C_{NO} and it is calculated as shown in Equation 7.

$$C_{NO} = (N_{BT} / N_{Bts}) \times C_{Bt} \quad (7)$$

where N_{BT} defines the total number of batteries, C_{Bt} specifies the capacity of each battery (kWh), N_{Bts} denotes the series connection of batteries to achieve the required DC bus voltage and calculated as shown in Equation 8 (Abbes, Martinez, & Champenois, 2014).

$$N_{Bts} = \frac{V_{Bus}}{V_{Bt}} \quad (8)$$

where V_{Bus} denotes the nominal DC bus voltage (48 V) and V_{Bt} defines the nominal voltage of each individual battery.

E_{BS}^{Min} is calculated using the maximum depth of discharge (DOD), as described in **Equation 9**.

$$E_{BS}^{Min} = (1 - DOD) \times C_{NO} \quad (9)$$

1.2. Objective Function Formulation of the Problem

The objective function for the optimization problem aims to minimize the NPC of the system while ensuring the LPSP remains within acceptable limits. The NPC comprises the total capital cost (C_{cap}), replacement cost (C_{rpl}) and maintenance cost (C_{mtc}). To determine the optimal system configurations, the objective function in **Equation 10** is solved using an optimization algorithm (Wankouo Ngouleu et al. (2023)).

$$\text{Minimization of NPC} = C_{Cap} + C_{Rpl} + C_{Mtc} \quad (10)$$

C_{Cap} is calculated as shown in Equation 11.

$$C_{Cap} = N_{PVS} \times C_{Cap}^{PV} + N_{WTS} \times C_{Cap}^{WT} + N_{BT} \times C_{Cap}^{BT} + C_{Cap}^{INV} \quad (11)$$

In Equation 11, C_{Cap}^{PV} , C_{Cap}^{WT} , C_{Cap}^{BT} and C_{Cap}^{INV} represent the unit costs of PV panels, wind turbines, batteries and inverters, while N_{PVS} , N_{WTS} , N_{BT} denote their respective numbers.

In the study, both the inverter and battery storage have an assumed lifespan of 10 years. To account for the replacement of these components, the single payment worth factor is used to determine the associated cost, as presented in Equation 12.

$$C_{Rpl} = [N_{BT} \times C_{Cap}^{BT} + C_{Cap}^{INV}] \times (1/(1+i)^{10}) \quad (12)$$

where i denote the inflation rate (The value of i is set to 0.05 in this study.)

The overall maintenance cost for the hybrid system during the system's lifetime is formulated in Equation (13).

$$C_{Mtc} = N_{PVS} \times \sum_{t=1}^x C_{Mtc}^{PV} + N_{WT} \times \sum_{t=1}^x C_{Mtc}^{WT} + N_{BT} \times \left(\frac{x}{LF_{BT}} \right) \times \sum_{t=1}^x C_{Mtc}^{BT} \quad (13)$$

where x denotes the project lifetime (The value of x is set to 20 in this study), LF_{BT} refers to lifetime of the battery, C_{Mtc}^{PV} , C_{Mtc}^{WT} , C_{Mtc}^{BT} indicate the unit annual maintenance costs associated with PV panels, wind turbine generators, and batteries, respectively. In this study, the maintenance cost of the inverter is neglected, and the lifetimes of PVS and WTS are assumed to be equal to the project lifetime ($x=20$).

The COE represents an important economic factor in hybrid systems and is obtained from the NPC through the Equation 14.

$$COE = \frac{NPC \times CRF}{\sum_{t=1}^{8760} P_{LD}(t) \times \Delta t} \quad (14)$$

where $\sum_{t=1}^{8760} P_{LD}(t) \times \Delta t$ defines the total load demand over a year, while **CRF** indicates the capital recovery factor, which is obtained from **Equation 15**.

$$CRF = \frac{i(1+i)^x}{(1+i)^x - 1} \quad (15)$$

1.3. Constraints of the Optimization Problem

In order to achieve an optimal configuration, the hybrid system is subject to constraints linked to the objective function. These constraints place upper and lower bounds on the number of PV panels, wind turbines and batteries as shown in Equation 16 (Wankouo Ngouleu et al. (2023)).

$$\begin{cases} 0 \leq N_{PVS} = Integer \leq N_{PVS}^{Max} \\ 0 \leq N_{WTS} = Integer \leq N_{WTS}^{Max} \\ 0 \leq N_{BT} = Integer \leq N_{BT}^{Max} \end{cases} \quad (16)$$

where the maximum allowable number of PV panels, wind turbines, and batteries are represented by N_{PVS}^{Max} , N_{WTS}^{Max} and N_{BT}^{Max} , respectively, which are predetermined system constraints.

In hybrid power generation systems, the LPSP is a critical reliability measure. It is defined as the ratio between the loss of power supply (LPS) and the total load demand. LPSP ranges from 0 to 1, where 0 signifies complete satisfaction of the load, and 1 indicates that no load demand is met. The LPSP is typically calculated using **Equation 17**.

$$LPSP = \frac{\sum_{t=1}^T LPS(t)}{\sum_{t=1}^T P_{LD}(t)} \quad (17)$$

where $\sum_{t=1}^T P_{LD}(t)$ signifies the total power consumed by the load throughout the year, while $\sum_{t=1}^T LPS(t)$ denotes the total energy shortfall over the same period. The definition of LPS is provided in **Equation 18**.

$$LPS(t) = \frac{P_{LD}(t)}{\eta_{Inv}} - \left(P_{PVS}(t) + P_{WTS}(t) + (E_{BS}(t-1) - E_{BS}^{Min}) \right) \quad (18)$$

Ensuring the reliability of the hybrid system requires the consideration of the LPSP as an inequality constraint, which is defined as shown in Equation 19.

$$LPSP \leq LPSP_{MAV} \quad (19)$$

where $LPSP_{MAV}$ specifies the maximum allowed value of the LPSP (The value of $LPSP_{MAV}$ is set to 0.05 in this study.).

2. GENETIC ALGORITHM (GA) OPTIMIZATION

The GA is utilized to optimize the sizing of the PV/Wind/Battery hybrid energy system with the dual objective of minimizing the Net Present Cost (NPC) and maintaining system reliability at an LPSP level of 5%. The optimal sizing problem and the energy balance of the hybrid system components are considered in the development of the objective function and constraints, which are implemented in a MATLAB m-file. The technical and economic attributes of the hybrid system components are included in these formulations. In this study, The GA optimization process utilizes the following parameters: a population size of 50, selection, crossover rate (0.80), mutation rate (0.20) and a stopping criterion defined by a maximum of 100 generations. For each generation, the LPSP is evaluated for every population and populations that fail to satisfy the LPSP constraint are removed from the subsequent generation. This process continues until the maximum number of generations is reached (Das, Hasan, & Rashid, 2021). Further details about the GA can be found in the literature (Ismail, Moghavvemi, & Mahlia, 2014).

3. SIMULATION STUDIES AND RESULTS

The proposed methodology, validated through case studies incorporating GA optimization, explored various hybrid system configurations, including PV-Battery, Wind-Battery, and PV/Wind/Battery systems.

The GA optimization approach has been developed and executed in MATLAB 2022a. A total of 20 independent runs are carried out and the associated results are reported.

3.1. Input data

The input data required for modeling the optimization problem has been gathered from various studies in the literature, as no single study containing all the necessary information has been available. The data of parameters and values of the hybrid system components is given in Table 1 (Wankouo Ngouleu et al. (2023); Maleki & Askarzadeh (2014)).

Table 1. The parameters and values of the components

Components	Parameters	Values
Wind	$P_{rt,WT}$	1 kW
	V_{in}	2.5 m/s
	V_{rt}	11 m/s
	V_{out}	13 m/s
	C_{Cap}^{WT}	3200\$
	C_{Mtc}^{WT}	(0.03*3200) (\$/y1l)
PV	$P_{rt,PV}$	0.305 kW
	η_{PVS}	90%
	C_{Cap}^{PV}	270\$
	C_{Mtc}^{PV}	(0.01*270) (\$/y1l)
Battery	η_{chr}	85%
	σ	0.0002
	DOD	80%
	C_{NO}	1.35 kWh
	V_{Bt}	12 V
	C_{Cap}^{BT}	130\$
	C_{Mtc}^{BT}	(0.01*130) (\$/y1l)
Inverter	η_{inv}	95%
	C_{Cap}^{INV}	1500\$

The hourly load demand, which represents the energy consumption pattern over a 24-hour period, is presented in the Figure 2 (Wankouo Ngouleu et al. (2023)).

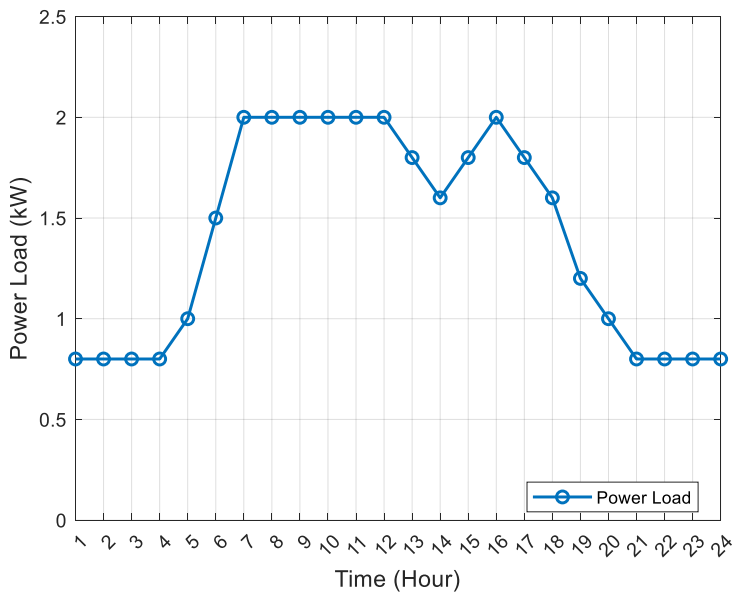


Figure 2. The hourly load demand

The hourly wind speed, which illustrates the variation in wind velocity throughout the day, is shown in Figure 3. (Wankouo Ngouleu et al. (2023)).

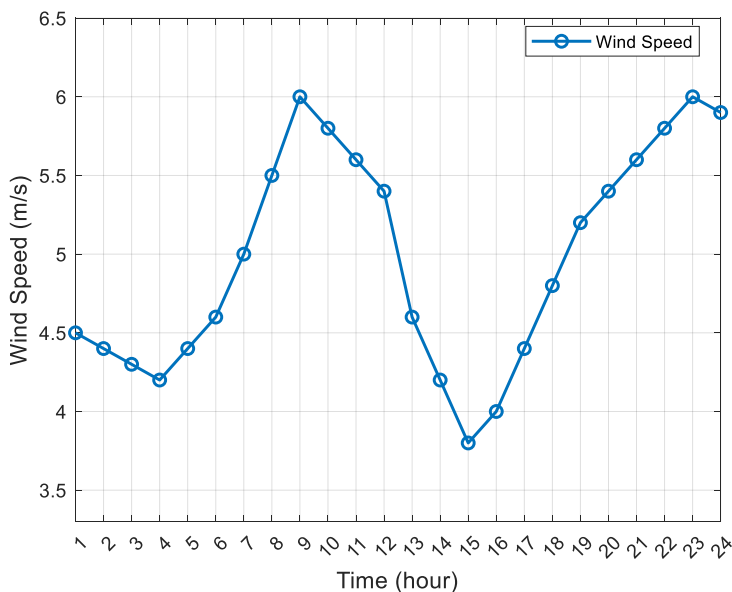


Figure 3. The hourly wind speed

The hourly solar radiation and ambient temperature, which highlight the variations in solar energy and atmospheric temperature throughout the day, are shown in Figure 4 (Wankouo Ngouleu et al. (2023); SoltaniNejad Farsangi, Hadayeghparast, Mehdinejad, & Shayanfar, 2018)).

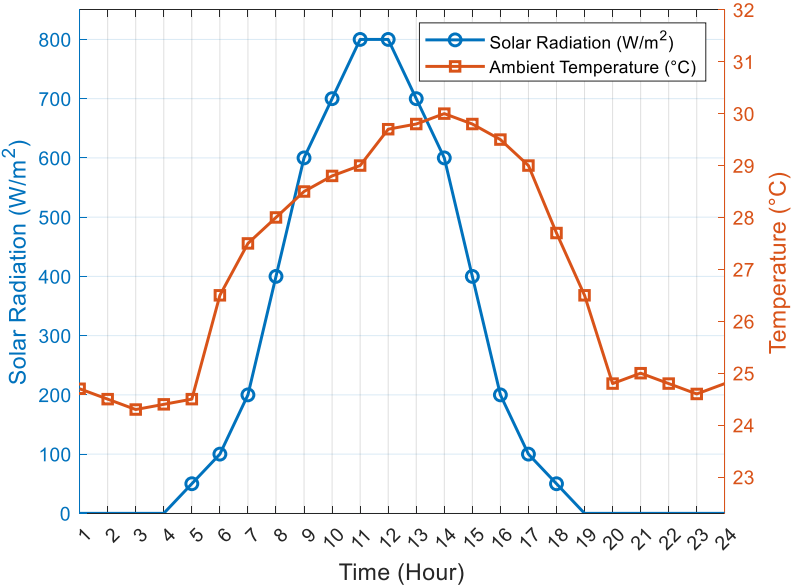


Figure 4. The hourly solar radiation and ambient temperature

3.2. Simulation Results

The GA has been executed iteratively and the best-performing solution among the 20 trials has been chosen as the optimal solution.

As a result of the study, for the PV-Battery hybrid system, NPC is found to be 18650 \$ and COE is found to be 0.1216 \$/kWh with $N_{PVS}=21$, $N_{BT}=36$, for Wind-Battery hybrid system, NPC is found to be 98332.9 \$ and COE is found to be 0.6412 \$/kWh with $N_{WTS}=15$, $N_{BT}=73$, for PV-Wind-Battery hybrid system, NPC is found to be 22660.6 \$ and COE is found to be 0.1478 with $N_{PVS}=20$, $N_{WTS}=1$, $N_{BT}=33$. The optimal solutions for the three type of hybrid energy system configuration are presented in the Table 2.

Table 2. Optimal solutions for PV-Battery, Wind-Battery, PV-Wind-Battery Hybrid Systems

	N _{PVS}	N _{WTS}	N _{BT}	NPC (\$)	COE(\$/kWh)
PV-Battery	21	-	36	18650	0.1216
Wind-Battery	-	15	73	98332.9	0.6412
PV-Wind-Battery	20	1	33	22660.6	0.1478

The analysis of the results reveals that the costs of the PV-Battery and PV-Wind-Battery hybrid systems are relatively similar, indicating that both configurations offer economic advantages. In the Wind-Battery system, a higher number of wind turbines are required to meet the load demand solely through wind power. This requirement is further exacerbated by the low wind speed, which resulted in reduced wind power output. Consequently, additional wind turbines are necessary to fulfill the energy demand. Given that wind turbines have a higher capital cost compared to other system components, the NPC of the Wind-Battery system is significantly higher. Therefore, the implementation of a Wind-Battery system in areas with low wind speeds would not be economically feasible.

Figure 5 illustrates the overall capital, replacement and maintenance costs associated with each hybrid energy system configuration.

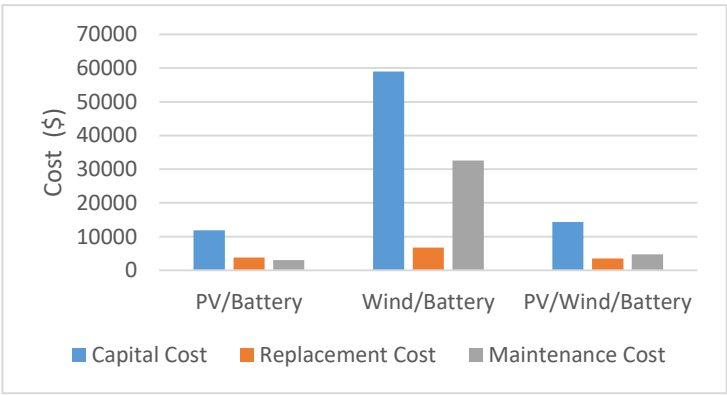


Figure 5. The overall capital, replacement and maintenance costs for each hybrid system

Figure 5 compares the costs of PV-Battery, Wind-Battery and PV-Wind-Battery hybrid systems. The Wind-Battery system has the highest overall costs due to expensive wind turbines and high maintenance. The PV/Battery system is the most cost-effective, with low capital, replacement and maintenance costs. The PV/Wind/Battery system balances cost and performance, offering a viable option in areas with both solar and wind resources.

The output power generated by the PVS and WTS for the PV-Wind-Battery hybrid energy system is illustrated in Figure 6, providing a comparative view of their hourly contributions to the hybrid energy system.

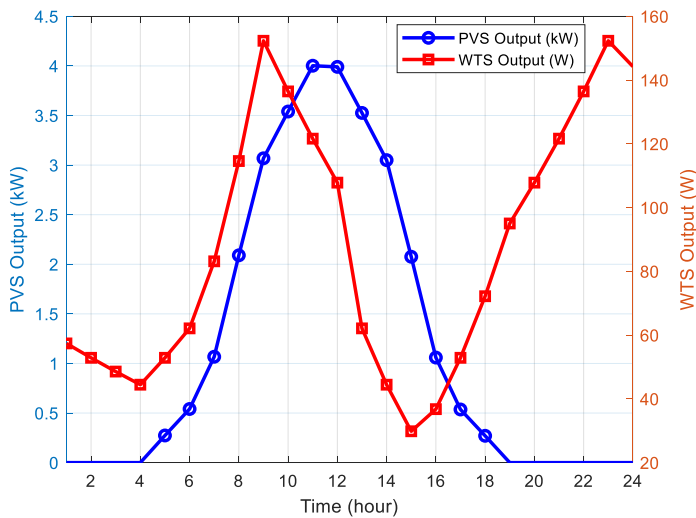
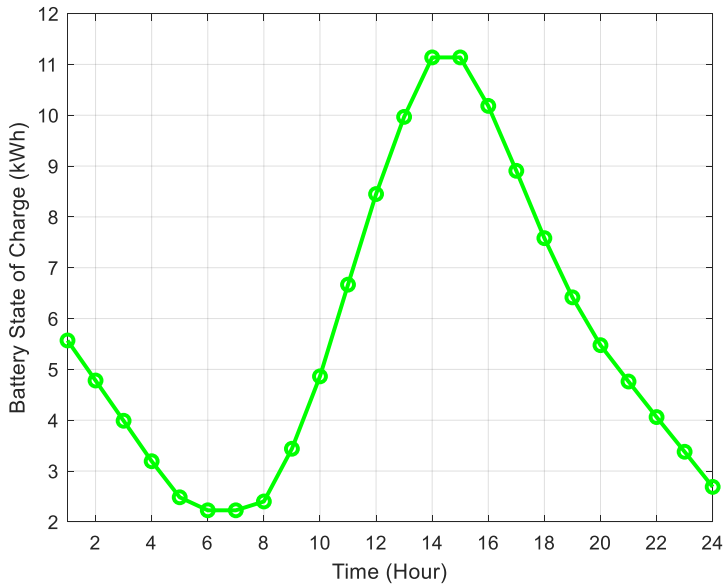


Figure 6. The output power of PVS and WTS for PV-Wind-Battery System

The Figure 6 illustrates the hourly output of the PVS and the WTS across a 24-hour period. The PVS demonstrates a distinct pattern, producing energy primarily during daylight hours, with its output peaking at midday when solar radiation is at its highest. Conversely, the WTS shows a more irregular power output, with significant production during early morning and evening hours, reflecting fluctuations in wind speed. This complementary relationship highlights the advantages of combining solar and wind energy systems to ensure a more stable and consistent power supply.

The hourly state of charge (SoC) of the battery throughout a 24-hour period is shown in Figure 7.



The Figure 7 illustrates the 24-hour battery SoC (kWh). The battery begins to discharge during the early morning hours as energy demand exceeds production, reaching its lowest level around 6-7 AM. As solar energy production increases, the battery starts charging from 8 AM, peaking at its maximum level in the afternoon. From the evening onward, as energy production declines, the battery discharges again. This indicates that the battery is effectively utilized to balance energy production and demand throughout the day.

4. CONCLUSION

This study demonstrates the feasibility and efficiency of utilizing hybrid renewable energy systems consisting of PV, wind turbines, and battery storage to meet load demands sustainably. The results indicate that both PV-battery and PV-wind-battery systems present significant advantages, particularly in scenarios with low wind speeds where wind turbine systems alone are insufficient. The PV-battery configuration proves to be cost-effective due to its relatively lower capital costs compared to systems involving wind turbines.

Furthermore, the NPC associated with wind-battery systems underscores the impact of high capital and maintenance costs of wind turbines, especially in regions with limited wind resources. This highlights the importance of carefully analyzing site-specific conditions, including wind and solar availability, before implementing hybrid energy systems.

The hourly performance analysis of the components, including PV output, wind output, and battery state of charge, provides valuable insights into the dynamic interactions between the system components and their ability to balance supply and demand efficiently. The findings also emphasize the need for strategic sizing of each component to optimize the overall system performance and minimize costs.

In conclusion, this study supports the implementation of hybrid renewable energy systems as a sustainable solution for energy generation while highlighting the necessity for detailed analysis and optimization tailored to specific environmental and economic conditions. Further research is encouraged to explore advanced optimization techniques and the integration of additional renewable sources to enhance system reliability and efficiency.

REFERENCES

- Abbes, D., Martinez, A., & Champenois, G. (2014). Life cycle cost, embodied energy and loss of power supply probability for the optimal design of hybrid power systems. *Mathematics and Computers in Simulation*, 98, 46–62. <https://doi.org/10.1016/j.matcom.2013.05.004>
- Al Afif, R., Ayed, Y., & Maaitah, O. N. (2023). Feasibility and optimal sizing analysis of hybrid renewable energy systems: A case study of Al-Karak, Jordan. *Renewable Energy*, 204, 229–249. <https://doi.org/10.1016/j.renene.2022.12.109>
- Das, B. K., Hasan, M., & Rashid, F. (2021). Optimal sizing of a grid-independent PV/diesel/pump-hydro hybrid system: A case study in Bangladesh. *Sustainable Energy Technologies and Assessments*, 44, 100997. <https://doi.org/10.1016/j.seta.2021.100997>
- Hermann, D. T., Donatien, N., Armel, T. K. F., & René, T. (2022). Techno-economic and environmental feasibility study with demand-side management of photovoltaic/wind/hydroelectricity/battery/diesel: A case study in Sub-Saharan Africa. *Energy Conversion and Management*, 258, 115494. <https://doi.org/10.1016/j.enconman.2022.115494>
- Ismail, M. S., Moghavvemi, M., & Mahlia, T. M. I. (2014). Genetic algorithm based optimization on modeling and design of hybrid renewable energy systems. *Energy Conversion and Management*, 85, 120–130. <https://doi.org/10.1016/j.enconman.2014.05.064>
- Khan, F. A., Pal, N., & Saeed, S. H. (2018). Review of solar photovoltaic and wind hybrid energy systems for sizing strategies, optimization techniques, and cost analysis methodologies. *Renewable and Sustainable Energy Reviews*, 92, 937–947. <https://doi.org/10.1016/j.rser.2018.04.107>
- Koholè, Y. W., Fohagui, F. C. V., Ngouleu, C. A. W., & Tchuen, G. (2024). An effective sizing and sensitivity analysis of a hybrid renewable energy system for household, multimedia, and rural healthcare centres power supply: A case study of Kaele, Cameroon. *International Journal of Hydrogen Energy*, 49(1321–1359). <https://doi.org/10.1016/j.ijhydene.2023.09.093>
- Maleki, A., & Askarzadeh, A. (2014). Comparative study of artificial intelligence techniques for sizing of a hydrogen-based stand-alone photovoltaic/wind hybrid system. *International Journal of Hydrogen Energy*, 39(29), 9973–9984. <https://doi.org/10.1016/j.ijhydene.2014.04.147>
- Maleki, A., & Pourfayaz, F. (2015). Optimal sizing of autonomous hybrid photovoltaic/wind/battery power system with LPSP technology by using evolutionary algorithms. *Solar Energy*, 115, 471–483. <https://doi.org/10.1016/j.solener.2015.03.004>
- Marsa, N., Houcine, L., Zaafour, A., & Chaari, A. (2021). Optimal sizing of stand-alone hybrid photovoltaic/wind system using BAT algorithm. *International Journal of*

- Moghaddam, S., Bigdeli, M., Moradlou, M., & Siano, P. (2019). Designing of stand-alone hybrid PV/wind/battery system using improved crow search algorithm considering reliability index. *International Journal of Energy and Environmental Engineering*, 10(3), 429–449. <https://doi.org/10.1007/s40095-019-00319-y>
- Montoya, O. D., Grisales-Noreña, L. F., Gil-González, W., Alcalá, G., & Hernandez-Escobedo, Q. (2020). Optimal location and sizing of PV sources in DC networks for minimizing greenhouse emissions in diesel generators. *Symmetry*, 12(2), 322. <https://doi.org/10.3390/sym12020322>
- Rajabi-Ghahnavieh, A., & Nowdeh, S. A. (2014). Optimal PV–FC hybrid system operation considering reliability. *International Journal of Electrical Power & Energy Systems*, 60, 325–333. <https://doi.org/10.1016/j.ijepes.2014.03.043>
- Rodríguez-Gallegos, C. D., Yang, D., Gandhi, O., Bieri, M., Reindl, T., & Panda, S. K. (2018). A multi-objective and robust optimization approach for sizing and placement of PV and batteries in off-grid systems fully operated by diesel generators: An Indonesian case study. *Energy*, 160, 410–429. <https://doi.org/10.1016/j.energy.2018.06.185>
- SoltaniNejad Farsangi, A., Hadayeghparast, S., Mehdinejad, M., & Shayanfar, H. (2018). A novel stochastic energy management of a microgrid with various types of distributed energy resources in presence of demand response programs. *Energy*, 160, 257–274. <https://doi.org/10.1016/j.energy.2018.06.136>
- Wankouo Ngouleu, C. A., Koholé, Y. W., Fohagui, F. C. V., & Tchuen, G. (2023). Techno-economic analysis and optimal sizing of a battery-based and hydrogen-based standalone photovoltaic/wind hybrid system for rural electrification in Cameroon based on meta-heuristic techniques. *Energy Conversion and Management*, 280, 116794. <https://doi.org/10.1016/j.enconman.2023.116794>
- Zhang, G., Shi, Y., Maleki, A., & Rosen, M. A. (2020). Optimal location and size of a grid-independent solar/hydrogen system for rural areas using an efficient heuristic approach. *Renewable Energy*, 156, 1203–1214. <https://doi.org/10.1016/j.renene.2020.04.010>



CHAPTER 23

Prediction of Surface Leakage Currents in High-Voltage Insulators By Machine Learning Approaches

Serhat Berat Efe¹

¹ Assoc. Prof. Dr., Bandırma Onyedi Eylül University, Dept. of Electrical Engineering,
ORCID: 0000-0001-6076-4166

INTRODUCTION

High voltage insulators, which are critical components of electrical power networks, are subjected to tremendous electrical stress due to their operating circumstances and also affect various electrical systems (Cengiz 2022a, 2024; Nacar, Öncü, and Kayfeci 2022). These elements, which run at high voltage levels under nominal settings, are subjected to greater stress in the event of faults caused by the nature of power systems or changes in the working environment (Cengiz 2022b).

There is a margin of error in the calculations because of both unanticipated external factors and transient situations that arise during operation, even though the continuous operating conditions of the related equipment in the areas where high voltage insulators will be used can be determined in general terms. Dust and humidity are the two most significant external elements that contaminate the insulator outside surface. This contamination eventually creates a permanent layer on the insulator surface and leads to the flow of currents known as leakage currents, which seriously impair safety and operation. One of the most critical factors influencing the working life of high voltage insulators is the surface leakage currents that occur during their operation. Surface leakage currents increase the size of the so-called dry band, resulting in dry band current hopping and deterioration of insulator performance.

Manufacturers of insulators are attempting to take preventative measures to address these and related issues by adding techniques like silicone coating to already-existing insulators and diversifying the materials used in insulator production (Pernebaveva et al. 2019). To get around the process complexity brought on by the high voltage insulators' many characteristics, researchers have created a variety of models. The intricacy of the jump mechanism, which fluctuates depending on operating conditions, makes mathematical techniques used to predict the discharge voltage challenging in this situation. Two theoretical model categories—dynamic and static models—have been used to analyze the discharge event (Arshad et al. 2019). Sundararajan - Gorur Model, Megriche-Beroual Model and Equivalent Cylindrical Insulator Model are classified as dynamic models while Wilkins Model, Rumeli Model, Circular Strip Model and Obenaus Model are classified as static models (El Amine Slama, Beroual, and Haddad 2020; Venkataraman and Gorur 2006). Compared to static models, dynamic models have certain advantages. For instance, dynamic models evaluate by taking into account immediate changes in parameters, whereas static models are predicated on steady-state operation (Bhuvir, Bhuvir, and Shah 2020; Salem et al. 2022; Slama et al. 2022).

Researchers have begun using intelligent system approaches to this problem in addition to mathematical methods in recent years because surface leakage currents with nonlinear structure have many parameters that are affected simultaneously. This is done in order to take advantage of artificial intelligence (AI) technologies, which have many benefits when it comes to solving nonlinear problems (Florkowski 2020; Nacar 2024; Nacar and Öncü 2019; Wang et al. 2019).

METHODOLOGY

Finding the discharge currents in high voltage insulators is essential for evaluating the functionality and condition of electrical systems. AI techniques can be used to track and forecast the discharge currents in high voltage insulators. Although there are several studies on surface leakage currents in the literature, recent advances in artificial intelligence and deep learning methodologies have helped researchers working in this field get more effective outcomes using the aforementioned models. Machine learning algorithms are one of the AI techniques that can be applied here such as done other research areas (Nacar and Öncü 2022). To forecast discharge currents based on a variety of input characteristics, including voltage, temperature, humidity, and pollution levels, regression models from machine learning techniques can be trained on historical data (Shaik and Karupaiyan 2019; Stefenon et al. 2020; Wang et al. 2023; Yang et al. 2012). Algorithms include support vector machines, decision trees, and linear regression (Cengiz 2019).

In the context of time series analysis, discharge currents are predicted using previous measurements and models using machine learning algorithms and time series forecasting techniques as LSTM (Long Short-Term Memory) neural networks and ARIMA (AutoRegressive Integrated Moving Average) (Fatima and Rahimi 2024; Ozer, Efe, and Ozbay 2021). Analyzing data with artificial neural networks (ANN) is an additional technique (Gençoğlu and Cebeci 2008; Patel, Parekh, and Kumar 2019; Schober and Schichler n.d.). In regression tasks, feed-forward ANNs can be utilized to forecast discharge currents. They are able to understand intricate connections between discharge current and input parameters. Recurrent neural networks (RNNs) can be used to anticipate discharge currents based on historical records since they are appropriate for processing time series data. Images can be utilized to monitor insulators and identify discharge events using Convolutional Neural Networks (CNN) (Han et al. 2019; Vigneshwaran et al. 2021). Areas with discharges can be identified by processing images of the insulators.

Comparable to this approach is data fusion, which offers a thorough understanding of insulating conditions by merging data from several sources, including heat sensors, ambient sensors, and visual cameras. This multimodal data can be integrated and analyzed using AI techniques like fusion networks and ensemble approaches. Unusual or unexpected discharge current patterns that point to possible issues with isolators can be found using AI-based anomaly detection methods like isolation forests or single-class support vector machines (SVM). It is possible to optimize isolator maintenance schedules by using Reinforced Learning (RL). RL algorithms can assist in deciding when to do maintenance or inspections by simulating the trade-off between maintenance expenses and the risk of discharge incidents (Barrios et al. 2019).

Data from devices and sensors connected to insulators can be analyzed using the Internet of Things (IoT) and sensor integration. Real-time temperature, humidity, and voltage data from these sensors can be utilized to forecast discharge events. In order to estimate discharge currents and make well-informed judgments regarding insulator maintenance, AI-driven expert systems integrate domain knowledge with expert rules and historical data (Fan, Xiao, and Zhao 2017; Haq and Ni 2019). If visual inspections are important, deep learning models, like CNNs, can be taught to examine insulator photos or videos for indications of discharge events, like flashovers or corona discharges. Real-time monitoring and discharge current prediction can be made possible by directly deploying AI models to end devices or power grid infrastructure, eliminating the need for centralized computing resources (Arshad et al. 2020; Valeriy and Iosif 2022).

Access to high-quality data for training and validation, as well as a strong infrastructure for data collection, preprocessing, and model deployment, are essential for the successful application of AI techniques for detecting discharge currents in high-voltage insulators (Abdullah et al. 2020). Additionally, for AI to be successfully included into the upkeep and monitoring of high voltage insulators, cooperation between electrical engineers, data scientists, and domain experts is essential.

Surface leakage current is influenced by several factors, including surface conductivity (σ_s), applied voltage (V), and the geometry of the insulator. Surface conductivity, measured in siemens per meter (S/m), represents the conductance per unit area on the insulator's surface. The applied voltage drives the leakage current along the surface, while the geometry of the insulator, such as the length of the leakage path (L) and the shape of the insulator (e.g., with sheds in high-

voltage applications), also plays a significant role. The basic relation for surface leakage current (I_s) is given by

$$I_s = \sigma_s \cdot E_s \cdot A \quad (1)$$

where $E_s = V/L$ is the electric field strength along the leakage path (V/m), and A is the cross-sectional area for current flow (m^2). For practical insulators, the design parameters such as leakage path length and surface area are critical in determining the leakage current.

For theoretical analysis, a range of σ_s values can be assumed or measured to represent different surface conditions, such as clean, partially polluted, and heavily polluted insulator surfaces. Clean surfaces typically have lower σ_s values due to minimal contamination, while partially polluted surfaces have intermediate values influenced by factors like humidity or light dirt deposits. Heavily polluted surfaces, on the other hand, exhibit high σ_s values as a result of dense contamination or wet conditions that enhance conductivity. Using the relationship

$$I_s = \sigma_s \cdot \frac{V}{L} \cdot A \quad (2)$$

where V is the applied voltage, L is the leakage path length, and A is the effective cross-sectional area for current flow, the surface leakage current I_s can be calculated. By substituting varying σ_s values into the formula, the corresponding I_s can be determined for each surface condition (Öztürk and Cebeci 2015). This approach allows for the evaluation of the impact of surface conductivity on leakage current, providing insights into how different contamination levels affect the performance of the insulator under specific voltage and geometric configurations.

EXPERIMENTAL RESULTS AND DISCUSSION

According to the equations given previous sections, a dataset of surface leakage currents was generated as a function of the applied voltage and pollution rate under Python environment by using necessary extensions. Since the fouling rate increases the surface conductivity of the insulator, it can be said that this dataset also expresses changes due to surface conductivity. The applied voltage was started at 5 kV and increased with a resolution of 1 kV step up to 400 kV,

and the dataset was created considering 10%, 15%, 25%, 40%, 60%, 75% and 90% pollution rates.

Using a dataset contained in an Excel file, this Python application applies a machine learning process to forecast leakage current. Assuming that the first seven columns represent the features (independent variables) and the eighth column represents the target variable (leakage current), it starts by loading the dataset using the pandas package. The “train_test_split” function is then used to divide the data into training and testing subsets, allocating 70% of the data for training and 30% for testing. While testing the model's generalization ability on unseen cases, this guarantees that the model is trained on the majority of the data.

To determine the correlation between the characteristics and the leakage current, the training data is fed into a RandomForestRegressor as the block diagram is shown in Figure 1, a powerful machine learning model. In order to increase accuracy and decrease overfitting, the Random Forest algorithm builds several decision trees during training and averages their predictions. Using metrics like Mean Squared Error (MSE), Root Mean Squared Error (RMSE), and Mean Absolute Error (MAE), the model's performance is assessed after it has been trained and applied to the testing set to generate predictions. These predictions are then contrasted with the actual values. With RMSE being especially helpful because it measures error in the same unit as the target variable, these metrics offer insightful information about the quality of the model.

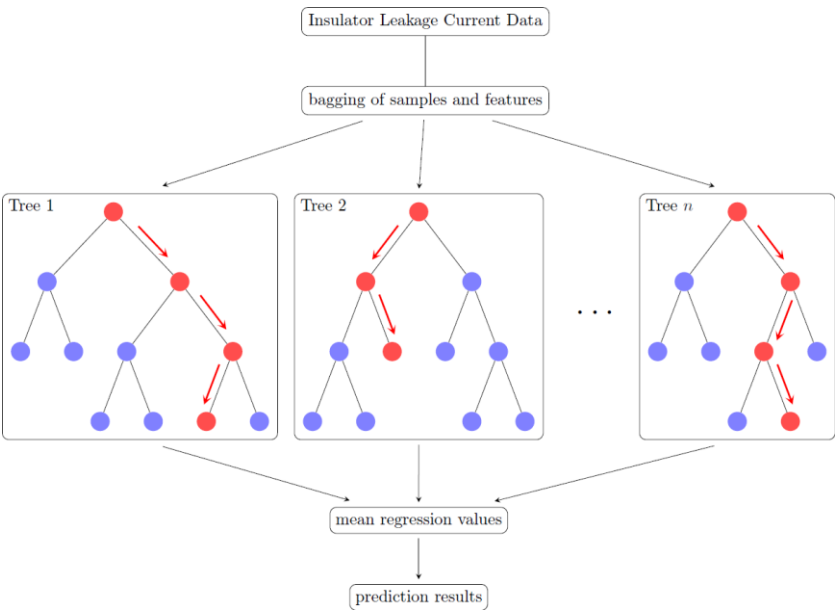


Figure 1. RandomForestRegressor block diagram

In order to allow engineers and researchers to analyze individual predictions and their deviations, the script additionally records the predictions, actual values, and absolute errors into an Excel file for in-depth examination. In order to give a clear and understandable comparison, the script also uses matplotlib to build a visualization that plots actual versus expected leakage current values on a line graph.

The model's performance is summarized in a text box inside the plot that highlights the important metrics. In engineering contexts, this workflow is especially useful for assessing and forecasting insulator performance, detecting possible insulation failure risks, streamlining maintenance plans, and enhancing electrical system dependability. The script makes sure that both technical and non-technical stakeholders can understand the results by providing both numeric insights and visual analysis.

Developed algorithm is performed by using the dataset and prediction performances for 25%, 60% and 90% pollution rates are given in Figure 2, Figure 3 and Figure 4 respectively.

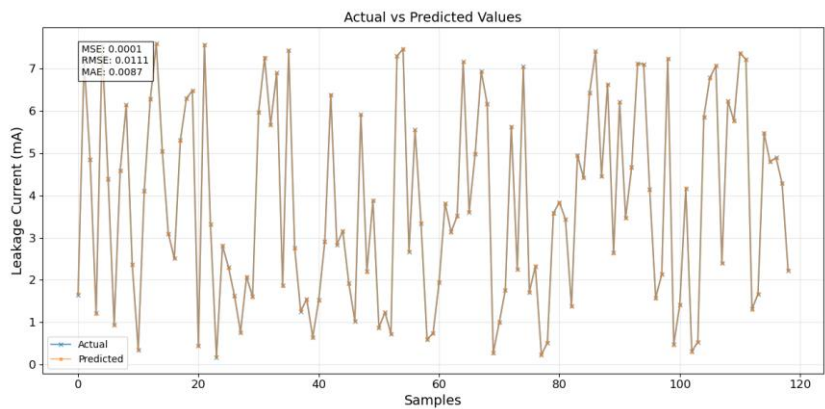


Figure 2. 25% pollution rate

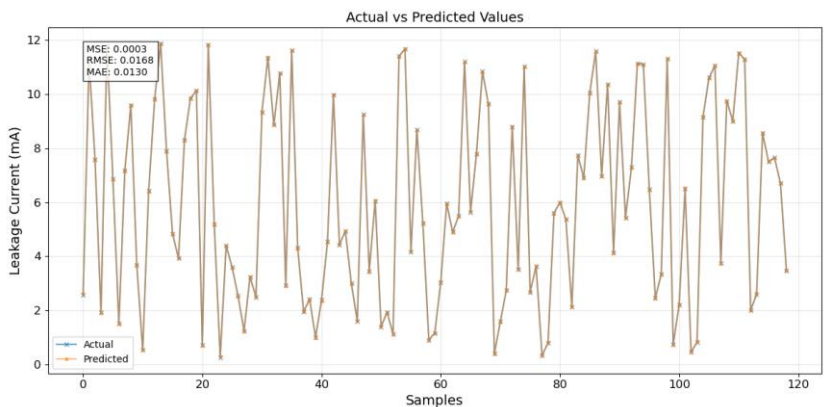


Figure 3. 60% pollution rate

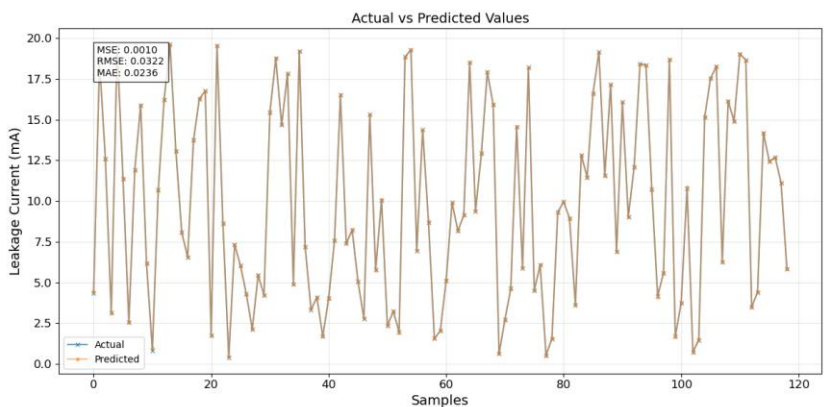


Figure 3. 90% pollution rate

CONCLUSION

The developed machine learning algorithm provides an effective approach to predict surface leakage currents in high-voltage insulators under varying conditions of pollution and applied voltage. By leveraging Random Forest regression, the model achieves high accuracy in forecasting leakage currents, accounting for factors such as surface conductivity, pollution rate, and applied voltage. The ability to simulate and analyze leakage currents under different pollution levels (e.g., 25%, 60%, and 90%) highlights the adaptability and practical application of the model in real-world scenarios.

This approach offers significant benefits for the electrical industry, including enhanced monitoring of insulator performance, identification of potential risks such as insulation failure, and optimization of maintenance schedules. By

recording predictions and metrics, and visualizing results in an intuitive manner, the algorithm ensures accessibility for both engineers and researchers. Additionally, the inclusion of key performance metrics like RMSE enables informed evaluation of the model's effectiveness. Overall, the integration of machine learning into the study of surface leakage currents represents a major step forward in understanding and mitigating the challenges posed by contamination and environmental factors, ultimately improving the reliability and safety of high-voltage electrical systems.

REFERENCES

- Abdullah, Farrah Salwani Binti, Mohamed Afendi Mohamed Piah, Nordiana Azlin Othman, and Asri Din. 2020. "Prediction of Surface Leakage Current of Overhead Insulators under Environmental and Electrical Stresses." *Bulletin of Electrical Engineering and Informatics* 9(5):1747–54. doi: 10.11591/eei.v9i5.2182.
- El Amine Slama, Mohammed, Abderrahmane Beroual, and Abderrahmane Haddad. 2020. "Surface Discharges and Flashover Modelling of Solid Insulators in Gases." *Energies* 13(3). doi: 10.3390/en13030591.
- Arshad, Jawad Ahmad, Ahsen Tahir, Brian G. Stewart, and Azam Nekahi. 2020. "Forecasting Flashover Parameters of Polymeric Insulators under Contaminated Conditions Using the Machine Learning Technique." *Energies* 13(15). doi: 10.3390/en13153889.
- Arshad, Azam Nekahi, Scott G. McMeekin, and Masoud Farzaneh. 2019. "Flashover Characteristics of Silicone Rubber Sheets under Various Environmental Conditions." *Energies* 9(9). doi: 10.3390/en9090683.
- Barrios, Sonia, David Buldain, María Paz Comech, Ian Gilbert, and Iñaki Orue. 2019. "Partial Discharge Classification Using Deep Learning Methods - Survey of Recent Progress." *Energies* 12(13).
- Bhuvir, Dhruvi, Dhruvi Bhuvir, and Prakruti Shah. 2020. "An Experimental Study on Pollution Flashover: A Review." *International Research Journal of Engineering and Technology*.
- Cengiz, Çiğdem. 2019. "Nonparametric Estimation of a Renewal Function in the Case of Censored Sample."
- Cengiz, Cigdem. 2024. "THE RELATIONSHIP BETWEEN ELECTRICITY CONSUMPTION FROM OUTDOOR LIGHTING AND ECONOMIC GROWTH." *Light and Engineering* 32(4):14–21. doi: 10.33383/2023-032.
- Cengiz, Mehmet Sait. 2022a. "LIGHTING MASTER PLAN APPLICATION IN LIVING AREAS." *Light and Engineering* 30(6):124–32. doi: 10.33383/2021-111.
- Cengiz, Mehmet Sait. 2022b. "USING ELECTRIC LIGHTING TO SUPPORT DAY-LIGHTING IN ARCHITECTURAL BUILDING DESIGNS." *Light and Engineering* 30(1):113–23. doi: 10.33383/2021-086.
- Fan, Cheng, Fu Xiao, and Yang Zhao. 2017. "A Short-Term Building Cooling Load Prediction Method Using Deep Learning Algorithms." *Applied Energy* 195:222–33. doi: 10.1016/j.apenergy.2017.03.064.
- Fatima, Syeda Sitara Wishal, and Afshin Rahimi. 2024. "A Review of Time-Series Forecasting Algorithms for Industrial Manufacturing Systems." *Machines* 12(6).
- Florkowski, Marek. 2020. "Classification of Partial Discharge Images Using Deep Convolutional Neural Networks." *Energies* 13(20). doi: 10.3390/en13205496.

- Gençoğlu, Muhsin Tunay, and Mehmet Cebeci. 2008. "The Pollution Flashover on High Voltage Insulators." *Electric Power Systems Research* 78(11):1914–21. doi: 10.1016/j.epsr.2008.03.019.
- Han, Jiaming, Zhong Yang, Qiuyan Zhang, Cong Chen, Hongchen Li, Shangxiang Lai, Guoxiong Hu, Changliang Xu, Hao Xu, Di Wang, and Rui Chen. 2019. "A Method of Insulator Faults Detection in Aerial Images for High-Voltage Transmission Lines Inspection." *Applied Sciences (Switzerland)* 9(10). doi: 10.3390/app9102009.
- Haq, Md Rashedul, and Zhen Ni. 2019. "A New Hybrid Model for Short-Term Electricity Load Forecasting." *IEEE Access* 7:125413–23. doi: 10.1109/ACCESS.2019.2937222.
- Nacar, Salih. 2024. "Hybrid-Controlled Class-E Resonant Converter with Synchronous Rectifier for LED Driver Applications." *Engineering Science and Technology, an International Journal* 56. doi: 10.1016/j.jestch.2024.101781.
- Nacar, Salih, and Selim Öncü. 2019. "Hydrogen Production System with Fuzzy Logic-Controlled Converter." *Turkish Journal of Electrical Engineering and Computer Sciences* 27(3):1885–95. doi: 10.3906/elk-1805-77.
- Nacar, Salih, and Selim Öncü. 2022. "Implementation of Hydrogen Generation System with Resonant Converter." *Journal of the Faculty of Engineering and Architecture of Gazi University* 37(4):2163–75. doi: 10.17341/gazimmfd.943982.
- Nacar, Salih, Selim Öncü, and Muhammet Kayfeci. 2022. "Induction Heated Metal Hydride Tube for Hydrogen Storage System." *Pamukkale University Journal of Engineering Sciences* 28(5):676–80. doi: 10.5505/pajes.2021.97692.
- Ozer, Ilyas, Serhat Berat Efe, and Harun Ozbay. 2021. "A Combined Deep Learning Application for Short Term Load Forecasting." *Alexandria Engineering Journal* 60(4):3807–18. doi: 10.1016/j.aej.2021.02.050.
- Öztürk, Dursun, and Mehmet Cebeci. 2015. "Calculation of Surface Leakage Currents on High Voltage Insulators by Ant Colony Algorithm-Supported FEM." *Turkish Journal of Electrical Engineering and Computer Sciences* 23(4):1009–24. doi: 10.3906/elk-1305-6.
- Patel, Krishna, Bhupendra Parekh, and Dinesh Kumar. 2019. "Leakage Current Prediction of Composite Insulator Using Artificial Neural Network." *International Journal of Recent Technology and Engineering* 8(2):6258–66. doi: 10.35940/ijrte.B3746.078219.
- Pernebayeva, Damira, Aidana Irmanova, Diana Sadykova, Mehdi Bagheri, and Alex James. 2019. "High Voltage Outdoor Insulator Surface Condition Evaluation Using Aerial Insulator Images." *High Voltage* 4(3):178–85. doi: 10.1049/hve.2019.0079.
- Salem, Ali Ahmed, Kwan Yiew Lau, Wan Rahiman, Zulkurnain Abdul-Malek, Samir A. Al-Gailani, R. Abd Rahman, and Salem Al-Ameri. 2022. "Leakage Current Characteristics in Estimating Insulator Reliability: Experimental Investigation and Analysis." *Scientific Reports* 12(1). doi: 10.1038/s41598-022-17792-x.
- Schober, B., and U. Schichler. n.d. *Application of Machine Learning for Partial Discharge Classification under DC Voltage*.

- Shaik, Mohamed Ghouse, and Vijayarekha Karuppaiyan. 2019. "Investigation of Surface Degradation of Aged High Temperature Vulcanized (HTV) Silicone Rubber Insulators." *Energies* 12(19). doi: 10.3390/en12193769.
- Slama, Mohammed El Amine, Adnan Krzma, Maurizio Albano, and Abderrahmane Manu Haddad. 2022. "Experimental Study and Modeling of the Effect of ESDD/NSDD on AC Flashover of SiR Outdoor Insulators." *Energies* 15(10). doi: 10.3390/en15103782.
- Stefenon, Stéfano Frizzo, Roberto Zanetti Freire, Leandro dos Santos Coelho, Luiz Henrique Meyer, Rafael Bartnik Grebogi, William Gouvêa Buratto, and Ademir Nied. 2020. "Electrical Insulator Fault Forecasting Based on a Wavelet Neuro-Fuzzy System." *Energies* 13(2). doi: 10.3390/en13020484.
- Valeriy, Ivanov, and Breido Iosif. 2022. *Predicting the Service Life of High-Voltage Insulators Using Actual Leakage Current Values*. Vol. 122.
- Venkataraman, S., and R. S. Gorur. 2006. "Prediction of Flashover Voltage of Non-Ceramic Insulators under Contaminated Conditions." *IEEE Transactions on Dielectrics and Electrical Insulation* 13(4):862–69. doi: 10.1109/TDEI.2006.1667747.
- Vigneshwaran, B., R. V. Maheswari, L. Kalaivani, Vimal Shanmuganathan, Seungmin Rho, Seifedine Kadry, and Mi Young Lee. 2021. "Recognition of Pollution Layer Location in 11 KV Polymer Insulators Used in Smart Power Grid Using Dual-Input VGG Convolutional Neural Network." *Energy Reports* 7:7878–89. doi: 10.1016/j.egy.2020.12.044.
- Wang, Jingang, Peiyuan Li, Xudong Deng, Na Li, Xi Xie, Hang Liu, and Juan Tang. 2019. "Evaluation on Partial Discharge Intensity of Electrical Equipment Based on Improved ANFIS and Ultraviolet Pulse Detection Technology." *IEEE Access* 7:126561–70. doi: 10.1109/ACCESS.2019.2938784.
- Wang, Qian, Zhixuan Fan, Zhirong Luan, and Rong Shi. 2023. "Insulator Abnormal Condition Detection from Small Data Samples." *Sensors* 23(18). doi: 10.3390/s23187967.
- Yang, Qing, Rui Wang, Wenxia Sima, Chilong Jiang, Xing Lan, and Markus Zahn. 2012. "Electrical Circuit Flashover Model of Polluted Insulators under Ac Voltage Based on the Arc Root Voltage Gradient Criterion." *Energies* 5(3):752–69. doi: 10.3390/en5030752.



CHAPTER 24

XRD and XRF Characterizations of Electrospun Nanofibers

Atike İnce Yardımcı¹ & Yaser Açıkbaş²

¹ Assoc. Prof. Dr. ; Usak University, Technology Transfer Office, Usak University, 64200 Usak, Turkey, No: <https://orcid.org/0000-0001-5482-4230>

² Prof. Dr. ; Usak University, Faculty of Engineering and Natural Science, Department of Electric-Electronic Engineering, ORCID No: <https://orcid.org/0000-0003-3416-1083>

1. INTRODUCTION

The electrospinning method is an effective method that allows the production of fibers with diameters ranging from a few nanometers to a few micrometers from polymer solutions under a high electric field (Nadaf et al., 2022). In the electrospinning method, a nanofibrous film is formed by the accumulation of nanofibers during the process. Nanofibers obtained by this method have been used in many different application areas with their low diameter, high surface area, porous structure, superior mechanical properties, and low density (Fadil et al., 2021). Biomedical applications, tissue engineering (Ince Yardimci, Aypek, et al., 2019; Ince Yardimci, Baskan, et al., 2019; Ince Yardimci et al., 2024), sensor technologies (Ince Yardimci et al., 2022; Yagmurcukardes et al., 2023), filter materials (Fahimirad, Fahimirad, & Sillanpää, 2021; T. Lu et al., 2021), and energy storage (Li et al., 2019; Yan, Liu, Yan, Guan, & Wang, 2021) are some of these applications (Zaarour, Zhu, & Jin, 2020).

Determining the performance of nanomaterials is crucial to determine which applications the material is suitable for and to optimize its design and performance (Saleh & Hassan, 2023). The composition of the material directly affects its performance. When determining the usage areas of nanofibers, it is necessary to examine their morphology, crystal structure, surface area, porosity, and chemical components. These properties of nanofibers affect application performance directly.

In this study, nanofiber synthesis by electrospinning method and characterization methods used in nanofiber synthesis in general were examined, but XRF and XRD methods used to examine the elemental analysis and crystal structure of nanofibers were also evaluated in detail. X-ray fluorescence (XRF) is a non-destructive analytical method used to examine the elemental composition of the material (Salem, Hammad, Mohamed, & El-DougDoug, 2022). X-ray diffraction (XRD) is used to determine the crystal structure, crystalline phases, and density of the material (Kumar et al., 2021).

2. Synthesis and Characterization of Electrospun Nanofibers

2.1 *Electrospinning Process of Nanofibers*

The electrospinning method was used to synthesize nanofibers. The electrospinning device consists of 3 main components; a high voltage power supply up to 40 kV, a syringe pump, and a metal collector. For the electrospinning process, the polymer solution is filled into a syringe and the solution is sprayed

into the metal collector at a certain speed with the syringe pump. A piece of Al foil is covered on the collector and nanofibers are collected on this foil.

2.2 Characterization Techniques of Nanofibers

Imaging the morphology of nanofibers is very important. For this, Scanning Electron Microscope (SEM) (Lopez Marquez, Gareis, Dias, Gerhard, & Lezcano, 2022) and Tunneling Electron Microscope (TEM) are used. The morphology and diameter of electrospun nanofibers can be analyzed by SEM. SEM is used for the analysis of nanofibers in secondary electron (SE) mode, at 5-7 kV and a spot size of 3 (Yardimci, Tanoğlu, Yilmaz, & Selamet, 2020). Depending on the polymer used, gold plating may be necessary before analysis. TEM allows to see the distribution of different materials added into electrospun nanofibers and to examine the crystal structure of the fiber (Zhao et al., 2023).

Structural properties of nanofibers are examined by Fourier Transform Infrared Spectroscopy (FT-IR) . No sample preparation is required for FT-IR analysis of electrospun nanofibers. FTIR-ATR mode is suitable for analysis. Nanofibers are placed directly on the diamond crystal platform of the spectrophotometer and the IR beam is focused on a small area of the nanofibrous mat to record FT-IR spectra. The resolution of FT-IR is 4 cm⁻¹, the number of scans collected is 32, suitable for analysis. To examine changes in molecular orientation, random and oriented nanofibers are analyzed by polarized FT-IR. In parallel polarization, the direction of the oscillating electric field of the IR beam is parallel to the alignment direction of the nanofibers, and in perpendicular polarization, it is perpendicular to the alignment direction of the nanofibers.

Since nanofibers generally have high surface areas, their thermal resistance may vary. Thermogravimetric analysis (TGA) is used to study the thermal stability of nanofibers (X. Liu, Wang, Cai, Hu, & Zhu, 2022). By recording the changes in the weight of nanofibers as the temperature increases, it allows determining in which temperature ranges the material decomposes. TGA shows the degradation temperatures of polymer nanofibers as well as the loss of volatile components. Additionally, this method can be used to understand how stable polymers remain at high temperatures and at what temperature structural deterioration occurs. In order to determine thermal properties of electrospun nanofibers TGA is generally carried out from 25 to 600 °C with the ramp rate of 10 °C/min in air atmosphere.

DSC is another extremely useful technique to study the thermal properties, phase changes, crystallization processes and thermal durability of nanofibers. DSC provides important information in evaluating the performance, safety and

efficiency of polymer nanofibers. Polymer nanofibers show thermal transitions in certain temperature ranges. These transitions can directly affect the physical and chemical properties of the material. DSC is used to determine the glass transition temperature (T_g), melting point (T_m) and crystallization temperatures of nanofibers. Nanofibers were heated from 25 to 400 °C with the ramp rate of 10 °C under N_2 atmosphere for DSC analysis (X. Liu et al., 2022).

Polymeric nanofibers may have characteristic Raman bands. These bands detect the polymer's chemical structure and chain structure. Carbon-based nanofibers show characteristic features such as the D band representing and the G band representing graphite bands in Raman spectroscopy (Pan, Bai, Pan, Liu, & Ramakrishna, 2023). The ratio of these bands to each other shows the graphitic structure and regularity of carbon structures. Raman spectroscopy was used with 514 nm Ar laser excitation to characterize the graphitic nature of nanofibers.

Surface hydrophobicity and hydrophilicity of nanofibers can be examined with the Water Contact Angle Test (Korkut & Aydin, 2024). The interaction of the surfaces of nanofibers with water determines their hydrophobic or hydrophilic properties. Water contact angle measures the angle at which a water droplet spreads on the surface of the film composed of nanofibers. This diffusion angle is observed as a high water contact angle on hydrophobic surfaces, usually 90° and above. On hydrophilic surfaces, a low water contact angle, below 90°, is observed. Hydrophilic surfaces tend to attract water, so water droplets spread on the surface. When nanofibers exhibit hydrophilic properties, the surface absorbs or interacts more with water.

Determining the flexibility and tensile properties of nanofibers is also very important in determining the application area of nanofibers. Tensile testing is performed to determine the flexibility of nanofibers. Tensile testing gives the stress-strain curves of nanofibers, showing how elastic they are and under what conditions they start to break. It is used to calculate Young's Modulus. Young's Modulus determines the sensitivity of the material to its deformation in response to applied stress. For nanofibers, this value varies depending on the production conditions and polymer type, especially for polymer nanofibers. Tensile tests of nanofibers were performed by using a texture analyser with a 5 kg load cell and 0,1 mm/s test speed (Ince Yardimci, 2022).

3. XRD and XRF Analysis of Electrospun Nanofibers

X-Ray Diffraction (XRD) is a widely used characterization method to analyze the crystal structure of materials (Q. Liu, Ouyang, Zhou, Jin, & Wu, 2021). It plays an extremely important role in determining the crystal structure, phases and

crystal sizes of nanofibers. Electrospun nanofibers can generally be found in an amorphous structure or a crystal structure. The crystal structure of nanofibers varies depending on the content of the electrospinning solution and the electrospinning parameters. XRD reveals the atomic arrangement of the material based on diffraction patterns while determining the crystalline properties of nanofibers. Therefore, XRD can determine whether the nanofiber is amorphous, microcrystalline or completely crystalline. Schematic representation of XRD is given in Fig.1.

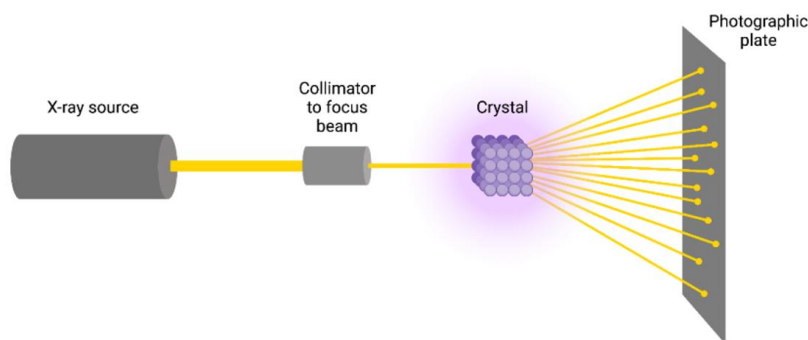


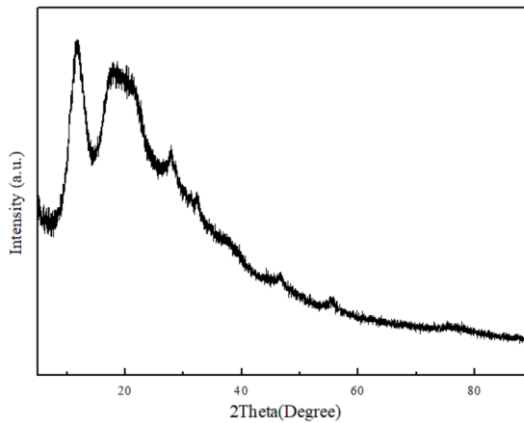
Figure 1 Schematic representation of XRD.

It is also possible to determine the presence of different phases in a material with XRD. Nanofibers can often consist of different crystalline phases. For example, the presence of different oxide phases such as Al_2O_3 , TiO_2 and ZnO in electrospun nanofibers containing metal or metal oxide can be determined by XRD. Like the crystal structure of nanofibers, crystal sizes also affect the mechanical, optical and electrical properties of the material. The average crystal sizes of nanofibers can be calculated using XRD and the Scherrer equation. Used to analyze small crystals in nanofibers, this equation serves to calculate crystal size using the width of XRD peaks. The crystal size of nanofibers is generally nanometer-sized. Crystal orientation within nanofibers can also be determined in XRD analysis. Crystal orientations also affect the macroscopic properties of nanofibers such as electrical conductivity, mechanical strength and thermal conductivity. With XRD, the properties of nanofibers, especially those with unidirectional or crystals arranged in a certain direction, can be easily analyzed.

Electrospun polymeric nanofibers may show amorphous structures. This can be observed by the width and intensity of the peaks in XRD. Amorphous Structures show a broad diffraction peak in XRD. This shows that nanofibers do

not have a regular crystal structure. Structural changes such as the transformation of the amorphous structure into a crystal structure during the electrospinning process or during the processing of nanofibers can also be observed by XRD.

XRD analysis was utilized to characterize the crystalline structure of electrospun nanofibrous mats and the XRD patterns of the polyacrylonitrile (PAN) nanofibers are illustrated in Fig. 2. XRD patterns of PAN indicated typical diffraction peaks at $2\theta=29^\circ$, respectively, corresponding to (110) plane of PAN (Y. Lu et al., 2013). Broad diffraction peaks of amorphous carbon were seen at around $10\text{--}12^\circ$, $27\text{--}29^\circ$, and $45\text{--}47^\circ$ in line with the literature (Pech & Maensiri, 2019).



In summary, XRD is a very important characterization method for material characterization used to examine the crystal structure, phases, crystal sizes, texture order, and amorphous structures of nanofibers. Understanding the crystal properties of the material obtained during the production of nanofibers is necessary to determine the usage areas of these materials. XRD provides a better understanding of the structural properties of nanofibers and thus more effective applications can be made in fundamental fields such as nanotechnology, materials science, engineering and health.

X-ray fluorescence (XRF) spectroscopy is used to analyze the chemical composition of materials (Machado, Fonseca, Teixeira, Catalani, & Rodrigues, 2023). It is also involved in the characterization study of electrospun nanofibers. With XRF, the chemical composition of the elements on the surface of nanofibers can be determined. This allows different types of materials and layers to be identified. When we examine the working principle if the atom is excited by high-energy radiation such as X-rays, this high-energy input raises the electrons in close orbits to a higher energy level. When the excited electrons return to their

initial energy levels, they give back the excess energy they gained in the form of X-rays with a wavelength of 0.1-50 Å. This secondary emission of X-rays is called fluorescence. The wavelength of these radiations given by the elements is different and distinctive for each element. Therefore, by determining the wavelength of the fluorescence radiation, the type of element and the concentration of the element are determined from the intensity of the fluorescence beam. One of the key advantages of XRF is that it determines the chemical composition of nanofibers without damaging them.

XRF is generally used to investigate the presence of metallic elements such as Fe, Cu, Ti, Al and some heavy elements such as Pb, Hg. XRF can also be used to detect the presence of harmful or toxic elements, especially in nanofibers. In this way, it can be evaluated whether nanofibers are harmful to the environment and health.

Thin coatings, additives and foreign substances on the nanofiber surface can be detected with XRF. Thus, the composition of the coating material applied to the nanofiber surface or the impurities used in the production process of the nanofiber can be analyzed. Homogeneity and elemental distribution of the material can also be tested with XRF. Additionally, if the nanofibrous film consists of different layers, XRF can also be used to determine the fundamental differences between the layers. XRF is an effective method in cases where a layer has a different chemical composition from the other layer.

In general, XRF is an analysis method that provides information about the determination of the chemical composition of nanofibers, surface analysis, examination of element distribution and layered structures. It has an important place in nanotechnology and material science. Quality control processes are of great importance in the production of nanofibers and their use in different applications.

4. Conclusions

In this chapter, nanofibers obtained by the electrospinning method are discussed and characterization methods of these nanomaterials are introduced. The importance of nanofiber characterization in determining nanofiber quality and application area has been evaluated. The physical, chemical, electrical, optical, magnetic, and mechanical properties of nanomaterials directly depend on their elemental content and crystal properties, as well as their size. For this reason, XRD and XRF analysis methods are specifically mentioned.

References

- Fadil, F., Affandi, N. D. N., Misnon, M. I., Bonnia, N. N., Harun, A. M., & Alam, M. K. (2021). Review on electrospun nanofiber-applied products. *Polymers*, 13(13), 2087.
- Fahimirad, S., Fahimirad, Z., & Sillanpää, M. (2021). Efficient removal of water bacteria and viruses using electrospun nanofibers. *Science of the total environment*, 751, 141673.
- Ince Yardimci, A. (2022). Comparative Study of the Structural, Mechanical and Electrochemical Properties of Polyacrylonitrile (PAN)-Based Polypyrrole (PPy) and Polyvinylidene Fluoride (PVDF) Electrospun Nanofibers. *Journal of Macromolecular Science, Part B*, 61(9), 1103-1115.
- Ince Yardimci, A., Aypek, H., Ozturk, O., Yilmaz, S., Ozcivici, E., Mese, G., & Selamet, Y. (2019). CNT incorporated polyacrylonitrile/polypyrrole nanofibers as keratinocytes scaffold. *Journal of Biomimetics, Biomaterials and Biomedical Engineering*, 41, 69-81.
- Ince Yardimci, A., Baskan, O., Yilmaz, S., Mese, G., Ozcivici, E., & Selamet, Y. (2019). Osteogenic differentiation of mesenchymal stem cells on random and aligned PAN/PPy nanofibrous scaffolds. *Journal of biomaterials applications*, 34(5), 640-650.
- Ince Yardimci, A., Mutlu, D., Istifli, E. S., Arslan, S., Mahaleh, S. P. G., Yagmurcukardes, N., . . . Liman, R. (2024). Polyacrylonitrile (PAN)/carbon nanotube (CNT) electrospun nanofibers: synthesis, characterization, their biocompatibility for L929 fibroblast cells and molecular docking studies. *International Journal of Polymeric Materials and Polymeric Biomaterials*, 73(16), 1418-1428.
- Ince Yardimci, A., Yagmurcukardes, N., Yagmurcukardes, M., Capan, I., Erdogan, M., Capan, R., . . . Acikbas, Y. (2022). Electrospun polyacrylonitrile (PAN) nanofiber: preparation, experimental characterization, organic vapor sensing ability and theoretical simulations of binding energies. *Applied Physics A*, 128(3), 173.
- Korkut, I., & Aydin, E. S. (2024). Electrospun PAN-PS membranes with improved hydrophobic properties for high-performance oil/water separation. *Separation and Purification Technology*, 331, 125590.
- Kumar, J. A., Krithiga, T., Manigandan, S., Sathish, S., Renita, A. A., Prakash, P., . . . Hosseini-Bandegharaei, A. (2021). A focus to green synthesis of metal/metal based oxide nanoparticles: Various mechanisms and applications towards ecological approach. *Journal of Cleaner Production*, 324, 129198.
- Li, S., Cui, Z., Li, D., Yue, G., Liu, J., Ding, H., . . . Zhao, Y. (2019). Hierarchically structured electrospinning nanofibers for catalysis and energy storage. *Composites Communications*, 13, 1-11.

- Liu, Q., Ouyang, W.-C., Zhou, X.-H., Jin, T., & Wu, Z.-W. (2021). Antibacterial activity and drug loading of moxifloxacin-loaded poly (vinyl alcohol)/chitosan electrospun nanofibers. *Frontiers in Materials*, 8, 643428.
- Liu, X., Wang, C., Cai, Z., Hu, Z., & Zhu, P. (2022). Fabrication and characterization of polyacrylonitrile and polyethylene glycol composite nanofibers by electrospinning. *Journal of Energy Storage*, 53, 105171.
- Lopez Marquez, A., Gareis, I. E., Dias, F. J., Gerhard, C., & Lezcano, M. F. (2022). Methods to characterize electrospun scaffold morphology: a critical review. *Polymers*, 14(3), 467.
- Lu, T., Cui, J., Qu, Q., Wang, Y., Zhang, J., Xiong, R., . . . Huang, C. (2021). Multistructured electrospun nanofibers for air filtration: a review. *ACS applied materials & interfaces*, 13(20), 23293-23313.
- Lu, Y., Li, Y., Zhang, S., Xu, G., Fu, K., Lee, H., & Zhang, X. (2013). Parameter study and characterization for polyacrylonitrile nanofibers fabricated via centrifugal spinning process. *European Polymer Journal*, 49(12), 3834-3845.
- Machado, R. C., Fonseca, K. T., Teixeira, V. C., Catalani, L. H., & Rodrigues, L. C. (2023). Development of a red persistent luminescent composite: Electrospun nanofiber polymer coating prevents emission quenching by water. *Materials Today Communications*, 35, 105965.
- Nadaf, A., Gupta, A., Hasan, N., Ahmad, S., Kesharwani, P., & Ahmad, F. J. (2022). Recent update on electrospinning and electrospun nanofibers: current trends and their applications. *RSC advances*, 12(37), 23808-23828.
- Pan, X., Bai, L., Pan, C., Liu, Z., & Ramakrishna, S. (2023). Design, fabrication and applications of electrospun nanofiber-based surface-enhanced raman spectroscopy substrate. *Critical Reviews in Analytical Chemistry*, 53(2), 289-308.
- Pech, O., & Maensiri, S. (2019). Electrochemical performances of electrospun carbon nanofibers, interconnected carbon nanofibers, and carbon-manganese oxide composite nanofibers. *Journal of Alloys and Compounds*, 781, 541-552.
- Saleh, H. M., & Hassan, A. I. (2023). Synthesis and characterization of nanomaterials for application in cost-effective electrochemical devices. *Sustainability*, 15(14), 10891.
- Salem, S. S., Hammad, E. N., Mohamed, A. A., & El-DougDoug, W. (2022). A comprehensive review of nanomaterials: Types, synthesis, characterization, and applications. *Biointerface Res. Appl. Chem*, 13(1), 41.
- Yagmurcukardes, N., Ince Yardimci, A., Yagmurcukardes, M., Capan, I., Erdogan, M., Capan, R., & Acikbas, Y. (2023). Electrospun polyacrylonitrile (PAN)/polypyrrole (PPy) nanofiber-coated quartz crystal microbalance for sensing volatile organic compounds. *Journal of Materials Science: Materials in Electronics*, 34(27), 1869.

- Yan, Y., Liu, X., Yan, J., Guan, C., & Wang, J. (2021). Electrospun nanofibers for new generation flexible energy storage. *Energy & Environmental Materials*, 4(4), 502-521.
- Yardimci, A. İ., Tanoğlu, M., Yilmaz, S., & Selamet, Y. (2020). Effect of CNT incorporation on PAN/PPy nanofibers synthesized by electrospinning method. *Turkish Journal of Chemistry*, 44(4), 1002-1015.
- Zaarour, B., Zhu, L., & Jin, X. (2020). A review on the secondary surface morphology of electrospun nanofibers: formation mechanisms, characterizations, and applications. *ChemistrySelect*, 5(4), 1335-1348.
- Zhao, J., Li, Z., Lv, S., Wang, M., Li, C., Li, X., . . . Wang, F. (2023). Electrospun advanced nanomaterials for in situ transmission electron microscopy: Progress and perspectives. *InfoMat*, 5(12), e12483.



CHAPTER 25

Chemometric Evaluation of Physicochemical Properties and Bioactive Compounds of Hot Air and Microwave Dried Potatoes by FTIR Spectroscopy

Katibe Sinem Coruk¹ & Hande Baltacıoğlu²

¹ Arş. Gör. Dr., Niğde Ömer Halisdemir Üniversitesi, Mühendislik Fakültesi, Gıda Mühendisliği Bölümü, <https://orcid.org/0000-0001-5645-7200>

² Doç. Dr., Niğde Ömer Halisdemir Üniversitesi, Mühendislik Fakültesi, Gıda Mühendisliği Bölümü, <https://orcid.org/0000-0003-0774-0872>

Introduction

Potato

Potatoes (*Solanum tuberosum* L), grown in about 160 countries worldwide with an annual production of 388 million metric tons, are an important staple food for humans and the fourth largest crop grown worldwide after rice, wheat, and maize (Singh and Saldaña, 2011; FAO 2024). After harvest, fresh potato tubers are composed of about 80% water and 20% dry content, of which is starch (60–80%) (Coruk and Baltacıoğlu, 2022). In addition to vitamins B1, B3, and B6, potatoes are a good source of minerals like potassium, phosphorus, and magnesium. They also include pantothenic acid, folate, and riboflavin (Ekin 2011; FAO 2008). Furthermore, some potato varieties that are fleshed in color contain important bioactives such as anthocyanins (Brown, 2005). The main class of visible polyphenols that give potatoes their red, purple, and blue colors is called anthocyanins (De Jong et al., 2004; Stushnoff et al., 2008). It has been demonstrated that genotypes of potatoes with pigments have far higher amounts of anthocyanins and antioxidant activity than cultivars with white and yellow tubers, particularly those with purple and red skin and/or flesh (Stushnoff et al., 2008; Thompson et al., 2009). As a result, a potato with a high anthocyanin content may be a novel cultivar with improved health advantages.

In addition to the nutritional value of potatoes, they can be processed into different products as fresh due to their many biofunctional properties, as well as reducing the risk of spoilage and increasing the nutritional value of the products, they can be dried and added to different products. For this reason, in recent years, drying methods that preserve the nutritional properties of potatoes in the best way have been developed (Waseem et al., 2022).

Drying

In addition to being used directly as a raw material, potatoes can also be dried to stop quality degradation and loss during post-harvest storage. The enzyme activity slows down and the microbial activity that causes spoiling ends as the potato's moisture level drops during the drying process (Sidhu et al., 2019). As a result, there is growing interest in various drying methods to reduce the potential quality losses in the finished product during drying.

Traditional drying techniques include hot air, vacuum, and freeze-drying. Each drying method has different advantages and disadvantages (Sun et al., 2019). In contrast to other drying methods, the microwave is a novel technique. In order to produce high-quality powders, it is utilized both alone and in

combination with other drying techniques, particularly in fruit, vegetable, and grain products (Coruk and Baltacıoğlu, 2024a, Coruk and Baltacıoğlu, 2024b). In these studies, physicochemical analysis were performed on potato powder samples obtained by different conditions with RSM during hot air and microwave drying (Coruk and Baltacıoğlu 2022; Coruk and Baltacıoğlu 2024a; Coruk and Baltacıoğlu 2024b), and comparisons of two different potato varieties and two different drying methods were made with the help of chemometric analysis and FTIR spectroscopy.

FTIR spectroscopy and chemometric analysis

FTIR spectroscopy is a vibrational spectroscopy technique that can easily determine the specific bands of molecules. In recent years, FTIR spectroscopy with chemometric analysis has been used to determine bioactive compounds and physicochemical properties of foods. Baltacıoğlu et al. (2024a) examined the changes in bioactive content in fried yellow and purple-fleshed potatoes with pulsed electric field (PEF) pretreatment by chemometric analysis. Uslu et al. (2024) analyzed the effects of different cooking techniques and oils on bioactive compounds in potatoes that have different flesh colors and were compared by the chemometric analysis method. The red cabbage was examined in terms of encapsulation ability and color value with hot air and freeze-drying methods and differences between drying methods were revealed with the help of chemometric analysis (Baltacıoğlu et al., 2024). In this chapter, the physicochemical properties and bioactive compounds of potato powders with different flesh colors obtained by optimization in previous studies were investigated using FTIR spectroscopy and chemometric analysis.

Material and Methods

Hot air and microwave dried potato powders (yellow and purple-fleshed) obtained by optimization in previous studies were used (Coruk, 2024).

Analysis of potato powders

Solvent extraction of bioactive compounds

Bioactive substances were extracted from potato powders using methanol (80%, Sigma) with 1% HCl (Honeywell, Germany). To extract the phenolic compounds, 0.25 g of yellow-fleshed potato powder was mixed with 10 mL of extraction solution, and 1 g of purple-fleshed potato powder was combined with 50 mL of extraction solution, and they were agitated at 40 rpm for 4 hours at 25 °C. To separate the clear portion, the mixture was centrifuged (Nüve brand NR

800R model NR 800R, Turkey) at 6000 g at 4°C for 15 minutes (Coruk and Baltacıoğlu 2022).

Determination of Total Phenolic Content (TPC)

The total amount of phenolic compounds in the extracts was calculated using the method suggested by Baltacıoğlu et al. (2021).

Determination of Antioxidant activity (AA)

The Horuz et al. (2018) approach was utilized to ascertain the samples' antioxidant activity (AA).

Determination of Total Monomeric Anthocyanin (TMA) content

The pH differential method was used to assess the total monomeric anthocyanin (TMA) content of dried potato powders (Coruk and Baltacıoğlu 2022).

Determination of Color

The Konica-Minolta (CR400, Osaka, Japan) colorimeter was used to measure the L^* , a^* , and b^* values (Horuz et al. 2017). In processes where enzymatic browning occurs, the browning index (BI) is a crucial quantity, and the brown hue indicates the product's degradation. To ascertain the impact of drying on the browning of the yellow-fleshed potatoes, BI values were computed using equations (1) and (2) (Maskan 2006). To find out how drying affected the purple-fleshed potatoes, chroma values were also computed using equation (3).

$$BI = [100(x - 0,31)] / 0,172 \quad (1)$$

$$x = (a^* + 1,75L^*) / (5,645L^* + a^* - 3,012b^*) \quad (2)$$

$$\text{Chroma} = C^* = [(a^*)^2 + (b^*)^2]^{1/2} \quad (3)$$

Determination of Starch Ratio

The approach of Coruk and Baltacıoğlu (2022) was utilized to ascertain the samples' starch ratio. To obtain the starch ratio (%), the calculated optical rotation degree was entered into equation (4).

$$\alpha_{20}^D = \frac{\alpha}{L \times C} \quad (4)$$

$$\% \text{ Starch ratio} = \frac{10000 \times \alpha}{\alpha_{20}^D \times L \times m}$$

- α : Degree of rotation read on the polarimeter
- C: Concentration of pure potato starch (g/100mL)
- α_{20}^D : Specific degree of conversion of potato starch
- L : Polarimetre tube length (dm)
- m: Sample quantity (g)

Determination of bioactive compounds by HPLC

The HPLC method was applied to determine the phenolic compounds of potato powders (Okur et al., 2019). Before injection, the extracts were passed through a 0.45 μ m Teflon membrane filter. The extracts were then injected into HPLC (LC-20A/Prominence, Shimadzu Corporation, Kyoto, Japan) in a volume of 20 μ l. The HPLC system consists of a pump, degasser, control oven (CTO-10AS VP, Shimadzu), and a detector (UV-VIS detector, SPD-20A, Shimadzu Corporation, Kyoto, Japan). Polyphenols were separated using a C18 column (GL Sciences, 250x4.60 mm, 5 micron, Japan). The column temperature is 30 °C. Separation for phenolic compounds was carried out by applying a gradient program with a binary solvent system. Colorless phenolic compounds were detected at 320 nm and colored phenolic compounds (anthocyanins) at 520 nm. The mobile phase consists of 5% formic acid (A) and 20% A + 80% acetonitrile ACN (B). The flow rate is 1.0 ml/min throughout the run. The gradient program for colorless phenolic compounds was applied as given in Table 1. Colored and colorless phenolic content retention times were defined by comparison with relevant standards. The gradient program for colored phenolic compounds was applied as given in Table 2.

Table 1. Gradient program for colorless phenolic compounds (Coruk, 2024)

Time (minute)	A (%)	B (%)
0	100	0
15	90	10
90	40	60
90,01	0	100
93	0	100
93,01	100	0
98	100	0

Table 2. Gradient program for colored phenolic compounds (Coruk, 2024)

Time (minute)	A (%)	B (%)
0	90	10
25	70	30
25,01	0	100
28	0	100
28,01	90	10
33	90	10

Determination of anthocyanins by LC-MS-MS

Extraction of anthocyanins

Twenty milliliters of methanol-water (80:20, v/v) were added to a centrifuge tube containing two grams of samples. Using a magnetic stirrer, the extraction process lasted for sixty minutes. The mixture was then centrifuged for 15 minutes at 4°C and 5500 rpm. Prior to injection, the supernatant was passed through a membrane filter with a hole size of 0.45 µm (Kelebek et al., 2020).

According to Keskin et al. (2021), the LC-DAD-ESI-MS/MS with negative and positive ionization modes was used to analyze anthocyanins. ChemStation software was utilized in conjunction with an Agilent 1100 HPLC system (Agilent Technologies, Palo Alto, CA, USA). A Beckman Ultrasphere ODS column (4.6 mm × 250 mm; Rossy CDG, France) was used for the analysis. Two solvents, Solvent A (water/formic acid, 99:1; v/v) and Solvent B (acetonitrile/solvent A,

60:40; v/v), made up the mobile phase. Kelebek and Selli (2011) employed a 0.5 ml/min flow rate at 25°C to elute the phenolic chemicals in the samples. The UV-VIS spectra's peaks (200–600 nm) were acquired and analyzed. Phenolic compounds were identified using the retention times as UV spectra were compared to authentic standards and then confirmed by using LC-MS/MS spectrometer (Agilent 6430) with a source of electrospray ionization (ESI) by using the following parameters: drying gas of N₂ at 12 l/min, capillary temperature of 400°C and nebulizer pressure of 45 psi of ESI/MS. For quantification, standard phenolic calibration curves were used (Kelebek et al., 2015). The limit of detection and quantification were calculated using signal-to-noise ratio (S/N) values of 10 and 3, respectively.

Fourier Transform Infrared (FTIR) spectroscopy

The functional bands in the potato powders were determined using Fourier transform infrared (FTIR) spectroscopy. For this purpose, the absorption spectra of the lyophilized samples were obtained in the 400-4000 cm⁻¹ region by performing 128 scans at a resolution of 2 cm⁻¹ using FTIR spectroscopy (Bruker, Germany) with an ATR cell in the Central Research Laboratory of Niğde Ömer Halisdemir University. Vector normalization was applied to all FTIR spectra before chemometric analysis by OPUS program (version 8.1, Bruker Optics, Germany).

Chemometric analysis

Principal component analysis (PCA) was used to discriminate different drying methods and potato varieties, and the results are presented as a score graph. PCA analysis was carried out using Minitab 17. The physicochemical properties and bioactive contents of the samples were estimated using FTIR spectral data with PLS regression. The FTIR spectral data were used as X variables (predictors), and each of the analysis results was used as a Y variable (responses) to generate PLS models as described previously (Baltacıoğlu et al., 2024b).

Statistical Analysis

One-way ANOVA was employed in the data analysis, and the Minitab 17 application was used to examine the physicochemical analysis results within a 95% confidence level. Tukey's multiple comparison test was used to find application-specific differences. At least three repetitions of each experiment were carried out, and for each repetition, the analysis was done three times.

Results and Discussion

Analysis results of the yellow-fleshed potato dried under optimum conditions were given in Table 3, while analysis results of the purple-fleshed potato were shown in Table 4.

Table 3. Results of analysis of yellow-fleshed potato powder obtained by different drying methods (Coruk, 2024)

	Yellow-fleshed potato powder dried with hot air	Yellow-fleshed potato powder dried with microwave
Total phenolic content (mg GAE/kg dry weight)	2290,24 ± 39,37 ^{de}	4656,19 ± 216,37 ^{ab}
Antioxidant activity (%)	34,30 ± 2,39 ^c	45,46 ± 1,16 ^b
Starch Ratio (%)	81,97 ± 1,22 ^a	84,06 ± 1,40 ^a
Browning Index (BI)	32,23 ± 0,34 ^b	44,21 ± 0,28 ^a

Table 4. Results of analysis of purple-fleshed potato powder obtained by different drying methods (Coruk, 2024)

	Purple-fleshed potato powder dried with hot air	Purple-fleshed potato powder dried with microwave
Total phenolic content (mg GAE/kg dry weight)	5122,14 ± 343,45 ^a	3527,05 ± 253,71 ^{bc}
Antioxidant activity (%)	56,99 ± 0,71 ^a	57,078 ± 0,85 ^a
Starch Ratio (%)	85,18 ± 3,86 ^a	86,37 ± 1,56 ^a
Chroma	11,58 ± 0,25 ^a	9,61 ± 0,073 ^a
Total Monomeric Ant-hocyanin Content (mg/kg)	2623,40 ± 288,90 ^a	2084.47 ± 67,77 ^a

It was seen that the total phenolic content and antioxidant activity of yellow-fleshed potato powder obtained by microwave drying was higher ($p\leq0.05$) than that obtained by hot air drying. However, the total phenolic content, antioxidant

activity, and the total monomeric anthocyanin value of purple-fleshed potato powder obtained by hot air drying were higher ($p \leq 0.05$) than those obtained by microwave drying. It was observed that different drying methods may have different effects on different potato varieties.

Bioactive component results determined by HPLC

Bioactive components identified and quantified in potato powders were shown in Table 5. Phenolic acids were found as chlorogenic acid, caffeic acid, p-coumaric acid, ferulic acid, rutin in yellow-fleshed potato powders. In addition to these phenolic compounds, neochlorogenic acid was found in purple-fleshed potato powders (Table 5, Figure 1). It has been reported in the literature that there is a wide variation in phenolic acid profile in different potato genotypes (Kim et al., 2019). The diverse phenolic acids in different genotypes can be attributed to the complex biosynthesis pathway of phenolic acids in potatoes (Shao et al., 2015). When anthocyanin analysis was performed for purple fleshed potatoes, the peaks could not be identified by HPLC and given as cyanidin-derivative, therefore anthocyanins were identified more precisely by LC-MS-MS (Table 6).

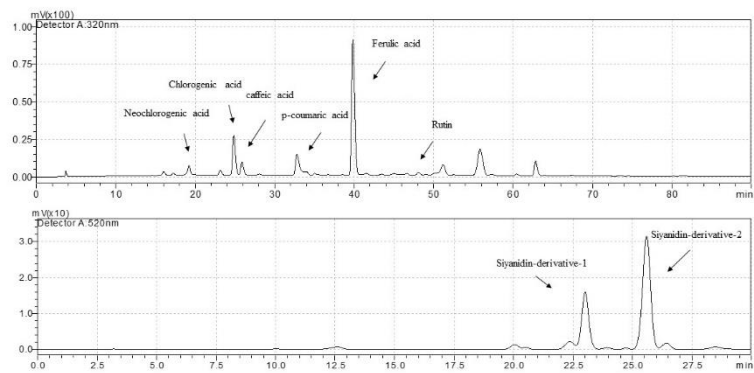


Figure 1. Identified bioactive components in potato powders (Coruk, 2024)

Table 5. Bioactive components identified and quantified in potato powders (Coruk, 2024)

Sample	Phenolic compounds (mg/100g dry weight)							Cyanidin-derivative-1 (cyanidin-3-glucoside equivalent)	Cyanidin-derivative-2 (cyanidin-3-glucoside equivalent)
	Neochlorogenic acid	Chlorogenic acid	Caffeic acid	p-coumaric acid	Ferulic Acid	Rutin			
Potato powder									
Yellow-fleshed potato powder dried with hot air	-	2.635 ± 0.017 ^c	1.452 ± 0.0009 ^d	1.200 ± 0.002 ^c	0.249 ± 0.00006 ^f	0.914 ± 0.005 ^{bc}	-	-	
Yellow-fleshed potato powder dried with MW	-	2.399 ± 0.023 ^{cd}	1.401 ± 0.008 ^d	1.200 ± 0.010 ^c	0.222 ± 0.078 ^f	0.891±0.029 ^{bc}	-	-	
Purple-fleshed potato powder dried with hot air	0.045 ±0.011 ^b	5.575 ± 0.365 ^a	0.973 ± 0.025 ^f	1.180 ± 0.061 ^c	9.955 ± 0.737 ^a	1.099 ±0.067 ^a	3.160 ± 0.30 ^a	6.370 ± 0.663 ^a	
Purple-fleshed potato powder dried with MW	0.130 ±0.007 ^a	5.722 ± 0.256 ^a	1.798 ± 0.033 ^b	1.587 ± 0.023 ^a	9.299 ± 0.056 ^{ab}	1.109 ±0.087 ^a	2.062 ± 0.331 ^b	3.957 ± 0.644 ^b	

As shown in Table 5, chlorogenic acid was the most abundant phenolic compound in potato varieties. In addition, more chlorogenic acid was detected in purple-fleshed potatoes than in yellow-fleshed potatoes. The excess of chlorogenic acid over other phenolic compounds is consistent with the comparisons made in the literature (Ru et al., 2019; Reddivari et al., 2007).

Anthocyanin compounds identified by LC-MS-MS

Anthocyanin compounds identified and quantified in potato powders obtained by hot air and microwave drying of purple-fleshed potatoes were shown in Table 6.

Table 6. Identified and quantified anthocyanin compounds in the samples by LC-MS-MS

Anthocyanins (mg/100g)	Retention time (min)	Purple-fleshed po- tato powder dried with MW	Purple-fleshed po- tato powder dried with hot air
Cy 3-(6'''-caffeoyl soph)-5-glc	42.51	0.68±0.02 ^b	0.74±0.01 ^a
Cy 3-feruloyl soph- 5-glc	45.29	11.10±0.06 ^b	18.63±0.06 ^a
Peo 3-feruloyl soph-5-glc	42.01	0.86±0.01 ^b	1.20±0.001 ^a
Peo 3-caf-fer soph- 5-glc	46.82	3.15±0.03 ^b	5.29±0.001 ^a
Cy 3-caf-p-hb soph-5-glc	43.61	1.98±0.04 ^b	3.08±0.01 ^a
Peo 3-caf-p-hb soph-5-glc	45.55	26.35±0.04 ^b	42.89±0.04 ^a
Peo 3-fer-p-hb soph-5-glc	47.85	0.37±0.001 ^b	0.46±0.001 ^a

As shown in Table 6 six different anthocyanin compounds were identified in purple-fleshed potato powders. Among these anthocyanin compounds, Peo 3-caf-p-hb soph-5-glc and Cy 3-feruloyl soph-5-glc were found the most abundant anthocyanins. It was seen that hot air drying preserves the anthocyanin content more than microwave drying methods and the quantity of anthocyanins was more than the potato powder obtained by the microwave drying method. In the studies conducted in the literature, it has been stated that the chemical structure of purple-fleshed potato has an excellent anthocyanin source consisting of cyanidin, peonidin, pelargonidin, and delphinidin derivatives in the form of monoacylation and diacetylation, but the most abundant anthocyanins are peonidin derivatives (Li et al.. 2019).

Result of FTIR spectroscopy analysis

The results of FTIR spectroscopy analysis of potato powders obtained under optimum conditions were shown in Figure 2.

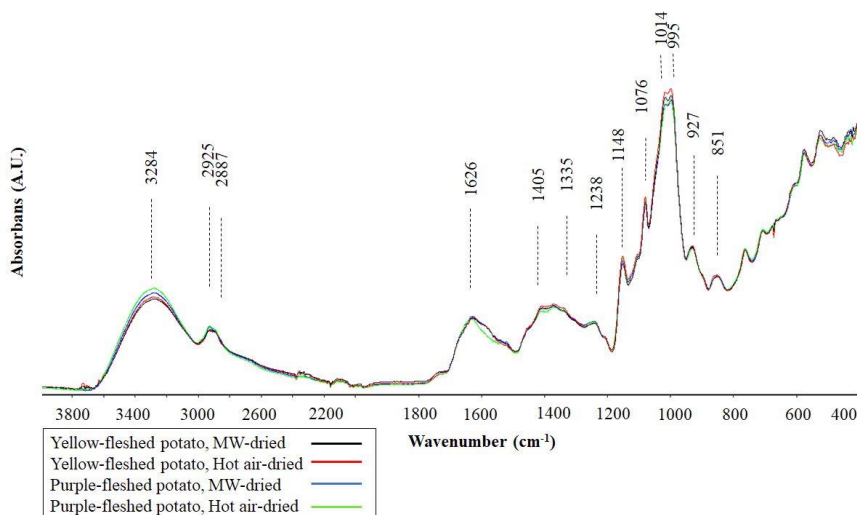


Figure 2. Results of FTIR spectroscopy analysis of potato powders

According to the FTIR spectra the peaks observed in the 3800 cm^{-1} - 3200 cm^{-1} region are due to the OH stretching groups and N-H stretching groups (Amide A) band of polysaccharides. The broad peak at 3280 cm^{-1} contains the amide A band. The region between 3000 - 2800 cm^{-1} includes asymmetric and symmetric vibrations of methylene groups of lipids. 1626 cm^{-1} was due to the amide I band. The peaks at 1500 - 1000 cm^{-1} were C-H and O-H vibrations of phenolic compounds. The bands at 1000 cm^{-1} - 800 cm^{-1} were the stretching vibrations of C-O, C-C and C-H polysaccharides. As seen from the peaks, different drying methods and potato varieties affected the peaks differently.

Chemometric analysis

Potato samples dried with hot air and microwave were differentiated using PCA analysis (Figure 3a). PCA showed four groups of yellow-fleshed potatoes dried with hot air, yellow-fleshed potatoes dried with microwave, purple-fleshed potatoes dried with hot air, purple-fleshed potatoes dried with microwave. The score plot for the first two components was shown in Figure 3a and accounted for 88.0% of the total variance. PC1 explained 56.1% of the total variance whereas PC2 explained 31.9% of the total variance. The purple-fleshed potato powders were mainly located on the negative axis of the first component (PC1), while the yellow-fleshed potato powders were located on the positive axis of PC1. In other words, powders obtained from different varieties were separated according to PC1. However, the powders obtained by different drying methods were also

separated according to PC2. PCA was successfully used to separate fried potato samples into groups using FTIR spectra (Baltacıoglu et al., 2024 a).

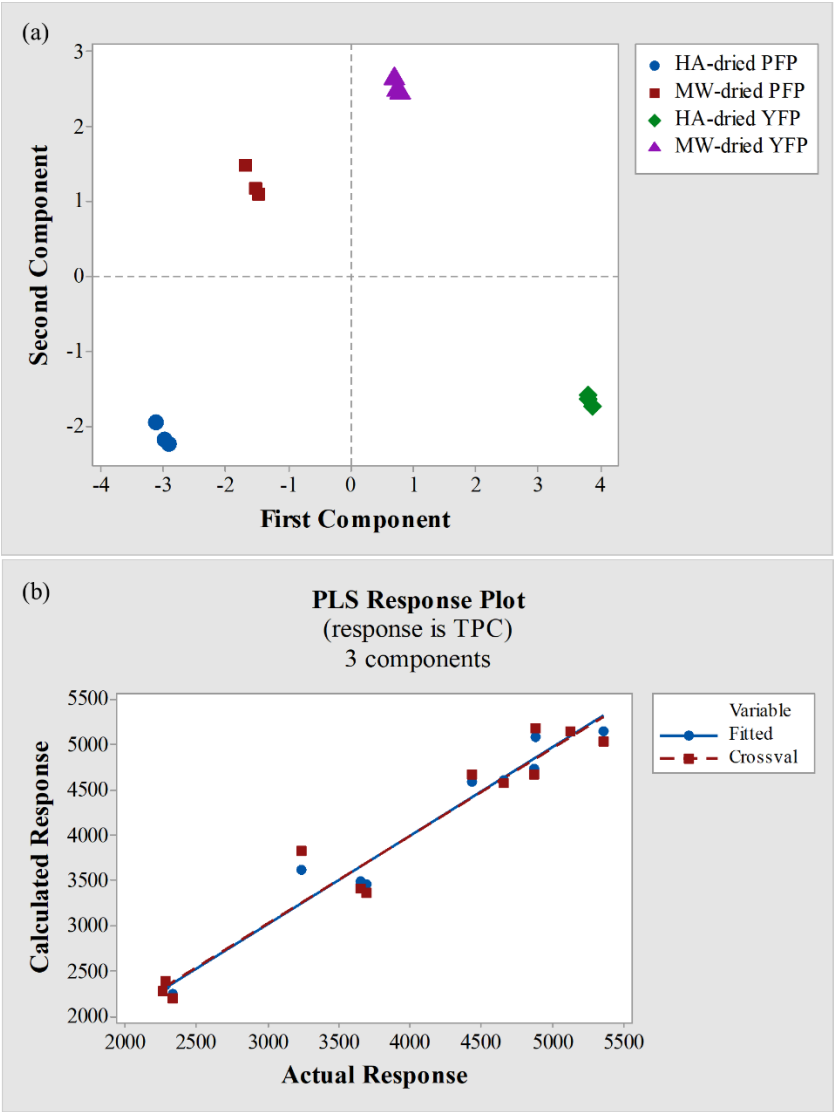


Figure 3. (a) PCA score plot of the FTIR spectra of potato powders, (b) PLS regression plot of actual versus predicted response for total phenolic content (TPC), HA: Hot air, MW: Microwave, YFP; Yellow-fleshed potato, PFP; Purple-fleshed potato

Partial least square (PLS) models were developed to determine the color, TPC, antioxidant activity, and TMA content of the samples using FTIR spectral data (Table 7), and all models showed a good correlation between the calculated and

predicted responses. The PLS response plot for the model of TPC was shown in Figure 3b. Moreover, models were statistically significant ($p \leq 0.05$), and the differences between the RMSE values were detected as small. Based on PLS regression analysis for fried potatoes was performed to develop good models by Baltacıoğlu et al. (2024a).

Table 1. PLS regression analysis for the prediction of the physicochemical properties and bioactive compounds of potato powders using FTIR spectral data

Parameters	Components	r _{cv}	r _{Pre}	RMSEC	RMSEP
TPC	3	0.9744	0.9421	194.346	185.302
Antioxidant activity	3	0.9848	0.9648	1.286	1.226
Color	6	0.99999	0.99992	0.058	0.055
TMA	6	0.9999	0.9991	12.872	12.273

Factors; set of orthogonal factors that account for most of the variation in the response.

r_{cv}; correlation coefficient of cross-validation

r_{Pre}; correlation coefficient of prediction

RMSEC; root mean square error of calibration

RMSEP; root mean square error of prediction

Conclusion

In terms of the methods used, microwave drying was found to be more effective in the production of yellow-fleshed potato powder in terms of preserving the color with short processing conditions. However, hot air drying was more effective for the production of purple-fleshed potato powder, especially in terms of preserving anthocyanin pigments. In addition, phenolic compounds and antioxidant activity were more preserved in purple-fleshed potatoes after hot air drying. It is thought that it will contribute to further studies in terms of showing that different drying methods may have different effects on different types of potatoes.

References

- Baltacıoğlu H. Baltacıoğlu C. Okur I. Tanrıvermiş A. Yalıcı M (2021). Optimization of microwave-assisted extraction of phenolic compounds from tomato: Characterization by FTIR and HPLC and comparison with conventional solvent extraction. *Vibrational Spectroscopy* 113:103204. <https://doi.org/10.1016/j.vibspec.2020.103204>
- Baltacıoğlu. C.. Yetişen. M.. Baltacıoğlu. H.. Karacabey. E.. & Buzrul. S. (2024a). Impacts of pulsed electric fields (PEF) pre-treatment on the characteristics of fried yellow-and purple-fleshed potatoes: a chemometric-assisted FTIR study. *Potato Research*. 67(3). 1027-1048.
- Baltacıoğlu. C.. Keskin. O.. Baltacıoğlu. H.. & Ağçam. E. (2024b). Encapsulation and drying methods in the production of powdered red cabbage (*Brassica oleracea* L.): Chemometrics and Fourier transform infrared spectroscopy. *Food Science and Technology International*. 10820132241238261.
- Brown. C.R. (2005). Antioxidants in Potato. *American Journal of Potato Research*. 82. 163-172. <https://doi.org/10.1007/BF02853654>
- Coruk KS. Baltacıoğlu H (2022). Determination of the effect of different drying methods on the physicochemical properties of potato powder using multivariate analysis. *Turkish J Agriculture-Food Sci Technol*. 10(7):1300-1307. <https://doi.org/10.24925/turjaf.v10i7.1300-1307.5243>
- Coruk. K.S. (2024). *Optimisation of hot air and microwave drying conditions for purple and yellow fleshed potatoes and application of dry powder to different products*. Doctoral thesis. Niğde Ömer Halisdemir University Institute of Science and Technology. Niğde.
- Coruk. K. S.. & BALTACIOĞLU. H. (2024a). Optimization of hot air drying conditions of purple-fleshed potato. *Niğde Ömer Halisdemir Üniversitesi Mühendislik Bilimleri Dergisi*. 13(2). 1-1.
- Coruk. K. S.. & Baltacıoğlu. H. (2024b). Optimization of Process Parameters for Microwave Drying of Yellow-and Purple-Fleshed Potatoes. *Potato Research*. 1-20.
- De Jong. W. S.. Eannetta. N. T.. De Jong. D. M.. & Bodis. M. (2004). Candidate gene analysis of anthocyanin pigmentation loci in the Solanaceae. *Theoretical and Applied Genetics*. 108. 423-432.
- Ekin. Z. (2011). Some analytical quality characteristics for evaluating the utilization and consumption of potato (*Solanum tuberosum* L.) tubers. *African J Biotechnol* 10(32):6001-6010.
- FAO (2008) Food and Agriculture Organization of the United Nations. International Year of the Potato: The Potato. Available from: <http://www.fao.org/potato-2008/en/potato/index.html>
- FAO (2024). Food and agriculture organization crop production report

- Horuz. E. Bozkurt. H. Karataş. H. & Maskan. M (2017). Effects of hybrid (microwave-convectional) and convectional drying on drying kinetics. total phenolics. antioxidant capacity. vitamin C. color and rehydration capacity of sour cherries. *Food Chem* 230:295–305. <https://doi.org/10.1016/j.foodchem.2017.03.046>
- Horuz. E. Bozkurt. H. Karataş. H. & Maskan. M. (2018). Comparison of quality. bioactive compounds. textural and sensorial properties of hybrid and convection-dried apricots. *J Food Measure Characteriz* 12(1):243–256. <https://doi.org/10.1007/s11694-017-9635-x>
- Kelebek. H.. & Selli. S. (2011). Characterization of phenolic compounds in strawberry fruits by RP-HPLC-DAD and investigation of their antioxidant capacity. *Journal of Liquid Chromatography & Related Technologies*. 34(20). 2495-2504.
- Kelebek. H.. Kesen. S.. & Selli. S. (2015). Comparative study of bioactive constituents in Turkish olive oils by LC-ESI/MS/MS. *International Journal of Food Properties*. 18(10). 2231-2245.
- Kelebek. H.. Selli. S.. Sevindik. O.. (2020). Screening of phenolic content and antioxidant capacity of Okitsu mandarin (*Citrus unshui* Marc.) fruits extracted with various solvents. *J Raw Mater. Proces. Food* 1. 7–12.
- Keskin. M.. Guclu. G.. Sekerli. Y. E.. Soysal. Y.. Selli. S.. Kelebek. H.. (2021). Comparative assessment of volatile and phenolic profiles of fresh black carrot (*Daucus carota* L.) and powders prepared by three drying methods. *Sci. Hortic*. 287. 110256. <https://doi.org/10.1016/j.scienta.2021.110256>.
- Kim. J.. Soh. S.Y.. Bae. H. and Nam. S.Y.. (2019). “Antioxidant and phenolic contents in potatoes (*Solanum tuberosum* L.) and micropropagated potatoes”. *Applied Biological Chemistry*. 62(1). 1-9.
- Li. A.. Xiao. R.. He. S.. An. X.. He. Y.. Wang. C.. & He. J. (2019). Research advances of purple sweet potato anthocyanins: extraction. identification. stability. bioactivity. application. and biotransformation. *Molecules*. 24(21). 3816.
- Maskan. M. (2006). Production of pomegranate (*Punica granatum* L.) juice concentrate by various heating methods: color degradation and kinetics. *J Food Eng*. 72(3):218-224. <https://doi.org/10.1016/j.jfoodeng.2004.11.012>
- Reddivari. L.. Hale. A.L. and Miller. J.C.. (2007). Determination of phenolic content. composition and their contribution to antioxidant activity in specialty potato selections. *American Journal of Potato Research*, 84. 275-282.
- Ru. W.. Pang. Y.. Gan. Y.. Liu. Q. and Bao. J.. (2019). “Phenolic compounds and antioxidant activities of potato cultivars with white. yellow. red and purple flesh”. *Antioxidants*, 8(10). 419.
- Shao. Y. and Bao. J.. (2015). Polyphenols in whole rice grain: Genetic diversity and health benefits. *Food Chemistry*, 180. 86-97.
- Singh. P. P.. & Saldaña. M. D. (2011). Subcritical water extraction of phenolic compounds from potato peel. *Food Research International*. 44(8). 2452-2458.

- Sidhu GK, Singh M, Kaur P (2019). Effect of operational parameters on physicochemical quality and recovery of spray-dried tomato powder. *J Food Proc Preserv.* 43. e14120. <https://doi.org/10.1111/jfpp.1412>.
- Stushnoff, C., Holm, D., Thompson, M. D., Jiang, W., Thompson, H. J., Joyce, N. I., & Wilson, P. (2008). Antioxidant properties of cultivars and selections from the Colorado potato breeding program. *American Journal of Potato Research.* 85. 267-276.
- Sun, Q., Zhang, M. and Mujumdar, A.S., (2019). Recent developments of artificial intelligence in drying of fresh food: A review. *Critical Reviews In Food Science And Nutrition*, 59(14). 2258-2275.
- Thompson, M. D., Thompson, H. J., McGinley, J. N., Neil, E. S., Rush, D. K., Holm, D. G., & Stushnoff, C. (2009). Functional food characteristics of potato cultivars (*Solanum tuberosum* L.): phytochemical composition and inhibition of 1-methyl-1-nitrosourea induced breast cancer in rats. *Journal of Food Composition and Analysis*, 22(6). 571-576.
- Uslu, D. Y., Coruk, K. S., Baltacıoğlu, H., & Tangüler, H. (2024). Effects of Cooking Methods and Oils on Bioactive Compounds, Sensory and Textural Properties of Yellow-Fleshed Potatoes (*Solanum tuberosum* L.). *Potato Research.* 1-22.
- Waseem M, Akhtar S, Ahmad N, Ismail T, Lazarte CE, Hussain M, Manzoor MF (2022). Effect of microwave heat processing on nutritional indices, antinutrients, and sensory attributes of potato powder-supplemented flatbread. *J Food Quality.* <https://doi.org/10.1155/2022/2103884>



CHAPTER 26

Biofilm Synthesis for Active Food Packaging

Mukaddes Karataş¹

¹ Dr., Department of Chemical Engineering, Engineering Faculty, Fırat University, Elazığ, Türkiye,
Corresponding Author ORCID: 0000-0001-5803-6821

1. Introduction

Active food packaging represents a significant advancement in food preservation technology, moving beyond the traditional role of packaging as a mere barrier to external factors. This innovative approach involves dynamic interactions between the packaging and the food, which can enhance shelf life, maintain freshness, and ensure safety. The increasing consumer demand for minimally processed and preservative-free foods has driven the development of active packaging solutions that mitigate spoilage, reduce foodborne illnesses, and minimize waste while preserving food quality and safety (Onyeaka et al., 2022; Bhowmik et al., 2022; Rahmadhia, 2023).

Biofilms, especially those originating from natural or biopolymer sources, are essential to the development of active packaging. These biofilms can be designed to include functional agents such as antimicrobials and antioxidants that specifically address spoilage factors like microbial growth and oxidative damage (Bhowmik et al., 2022; Abdullah et al., 2022; Atarés & Chiralt, 2016). For example, biofilms made from gelatin have demonstrated a capacity to effectively integrate nanoparticles that boost their antioxidant and antimicrobial characteristics, thus enhancing food safety and prolonging shelf life (Abdullah et al., 2022). Additionally, using biodegradable polymers for food packaging tackles the environmental issues linked to conventional plastics and supports sustainability objectives by offering a greener option (Pleva et al., 2021; Шершнева, 2022).

The incorporation of essential oils into biofilms has also garnered attention due to their antimicrobial properties. Research indicates that essential oils can be integrated into biodegradable films to enhance their functionality, providing a natural means of preserving food and preventing spoilage (Atarés & Chiralt, 2016; Bhowmik et al., 2022). As an illustration, research has shown that incorporating ginger oil and anthocyanins from natural origins can produce smart packaging that can identify alterations in food pH, thereby acting as a freshness indicator (Mahatmanti, 2024). This multifunctionality is essential for modern food packaging, as it not only protects the food but also provides real-time information about its condition.

Furthermore, the mechanical properties of biofilms are critical for their application in food packaging (Figure 1). The flexibility, barrier properties, and water resistance of these films must be optimized to ensure they effectively preserve food quality (Wahab, 2023). Research has shown that incorporating materials like chitosan and carbon quantum dots into biofilms can enhance their

mechanical strength and functional capabilities, making them suitable for various food packaging applications (Riahi et al., 2022; Bhowmik et al., 2022). The development of such advanced materials is vital for addressing the challenges posed by food spoilage and contamination, particularly in environments where biofilm formation can lead to significant health risks (Carvalho et al., 2021; Wang et al., 2022).



Figure 3.Food packaging applications.

In conclusion, active food packaging, particularly through the use of biofilms, represents a promising direction in food preservation technology. By integrating functional agents and focusing on biodegradable materials, this approach not only meets consumer demands for safety and quality but also contributes to sustainability efforts in the food industry. The ongoing research and development in this field are crucial for creating effective, environmentally friendly packaging solutions that can significantly reduce food waste and enhance food safety.

2. Principles of Biofilm Synthesis

Biofilms are cohesive matrices composed of biological materials, primarily polysaccharides, proteins, lipids, and sometimes nucleic acids. They form through the self-aggregation of cells or biopolymers, often produced via microbial activity or extracted from natural sources such as plants, algae, or animal byproducts. This organized structure encapsulates active agents within a customizable matrix, allowing for the achievement of desired properties such as antimicrobial activity, gas permeability, and mechanical strength, which are essential for effective active food packaging (Valdés et al., 2017). The

mechanical properties of biofilms are also a critical factor in their application for food packaging. The flexibility, tensile strength, and barrier properties of these films must be optimized to ensure they effectively preserve food quality while being easy to handle and process (Roy & Rhim, 2020; Aider, 2010). Recent studies have demonstrated that the incorporation of nanoparticles or other functional additives can significantly enhance the mechanical and barrier properties of biofilms, making them suitable for a wider range of food packaging applications (Sapalina & Retnaningrum, 2020; Souza et al., 2020).

Adhesion is the initial stage where cells or biopolymeric components adhere to a surface or to each other. This step is crucial as it establishes the foundation for biofilm development. Various studies have highlighted that the adhesion process can be influenced by surface properties, bacterial motility, and environmental conditions (Zheng et al., 2021; Jiang et al., 2021). For instance, Zheng et al. emphasize that biofilm development begins with a loose association of microorganisms to a surface, which then transitions to strong adhesion as extracellular polymeric substances (EPS) are produced (Zheng et al., 2021). This initial attachment is often mediated by the production of EPS, which serves as an adhesive material (Kolappan & Satheesh, 2011).

Following adhesion, the **maturation** phase occurs, characterized by cell proliferation and the further cross-linking of biopolymeric components. This leads to the formation of a cohesive and stable biofilm structure. The maturation process is marked by the development of microcolonies, where cells grow and multiply, contributing to the overall density and robustness of the biofilm (Vera et al., 2013; Han et al., 2022). Research by Kimani et al. indicates that biofilm maturation involves complex signaling pathways that regulate the growth and organization of microbial communities (Kimani et al., 2016).

The next stage, **matrix production**, involves the secretion of EPS, which fill in the matrix and provide protective and adhesive properties to the biofilm. EPS are primarily composed of polysaccharides, proteins, and nucleic acids, and they play a vital role in maintaining the structural integrity of the biofilm (Taglialegna et al., 2016; Guo, 2023). According to Taglialegna et al., the production of EPS is essential for forming a stable biofilm matrix that can resist environmental stresses and antimicrobial treatments (Taglialegna et al., 2016). This matrix not only protects the embedded microorganisms but also facilitates nutrient exchange and waste removal.

Finally, **customization** of biofilms allows for tailoring their properties for specific functions. This can be achieved by incorporating active agents, adjusting

cross-linking, or combining various biopolymers to enhance functionality. For example, the addition of antimicrobial agents into the biofilm matrix can significantly improve its ability to inhibit microbial growth, making it particularly useful in food packaging applications (Park et al., 2019). The ability to customize biofilms is crucial for developing targeted solutions that meet specific needs in various industries, including food safety and preservation (Martínez et al., 2020; Borowski et al., 2018). Each stage plays a critical role in the development of biofilms, particularly in applications such as active food packaging, where the properties of the biofilm can be tailored to enhance food safety and quality.

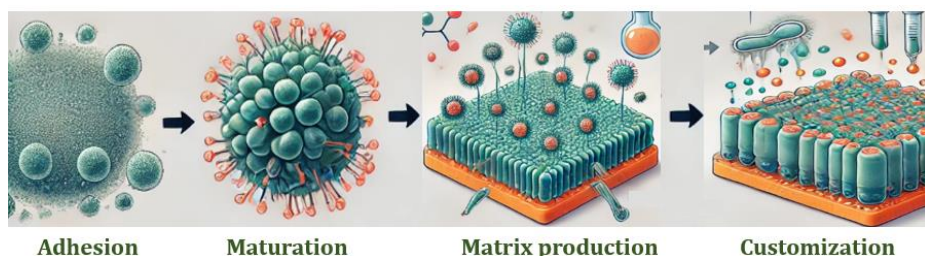


Figure 4. The biofilm synthesis steps.

The synthesis of biofilms for food packaging utilizes a variety of materials, each contributing unique properties that enhance the functionality and effectiveness of the packaging. The primary materials include polysaccharides, proteins, lipids, and composite biofilms, which combine these components for improved performance.

Polysaccharides such as alginate, starch, and cellulose are commonly used in biofilm synthesis due to their excellent film-forming capabilities and biodegradability. These materials provide flexible films with moderate to high water and gas barrier properties, making them suitable for preserving food quality. For instance, Kannan et al. highlight the role of extracellular polysaccharides in biofilm formation, noting that they act as a cement to hold cells together, which is crucial for the structural integrity of the biofilm (Kannan & Pennathur, 2015). Additionally, polysaccharides significantly contribute to the water-binding capacity of biofilms, which is essential for maintaining moisture levels in food products (Liu & Wang, 2022).

Proteins such as gelatin, whey protein, and soy protein are also integral to biofilm formation. These proteins provide excellent film-forming capabilities and are also suitable for integrating active agents, improving the functionality of the biofilm. The mechanical strength provided by proteins is particularly important in applications where durability is required. Research indicates that the presence

of proteins in biofilms can enhance their resistance to environmental stresses, thereby improving the shelf life of packaged foods. For example, Wyrwa and Barska discuss how protein-based biofilms can be tailored to provide specific barrier properties while maintaining flexibility (Wyrwa & Barska, 2017).

Lipids, including waxes and oils, are often used as coatings within biofilms to improve moisture barrier properties. This is especially beneficial for packaging moist or perishable food products, as lipids help to prevent moisture loss and maintain product freshness. The incorporation of lipids into biofilms can enhance their overall performance by providing additional layers of protection against environmental factors (Reichling, 2020).

Composite biofilms, which combine polysaccharides, proteins, and lipids, offer enhanced properties that allow for customization of the film's strength, flexibility, and barrier capabilities. By integrating different materials, researchers can create biofilms that meet specific requirements for various food products. For instance, the combination of alginate and protein can yield a biofilm with improved mechanical strength and moisture resistance, making it suitable for a wider range of applications (Wang et al., 2022; González-Machado et al., 2018). Studies have shown that such composite materials can effectively inhibit biofilm formation by pathogenic bacteria, thereby enhancing food safety (Jiang et al., 2011).

3. Biological and Chemical Methods for Biofilm Synthesis

The development of biofilm-based active packaging for food necessitates that the biofilms exhibit specific qualities such as flexibility, durability, barrier properties, and the ability to incorporate active agents for food preservation. Achieving these qualities can be accomplished through two broad categories of methods: biological and chemical synthesis (Figure 3). Each method offers unique advantages that enable the tailoring of properties and functionalities in the resulting biofilms.

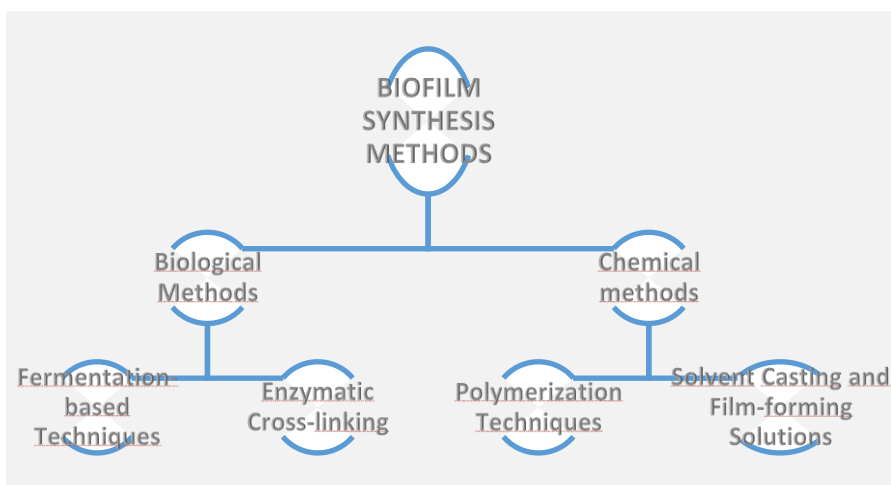


Figure 5. Scheme of biofilm synthesis methods.

3.1. Biological Methods

Biological methods for synthesizing biofilms typically involve the use of microorganisms or natural biopolymers. These methods capitalize on the inherent properties of biological materials, which can be modified to enhance their performance in food packaging applications.

Microbial biofilm formation is a critical process in various applications, including food packaging, where biofilms can provide structural integrity and protective properties. Microorganisms such as bacteria and fungi naturally produce biofilms composed of extracellular polymeric substances (EPS). These substances play a vital role in functionality of the biofilm, particularly in enhancing barrier properties and incorporating antimicrobial agents.

3.1.1. Fermentation-based Techniques

Fermentation-based techniques utilize microorganisms to produce biofilm matrices through controlled cultivation processes. These methods leverage the natural abilities of various microorganisms, such as lactic acid bacteria, yeasts, and certain bacterial strains, to synthesize extracellular matrices during their growth cycles. The following references provide insights into the mechanisms, properties, and applications of fermentation-based biofilm production for food packaging.

Lactic acid bacteria (LAB) play a significant role in biofilm formation, which has critical implications for food safety. This not only helps in food preservation but also imparts antimicrobial properties to the biofilm. LAB, such as

Lactobacillus rhamnosus and *Lactobacillus acidophilus*, can enhance biofilm formation under stress conditions like nutrient deficiency, as shown by Liu et al. (2024). In particular, *L. acidophilus* has demonstrated the ability to integrate into biofilms within cheese whey environments, where it plays a role in inhibiting gram-negative bacteria and contributes to the structural integrity of the biofilm (Al-Mathkhury et al., 2011). Additionally, environmental factors such as temperature and humidity significantly impact biofilm strength and pathogen transfer, with higher temperatures resulting in more robust biofilms, which may influence the persistence of LAB and other organisms within these communities (Nan et al., 2023). Together, these findings underscore the resilience and functional adaptability of LAB in biofilm formation, especially under varying environmental stresses.

Yeasts, particularly *Saccharomyces cerevisiae*, produce polysaccharides that possess a high water-binding capacity, a property that makes them highly effective for creating moisture-retentive films in various applications. These polysaccharides have garnered interest for their potential in enhancing the mechanical and functional properties of food packaging materials, as they can improve moisture retention and prolong shelf life by forming a protective barrier. Huang et al. (2019) emphasize the role of these yeast-derived polysaccharides in improving food packaging, noting that their natural origins and biodegradability make them an attractive alternative to synthetic materials in eco-friendly packaging (Huang et al., 2019). Furthermore, the integration of such polysaccharides in packaging not only supports moisture regulation but can also contribute to the overall strength and flexibility of the material, creating safer, more sustainable packaging solutions for the food industry.

Certain bacterial strains, such as *Bacillus subtilis*, are known for their ability to produce robust biofilms made up of diverse biopolymers. These biofilms are not only resilient but also highly versatile, comprising proteins, polysaccharides, and other organic compounds that enhance their structural integrity and functionality. *B. subtilis* biofilms, in particular, exhibit properties that make them suitable for potential applications in areas requiring durability and resistance, such as food packaging. Kausar (2019) reviews the potential of high-performance polymer nanocomposites, including those derived from bacterial sources, for advanced packaging applications, highlighting how bacterial biopolymers can improve material strength, flexibility, and barrier properties (Kausar, 2019). Such biopolymer-based nanocomposites offer a sustainable alternative to synthetic materials, providing eco-friendly options that can reduce environmental impact while meeting industry demands for durable, protective, and versatile packaging

solutions. The use of bacterial biofilms in this context also promotes the exploration of biodegradable, renewable sources, aligning with the growing focus on sustainable materials in packaging technologies.

The production of biofilms through fermentation involves a series of carefully managed steps to achieve films with specific qualities. First, the selection of the microorganism plays a key role in determining the final biofilm properties, with strains like *Lactobacillus* often chosen for their natural antimicrobial and preservative benefits. Once selected, the microorganism undergoes cultivation in a controlled fermentation environment where factors such as pH, temperature, and nutrient availability are optimized to encourage robust matrix production. Li et al. (2021) highlight how these environmental conditions directly impact biofilm formation and its final properties, underscoring the importance of precise control during growth (Li et al., 2021). Following the cultivation phase, the biofilm matrix produced by the microorganisms is carefully harvested and purified. Understanding the composition and structure of the microbial community within the biofilm, as detailed by Fish et al. (2015), is crucial for effective extraction and refinement. Lastly, the purified matrix is transformed into films through processes like solvent casting or drying, resulting in a material suitable for applications such as edible coatings (Fish et al., 2015). Popescu et al. (2022) discuss how these edible films, derived from fermentation processes, are beneficial in extending the shelf life and quality of fresh produce, illustrating the practical applications of fermentation-based biofilm production (Popescu et al., 2022).

3.1.2. Enzymatic Cross-linking

Enzymatic cross-linking is an effective method for stabilizing and strengthening biofilm structures by forming covalent bonds between biopolymer chains. This technique enhances the durability, flexibility, and moisture resistance of biofilms, making them more suitable for food packaging applications. By utilizing different enzymes tailored to specific biopolymers, it is possible to produce biofilms with properties that meet a variety of packaging needs.

One commonly used enzyme is transglutaminase, which effectively cross-links proteins by forming covalent bonds between amino groups, significantly enhancing the tensile strength and elasticity of biofilms. This enzyme-induced cross-linking not only improves the structural resilience of protein-based films but also increases their flexibility, making them ideal for applications requiring durable yet adaptable materials. Jiang et al. (2019) highlight the role of

transglutaminase in enhancing the mechanical properties of protein-based films, emphasizing its utility in the food packaging industry, where robust and safe packaging materials are essential (Kandarakis et al., 2022). Transglutaminase promotes stronger bonds within the protein matrix, allowing for the formation of biofilms that can endure handling and environmental stresses, thus decreasing the risk of tearing or degradation. The use of transglutaminase in biofilm production also aligns with the shift towards biodegradable, protein-based packaging materials, providing an eco-friendly alternative to conventional synthetic options while ensuring product integrity and extending shelf life in food applications.

For biofilms containing phenolic compounds or other bioactive molecules, enzymes like laccase and peroxidase are pivotal in enhancing structural integrity and functional properties through their cross-linking role. These enzymes facilitate covalent bonding among phenolic structures, which not only strengthens the biofilm matrix but also imparts valuable antimicrobial properties. Özkul (2023) specifically highlight the application of laccase in biofilm production, noting its dual benefit of reinforcing the biofilm structure while simultaneously providing antimicrobial effects that are advantageous for food preservation (Özkul, 2023). This is particularly relevant in extending the shelf life of food products by inhibiting microbial growth, thereby reducing spoilage. The incorporation of laccase and peroxidase into biofilm production aligns with sustainable practices in food packaging. These enzymes offer a natural and eco-friendly method to enhance biofilm performance, which is becoming more crucial in the context of environmental sustainability. For instance, laccases have been recognized for their ability to oxidize a wide range of substrates, including phenols and arylamines, which can lead to the formation of bioactive compounds with antimicrobial properties (Bassanini et al., 2020). This characteristic is particularly beneficial for developing bio-based, functional packaging materials that not only protect food but also contribute to food safety by reducing the risk of microbial contamination. Moreover, the structural properties of biofilms enhanced by laccase and peroxidase make them more resistant to environmental stressors and degradation. The biofilm matrix acts as a physical barrier that limits the penetration of harmful agents, thereby enhancing the overall durability and effectiveness of the packaging. This is crucial in applications where maintaining the integrity of the food product is essential. The ability of these enzymes to incorporate antimicrobial properties directly into the biofilm structure allows for the creation of safer, longer-lasting protective films, which is a significant advancement in the field of food technology and packaging (Polak et al., 2020).

In biofilms derived from pectin or cellulose, enzymes like pectinase and cellulase play a crucial role by enhancing moisture resistance and overall cohesiveness. These enzymes catalyze specific reactions within the polysaccharide structures, leading to improved integrity and stability of the biofilm matrix. The cross-linking action of pectinase and cellulase not only increases the biofilm's resistance to moisture but also reduces its susceptibility to breaking or tearing, which is essential for applications requiring durability, such as food packaging. The role of pectinase in enhancing the properties of biofilms is well-documented. For instance, Al-Rousan et al. (2021) demonstrated that pectinase, when used in conjunction with cellulase, significantly improves the extraction of bioactive compounds from olive oil, indicating its effectiveness in breaking down cell walls and facilitating the release of polysaccharides (Al-Rousan et al. 2021). This enzymatic action is crucial for creating cohesive films that can withstand environmental stresses. Similarly, Zouari-Ellouzi et al. (2018) explored the use of starch extracted from pasta by-products in biodegradable film production, noting that the incorporation of enzymes like pectinase can enhance the film's moisture resistance and overall performance (Zouari-Ellouzi et al., 2018). Cellulase also plays a vital role in biofilm formation by breaking down cellulose into smaller polysaccharides, which can then be cross-linked to improve film properties. Jiao et al. highlighted that cellulase treatment can lead to the formation of films with enhanced mechanical properties, including increased tensile strength and reduced brittleness (Jiao et al., 2020). This is particularly beneficial in food packaging applications, where the integrity of the packaging is critical for preserving food quality. Furthermore, the combination of cellulase and pectinase has been shown to optimize the extraction and clarification of fruit juices, which underscores their synergistic effects in enhancing polysaccharide-based films (Jiao et al., 2020). The moisture resistance provided by these enzyme-treated biofilms is essential for food preservation. As noted by Yuvaraj et al., (2021) biodegradable packaging materials derived from biopolymers can significantly minimize moisture loss, thereby extending the shelf life of food products (Yuvaraj et al., 2021). The smoother and more uniform surfaces of films produced with pectinase and cellulase also contribute to their aesthetic appeal and functionality in packaging applications, making them suitable for consumer products where appearance is important (Bátori et al., 2019).

3.2. Chemical Methods

Chemical synthesis methods are essential for producing biofilms with specific barrier properties, durability, and compatibility with active agents. Among these

methods, polymerization techniques play a crucial role in forming biofilms with controlled thickness, uniformity, and stability.

3.2.1. Polymerization Techniques

Polymerization is a foundational technique in biofilm synthesis, involving the chemical bonding of monomers to form long-chain polymers that can be processed into biofilm layers. Researchers can produce biofilms with exact thickness, consistency, and stability by choosing particular monomers and managing the polymerization process. These properties are essential for applications requiring consistent film strength, flexibility, and resistance to environmental factors like moisture or temperature variations.

Through the process of polymerization, monomers such as lactic acid, acrylates, and natural polysaccharides can be converted into biofilms with specific characteristics tailored to meet the requirements of various applications. This transformation facilitates the production of biofilms exhibiting diverse properties, including durability, moisture resistance, and structural integrity, which are essential for uses such as food packaging and biodegradable coatings. By manipulating the type and arrangement of monomers, as well as incorporating cross-linking agents or catalysts, polymerization techniques provide substantial versatility in the design and development of biofilms. This adaptability enables the creation of materials that not only fulfill functional requirements but also align with environmental sustainability objectives.

The processes of polymerization that contribute to biofilm production encompass free radical polymerization, emulsion polymerization, and the development of cross-linked polymer networks.

Free radical polymerization is a widely utilized technique in the synthesis of biofilms, particularly noted for its effectiveness in producing materials with high durability and superior barrier properties. This method involves the initiation of polymerization through free radicals, which facilitates the formation of strong covalent bonds between polymer chains. As a result, biofilms generated via free radical polymerization exhibit remarkable resistance to physical stresses, environmental exposure, and moisture penetration. Such characteristics render this technique particularly suitable for applications where biofilms must endure handling and provide a robust barrier against contaminants, thereby ensuring the integrity and safety of the packaged products (Jähnert et al., 2014).

Emulsion polymerization is recognized for its ability to produce polymers with a high degree of uniformity, which significantly contributes to the even

texture and consistent performance of the resulting biofilms. This process involves dispersing the monomer within a water-based solution, leading to the formation of polymers that exhibit enhanced moisture resistance. Consequently, biofilms synthesized through emulsion polymerization are particularly advantageous for applications requiring effective water barrier properties. These films play a crucial role in maintaining food quality by preventing moisture exchange, thereby extending shelf life and preserving the sensory attributes of food products (Zhang et al., 2014).

The incorporation of cross-linking agents in polymer networks is a pivotal method for enhancing the structural integrity and thermal stability of biofilms. **Cross-linked polymer networks** create a three-dimensional framework that bonds polymer chains together, resulting in increased strength and resilience. This method significantly enhances the biofilm's resistance to deformation, heat, and physical stress. Cross-linked biofilms are especially valuable in applications where packaging must withstand varying temperatures or maintain its shape and strength over extended periods. The ability to endure such conditions is critical for ensuring the reliability and effectiveness of packaging solutions in diverse environments (Panahi et al., 2019).

Steps in polymerization for biofilm synthesis:

1. Selection of Monomers and Cross-linkers: The polymerization process begins with the careful selection of suitable monomers and, if necessary, cross-linkers to create a cohesive polymer network. Common monomers include lactic acid, acrylates, and natural polysaccharides, each offering distinct properties that influence the final characteristics of the biofilm. Cross-linkers are often incorporated to strengthen the bonds between polymer chains, resulting in a durable film. The choice of monomers and cross-linkers is crucial as it directly affects the mechanical properties and functionality of the biofilm (Kapil et al., 2022)

2. Initiation of Polymerization: After choosing the monomers and cross-linkers, the polymerization process begins by adding a catalyst or using heat. This step triggers the bonding of monomers into long polymer chains, forming the foundation of the biofilm structure. Controlled initiation allows for customization of the film's properties, such as flexibility and toughness, which are essential for specific applications (Guo, 2023).

3. Cross-linking and Film Formation: Cross-linkers are incorporated to stabilize and fortify the polymer network, interlinking the polymer chains and improving cohesion and resilience of the biofilm. After the polymer solution is

cross-linked, it is cast onto a surface or mold to form a thin, uniform layer. This film-forming process determines the thickness and uniformity of the biofilm, which are essential for achieving consistent performance in applications such as food packaging and coatings (Sondari et al., 2019).

4. Curing: The last step in biofilm synthesis is curing, in which the film undergoes controlled conditions, like heat or ultraviolet (UV) light, to solidify and complete the polymerization process. This curing stage forms a stable, long-lasting biofilm that demonstrates the required physical and functional characteristics. The produced biofilm is appropriate for numerous packaging uses, providing protection, structural strength, and frequently biodegradability, which corresponds with sustainable packaging efforts (Liu et al., 2014).

3.2.2. Solvent Casting and Film-forming Solutions

Solvent casting is a widely employed technique in biofilm production, particularly appreciated for its simplicity and the precise control it offers over the properties of the resulting films. The process encompasses several critical steps, including the preparation of film-forming solutions, incorporation of active agents, casting, drying, and processing of the biofilm.

Steps in solvent casting method for biofilm synthesis:

1. Preparation of Film-forming Solution: The initial step involves selecting appropriate solvents and polymers to create a homogeneous film-forming solution. Various biopolymers such as starch, chitosan, gelatin, and alginate are commonly used in solvent casting. The choice of biopolymer is determined by the desired properties of the final biofilm. For example, in chitosan-gelatin biofilms, chitosan provides antimicrobial properties, while gelatin contributes to flexibility and barrier properties (Benbettaïeb et al., 2014). The choice of solvent is crucial for dissolving the selected biopolymer. Choi et al. (2016) examine how pH and salts affect the physical and mechanical properties of pea starch films, indicating that solvent selection can influence the solubility and integrity of the film (Choi et al., 2016). Additionally, the concentration of the biopolymer in the solvent determines the viscosity of the film-forming solution and, consequently, the thickness and consistency of the final film. Typically, biopolymer concentrations range from 1-10% (w/v), though adjustments are made based on molecular weight of the polymer and intended application.

2. Incorporation of Active Agents : Once the film-forming solution is prepared, active agents can be incorporated into the film-forming solution to impart specific functionalities to the biofilm, such as antimicrobial, antioxidant,

or UV-protective properties. Pinto et al. (2012) showed that incorporating graphene oxide into poly(lactic acid) films made through solvent casting enhanced mechanical properties and gas permeability, highlighting the adaptability of this technique in customizing film attributes (Pinto et al., 2012).

Antimicrobial agents are integral to biofilms used in food packaging, as they inhibit the growth of pathogens and spoilage organisms, enhancing the safety and shelf life of perishable items. Common antimicrobial agents include natural extracts, such as essential oils (EOs) from plants like thyme, oregano, and rosemary, which contain bioactive compounds like thymol, carvacrol, and eugenol that disrupt microbial cell membranes. These EOs are often encapsulated in nanoemulsions or liposomes within the biofilm matrix to control their release rates and prevent oxidation (Burt, 2004). Additionally, metal nanoparticles such as silver, zinc oxide, and titanium dioxide provide antimicrobial effects by releasing ions that damage bacterial cell walls and disrupt cellular functions; these nanoparticles are typically embedded in biofilms during synthesis for uniform distribution and sustained release (Kalpana and Rajeswari, 2017). Organic acids, including citric, lactic, and acetic acid, serve as natural preservatives by lowering pH and inhibiting microbial growth, while also contributing to flavor profiles, making them suitable for incorporation into edible biofilms (Coban, 2020).

Antioxidant agents play a crucial role in preventing oxidative spoilage in foods, particularly those high in fats and oils, such as meats and dairy products. Effective antioxidants like Vitamin C (ascorbic acid) and tocopherols (vitamin E) are commonly incorporated into biofilms used in food packaging to neutralize free radicals and reduce oxidative damage (Chu et al., 2023). These antioxidants can be integrated into the biofilm matrix through direct mixing or encapsulation techniques, which protect them from premature oxidation and facilitate controlled release. Their mechanism of action involves scavenging reactive oxygen species (ROS) that contribute to lipid oxidation and discoloration, thereby preserving the aesthetic quality of food and extending its shelf life by preventing rancidity.

Biofilms can be categorized into edible and non-edible variants based on their intended applications and regulatory standards concerning direct food contact. Edible biofilms are formulated to be safe for consumption, often serving as direct coatings on food products. They are made from food-grade biopolymers such as starch, gelatin, and chitosan, along with additives that have been approved by food safety authorities. The active agents incorporated into these biofilms, including natural extracts and organic acids, must originate from safe sources and adhere to permissible concentrations to comply with food safety regulations.

Conversely, non-edible biofilms function as outer packaging layers and may contain more potent antimicrobial agents, such as metal nanoparticles, which are not meant for direct contact with food. These biofilms are required to meet environmental and safety standards, emphasizing biodegradability and minimal environmental impact (Han et al., 2018).

4. Properties and Characterization of Biofilms for Food Packaging

In order to confirm that biofilms adhere to the specific requirements for food packaging, their properties must undergo strict evaluation in various essential categories. This assessment is vital for determining the efficacy of biofilms in preserving food quality, resisting degradation, and minimizing environmental impact when compared to traditional packaging materials. The primary properties of interest include mechanical strength, barrier effectiveness, antimicrobial and antioxidant activities, and biodegradability.

4.1. Mechanical Properties

The mechanical properties of biofilms are critical in determining their effectiveness as food packaging materials, particularly regarding their ability to withstand handling, storage, and transport without compromising food safety or quality.

Tensile strength is a key indicator of the maximum stress that a biofilm can endure while being stretched. This property is essential for packaging materials, as higher tensile strength enables biofilms to resist breaking, tearing, or rupturing when handling heavier or awkwardly shaped items. Standardized mechanical stress testing, such as ASTM D882, is employed to evaluate this property, wherein a sample film is subjected to tensile forces until it breaks. The resulting force-displacement data provide insights into tensile strength of the film and its resistance to breaking under stress (Powell et al., 2013).

Flexibility allows biofilms to conform to the shape of the food they package, which is particularly beneficial for semi-solid or moisture-rich foods like cheese, meat, and baked goods. **Elasticity** testing is often conducted alongside tensile tests, focusing on the biofilm's ability to recover its shape after deformation. A high level of elasticity is desirable as it reduces the likelihood of tears and maintains the integrity of the packaging during handling (Fabbri and Stoodley, 2016).

Puncture resistance is another vital mechanical property for food packaging applications. Packaging materials frequently encounter pointed forces, such as when stored near hard surfaces or transported with other items. Testing methods

for puncture resistance involve pressing a probe against the biofilm until it punctures, allowing for quantification of the film's resistance. A higher puncture resistance indicates that the biofilm can better protect against potential contamination or spoilage (Briassoulis and Giannoulis, 2018).

4.2. Barrier Properties

Barrier properties of biofilms are critical in food packaging, particularly in regulating moisture and gas transfer, which directly impacts food quality and shelf life. Two key metrics for assessing these properties are Water Vapor Permeability (WVP) and Oxygen Permeability (OP).

WVP assesses the efficiency of a biofilm in hindering moisture transfer. Low WVP is essential for foods sensitive to moisture fluctuations, such as bread and crackers, as it helps maintain texture and prevents spoilage. This can be quantified using gravimetric or cup methods, where the biofilm separates two compartments with different humidity levels, and the moisture transfer rate is recorded. Studies have shown that various biofilm materials, including those derived from chitosan and polyvinyl alcohol (PVA), exhibit favorable WVP characteristics. For instance, Nazreen et al. (2020) emphasized that bioplastic films serve as effective moisture barriers, crucial for preventing moisture loss in food products (Nazreen et al., 2020). Furthermore, the incorporation of glycerin-plasticized PVA in LDPE blends has been shown to enhance barrier properties, making them suitable for food packaging applications (Kim et al., 2015).

OP is equally important, particularly for foods susceptible to oxidative spoilage, such as oils and meats. OP is tested using specialized equipment that measure the rate of oxygen passage through the biofilm under controlled conditions. Lower OP values correlate with reduced oxygen exposure, which can slow down lipid oxidation and microbial growth. Kim et al. demonstrated that the addition of PVA to LDPE matrices significantly improved oxygen barrier properties, making these materials more effective for food packaging (Kim et al., 2015). Additionally, studies on chitosan-based films have shown that they possess inherent oxygen barrier properties, which can be further enhanced through modifications (Quyen et al., 2012). The development of biodegradable films, such as those reinforced with essential oils, has also been noted for their ability to maintain low OP, thereby extending the shelf life of food products (Liu et al., 2024).

Gas barrier properties are particularly vital for fresh produce, which continues to respire after harvest. Biofilms that allow for controlled gas exchange can help maintain the freshness of fruits and vegetables by regulating oxygen and carbon

dioxide levels. Barrier properties for O₂ and CO₂ are tested using similar methods to those for OP, ensuring that the packaging meets the specific respiration requirements for the produce.

4.3. Antimicrobial and Antioxidant Activity

Biofilms frequently include antimicrobial and antioxidant agents to avoid spoilage and prolong shelf life. These active compounds play a significant role in inhibiting microbial growth and oxidative reactions, which are common causes of food spoilage.

Antimicrobial efficacy tests are crucial for assessing the effectiveness of biofilms in reducing microbial loads on food surfaces. One common method is the Disk Diffusion Assay, where biofilm samples containing antimicrobial agents are placed on agar plates inoculated with bacteria. The inhibition zone around the biofilm disc indicates its effectiveness in preventing bacterial growth. For instance, Essential oils, such as those from *Thymbra capitata* and *Thymus pallescens*, have shown significant inhibition zones (up to 50 mm) against pathogens like *Staphylococcus aureus* (Bouguenoun et al., 2023). Additionally, the Direct Contact Method allows for testing biofilms on actual food samples, providing insights into their performance under real-world conditions. Studies have shown that biofilms enriched with compounds like ethyl lauroyl arginate (LAE) can significantly reduce biofilm formation of pathogens such as *E. coli* and *Listeria* (Sadekuzzaman et al., 2017).

Antioxidant activity is another critical aspect of biofilms designed to prevent oxidative spoilage. The DPPH (2,2-Diphenyl-1-picrylhydrazyl) radical scavenging assay is a widely utilized method for evaluating the antioxidant capacity of various compounds, including those incorporated into biofilms. This assay is particularly significant in the context of food packaging, as it quantifies the ability of biofilms to neutralize free radicals, thereby preventing oxidative spoilage. The Thiobarbituric Acid Reactive Substances (TBARS) assay is commonly used to evaluate the effectiveness of biofilms in reducing lipid oxidation, a primary cause of rancidity in high-fat foods. This test measures malondialdehyde (MDA), the main byproduct of lipid peroxidation, where biofilm-packaged and control food samples are kept under identical conditions and MDA levels are evaluated at regular intervals. For example, Glaser et al. utilized the TBARS method to assess the oxidative behavior of fresh meat packaged with active films containing chitosan nanoparticles, demonstrating a significant reduction in lipid oxidation (Glaser et al., 2019).

4.4. Biodegradability and Environmental Impact

The development of biofilms as sustainable packaging solutions necessitates a thorough assessment of their biodegradability and environmental impact. This evaluation involves standardized tests to measure the decomposition rates of biofilms in various environments and a life cycle analysis (LCA) to understand their ecological footprint.

Biodegradability Tests: Several standardized tests are employed to assess the biodegradability of biofilms. The Soil Burial Test is one such method, where biofilms are buried in soil under controlled conditions, and their weight loss or structural changes are periodically measured. This test simulates natural environmental conditions, providing insights into how well biofilms can decompose. For instance, studies have shown that starch-based biofilms exhibit significant biodegradation in soil, indicating their potential as eco-friendly packaging materials (Sun et al., 2023).

Composting tests are also critical, particularly for biofilms designed for industrial composting. Samples are placed in compost at specific temperatures, and their degradation is monitored. Certifications such as ASTM D6400 indicate that a biofilm can decompose fully and safely in industrial composting settings. Research has demonstrated that biofilms made from natural polymers, such as chitosan and starch, can meet these compostability standards, thus contributing to waste reduction.

Conclusion

Biofilm-based active packaging represents a significant advancement in the field of food preservation, offering a multifaceted solution that addresses critical challenges within the food industry. By integrating principles of advanced materials science with sustainable practices, biofilm technology not only enhances food safety and quality but also aligns with the increasing demand for environmentally sustainable packaging alternatives. One of the most notable advantages of biofilm-based packaging is its inherent adaptability. Manufacturers can tailor the mechanical, barrier, antimicrobial, and antioxidant properties of biofilms to create packaging solutions that are optimized for the specific requirements of various food categories. Additionally, the incorporation of antimicrobial agents can effectively inhibit microbial growth in perishable items, including seafood and dairy products.

The integration of active agents into biofilms—such as natural plant extracts, essential oils, and metal nanoparticles—further enhances their functional

capabilities. These agents operate synergistically to inhibit spoilage, reduce microbial contamination, and preserve the sensory qualities of packaged foods. Moreover, biofilm-based packaging significantly contributes to sustainability initiatives. By offering a viable alternative to petroleum-based plastics, biodegradable biofilms can reduce environmental pollution and provide a lower ecological footprint.

The application of biofilm-based active packaging encompasses a diverse range of food products, including dairy, meats, seafood, fresh produce, and baked goods. Its capacity to extend shelf life plays a crucial role in reducing food waste, which is a pressing concern in global food systems. By prolonging the freshness of food items, biofilms facilitate global distribution chains, enabling high-quality products to reach consumers in distant markets.

As the food industry increasingly prioritizes health, safety, and sustainability, biofilm-based active packaging is positioned to play a pivotal role in the future of food preservation. Ongoing research and development efforts focused on biofilm synthesis, the integration of novel active agents, and the enhancement of testing protocols are likely to expand the potential applications of this innovative technology. By addressing both consumer demands and environmental challenges, biofilm-based packaging not only ensures food safety and quality but also contributes to a more sustainable future for the food packaging industry.

References

- Abdullah, J. A. A., Jiménez-Rosado, M., Guerrero, A., & Romero, A. (2022). Gelatin-based biofilms with fexoy-nps incorporated for antioxidant and antimicrobial applications. *Materials*, 15(5), 1966. <https://doi.org/10.3390/ma15051966>
- Aïder, M. (2010). Chitosan application for active bio-based films production and potential in the food industry: review. *LWT - Food Science and Technology*, 43(6), 837-842. <https://doi.org/10.1016/j.lwt.2010.01.021>
- Al-Mathkhury, H. J. F., Ali, A. S., & Ghafil, J. A. (2011). Antagonistic effect of bacteriocin against urinary catheter associated pseudomonas aeruginosa biofilm. *North American Journal of Medical Sciences*, 367-370. <https://doi.org/10.4297/najms.2011.3367>
- Al-Rousan, W. M., Al-Marazeeq, K. M., Abdullah, M. A., Khalaileh, N. I. A., Angor, M., & Ajo, R. (2021). Use of enzymatic preparations to improve the productivity and quality of olive oil. *Jordan Journal of Agricultural Sciences*, 17(4), 455-469. <https://doi.org/10.35516/jjas.v17i4.97>
- Atarés, L. and Chiralt, A. (2016). Essential oils as additives in biodegradable films and coatings for active food packaging. *Trends in Food Science & Technology*, 48, 51-62. <https://doi.org/10.1016/j.tifs.2015.12.001>
- Bassanini, I., Ferrandi, E. E., Riva, S., & Monti, D. (2020). Biocatalysis with laccases: An updated overview. *Catalysts*, 11(1), 26. <https://doi.org/10.3390/catal11010026>
- Bátori, V., Lundin, M., Åkesson, D., Lennartsson, P. R., Taherzadeh, M. J., & Zamani, A. (2019). The effect of glycerol, sugar, and maleic anhydride on pectin-cellulose thin films prepared from orange waste. *Polymers*, 11(3), 392. <https://doi.org/10.3390/polym11030392>
- Benbettaïeb, N., Kurek, M., Bornaz, S., & Debeaufort, F. (2014). Barrier, structural and mechanical properties of bovine gelatin–chitosan blend films related to biopolymer interactions. *Journal of the Science of Food and Agriculture*, 94(12), 2409-2419. <https://doi.org/10.1002/jsfa.6570>
- Bhowmik, S., Agyei, D., & Ali, A. (2022). Bioactive chitosan and essential oils in sustainable active food packaging: recent trends, mechanisms, and applications. *Food Packaging and Shelf Life*, 34, 100962. <https://doi.org/10.1016/j.fpsl.2022.100962>
- Borowski, R. G. V., Gnoatto, S. C. B., Macêdo, A. J., & Gillet, R. (2018). Promising antibiofilm activity of peptidomimetics. *Frontiers in Microbiology*, 9. <https://doi.org/10.3389/fmicb.2018.02157>
- Bouguenoun, W., Benbelaid, F., Mebarki, S., Bouguenoun, I., Boulmaiz, S., Khadir, A., ... & Muselli, A. (2023). Selected antimicrobial essential oils to eradicate multi-drug resistant bacterial biofilms involved in human nosocomial infections. *Biofouling*, 39(8), 816-829. <https://doi.org/10.1080/08927014.2023.2269551>

- Briassoulis, D., & Giannoulis, A. J. P. T. (2018). Evaluation of the functionality of bio-based food packaging films. *Polymer Testing*, 69, 39-51. <https://doi.org/10.1016/j.polymertesting.2018.05.003>
- Burt, S. (2004). Essential oils: their antibacterial properties and potential applications in foods—a review. *International journal of food microbiology*, 94(3), 223-253. <https://doi.org/10.1016/j.ijfoodmicro.2004.03.022>
- Carvalho, L. G., Alvim, M. M. A., Fabri, R. L., & Apolônio, A. C. M. (2021). staphylococcus aureus biofilm formation in minas frescal cheese packaging. *International Journal of Dairy Technology*, 74(3), 575-580. <https://doi.org/10.1111/1471-0307.12783>
- Choi, W. S., Patel, D., & Han, J. H. (2016). Effects of pH and salts on physical and mechanical properties of pea starch films. *Journal of food science*, 81(7), E1716-E1725. <https://doi.org/10.1111/1750-3841.13342>
- Chu, C. C., Chew, S. C., Liew, W. C., & Nyam, K. L. (2023). Review article vitamin E: a multi-functional ingredient for health enhancement and food preservation. *Journal of Food Measurement and Characterization*, 17(6), 6144-6156. <https://doi.org/10.1007/s11694-023-02042-z>
- Coban, H. B. (2020). Organic acids as antimicrobial food agents: applications and microbial productions. *Bioprocess and Biosystems Engineering*, 43(4), 569-591. <https://doi.org/10.1007/s00449-019-02256-w>
- Fabbri, S., & Stoodley, P. (2016). Mechanical properties of biofilms. The perfect slime—microbial extracellular polymeric substances, 153-178.
- Fish, K. E., Collins, R., Green, N., Sharpe, R., Douterelo, I., Osborn, A. M., ... & Boxall, J. (2015). Characterisation of the physical composition and microbial community structure of biofilms within a model full-scale drinking water distribution system. *Plos One*, 10(2), e0115824. <https://doi.org/10.1371/journal.pone.0115824>
- Glaser, T. K., Plohl, O., Vesel, A., Ajdnik, U., Ulrih, N. P., Chen, L., ... & Zemljč, L. F. (2019). Functionalization of polyethylene (pe) and polypropylene (pp) material using chitosan nanoparticles with incorporated resveratrol as potential active packaging. *Materials*, 12(13), 2118. <https://doi.org/10.3390/ma12132118>
- González-Machado, C., Capita, R., Riesco-Peláez, F., & Alonso-Calleja, C. (2018). Visualization and quantification of the cellular and extracellular components of salmonella agona biofilms at different stages of development. *Plos One*, 13(7), e0200011. <https://doi.org/10.1371/journal.pone.0200011>
- Guo, H., Takemura, Y., Tange, D., Kurata, J., & Aota, H. (2023). Redox-active ferrocene polymer for electrode-active materials: step-by-step synthesis on gold electrode using automatic sequential polymerization equipment. *Polymers*, 15(17), 3517. <https://doi.org/10.3390/polym15173517>

- Guo, W., Xu, Y., Yang, Y., Xiang, J., Chen, J., Luo, D., ... & Xie, Q. (2023). Antibiofilm effects of oleuropein against staphylococcus aureus: an in vitro study. *Foods*, 12(23), 4301. <https://doi.org/10.3390/foods12234301>
- Han, J. W., Ruiz-Garcia, L., Qian, J. P., & Yang, X. T. (2018). Food packaging: A comprehensive review and future trends. *Comprehensive Reviews in Food Science and Food Safety*, 17(4), 860-877. <https://doi.org/10.1111/1541-4337.12343>
- Han, x., Lou, Q., Feng, F., Xu, G., Hong, S., Yao, L., ... & Wang, X. (2022). Spatiotemporal release of reactive oxygen species and no for overcoming biofilm heterogeneity. *Angewandte Chemie International Edition*, 61(33). <https://doi.org/10.1002/anie.202202559>
- Huang, T., Qian, Y., Wei, J., & Zhou, C. (2019). Polymeric antimicrobial food packaging and its applications. *Polymers*, 11(3), 560. <https://doi.org/10.3390/polym11030560>
- Jähnert, T., Häupler, B., Janoschka, T., Hager, M. D., & Schubert, U. S. (2014). Polymers based on stable phenoxyl radicals for the use in organic radical batteries. *Macromolecular Rapid Communications*, 35(9), 882-887. <https://doi.org/10.1002/marc.201300791>
- Jiang, P., Li, J., Han, F., Duan, G., Lu, X., Gu, Y., ... & Yu, W. (2011). Antibiofilm activity of an exopolysaccharide from marine bacterium vibrio sp. qy101. *PLoS ONE*, 6(4), e18514. <https://doi.org/10.1371/journal.pone.0018514>
- Jiang, S. J., Zhang, T., Song, Y., Qian, F., Tuo, Y., & Mu, G. (2019). Mechanical properties of whey protein concentrate based film improved by the coexistence of nanocrystalline cellulose and transglutaminase. *International journal of biological macromolecules*, 126, 1266-1272. <https://doi.org/10.1016/j.ijbiomac.2018.12.254>
- Jiang, Z., Nero, T., Mukherjee, S., Olson, R., & Yan, J. (2021). Searching for the secret of stickiness: how biofilms adhere to surfaces. *Frontiers in Microbiology*, 12. <https://doi.org/10.3389/fmicb.2021.686793>
- Jiao, S., You, L., Wang, Z., Sun-Waterhouse, D., Waterhouse, G. I., Liu, C., ... & Wang, X. (2020). Optimization of enzyme-assisted extraction of bioactive-rich juice from chaenomeles sinensis (thouin) koehne by response surface methodology. *Journal of Food Processing and Preservation*, 44(9). <https://doi.org/10.1111/jfpp.14638>
- Kalpana, V. N., & Rajeswari, V. D. (2017). Biosynthesis of metal and metal oxide nanoparticles for food packaging and preservation: a green expertise. In *Food biosynthesis* (pp. 293-316). Academic Press. <https://doi.org/10.1016/B978-0-12-811372-1.00010-5>
- Kannan, A. and Pennathur, G. (2015). A quantitative study on the formation of pseudomonas aeruginosa biofilm. *SpringerPlus*, 4(1). <https://doi.org/10.1186/s40064-015-1029-0>

- Kausar, A. (2019). A review of high performance polymer nanocomposites for packaging applications in electronics and food industries. *Journal of Plastic Film & Sheeting*, 36(1), 94-112. <https://doi.org/10.1177/8756087919849459>
- Kimani, V. N., Chen, L., Liu, Y., Raza, W., Zhang, N., Mungai, L. K., ... & Zhang, R. (2016). Characterization of extracellular polymeric substances of *Bacillus amyloliquefaciens* *sqr9* induced by root exudates of cucumber. *Journal of Basic Microbiology*, 56(11), 1183-1193. <https://doi.org/10.1002/jobm.201600104>
- Kolappan, A. and Satheesh, S. (2011). Efficacy of uv treatment in the management of bacterial adhesion on hard surfaces. *Polish Journal of Microbiology*, 60(2), 119-123. <https://doi.org/10.33073/pjm-2011-016>
- Li, F., Xiong, X., Yang, Y., Wang, J., Wang, M., Tang, J., ... & Gu, B. (2021). Effects of nacl concentrations on growth patterns, phenotypes associated with virulence, and energy metabolism in *Escherichia coli* *bw25113*. *Frontiers in Microbiology*, 12. <https://doi.org/10.3389/fmicb.2021.705326>
- Liu, R., Chen, X., Falk, S. P., Mowery, B. P., Karlsson, A. J., Weisblum, B., ... & Gellman, S. H. (2014). Structure–activity relationships among antifungal nylon-3 polymers: identification of materials active against drug-resistant strains of *Candida albicans*. *Journal of the American Chemical Society*, 136(11), 4333-4342. <https://doi.org/10.1021/ja500036r>
- Liu, Y. and Wang, L. (2022). Antibiofilm effect and mechanism of protocatechuic aldehyde against *Vibrio parahaemolyticus*. *Frontiers in Microbiology*, 13. <https://doi.org/10.3389/fmicb.2022.1060506>
- Liu, Y., Shen, K., Liu, Q., Diao, X., Ma, W., & Liu, G. (2024). Transcriptomics analysis of the mechanism behind *Lactobacillus rhamnosus* Gr18 biofilm formation in an Mn²⁺-deficient environment. *LWT*, 200, 116163. <https://doi.org/10.1016/j.lwt.2024.116163>
- Liu, Z., Wang, S., Liang, H., Zhou, J., Zong, M., Cao, Y., & Lou, W. (2024). A review of advancements in chitosan-essential oil composite films: Better and sustainable food preservation with biodegradable packaging. *International Journal of Biological Macromolecules*, 133242. <https://doi.org/10.1016/j.ijbiomac.2024.133242>
- Mahatmanti, F. W., Alauhdin, M., & Kusumaningrum, S. B. C. (2024). Smart and green packaging made from chitosan-based biofilm with the addition of ginger oil and anthocyanins from butterfly pea flower extract (*Clitoria ternatea* L). *Jurnal Kimia Sains Dan Aplikasi*, 27(2), 53-63. <https://doi.org/10.14710/jksa.27.2.53-63>
- Martínez, S. R., Ibarra, L. E., Ponzio, R. A., Forcone, M. V., Wendel, A., Chesta, C. A., ... & Palacios, R. E. (2020). Photodynamic inactivation of escape group bacterial pathogens in planktonic and biofilm cultures using metallated porphyrin-doped conjugated polymer nanoparticles. *ACS Infectious Diseases*, 6(8), 2202-2213. <https://doi.org/10.1021/acsinfecdis.0c00268>

- Nan, Y., Rodas-Gonzalez, A., Stanford, K., Nadon, C., Yang, X., McAllister, T., & Narváez-Bravo, C. (2024). Lactic acid bacteria and spoilage bacteria: Their interactions in *Escherichia coli* O157: H7 biofilms on food contact surfaces and implications for beef contamination. *Journal of Food Safety*, 44(1), e13101. <https://doi.org/10.1111/jfs.13101>
- Nazreen, A. Z., Jai, J., Ali, S. A., & Manshor, N. M. (2020). Moisture adsorption isotherm model for edible food film packaging—a review. *Scientific Research Journal*, 17(2), 221-245. <https://doi.org/10.24191/srj.v17i2.10160>
- Onyeaka, H., Obileke, K., Makaka, G., & Nwokolo, N. (2022). Current research and applications of starch-based biodegradable films for food packaging. *Polymers*, 14(6), 1126. <https://doi.org/10.3390/polym14061126>
- Özkul, G., Kehribar, E. Ş., & Şeker, U. Ö. Ş. (2023). An Antibiotic Degrading Engineered Living Material Platform to Combat Environmental Antibiotic Resistance. *bioRxiv*, 2023-10. <https://doi.org/10.1101/2023.10.19.563050>
- Panahi, Y., Gharekhani, A., Hamishehkar, H., Zakeri-Milani, P., & Gharekhani, H. (2019). Stomach-specific drug delivery of clarithromycin using asemi interpenetrating polymeric network hydrogel made ofmontmorillonite and chitosan: synthesis, characterization and invitro drug release study. *Advanced Pharmaceutical Bulletin*, 9(1), 159-173. <https://doi.org/10.15171/apb.2019.019>
- Park, S., Lee, M. Y., Kim, J., Kim, H., Jung, M., Shin, M., ... & Jang, M. (2019). Antibiofilm effects of synthetic antimicrobial peptides against drug-resistant pseudomonas aeruginosa and staphylococcus aureus planktonic cells and biofilm. *Molecules*, 24(24), 4560. <https://doi.org/10.3390/molecules24244560>
- Pinto, A. M., Cabral, J., Tanaka, D. A. P., Mendes, A., & Magalhães, F. D. (2012). Effect of incorporation of graphene oxide and graphene nanoplatelets on mechanical and gas permeability properties of poly(lactic acid) films. *Polymer International*, 62(1), 33-40. <https://doi.org/10.1002/pi.4290>
- Pleva, P., Bartošová, L., Máčalová, D., Zálešáková, L., Sedlaříková, J., & Janalíková, M. (2021). Biofilm formation reduction by eugenol and thymol on biodegradable food packaging material. *Foods*, 11(1), 2. <https://doi.org/10.3390/foods11010002>
- Polak, J., Wlizio, K., Pogni, R., Petricci, E., Graż, M., Szałapata, K., ... & Jarosz-Wilkołazka, A. (2020). Structure and bioactive properties of novel textile dyes synthesised by fungal laccase. *International Journal of Molecular Sciences*, 21(6), 2052. <https://doi.org/10.3390/ijms21062052>
- Popescu, P. A., Palade, L. M., Nicolae, I., Popa, E. E., Miteluţ, A. C., Drăghici, M., ... & Popa, M. E. (2022). Chitosan-based edible coatings containing essential oils to preserve the shelf life and postharvest quality parameters of organic strawberries and apples during cold storage. *Foods*, 11(21), 3317. <https://doi.org/10.3390/foods11213317>

- Powell, L. C., Sowedan, A., Khan, S., Wright, C. J., Hawkins, K., Onsøyen, E., ... & Thomas, D. W. (2013). The effect of alginate oligosaccharides on the mechanical properties of Gram-negative biofilms. *Biofouling*, 29(4), 413-421. <https://doi.org/10.1080/08927014.2013.777954>
- Quyen, D. T. M., Adisak, J., & Rachtanapun, P. (2012). Relationship between solubility, moisture sorption isotherms and morphology of chitosan/methylcellulose films with different carbendazim content. *Journal of Agricultural Science*, 4(6). <https://doi.org/10.5539/jas.v4n6p187>
- Rahmadhia, S. N. (2023). Physicochemical properties and microbial inhibition on biofilms cassava starch with green cayenne pepper leaf extract (*capsicum frutescens* L). *Jurnal Keteknikan Pertanian*, 11(2), 153-164. <https://doi.org/10.19028/jtep.011.2.153-164>
- Reichling, J. (2020). Anti-biofilm and virulence factor-reducing activities of essential oils and oil components as a possible option for bacterial infection control. *Planta Medica*, 86(08), 520-537. <https://doi.org/10.1055/a-1147-4671>
- Riahi, Z., Rhim, J., Bagheri, R., Pircheraghi, G., & Lotfali, E. (2022). Carboxymethyl cellulose-based functional film integrated with chitosan-based carbon quantum dots for active food packaging applications. *Progress in Organic Coatings*, 166, 106794. <https://doi.org/10.1016/j.porgcoat.2022.106794>
- Roy, S. and Rhim, J. (2020). Fabrication of copper sulfide nanoparticles and limonene incorporated pullulan/carrageenan-based film with improved mechanical and antibacterial properties. *Polymers*, 12(11), 2665. <https://doi.org/10.3390/polym12112665>
- Sadekuzzaman, M., Yang, S., Kim, H. S., Mizan, M. F. R., & Ha, S. D. (2017). Evaluation of a novel antimicrobial (lauric arginate ester) substance against biofilm of *Escherichia coli* O157: H7, *Listeria monocytogenes*, and *Salmonella* spp. *International Journal of Food Science & Technology*, 52(9), 2058-2067. <https://doi.org/10.1111/ijfs.13484>
- Sapalina, F. and Retnaningrum, E. (2020). Molecular characterization of lactic acid bacteria producing edible biofilm isolated from kimchi. *Biodiversitas Journal of Biological Diversity*, 21(3). <https://doi.org/10.13057/biodiv/d210315>
- Sondari, D., Falah, F., Suryaningrum, R., Sari, F. P., Septefani, A. A., Restu, W. K., ... & Sampora, Y. (2019). Biofilm based on modified sago starch: preparation and characterization. *Reaktor*, 19(3), 125-130. <https://doi.org/10.14710/reaktor.19.3.125-130>
- Souza, V. V. M. A. d., Crippa, B. L., Almeida, J. M. d., Iacuzio, R., Setzer, W. N., Sharifi-Rad, J., ... & Silva, N. C. C. (2020). Synergistic antimicrobial action and effect of active chitosan-gelatin biopolymeric films containing *thymus vulgaris*, *ocimum basilicum* and *origanum majorana* essential oils against *escherichia coli* and *staphylococcus aureus*. *Cellular and Molecular Biology*, 66(4), 214-223. <https://doi.org/10.14715/cmb/2020.66.4.26>

- Sun, X., Li, Q., Wu, H., Zhou, Z., Su, F., Deng, P., ... & Lu, C. (2023). Sustainable starch/lignin nanoparticle composites biofilms for food packaging applications. *Polymers*, 15(8), 1959. <https://doi.org/10.3390/polym15081959>
- Taglialegna, A., Navarro, S., Ventura, S., Garnett, J. A., Matthews, S., Penadés, J. R., ... & Valle, J. (2016). Staphylococcal bap proteins build amyloid scaffold biofilm matrices in response to environmental signals. *PLOS Pathogens*, 12(6), e1005711. <https://doi.org/10.1371/journal.ppat.1005711>
- Valdés, A., Ramos, M., Beltrán, A. M., Jiménez, A., & Garrigós, M. C. (2017). State of the art of antimicrobial edible coatings for food packaging applications. *Coatings*, 7(4), 56. <https://doi.org/10.3390/coatings7040056>
- Vera, M., Krok, B., Bellenberg, S., Sand, W., & Poetsch, A. (2013). Shotgun proteomics study of early biofilm formation process of *acidithiobacillus ferrooxidans* atcc 23270 on pyrite. *Proteomics*, 13(7), 1133-1144. <https://doi.org/10.1002/pmic.201200386>
- Wahab, D. N. A., Siddique, M. B. M., Chew, J. J., Su, H. T., Khairuddin, N., Khaerudini, D. S., ... & Sunarso, J. (2023). Characterization of starch biofilm reinforced with cellulose microfibrils isolated from *Musa saba* midrib residue and its application as an active packaging film. *Journal of Applied Polymer Science*, 140(48). <https://doi.org/10.1002/app.54720>
- Wang, H., Zou, H., Wang, Y., Jin, J., Wang, H., & Zhou, M. (2022). Inhibition effect of epigallocatechin gallate on the growth and biofilm formation of *Vibrio parahaemolyticus*. *Letters in Applied Microbiology*, 75(1), 81-88. <https://doi.org/10.1111/lam.13712>
- Wang, X., Wang, K., Pu, H., & Sun, D. (2022). Formation of *Shewanella putrefaciens* biofilms on nylon film and effects on putrefaction of large yellow croaker. *Journal of Food Processing and Preservation*, 46(11). <https://doi.org/10.1111/jfpp.17133>
- Wyrwa, J. and Barska, A. (2017). Innovations in the food packaging market: active packaging. *European Food Research and Technology*, 243(10), 1681-1692. <https://doi.org/10.1007/s00217-017-2878-2>
- Yuvaraj, D., Iyyappan, J., Gnanasekaran, R., Ishwarya, G., Harshini, R., Dhithya, V., ... & Gomathi, K. (2021). Advances in bio food packaging – an overview. *Heliyon*, 7(9), e07998. <https://doi.org/10.1016/j.heliyon.2021.e07998>
- Zhang, W., Xiao, P., & Wang, D. (2014). Central treatment of different emulsion wastewaters by an integrated process of physicochemically enhanced ultrafiltration and anaerobic-aerobic biofilm reactor. *Bioresource Technology*, 159, 150-156. <https://doi.org/10.1016/j.biortech.2014.02.067>
- Zheng, S. L., Bawazir, M., Dhall, A., Kim, H., He, L., Heo, J., ... & Hwang, G. (2021). Implication of surface properties, bacterial motility, and hydrodynamic conditions on bacterial surface sensing and their initial adhesion. *Frontiers in Bioengineering and Biotechnology*, 9. <https://doi.org/10.3389/fbioe.2021.643722>

- Zouari-Ellouzi, S., Châari, F., Bouaziz, A., Kallel, F., Mechim, M., Jaziri, M., ... & El-louze-Ghorbel, R. (2018). Suitability of starch extracted from fresh pasta by-product in biodegradable film production. *Environmental Progress & Sustainable Energy*, 38(2), 527-533. <https://doi.org/10.1002/ep.13012>
- Шершнева, Е. Г. (2022). Biodegradable food packaging: benefits and adverse effects. *IOP Conference Series: Earth and Environmental Science*, 988(2), 022006. <https://doi.org/10.1088/1755-1315/988/2/022006>



CHAPTER 27

Carbon Capture and Sequestration Via Torrefied Biomass

Zuhal Akyürek¹

¹ Assoc. Prof. Dr., Burdur Mehmet Akif Ersoy University, ORCID ID: 0000-0003-3102-4278

1. INTRODUCTION

The rising demand for energy and the concerns on climate change related to fossil fuel utilization in energy generation sector require immediate transition to sustainable energy alternatives. The electricity production in the World has increased from 11896 TWh to 29479 TWh in the last three decades (Figure 1, Statistica,2024). According to IPCC 4th Assessment (2021) anthropogenic greenhouse gas emissions have significant influence on global average temperature rise since the mid-20th century. If energy production from fossil fuels continues to rise by the same rate, it would not be possible to limit the average global temperature rise to 1.5 °C value, and to reach the Paris Agreement goals (IEA, World Energy Outlook 2023).

Renewable energy sources play a key role in mitigating global environmental problems and climate change. Given the detrimental impacts of global climate change, accelerating the transition from fossil fuels to renewable energy (RE) sources has become utmost important. Currently, about 60% of global electricity generation is produced from fossil fuels resources (Figure 2). To meet rising global energy demands and to reduce the global warming effect, fossil fuel energy must be replaced at least by an equal amount of clean fuel substitutes and renewable energy.

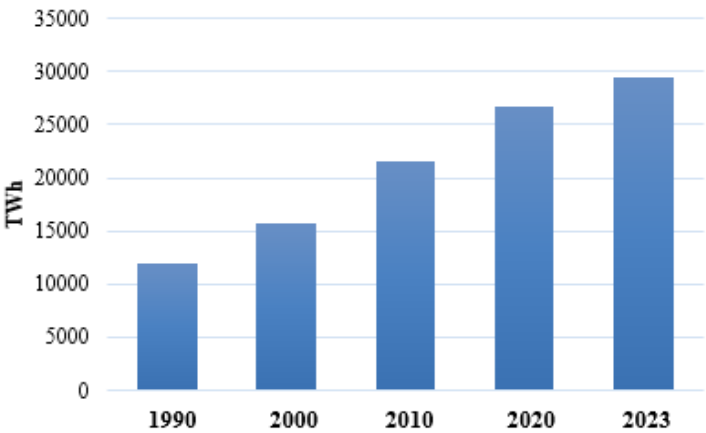


Figure 1. World electricity generation, (Statistica, 2024).

Biomass emerge as a promising option ensuring energy security of nations. Biomass is a carbon neutral energy source that accounts for approximately 14% of the global energy consumption (Siwal et al., 2022). Diversifying the world energy matrix with biomass energy sources not only reduce greenhouse gas emissions and climate change impacts, but also provide local energy supply and socio-economic growth in rural areas to improve the resilience of the society (IEA Bioenergy Report, 2023). Bioenergy has also significant contribution to environmental sustainability by protection of natural sources and biodiversity (Rial, 2024).

The most effective promotion of biomass utilization in energy sector can be achieved by governmental policies (Saravanan et al., 2020). For instance, in the United States, Canada, Brazil, and the European Union Countries, there are many policy actions that support motivation for bioenergy production with incentives, subsidies, tax exemptions, etc. and establish a stable economic environment to investors (Ebedian et al., 2020).

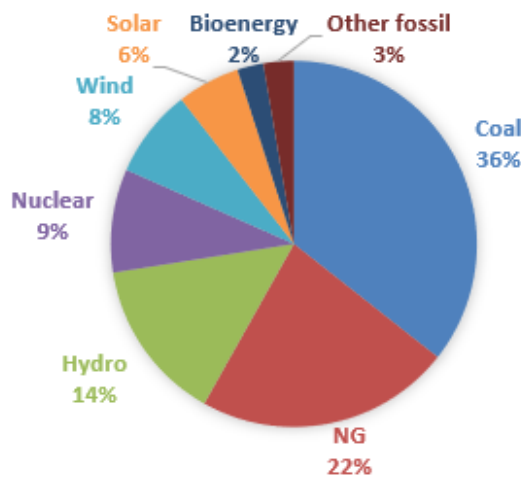


Figure 2. The distribution of energy sources for global electricity generation in 2023 (Statistica, 2024).

2. BIOMASS CARBON CAPTURING AND SEQUESTRATION

Carbon capture and storage (CCS) term describes separation of carbon dioxide gas from power generation plants and industry, its transportation and storage in the geological layers (IPCC, 2014). CCS methods are generally used for reducing carbon dioxide produced from fossil fuel resources. Carbon capturing for bioresources is more advantageous in terms of climate change impact. As biomass is a carbon neutral source, its energy conversion has zero carbon dioxide emission impact. Moreover, it is capturing and storing underground, results in carbon negative emissions (Kemper, 2015).

Biomass energy generation with CCS plays significant role in decarbonization strategies of the 2050 Net Zero Emissions (NZE) targets. In the NZE Scenario, the electricity sector accounts for almost 20% of the carbon dioxide emissions captured from coal fired power plants, bioenergy production plants and gas fired power plants in 2050 (IEA, 2021). Figure 3 illustrates the comparison of total carbon reduction in 2020 with predictions till 2050. The captured carbon dioxide is expected to reach 7600 million tons by 2050.

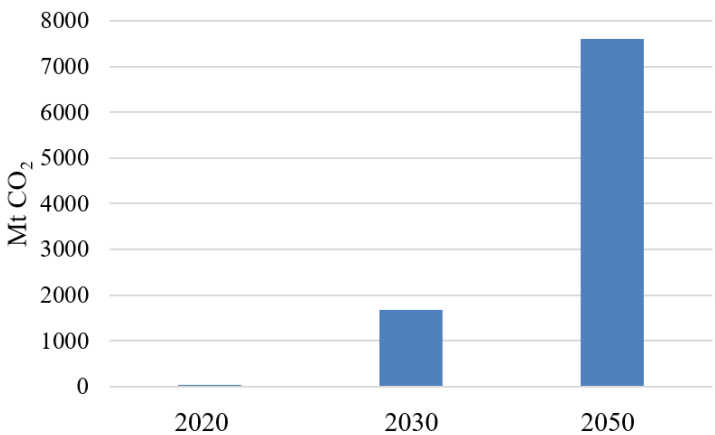


Figure 3. Energy-related and process CO₂ emission reduction targets

Transition process to bioenergy generation has some challenges, such as high investment costs, energy storage problems, etc. There occur some problems that limit biomass utilization in energy production systems related to its characteristics. Heterogeneous feature of bioresources, their low bulk density, high moisture content, low heating value, etc. harden biomass to energy

conversion. In addition, these characteristics increase the cost of their handling, transport, and storage.

Some of the biofuels can be directly utilized in energy systems as a renewable solid fuel substitute due to their properties, while some others may require pre-treatment methods to be used effectively (Akyürek, 2021; Shahbaz et al., 2021; Mignogna et al., 2024). Pre-treatment methods are essential for biofuel upgrading to increase their calorific value and fuel characteristics to develop sustainable energy systems based on biomass feedstocks.

2.1. PRE-TREATMENT VIA TORREFACTION METHODS

Biomass is a renewable and carbon neutral resource, and is recognized as clean fossil fuel substitute (Dacres et al. 2019). Torrefaction is an emerging technology for the pretreatment of biomass and upgrading its fuel properties. Torrefaction can be carried out under wet and dry torrefaction conditions according to the biofuel characteristics.

Dry torrefaction (DT) refers to biomass upgrading by thermal treatment in the absence of oxygen under atmospheric pressure and in a temperature range of 200-300 degrees Celsius. Wet torrefaction on the other hand refers to hydrothermal treatment of biomass carried out in the presence of water medium under autogenous pressure within temperature range of 180-300 °C (Akyürek, 2021a). The solid products obtained from wet torrefaction and dry torrefaction processes are called biochar\bio-coal and hydro-char, respectively.

Torrefied biomass poses higher energy density and enhanced fuel properties (Chen, 2018). The type of torrefaction process (wet\dry) mainly depends on the fuel characteristics. Biofuels with high moisture content are more appropriate for wet torrefaction pre-treatment process. Torrefaction produces higher carbon content solid product which exhibit high carbon capturing and sequestration potential.

In this study, carbon capturing potential of olive residues from olive oil production industry in Turkey is estimated by wet and dry torrefaction pretreatment methods. Torrefaction process performed in the temperature range of 200-250 °C are considered for comparison.

3. CARBON CAPTURE POTENTIAL OF TORREFIED OLIVE RESIDUES

Olive production has high economic value in Turkey. In 2023, olive production reached nearly 1.5 million tons (Statistica, 2023). Olive residues can be converted into carbon rich biofuel via torrefaction process. Biochar and hydro char have higher potential for carbon dioxide sequestration.

The theoretical carbon sequestration potential of olive residues (OR) is determined by using the experimental results of previous studies. Wet and dry torrefaction processes have carried out at 200 and 250 °C. Characteristics of fuels obtained at different temperatures from wet torrefaction (WOR-200, WOR-250) and dry torrefaction (DOR-200, DOR-250) processes are presented in Table 1.

The fuel characteristics of torrefied biomass in wet and dry torrefaction processes have shown that dry torrefaction pretreatment of olive residues resulted in higher energy density products compared to wet torrefaction process.

Table 1. Proximate and ultimate analyses of raw and torrefied olive residues (Bena-vente and Fullana, 2015; Volpe et al., 2016; Missaoui et al., 2017).

	Raw OR	WOR- 200	WOR- 250	DOR- 200	DOR- 250
Proximate Analysis (as received basis, wt. %)					
Moisture	4.3	1.6	0.8	2.6	1.2
Volatile Matter	75	77.1	72.8	78.2	71.8
Fixed Carbon	16.8	16.5	21.7	16.1	23
Ash	3.9	4.7	4.7	3.2	3.2
Elemental Analysis (Dry basis, wt. %)					
C	53.5	60.7	67.8	66.3	68.2
H	6.8	6.6	6.5	8.9	8
N	1.1	1.4	1.4	1.7	1.6
O	38.6	31.2	24.3	16.2	14
HHV, MJ/kg	19.8	20.9	23.3	23.2	27.2

From the carbon content and mass yield, the carbon yield % representing the amount of carbon remaining in the solid biochar\hydro char was calculated.

$$\% Carbon\ yield = \frac{BC_{Carbon}}{B_{Carbon}} \times 100 \qquad (1)$$

BC represents the carbon content in biochar/hydrocahr and B refers to carbon content in the biomass feedstock.

The increase in temperature from 200 to 250 °C has also shown positive influence on calorific value. Figure 4 presents carbon yields of the wet and dry torrefaction process products. As can be seen from the figure dry torrefaction of olive residue has higher carbon yield than wet torrefaction pretreatment products.

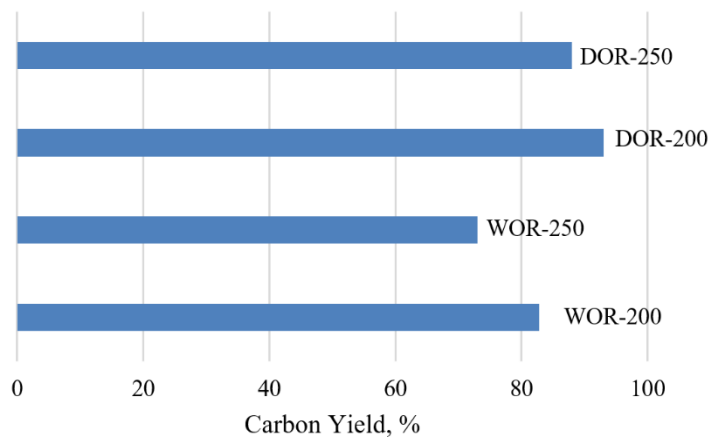


Figure 4. Carbon recovery of wet and dry torrefaction products.

Van Krevelen Plot is useful and simple method for predicting the chemical structure of biomass and biochar\hydro char by using chemical data. Van Krevelen diagram (H/C molar ratio vs O/C molar ratio) of olive residue and biochar and hydrochars produced at 200 and 250 °C are presented in Fig. 5. Examination of the plot of revealed H/C and O/C molar ratios of biochars\hydro chars were lower those of raw olive residue. Lower molar ratios indicate higher calorific value and higher stability of the material in soil (Akyürek, 2021b).

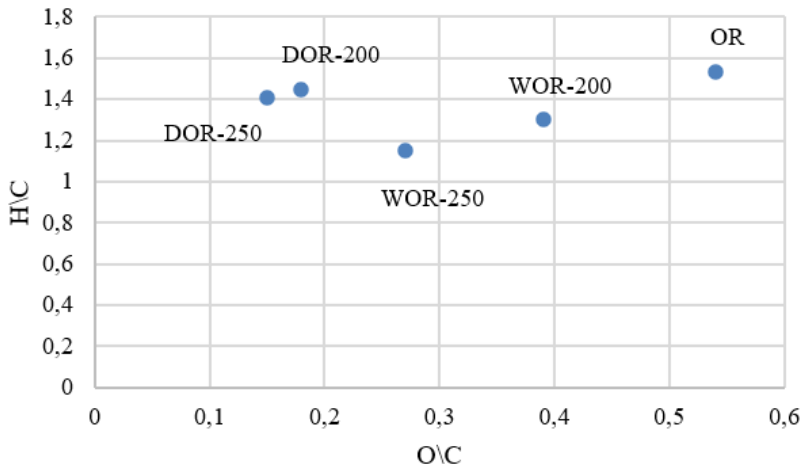


Figure 5. The Van Krevelen plot of raw olive residue and wet\dry torrefied products at 200 and 250 °C.

Carbon dioxide sequestration potential was determined by;

$$CO_{2\text{ }Eq} = BC_{Carbon} \times \frac{MW_{CO_2}}{MW_C} \quad (2)$$

where MW_C and MW_{CO_2} are the molecular weight of carbon and carbon dioxide, respectively.

The carbon dioxide sequestration potential of torrefied olive residue in Turkey have illustrated in Figure 6. As can be seen from the figure, dry torrefaction of olive residue at 200 °C has shown the highest annual carbon capturing potential of 2.04 million tons. Biochar produced at 250 °C has shown 1.74 carbon dioxide capturing capacity followed by hydro chars produced at 200 and 250 °C.

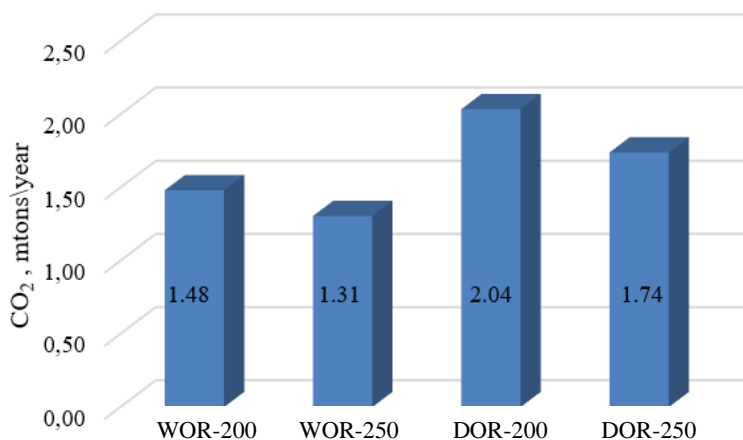


Figure 6. Carbon dioxide sequestration potential of wet and dry torrefaction of olive residue at 200 and 250 °C.

4. CONCLUDING REMARKS

The concerns on global climate change have raised the interest on carbon dioxide capturing and sequestration (CCS) of biomass in soil or underground. To reduce the anthropogenic gaseous emissions, utilization of biochar and hydro chars has become simple and effective options. This study provides the theoretical carbon dioxide sequestration potential of biochar and hydro chars produced from olive residue at two different temperatures (200 °C and 250 °C). The results revealed that dry torrefaction pretreatment products have greater carbon dioxide sequestration capacity compared to those of wet torrefaction pretreatment products. The increase in temperature from 200 to 250 °C has shown positive impact on energy density of the solid products however, carbon sequestration potential has seen to reduce with temperature in the case for both biochar and hydro chars. In conclusion, torrefaction is a useful pretreatment method to enhance the fuel properties of biofuels and soil application of biochar and hydro chars has high potential for reducing atmospheric carbon dioxide emissions and producing a carbon negative environment.

Acknowledgement

Financial supports provided by Burdur Mehmet Akif Ersoy University through a research project MAKÜ-BAP-0957-YL-23 in aid of this research gratefully acknowledged.

REFERENCES

- Akyürek Z. (2021a) Torrefaction for Energy Valorization of Animal Waste: Combustion Performances, Kinetics, Thermodynamics. *Solid Fuel Chemistry*, 55(S1), S1-S10. <https://doi.org/10.3103/S0361521921070028>
- Akyürek Z., (2021b) Carbon Dioxide Sequestration Assessment through Pyrogenic Biomass: Case for Turkey, *Polish Journal of Environmental Studies* 30 (3) 2467–2475. <https://dx.doi.org/10.15244/pjoes/129688>
- Benavente V., Fullana A. (2015) Torrefaction of olive mill waste Biomass and Bioenergy 73, 186-194. <https://doi.org/10.1016/j.biombioe.2014.12.020>
- Chen Z.W., Wang M, Ren Y., Jiang E., Jiang Y., Li W. (2018). Biomass torrefaction: A promising pretreatment technology for biomass utilization. *IOP Conf. Ser.: Earth Environ. Sci.* 113 012201. <https://doi.org/10.1088/1755-1315/113/1/012201>
- Dacres O.D., Tong S., Li X., Zhu X., Edreis E.M.A., Liu H., Luo G., Worasuwannarak N., Kerdsuwan S., Fungtammasan B., Yao H. (2019) Pyrolysis kinetics of biomasses pretreated by gas-pressurized torrefaction. *Energy Convers Manag*, 182, 117-125, <https://doi.org/10.1016/j.enconman.2018.12.055>
- Ebadian M, van Dyk S, McMillan JD, Saddler J. Biofuels policies that have encouraged their production and use: an international perspective. *Energy Policy*, 147,111906. <https://doi.org/10.1016/j.enpol.2020.111906>
- International Energy Agency (IEA) World Energy Outlook, 2023. <https://www.iea.org/reports/world-energy-outlook-2023>
- International Energy Agency (IEA) IEA Bioenergy Report 2023. How bioenergy contributes to a sustainable future. https://www.ieabioenergyreview.org/wp-content/uploads/2022/12/IEA_BIOENERGY_REPORT.pdf
- IPCC (Intergovernmental Panel on Climate Change) (2021) Climate change 2021: The physical science basis. Working Group I contribution to the IPCC Sixth Assessment Report. Cambridge, United Kingdom: Cambridge University Press. www.ipcc.ch/assessment-report/ar6
- IPCC (Intergovernmental Panel on Climate Change) (2014) Mitigation of Climate Change. Contribution of Working Group III to the Fifth Assessment Report of the Intergovernmental Panel on Climate Change Cambridge University Press, Cambridge, United Kingdom, and New York, NY, USA.
- Kemper J. (2015) Biomass and carbon dioxide capture and storage: A review. *International Journal of Greenhouse Gas Control* 40, 401-430. <https://doi.org/10.1016/j.ijggc.2015.06.012>
- Mignogna, D., Szabó, M., Ceci, P., & Avino, P. (2024). Biomass Energy and Biofuels: Perspective, Potentials, and Challenges in the Energy Transition. *Sustainability*, 16(16), 7036. <https://doi.org/10.3390/su16167036>

- Missaoui A., Bostyn S., Belandria V., Cagnon B., Sarh B., Gökalp İ. (2017) Journal of Analytical and Applied Pyrolysis 128, 281-290. <https://doi.org/10.1016/j.jaap.2017.09.022>
- Rial R.C. (2024) Biofuels versus climate change: Exploring potentials and challenges in the energy transition. Renewable and Sustainable Energy Reviews 196, 114369. <https://doi.org/10.1016/j.rser.2024.114369>
- Saravanan AP, Pugazhendhi A, Mathimani T. (2020) A comprehensive assessment of biofuel policies in the BRICS nations: implementation, blending target and gaps. Fuel 272, 117635. <https://doi.org/10.1016/j.fuel.2020.117635>.
- Shahbaz, M.; AlNouss, A.; Ghiat, I.; McKay, G.; Mackey, H.; Elkhailifa, S.; Al-Ansari, T. A Comprehensive Review of Biomass Based Thermochemical Conversion Technologies Integrated with CO₂ Capture and Utilisation within BECCS Networks. Resour. Conserv. Recycl. 2021, 173, 105734.
- Siwal, S.S.; Zhang, Q.; Devi, N.; Saini, A.K.; Saini, V.; Pareek, B.; Gaidukovs, S.; Thakur, V.K. Recovery Processes of Sustainable Energy Using Different Biomass and Wastes. TIDEE TERI Inf. Dig. Energy Environ. 2022, 21, 162–163
- Statistica, Generation of electricity worldwide from 1990 to 2023, by energy source (2023). <https://www.statista.com/statistics/273273/world-electricity-generation-by-energy-source/>
- Volpe M., Fiori L., Volpe R., Messineo A. (2016) Upgrading of Olive Tree Trimmings Residue as Biofuel by Hydrothermal Carbonization and Torrefaction: a Comparative Study. Chemical Engineering Transactions, 50, 13-18. <https://doi.org/10.3303/CET1650003>



CHAPTER 28

Review of AI-Powered Digital Twin Technology for Real-Time Mechanical System Simulation and Optimization

Hamid Zamanlou¹ & Filiz Karabudak²

¹ Dr., Ataturk University, Faculty of Engineering, Department of Mechanical engineering, ORCID: 0000-0002-9780-8924

² Associate professor. Gumushane University, Faculty of Engineering and Natural Science, Department of Mechanical Engineering, ORCID: 0000-0002-7365-0333

INTRODUCTION

Digital Twin Technology (DTT), is a virtual model that replicates the characteristics, behavior, and performance of its physical counterpart in real time

or over time. Digital twin technology is used in various industries such as manufacturing systems, aerospace, energy, healthcare, transportation, etc. This technology allows engineers, designers, and operators to simulate, monitor, and optimize the performance of a physical system in a virtual environment. The concept has found widespread application in the field of mechanical systems, where it is used to model the behavior of machines, structures, and components under a wide range of conditions. Offering unrivaled insight into system performance, the real-time simulation of the operational dynamics of mechanical systems by digital twins enables early fault detection, better design methodologies, and enhanced maintenance strategies (Hao et al., 2024).

Using digital twin technology has many benefits, the most important of which are discussed in this section:

Productivity: By creating a DT of a physical system, engineers and operators can identify and address potential issues before they occur, optimizing performance and reducing downtime and maintenance costs (Rojek et al., 2024).

Decision-making: DT provide real-time data and analytics, enabling better decision-making and more informed actions (Granacher et al., 2022). This can lead to improved productivity, reduced costs and increased profitability.

Safety and sustainability: Digital twins can be used to identify potential safety hazards and environmental impacts, allowing operators to take corrective action before incidents occur (Agnusdei, 2021).

Overall, DTT has the potential to revolutionize the way physical systems are designed, operated, and maintained, leading to improved efficiency, safety, and sustainability, as well as increased profitability and customer satisfaction.

Digital twin frameworks can take advantage of this technology, and its potential is even greater when AI is integrated. Giving AI the capacity to analyze large volumes of data, use inference, and make decisions in real time offers a whole new level of intelligence in the digital twin space. Machine learning models in digital twin systems, in conjunction with deep learning and reinforcement learning algorithms, are now used not only to increase the accuracy of simulations, but also to predict future system behavior, optimize performance,

and provide actionable insights. The collaboration of AI and digital twins is already transforming industries such as aerospace, automotive, manufacturing, and energy by enabling better operational efficiency, reduced downtime, and solidified data-driven decision-making.

In mechanical system simulation and optimization, AI-driven digital twins offer a solution to many long-standing problems. Most traditional simulation techniques require huge amounts of time and resources for physical prototyping and testing, hence placing a limit on how the product development cycle can be accelerated while trying to maintain minimal costs. By unleashing advanced artificial intelligence in digital twins, engineers and researchers can create virtual models of mechanical systems in real time and study various scenarios with the aim of optimizing design parameters rather than taking expensive and time-consuming physical testing. Also, artificial intelligence allows models to learn from real-world data continuously, thereby constantly improving their accuracy and predictions (Vijayakumar et al., 2019).

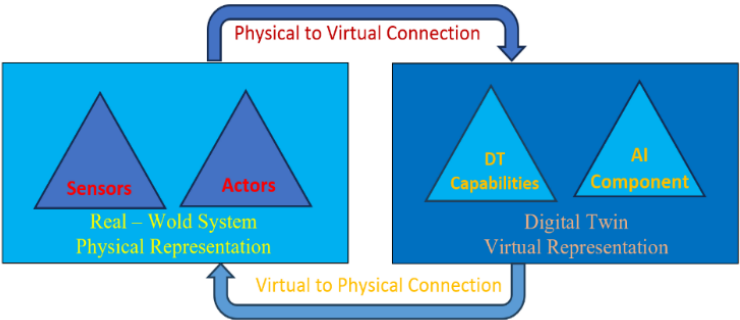


Fig. 1. Diagram illustrating the structure of a digital twin integrated with an AI component (Kreuzer, 2024).

Digital twins can be divided into three broad types that represent different times in the process for use:

Digital Twin Pre-production (DTP): Takes place before the physical product is created.

Digital Twin Application (DTI): This digital twin is used when a product is manufactured to run tests in different scenarios.

Digital Twin Aggregation (DTA): Collects previous model information (DTI) to determine a product’s capabilities, run prototypes, and test operating variables.

This breadth and variety of digital twin models can provide professionals with a wide range of applications including logistics planning, product development and redesign, quality control/management, and systems planning.

DT with AI and FEM

Integrating FEM with Digital Twin Technology and AI indeed provides a potent means to simulate and optimize mechanical systems in real time. Here, the digital twin refers to a virtual replica of a physical system but updated continuously with live data. The value added by AI to this process is being able to sense the data and predict performance characteristics intelligently, also guiding further improvement of the system. On the other hand, FEM is a numerical method for solving problems in engineering and physics, which has now been integrated into the digital twin for virtually analyzing any complex mechanical systems for any kinds of loads by preparing detailed reports on stresses, deformations, and thermal behavior (Dos Santos et al., 2022).

The interaction of AI and FEM enables iteration toward optimization. The results thrown by FEM simulations could be analyzed by the AI system itself in order to evidence design flows, optimize materials, or predict performance for different variables of operation. This might also involve the AI component making recommendations for design changes or operational adjustments that would result in higher performance, lower energy consumption, or increased component lifetimes. In this way, FEM-based simulations can be updated iteratively as new data arrives in the system, allowing real-time optimization and refinement.

By integrating AI with FEM within the digital twin framework, predictive maintenance strategies become more effective. AI analyzes data trends and FEM-based simulation results to identify early signs of wear, fatigue, or potential failure. This predictive capability enables timely maintenance interventions, preventing unplanned downtime and reducing repair costs (Nouzil et al., 2023).

Benefits of Integrating AI and FEM with DT

Accuracy and Reliability: AI's ability to learn and adapt enhances the precision of FEM simulations, providing more accurate predictions of system behavior (Zhang et al., 2022). Real-time data integration ensures that the digital twin remains a close reflection of the physical system.

Cost and Time Efficiency: The application of FEM simulations in the context of a digital twin enables engineers to evaluate various scenarios without necessitating physical prototypes or testing. Moreover, the integration of AI

accelerates the optimization procedure, thereby diminishing the time and financial resources required for conventional design iterations.

Real-Time Decision-making: Real-time data from the physical system, AI-driven analytics, and FEM-based simulations allow for instantaneous input to decision-making. Such is of key importance in cases where the system necessitates high performance and instant respond, like those in Aerospace, Automotive, or industries (Wang et al., 2021).

System performance: Continuous tuning using real-time FEM simulations guided by AI enhances the improved efficiency, safety, and life of the system, allowing it to operate optimally throughout its lifecycle.

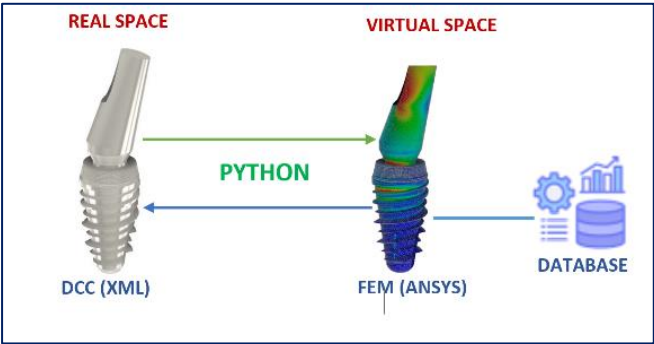


Figure 2. *Schematic View of Digital Twin with AI and FEM*
(Baer et al., 2023)

Challenges and Future Directions

Although the great promise that this technology holds, a number of critical challenges remain that need to be overcome to fully harness the functionalities of AI-driven digital twin technology for real-time simulation and optimization in mechanical systems. These challenges involve data, computation limitations, cybersecurity threats, and the need for an advanced technological framework (Fuller et al., 2021). Meeting these challenges is critical to ensuring the continued growth and widespread adoption of digital twins in the field of mechanical engineering and beyond.

Data Quality and Integration: The effectiveness of a digital twin is essentially anchored in the quality, consistency, and accuracy of the data it captures. Complex mechanical systems, especially, produce huge amounts of sensor data in real time, and the reliability of simulations and optimizations depends to a great degree on the level at which this data is integrated into the digital twin framework. Inaccurate or incomplete data can lead to biased

predictions, incorrect simulations of system behavior, and poor decision-making. The problem is further complicated by the diversity of sources since a mechanical system usually integrates several sensors, devices, and formats of data, each with its unique characteristics.

Computational Complexity

Real-time simulation and optimization of the mechanical systems using AI-enabled digital twins can be very demanding in terms of computational requirements. Mechanical systems, at scale, have very complex interactions among components, materials, and environmental variables. Modeling and simulation of such systems, especially in real-time applications, require significant computational resources, especially when AI-based methodologies such as deep learning, reinforcement learning, and optimization algorithms are used. These algorithms need to process large volumes of data, run iterative simulations, and make decisions in real time, all of which put heavy loads on today's computational infrastructure (Jafari et al., 2023). As systems grow in size and complexity, as with industrial-scale manufacturing lines, aerospace applications, or large structural components, the computational resources required to carry out real-time simulations and optimization grow exponentially.

CONCLUSION

The convergence of AI, FEM, and Digital Twin Technology is bound to a solid change in simulation, optimization, and maintenance processes of mechanical systems. The development of unprecedented capabilities for studying complex dynamics of systems, design optimization, and continual improvement of performance were due to the combination of real-time data gathering, predictive analytics, and highly complicated numerical simulations into one synergetic digital twin empowered by AI. FEM incorporation allows advanced simulation of mechanical conditions of stress, deformation, and other phenomena important to engineers for gaining better insight importance into the dynamic aspect of the systems in the virtual design environment without any physical prototyping.

The combination of AI and FEM within a digital twin framework brings as much accuracy and reliability to the simulation results as to the possibility of continuous optimization and up to predictive maintenance. The real-time 'smart' data from integrated analytics feeding on physics will automatically keep changing and adapting the digital twin and provide near-instant decisions in favor of efficiency and overall system safety.

Using sensor data and IoT devices, digital twins can be used to monitor the behavior and health of a system in real time. Digital twins also allow companies to quickly identify and act on potential problems. For example, a digital twin engine might contain information about its performance characteristics, allowing engineers to run simulations to test new designs or measure the impact of future changes. In other words, many digital twins are connected to physical devices that are part of an Internet of Things (IoT) network.

The challenges of data integration, computational complexity, and threats to systems associated with cybersecurity pose several hurdles to AI-driven development of digital twins. Continual innovations in computational technologies coupled with developments in emerging technologies like the 5G and Edge Computing, and Quantum Computing are providing a ray of hope for digital twin technologies acquisition in the modeling and optimization of mechanical systems, and such collaborations would further scale the growth. (Liu et al., 2019).

REFERENCES

- Hao, N., Li, Y., Liu, K., Liu, S., Lu, Y., Xu, B., ... & Zhao, Y. (2024). Artificial Intelligence-Aided Digital Twin Design: A Systematic Review.
- Rojek, I., Marciniak, T., & Mikołajewski, D. (2024). Digital twins in 3D printing processes using artificial intelligence. *Electronics*, 13(17), 3550.
- Granacher, J., Nguyen, T. V., Castro-Amoedo, R., & Maréchal, F. (2022). Overcoming decision paralysis—A digital twin for decision making in energy system design. *Applied Energy*, 306, 117954.
- Agnusdei, G. P., Elia, V., & Gnani, M. G. (2021). Is digital twin technology supporting safety management? A bibliometric and systematic review. *Applied Sciences*, 11(6), 2767.
- Vijayakumar, K., Dhanasekaran, C., Pugazhenthir, R., & Sivaganesan, S. (2019). Digital Twin for factory system simulation. *International Journal of Recent Technology and Engineering*, 8(1), 63-68.
- Kreuzer, T., Papapetrou, P., & Zdravkovic, J. (2024). Artificial intelligence in digital twins—A systematic literature review. *Data & Knowledge Engineering*, 102304.
- Dos Santos, J. F., Tshoombe, B. K., Santos, L. H., Araújo, R. C., Manito, A. R., Fonseca, W. S., & Silva, M. O. (2022). Digital twin-based monitoring system of induction motors using iot sensors and thermo-magnetic finite element analysis. *IEEE Access*, 11, 1682-1693.
- Nouzil, I., Eltaggaz, A., Deiab, I., & Pervaiz, S. (2023). Numerical CFD-FEM model for machining titanium Ti-6Al-4V with nano minimum quantity lubrication: A step towards digital twin. *Journal of Materials Processing Technology*, 312, 117867.
- Zhang, R., Wang, F., Cai, J., Wang, Y., Guo, H., & Zheng, J. (2022). Digital twin and its applications: A survey. *The International Journal of Advanced Manufacturing Technology*, 123(11), 4123-4136.
- Wang, K. J., Lee, Y. H., & Angelica, S. (2021). Digital twin design for real-time monitoring—a case study of die cutting machine. *International Journal of Production Research*, 59(21), 6471-6485.
- Baer, O., Giusca, C., Kumme, R., Prato, A., Sander, J., Mirian, D., & Hauschild, F. (2023). Digital Twin concept of a force measuring device based on the finite element method. *Acta IMEKO*, 12(1), 1-5.
- Fuller, A., Fan, Z., Day, C., & Barlow, C. (2020). Digital twin: Enabling technologies, challenges and open research. *IEEE access*, 8, 108952-108971.
- Jafari, M., Kavousi-Fard, A., Chen, T., & Karimi, M. (2023). A review on digital twin technology in smart grid, transportation system and smart city: Challenges and future. *IEEE Access*, 11, 17471-17484.
- Liu, G. R. (2019). FEA-AI and AI-AI: Two-way deepnets for real-time computations for both forward and inverse mechanics problems. *International Journal of Computational Methods*, 16(08), 1950045.



CHAPTER 29

Developing a Monitoring and Warning System for Cold Storage of Hotels for Sustainable Tourism

Ahmet oşgun¹

¹ Dr.Öğr.Üyesi., Akdeniz Üniversitesi Mühendislik Fakültesi Makine Mühendisliği Bölümü Kampüs/
ANTALYA

1. INTRODUCTION

The history of storing products is as old as human history. Mankind has attached great importance to the storage, preservation, and storage of products in order to consume or commercially utilize the agricultural products obtained in the following days, weeks and months. The storage of products was previously carried out in simply prepared containers, wells and cellars without temperature and humidity control. Today, storage activities have entered a very rapid development process with the help of science and technology. Now, long-term storage of products is carried out in modern facilities, with the help of machines, by controlling the temperature and humidity composition of the cooling environment in a way to minimize the deterioration and decay of the product (Sargin and Okudum 2014).

Today, a rapid development has been observed in storage activities thanks to the developments in science and technology. In cold storage of vegetables and fruits, spoilage and decay can be prevented with the help of modern and long-term storage machines. In addition, the commercial return of the stored product increases, the products can be stored longer, quality losses are reduced, it is possible to find fresh fruits and vegetables at affordable prices in all seasons and these activities provide employment in many sectors from packaging to transport (Katrancı and Kundakcı 2020).

The supply and continuous storage of food has always been a problem for humanity. To access food at the desired time based on needs, it is needed to store it. Because some foods are products that are grown once a year, these foods are stored by drying, fermenting, or in the form of traditional product such as jams. Moreover, while the overabundance of products when they first enter the market leads to price drops, their prices increase excessively when they are available outside their season, and this issue has paved the way for the emergence of the storage of foods in cold storage rooms (Devres *et al.* 2013).

Cold storage is a very important ring of the cold chain. In the last decade, the rate of energy consumption in cold storage has risen fastly. The coordination of technologies on solar electricity generation and demand side management (DSM) is very important for energy saving and cost adjusting (Deng *et al.* 2022).

The following parameters must be considered regarding cold storage rooms:

a) Temperature: The temperature of the cold storage room should be determined based on the properties of the products that will be stored. In general, products are stored at temperatures that are very close to their freezing point. On

the other hand, like some tropical fruits, some products may need to be stored at higher temperatures.

b) Thermal Insulation: To preserve energy in the storage of products (foods) in cold storage rooms, a homogeneous temperature profile should be provided. In this case, the thermal insulation coefficient should be optimized. Accordingly, by using insulation materials at a suitable thickness, it should be ensured that the temperature difference between the room and its interior surfaces is lower than 2°C. In general, a cold storage room contains a space heater with a fan, an evaporator, thermostatic and digital valves, and interior lighting equipment. There is also a control panel outside the room.

c) Relative Humidity: The relative humidity of the cooling environment is as important as the effectiveness of cooling. High relative humidity values inside cold storage rooms are inevitable when fresh fruits and vegetables are being stored. Evaporators, which are named internal units, can create a high relative humidity inside the cold storage room. Although this issue can be minimized using an effective design set by air conditioning engineers, it should be kept in mind that absolute humidity transfer around an evaporator is inevitable (Erkan 2011, Devres *et al.* 2013).

As in the case of all industrial firms, firms that are involved in cold storage room construction and installation also aim at effectiveness and efficiency with the minimum investment and operating cost. In commercial cold storage operations, food items are kept in fresh or frozen form. The fresh storage of food items involves temperatures around $\pm 0^{\circ}\text{C}$ to $+15^{\circ}\text{C}$, while their frozen storage involves temperatures lower than -30°C to -10°C . The fresh or frozen storage of a food item is dependent on the type of the item and its storage duration. For example, lean beef to be consumed within 1 week to 3 weeks is stored fresh at around $\pm 0^{\circ}\text{C}$, while it is stored frozen under -10°C or -30°C depending on its storage duration for consumption within 4 weeks to 12 months. Fruits like apples, pears, and quinces are stored fresh at around $\pm 1^{\circ}\text{C}$, while citrus fruits such as oranges, tangerines, and grapefruit are stored fresh at temperatures under $+10^{\circ}\text{C}$ to $+15^{\circ}\text{C}$ for consumption times from 6 to 8 months (Gazette 2023).

Commercial cooling systems include cooled cabins that contain products and foods that have commercial value, and portable cold storage rooms up to a volume of 60 m³ are also in this class. These cabins are categorized based on their storage temperatures as positive products (0°C to 15°C) or negative products (-18°C to -5°C). Whether foods are cooled or frozen, the effect of every single day spent outside before they are put in cold storage on the reduction in their

storage life is substantial. When fruits are collected from a tree and stored at 20°C-25°C for three or four days,

their storage life is shortened by 3-4 weeks. If they will be stored fresh, most products should be stored at temperatures close to but higher than their freezing point. In cold storage, relative humidity and ventilation are also critically important. Relative humidity should be high enough to prevent the product from losing moisture and low enough to prevent the development of microorganisms on the surface of the product (Bulgurcu 2015).

The Turkish Standards Institute (TSE) published the “ISO 22000:2018 Food Safety Management Systems” (GGYS) standard on 02.05.2019. The scope of this standard was explained as ensuring that:

a) A food safety management system that provides goods and services in a way suitable for their usage purposes and safe is planned, implemented, operated, maintained, and updated,

b) Its suitability for applicable legal and regulatory food safety requirements is demonstrated,

c) Mutually agreed-upon consumer food safety requirements are examined and evaluated, and compliance with these requirements is demonstrated,

d) Matters associated with food safety are communicated to the relevant stakeholders inside the food chain effectively,

e) The compliance of the firm with the specified food safety policy is provided,

f) The compliance status of operations is demonstrated to the relevant parties,

g) The food safety management system of the firm is certified or approved by an independent institution, or an internal assessment or declaration on the compliance of the system with such documents is made (TSE 2019).

Furthermore, in the “Food Hygiene Directive” of the Turkish Ministry of Food, Agriculture and Livestock published in the Official Gazette issue 28145 on 17.12.2011, Article 2 covers the procedures and principles regarding the responsibilities of food businesses about general rules of food hygiene to be followed at every stage of production, processing, and delivery, including primary production. In the same directive, Article 6 states the following:

a) The main responsibility of ensuring food safety belongs to the food business.

b) Food safety must be provided throughout the food chain from primary production to the end consumer.

c) A cold chain must be in place for food items that cannot be stored safely at ambient temperature and need to be stored under cooling.

d) The food business is responsible for the implementation of procedures founded on hazard analysis and critical control points (HACCP) principles in the context of best hygiene practices.

e) Guidelines for best practices are an important tool that is helpful to the food business for its compliance with food hygiene rules and HACCP principles at every stage of the food chain.

f) Microbiological criteria based on scientific risk assessment and temperature control requirements must be determined.

Article 7 of the same directive makes it compulsory to comply with temperature control requirements, protect the cold chain and document the cold chain for meeting specific hygiene requirements.

The document titled Guidelines for Hygiene Principles and Best Practices for Facilities Producing Food Contact Substances and Materials particularly states the responsibilities of firm managers, and especially traceability, documentation, and record-checking are emphasized. These outputs must be provided to inspection personnel during an inspection. Especially in cold storage areas, it is a legal requirement to provide the appropriate storage conditions including storage temperature, humidity, other ambient factors, and substances and materials in contact with food (Association 2014).

The legal requirements in place in Turkey are described above. Moreover, highly complicated management systems are being used in the control of automated air conditioning and cooling systems in cold storage rooms (Bulgurcu 2005).

Additionally, a change was made by the Pharmaceuticals and Medical Devices Agency in Turkey in the directive dated 31.12.2018 and numbered 30642 (4 redundant) about pharmacists and pharmacies, and it was stated as a requirement to regularly keep records to ensure the monitoring of temperature and humidity data inside pharmacies and refrigerators, have early warning systems that will set alarms in critical situations and thermometers with data logging capacity in place, and regularly inspect/calibrate all devices that need to be available in a pharmacy (Savaş and Bayboz 2022).

In the literature, it is seen that various research have been carried out for the follow-up and monitoring of cold storages.

Üçüncü emphasised the importance of humidity control in cold storage. The humidity levels are extremely important as well as the storage method and storage temperature of the substances to be stored in cold rooms. Therefore, necessary measures must be taken to keep the humidity at the desired level as well as the temperature in cold rooms. Thus, the quality, appearance and other properties of the goods to be stored will be protected (Üçüncü 2003).

Bugarski et al. describes the implementation of a remote supervisory control system for fruit reception in cold stores. One purpose of the software was remote supervision and control of the entire plant from a control room. Also, a graphical representation of the relevant data is available in the laboratory at the remote workstation (technological station) (Bugarski *et al.* 2008).

The Lim and Ryoo study describes a remote monitoring system for temperature control for cold storage of farm products. When the operator leaves the cold storage, the temperature may change for various causes, for instance a valve of the cooler is broken down. The temperature change causes a critical problem with the quality of farm products. To avoid the problem, the operator should look at the present status of the cold store temperature, even when he is away. For this reason, it is necessary to monitorize the system for the operator who can move to observe the temperature (Lim and Ryoo 2004).

Kintner-Meyer and Sandpaper performed a comprehensive analysis of the optimal control protocol to minimize the daily operating cost of an air conditioning system in a 600 m² building. The system consists of two chillers, one designated for cold storage charging and the other for direct cooling, an air handling unit, a cooling tower and water pumps. This analysis determines the optimal protocol for internal temperature and humidity control as well as operating point settings for chiller control, considering two sources of thermal storage (Kintner-Meyer and Emery 1995).

Mohammed et al. aimed to design and evaluate an IoT-BC system to remotely control, risk alert and monitor microclimate parameters such as relative humidity, temperature, CO₂, C₂H₄, and light, and some operating parameters, i.e., temperature of the refrigeration compressor, electric current, and energy consumption for a modified CSR (MCSR). Furthermore, the effects of the designed IoT-BC system on the quality of dates during cold storage were investigated as a case study by comparing it with a conventional CSR (TCSR). The results showed that the designed IoT-BC system precisely controls the

MCSR, provides reliable data on the internal microclimate atmosphere, applied electric current and energy consumption of the MCSR, and sends necessary alerts in case of an emergency based on real-time data (Mohammed *et al.* 2022).

Guo mentioned the importance of intelligent technology of cold storage control system. The application of intelligent technology in the cold storage control system is conducive to the optimized operation of the cold storage. It not only reduces energy consumption, energy saving and environmental protection, but also has networked and humanized management in control management. Therefore, cold storage control technology has developed rapidly. This paper analyses the application of the current cold storage control system and focuses on the application and development of the main intelligent technologies in the cold storage control system (Guo 2020).

A new solar cold storage system for energy efficiency in cold storage is proposed in the study of Yang and Jia. The refrigeration cycle is driven by low-priced electricity at night and electricity generated by PVs. The refrigeration capacity is stored in the cold storage and used when needed and thus the electricity price is minimized by this control strategy (Deng *et al.* 2022).

In this case, similarly to the food sector, it becomes possible to prevent the degradation of drugs in the cold chain in cold storage rooms in all pharmacies, hospitals, and other facilities in the pharmaceutical sector. Therefore, both control systems and programming are crucial for cold storage rooms.

The main purpose of this study is to remotely control the changing parameters such as temperature and humidity of cold storages and to develop an alarm system. Thus, businesses, especially the tourism sector, will gain labor, time and cost savings. The biggest feature that differs from similar studies is that it can be adapted to existing cold storages at very low costs and can operate more stably. The studies carried out have obtained results that support the purpose of the article.

In the first section of the study, the introduction, the importance of the study and the literature are mentioned. In the second section of the study, material and method section, the developed system is explained in detail. Here, the hardware and software features of the system are discussed. In the third section of the study, the findings of the study are discussed and the features that differ from similar ones are mentioned. In the last section of the study, the results of the study are discussed and the contributions of the study to the literature are mentioned.

2. MATERIAL AND METHOD

It supports many domains, including digital applications, the private sphere and the world of work. In this study, the following components were used as hardware:

- Temperature sensor on an electronic circuit board,
- ESP-based processor,
- Wi-Fi adapter,
- Ethernet adapter,
- LoRaWAN adapter

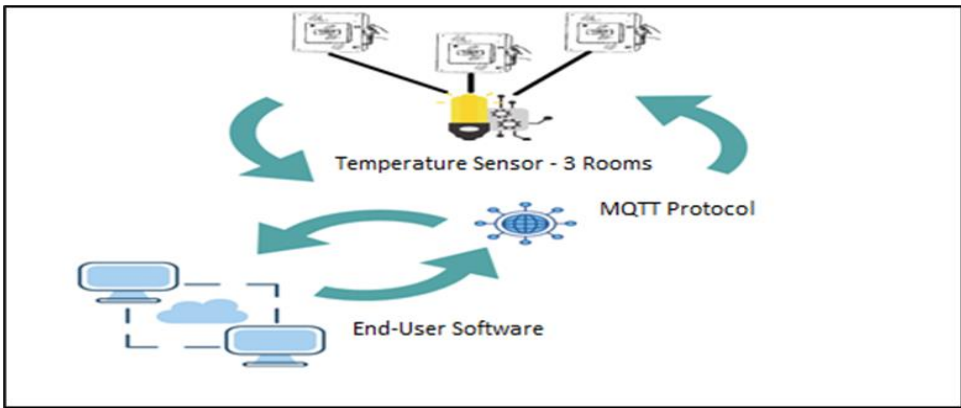


Figure 1. Operational model of the temperature log monitoring and warning system

Using these five pieces of hardware, the circuit board given in Figures 2, 3, and 4 was produced.

The software development process and main components were as follows:

1. Web-based software responsive to mobile screens that can be accessed on an internet browser,
2. Web service software developed using the Node.js programming language to connect the device, the web-based software, and the database,
3. MQTT device network protocol.

While developing the hardware components, because nested types of cold storage rooms were considered, the components were designed in a way to allow a minimum of one temperature-humidity sensor and a maximum of three

temperature-humidity sensors, as well as door status monitoring sensors, to be connected to each device. Open-source libraries were utilized while developing the software. All algorithms were specifically developed for this study.

2.1. Hardware

The most important property of the hardware components was that they were very inexpensive. The most significant aspect of the integrated circuit was that it had an adapter-based structure to send data to the network, and it was able to transfer

data over Wi-Fi, ethernet, or LoRaWAN depending on the adapter used. The main purpose of using a multi-adapter system here was to create a design suitable for any kind of infrastructure in each business.

2.2. Embedded system

The algorithm of the system is shown below.

1. Start
2. Start DataLogger
3. Initialise Mqtt;
 1. Connect To Mqtt Server Read Connection Info From EEPROM;
4. Initialise Setup;
 1. Read Sensor Pin Numbers, Network Config, Serial Info vs From EEPROM;
 2. If cannot find config at eeprom, go to CheckConfig;
5. CheckConfig;
 1. Start at ap mode device for config;
6. StartLogger;
 1. Start Data Logger, Read Data and share device data with Share-Data Method;
7. ShareData;
 1. Share Data using MqttConfig with Server;
8. ReciveMsg(Get Msg From Servers for manage device from remote);
 1. Close Device;
 2. ReShare Last Read data;

3. Restart Device;
4. Update Configuration From Remote;
9. Finish Program;

// Wi-Fi Bağlan

wifi_server.handleClient();

unsigned long simdiki_zaman = millis();

//unsigned long simdiki_zaman1 = millis();

//unsigned long simdiki_zaman2 = millis();

// Read Sensors

reed_status1 = digitalRead(reed_switch1);

reed_status2 = digitalRead(reed_switch2);

reed_status3 = digitalRead(reed_switch3);

Temperature1 = dht1.readTemperature(); // Gets the values of the temperature

Humidity1 = dht1.readHumidity(); // Gets the values of the humidity

Temperature2 = dht2.readTemperature(); // Gets the values of the temperature

Humidity2 = dht2.readHumidity(); // Gets the values of the humidity

Temperature3 = dht3.readTemperature(); // Gets the values of the temperature

Humidity3 = dht3.readHumidity(); // Gets the values of the humidity

//Read Multiple Temp Sensors

if (isnan(Temperature1)) {

Temperature1 = 500;

Humidity1 = 500;

}

if (isnan(Temperature2)) {

Temperature2 = 500;

```

    Humidity2 = 500;
}
if (isnan(Temperature3)) {
    Temperature3 = 500;
    Humidity3 = 500;
}
// Gate Control
doorCheck(doorOpened1, Temperature1, Humidity1, reed_status1, 1);
doorCheck(doorOpened2, Temperature2, Humidity2, reed_status2, 2);
doorCheck(doorOpened3, Temperature3, Humidity3, reed_status3, 3);
if(sendWebService){
    webService(Temperature1, Humidity1, reed_status1, 1);
    webService(Temperature2, Humidity2, reed_status2, 2);
    webService(Temperature3, Humidity3, reed_status3, 3);
    sendWebService= false;
}
if (simdiki_zaman - eskizaman >= unsigned((wifi.sendTime.toInt()) * 60 *
1000)) {
    shareDataRead(Temperature1, Humidity1, reed_status1, 1);
    shareDataRead(Temperature2, Humidity2, reed_status2, 2);
    shareDataRead(Temperature3, Humidity3, reed_status3, 3);
    eskizaman = millis();
}

```

Additionally, Figure 2 shows the two-layer circuit diagram of the temperature logging circuit, and its 2D and 3D outputs.

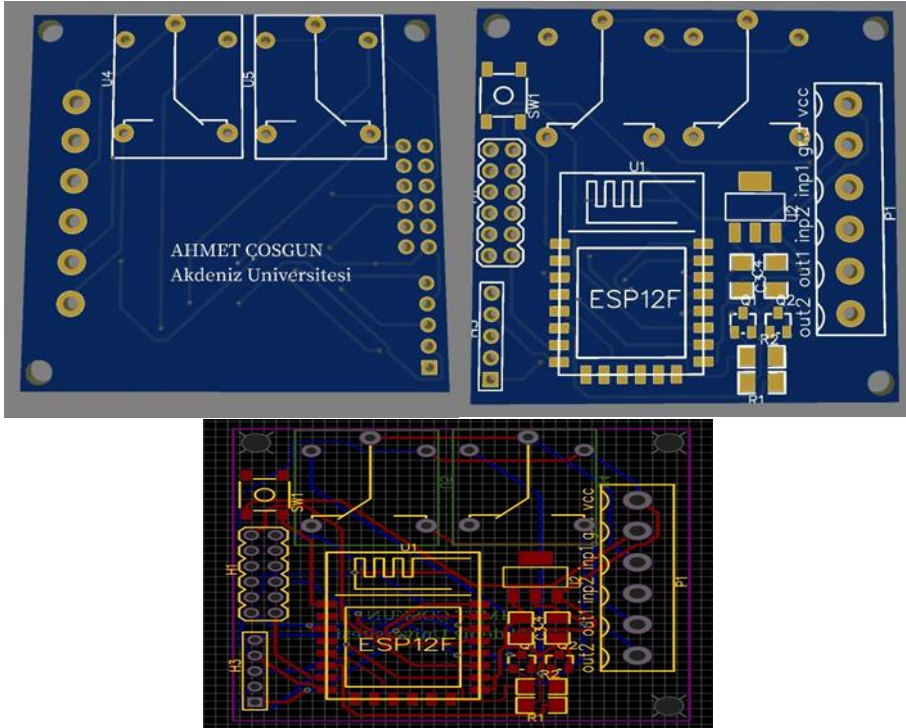


Figure 2. Two-layer circuit diagram of the temperature logging circuit, 2D and 3D outputs

Figure 3 shows the electrical circuit schematic of a cold storage room in a hotel named Megasaray in the province of Antalya in Turkey.

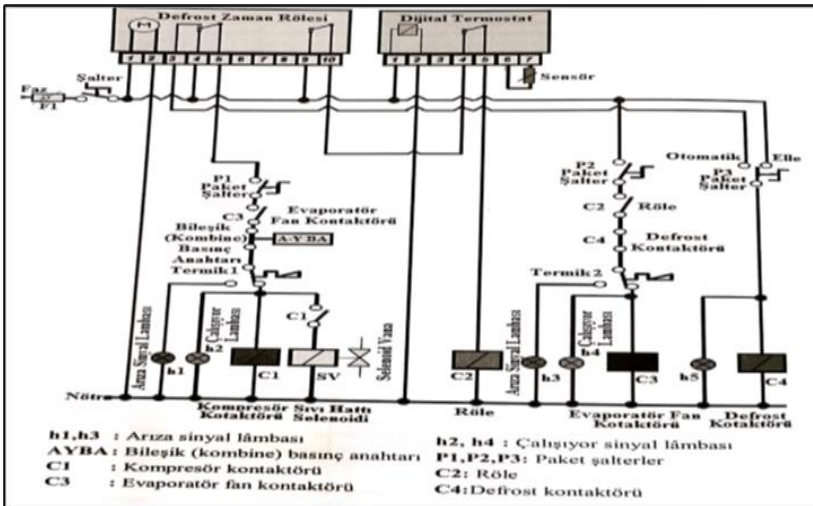


Figure 3. Control circuit of a cold storage room (Bulgurcu *et al.* 2012)

Figure 4 shows the electrical circuit schematic of the design that was created in this study as a cold storage room control system.

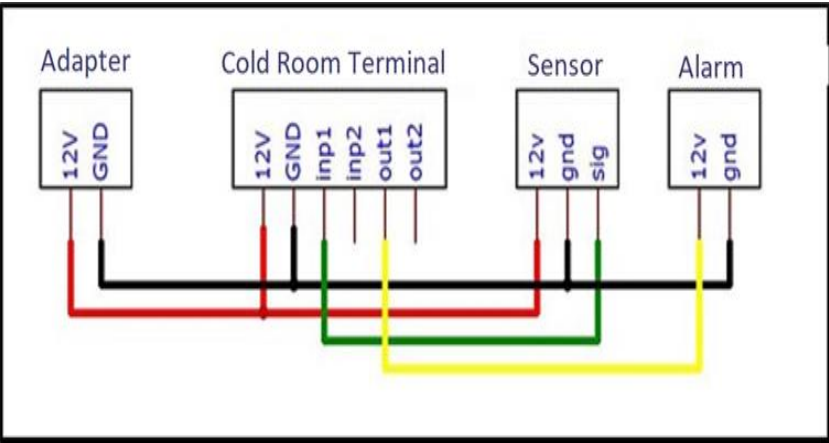


Figure 4. Electrical circuit diagram of the system

3. RESULT AND DISCUSSION

The positions of the temperature logging and monitoring system components applied to a cold storage room in the Megasaray Hotel in Antalya in this study are shown in Figure 5.



Figure 5. Installation photographs of the system in the cold storage room

The web-based software output screens for the temperature logging and monitoring system that was developed in this study for the Megasaray Hotel in Antalya are presented in Figures 6, 7, and 8

Mega Test

megasaray@gmail.com

Çıkış Yap

Ana Sayfa

Sensörler

Konumlar

Konum Grupları

Raporlar

Ayarlar

Kullanıcılar

Konum Ara

Konum Ekle

#	Konum Adı	Konum Grubu	Sıra Numarası	Bek. Sıcaklık	Okunan Sıcaklık	S. Sapma
1	TestOda	Megasaray	1	5	20.1	15.10

Figure 6. Temperature values on the output screens of the web-based software for the temperature logging and monitoring system developed for the Megasaray Hotel.

Mega Test

megasaray@gmail.com

Çıkış Yap

Ana Sayfa

Sensörler

Konumlar

Konum Grupları

Raporlar

Ayarlar

Kullanıcı

2021-03-09

2021-03-02

Kayıt Adı

Filtri

#	Adı	Konum	Kapı	Sıcaklık	Sıcaklık (Kalibre edilmiş)	Nem	Nem (Kalibre edilmiş)	Durum	Tarih
1	Mgrya-01	TestOda	Açık	26.1	20.1	26.1	26.1	Açık	2021-01-21 13:23
2	Mgrya-01	TestOda	Açık	26.1	20.1	26.1	26.1	Kapalı	2021-01-21 11:57
3	Mgrya-01	TestOda	Açık	26.1	20.1	26.1	26.1	Kapalı	2021-01-21 11:50
4	Mgrya-01	TestOda	Açık	26.1	20.1	26.1	26.1	Kapalı	2021-01-21 11:49
5	Mgrya-01	TestOda	Açık	26.1	20.1	26.1	26.1	Kapalı	2021-01-21 11:48
6	Mgrya-01	TestOda	Açık	26.1	20.1	26.1	26.1	Kapalı	2021-01-21 11:47
7	Mgrya-01	TestOda	Açık	26.1	20.1	26.1	26.1	Kapalı	2021-01-21 11:46
8	Mgrya-01	TestOda	Açık	26.1	20.1	26.1	26.1	Kapalı	2021-01-21 11:45
9	Mgrya-01	TestOda	Açık	26.1	20.1	26.1	26.1	Kapalı	2021-01-21 11:45

1

2

3

Figure 7. Megasaray hotel web-based temperature logging and warning system software output (temperature and relative humidity) values

#	Rapor Adı	Oluşturulma Tarihi	Uyan
1	1.hafta 2.gün ölçüm	2021-01-19 13:45	Hayır
2	Genel Rapor	2021-01-12 12:52	Hayır
3	f	2021-01-12 12:22	Hayır
4	Skasın2020-ortalama	2020-11-05 15:05	Hayır
5	Skasın2020-uyarı	2020-11-05 15:04	Evet

Figure 8. Output screens of the web-based software for the temperature logging and monitoring system developed for the Megasaray Hotel

As seen in the results on the screens, 1st output report: The report presents data on the average temperature, humidity, and door status (open or closed) values in the date interval selected on the screen. 2nd output report: The warning report presents values showing the number of warnings and warning categories in the system depending on preset warning scenarios.

These output reports could be downloaded in PDF or .xlsx format. The design that was made in this study also provided the opportunity to e-mail the outputs to different departments of the hotel for them to follow the results over the system.

In such studies, it is aimed to provide the consumer with quality energy at the lowest cost (Tanaka *et al.* 2015, Aybers and Şahin 1995).

Accordingly, the optimal design of cold storage rooms is increasingly becoming more important day by day. For example, in the design developed in this study, in cases where someone forgets to close the door to the cold storage room, this information is sent to the relevant technical department in the hotel, and thus, it is possible to prevent additional energy costs to be brought about by leaving this door open.

The greatest advantage of the system is its cost compared to current temperature logging and warning systems used in cold storage rooms. By 2023, under normal conditions, the cost of the system is around 50 TL including the required spending items and some electronic components (transistors, resistors, capacitors, inductors). Considering the implementation of this system for 40 cold

storage rooms, the cost including the programming labor of an expert engineer adds up to 16,000 TL.

On the other hand, the manufacturer firm of these rooms charges 2000 TL for such a system for each cold storage room. For 40 rooms, the cost adds up to 80,000 TL.

a) Total cost of temperature logging, warning, and monitoring systems for 40 cold storage rooms in this study: $2000 \text{ TL/per unit} \times 40 \text{ units} = 16,000 \text{ TL}$.

b) Average cost of similar systems for 40 cold storage rooms provided by cold storage room manufacturing companies is 80,000 TL.

In this case, the saving in costs becomes $a-b = 80,000 \text{ TL} - 16,000 \text{ TL} = 64,000 \text{ TL}$.

As seen here, using the design that was developed in this study, the expenditures of five-star hotels on these items would decrease significantly. This study will be guiding for similar design studies around the world.

The design that was developed in this study can also be used in cold storage rooms in other sectors, especially pharmacies and hospitals, in addition to the food sector. An example of problems that could be prevented by using this design at very low installation costs is the potential of chemotherapy drugs worth millions of dollars becoming unusable in case of failure to intervene with malfunctions in a cold storage room that is used to store drugs for lung cancer patients in the cold chain. This design also offers a good warning and monitoring system to ensure that cold storage rooms are not operated under unsuitable conditions.

4. CONCLUSIONS

With the rapid development of technology, developments in the internet of things and rapid information technologies will be seen more widely following Industry 4.0. In this study, hotel, and accommodation

Developed for the continuation of sustainability in its facilities, the design enables data records of cold storage warehouses to be accessed remotely via a web-based platform. Temperature measurements can be reported in real time or according to date and time intervals. This system also allows sending notifications to the relevant parties according to the warning thresholds created in the warning scenarios created on the integrated software.

For example, the system may send a warning if the temperature in the cold storage exceeds -5°C . In this integrated platform, it is ensured that these alerts are

sent to the control centers in tourism and accommodation facilities in an instant and sustainable manner via instant notifications, e-mail, or SMS.

The designed device allows the connection of three sensors to log and monitor temperature data. With this property, it is possible to collect information on nested cold storage room systems.

The temperature logging and warning system provides the opportunity to remotely monitor the parameters measured in the hotel and receive notifications (via SMS, e-mail, etc.), offer objectively measured data for inspections, and allow faster and more accurate communication among different users registered to the system via the software.

The risk of workers catching life-threatening diseases can be minimized by collecting data on temperature, humidity, and other parameters in cold storage without the need to involve people in the process. In this case, it will be possible for employers in Turkey to protect the health of their employees in five-star hotels within the scope of the Occupational Health and Safety Law No. 6331.

In order to monitor the temperature and humidity values in refrigerators and pharmacies, records should be kept regularly, early warning systems should be used to set an alarm in critical situations, and thermometers with data recording capacity should be available in the field.

By using this temperature recording and monitoring system, which we designed in this study, in sustainable tourism and accommodation facilities, as well as in cold storages of all pharmacies and hospitals, it will be possible to reduce the number of employees and prevent the deterioration of drugs. In the cold chain in the pharmaceutical industry with digital sustainability.

In this study, it is aimed to establish a basis for similar studies in sustainable tourism and accommodation facilities, pharmaceutical industry by developing temperature recording and monitoring design.

5. REFERENCES

- Aybers, N. ve Şahin, B., 1995. Energy Cost. Yildiz Technical University Printing.
- Bugarski, V., Kulic, F., Francuski, L. ve Vasic, V., 2008. The implementation of a distributed system for supervision and control of cold storages. PTEP (Serbia), cilt 12, 3, ss. 168-170.
- Bulgurcu, H., 2005. Automatic control in Air Conditioning and Refrigeration Systems. 3, Istanbul, Türkiye: Doğa Publishing, Technical Books.
- Bulgurcu, H., 2015. Cooling systems. Miem yayınları, MMO/645.
- Bulgurcu, H., Şimşek, E. ve Basalak, A., 2012. Air Conditioning Refrigeration Electricity and Control Circuits. 7, Istanbul, Türkiye: Iskav publication.
- Deng, Q., Yang, Z., Zhang, L. ve Jia, M., 2022. The control strategy and economic analysis of a new type of solar cold storage. Journal of Energy Storage, cilt 52, p. 104865.
- Devres, O., 2013. Food safety and cold chain. Iskid Publishing.
- E. E. o. P. M. Association, 2014. Hygiene principles and good practice guide for workplaces producing substances and materials in contact with food. Türkiye.
- Erkan, T., 2011. To shed light on common misconceptions in cold storage application. Presented at the X. National congress of installation engineering, İzmir, Türkiye.
- Guo, C., 2020. Application of intelligent technology in cold storage control system. In IOP Conference Series: Earth and Environmental Science, 571, 1, IOP Publishing, p. 012026.
- Kintner-Meyer, M. ve Emery, A. F., 1995. Optimal control of an HVAC system using cold storage and building thermal capacitance. Energy and Buildings, 23, 1, pp. 19-31.
- Katrancı, A. ve Kundakçı, N., 2020. Selection of Cold Storage by SWARA Based Fuzzy COPRAS Method. Optimum Journal of Economics and Management Sciences, 7, 1, pp. 63-80.
- Lim, D.-Y. ve Ryoo, Y.-J., 2004. Development of remote monitoring system for cold-storage. In 30th Annual Conference of IEEE Industrial Electronics Society, IECON 2004, 3, IEEE, pp. 2252-2254.
- Mohammed, M., Riad, K. ve Alqahtani, N., 2022. Design of a Smart IoT-Based Control System for Remotely Managing Cold Storage Facilities. Sensors, 22, 13, p. 4680.
- Ö. Üçüncü, 2003. Humidity control in cold storage. Presented at the VI. National Plumbing Engineering Congress and Exhibition, İzmir, Türkiye.

- Sargın, S. ve Okudum, R., 2014. Construction and Development of Cold Stores and the Determining Factors on them in Isparta Province. SDU Faculty of Arts and Sciences Sosyal Bilimler Dergisi Journal of Social Sciences, 2014, 31, pp. 111-132.
- Savaş, S. ve Bayboz, B., 2022. Refrigeration technique and cold storage applications. Presented at the IV. National Plumbing Engineering Congress and Exhibition, İzmir, Türkiye.
- Tanaka, R., Sekizaki, S., Nishizaki, I. ve Hayashida, T., 2015. The multi-objective optimization of Distribution System management in deregulated electricity market. In 2015 IEEE 8th International Workshop on Computational Intelligence and Applications (IWCIA): IEEE, pp. 155-160.

İnternet References

- 1- O. Gazette. Directive on the Amendment of the Directive for Pharmacists and Pharmacies. <https://www.resmigazete.gov.tr/eskiler/2018/12/20181231M4-9.htm> (accessed 2023).
- 2- T. S. E. (TSE), ISO 22000:2018 Gıda Güvenliği Yönetim Sistemleri. 2019. [Online]. Available: <https://intweb.tse.org.tr/Standard/Standard/Standard.aspx?>
- 3- R. I. market. Temperature and Humidity Sensor Datasheet. <https://www.robo-linkmarket.com/dht21-isi-ve-nem-sensoru> (accessed).
- 4- LoRaWAN. LoRaWAN Module. <https://www.direnc.net/lora-sx1278-433-mhz-transceiver-modulu?language=tr&h=4064ceb8> (accessed).



CHAPTER 30

Applications of Hybrid Laser Welding in Titanium Materials

Ferit Artkin¹

¹ Lect. Dr., Kocaeli University, ORCID: 0000-0002-8543-6334

Introduction

Environmental and energy challenges are getting more severe, and material lightweighting is becoming a critical component of green production, resulting in increased demand and interest in lightweight, high-strength materials. Titanium alloys are commonly utilized in the aerospace sector owing to their high specific strength, corrosion resistance, and high temperature performance.

The aerospace and medical sectors are only two of the many businesses that may benefit from titanium alloys' exceptional corrosion resistance and high strength-to-weight ratio. To produce dependable welds with little distortion for the production of components in these sectors, a number of methods have been examined. Laser welding is one of these methods that may be quite helpful for welding titanium alloys because of its accuracy and speed of processing.

The medical, aerospace, automotive, petrochemical, nuclear, and power generation industries have found a wide range of successful applications for titanium and titanium alloys due to their low density, good high-temperature mechanical properties, and good corrosion resistance. In applications like the outer shells of turbines, avionics power units, and landing gear structural components on the some commercial jet airliners, titanium alloys can be used in place of aluminum-based materials when the perating temperature rises above a particular point. This allows for the achievement of better mechanical properties at high temperatures. Alternative uses for titanium in the medical field include pacemaker cases, artificial heart pumps, prosthetic devices like heart valve components, and load-bearing bones like hip bone replacements because of its extremely low corrosion rates in bodily fluids.

Specifications for Hybrid Laser Welding

Hybrid laser arc welding (HLAW) is another name for hybrid welding. In order to make up for the drawbacks, this welding technique was created to utilize the benefits of both arc welding (such as TIG, MAG, or MIG welding) and laser welding concurrently.

More gap control tolerance, deeper penetration, less heat input, less deformation and shrinkage, increased weld hardness and strength, more fatigue resistance, better welding speed and quality, and reduced costs are all thought to be achievable with hybrid welding.



Figure 1. Laser Welding on the Left, Hybrid Welding Schematic on the Right.

Because of the narrow laser beam spot diameter, butt-to-butt welding necessitates precise gap control, or groove precision. Countermeasures like slower cutting rates are necessary in broader grooves. Generally speaking, laser welding works well for joining thin plates, but not for joining thicker ones. On the other hand, thick plates can be welded using arc welding; however, high-speed welding is not advised due to the huge weld spot diameter and shallow penetration.

Laser welding offers the following benefits: minimal distortion, deep penetration, and fast welding rates. The drawbacks include impossibility of build-up and weakness to vacancies. Fast welding rates with little distortion, deep penetration, and strong void resistance are the benefits of hybrid welding (keyence.com/ss/products/measure/welding, 2024).

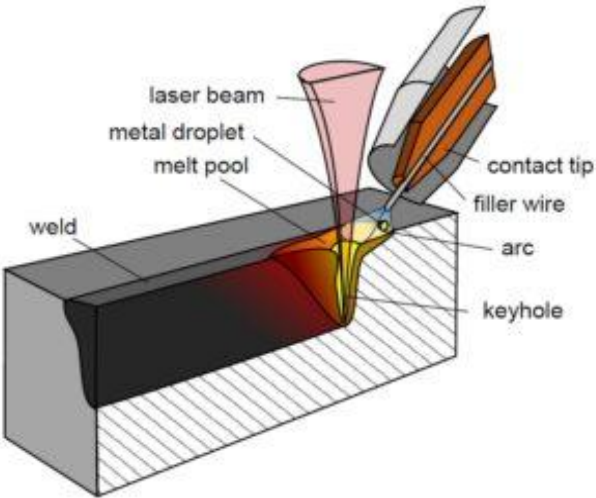


Figure 2. Hybrid Laser Source Detailed Diagram.

Arc welding, which is best suited for thick sheets and provides excellent gap management with high groove precision, and laser welding, which is best for thin

sheets and detailed welding, are both done concurrently in high-speed, high-quality hybrid welding. Hybrid welding is gaining popularity in applications that need high process speeds even in complex situations. Examples of these include welding materials with different melting points and welding base material thicknesses during the machining of custom blanks in the automotive industry (twi-global.com/technical-knowledge, 2024).

Deep-penetration keyhole laser welding and arc welding are combined in a single process zone in hybrid laser arc welding, which was first suggested in the 1970s but has lately attracted renewed interest. Some of the accompanying drawbacks, such the poorer tolerance of laser welding to joint fit or the higher heat input of arc welding, which increases distortion and consequent rework costs, are solved by the hybrid method, which combines the benefits of different procedures. According to estimates, these expenses may make up as much as 15–30% of the labor costs associated with new building. Hybrid welding is therefore being thoroughly researched for a variety of materials and industrial applications, and is being used in several industries, such as shipbuilding (ionix.fi/en/technologies, 2024).

Welding Processes of Titanium Materials with Laser Hybrid Welding Method

The majority of commercially pure titanium and titanium alloys can be joined using the same welding techniques and tools used for austenitic stainless steels and aluminum alloys; however, extra care must be taken to protect the molten weld pool because of their increased reactivity with atmospheric elements at high temperatures. Nonetheless, laser welding offers a great deal of versatility when it comes to connecting titanium alloys automatically or with the use of flux or filler wire. Because laser welding can create a keyhole that efficiently concentrates energy input into a small area, limiting microstructural changes to the weld zone and a narrow heat-affected zone, it has good potential for joining titanium alloys. Additionally, it has been experimentally shown to maintain the mechanical strength and corrosion resistance of the weld bead.

During laser welding, gas shielding is crucial to maintaining the mechanical qualities of titanium alloys by preventing the weld zone from getting bitter and the consequent loss of ductility. Shielding gas is used to protect the weld pool from air pollution, which is said to enhance the laser's ability to adhere to the material (Wang et al., 2007).

The behavior of the molten pool was concurrently investigated by Kawakito et al. (2007) in order to comprehend the laser welding phenomena of

commercially available pure titanium. To minimize spatter or porosity, the possibility of adaptive regulation of laser peak power and pulse duration was examined, taking into account the link between the welding outcomes and the in-process monitoring signals. According to reports, when compared to titanium alloys, laser welding has the thinnest weld bead and the greatest aspect ratio among the three welding processes (TIG, plasma, and laser).

The pulsed and continuous wave (CW) mode laser can be used to weld titanium alloys. In applications involving pulsed lasers, each laser pulse creates a little pool of molten material that solidifies again in a matter of milliseconds. A shallow and smooth weld pool is created when welding takes place in the conduction mode, which is triggered by low peak power or increased spot size. Alternatively, a significantly deeper weld pool is produced by increasing the peak power or decreasing the spot size; this is said to be known as penetration or keyhole mode welding.

In order to weld 1.5 mm thick commercially pure titanium (CP-Ti), the fiber laser-gas metal arc (GMA) hybrid welding technology was experimentally demonstrated. In comparison to the fiber laser welded joint, the impact of the welding settings on the hybrid weldability was examined in terms of the welded joints' microstructure, tensile characteristics, hardness, and bead form.

Consequently, it was shown that the fiber laser-GMA hybrid welding technique can weld CP-Ti sheets that are 1.5 mm thick at up to 9 m/min. Additionally, compared to the base metal, the fiber laser-GMA hybrid welding yields greater Vickers hardness and tensile strength. It is evident that hybrid welded connections offer a superior blend of strength and ductility when contrasted with laser welded joints.

Fiber lasers have outstanding performance, power scalability, dependability, efficiency, and operational life. They are also incredibly small and sturdy. In comparison to traditional solid-state lasers, the lasers are more than 20% efficient, need less electricity, and provide superior beam quality. The literature on fiber laser-laser hybrid welding is somewhat limited because kilowatt-level fiber lasers have just been around for a few years (Kancharla V., 2006).

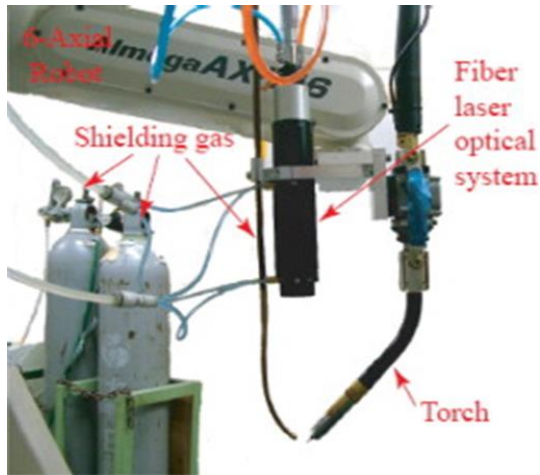


Figure 3. Fiber laser-GMAW hybrid welding system.

In comparison to the fiber laser welded connections, Fig. 4 displays the cross-section and bead appearance of the laser-GMA hybrid welded junction at a speed of 9 m/min. These two welding techniques provide full penetration welds with consistent weld patterns at a 9 m/min travel speed. A crucial finding is that the weld surfaces are smooth, brilliant silver, and exhibit minimal deformation, all of which suggest that the molten pool is adequately shielded. The thin heat affected zone (HAZ) and narrow butt joints welded by fiber laser welding have a nearly parallel weld pattern and result in little workpiece deformation. The laser welds do, however, have a little depression in the weld bead. When using the fiber laser-GMA hybrid welding method, the welded connection of CP-Ti has a much broader HAZ and a slightly projecting top surface.

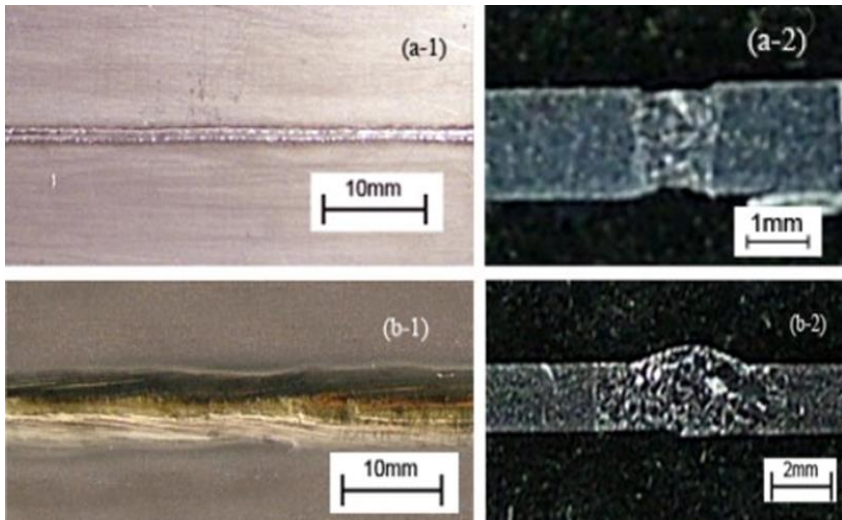


Figure 4. Comparison of joints welded at a m/min welding speed: The top bead appearance in the fiber laser welded junction is shown in (a-1) and the cross-section in the fiber laser welded joint is shown in (a-2). The top bead appearance in the laser-GMA hybrid welded joint is shown in (b-1).

The hybrid welding technique, thus, produced complete penetration welds without recesses with the same high travel speeds as the laser welding process, but with a wider HAZ. Vickers hardness indentations are seen along two welds (from the base metal to the HAZ and the weld centerline). The base metal has a hardness of around 150 HV, but the weld metal has a somewhat greater hardness, ranging from 160 to 220 HV. Since the HAZ's hardness is comparable to that of the base metal, it may be concluded that the HAZ has minimal influence on the total hardness. The peak hardness of laser and hybrid welding reaches 190 and 212 HV, respectively, and the hardness increases sharply as the HAZ gets closer to the center of the weld metal.

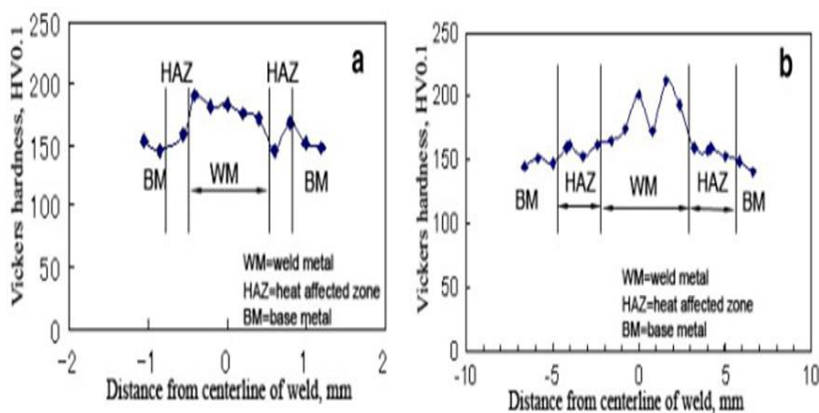


Figure 5. Hardness graph along the welded joint with laser power $P = 2$ kW and welding speed $v = 9$ m/min: (a) fiber laser source; (b) hybrid source, with defocus distance = 0 mm, arc-laser distance = 1 mm, arc voltage = 20 V, and welding current = 220 A.

The weld hardness for a particular cooling rate is not only determined by the oxygen level of titanium, despite it being the primary component. The ultimate hardness outcome is determined by how the cooling rate interacts with the composition's nitrogen and oxygen concentrations. Thus, it is evident from these results that the microhardness of the welded joints is significantly influenced by the interaction between the cooling rate and the composition that contains nitrogen and oxygen (X. Li., et al., 2005).

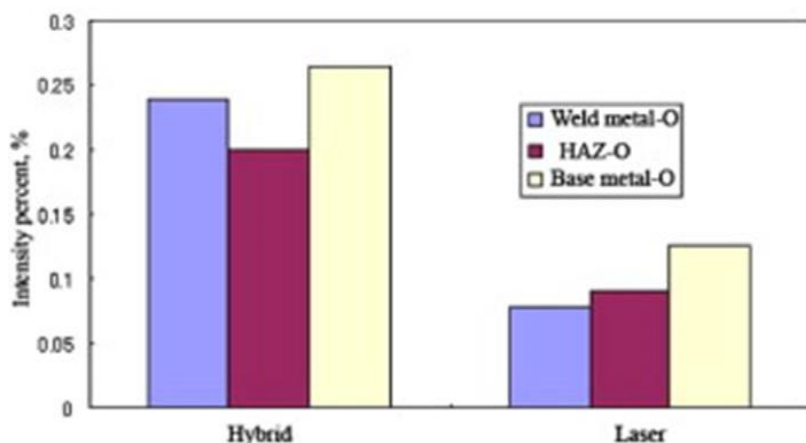


Figure 6. Comparison of the welded joints' oxygen profiles.

Tensile characteristics The elongation and tensile strength of two welded connections in relation to the base metal are displayed in Figure 7. The fracture happens in the weld metal in laser-welded joints, whereas it happens in the base metal in laser-GMA hybrid welded junctions. It is evident that the two welded connections attain the majority of the base metal's tensile strength, but the finer microstructure created in the fusion zone causes a minor loss of ductility. In contrast to fiber laser-welded joints, hybrid welded joints exhibit more elongation. Consequently, compared to fiber laser-welded joints, hybrid welded joints exhibit superior elongation and greater tensile strengths.

The hybrid welded joints clearly offer a superior mix of strength and ductility than the laser-welded ones. The microstructure and chemical makeup of the welds have a significant impact on their mechanical qualities, just like they do for any other material (S. Lathabai et al. 2001).

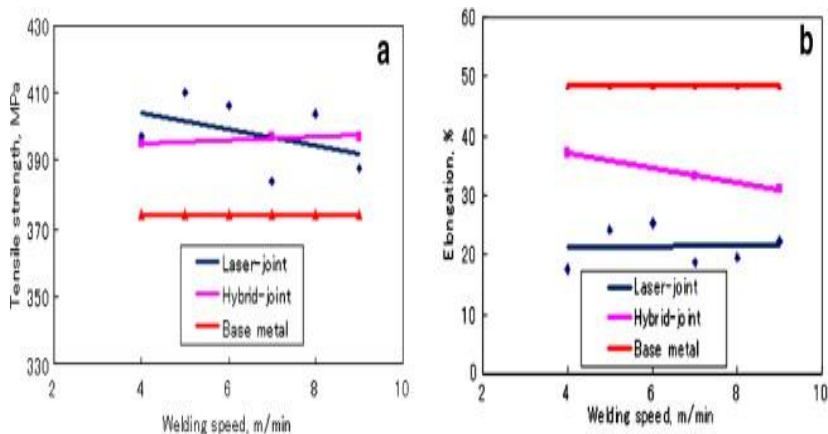


Figure 7. Tensile characteristics of welded joints and base metal are compared: (a) strength under tension; (b) lengthening.

The welded joints' microstructure α (HCP) \rightleftharpoons β (BCC) is the allotropic phase transition that titanium goes through at 882 °C (Eboo M., et al., 1978). A transition to the β phase occurs when the material in the fusion zone is heated to 882 °C or higher during welding. As the weld cools via the β transus, the resultant microstructure in a CP-Ti is controlled by the cooling rate from the β phase area (R. I. Jaffee, 1973). Titanium microstructure can therefore differ significantly based on processing settings. Thus, by examining the related diffraction patterns, XRD analysis of the base metal and the welded joints was carried out to identify whether phases (α -Ti or β -Ti) were present. Fig. 8 displays phase measurements made with Cu K α radiation at 40 kV and 20 mA in the 2θ window from 20 to 80°. The existence of α -Ti hcp phase is shown by the base metal's primary

diffraction peaks. According to (Cui Li et al., 2009), alpha phases are found for the HAZ and weld metal in two welded connections when compared to the base metal's diffraction pattern.

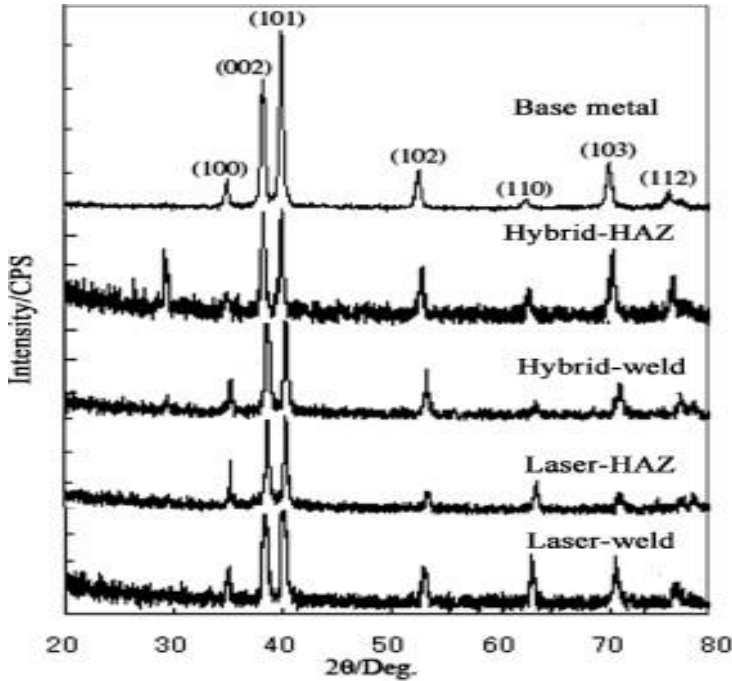


Figure 8. Diffraction patterns in base metal and welded joints were calculated.

Conclusion

The creation of hybrid structures with significant uses in the automotive and aerospace sectors has also been aided by the laser welding of titanium materials with other materials, such as various titanium and aluminum alloys. When titanium materials are subjected to hybrid welding, excessively high peak power increases cause the workpieces' temperature to rise over the material's evaporation point, which encourages the creation of craters on the materials' surface. The pulse length is increased with constant peak power to enhance the penetration depth without craters. The weld pool will expand at the same penetration depth as the pulse length increases the diameter of the heat-affected zone. The two weld zones have extremely high hardness as a result of the quick cooling. The hardness distribution in the fusion zone is greater than that of the base metal and the HAZ, according to the microhardness profile along the weld. Furthermore, for high peak powers, the hardness values are greater. The cooling and hardness values are decreased, though, as the increase in average power raises the target's overall heat input.

Because new and innovative materials are constantly being created for crucial engineering applications, particularly in the automotive and aerospace sectors, laser welding titanium alloys presents growing research opportunities and chances for creating lightweight parts.

Acknowledge

In the preparation of this study, I contributed to the MAK579 Advanced Welding and 3D Additive Manufacturing lecture notes that I received from Prof. Dr. Mustafa KOÇAK during the Mechanical Engineering graduate course phase. I would like to thank Prof. Dr. Mustafa Koçak.

References

- Cui Li, Kutusna Muneharua, Simizu Takao, Horio Kouji, Fiber laser-GMA hybrid welding of commercially pure titanium, *Materials & Design*, Volume 30, Issue 1, 2009, Pages 109-114.
- Eboo M., Steen WM., Clarck J. Arc. augmented laser processing of materials. In: *Proceedings of conference advances in welding processes*. Harrogate, UK, 9–11(May); 1978. p. 257–65.
- <https://www.ionix.fi/en/technologies/laser-processing/hybrid-laser-welding/> Accessed 20 December 2024.
- <https://www.twi-global.com/technical-knowledge/published-papers/hybrid-laser-mag-welding-procedures-and-weld-properties-in-4mm-6mm-and-8mm-thickness-cmn-steels> Accessed 19 December 2020.
- <https://www.keyence.com/ss/products/measure/welding/laser/>
- Kancharla Vijay. Applications review: materials processing with fiber lasers under 1 kW. In: *Proceedings of 25th international congress on applications of lasers and electro-optics (ICALEO)*; 2006. p. 579–85.
- Kawahito Y., Masami M., Seiji K., Elucidation of high-power fibre laser welding phenomena of stainless steel and effect of factors on weld geometry (2007), *J. Phys. D: Appl. Phys.* 40 5854, DOI 10.1088/0022-3727/40/19/009.
- Kocak M., MAK279 Advanced Welding and 3D Additive Manufacturing Mechanical Engineering Master's Degree Lecture Notes, 2024.
- R.I. Jaffee, H.M. Burte (Eds.), *Metallurgical synthesis, Titanium science and technology*, vol. 3, Pleunum Press, London (1973), pp. 1665-1693
- S. Lathabai, B.L. Jarvis, K.J. Barton, Comparison of keyhole and conventional gas tungsten arc welds in commercially pure titanium, *Mater Sci Eng A*, 299 (2001), pp. 81-93.
- X. Li, J. Xie, Y. Zhou, Effects of oxygen contamination in the argon shielding gas in laser welding of commercially pure titanium thin sheet, *J Mater Sci*, 40 (2005), pp. 3437-3443.
- Zhang W, Wang S. Investigation of Laser-MIG Hybrid Welding of Al-Mg-Si Aluminum Alloy. *Metals*. 2024; 14(6):729. <https://doi.org/10.3390/met14060729>.
- Zhang, C.; Gao, M.; Wang, D.Z.; Yin, J.; Zeng, X.Y. Relationship between pool characteristic and weld porosity in laser arc hybrid welding of AA6082 aluminum alloy. *J. Mater. Process. Technol.* 2017, 240, 217–222.



CHAPTER 31

The Effect of Hybrid Laser Welding Technology on Aluminum Alloys

Ferit Artkin¹

¹ Lect. Dr., Kocaeli University, ORCID: 0000-0002-8543-6334

Introduction

The need for resource conservation and energy consumption reduction is growing daily in order to satisfy the expectations of sustainable development. In order to lower energy and resource consumption, structural lightness is one of the key development objectives for global manufacturing.

The concept of hybrid laser-arc welding dates back to the 1970s. Nevertheless, there hasn't been enough research done on this topic in the years thereafter. Researchers are now focusing on this topic once again and are attempting to combine the benefits of arc and laser welding techniques. In recent years, high-quality laser systems have become a typical component of production systems, despite the fact that challenges with balanced laser production made practice difficult in the early days. The process known as laser-arc hybrid welding, which blends arc and laser welding, allows both techniques to influence and support one another by applying them simultaneously in the same welding region.

The industrial and academic groups have been paying more and more attention to hybrid laser arc welding of aluminum alloys. The literature has shown that laser arc welded joints with comparable Al alloys have exceptional mechanical and fatigue characteristics. The microstructures and characteristics of laser arc welded joints made of various Al alloys have not been extensively studied, despite their growing use in contemporary engineering projects. Because of their excellent strength-to-weight ratio and corrosion resistance, aluminum alloys are utilized extensively in a variety of sectors. These alloys are challenging to weld because of their unique thermophysical characteristics and intricate physical metallurgy.

Hybrid Laser Welding Technology

Hybrid laser welding is a frequently used hybrid technology that combines gas metal arc welding (GMAW) with laser beam techniques. This process makes use of a head that contains the laser focusing optics and GMAW gun. The laser beam creates a keyhole close to the puddle's leading edge. Furthermore, hybrid methods that combine laser and gas metal arc welding (GMAW) have been developed for usage in permanent places. Additionally, the instruments needed to develop the joint design are no longer necessary. Specially designed alloys of filler metal are used to create a physically smooth junction. Laser-GMAW hybrid welding combines the LBW and GMAW techniques. One potential application for this combination is welding lightweight structures, particularly aluminum alloys.

The effectiveness, resilience, and versatility of this hybrid welding technique are widely recognized. By combining the high fillet feed of GMAW with a deep-penetrating laser beam, the primary applications of LBW and GMAW may be significantly enhanced. This technique's main benefits are excellent gap bridging capabilities, deep and consistent weld penetration, minimum deformation, and quick filler metal addition. Wider groove tolerances are possible with this hybrid process than with LBW of some metals, such as aluminum alloys.

Laser welding is more cost-effective and robotic than electron beam welding since it doesn't require a vacuum atmosphere to function and the beam can be optically focussed like other light beams. High operating speeds and extremely little workpiece deformation are made possible by the focused heat source that is the laser beam. Unfortunately, high-power lasers are both costly and huge. Additionally, the beam must somehow reach the joint. In contrast to CO₂ lasers, which require mirrors to transfer their light, Nd:YAG lasers can transport their light through thin glass fibers, which makes them appealing for use in robotic welding.

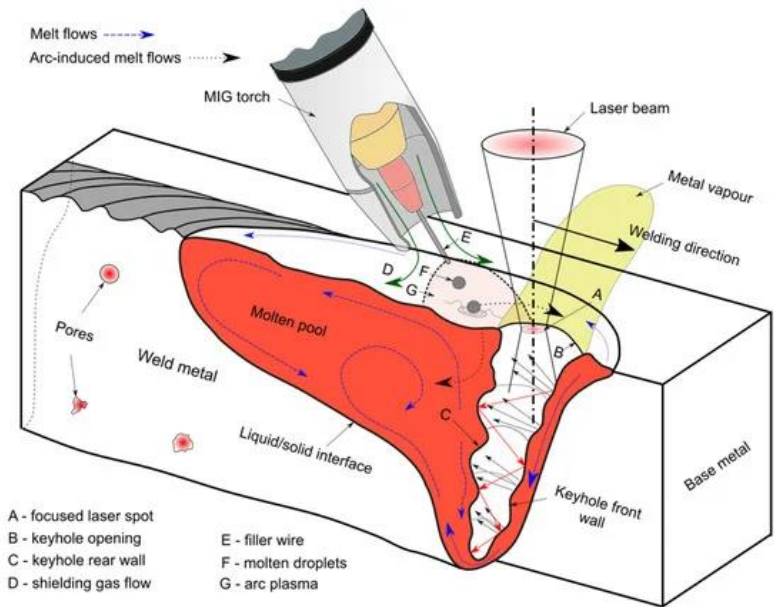


Figure 1. Depicts the melt flow characteristics of LAHW in a paraxial arrangement with a leading laser beam/trailing arc.

Laser-Arc Combination Welding The laser beam and the arc are combined in the same weld pool using LAHW (Figure 1). This technique, which was created and initially published in the 1970s, aimed to lessen the drawbacks of LBW and

issues including poor bridgeability, high sample preparation requirements, and issues with filler material addition. It is conceivable to combine both heat sources to create a hybrid weld because the electric arc and the high-energy-density laser beam both function in a gaseous shielding environment at room pressure. Deeper penetration is accomplished by the laser beam heat source, while additional benefits including increased productivity, process stability, and dependability are offered by the arc, which serves as a secondary heat source. This approach is known as laser-enhanced or laser-assisted arc welding if the arc serves as the main source of heat (Bunaziv I., et al., 2021).

The practice of combining laser welding with other welding techniques, such as MAG welding, into a single operation is known as hybrid laser welding. Although electric arcs and laser beams are quite distinct welding heat sources, they may both function in a gaseous shielding environment at room pressure, allowing for the combination of these heat sources in a special welding process known as hybrid laser-arc welding. In recent years, hybrid laser-arc processes—particularly hybrid laser-MAG welding—have been used more and more in welding applications. Many of the autogenous laser welding and arc welding process mechanisms are evident in hybrid laser-arc welding. Additionally, the combination of the two distinct processes has certain synergistic benefits.

The combination of arc and laser welding is known as hybrid laser-arc welding. Along the weld pass, the procedures produce a shared weld pool. There are instances where the arc and laser beam are so far apart that the operations produce distinct weld pools. Occasionally, this procedure is referred to as tandem laser-arc welding rather than hybrid laser-arc welding. There are intricate physical interactions between the two heat sources in the hybrid process, which goes beyond just combining the laser beam and the arc. In hybrid laser-arc welding processes, the arc acts as a secondary heat source to increase stability and dependability, while the laser beam, which has a high energy density, often acts as the primary heat source to enable deep penetration mode welding and efficiency of the welding process, as well as the weld quality.

The TIG process is a non-consumable electrode method, while the MAG process is a consumable electrode process that may be used as a secondary heat source. Consumable electrode processes are recommended if filler material needs to be added; non-consumable electrode arcs are the preferable option. Both arc-like and laser-like properties can be found in the hybrid process, depending on the energy ratio of the two heat sources. The weld breadth grows with arc energy, whereas the weld penetration increases with laser energy. The ideal ratio of laser

beam and arc strengths varies depending on the application (www.ionix.fi/en/technologies/laser-processing, 2024).

Welding Technology Applications on Aluminum Alloys

It may be used to combine disparate materials and weld thin metal sheets to create lightweight structural designs, such as those seen in the automobile sector. A laser riveting procedure is proposed to replace existing thermal joining processes, where the primary difficulty is the development of intermetallic phases from distinct alloying elements (E. Schubert et al. 2001). The concept of laser riveting is demonstrated in Figure 2, along with an example of connecting steel to aluminum—a task that is sometimes thought to be challenging or impossible using conventional thermal techniques. Steel and other nonmetallic materials like resin and carbon fiber reinforced plastic (CFRP) can also be joined using this laser riveting technique.

An arc and a laser are the two heat sources used in laser-MIG hybrid welding (Yan, S.H et al. 2014, Su, J., et al. 2023, Vorontsov, A., 2022). Aluminum alloys' laser energy reflection may be decreased by efficiently lowering the plasma's inhibitory impact on the laser through the coupling effect between the arc and the laser. To optimize the energy consumption ratio of the two heat sources at the same time, the laser also stabilizes, compresses, and increases the energy density of the arc.

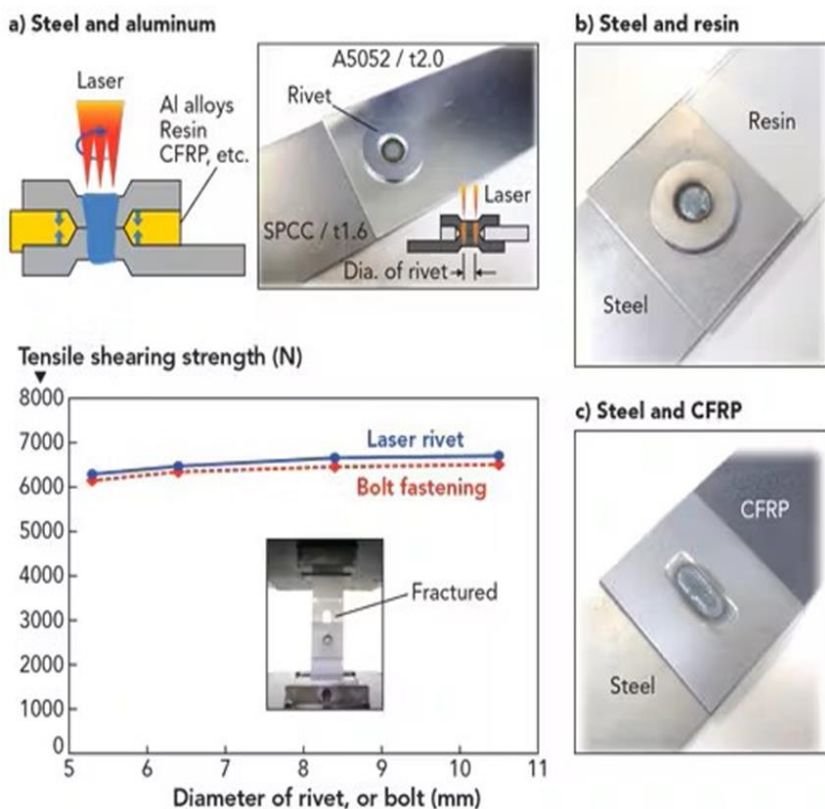


Figure 2. Steel can be joined to CFRP, aluminum, or resin using the laser riveting process (laserfocusworld.com, 2024).

Zhang et al. (Zhang, C., et al., 2017) studied the effect of laser-arc hybrid welding parameters on the porosity of 8 mm thick AA6082-T6 aluminum alloy. The weld porosity was less than 0.5% under the optimized welding parameters, and there was a certain relationship between the properties of the molten pool and the weld porosity. When the arc current or laser power was increased or the welding speed was reduced, the weld cross-section gradually changed from Y-shape to V-shape, and the weld porosity decreased. Another study by Huang et al. (Huang, L.J., et al. 2018) carried out laser-MIG hybrid welding of 10 mm thick 5083 aluminum alloy. The order of laser and MIG heat sources was studied on the effect of weld forming and joint mechanical properties. The effects of laser and MIG heat sources on joint mechanical characteristics and weld formation were examined. It shown that weld porosity was clearly reduced and weld formation was improved when the laser heat source was in the front. Additionally, the weld metal's mechanical characteristics improved due to the homogenous distribution of second phase particles. (Cai, et al. 2019) welded an aluminum

alloy using a laser-MIG hybrid process. The impact of varying volume ratios of He and Ar-He mixed gases on the porosity flaws, plasma physical characteristics, and weld penetration depth was investigated.

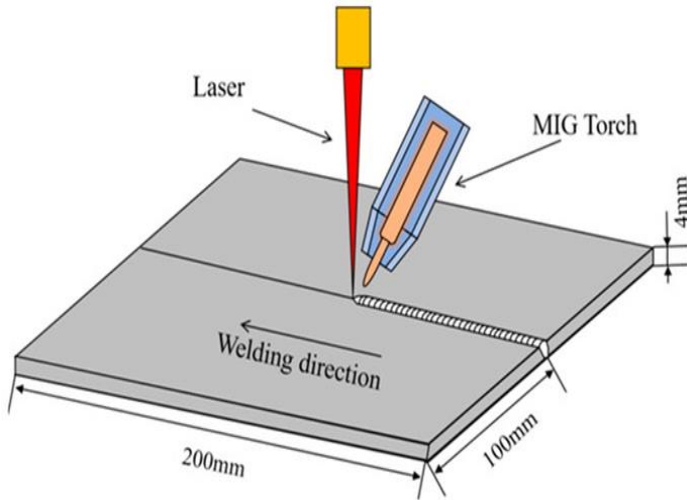


Figure 3. Schematic Diagram of Laser-MIG Hybrid Al Welding Process

Aluminum alloys with low boiling point components, such as magnesium, may evaporate and burn when fused by a laser beam. In 6XXX aluminum alloys, the constituent element of the strengthening phase Mg_2Si is magnesium.

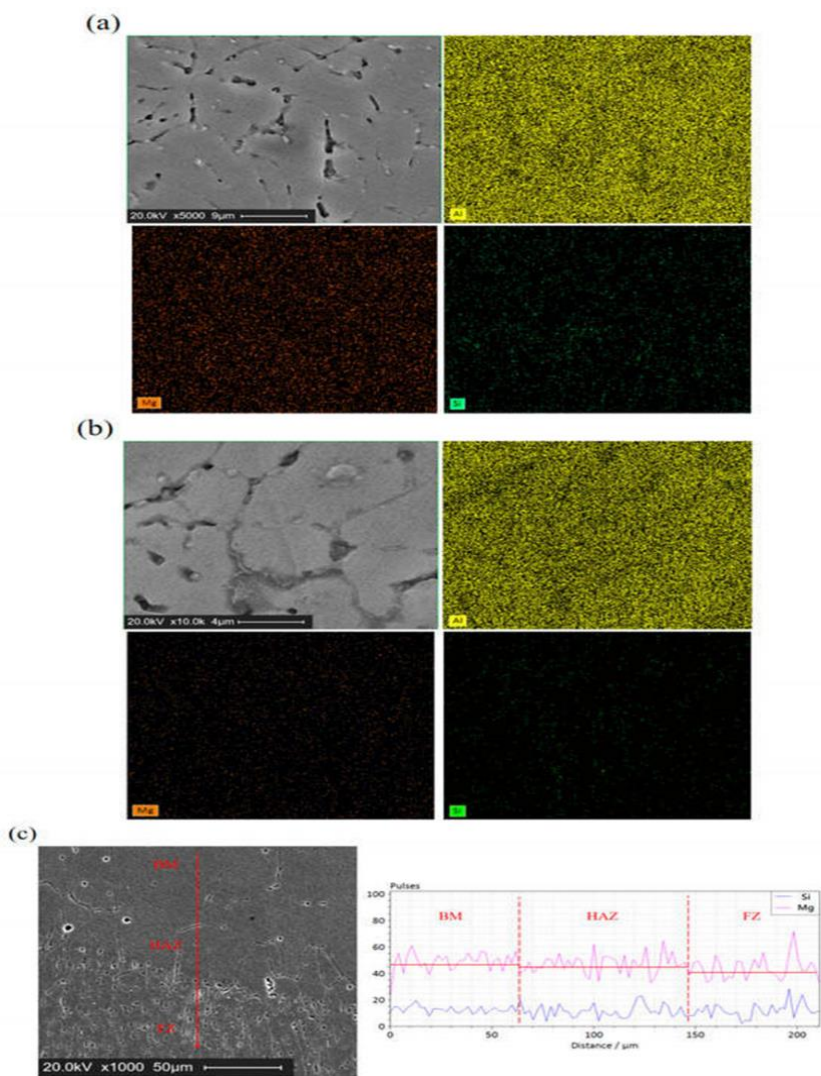


Figure 4. SEM Observation and Analysis of L and H1 joints: (a) Weld center morphology and Al, Mg and Si element distribution of L joint (Zhang, W.,et al. 2024).

The reduction in the strengthening phase of the joints due to the burning loss of magnesium would result in a decline in the mechanical characteristics of the joints. The filler wire, which is added to the laser-MIG hybrid welding technique, can somewhat enhance the alloying components. The location and composition of alloying materials have a significant impact on the welded joints' mechanical characteristics. The SEM of FZ of the L and H1 joints displays the distributions of the Mg and Si elements for the L and H1 joints, respectively, as seen in Figure 4. In the weld of two joints, the magnesium element is evenly dispersed without

any discernible segregation. In the grain boundary, the Si element is somewhat segregated and mostly concentrated in the white particle phase. White particles enhance the resistance of dislocation movement when it reaches the grain boundary, improving the mechanical characteristics of the welded joint (Kocak, M., 2024).

Conclusion

Porosity may be reduced by adjusting the process parameters, which is especially difficult for laser-arc hybrid welding because there are a lot of variables to change. The process of adjusting parameters might be laborious and involve interactions. A laser welding strategy may be quickly developed in demanding sectors if the influence of process factors is clearly understood. The broader process window provided by filler wire and heat input manipulation can make laser-arc hybrid welding advantageous. New filler materials must be developed in order to improve strength and resistance to corrosion. New technologies including grain refiners, electromagnetic support, shorter wavelength diode laser sources, laser beam oscillations, and nanoparticles in filler wire can be used to further enhance weld quality and attain strength comparable to the base metal. Vacuum may be used to solve a lot of processing issues, leading to new manufacturing possibilities and notable productivity gains. The process of producing a vacuum is complicated and expensive, particularly for small and medium-sized businesses. Compared to fusion welding processes, the evolution of aluminum alloys towards greater strength occurs significantly more quickly. Therefore, in order to be more competitive with friction stir and arc welding, it is important to research and evaluate the application of laser welding and laser arc hybrid welding capabilities.

Acknowledge

In the preparation of this study, I contributed to the MAK579 Advanced Welding and 3D Additive Manufacturing lecture notes that I received from Prof. Dr. Mustafa KOÇAK during the Mechanical Engineering graduate course phase. I would like to thank Prof. Dr. Mustafa Koçak.

References

- Bunaziv I, Akselsen OM, Ren X, Nyhus B, Eriksson M. Laser Beam and Laser-Arc Hybrid Welding of Aluminium Alloys. *Metals*. 2021; 11(8):1150. <https://doi.org/10.3390/met11081150>
- Cai, C.; He, S.; Chen, H.; Zhang, W.H. The influences of Ar–He shielding gas mixture on welding characteristics of fiber laser-MIG hybrid welding of aluminum alloy. *Opt. Laser Technol.* 2019, 113, 37–45. <https://www.ionix.fi/en/technologies/laser-processing/hybrid-laser-welding/>
- Huang, L.J.; Hua, X.M.; Wu, D.S. Relationship between the weld pool convection and metallurgical and mechanical properties in hybrid welding for butt joint of 10-mm-thick aluminum alloy plate. *Weld. World* 2018, 62, 895–903.
- Kocak M., MAK279 Advanced Welding and 3D Additive Manufacturing Mechanical Engineering Master's Degree Lecture Notes, 2024.
- Su, J.; Dong, J.W.; Luo, Z.; Yang, Y.; Bi, Y.B.; Zhang, Y.X. Effect of laser-arc synergy on melting energy in laser-CMT hybrid welding of aluminum alloy. *Optik* 2023, 292, 171406.
- Vorontsov, A.; Zykova, A.; Chumaevskii, A.; Kolubaev, E. Outstanding features of high-speed hybrid laser-arc welding compared to high-speed laser welding of AA5059 aluminum alloys. *Vacuum* 2022, 196, 110736.
- Yan, S.H.; Chen, H.; Zhu, Z.T.; Gou, G.Q. Hybrid laser-metal inert gas welding of Al-Mg-Si alloy joints: Microstructure and mechanical properties. *Mater. Des.* 2014, 61, 160–167.
- Zhang W, Wang S. Investigation of Laser-MIG Hybrid Welding of Al-Mg-Si Aluminum Alloy. *Metals*. 2024; 14(6):729. <https://doi.org/10.3390/met14060729>.
- Zhang, C.; Gao, M.; Wang, D.Z.; Yin, J.; Zeng, X.Y. Relationship between pool characteristic and weld porosity in laser arc hybrid welding of AA6082 aluminum alloy. *J. Mater. Process. Technol.* 2017, 240, 217–222.
- Zhang, W., & Wang, S. (2024). Investigation of Laser-MIG Hybrid Welding of Al-Mg-Si Aluminum Alloy. *Metals*, 14(6), 729. <https://doi.org/10.3390/met14060729>.



CHAPTER 32

Biomechanical Workload Analysis of Aircraft Technicians

Haşim Kafalı¹ & İbrahim Güçlü²

¹ Associate Professor, Muğla Sıtkı Koçman University, ORCID: 0000-0002-7740-202X)

² Lecturer Cappadocia University, ORCID: 0000-0003-0977-3862

Introduction

The aviation industry started with Hazerfen Ahmet Çelebi in 1632, continued with the Wright brothers at the beginning of the 20th century, and has come to the present day as a result of a long process and efforts (Kanbur and Gökalp, 2014). With the developments in the aviation sector from the past to the present, the need for aircraft has increased due to the fact that the aircraft have become more technological, large, and complex in this field, as well as the desire of states to be in a strong position in line with their political and military interests, which means an increase in the need for aircraft workers. Increased competition in the marketplace has increased the value of human capital, especially in order to improve quality and achieve greater customer satisfaction.

The increase in the number of people working in the aviation sector, together with the increasing competition around the world, has increased the points to be considered and emphasized in this field. An intensive working process, heavy and fast-paced shifts, the necessity to work in a narrow space, and the necessary maintenance equipment and environmental impacts during the work process can be given as examples. In addition, the working individual also has responsibilities in this process. It is necessary to position the body correctly, select appropriate hand tools, and take individual precautions against hazards that may come from the environment in the workplace. In this regard, especially in aircraft workers, aircraft maintenance technicians face injuries and injuries as a result of the workloads encountered in the aircraft maintenance process. Since injuries can occur, the correct working positions, appropriate equipment, and safety measures for people working in this field are important for the continuity of a healthy process.

1. Aircraft Employees

When aircraft employees are classified according to criteria that require technical knowledge and experience, they are divided into general classes as pilot, mechanical maintenance technician, and avionics technician. Aircraft require maintenance and replacement of necessary parts to ensure safe flight. Aircraft mechanical and avionics maintenance technicians carry out planned maintenance, repair, and inspections in accordance with the required standards and rules in order to keep the aircraft airworthy. From a physical point of view, aircraft maintenance technicians also face physical challenges in this process; pilots, on the other hand, are not exposed to physical work challenges compared to those working in avionics and mechanical maintenance. Pilots are more likely to suffer from neck, back, and lower back pain due to incorrect posture. Aircraft

maintenance technicians, on the other hand, are exposed to heavy physical work, heavy lifting and lowering, pushing-pulling movements, frequent bending and turning, repetitive periodic movements, incorrect movements during work, load on the muscles during the work process, speed and duration of the work, the force and magnitude used during the movement, standing with arms above the shoulders during work, etc. (Yeşil, 2013). The musculoskeletal structure of the body gives rise to the disorders that pilots and aircraft maintenance technicians encounter.

2. Musculoskeletal Disorders

Through the musculoskeletal system, humans fulfill the necessary vital and actional functions with the nerve and brain commands that physically direct the body. Muscles and the skeletal system play a major role in fulfilling the tasks required in the working process. Muscles are the part that uses the chemical energy obtained by the body as mechanical energy. There are types of striated, smooth, and cardiac muscles. Striated muscles are the structures that can provide movement with voluntary control that surround the bone structure in the body. Smooth muscles are involuntary structures found in the internal organs of the body. Although the heart muscle is similar in structure to the striated muscles, it works involuntarily, and unlike other muscles, it fulfills its function not with signals from the brain but with the signals it generates. It only receives its operating frequency from the brain (Serbest and Eldoğan, 2014). Muscles surround the joints and provide a smooth appearance and defense against impacts. The muscles surrounding the joints are connected to the bones with tendons as shown in Figure 1.

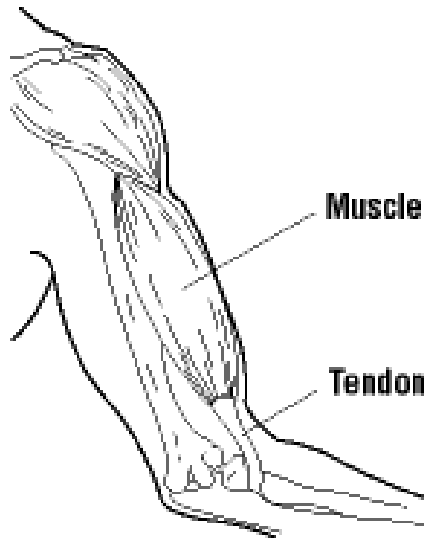


Figure 6.Combination of muscles and bones(URL-1)

The musculoskeletal and skeletal workings of the living body operate on the principle of mechanics as found in physics. Mechanics is one of the five classical fields of physics and studies motion, work, and energy (Karakoç, 2020). Biomechanics also involves the analysis of the principle of mechanics in physics on living organisms. Having different aspects of biomechanics helps to understand different areas of mechanics. For example, while static principles can be used to study force effects in the musculoskeletal system, dynamic principles are used in gait and movement analysis, especially in sports mechanics (Karakoç, 2020). During work, a mechanical action occurs in the striated muscle tissue and skeletal structure as a result of the individual performing actions that require labor. Here the correct body position should be ensured. As shown in Figure 2, an incorrect body position and behavior will cause excessive load on the skeletal structure and cause musculoskeletal disorders.

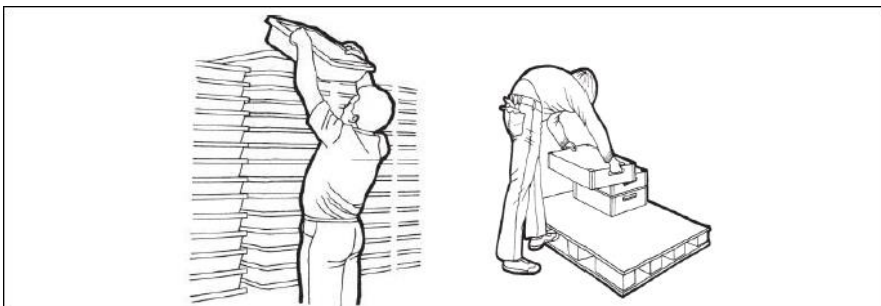


Figure 7.Wrong posture positions(Stephen,2003)

Musculoskeletal disorders are referred to as work-related musculoskeletal disorders in the International Commission on Occupational Health and Safety. The term work-related is used by WHO (World Health Organization) to investigate disorders that may occur due to work performance and the working environment. Musculoskeletal and tendon disorders in working life are caused by holding, compressing, bending, applying torque, reaching somewhere, and repeating this. The negative effects of these actions, which are normally harmless, are caused by repetition and repetition in less time than the time required for the body. At this point, possible risk factors emerge. Although they do not pose a serious risk on their own, the combination of risks at the same time increases the extent of the discomfort. Risks can be listed as body posture, repetition of movement, continuous work, applied force, working speed, ambient temperature, vibration, and working standards.

Fixed shoulders and necks cause discomfort in that area. Because in order to achieve the desired balance in that area, it is necessary to work continuously, and this causes the vessels in that area to be compressed and causes discomfort. In repetitive movements, discomfort occurs due to constant repetition and force application, especially in the moving points of the body, such as the shoulder, wrist, and elbow joints. Working continuously without a break, no matter how light the work is, keeping the muscles constantly working and not taking enough breaks causes injuries. For example, in short-term work (less than 1 hour) in lifting action, a rest period of 1.2 times the working time is given as a rest period. As can be seen in Table 1, studies have been carried out on the periods to be rested for light, medium, and heavy analysis of the work done.

Table 2: Rest time depending on the working interval (sec)(Reinhold,1986)

Operation Time (sec)	Light Operation	Medium Operation	Hard Operation
1	0	1	1
2	1	2	3
3	1	2	4
4	1	3	5
5	1	3	9
6	1	4	14
7	1	5	18
8	1	8	27
9	1	11	35
10	2	14	49
11	2	17	57
12	3	20	62
13	3	24	74
14	3	28	97
15	3	32	111
16	3	36	135
17	3	43	149
18	4	48	158
19	4	53	167
20	5	57	186
21	5	62	220
22	5	67	
23	5	73	
24	5	79	
25	5	86	
30	11		
35	13		
40	15		
45	17		
50	20		
55	25		
60	40		

For long-term work, a morning break, lunch, and afternoon break are also indicated. Lifting, carrying, and applying excessive force will cause too much effort. In this process, overloading the body and continuing uninterruptedly causes the discomfort to occur more quickly. The speed of work will invite musculoskeletal disorders when the individual wants to go above his/her body capacity in order to finish the work on time and wants to do it without a break. Apart from employee-related risks, ambient temperature and humidity are also risk factors in the emergence of disorders. High temperature and humidity tire the worker more, while low humidity causes discomfort during work due to decreased flexibility of the muscles. The minimum temperature values required for working are given below (Table 2).

Table 3: Operating Temperatures(Can, 2013)

Type of Work Performed	Temperature °C
Seated work	19
Standing work	17
Heavy physical labor	12
Offices	20
Indoor sales outlets	19

The use of vibrating tools and instruments will also cause damage to the hand and nerves, leading to numbness of the fingertips and senses. For example, using a heavy hand tool, such as a hammer, will cause vibration, leading to the common Raynaud's Syndrome. As a result of the aforementioned risk factors, the main musculoskeletal disorders resulting from work are back pain, muscle strain, stiff neck, cervical disc herniation, lumbar disc herniation, carpal tunnel syndrome, stiff neck syndrome, and muscle strength imbalances(Esen and Fırlalı, 2013).The most obvious sign of musculoskeletal disorders is pain. In some cases, symptoms such as swelling, edema, redness, stiffness, and numbness also occur in the relevant area.

Bursitis: It occurs in the soft tissues between bone-tendon or skin-bone. Swelling and pain symptoms occur in the relevant area. Repeated shoulder movements and mechanical pressure on the elbow cause this condition.

Carpal Tunnel Syndrome: It is caused by compression of the nerves passing through the wrist. It shows symptoms in the form of tingling and numbness in the fingers at night. Working with a bent wrist and using vibrating hand tools cause this condition.

Cellulitis: It occurs as a result of repeated injuries to the palm. Pain and swelling in the palm are the most common symptoms. Using impact-causing tools such as hammers, etc., can cause this condition.

Epicondylitis: It occurs as inflammation occurring at the bone-tendon junction. It shows symptoms as pain and swelling in the relevant place. Repetitive movements in jobs requiring force cause this discomfort.

Ganglion: It occurs as a result of cyst structures that occur in the sheath of joints or tendons. It shows a painless symptom in a small area. Discomfort occurs as a result of repetitive hand movements.

Osteoarthritis: Inflammation of the joint and bone surfaces. It shows symptoms in the form of stiffness and pain in the spine, neck, and other joint areas. Prolonged loading of the spine and related joints causes this condition.

Tendonitis: It occurs as tendon inflammation. It is manifested by symptoms such as redness, pain, swelling, and tenderness in the upper arm, wrist, or hand, as well as an inability to get full efficiency when using the hand. Repetitive working movements cause this discomfort.

Tenosynovitis: It is a discomfort due to inflammation in tendons and their sheaths. It shows symptoms such as pain, swelling, extremely severe pain, and difficulty in using the hand. Sudden increases in workload cause this condition.

Pressure on the Neck and Shoulder: It is a condition that occurs with inflammation in the neck and shoulder muscles and tendons. It manifests as local pain in the neck and shoulder area. Constantly working in the same position causes this discomfort.

Trigger Finger: Inflammation of the tendons and sheaths of the fingers. It shows symptoms such as inability to move the fingers comfortably, locking when the finger is curled, and pain when moving it. Squeezing and grasping a tool for a long time with repetitive movements causes this discomfort.

White Finger Vibration: It is stated as neural changes and vascular contractions in the finger and forearm. It usually shows symptoms as numbness and tingling in cold weather. Using vibrating hand tools causes this discomfort.

Back and Waist Disorders: They are tensions and strains that occur in the structure of the spine. It usually shows symptoms with pain in the strained part and forcing movement. Behaviors such as lifting more than necessary, standing in an incorrect body position, and straining cause this discomfort.

Lumbar Hernia: It occurs when the anatomical integrity of the layer outside the elastic cartilage structure between the vertebrae in the lumbar region is disrupted due to the compression of the vertebrae, and the soft part inside protrudes outward (Çevikcan and Kara, 2007). Behaviors such as working in the wrong position, lifting heavy loads, and working from a seated position cause this discomfort.

For this reason, the movement management of the musculoskeletal system should be provided with the correct position and force to avoid permanent damage to the body or damage that affects the quality of life. Another situation to be considered is that the equipment used during work should be suitable for the working individual. At this point, we come across anthropometry. The fact that the equipment is suitable for the working individual will also increase the efficiency at work. Because the physical comfort of working people and their ability to use their physical abilities at the maximum level depend on the suitability of the materials, work surfaces, and volumes they use with their own dimensions (Bulut and Kıran, 2015).

3. Anthropometry

Anthropometry is a term that comes from the Greek words *anthropos* and *metrikos*. It can be called human measurement. Anthropometry measures the body according to some standards and analyzes it statistically (Figure 3). It is based on determining the measurement of all kinds of independent equipment, hand tools, and clothes, especially in business areas, and designing them in accordance with human beings.

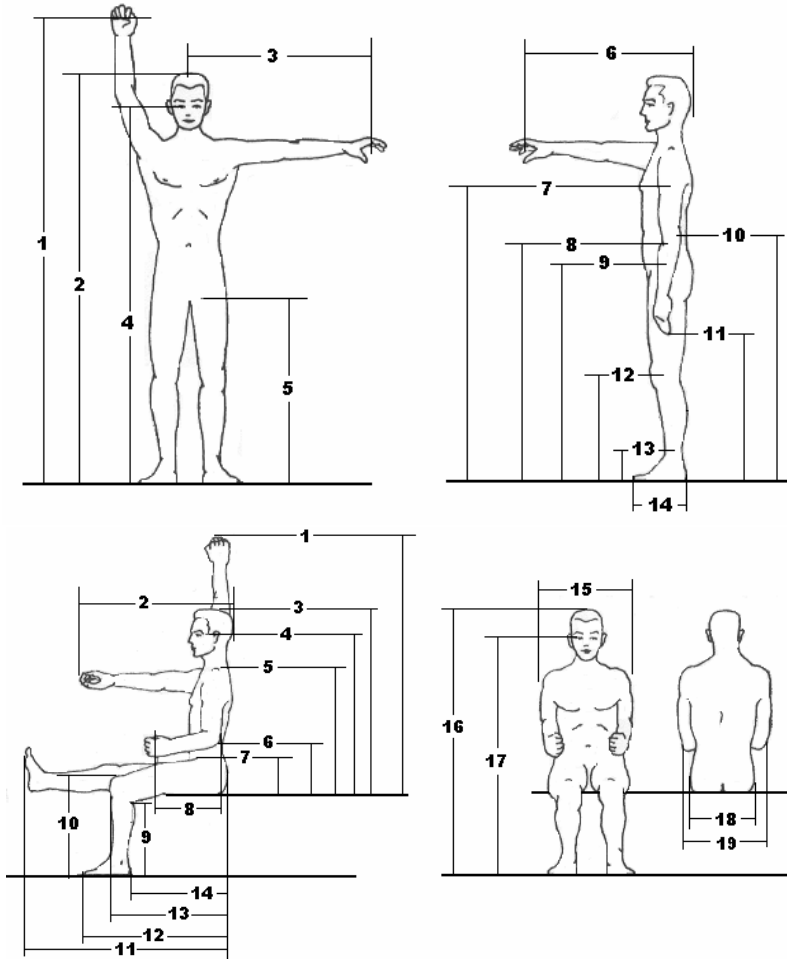


Figure 8: Dimensions used in static anthropometry studies(Kaya,2008)

Today, with the rapidly developing technology, business life is also undergoing changes. Employees who take an active role in the front field are physically and psychologically burdened due to the intense and heavy work pace. One of the reasons for this is that the equipment and hardware used are not suitable for the working individual. As a result, the working individual will have to bend, reach, or apply more force than they should, and problems due to strain will appear. It should not be forgotten that the musculoskeletal system of the working person has a certain limit strength. Therefore, compatibility between human and work should be ensured. Expecting people to do more than the work

they can do will have negative consequences and will reduce the quality of the employee and the work.

It is accepted that approximately 80% of occupational accidents are related to people, 18% to physical and mechanical environmental conditions, and 2% to unexpected events (Camkurt,2007). This shows that unwanted mishaps can be avoided to a great extent. What needs to be done here is to achieve compatibility between work and people. However, the key point here is to make the work suitable for people, not people for work. During the inspection, there are many different criteria ranging from the work area, the equipment used, to the physical condition of the environment. The use of appropriate equipment and tools during work is one of these criteria. Therefore, it can be said that the goal of anthropometry is to ensure that the right equipment is suitable for the individual during the work and that the working individual can devote himself to his work with full efficiency and health.

3.1. Anthropometric Design Approach To Equipment

Equipment is expected to perform the task for which it is designed well, to meet the needs of the maximum possible number of users, and to be inexpensive. This means that a piece of equipment is designed for potentially all users. It is also expected to provide good comfort and reduce biomechanical demands. The use of hand tools, in particular, covers a wide range of industries, and it is mostly the upper musculoskeletal region where accidents and injuries occur (Aptel at al.,2002). A study has shown that 24% of musculoskeletal accidents are related to hand tools (Myers and Trent, 1988) When designing a hand tool, it should not be overlooked that the user, the tool, and the working environment are an inseparable whole. Each of them is in a relationship with the other two, and the design of the hand tool is realized with an ergonomic approach. In general, three basic processes emerge in the design of hand tools (Aptel at al.,2002):

- Determining the needs and requirements of the employee according to anthropometric measurement criteria after observing the work process and work context
- After the initial process, testing of new prototypes according to tool specifications and laboratory simulations and examination of their biomechanical demands
- After the second stage, the new prototypes are tested in the real business sector over a long period of time. When satisfactory results are obtained, the prototype is accepted and approved.

The important point here is that users carefully test these new tools for a long time before making a final decision.

4. Biomechanics

Biomechanics studies the physical structure of the musculoskeletal and biological movement systems. Therefore, biomechanics can be considered as a part of mechanics. Because the working principle of some parts of the human body is similar to the working principle of a machine (Çalışkan and Fındık, 2012). Today, biomechanics covers the force-motion relationship of organs, load lifting, the operation and modeling of joints, diagnosis, and treatment studies in the field of sports and health. Research on biomechanics is basically divided into three separate sections: experimental research, applied research, and model analysis research. Experimental research includes studies on organs such as muscles and bones. Applied and model analysis research includes studies that are carried out by modeling existing research and studies without the need for experiments. Applied research includes useful research obtained by putting existing knowledge into practice. Biomechanical research can be in the field of occupational health and sports. Biomechanical research in the field of sports is carried out to ensure the highest efficiency and success of the athlete. Biomechanical research in the field of health includes injuries, musculoskeletal movements, and treatments of the human body. Occupational biomechanical research is carried out to reduce occupational accidents and physical difficulties while working in a healthier and more comfortable work environment (Karakoç,2020).

4.1 Musculoskeletal Biomechanics

The realization of movement in the human body is the result of the joint work of the muscular, skeletal, and nervous systems. The skeletal system protects the internal organs, acts as a place to attach to the muscles through tendons, shapes the body and provides uprightness, and has an important role in the movement of the body. The bones that make up the building blocks of the skeletal system are resistant to compression and can regenerate themselves after damage. Cartilage tissues, another element of the skeletal system, are three in number. Hyaline cartilage is found at the ends of long bones, elastic cartilage is found in places that do not ossify, such as the ear, and fibrous cartilage is found in the discs between the vertebrae and at the points where tendons and bones meet. In the muscular system, they are the structures that provide movement with the skeletal system. There are striated, smooth, and cardiac muscle types, and the striated cardiac muscle accounts for approximately 40-45% of body weight. Striated

muscles provide a regular distribution of the load on the body and protect the skeleton during movement (Karakoç,2020).

Conclusion

Aircraft maintenance technicians perform actions such as transportation, maintenance, repair, etc., and as a result, the risk of musculoskeletal injuries is quite high. Approximately 35.4% of the cases reported in this field are musculoskeletal disorders, and the neck, back, head, and lower parts are the most affected parts (Asadi, 2019)

REFERENCES

- Kanbur, E., & Gökalp, Ç. (2014). Havacılıkta Ekip Kaynak Yönetimi (CRM): Türkiye ve Dünyada Yapılan Araştırmalardan Seçmeler. V. Ulusal Havacılık Ve Uzak Konferansı, Kayseri.
- Yeşil, H. (2013). Metal Sektöründe Faaliyet Gösteren Bir İşyerinde Bel Ağrısı Prevelansını Etkileyen Fiziksel, Psikososyal ve Ergonomik Faktörler. Yüksek Lisans Tezi, İstanbul, Marmara Üniversitesi, Sağlık Bilimleri Enstitüsü
- Serbest, K., & Eldoğan O. (2014). İskelet Kaslarının Yapısı Ve Biyomekaniği. *Akademik Platform Mühendislik Ve Fen Bilimleri Dergisi*, 2(3), 41-51.
- Karakoç, Y. , Naderi, S. (2020), *Biyomekaniğin Temelleri*, Sağlık Bilimleri Üniversitesi Yayınları
- P. Stephen (2003), *Body Space Anthropometry, Ergonomics And The Design Of Work*, Taylor & Francis
- V. N. Reinhold (1986), *Ergonomic Design For People At Work*. Vol. 2, By Eastman Kodak Company,
- Can, G. F. (2013). Rula Yönteminin Görüntü İşleme Desteği İle Geliştirilmesi. Doktora Tezi, Kocaeli, Kocaeli Üniversitesi, Fen Bilimleri Enstitüsü
- Esen, H., Fırlı, N. (2013). Çalışma Duruşu Analiz Yöntemleri Ve Çalışma Duruşunun Kas-İskelet Sistemi Rahatsızlıklarına Etkileri. *Sakarya University Journal Of Science*, 17(1), 41-51.
- Çevikcan, B., & Kara, S. (2007). Bel Fıtığı Hastalığı Bulunan Bireylerin Bel Ve Karın Kası Fonksiyonlarının Elektromiyografik Analizi. Elektrik-Elektronik, Bilgisayar, Biyomedikal Mühendisliği XII. Ulusal Kongresi Ve Fuarı.
- Bulut, Ç., & Kıran, S. (2015). Antropometrinin Ergonomide Kullanımı. *Mesleki Sağlık ve Güvenlik Dergisi (MSG)*, 6(21).
- Kaya, N. A. (2008). Eskişehir Kent Merkezinde Kullanılan Dış Mekan Fitness Spor Aletlerinin Antropometrik Ölçülerinin Değerlendirilmesi ve Bir Tasarım Önerisi Geliştirilmesi, Yüksek Lisans Tezi, Eskişehir, Anadolu Üniversitesi.
- Camkurt, M. Z. (2007). İşyeri Çalışma Sistemi Ve İşyeri Fiziksel Faktörlerinin İş Kazaları Üzerindeki Etkisi. *TÜHİS İş Hukuku Ve İktisat Dergisi*, 21(1), 80-106.
- Aptel, M., Claudon, L., & Marsot, J. (2002). Integration Of Ergonomics Into Hand Tool Design: Principle And Presentation Of An Example. *International Journal Of Occupational Safety And Ergonomics*, 8(1), 107-115.
- Myers, J. R., & Trent, R. B. (1988). Hand Tool Injuries At Work: A Surveillance Perspective. *Journal Of Safety Research*, 19(4), 165-176.
- Çalışkan, M., & Fındık, F. (2012). Malzeme, Ergonomi ve Biyomekanik İlişkisi. *Sakarya University Journal Of Science*, 16(3), 273-282.
- Asadi, H., Yu, D., & Mott, J. H. (2019). Risk Factors For Musculoskeletal Injuries In Airline Maintenance, Repair & Overhaul. *International Journal Of Industrial Ergonomics*, 70, 107-115.
- URL-1 Work-Related Musculoskeletal Disorders,. <https://www.ccohs.ca/oshanswers/diseases/rmirsi.html> [Online]. Access Date: 10.10.2024



CHAPTER 33

Production Methods of Fiber Reinforced Composites

Sümeyye Erdem Korkmaz¹

¹ Öğr. Gör., Karamanoglu Mehmetbey University Vocational School of Technical Sciences,
ORCID: 0000-0002-5518-2716

1. Introduction

Fiber-reinforced composites are important building blocks of modern engineering and materials science, capable of providing strong and lightweight materials for various industries. These composites usually consist of a matrix material (polymer, metal or ceramic) and fibers that reinforce this matrix [1]. The fibers optimize the performance of the matrix material by increasing the mechanical properties of the composites [2]. The manufacturing methods of fiber reinforced composites are critical factors that determine the final properties and performance of the material [3]. Figure 1 shows a fiber reinforced composite.

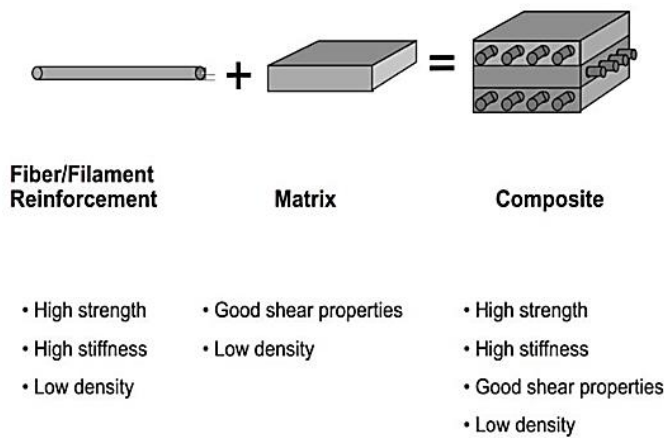


Figure 1. Fiber Reinforced Composites [4]

One of the basic methods used in the production of fiber-reinforced composites involves the process of combining fibers with a matrix material. This process is usually divided into two main categories: wet and dry methods [5]. Wet methods are those in which the fibers are saturated with liquid resins and then cured. These methods ensure complete coverage of the fibers with the matrix material, thus achieving high bonding and durability [6]. In dry methods, the fibers are combined with the matrix material in a drier environment and then cured by process temperature and pressure. These methods generally offer faster production cycles and lower costs, but can have limitations on resin penetration and thus bond quality [7].

Another important production method is the production of elastomeric fiber reinforced composites. This method is particularly suitable for applications where high flexibility and impact resistance are required [8]. Elastomeric composites are produced using fibers reinforced with elastomeric matrices. Such composites provide high impact resistance and flexibility by utilizing flexible materials such

as rubber. The manufacturing process of these composites usually involves molding and vulcanization [9]. For example, a rubber-based elastomeric composite requires a vulcanization process at 160°C for 30-60 minutes. This process allows the elastomeric matrix to harden and the fibers to fully bond, which improves the durability and performance of the composite [10].

Vacuum infusion is the preferred technique for the production of fiber-reinforced composites, especially for large and complex shapes. In this method, the fibers are placed in a mold and covered with a vacuum bag. The resin is then infused into the cavities under vacuum [11]. The vacuum infusion method produces high quality and homogeneous composites and minimizes air bubbles [12]. For example, a vacuum infusion system can infuse epoxy resins onto the fibers at a temperature of 60-80°C under a vacuum of 50-70 bar [13]. This method has a wide range of applications in the production of high performance and low cost composites and is often used in the marine and aerospace industries [14].

Pultrusion is another important method used in continuous profile production of fiber reinforced composites. This method involves the process of dipping reinforcing elements (usually glass or carbon fibers) into a resin pool and then drawing them through a die [15]. Pultrusion is suitable for the production of high-strength and long profiles and is often used in construction and industrial applications [16].

Injection molding is the preferred technique for the production of small, complex and high-volume parts. In this method, polymer-based matrix materials are melted and injected into a mold under high pressure. Widely used in the production of thermoplastic composites, injection molding offers precision and speed [17].

Molding and pressing methods are other important techniques used in the production of fiber-reinforced composites. These methods are usually based on placing the fibers and matrix materials in a mold and then curing them under heat and pressure. This method provides a homogeneous product and high mechanical performance [18]. Molding and pressing methods are generally used in high performance applications such as automotive, aerospace and sports equipment [19].

Sol-gel methods are a preferred technique, especially in the production of ceramic and polymer-based composites. This method involves the process of gelation of a solution and subsequent curing by thermal treatment [20]. The sol-gel process produces detailed and high-performance composites [21]. For example, silica solutions are gelled at 25-50°C and cured by drying at 100-150°C

[22]. The sol-gel method has wide application in applications such as nanotechnology and thin coatings, providing high uniformity and detailed structures [23].

The production methods of fiber-reinforced composites determine the advantages and limitations of each technique [24]. Methods such as injection molding and extrusion provide high speed and precision production, while methods such as vacuum infusion and pultrusion are used to produce large and high performance composites [25]. Sol-gel methods are preferred in applications requiring high detail and performance [26].

2. Elastomeric Fiber Reinforced Composite

Elastomeric fiber reinforced composites are a very special type of composites that offer a combination of flexibility and durability in materials engineering [27]. These composites are usually produced by reinforcing rubber-based elastomers with high-strength fibers. Elastomeric materials are particularly known for their high resilience and impact resistance properties. These properties make elastomeric composites ideal for applications requiring shock absorption and vibration isolation. The manufacturing process and material properties of these composites are critical factors affecting their technical properties and application areas [28].

The manufacturing process of elastomeric fiber reinforced composites usually includes molding and vulcanization steps. The molding process involves placing the elastomer into a specific mold and processing it at high temperature. This process allows the elastomer to take shape and bond with the fibers [29]. Vulcanization is a process that chemically hardens the elastomer and usually takes place at high temperature (150-200°C) and over a period of time. During this process, the sulfur atoms present in the elastomer form cross-linked structures between the polymer chains. These cross-links increase the elasticity and durability of the elastomer, so that the end product of the composite is both flexible and durable [30].

The properties of elastomeric fiber reinforced composites vary greatly depending on the type of elastomer used and the properties of the fiber [31]. Rubber-based elastomers can be natural rubber (NR) or synthetic rubbers (SBR, BR). Each type of elastomer offers different properties and performance. Natural rubber offers excellent elasticity and impact resistance, but may be limited in chemical resistance [32]. Synthetic rubbers, on the other hand, offer higher

resistance to various chemicals and can better withstand various environmental conditions [33].

The mechanical properties of composites vary according to the type, orientation and proportion of fibers [34]. Glass fiber composites offer good mechanical resistance and low cost, so they are widely used in the automotive and construction industries [35]. Carbon fiber composites, on the other hand, provide higher strength and lightweight properties, making them a preferred choice in aerospace and high-performance automotive applications. The proportion of carbon fibers in the composite greatly influences the mechanical properties of elastomeric composites and can typically range from 30-50% [36]. The orientation of the fibers is also important; longitudinally oriented fibers increase the tensile strength of the composite, while transversely oriented fibers increase the shear strength of the composite [37].

The advantages of elastomeric composites are related to their flexibility and impact resistance, as well as their vibration isolation and noise reduction properties [38]. These composites are used in applications such as vehicle suspension systems, tires and sports equipment. Elastomeric composites used in tire production are specially formulated to increase ride comfort and improve handling [39]. In sports equipment, elastomeric composites provide shock absorption and flexibility, which improves athletes' performance and reduces the risk of injury [40].

The production methods of elastomeric fiber reinforced composites require customized processes and materials for each application [3]. Molding, vulcanization, and material selection are important factors that determine the final properties of composites [41].

3. Vacuum Infusion

Vacuum infusion is a precise and efficient method commonly used in the production of composite materials. This manufacturing technique is particularly effective in the production of large-scale parts with complex geometries. The basic principle of vacuum infusion is that the resin is injected between the fibers under vacuum to ensure a homogeneous distribution. This process allows the production of high quality composites and significantly improves the mechanical properties of the material [42]. Figure 2 shows a schematic representation of the vacuum infusion process.

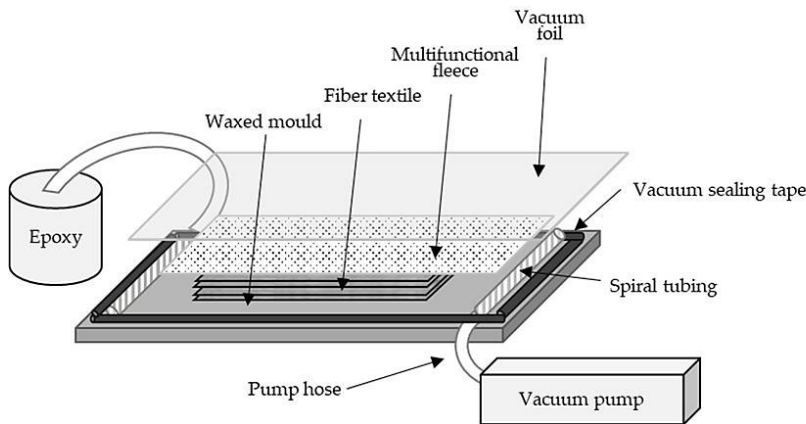


Figure 2. Schematic representation of the vacuum infusion process [43]

The basic stages of vacuum infusion include preparation, vacuum application, resin infusion and curing [44]. First, the appropriate mold for composite production is prepared. The mold usually consists of two parts: a support mold and a cover mold. The support mold determines the shape of the composite part, while the cap mold allows the vacuum and resin to be controlled. The mold is usually made of fiberglass, carbon fiber or other composite materials and must have high temperature and chemical resistance properties [45].

In the fiber placement stage, high-strength fibers are carefully placed in the mold [46]. The fibers can be of various types such as glass fibers, carbon fibers or aramid fibers [47]. Glass fibers are widely used due to their generally low cost and good mechanical properties, while carbon fibers offer high strength and lightweight properties [48]. The placement of the fibers in the mold must be done carefully because the proper placement of the fibers directly affects the final performance of the composite. The fibers are placed in the mold according to the desired directions and layers. Each layer of fibers determines the mechanical properties of the composite and therefore must be carefully placed [49].

The next step in the vacuum infusion process is vacuum application. The mold is covered with a special vacuum bag or pouch and negative pressure is applied inside using vacuum pumps. At this stage, the application of vacuum ensures that air and moisture inside the mold are completely removed. Under vacuum, air bubbles and other impurities are removed, allowing better penetration of the resin into the fibers [50].

In the resin infusion stage, the resin is injected into the mold under vacuum. The resin can be of various types, usually epoxy, polyester or vinyl ester. Each type of resin offers different mechanical and chemical properties and should be

selected according to the intended use [11]. The resin is injected into the mold under vacuum and completely penetrates between the fibers. During the resin infusion process, it must be carefully controlled so that the resin is homogeneously dispersed. The movement of the resin in the mold is usually controlled by vacuum systems, which ensure that the resin is evenly distributed over all fiber layers [51].

In the curing phase, the infused resin cures under temperature and pressure over a period of time. Curing usually takes place at high temperature and for a certain period of time, and this process allows the resin to harden chemically. This process improves the mechanical properties of the composite and increases the durability of the final product. During the curing process, the resin is fully cured and the composite part is left for a sufficient time before it is demolded [52].

The vacuum infusion method offers many advantages. In particular, this method keeps air bubbles and voids inside the composites to a minimum, which significantly improves the mechanical performance of the composites. Furthermore, the vacuum infusion method is effective in the production of large and complex parts, resulting in high quality composites. However, this method also has some limitations [53]. Vacuum infusion can require costly equipment and can be time-consuming in large-scale production processes. Also, the mold preparation and resin infusion process must be carefully controlled, otherwise it may affect the quality of the composites [54].

4. Pultrusion

Pultrusion is a method used in the production of continuous profiles and long composite parts. This technique enables the economical and efficient production of composite materials with high strength and light weight properties. The pultrusion process is based on the principle of coating fibers with resins and passing them through a mold to form a specific profile [15].

The pultrusion process usually consists of three main stages: coating the fibers with resin, passing through the die and curing. In the first stage, the fibers are immersed in a resin pool. Various types of resins can be used in this pool. Each type of resin provides different mechanical and chemical properties and is selected according to the intended use [55]. Figure 3 shows the pultrusion process.

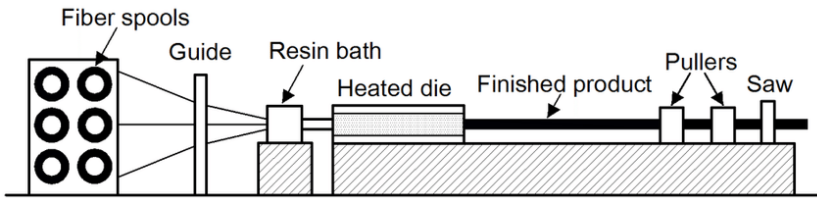


Figure 3. Pultrusion process [56]

After coating the fibers with resin, these coated fibers are fed into a pultrusion machine [57]. The pultrusion machine guides the fibers through a series of stages. First, the coated fibers are directed to a heating zone. In the heating zone, the viscosity of the resin is reduced, allowing better penetration of the fibers. This zone, usually at a temperature of 80-120°C, increases the fluidity of the resin and facilitates its passage through the mold. After heating, the fibers are passed through a mold. The mold is usually made of metal or aluminum and gives the desired profile shape. The mold allows the fibers to be formed into a specific shape and this stage determines the final shape of the composite [58].

The die passage stage is one of the most critical stages of pultrusion. The fibers in the mold, coated with resin, take on a specific profile and are pulled through the mold. This process creates the longitudinal profile of the composite material [59]. In the curing stage, the demolded composite material is cooled and cured for a certain period of time. This stage usually takes place in a cooling zone and allows the composite to fully cure [60]. The advantages of pultrusion include high production speed, low cost and high strength. This method allows large and long profiles to be produced quickly, and the mechanical properties of these profiles can be optimized depending on the ratio of fibers and resin [15].

5. Injection Molding

Injection molding is a sophisticated manufacturing method that is one of the cornerstones of industrial production and is used to produce many of the products that surround us every day. This process is carried out by liquefying plastics and injecting them into special molds under high pressure and then curing them in these molds [61]. Offering high precision, fast production and excellent repeatability, injection molding is an indispensable part of modern manufacturing technologies [62]. Figure 4 shows the injection molding process.

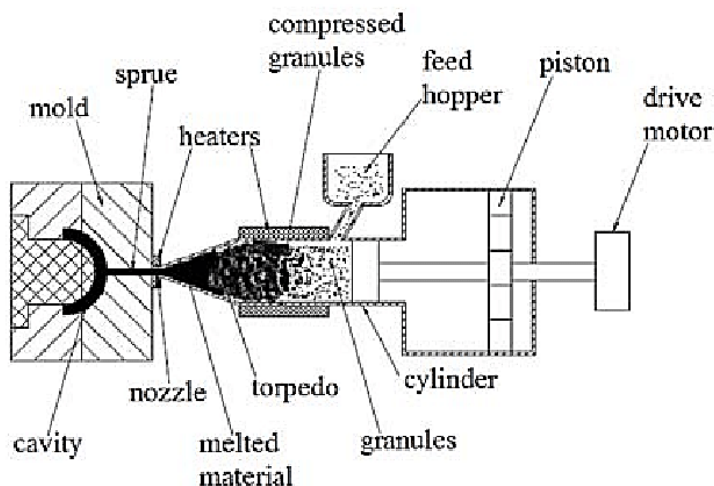


Figure 4. Injection molding process [63]

The first step in injection molding is the preparation of the material to be used. At this stage, plastic granules or powders are fed into an injection molding machine. Plastic materials can usually be polyethylene, polypropylene, polystyrene or various other thermoplastics. Granules are usually selected in accordance with precise quality control standards, as these standards directly influence the success of the production process [64]. Once the granules are placed in the feed hopper of the injection molding machine, they are transferred to the heating cylinder. The heating cylinder is used to melt the plastic granules. During the heating process, the granules are mixed and melted by a screw system. The heating process reduces the viscosity of the material and increases its fluidity so that the material can pass through the mold homogeneously [65]. The heated and liquidized plastic is injected into the mold by the injection machine. This stage involves injecting the material into the mold under high pressure [64].

The injection molding machine usually consists of two main parts: a fixed half mold and a movable half mold. The plastic material is injected between these two mold parts. The mold design is determined by the shape and characteristics of the product and is usually made with high precision. The plastic material inside the mold contains various inlets and channels to ensure its homogeneous distribution while in liquid form. These channels allow the plastic material to spread evenly inside the mold and prevent the formation of air bubbles [66]. After the injection process is complete, the plastic material is cooled and cured before being ejected from the mold [67]. The cooling process usually ranges from 10-60 seconds, which allows the plastic material to harden completely. During the cooling

process, the temperature in the mold and the cooling rate are carefully controlled. The demolded parts are usually cooled in the mold for a certain period of time and then removed from the mold. The cooling process determines the mechanical properties of the plastic material and affects the quality of the final product [68].

After cooling and hardening, the mold is opened and the final part is ejected. Part ejection is usually performed by automated systems or robots. This stage ensures that the product is produced quickly and efficiently. The demolded parts are usually cleaned of overflow and excess materials. The produced parts are subjected to quality control processes, which include the accuracy of the part's measurements, surface quality and mechanical properties [68]. Injection molding has many advantages. First of all, this method provides high production speeds and makes it possible to produce large quantities of parts in a short period of time. Injection molding also offers high precision and repeatability, which ensures consistent production of products. Furthermore, complex shapes and fine details can be created with injection molding, which provides design flexibility [64].

However, injection molding also has some limitations. First, mold costs can be high and mold design is often time-consuming and complex. Furthermore, the injection molding process requires careful design and maintenance of the mold for each production part [17]. The environmental impacts of injection molding must also be considered. The production and processing of plastic materials can increase energy consumption and requires waste management. However, modern injection molding machines and technologies can reduce these impacts by improving energy efficiency. Furthermore, the use of recycled plastics can help minimize environmental impacts [69].

6. Molding and Pressing

Molding and pressing are two fundamental technologies that play a critical role in modern industrial manufacturing processes. These methods are commonly used to mold various materials such as metals, plastics and composite materials into specific shapes and sizes. The molding and pressing processes provide high precision, repeatability and production efficiency [70]. Mold technology involves the process of passing material through a mold to produce a specific shape and size. Mold design requires great precision and engineering knowledge depending on the complexity of the part to be produced. The mold usually consists of two main parts: a fixed half mold and a movable half mold. Molds used in various production methods such as plastic injection molding, casting and stamping are usually made of durable materials such as steel, aluminum or hardened alloys [71]. Figure 5 shows the schematic setup of the compression molding process.

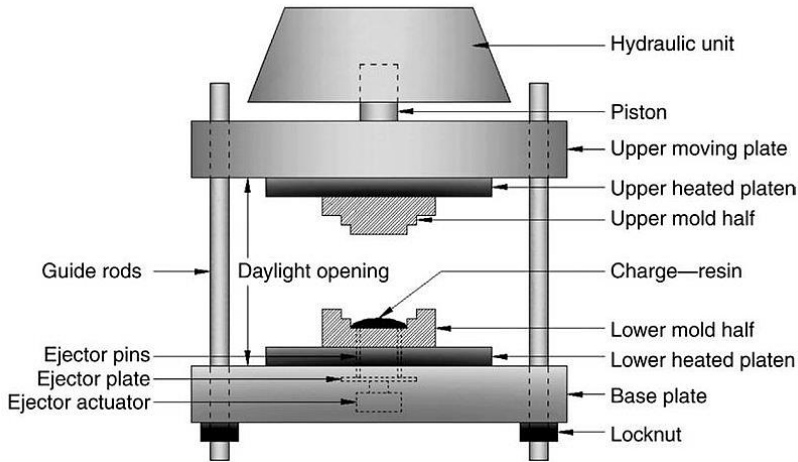


Figure 5. Schematic setup of compression molding process [72]

During the mold design process, part shape, dimensions and tolerances are taken into account. To ensure the precision of the parts coming out of the mold, the internal surfaces of the molds must usually have very high surface roughness standards. This ensures the smoothness of the part surface and clarity of detail. The temperature distribution inside the mold is also a critical factor, as an even temperature distribution ensures that the plastic or metal material flows smoothly through the mold [73].

Pressing is a method used to bring the material into a specific form under high pressure. The pressing process can be applied in a wide range of applications for the forming of metal sheets, plastics and composite materials. The most commonly used types of pressing include cold pressing, hot pressing and hydrogen pressing [74]. Cold stamping is the process of processing material at room temperature. This method allows metal sheets to be shaped under high pressure and is commonly used in the production of automotive parts, electronic components and packaging materials. The cold stamping process can increase the strength of the material and improve the deformation property of the metal [75]. Hot stamping is the process of processing the material at high temperature. This method is used to shape metal and ceramic materials and increases the fluidity of the material, allowing more complex shapes to be formed. During the hot pressing process, metal sheets are usually heated to temperatures of 800-1200°C and then extruded under high pressure [76].

Hydrogen pressing is a method used especially in the forming of composite materials. In this process, the material is exposed to high-pressure hydrogen in

the mold, which allows the material to be shaped [77]. Hydrogen pressing is used in the production of composite materials known for their high strength and lightweight properties [78]. The performance of the mold and pressing processes varies depending on many factors. These factors include material properties, mold design, pressing parameters and cooling/hardening process. In mold design, the fluidity and temperature distribution of the material are taken into account to ensure a uniform production quality. In the pressing process, parameters such as material pressure, temperature and time are carefully controlled [79].

Molding and pressing technologies have many advantages. They offer economical solutions for high-volume production and enable the production of parts with complex geometries. They also improve production quality by providing high precision and repeatability. In economic terms, molding and pressing technologies provide cost advantages in large-scale production. However, costs can be high at low production volumes and this can affect economic efficiency in small-scale production [80]. Therefore, molding and pressing methods perform best in large-scale production and provide cost advantages [81].

7. Sol-Gel Method

The sol-gel method is a process that enables the synthesis of various materials, especially ceramics and thin films, at low temperatures [82]. This method consists in the controlled transformation of the initially liquid mixture “sol” into a solid, network-like structure “gel”. The process usually starts with hydrolysis and polycondensation of metal alkoxides [83]. Figure 6 shows the steps of the sol-gel method.

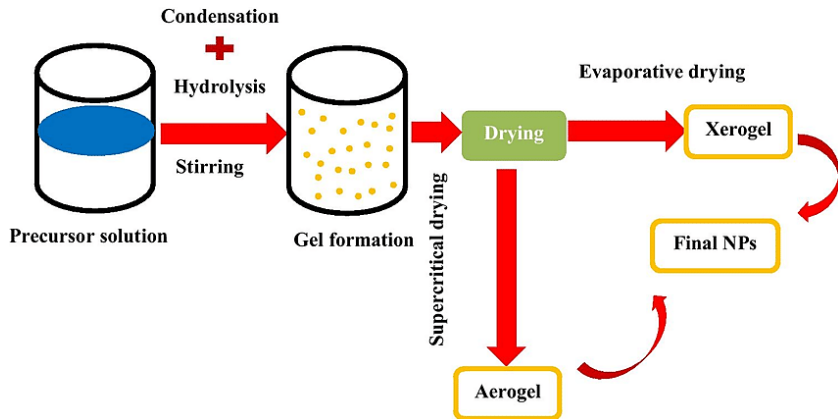


Figure 6. The steps of the sol–gel method [84]

Gelation is a critical stage where the particles in the sol come together to form a three-dimensional network structure. At this stage, the viscosity of the sol increases and a solid-like structure is obtained. This process is controlled by various factors such as temperature, pH and sol concentration [85]. The formed gel is dried by evaporation of the solvent. During the drying process it needs to be carefully controlled to avoid the formation of cracks in the gel. Then, the dried gel is subjected to sintering at high temperatures to give it a more robust and durable structure. This is a critical step that determines the final properties of the material [86]. The sol-gel method is used in a wide range of applications, from optical materials to biomedical applications. In addition, ceramics and glasses produced by this method exhibit superior mechanical and chemical resistance properties [26]. The sol-gel method offers advantages such as low temperature production and high purity materials. However, it also brings some challenges such as crack formation during drying and sintering processes. Furthermore, the implementation of the sol-gel process on industrial scales can present challenges in terms of process control [87].

8. Filament Winding

Filament winding is an advanced method used in the production of high-strength, lightweight and durable composite materials. This method involves winding fibers (filaments) onto a mandrel in a controlled manner. This process ensures proper alignment of the fibers and optimizes the mechanical properties of the final product [88]. Filament winding is widely used in various industries such as aerospace, automotive, energy and sports equipment [89]. Figure 7 shows the filament winding process.

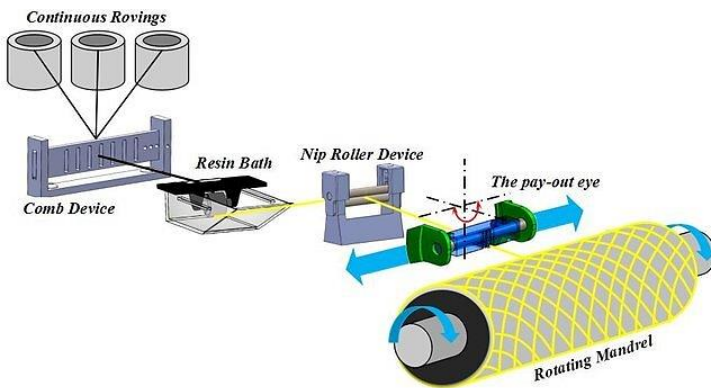


Figure 7. The process of filament winding [90]

The fibers used in filament winding are usually carbon, glass or aramid fibers. These fibers are prepared in spools and coated with resin before the winding

process begins. The resin ensures that the fibers stick together and the structure is strong [91]. The resin can be chosen from different materials such as polyester, epoxy or vinylester, and the type of resin chosen significantly affects the properties of the end product [92]. The mandrel is a shaping mold in which the filaments are wound. The size and shape of the mandrel determines the final form of the composite material to be produced [93]. The filaments are wound on the mandrel at a certain angle and tension. The winding angle is adjusted so that the fibers determine the strength, stiffness and flexibility of the final product. The smooth and tight winding of the fibers during the winding process affects the quality and durability of the end product [94].

After the winding process is completed, the resin is cured (hardened). The curing process can be done at room temperature or at elevated temperatures, depending on the properties of the resin. This process allows the resin to form a strong bond between the fibers and helps the composite to gain its final mechanical properties [95]. After the curing process is complete, the composite structure is carefully removed from the mandrel. This should be done carefully to avoid damage to the composite. The composite removed from the mandrel is ready for use as a final product [96].

9. Band Method

The tape method is a high-tech and highly precise process used in the production of composite materials. It is carried out by automatically or manually placing continuous bands of fibers pre-impregnated with resin on a mold [97]. The materials used in the production by the tape method consist of high-strength fibers such as carbon, glass or aramid combined with resin [98]. The tapes, which are pre-impregnated with resin, are placed on the mold at a certain angle and tension. The process of placing the tapes on the mold, when performed by automated machines, ensures that each layer has exactly the same thickness and pattern, making repeatable and high-quality production possible [99]. Once the placement of the tapes is complete, the composite structure is subjected to a curing process [49]. Curing allows the resin of the composite to harden, allowing the structures to gain their final form and strength. During this process, temperature and pressure are usually applied [100].

After the curing process is complete, the composite structure is removed from the mold and subjected to finishing. This process is important for finalizing the composite and improving the surface quality [101]. The tape method ensures high quality and consistency due to full control of the layers and automatic placement [102].

10. Conclusions

In this book chapter, we discuss the production methods of fiber-reinforced composites in detail and examine the advantages and limitations of each method. These various methods used in the production of composite materials are critical in determining the properties of parts used in different application areas. The methods chosen vary depending on the end-use of the composite, the desired properties and economic factors.

- New materials and technologies are constantly being developed in the production of composite materials. For example, fiber-reinforced composites developed with the use of nanomaterials can offer higher mechanical and thermal properties compared to conventional materials. Furthermore, the use of 3D printing technologies in composite material production facilitates the production of parts with complex shapes and geometries. Such developments provide innovative solutions in the composite materials industry, contributing to the development of more efficient and sustainable production methods.
- Nowadays, sustainability and environmental impacts play an important role in the production of composite materials. The recyclability of materials used in the production of fiber-reinforced composites and the environmental impact of production processes are becoming increasingly important in the industry. In this context, the use of biodegradable resins and fibers from renewable resources can be effective in reducing the environmental footprint of composite material production. In the future, developments in this area will enable composite materials to be produced in a more sustainable way and to be recycled at the end of their life cycle.
- Fiber reinforced composites are preferred in various industries thanks to their high strength and low weight properties. These materials, especially used in sectors such as aerospace, automotive and construction, offer significant advantages in terms of energy saving and performance. However, production costs and processes are important factors to be considered in the industrial applications of these materials. Improvements in production methods and technological innovations can reduce production costs and enable these materials to be used more widely.

- In a world where the methods and materials used in the production of fiber-reinforced composites are constantly evolving, the application areas of these materials will continue to expand. New technologies and materials will make composite materials more durable, lightweight and environmentally friendly. These developments will lead to significant changes in various industries such as aerospace, automotive, construction, energy and sports equipment.
- The production methods of fiber-reinforced composites are a dynamic and innovative area of materials science. In the future, advances in this field will allow the production of composite materials with higher performance, more efficient and more sustainable. This will increase the use and importance of composite materials in a world where technological advances and environmental awareness are becoming increasingly important.

References

- [1] Valorosi, F., De Meo, E., Blanco-Varela, T., Martorana, B., Veca, A., Pugno, N., et al. (2020). Graphene and related materials in hierarchical fiber composites: Production techniques and key industrial benefits. *Composites Science and Technology*, 185, 107848. <https://doi.org/10.1016/j.compscitech.2019.107848>
- [2] Herrera-Franco, P. J., & Valadez-González, A. (2005). A study of the mechanical properties of short natural-fiber reinforced composites. *Composites Part B: Engineering*, 36(8), 597–608. <https://doi.org/10.1016/j.compositesb.2005.04.001>
- [3] Rajak, D. K., Pagar, D. D., Menezes, P. L., & Linul, E. (2019). Fiber-reinforced polymer composites: Manufacturing, properties, and applications. *Polymers*, 11(10), 1667. <https://doi.org/10.3390/polym11101667>
- [4] Yadav, K. K., & Lohchab, D. S. (2016). Influence of aviation fuel on mechanical properties of glass fiber-reinforced plastic composite. *International Advanced Research Journal in Science, Engineering and Technology*, 3(4), 58. <https://doi.org/10.17148/IARJSET.2016.3413>
- [5] Erden, S., & Ho, K. (2017). Fiber reinforced composites. In *Fiber Technology for Fiber-Reinforced Composites* (pp. 51–79). Woodhead Publishing Series in Composites Science and Engineering. <https://doi.org/10.1016/B978-0-08-101871-2.00003-5>
- [6] Francucci, G., & Rodriguez, E. (2014). Processing of plant fiber composites by liquid molding techniques: An overview. *Polymer Composites*. <https://doi.org/10.1002/pc.23229>
- [7] Nechita, P., & Panaitescu, D. M. (2013). Improving the dispersibility of cellulose microfibrillated structures in polymer matrix by controlling drying conditions and chemical surface modifications. *Cellulose Chemistry and Technology*, 47(9-10), 711–719.
- [8] Mahesh, V., Joladarashi, S., & Kulkarni, S. M. (2021). Damage mechanics and energy absorption capabilities of natural fiber reinforced elastomeric based bio composite for sacrificial structural applications. *Defense Technology*, 17(1), 161–176. <https://doi.org/10.1016/j.dt.2020.02.013>
- [9] O'Connor, J. E. (1977). Short-fiber-reinforced elastomer composites. *Rubber Chemistry and Technology*, 50(5), 945–958. <https://doi.org/10.5254/1.3535189>
- [10] Zimny, A. (2023). Processing and characterization of elastomers and elastomer composites using waste rubber [Master's thesis]. In R. MasPOCH Rulduà & N. Candau (Eds.). Available from: <http://hdl.handle.net/2117/386214>
- [11] Agwa, M. A., Youssef, S. M., & Megahed, M. (2020). Integrated vacuum assisted resin infusion and resin transfer molding technique for manufacturing of nano-filled glass fiber reinforced epoxy composite. *Journal of Industrial Textiles*. <https://doi.org/10.1177/1528083720932337>

- [12] Romero, M. A. T. (2014). State of the art of degasification techniques in the shaping processes of composite materials prepared by resin infusion [Master's thesis]. Supervisor: M. N. Salán Ballesteros. Universitat Politècnica de Catalunya - BarcelonaTECH.
- [13] Mazzuca, P., Firmo, J. P., Correia, J. R., & Castilho, E. (2022). Influence of elevated temperatures on the mechanical properties of glass fibre reinforced polymer laminates produced by vacuum infusion. *Construction and Building Materials*, 345, 128340. <https://doi.org/10.1016/j.conbuildmat.2022.128340>
- [14] Alam, M. I., Maraz, K. M., & Khan, R. A. (2022). A review on the application of high-performance fiber-reinforced polymer composite materials. *GSC Advanced Research and Reviews*, 10(02), 20–36. <https://doi.org/10.30574/gscarr.2022.10.2.0036>
- [15] Volk, M., Yuksel, O., Baran, I., Hattel, J. H., Spangenberg, J., & Sandberg, M. (2022). Cost-efficient, automated, and sustainable composite profile manufacture: A review of the state of the art, innovations, and future of pultrusion technologies. *Composites Part B: Engineering*, 246, 110135. <https://doi.org/10.1016/j.compositesb.2022.110135>
- [16] Minchenkov, K., Vedernikov, A., Safonov, A., & Akhatov, I. (2021). Thermoplastic pultrusion: A review. *Polymers*, 13(2), 180. <https://doi.org/10.3390/polym13020180>
- [17] Sharifi, E., Chaudhuri, A., Waehrens, B. V., Staal, L. G., & Farahani, S. D. (2021). Assessing the suitability of freeform injection molding for low volume injection molded parts: A design science approach. *Sustainability*, 13(3), 1313. <https://doi.org/10.3390/su13031313>
- [18] Lotfi, A., Li, H., & Prusty, G. (2019). Natural fiber-reinforced composites: A review on material, manufacturing, and machinability. *Journal of Thermoplastic Composite Materials*, 34(2). <https://doi.org/10.1177/0892705719844546>
- [19] Sreejith, M., & Rajeev, R. S. (2021). Fiber reinforced composites for aerospace and sports applications. In *Fiber Reinforced Composites: Constituents, Compatibility, Perspectives, and Applications* (pp. 821–859). Woodhead Publishing Series in Composites Science and Engineering. <https://doi.org/10.1016/B978-0-12-821090-1.00023-5>
- [20] Parvej, M. S., Khan, M. I., & Hossain, M. K. (2022). Preparation of nanoparticle-based polymer composites. In *Nanoparticle-Based Polymer Composites* (pp. 55–94). Woodhead Publishing Series in Composites Science and Engineering. <https://doi.org/10.1016/B978-0-12-824272-8.00013-0>
- [21] Li, F., Huang, X., Liu, J. X., & Zhang, G. J. (2020). Sol-gel derived porous ultra-high temperature ceramics. *Journal of Advanced Ceramics*, 9, 1–16. <https://doi.org/10.1007/s40145-020-0370-z>

- [22] Gonzalez-Oliver, C. J., James, P. F., & Rawson, H. (1982). Silica and silica-titania glasses prepared by the sol-gel process. *Journal of Non-Crystalline Solids*, 48(1), 129–152. [https://doi.org/10.1016/0022-3093\(82\)90251-4](https://doi.org/10.1016/0022-3093(82)90251-4)
- [23] Schmidt, H. (2006). Considerations about the sol-gel process: From the classical sol-gel route to advanced chemical nanotechnologies. *Journal of Sol-Gel Science and Technology*, 40, 115–130. <https://doi.org/10.1007/s10971-006-6950-9>
- [24] Komanduri, R. (1993). Machining fiber-reinforced composites. *Mechanical Engineering*, 115(4), 58.
- [25] Advani, S. G., & Hsiao, K. T. (2012). Introduction to composites and manufacturing processes. In *Manufacturing Techniques for Polymer Matrix Composites (PMCs)* (pp. 1–12). Woodhead Publishing Series in Composites Science and Engineering. <https://doi.org/10.1533/9780857096258.1.1>
- [26] Owens, G. J., Singh, R. K., Foroutan, F., Alqaysi, M., Han, C. M., Mahapatra, C., Kim, H. W., & Knowles, J. C. (2016). Sol–gel based materials for biomedical applications. *Progress in Materials Science*, 77, 1–79. <https://doi.org/10.1016/j.pmatsci.2015.12.001>
- [27] Maiti, S., Islam, M. R., Uddin, M. A., Afroj, S., Eichhorn, S. J., & Karim, N. (2022). Sustainable fiber-reinforced composites: A review. *Advanced Sustainable Systems*, 6(11), 2200258. <https://doi.org/10.1002/adsu.202200258>
- [28] Rajeev, R. S. (2008). Fiber-reinforced elastomers. In *Current Topics in Elastomers Research* (pp. 351–394). CRC Press.
- [29] Goettler, L. A., & Shen, K. S. (1983). Short fiber reinforced elastomers. *Rubber Chemistry and Technology*, 56(3), 619–638. <https://doi.org/10.5254/1.3538144>
- [30] Bhowmick, A. K., & Mangaraj, D. (1994). Vulcanization and curing techniques. In *Rubber Products Manufacturing Technology* (1st ed., p. 82). Routledge. eBook ISBN: 9780203740378.
- [31] Ashida, M., Noguchi, T., & Mashimo, S. (1985). Effect of matrix's type on the dynamic properties for short fiber-elastomer composite. *Journal of Applied Polymer Science*, 30(3), 1011–1021. <https://doi.org/10.1002/app.1985.070300311>
- [32] Coveney, V. (2013). Natural and synthetic rubbers. In *Construction Materials Reference Book* (2nd ed., p. 18). Routledge. <https://doi.org/10.4324/9780080940380>
- [33] Blackley, D. C. (2012). *Synthetic Rubbers: Their Chemistry and Technology*. Springer Science & Business Media.
- [34] Young, K., Blighe, F. M., Vilatela, J. J., Windle, A. H., Kinloch, I. A., Deng, L., Young, R. J., & Coleman, J. N. (2010). Strong dependence of mechanical properties on fiber diameter for polymer–nanotube composite fibers: Differentiating defect from orientation effects. *ACS Nano*, 4(11), 6989–6997. <https://doi.org/10.1021/nn102059c>

- [35] Singh, J., Kumar, M., Kumar, S., & Mohapatra, S. K. (2017). Properties of glass-fiber hybrid composites: A review. *Polymer-Plastics Technology and Engineering*, 56(5), 455–469. <https://doi.org/10.1080/03602559.2016.1233271>
- [36] Sayam, A., Rahman, A. N. M., Rahman, M. S., Smriti, S. A., Ahmed, F., Rabbi, M. F., Hossain, M., & Faruque, M. O. (2022). A review on carbon fiber-reinforced hierarchical composites: Mechanical performance, manufacturing process, structural applications and allied challenges. *Carbon Letters*, 32, 1173–1205. <https://doi.org/10.1007/s42823-022-00399-3>
- [37] Almeida, J. H. S. Jr, Angrizani, C. C., Botelho, E. C., & Amico, S. C. (2015). Effect of fiber orientation on the shear behavior of glass fiber/epoxy composites. *Materials & Design*, 65, 789–795. <https://doi.org/10.1016/j.matdes.2014.10.003>
- [38] Kumbhar, S., Maji, S., & Kumar, B. (2014). Automotive vibration and noise control using smart materials: A state of art and challenges. *World Journal of Engineering*, 11(4), 413–420.
- [39] Sahu, B. B., Moharana, S., & Behera, P. K. (2024). Elastomeric-based composite materials for engineering applications. In *Polymer Composites (Engineering Materials series*, pp. 329–355). First Online: 04 May 2024.
- [40] Fan, Q., Duan, H., & Xing, X. (2024). A review of composite materials for enhancing support, flexibility and strength in exercise. *Alexandria Engineering Journal*, 94, 90–103. Available under a Creative Commons license. <https://doi.org/10.1016/j.aej.2024.03.048>
- [41] Trifkovic, M., Sheikhzadeh, M., Choo, K., & Rohani, S. (2010). Experimental and statistical study of the effects of material properties, curing agents, and process variables on the production of thermoplastic vulcanizates. *Journal of Applied Polymer Science*, 118(2), 764–777. <https://doi.org/10.1002/app.32316>
- [42] Menta, V. G. K., Vuppalapati, R. R., & Schuman, T. (2014). Manufacturing of transparent composites using vacuum infusion process. *Polymers and Polymer Composites*, 22(9). <https://doi.org/10.1177/096739111402200912>
- [43] Wakeman, M. D., & Dilsiz, N. (2019). Manufacture of hybrid natural/synthetic fiber woven textiles for use in technical biocomposites with maximum biobased content. *Journal of Composites Science*, 3(2), 43. <https://doi.org/10.3390/jcs3020043>
- [44] Zhang, K., Gu, Y., Li, M., & Zhang, Z. (2014). Effect of rapid curing process on the properties of carbon fiber/epoxy composite fabricated using vacuum assisted resin infusion molding. *Materials & Design*, 54, 624–631. <https://doi.org/10.1016/j.matdes.2013.08.065>
- [45] Hoa, S. V. (2009). *Principles of the manufacturing of composite materials*. Lancaster (PA): DEStech Publications, Inc.
- [46] Yoo, D. Y., Zi, G., Kang, S. T., & Yoon, Y. S. (2015). Biaxial flexural behavior of ultra-high-performance fiber-reinforced concrete with different fiber lengths

- and placement methods. *Cement and Concrete Composites*, 63, 51–66. <https://doi.org/10.1016/j.cemconcomp.2015.07.011>
- [47] Aydin, M. R., Acar, V., Cakir, F., Gündoğdu, Ö., & Akbulut, H. (2022). Comparative dynamic analysis of carbon, aramid and glass fiber reinforced interply and intraply hybrid composites. *Composites Structures*, 291, 115595. <https://doi.org/10.1016/j.compstruct.2022.115595>
- [48] Sanjay, M. R., Arpitha, G. R., & Yogesha, B. (2015). Study on mechanical properties of natural-glass fiber reinforced polymer hybrid composites: A review. *Materials Today: Proceedings*, 2(4–5), 2959–2967. <https://doi.org/10.1016/j.matpr.2015.07.264>
- [49] Yassin, K., & Hojjati, M. (2017). Processing of thermoplastic matrix composites through automated fiber placement and tape laying methods: A review. *Journal of Thermoplastic Composite Materials*, 31(12). <https://doi.org/10.1177/0892705717738305>
- [50] Modi, D., Correia, N., Johnson, M., Long, A., Rudd, C., & Robitaille, F. (2007). Active control of the vacuum infusion process. *Composites Part A: Applied Science and Manufacturing*, 38(5), 1271–1287. <https://doi.org/10.1016/j.compositesa.2006.11.012>
- [51] Hsiao, K. T., & Heider, D. (2012). Vacuum assisted resin transfer molding (VARTM) in polymer matrix composites. In *Manufacturing Techniques for Polymer Matrix Composites (PMCs)* (pp. 310–347). Woodhead Publishing Series in Composites Science and Engineering. <https://doi.org/10.1533/9780857096258.3.310>
- [52] Gu, Y., Qin, X., & Zhang, Z. (2015). Temperature distribution and curing behaviour of carbon fibre/epoxy composite during vacuum assisted resin infusion moulding using rapid heating methods. *Polymers and Polymer Composites*, 23(1). <https://doi.org/10.1177/096739111502300102>
- [53] Afendi, M., Banks, W. M., & Kirkwood, D. (2005). Bubble free resin for infusion process. *Composites Part A: Applied Science and Manufacturing*, 36(6), 739–746. <https://doi.org/10.1016/j.compositesa.2004.10.030>
- [54] Land, P., Crossley, R., Branson, D., & Ratchev, S. (2016). Technology review of thermal forming techniques for use in composite component manufacture. *SAE International Journal of Materials and Manufacturing*, 9(1). <https://doi.org/10.4271/2015-01-2610>
- [55] Talabi, S. I., Tobin, J., Strom, B., Brownstein, I., Kunc, V., & Hassen, A. A. (2024). Recent and future developments in pultrusion technology with consideration for curved geometries: A review. *Composites Part B: Engineering*, 283, 111678. <https://doi.org/10.1016/j.compositesb.2024.111678>
- [56] Barkanov, E., Akishin, P., Emmerich, R., & Graf, M. (2016). Numerical simulation of advanced pultrusion processes with microwave heating. In *VII European*

Congress on Computational Methods in Applied Sciences and Engineering (pp. 5953). Crete Island, Greece. <https://doi.org/10.7712/100016.2368.5953>

- [57] Irfan, M. S., Shotton-Gale, N., & Fernando, G. F. (2016). A modified pultrusion process. *Journal of Composite Materials*, 51(13). <https://doi.org/10.1177/0021998316666653>
- [58] Shaw-Stewart, D., & Sumerak, J. E. (2000). The pultrusion process. In *Pultrusion for Engineers* (1st ed., pp. 19–65). Abington Cambridge: Woodhead Publishing Ltd.
- [59] Mukherji, A., & Njuguna, J. (2022). An assessment on the effect of process parameters on pull force during pultrusion. *International Journal of Advanced Manufacturing Technology*, 121, 3419–3438. <https://doi.org/10.1007/s00170-022-09975-1>
- [60] Huda, Z. (2017). Composite processing technology. In *Foundations of Materials Science and Engineering* (pp. 279–297).
- [61] Kennedy, P. K. (2008). Practical and scientific aspects of injection molding simulation [PhD thesis]. Eindhoven: Technische Universiteit Eindhoven. <https://doi.org/10.6100/IR634914>
- [62] Zhao, P., Zhang, J., Dong, Z., Huang, J., Zhou, H., Fu, J., & Turng, L. S. (2020). Intelligent injection molding on sensing, optimization, and control. *Advances in Polymer Technology*, 2020, 7023616. <https://doi.org/10.1155/2020/7023616>
- [63] Hrițuc, A. (2018). Simple equipment for studying the injection molding process. *MATEC Web of Conferences*, 178, 02001. <https://doi.org/10.1051/matec-conf/201817802001>
- [64] Fu, H., Xu, H., Liu, Y., Yang, Z., Kormakov, S., Wu, D., & Sun, J. (2020). Overview of injection molding technology for processing polymers and their composites. *ES Materials and Manufacturing*, 8, 3–23. <https://doi.org/10.30919/esmm5f713>
- [65] Whelan, A. (2012). *Injection Moulding Materials*. Springer Science & Business Media.
- [66] Dym, J. B. (1987). *Injection molds and molding: A practical manual*. Springer Science & Business Media.
- [67] Rosato, D. V., & Rosato, M. G. (2012). *Injection molding handbook*. Springer Science & Business Media.
- [68] Dealey, R. (1991). Injection mold manufacturing. In M. L. Berins (Ed.), *SPI Plastics Engineering Handbook of the Society of the Plastics Industry, Inc.* (pp. 201–238). Boston, MA: Springer. https://doi.org/10.1007/978-1-4615-7604-4_7
- [69] Elduque, A., Elduque, D., Javierre, C., Fernández, Á., & Santolaria, J. (2015). Environmental impact analysis of the injection molding process: Analysis of the processing of high-density polyethylene parts. *Journal of Cleaner Production*, 108(Pt A), 80–89. <https://doi.org/10.1016/j.jclepro.2015.07.119>

- [70] Koç, M., & Özel, T. (Eds.). (2019). *Modern manufacturing processes*. John Wiley & Sons.
- [71] Fernandes, C., Pontes, A. J., Viana, J. C., & Gaspar-Cunha, A. (2016). Modeling and optimization of the injection-molding process: A review. *Advances in Polymer Technology*. <https://doi.org/10.1002/adv.21683>
- [72] Billah, M. M., Rabbi, M. S., & Hasan, A. (2021). A review on developments in manufacturing process and mechanical properties of natural fiber composites. *Journal of Engineering Advances*, 2(1), 13–23. <https://doi.org/10.38032/jea.2021.01.003>
- [73] Zemel, M. I., & Otto, K. N. (1996). Use of injection molding simulation to assess critical dimensions and assign tolerances. In *Proceedings of the ASME 1996 Design Engineering Technical Conferences and Computers and Information in Engineering Conference* (Paper No: 96-DETC/DFM-1277, V001T01A013). Irvine, CA. Published online 2021 Feb 25. <https://doi.org/10.1115/96-DETC/DFM-1277>
- [74] Atkinson, H. V., & Davies, S. (2000). Fundamental aspects of hot isostatic pressing: An overview. *Metallurgical and Materials Transactions A*, 31, 2981–3000.
- [75] Liu, K., Tang, X., Liu, Y., Xu, Z., Yuan, Z., & Zhang, Z. (2020). Enhancing the performance of fully-scaled structure-adjustable 3D thermoelectric devices based on cold-press sintering and molding. *Energy*, 206, 118096. <https://doi.org/10.1016/j.energy.2020.118096>
- [76] Rezaie, A., Fahrenholtz, W. G., & Hilmas, G. E. (2007). Effect of hot pressing time and temperature on the microstructure and mechanical properties of ZrB₂–SiC. *Journal of Materials Science*, 42, 2735–2744.
- [77] Khodabakhshi, F., Ekrt, O., Abdi, M., Gerlich, A. P., Mottaghi, M., Ebrahimi, R., Nosko, M., & Wilde, G. (2022). Hydrogen storage behavior of Mg/Ni layered nanostructured composite materials produced by accumulative fold-forging. *International Journal of Hydrogen Energy*, 47(2), 1048–1062. <https://doi.org/10.1016/j.ijhydene.2021.10.096>
- [78] Fan, J., & Njuguna, J. (2016). An introduction to lightweight composite materials and their use in transport structures. In *Lightweight Composite Structures in Transport: Design, Manufacturing, Analysis and Performance* (pp. 3–34). <https://doi.org/10.1016/B978-1-78242-325-6.00001-3>
- [79] Ho, M., Wang, H., Lee, J. H., Ho, C. K., Lau, K. T., Leng, J., & Hui, D. (2012). Critical factors on manufacturing processes of natural fibre composites. *Composites Part B: Engineering*, 43(8), 3549–3562. <https://doi.org/10.1016/j.compositesb.2011.10.001>
- [80] Sarfraz, M. S., Hong, H., & Kim, S. S. (2021). Recent developments in the manufacturing technologies of composite components and their cost-effectiveness in the automotive industry: A review study. *Composite Structures*, 266, 113864. <https://doi.org/10.1016/j.compstruct.2021.113864>

- [81] Gates, B. D., Xu, Q., Stewart, M., Ryan, D., Willson, C. G., & Whitesides, G. M. (2005). New approaches to nanofabrication: Molding, printing, and other techniques. *Chemical Reviews*, 105(4), 1171–1196. <https://doi.org/10.1021/cr030076o>
- [82] Chilibon, I., & Marat-Mendes, J. N. (2012). Ferroelectric ceramics by sol–gel methods and applications: A review. *Journal of Sol-Gel Science and Technology*, 64, 571–611. <https://doi.org/10.1007/s10971-012-2795-8>
- [83] Danks, A. E., Hall, S. R., & Schnepf, Z. (2016). The evolution of ‘sol–gel’ chemistry as a technique for materials synthesis. *Materials Horizons*, 3, 91–112. <https://doi.org/10.1039/C5MH00260E>
- [84] Jazie, A. A., Albaaji, A. J., & Abed, S. A. (2021). A review on recent trends of antiviral nanoparticles and airborne filters: Special insight on COVID-19 virus. *Air Quality, Atmosphere & Health*, 14, 1811–1824. <https://doi.org/10.1007/s11869-021-01055-1>
- [85] Flory, P. J. (1942). Constitution of three-dimensional polymers and the theory of gelation. *The Journal of Physical Chemistry*, 46(1), 132–140. <https://doi.org/10.1021/j150415a016>
- [86] Boulogne, F., Pauchard, L., & Giorgiutti-Dauphiné, F. (2012). Effect of a non-volatile cosolvent on crack patterns induced by desiccation of a colloidal gel. *Soft Matter*, 8, 8505–8510. <https://doi.org/10.1039/C2SM25858G>
- [87] Bokov, D., Jalil, A. T., Chupradit, S., Suksatan, W., Ansari, M. J., Shewael, I. H., Valiev, G. H., & Kianfar, E. (2021). Nanomaterial by sol-gel method: Synthesis and application. *Advances in Materials Science and Engineering*, 2021, 5102014. <https://doi.org/10.1155/2021/5102014>
- [88] Quanjin, M., Rejab, M. R., Idris, M. S., Zhang, B., & Kumar, N. M. (2019). Filament winding technique: SWOT analysis and applied favorable factors. *SCIREA Journal of Mechanical Engineering*, 3(1), 1–25. Available from: <http://www.scirea.org/journal/Mechanical>
- [89] Azeem, M., Ya, H. H., Alam, M. A., Kumar, M., Stabla, P., Smolnicki, M., et al. (2022). Application of filament winding technology in composite pressure vessels and challenges: A review. *Journal of Energy Storage*, 49, 103468. <https://doi.org/10.1016/j.est.2021.103468>
- [90] ter Harmsel, J. M., El Amien, N. P., & Popa, I. B. (2023). Relevant mechanical characterization methods of hybrid composites joints - A review. Enschede: University of Twente, Faculty of Engineering Technology; November 2023.
- [91] Xu, J., Ma, Y., Zhang, Q., Sugahara, T., Yang, Y., & Hamada, H. (2016). Crashworthiness of carbon fiber hybrid composite tubes molded by filament winding. *Composite Structures*, 139, 130–140. <https://doi.org/10.1016/j.compstruct.2015.11.053>

- [92] Nodehi, M. (2022). Epoxy, polyester and vinyl ester based polymer concrete: A review. *Innovative Infrastructure Solutions*, 7, 64. Published online October 17, 2021. <https://doi.org/10.1007/s41062-021-00664-2>
- [93] Vargas-Rojas, E. (2022). Prescriptive comprehensive approach for the engineering of products made with composites centered on the manufacturing process and structured design methods: Review study performed on filament winding. *Composites Part B: Engineering*, 243, 110093. <https://doi.org/10.1016/j.compositesb.2022.110093>
- [94] Peters, S. T., & Tarnopol'skii, Y. M. (1997). Filament winding. In *Composites Engineering Handbook* (1st ed., pp. 34). CRC Press.
- [95] Hübner, F., Brückner, A., Dickhut, T., Altstädt, V., Rios de Anda, A., & Ruckdäschel, H. (2021). Low temperature fatigue crack propagation in toughened epoxy resins aimed for filament winding of type V composite pressure vessels. *Polymer Testing*, 102, 107323. <https://doi.org/10.1016/j.polymertesting.2021.107323>
- [96] Du, H., Liu, L., Leng, J., Peng, H., Scarpa, F., & Liu, Y. (2015). Shape memory polymer S-shaped mandrel for composite air duct manufacturing. *Composite Structures*, 133, 930–938. <https://doi.org/10.1016/j.compstruct.2015.08.005>
- [97] Schmitt, R., Mersmann, C., & Damm, B. (2010). In-process 3D laser measurement to control the fiber tape-laying for composite production. In *Optics, Photonics, and Digital Technologies for Multimedia Applications (Proceedings of SPIE; Vol. 7723, 77230R)*. <https://doi.org/10.1117/12.853882>
- [98] Song, J. H. (2015). Pairing effect and tensile properties of laminated high-performance hybrid composites prepared using carbon/glass and carbon/aramid fibers. *Composites Part B: Engineering*, 79, 61–66. <https://doi.org/10.1016/j.compositesb.2015.04.015>
- [99] Grove, D. A. (2005). Composite processes. In C. A. Harper (Ed.), *Handbook of Plastic Processes* (1st ed.). <https://doi.org/10.1002/0471786586.ch8>
- [100] Mgbemena, C. O., Li, D., Lin, M. F., Liddel, P. D., Katnam, K. B., Thakur, V. K., & Yazdani Nezhad, H. (2018). Accelerated microwave curing of fibre-reinforced thermoset polymer composites for structural applications: A review of scientific challenges. *Composites Part A: Applied Science and Manufacturing*, 115, 88–103. <https://doi.org/10.1016/j.compositesa.2018.09.012>
- [101] Walczyk, D., Kupperts, J., & Hoffman, C. (2011). Curing and consolidation of advanced thermoset composite laminate parts by pressing between a heated mold and customized rubber-faced mold. *Journal of Manufacturing Science and Engineering*, 133(1), 011002. <https://doi.org/10.1115/1.4003125>
- [102] Qureshi, Z., Swait, T., Scaife, R., & El-Dessouky, H. M. (2014). In situ consolidation of thermoplastic prepreg tape using automated tape placement technology: Potential and possibilities. *Composites Part B: Engineering*, 66, 255–267. <https://doi.org/10.1016/j.compositesb.2014.05.025>



CHAPTER 34

Applications and Developments of Vacuum Infusion Method in Mechanical Engineering

Sümeyye Erdem Korkmaz¹

¹ Öğr. Gör., Karamanoglu Mehmetbey University Vocational School of Technical Sciences,
ORCID: 0000-0002-5518-2716

1. Introduction

The vacuum infusion method stands out as a modern technology that represents an important stage in the evolution of composite material production [1]. In mechanical engineering, this method has radically changed not only manufacturing processes, but also product performance and economic efficiency. The advantages offered by vacuum infusion are increasingly recognized, especially in industrial applications requiring high durability, low weight and cost effectiveness [2].

Vacuum infusion technology is essentially a method used in the production of composite materials, which is based on the infiltration of resin into the reinforcing material (usually fibers) under vacuum. This process removes both air and other contaminants from the composite material structure, resulting in a more homogeneous and durable structure. The mechanical properties of composites produced by vacuum infusion are significantly improved compared to conventional methods [3]. For example, the tensile strength of a carbon fiber composite produced by vacuum infusion method can reach up to 1000 MPa in some cases, while this value usually remains around 700 MPa in conventional fiber reinforcement methods [4].

In recent years, the impact of vacuum infusion in industrial applications has grown remarkably. According to a 2022 industry report, the use of vacuum infusion technology in the automotive sector has reduced the production costs of composite parts by 35% and shortened production time by 30%. These developments have greatly facilitated the automotive industry to achieve its lightweighting and fuel efficiency goals. The same report revealed that vacuum infusion technology increases the durability of automotive parts by 20%, resulting in longer life [5].

The aerospace industry is another sector that benefits from the advantages offered by vacuum infusion technology. Due to the critical importance of material performance and safety in aerospace applications, the high durability and low weight properties provided by vacuum infusion are extremely valuable. A 2023 study reported that the weight of aircraft parts produced using vacuum infusion was reduced by 25% and fuel consumption was reduced by 15%. Furthermore, the success of this method in the production of large structural parts such as fuselage and wings makes it possible for the aviation industry to produce more efficient and environmentally friendly aircraft [6].

The maritime industry, especially in the production of yachts and boats, greatly benefits from the advantages of lightness and durability provided by the vacuum infusion method. In this sector, the resistance of composite materials produced using vacuum infusion technology to marine conditions has been increased and maintenance costs have been reduced [7]. In a study conducted in 2024, it was reported that the structural strength of a sailboat produced using vacuum infusion technique was increased by 40% and its longevity was significantly extended [8].

The development of vacuum infusion is important not only for materials science and engineering, but also for environmental sustainability. This method minimizes the negative impact on the environment by reducing the amount of resin and waste used in the production of composite materials [9]. An environmental impact assessment conducted in 2024 showed that the vacuum infusion method reduces carbon emissions in composite production by 20%, thus contributing to the reduction of the industrial carbon footprint. Furthermore, the use of recyclable materials was increased by 15% with the use of this technology [10].

Vacuum infusion plays an important role in mechanical engineering and industrial production processes. It is reshaping industry standards with its advantages in the production of high-performance and economical composite materials and offers innovative solutions in many sectors. Developing technology and continuous innovations will make the vacuum infusion method even more effective and sustainable, which will create a wider usage area in industrial applications [11]. In this study, current applications, technological developments and potential future research areas of the vacuum infusion method will be examined in detail.

2. Basic Principles of Vacuum Infusion Method

Vacuum infusion is recognized as a highly effective and widespread process in the production of composite materials. Its basic principles are critical elements that directly affect both the efficiency of the processes and the quality of the results [12]. The basic principles of the vacuum infusion process generally consist of three main stages: material preparation, vacuum application and resin infusion [13]. In the first stage, the reinforcing materials, usually fiber fabrics of various types (such as carbon fiber, aramid fiber, fiberglass), are placed in a suitable mold. This mold is of great importance for the final shape and properties of the composite material. During material preparation, the correct placement of the fiber layers is a critical step for the homogeneity and structural integrity of the

material. In addition, the orderly placement of the materials in the mold ensures that the vacuum infusion process is carried out properly [14].

The second stage, vacuum application, is another important step that affects the quality of the process. At this stage, air and moisture are completely removed from the mold. By means of a vacuum pump, the atmosphere inside the mold is kept under low pressure, providing the necessary environment for the resin to penetrate the pores in the material. Successful vacuum treatment ensures that the material is free of all voids and the resin is evenly distributed. This step increases the strength and homogeneity of the composite material, resulting in a high quality product [15].

The last stage is resin infusion. The resin is usually used as a two-component system and these components are mixed with each other during infusion. The resin is injected into the mold under vacuum and systematically diffuses into the reinforcement materials. This process ensures that the resin fully penetrates the reinforcement materials and fills all voids. The infusion process of the resin is usually carried out through a series of injection points and the strategic placement of these points ensures an even distribution of the resin throughout the material [16]. Figure 1 shows a schematic of the Vacuum Infusion Method (VIM).

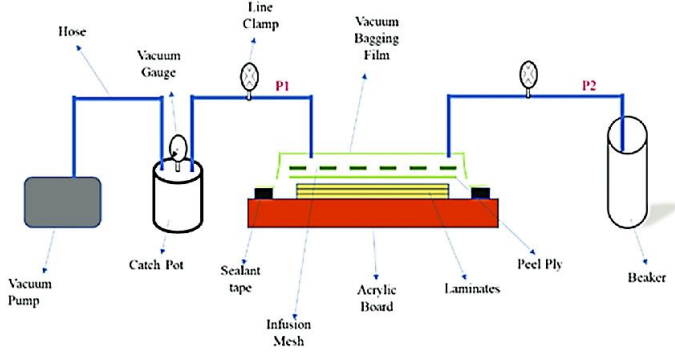


Figure 1. Schematic of the Vacuum Infusion Method (VIM) [17]

The materials and equipment used in vacuum infusion are critical to the success of the process. Key materials include high-strength fiber reinforcement materials and special resins [18]. Reinforcing materials such as carbon fiber, aramid fiber and fiberglass enhance the mechanical properties of composite materials, providing high durability and low weight [19]. Resins can usually be epoxy, polyester or vinylester based, and these resins ensure the hardening and structural integrity of the material [20]. Equipment includes vacuum pumps, resin injection systems, molds and vacuum beds. Vacuum pumps remove air and moisture from the mold, creating a low pressure environment. Resin injection

systems allow resin to be infused into the material in a controlled manner. Molds are the building blocks that determine the final shape of the composite material and are usually made of special materials with high durability [21].

The advantages and limitations of the vacuum infusion method determine the areas of application and impact of this process. The advantages of the process include increasing material homogeneity and minimizing air bubbles. The vacuum infusion method can reduce air voids inside composite materials by 90%, which significantly improves the mechanical properties of the materials. Furthermore, this method results in high quality and aesthetically superior surfaces. Another advantage of vacuum infusion is the reduction of resin quantity and waste. This increases environmental sustainability and reduces production costs [22].

However, the vacuum infusion method also has some limitations. The applicability of the process depends on factors such as mold design and control of resin flow. Mold design and preparation can often be costly and must be done correctly at the initial stage of the process. Furthermore, any errors during resin infusion can adversely affect the quality of the composite material. The lengthy curing stages of the process can also extend the production time, which can create challenges in terms of time management. In some specific cases, the vacuum infusion method may have application difficulties due to limitations such as material thickness and geometry [23].

3. Material and Resin Selection

The choice of materials and resins used in the vacuum infusion process are critical factors that directly affect the mechanical performance, durability and cost effectiveness of composites. Material selection usually starts with fiber reinforcement materials and the type of these materials varies according to the application requirements [24]. Carbon fiber is preferred especially in aerospace and automotive industries due to its combination of high strength and low weight. Carbon fiber composites can reach 800-1000 MPa in tensile strength and provide high performance in structural applications thanks to these properties [25]. Aramid fiber is known for its high impact toughness and excellent energy absorption and is therefore often used in protective equipment [26]. Fiberglass is suitable for many industrial applications due to its cost effectiveness and good overall durability [27]. Each type of fiber material offers different mechanical properties and performance criteria, so the suitability of the material for the end use should be carefully evaluated during the selection process [28].

Resin selection is another important factor determining the success of the vacuum infusion process [29]. Epoxy resins are known for their high bond strength, excellent chemical resistance and low shrinkage rate, making them ideal for high performance composites [30]. In particular, epoxy resins are preferred for critical applications such as aircraft and sports car parts [31]. Polyester resins, on the other hand, are characterized by their lower cost and ease of processing, which is why they are often used in less load-bearing and cost-oriented applications [32]. Vinyl ester resins combine the advantages of both epoxy and polyester resins and offer good chemical resistance and moderate mechanical properties, making them suitable for marine and chemical tank construction [33]. Factors such as curing time, viscosity and fluidity properties of the material should also be considered when selecting the resin. These parameters affect the homogeneous distribution of the resin in the material and the efficiency of the infusion process. In addition, resin and fiber material compatibility directly affects the overall performance and durability of the composite; therefore, material and process compatibility should be ensured by selecting the appropriate resin type [34].

3.1. Resins Used in Vacuum Infusion

The resins used in vacuum infusion are critical components that determine the mechanical properties and performance of composite materials [35]. These resins are generally divided into three main categories: epoxy, polyester and vinylester resins. Each type of resin is characterized by different properties and application advantages [36].

Epoxy resins are one of the most widely used resin types in the vacuum infusion process and are preferred in many industrial applications. The chemical structure of epoxy resins provides excellent adhesion strength, low shrinkage and high mechanical strength. These resins are particularly preferred in applications requiring high performance, for example in the aerospace and automotive sectors. Epoxy resins have high tensile strength, which can range from 800-1000 MPa, making them ideal for structures requiring high strength. Furthermore, epoxy resins offer excellent chemical and temperature resistance, making them usable in harsh environmental conditions. However, the curing time of epoxy resins can often be longer and this can lengthen the manufacturing process [37]. Figure 2 shows the flow diagram of epoxy resin sample preparation.

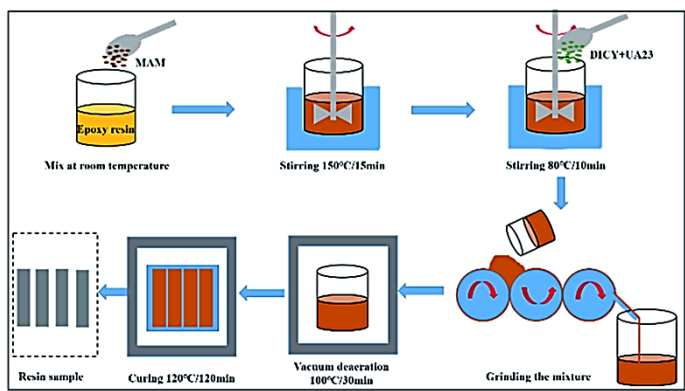


Figure 2. The flow diagram of preparing an epoxy resin sample [38]

Polyester resins generally offer lower cost and faster cure times. The chemical structure of polyester resins offers a wide viscosity range and favorable flowability properties, making them suitable for large-scale and cost-oriented production. Polyester resins are widely used, especially in the automotive and marine industries. These resins are generally less durable and less chemically resistant than epoxy resins, but their cost-effectiveness and fast cure time can speed up the production process. The mechanical properties of polyester resins generally exhibit lower tensile strength and fracture toughness, making them more suitable for lighter weight and low load bearing applications [39]. Figure 3 shows the coral-like structure of polyester resin based on microgel formation.

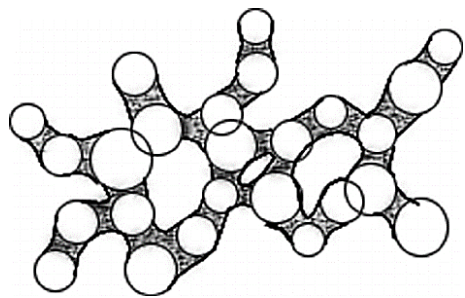


Figure 3. Structures of polyester resin based on microgel formation, coral-like structure [40]

Vinyl ester resins are an option that combines the advantages of epoxy and polyester resins. Vinyl ester resins offer both high chemical resistance and good mechanical properties. These resins are widely used in marine and chemical processing applications because they provide both high abrasion resistance and excellent water resistance. The mechanical properties of vinylester resins are better than those of polyester resins, generally offering tensile strength in the

range of 600-800 MPa, and their chemical resistance is comparable to epoxy resins. Vinyl ester resins also cure faster than epoxy resins, which shortens the production process, but their cost can often be lower than epoxy resins. The use of vinylester resins is particularly suitable for applications with long service life and resistance to harsh environmental conditions [41]. Figure 4 shows the mechanical properties of vinylester resin.

Properties	Value
Tensile Strength	80 MPa
Elongation at break	5%
Viscosity at 25°C	520-620 MPa s
Pot life at 25°C	14 – 24 Min

Figure 4. Properties of vinyl ester [42]

All three resin types offer certain advantages and limitations in the vacuum infusion method. The choice of resin is usually based on the specific requirements of the application, the desired mechanical properties and the budget. The viscosity, flowability and curing properties of the resin directly affect the efficiency of the vacuum infusion process and the final quality of the composite material. Furthermore, the chemical compatibility between the resin and fiber reinforcement materials is a critical factor to improve the durability and performance of the material. Proper resin selection ensures high performance, durable and economical solutions in composite production [43].

3.2. Reinforcement Materials

Reinforcing materials are critical components that enhance the performance and improve the mechanical properties of composite materials. These materials are usually combined with matrix materials (such as resins) to form high-strength and lightweight structures [44]. Fiberglass, carbon fiber, and aramid fiber are the most common of these types of reinforcing materials, each offering unique properties [45].

Fiberglass is a reinforcing material made of glass fiber and is highly effective in increasing the strength of composites. Fiberglass offers excellent mechanical properties and low cost, making it a popular choice in many industrial applications. Glass fibers have high tensile strength and good flexibility properties, which reduces their risk of fracture. In addition, fiberglass's chemical resistance makes it resistant to moisture and temperature changes. These properties make fiberglass widely used in the automotive, marine and

construction industries. However, the strength of fiberglass is not as high as that of carbon fiber and aramid fiber and therefore may show limitations in lighter weight and high performance applications [46].

Carbon fiber is known for its high strength and low weight properties, making it ideal for high performance composites. Carbon fibers generally have high tensile strengths, up to 1000 MPa, and their very low density makes them preferred for aerodynamic and structural applications. The planar structure and ordered molecular structure of carbon fibers support their high stiffness and rigidity properties. This material is widely used in high-performance applications such as aerospace, automotive and sports equipment. The disadvantage of carbon fibers is their generally high cost and limited long-life performance in some environmental conditions. However, the superior performance characteristics of carbon fibers provide a wide range of uses despite the cost factor [47].

Aramid fiber is particularly known for its high impact toughness and excellent energy absorption. Aramid fibers are commonly known as Kevlar, and this material is used in applications such as ballistic armor and protective clothing. Aramid fibers offer high tensile strength and excellent temperature resistance, making them particularly usable in harsh conditions. Furthermore, the high impact resistance of aramid fibers also makes them effective in structural applications. However, the cost of aramid fibers is often high and these materials can show a loss of performance in some chemical and moisture conditions. However, the superior protection and durability properties provided by aramid fibers make them a valuable material in a variety of applications [48]. Figure 5 shows images of (a) glass fiber fabric, (b) aramid fiber fabric and (c) carbon fiber fabric samples.

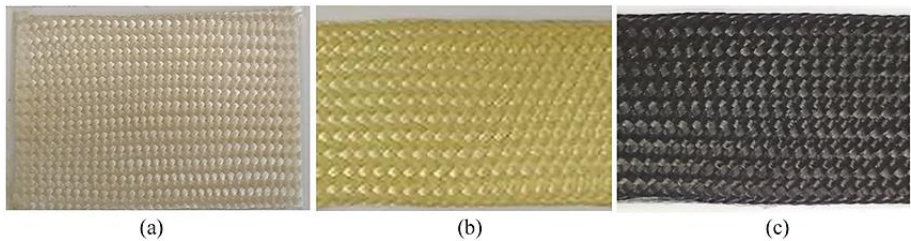


Figure 5. Fabric sample: (a) glass-fiber fabric, (b) aramid-fiber fabric, and (c) carbon-fiber fabric [49]

Other reinforcing materials include natural fibers such as basalt fibers, jute fibers and kenaf fibers. Basalt fibers offer high heat resistance and excellent chemical resistance properties and are used in high-performance applications [50]. Jute and kenaf fibers are advantageous in terms of environmental sustainability; these natural fibers are derived from biodegradable and renewable resources, making them environmentally friendly alternatives. Although natural fibers are generally low cost and lightweight, their mechanical properties are generally not as high as synthetic fibers [51].

In the selection of reinforcement materials, it is vital to balance between the performance characteristics of the material and the application requirements [52]. Common reinforcement materials, such as fiberglass, carbon fiber and aramid fiber, each stand out with their own advantages and limitations. Fiberglass is particularly noted for its cost effectiveness and good overall durability; it offers high tensile strength and good flexibility, making it ideal in the automotive and construction sectors. However, the mechanical properties of fiberglass are not as high as carbon fiber and aramid fiber and therefore may be limited in high-performance applications [53]. Carbon fibers stand out for their combination of high tensile strength and low weight; their tensile strength can be up to 1000 MPa, making them indispensable in applications such as aerospace and sports equipment. However, carbon fibers have high costs and performance limitations in some environmental conditions [54]. Aramid fibers offer high impact toughness and excellent energy absorption; these fibers, known under the brand name Kevlar, are used in armor and protective equipment. The high temperature resistance and impact absorption of aramid fibers make them effective in harsh conditions, but their cost is often high and they can experience performance degradation under some chemical environments [55].

Another important factor to consider in material selection is the application requirements and environmental conditions [56]. The environment in which composites will be used plays a decisive role in material selection; factors such as humidity, temperature, chemical interactions and mechanical loads directly affect the performance of reinforcing materials [57]. For example, marine and aerospace applications require high temperature and moisture resistance; therefore, high-performance carbon fiber or vinylester resins are often preferred in these areas [54]. On the other hand, for applications seeking low-cost and environmentally friendly solutions, options such as natural fibers, jute or kenaf can be considered. Furthermore, cost and production processes also play an important role in material selection; high-performance materials are generally more expensive and can affect production processes [58]. Consequently, the

selection of reinforcement materials requires careful consideration of performance characteristics as well as cost, environmental conditions and application requirements. This comprehensive approach ensures that the most suitable material is selected and composites perform optimally [59].

4. Vacuum Infusion Process and Procedures

The vacuum infusion process is an effective method for the production of high-performance composite materials and is carried out in several steps. First, a mold is prepared to create the shape and surface of the composite material. Then, the fiber reinforcement materials (carbon fiber, fiberglass, aramid fiber, etc.) are placed into the mold in an orderly manner. Then, the vacuum bag is closed over the mold and the vacuum system is connected. The vacuum pump removes all air and moisture from the system by drawing the air out of the bag, thus ensuring homogeneous penetration of the resin between the fibers. The resin is prepared to a certain viscosity and infused between the fibers under vacuum. Once the resin is completely dispersed between the fibers, the material remains under vacuum while waiting for a certain time for the resin to cure. Once the time is complete, the composite material is removed from the mold and the strength, durability and surface quality of the final product is checked. These steps ensure the production of high quality and robust composite materials [60].

The vacuum infusion process is a complex technique that guarantees high quality and durability in the production of composite materials, and each stage of this process requires careful planning and execution. The first stage of the process is mold preparation, which forms the basis for the entire production process. The mold surface is meticulously cleaned and, if necessary, coated with a release agent. The mold surface needs to be clean and smooth; any dirt, dust or surface irregularities can interfere with the proper dispersion of the resin, which can adversely affect the quality of the final composite material. The mold is usually made of high-quality and durable materials, as this material must be resistant to the effects of both the fiber reinforcements and the resin. The mold surface can be protected with a special coating or covered with a series of protective layers, which prevents the resin from sticking to the mold surface and ensures a smooth surface after the mold is removed [61].

The next step is to place the fiber reinforcement materials in the mold. At this stage, care is taken to ensure that the fibers are properly covered and placed in the desired ratio. Then, the vacuum bag is closed over the mold and the vacuum system is connected. The vacuum pump draws the air out of the bag, eliminating all air and moisture from the system, thus ensuring homogeneous penetration of

the resin between the fibers [62]. These materials usually consist of materials such as carbon fiber, fiberglass or aramid fiber, which offer high strength and low weight properties [63]. The most important factor to be considered during the placement of fibers is to place the fibers properly and according to the desired directions [62]. The regular placement of fiberglass and carbon fibers optimizes the mechanical properties of the material and improves the overall performance of the composite [64]. After placement of the fibers, the vacuum bag is covered and the vacuum system is activated to completely remove air and moisture from the mold. The vacuum draws air and moisture from the mold, allowing the resin to fully penetrate between the fibers. The proper application of vacuum eliminates air pockets and voids in the internal structure of the composite material, which improves the durability and mechanical performance of the final product [65].

In the resin infusion stage, the resin is slowly drawn between the fibers by the pressure created by the vacuum. The resin is prepared to have a certain viscosity and infused between the fibers under vacuum. After the resin is completely dispersed between the fibers, the material remains under vacuum while waiting for a certain period of time for the resin to cure. Resin selection is a critical factor affecting the success of the infusion process; the viscosity of the resin determines the infusion rate and quality. If the resin is too dense, it may not be able to penetrate well enough between the fibers, resulting in a weak composite material. On the other hand, if the resin is too fluid, this can lead to uncontrolled spreading of the resin and potentially a weak structure. During resin infusion, it must be ensured that the system is under vacuum and that all connection points are sealed. The pressure of the vacuum system should be continuously monitored and all connections in the vacuum bag should be checked regularly [66]. After the infusion is complete, a certain amount of time should be allowed for the resin to cure completely. The curing process allows the resin to fully cure and maximize the mechanical properties of the composite material. This stage is critical for the composite material to gain high strength, durability and performance properties [67].

The final stage of the vacuum infusion process is the demolding of the composite material, which must ensure that the resin has fully cured and all air pockets have been removed. The material must be carefully removed from the mold and checked for any defects or deformations. At this stage, the mechanical and physical properties of the composite material are evaluated and any necessary improvements are made. The meticulous execution of each stage throughout the vacuum infusion process directly affects the quality and performance of the final product. The care and attention provided at each stage of the process ensures the

production of high quality and durable composite materials, which offer reliability and high performance in industrial applications [68]. Figure 6 shows a schematic representation of the vacuum infusion process.

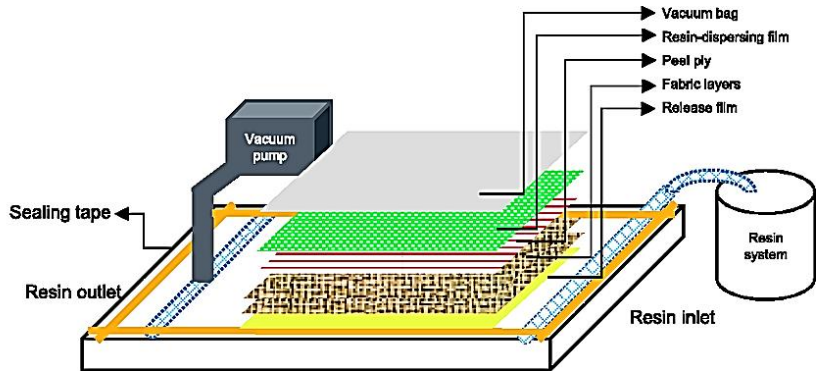


Figure 6. Schematic representation of vacuum infusion process [69]

4.1. Possible Errors and Solution Suggestions

Although the vacuum infusion process has emerged as a successful method for producing high quality composite materials, problems that may be encountered at various stages can affect the efficiency of the process and the quality of the final product. Errors and their solutions should be carefully addressed at each stage of the process [70]. In the first stage, during mold preparation and fiber placement, a common error is dirt, dust or oil residues on the mold surface [71]. Such contaminants can prevent the resin from properly passing through the mold, which can lead to the formation of air bubbles and weak spots. As a solution, the mold surface needs to be thoroughly cleaned, properly sanded and protected with a suitable coating material where necessary. It is also critical that the fibers are properly positioned in the mold; ensuring that the fibers do not overlap and are positioned in the correct orientation optimizes the mechanical properties of the composite. If the fibers are placed incorrectly, this can adversely affect the strength and performance of the composite. Therefore, fiber placement should be meticulous and regular checks should be performed [72].

Another important problem that can be encountered in the vacuum infusion process is related to the sealing of the vacuum system [66]. Any leakage in the vacuum bag can cause air bubbles and moisture to enter the mold, which prevents the resin from penetrating properly between the fibers. This can lead to the formation of weak zones and voids in the composite material. As a solution, all joints and seals of the vacuum system need to be regularly checked and rigorously

tested for leaks. Furthermore, the pressure of the vacuum system should be continuously monitored to ensure that the vacuum is effectively maintained [73]. Another problem encountered in resin infusion is the viscosity of the resin. If the resin is too viscous or too dense, it can affect the infusion process; too viscous resin can spread uncontrollably between the fibers, while too dense resin may not provide sufficient saturation. The resin consistency needs to be adjusted to suit the application requirements and the infusion process optimized accordingly. To ensure that the resin has the correct consistency, it is recommended to carefully prepare and pre-test the resin mixture [74].

Finally, defects in the curing process are also important. The complete curing of the resin is critical to ensure the mechanical properties and durability of the composite material. Insufficient curing time can cause the resin not to cure sufficiently, which can lead to a weak material. To avoid this, the time required for the resin to fully cure should be observed and it should be ensured that this time is determined in accordance with the properties of the material. In addition, the curing conditions (such as temperature and humidity) must be properly controlled and stabilized. Once the curing process is complete, the composite material must be carefully inspected before it is removed from the mold, making sure that the resin is fully cured and that all air pockets have been removed. Rigorous evaluation and testing at this stage improves the quality of the final product and ensures the successful completion of the process [75].

5. Effects of Vacuum Infusion on Performance and Quality

Vacuum infusion is a technique that significantly improves performance and quality in the production of composite materials. To understand the effects of this process on performance, it is necessary to take a detailed look at how the material quality, the manufacturing process and the physical properties of the final product are affected [76]. First, the vacuum infusion method minimizes air bubbles and other defects in the internal structure of composite materials. The infusion process under vacuum allows the resin to perfectly penetrate into all pores and voids of the fibers, which increases the density and homogeneity of the material. This homogeneity leads to an improvement of the mechanical properties of the final composite material, i.e. the composite material gains higher tensile and flexural strength, thus increasing its structural durability. Furthermore, composites with the vacuum infusion process usually contain fewer pores, which increases the overall strength and longevity of the material [77].

The effects on quality are due to the ability of the vacuum infusion method to ensure a proper combination of resin and fibers. The process ensures that the resin

is accurately dispersed and the fibers are fully coated, thus minimizing weak spots and heterogeneous regions within the material. As a result, the composites produced have a higher surface quality, which is a great advantage, especially in applications where aesthetic and functional requirements are critical [78]. In addition, composites obtained by the vacuum infusion process generally show lower porosity and better chemical resistance properties, because the vacuum environment has the capacity to attract air bubbles and other impurities into the resin. These properties improve the performance and durability of the material, especially in applications exposed to harsh environmental conditions [79].

6. Application Areas in Mechanical Engineering

The vacuum infusion method offers a wide range of uses in various application areas in mechanical engineering, and innovations in this field have significantly transformed materials science and engineering design [80]. This method plays a critical role, especially in industrial applications and advanced engineering designs, thanks to its ability to produce high-performance and lightweight composite materials [81]. Firstly, in the automotive industry, vacuum infusion is used to lighten and increase the durability of vehicle parts. This method is widely preferred in the production of lightweight composite panels, body parts, and structural components that increase the fuel efficiency of vehicles, improve their performance, and enhance safety [82]. For example, high-performance automobiles such as sports vehicles and electric vehicles improve their aerodynamic properties and overall durability by using carbon fiber or aramid fiber reinforced composite materials [83].

In the aerospace industry, the importance of vacuum infusion becomes even more evident. Here, lightweight but high-strength composites are integrated into aircraft wings, tail structures and other critical components [84]. Vacuum infusion allows composites used in the aerospace industry to produce long-lasting components that improve aerodynamic performance while reducing fuel consumption [85]. In particular, carbon fiber and ceramic matrix composites are used in rocket engines and other spacecraft due to their high temperature and corrosion resistance. These materials help engineers meet both performance and safety standards [86].

In the yacht and marine industries, vacuum infusion is used to produce composite materials that make marine vessels both lightweight and durable. This process provides significant advantages, especially in underwater structures and components under high stress [7]. For example, parts such as boat hulls and sails are designed to be resistant to the harsh conditions in the marine environment

[87]. In these applications, vacuum infusion improves performance and safety by increasing both the light weight and durability of marine products [88].

Vacuum infusion plays an important role in the energy sector, especially in wind turbine blades. Wind turbine blades must be designed to withstand large dimensions and continuous wind loads. Vacuum infusion provides high-strength and lightweight materials for manufacturing such large composite structures, improving turbine performance and lifetime. In addition, this method is also used in the production of composites used in solar energy panels, increasing the durability and efficiency of the panels [89].

7. Conclusions

The vacuum infusion method has introduced innovations in material production and composite processing in the field of mechanical engineering. The industrial applications and benefits of this method can be detailed as follows:

- Vacuum infusion plays a critical role in the production of composite materials with desirable properties such as high strength and low weight. This method can produce lightweight and durable materials used in the automotive, aerospace, marine and energy sectors. The uniform and homogeneous resinization of composites significantly improves material performance and durability.
- Compared to traditional methods, the vacuum infusion process offers a more cost-effective and efficient production method. High production speeds, the ability to produce large and complex parts in a single run, and low labor costs make vacuum infusion attractive. Especially in large-scale projects, the cost advantages of this method become apparent.
- Vacuum infusion offers a production process compatible with environmentally friendly resins and low waste production methods. The use of recycled materials and resins with low VOC (volatile organic compounds) minimizes environmental impact and promotes sustainable production practices. In this way, vacuum infusion complies with environmental protection standards and contributes to green manufacturing goals.
- In vacuum infusion, process control ensures precision at every stage, from material fluidity to resin introduction. Automated vacuum systems and intelligent control mechanisms minimize variations in

the production process and improve product quality. This process reduces error rates and ensures high quality end products.

- The vacuum infusion method enables the integration of advanced material technologies such as nanotechnology, smart materials and high-performance polymers. These innovations expand the application areas of vacuum infusion and improve the performance of materials. For example, composites produced using nanomaterials provide additional advantages such as higher strength and reduced weight.
- Vacuum infusion is particularly effective in the production of large and complex structures. This process ensures homogeneous resin distribution in large parts, improving material properties and enhancing structural integrity. Advanced vacuum systems and mold designs minimize the challenges of this type of production.
- The fact that vacuum infusion is a constantly evolving technology increases the need for research and development activities. Studies in areas such as new resin formulations, improved vacuum systems and innovative mold designs further increase the potential of this method and expand its industrial application areas.

The vacuum infusion method plays an important role in industrial processes with its various advantages in material production in mechanical engineering. The high performance materials, low costs, environmentally friendly production characteristics and advanced automation capabilities have positioned this method as a critical tool in industrial design and manufacturing processes. Future research and technological developments will further expand the effectiveness and application areas of vacuum infusion and provide innovative solutions in engineering applications.

References

- [1] Goren, A., & Atas, C. (2008). Manufacturing of polymer matrix composites using vacuum assisted resin infusion molding. *Archives of Materials Science and Engineering*, 34(2), 117-120. Retrieved from <http://www.archivesmse.org/>
- [2] Ouezgan, A., Adima, S., Maziri, A., Mallil, E., & Echaabi, J. (2019). An innovative methodology to design LCM mold for aeronautic and automotive industries. In A. Ouezgan, S. Adima, A. Maziri, E. Mallil, & J. Echaabi (Eds.), *New opportunities for innovation breakthroughs for developing countries and emerging economies* (Vol. 572, pp. 472-485). Berlin, Heidelberg: Springer. <https://doi.org/10.1007/978-3-030-27068-4>
- [3] Hindersmann, A. (2019). Confusion about infusion: An overview of infusion processes. *Composites Part A: Applied Science and Manufacturing*, 126, 105583. <https://doi.org/10.1016/j.compositesa.2019.105583>
- [4] Shah, D. U., Schubel, P. J., Clifford, M. J., & Licence, P. (2014). Mechanical property characterization of aligned plant yarn reinforced thermoset matrix composites manufactured via vacuum infusion. *Polymer-Plastics Technology and Engineering*, 53(3), 239–253. <https://doi.org/10.1080/03602559.2013.843710>
- [5] Dolz, M., Martinez, X., Sá, D., Silva, J., & Jurado, A. (2023). Composite materials, technologies and manufacturing: Current scenario of European Union shipyards. *Ships and Offshore Structures*. Advance online publication. <https://doi.org/10.1080/17445302.2023.2229160>
- [6] Silva, D., Rocha, R., Ribeiro, F., & Monteiro, H. (2024). Environmental impact of an innovative aeronautic carbon composite manufactured via heated vacuum-assisted resin transfer molding. *Sustainability*, 16(8), 3253. <https://doi.org/10.3390/su16083253>
- [7] Cucinotta, F., Guglielmino, E., & Sfravara, F. (2017). Life cycle assessment in the yacht industry: A case study of comparison between hand lay-up and vacuum infusion. *Journal of Cleaner Production*, 142(4), 3822–3833. <https://doi.org/10.1016/j.jclepro.2016.10.080>
- [8] Baley, C., Davies, P., Troalen, W., Chamley, A., Dinham-Price, I., Marchandise, A., & Keryvin, V. (2024). Sustainable polymer composite marine structures: Developments and challenges. *Progress in Materials Science*, 145, 101307. <https://doi.org/10.1016/j.pmatsci.2024.101307>
- [9] Xia, C., Wu, Y., Qiu, Y., Cai, L., Smith, L. M., Tu, M., Zhao, W., Shao, D., Mei, C., Nie, X., & Shi, S. Q. (2019). Processing high-performance woody materials by means of vacuum-assisted resin infusion technology. *Journal of Cleaner Production*, 241, 118340. <https://doi.org/10.1016/j.jclepro.2019.118340>
- [10] Shahid, A. T., Silvestre, J. D., Hofmann, M., Garrido, M., & Correia, J. R. (2024). Life cycle assessment of an innovative bio-based unsaturated polyester resin

- and its use in glass fibre reinforced bio-composites produced by vacuum infusion. *Journal of Cleaner Production*, 441, 140906. <https://doi.org/10.1016/j.jclepro.2024.140906>
- [11] Gajjar, T., Shah, D. B., Joshi, S. J., & Patel, K. M. (2020). Analysis of process parameters for composites manufacturing using vacuum infusion process. *Materials Today: Proceedings*, 21(2), 1244–1249. <https://doi.org/10.1016/j.matpr.2020.01.112>
- [12] Salman, S. D., Sharba, M. J., Leman, Z., Sultan, M. T. H., Ishak, M. R., & Cardona, F. (2015). Physical, mechanical, and morphological properties of woven kenaf/polymer composites produced using a vacuum infusion technique. *International Journal of Polymer Science*, 2015, 894565. <https://doi.org/10.1155/2015/894565>
- [13] Wang, T., Huang, K., Guo, L., Zheng, T., & Zeng, F. (2023). An automated vacuum infusion process for manufacturing high-quality fiber-reinforced composites. *Composite Structures*, 309, 116717. <https://doi.org/10.1016/j.compstruct.2023.116717>
- [14] Masuelli, M. A. (2013). Introduction of fibre-reinforced polymers – Polymers and composites: Concepts, properties and processes. In M. A. Masuelli (Ed.), *Fiber reinforced polymers - The technology applied for concrete repair* [Internet]. In-techOpen. <https://doi.org/10.5772/54629>
- [15] Kedari, V. R., Farah, B. I., & Hsiao, K. T. (2011). Effects of vacuum pressure, inlet pressure, and mold temperature on the void content and volume fraction of polyester/e-glass fiber composites manufactured with the VARTM process. *Journal of Composite Materials*, 45(26), 2977–2989. <https://doi.org/10.1177/0021998311415442>
- [16] Wang, Y., Liu, W., Qiu, Y., & Wei, Y. (2018). A one-component, fast-cure, and economical epoxy resin system suitable for liquid molding of automotive composite parts. *Materials*, 11(5), 685. <https://doi.org/10.3390/ma11050685>
- [17] Maharshi, K., & Patel, S. (2022). Experimental statistical analysis of tensile and shear properties of jute fabric epoxy composites. *Journal of Natural Fibers*, 19(14), 1–13. <https://doi.org/10.1080/15440478.2021.1966572>
- [18] Modi, D., Correia, N., Johnson, M., Long, A., Rudd, C., & Robitaille, F. (2007). Active control of the vacuum infusion process. *Composites Part A: Applied Science and Manufacturing*, 38(5), 1271–1287. <https://doi.org/10.1016/j.compositesa.2006.11.012>
- [19] Ekşi, S., & Genel, K. (2017). Comparison of mechanical properties of unidirectional and woven carbon, glass, and aramid fiber reinforced epoxy composites. *Acta Physica Polonica A*, 132(3-II), 879–884. <https://doi.org/10.12693/APhys-PolA.132.879>

- [20] Nodehi, M. (2022). Epoxy, polyester, and vinyl ester based polymer concrete: A review. *Innovative Infrastructure Solutions*, 7, 64. Published online October 17, 2021. <https://doi.org/10.1007/s40940-021-00112-8>
- [21] Schwartz, M. (2010). Resin transfer molding and associated closed molding and infusion processes. In *Innovations in materials manufacturing, fabrication, and environmental safety* (1st ed., pp. 1–28). CRC Press. <https://doi.org/10.1201/9780429139499>
- [22] Hammami, A., & Gebart, B. R. (2004). Analysis of the vacuum infusion molding process. *Polymer Composites*, 25(1), 28–40. <https://doi.org/10.1002/pc.10162>
- [23] Swift, K. G., & Booker, J. D. (2003). *Process selection: From design to manufacture*. Oxford: Elsevier.
- [24] Bader, M. G. (2001). Polymer composites in 2000: Structure, performance, cost, and compromise. *Journal of Microscopy*, 201(2), 110–121. <https://doi.org/10.1046/j.1365-2818.2001.00761.x>
- [25] Zhang, J., Lin, G., Vaidya, U., & Wang, H. (2023). Past, present, and future perspective of global carbon fibre composite developments and applications. *Composites Part B: Engineering*, 250, 110463. <https://doi.org/10.1016/j.compositesb.2022.110463>
- [26] Gore, P. M., & Kandasubramanian, B. (2018). Functionalized aramid fibers and composites for protective applications: A review. *Industrial & Engineering Chemistry Research*, 57(49), 16537–16563. <https://doi.org/10.1021/acs.iecr.8b04903>
- [27] Wallenberger, F. T., & Bingham, P. A. (2010). Fiberglass and glass technology. In *Energy-friendly compositions and applications*.
- [28] Ahmad, F., Choi, H. S., & Park, M. K. (2015). A review: Natural fiber composites selection in view of mechanical, lightweight, and economic properties. *Macromolecular Materials and Engineering*, 300(1), 10–24. <https://doi.org/10.1002/mame.201400089>
- [29] Verma, K. K., Dinesh, B. L., Singh, K., Gaddikeri, K. M., Srinivasa, V., Kumar, R., & Sundaram, R. (2013). Development of vacuum enhanced resin infusion technology (VERITy) process for manufacturing of primary aircraft structures. *Indian Institute of Science Journal*, 93(4), 429–448.
- [30] Mi, X., Liang, N., Xu, H., Wu, J., Jiang, Y., Nie, B., & Zhang, D. (2022). Toughness and its mechanisms in epoxy resins. *Progress in Materials Science*, 130, 100977. <https://doi.org/10.1016/j.pmatsci.2022.100977>
- [31] Bello, S. A., Agunsoye, J. O., Hassan, S. B., Zebase Kana, M. G., & Raheem, I. A. (2015). Epoxy resin based composites, mechanical and tribological properties: A review. *Tribology in Industry*, 37(4), 500–524. Available from: www.tribology.fink.rs

- [32] Malik, M., Choudhary, V., & Varma, I. K. (2000). Current status of unsaturated polyester resins. *Journal of Macromolecular Science, Part C: Polymer Reviews*, 40(2–3), 139–165. <https://doi.org/10.1081/MC-100100582>
- [33] Anderson, T. F., & Messick, V. B. (1980). Vinyl ester resins. In *Developments in Reinforced Plastics—1: Resin Matrix Aspects (The Development Series, POLS, Vol. 30, pp. 29–58)*.
- [34] Cho, K., Rajan, G., Farrar, P., Prentice, L., & Prusty, B. G. (2022). Dental resin composites: A review on materials to product realizations. *Composites Part B: Engineering*, 230, 109495. <https://doi.org/10.1016/j.compositesb.2021.109495>
- [35] Kim, S.-Y., Shim, C.-S., Sturtevant, C., Kim, D., & Song, H.-C. (2014). Mechanical properties and production quality of hand-layup and vacuum infusion processed hybrid composite materials for GFRP marine structures. *International Journal of Naval Architecture and Ocean Engineering*, 6(3), 723–736. <https://doi.org/10.2478/IJNAOE-2013-0208>
- [36] Jaswal, S., & Gaur, B. (2014). New trends in vinyl ester resins. *Reviews in Chemical Engineering*, 30(6), 1–14. <https://doi.org/10.1515/revce-2014-0012>
- [37] Parameswaranpillai, J., Pulikkalparambil, H., Rangappa, S. M., & Siengchin, S. (Eds.). (2021). *Epoxy Composites*. Hoboken, NJ: Wiley. <https://doi.org/10.1002/9783527824083>
- [38] Tao, L., Sun, Z., Min, W., Ou, H., Qi, L., & Yu, M. (2020). Improving the toughness of thermosetting epoxy resins via blending triblock copolymers. *RSC Advances*, 10(3), 1603–1612. <https://doi.org/10.1039/c9ra09183a>
- [39] Haider, M., Hubert, P., & Lessard, L. (2007). Cure shrinkage characterization and modeling of a polyester resin containing low profile additives. *Composites Part A: Applied Science and Manufacturing*, 38(3), 994–1009. <https://doi.org/10.1016/j.compositesa.2006.06.020>
- [40] Yang, Y. S., & Lee, L. J. (1988). Microstructure formation in the cure of unsaturated polyester resins. *Polymers*, 29, 1793–1800.
- [41] Kandelbauer, A., Tondi, G., Zaske, O. C., & Goodman, S. H. (2022). Unsaturated polyesters and vinyl esters. In *Handbook of Thermoset Plastics* (4th ed., pp. 97–158). *Plastics Design Library*. <https://doi.org/10.1016/B978-0-12-821632-3.00015-4>
- [42] Alia, C., Jofre-Reche, J. A., Suarez, J. C., Arenas, J. M., & Martin-Martinez, J. M. (2018). Polymer degradation and stability. *Polymer Degradation and Stability*, 153, 88–99.
- [43] Shevtsov, S., Zhilyaev, I., Chang, S.-H., Wu, J.-K., & Snezhina, N. (2022). Multi-criteria decision approach to design a vacuum infusion process layout providing the polymeric composite part quality. *Polymers*, 14(2), 313. <https://doi.org/10.3390/polym14020313>

- [44] Khan, A., & Saxena, K. K. (2022). A review on enhancement of mechanical properties of fiber reinforcement polymer composite under different loading rates. *Materials Today: Proceedings*, 56(4), 2316–2322. <https://doi.org/10.1016/j.matpr.2021.12.009>
- [45] Prashanth, S., Subbaya, K. M., Nithin, K., & Sachhidananda, S. (2017). Fiber reinforced composites - A review. *Journal of Materials Science and Engineering*, 6(3), 1000341. <https://doi.org/10.4172/2169-0022.1000341>
- [46] Sathishkumar, T. P., Satheeshkumar, S., & Naveen, J. (2014). Glass fiber-reinforced polymer composites – A review. *Journal of Reinforced Plastics and Composites*, 33(13), 1211–1235. <https://doi.org/10.1177/0731684414530790>
- [47] Manocha, L. M. (2003). High performance carbon-carbon composites. *Sadhana*, 28, 349–358.
- [48] Moure, M. M., Rubio, I., Aranda-Ruiz, J., Loya, J. A., & Rodríguez-Millán, M. (2018). Analysis of impact energy absorption by lightweight aramid structures. *Composite Structures*, 203, 917–926. <https://doi.org/10.1016/j.compstruct.2018.06.092>
- [49] Pei, L., Xiao, Z., Lei, G., Wu, J., Zhang, F., & Sun, Y. (2019). Surface parameters measurement for braided composite preform based on gray projection. *Journal of Engineered Fibers and Fabrics*, 14(3), 155892501988762. <https://doi.org/10.1177/1558925019887621>
- [50] Al-Ghazali, N. A., Abdul Aziz, F. N. A., Abdan, K., Mohd Nasir, N. A., & Norizan, M. N. (2022). Kenaf fibre reinforced cementitious composites. *Fibers*, 10(1), 3. <https://doi.org/10.3390/fib10010003>
- [51] Kumar, P. S., & Allamraju, K. V. (2019). A review of natural fiber composites [jute, sisal, kenaf]. *Materials Today: Proceedings*, 18(7), 2556–2562. <https://doi.org/10.1016/j.matpr.2019.07.113>
- [52] Ashby, M. F., & Jones, D. R. H. (2012). *Engineering materials 1: An introduction to properties, applications and design* (1st ed.). Elsevier.
- [53] Maiti, S., Islam, M. R., Uddin, M. A., Afroj, S., Eichhorn, S. J., & Karim, N. (2022). Sustainable fiber-reinforced composites: A review. *Advanced Sustainable Systems*, 6(11), 2200258. <https://doi.org/10.1002/adsu.202200258>
- [54] Rebouillat, S., Peng, J. C., Donnet, J. B., & Ryu, S. K. (1998). Carbon fiber applications. In *Carbon fibers* (pp. 463–541).
- [55] Tanner, D., Dhingra, A. K., & Pigliacampi, J. J. (1986). Aramid fiber composites for general engineering. *JOM*, 38, 21–25.
- [56] Holloway, L. (1998). Materials selection for optimal environmental impact in mechanical design. *Materials & Design*, 19(4), 133–143. [https://doi.org/10.1016/S0261-3069\(98\)00031-4](https://doi.org/10.1016/S0261-3069(98)00031-4)

- [57] Sethi, S., & Ray, B. C. (2015). Environmental effects on fibre reinforced polymeric composites: Evolving reasons and remarks on interfacial strength and stability. *Advances in Colloid and Interface Science*, 217, 43–67. <https://doi.org/10.1016/j.cis.2014.12.005>
- [58] Elfaleh, I., Abbassi, F., Habibi, M., Ahmad, F., Guedri, M., Nasri, M., & Garnier, C. (2023). A comprehensive review of natural fibers and their composites: An eco-friendly alternative to conventional materials. *Results in Engineering*, 19, 101271. <https://doi.org/10.1016/j.rineng.2023.101271>
- [59] Zaman, A., Gutub, S. A., & Wafa, M. A. (2013). A review on FRP composites applications and durability concerns in the construction sector. *Journal of Reinforced Plastics and Composites*, 32(24). <https://doi.org/10.1177/0731684413492868>
- [60] Fang, X., Bi, C., Hong, Y., Cho, K. H., Park, M. S., Wang, Y., et al. (2016). Rapid vacuum infusion and curing of epoxy composites with a rubber-cushioned mold design. *Composites Part A: Applied Science and Manufacturing*, 83, 1030–1038. <https://doi.org/10.1080/03602559.2015.1132453>
- [61] Vogt, C. (2011). An experimental cost model for composite parts using vacuum assisted resin transfer moulding (VARTM). Stellenbosch: University of Stellenbosch. Available from: <http://hdl.handle.net/10019.1/6579>
- [62] Kennedy, M. A. D. (2018). Development of cost effective composites using vacuum processing technique [dissertation]. Athens (OH): Ohio University. Available from: http://rave.ohiolink.edu/etdc/view?acc_num=ohiou1523633403784733
- [63] Al-Furjan, M. S. H., Shan, L., Shen, X., Zarei, M. S., Hajmohammad, M. H., & Kolahchi, R. (2022). A review on fabrication techniques and tensile properties of glass, carbon, and Kevlar fiber reinforced polymer composites. *Journal of Materials Research and Technology*, 19, 2930–2959. <https://doi.org/10.1016/j.jmrt.2022.06.008>
- [64] Burley, A., & Aitharaju, V. (2023). Enhanced ductility in in-layer glass-carbon fiber/epoxy hybrid composites produced via tailored fiber placement. *Composites Part A: Applied Science and Manufacturing*, 168, 107488. <https://doi.org/10.1016/j.compositesa.2023.107488>
- [65] Ricciardi, M. R., Antonucci, V., Langella, A., et al. (2013). A new cost-saving vacuum infusion process for fiber-reinforced composites: Pulsed infusion. *Journal of Composite Materials*, 48(11). <https://doi.org/10.1177/0021998313485998>
- [66] Sevostianov, I. B., Verijenko, V. E., von Klemperer, C. J., & Chevallereau, B. (1999). Mathematical model of stress formation during vacuum resin infusion process. *Composites Part B: Engineering*, 30(5), 513–521. [https://doi.org/10.1016/S1359-8368\(99\)00012-8](https://doi.org/10.1016/S1359-8368(99)00012-8)
- [67] Afendi, M., Banks, W. M., & Kirkwood, D. (2005). Bubble free resin for infusion process. *Composites Part A: Applied Science and Manufacturing*, 36(6), 739–746. <https://doi.org/10.1016/j.compositesa.2004.10.030>

- [68] Tarazona Romero, M. A. (2014). State of the art of degasification techniques in the shaping processes of composite materials prepared by resin infusion [thesis]. Barcelona: Universitat Politècnica de Catalunya. Available from: <http://hdl.handle.net/2117/86346>
- [69] Okur, N., & Yaradanakul, M. C. (2022). Development of hybrid layered structures based on natural fabric reinforced composites and warp knitted spacer fabric for acoustic applications. *Journal of Industrial Textiles*, 51(2_suppl), 152808372199467. <https://doi.org/10.1177/1528083721994677>
- [70] Khan, L. A., Mahmood, A. H., Hassan, B., Sharif, T., Khushnod, S., & Khan, Z. M. (2014). Cost-effective manufacturing process for the development of automotive from energy efficient composite materials and sandwich structures. *Polymer Composites*, 35(1), 97–104. <https://doi.org/10.1002/pc.22638>
- [71] Xiao, H., Sultan, M. T. H., Shahar, F. S., Nayak, S. Y., Yidris, N., & Md Shah, A. U. (2024). Development of hybrid aluminum/carbon fiber/pineapple leaf fiber laminates using vacuum-assisted resin transfer molding (VARTM) for automotive applications. *Applied Composite Materials*, 31, 561–581. <https://doi.org/10.1007/s10443-023-10183-z>
- [72] Ribeiro, A. C. (2023). Surface coating of steel molds and their components for plastic injection molding [dissertation]. Porto: Faculdade de Engenharia da Universidade do Porto. Supervisor: Parente, M.
- [73] Cender, T. A. (2017). Process analysis of manufacturing composite structures with vacuum-bag-only prepreps: Quantifying partial resin impregnation and its effect on gas evacuation [dissertation]. Newark (DE): University of Delaware. Available from: ProQuest Dissertations & Theses. Number: 10602895.
- [74] George, A. (2011). Optimization of resin infusion processing for composite materials: Simulation and characterization strategies [thesis]. Stuttgart: University of Stuttgart. [cited 2024 Aug 8]. Available from: Institute of Aircraft Design, University of Stuttgart.
- [75] Krämer, N., Lohbauer, U., García-Godoy, F., & Frankenberger, R. (2008). Light curing of resin-based composites in the LED era. *American Journal of Dentistry*, 21, 135–142.
- [76] Menta, V. G. K., Vuppalapati, R. R., Schuman, T., et al. (2014). Manufacturing of transparent composites using vacuum infusion process. *Polymers and Polymer Composites*, 22(9), 1–12. <https://doi.org/10.1177/096739111402200912>
- [77] Meier, R., Kahraman, I., Seyhan, A. T., Zaremba, S., & Drechsler, K. (2016). Evaluating vibration assisted vacuum infusion processing of hexagonal boron nitride sheet modified carbon fabric/epoxy composites in terms of interlaminar shear strength and void content. *Composites Science and Technology*, 128, 94–103. <https://doi.org/10.1016/j.compscitech.2016.03.022>
- [78] Liu, Y.-N., Yuan, C.-X., Liu, C.-X., Pan, J., & Dong, Q.-H. (2019). Study on the resin infusion process based on automated fiber placement fabricated dry fiber

- preform. *Scientific Reports*, 9, 7440. <https://doi.org/10.1038/s41598-019-43783-0>
- [79] Dilascio Vial, E., da Silva, R. J., dos Santos, J. C., da Silva, L. J., del Pino, G. G., Christoforo, A. L., Panzera, T. H., & Scarpa, F. (2023). Glass and aramid fibre-reinforced bio-based polymer composites manufactured by vacuum infusion: A statistical approach to their physical and mechanical properties. *Applied Composite Materials*, 30, 1627–1644.
- [80] Chawla, K. K. (2012). *Composite materials: Science and engineering* (2nd ed.). Berlin: Springer Science & Business Media.
- [81] Yi, X.-S., Du, S., & Zhang, L. (Eds.). (2018). *Composite materials engineering, volume 1: Fundamentals of composite materials*. Beijing: Chemical Industry Press.
- [82] Khan, L. A., & Mehmood, A. H. (2016). Cost-effective composites manufacturing processes for automotive applications. In L. Cernuschi (Ed.), *Lightweight composite structures in transport: Design, manufacturing, analysis and performance* (pp. 93–119). Amsterdam: Elsevier. <https://doi.org/10.1016/B978-1-78242-325-6.00005-0>
- [83] Wazeer, A., Das, A., Abeykoon, C., Sinha, A., & Karmakar, A. (2023). Composites for electric vehicles and automotive sector: A review. *Green Energy and International Transport*, 2(1), 100043. <https://doi.org/10.1016/j.geits.2022.100043>
- [84] Grimsley, B. W. (2005). *Characterization of the vacuum assisted resin transfer molding process for fabrication of aerospace composites* [thesis]. Blacksburg (VA): Virginia Tech. Available from: <http://hdl.handle.net/10919/36062>
- [85] Mrazova, M. (2013). Advanced composite materials of the future in aerospace industry. *INCAS Bulletin*, 5(3), 139–150. <https://doi.org/10.13111/2066-8201.2013.5.3.14>
- [86] Dhanasekar, S., Ganesan, A. T., Rani, T. L., Vinjamuri, V. K., Rao, M. N., Shankar, E., Dharamvir, & Kumar, P. S., Golie, W. M. (2022). A comprehensive study of ceramic matrix composites for space applications. *Advances in Materials Science and Engineering*, 2022, 6160591. <https://doi.org/10.1155/2022/6160591>
- [87] Rubino, F., Nisticò, A., Tucci, F., & Carlone, P. (2020). Marine application of fiber reinforced composites: A review. *Journal of Marine Science and Engineering*, 8(1), 26. <https://doi.org/10.3390/jmse8010026>
- [88] Barsotti, B., Gaiotti, M., & Rizzo, C. M. (2020). Recent industrial developments of marine composites: Limit states and design approaches on strength. *Journal of Marine Science and Application*, 19, 553–566.
- [89] Schubel, P. J. (2010). Technical cost modelling for a generic 45-m wind turbine blade produced by vacuum infusion (VI). *Renewable Energy*, 35(1), 183–189. <https://doi.org/10.1016/j.renene.2009.02.030>



CHAPTER 35

Negative Effects of Salt Stress On Plants

Gözde Hafize Yıldırım¹

¹ Research Assistant Dr., Recep Tayyip Erdoğan University, Faculty of Agriculture, Department of Field Crops, Rize/Turkey, 0000-0002-0557-6442

INTRODUCTION

The salinity problem observed in agricultural lands is one of the most significant environmental issues threatening agricultural production worldwide. Salinity, exacerbated by uncontrolled irrigation and poor soil management practices, drastically reduces the productivity of agricultural areas. Increasing incidents of floods and droughts globally (Hirabayashi et al., 2013), rising sea levels in coastal regions (Carter et al., 2006; Martin et al., 2011), and the widespread presence of sodium-rich soils (Ghassemi et al., 1995) contribute to combined flooding and salinity stress on plants (Bennett et al., 2009). Salt stress is recognized as one of the most critical abiotic factors affecting agricultural production, with approximately 50% of irrigated lands worldwide confronting this issue. This leads to the accumulation of toxic sodium and chloride ions in plant tissues (Zhang & Shi, 2013; Maathuis et al., 2014; Estaji et al., 2018).

The physiological and biochemical effects of salt stress on plants hinder growth and development, resulting in reduced yield and quality. High salt concentrations disrupt metabolic processes by causing osmotic stress, ion toxicity, mineral imbalances, and oxidative stress in plants. This condition limits water uptake capacity, increases energy consumption, and imposes significant pressure on agricultural sustainability. Soil salinity adversely affects plant membrane integrity, pigment content, osmotic regulation, water retention capacity, and photosynthetic activity, thereby impairing plant growth and productivity. In crops like peanuts, these effects create a complex scenario of abiotic stress (Benjamin & Nielsen, 2006; Bhatnagar-Mathur et al., 2009). Salinity increases ROS (reactive oxygen species) accumulation and suppresses antioxidant enzyme activities, negatively influencing metabolic and morphological processes in plants (Parvin et al., 2014). Polyamines help mitigate the effects of salinity stress by reducing Na^+ accumulation while enhancing antioxidant activities and photosynthetic capacity (Alcázar et al., 2020; Yılmaz and Çiftçi, 2021). Salinity is one of the most prevalent factors causing yield losses in agricultural lands, posing an even greater threat in arid and semi-arid regions. This review aims to examine the causes and effects of salinity issues, providing a general explanation of the adverse effects of salt stress on plant development.

SALINITY PROBLEM

Soil salinity typically arises from the accumulation of Na , Cl , SO_4 , and CO_3 ions. Factors such as excessive fertilizer use, the application of saline irrigation water, rapid evaporation, and poor drainage are the primary causes of this issue. Increased soil salinity prevents plants from adequately absorbing water or

exposes them to toxic effects from excessive ions in the water. This results in symptoms like yellowing and drying of plants, ultimately leading to yield and quality losses (Ağaoğlu et al., 2001; Şen, 2008; Doğan et al., 2024). Salt stress adversely affects plant growth and development throughout their life cycles. Plants attempt to adapt to such stress factors by developing defense mechanisms. However, salt stress disrupts ion balance, water uptake, and metabolic processes, causing significant damage. These damages result in substantial reductions in physiological activities and crop quality.

Plants are exposed to various abiotic stress factors that pose significant threats to agricultural systems. Among these, salt stress is considered a major problem, especially in arid and semi-arid regions, as it severely affects plant growth and productivity (Muneer & Jeong, 2015). Approximately 800 million hectares of land worldwide are affected by salinity, accounting for about 6% of the Earth's surface (Abbasi et al., 2015; Shah & Thivakaran, 2014). In Turkey, salinity and alkalinity issues affect approximately 1.5 million hectares, which constitutes 32.5% of irrigable lands (Uras & Sönmez, 2010; Ekmekçi et al., 2005). Salinity has been reported to reduce the availability of plant nutrients and adversely affect their uptake, transportation, and distribution, leading to nutritional disorders (Munns & Tester, 2008; Talaat et al., 2015). Salts increase the osmotic pressure of the environment, hindering water absorption or complicating the uptake of nutrients due to the excessive presence of ions such as Na^+ and Cl^- , thereby disrupting metabolism and harming plants (Hao et al., 2021; Zhao et al., 2021). The effects of salt stress typically manifest through two mechanisms: osmotic and ionic effects. The osmotic effect of salt reduces growth rates, alters leaf coloration, changes the root-to-shoot ratio, and affects maturation speed. Ionic effects damage meristematic tissues and leaves, negatively impacting plant development. Salt stress inhibits transpiration and the transportation of ions to roots, creating competition among ions, resulting in unbalanced nutrition and nutritional deficiencies (Nefissi Ouertani et al., 2021; Kınay & Erdem, 2021).

The need for effective practices to mitigate the negative impacts of salinity on plants is becoming increasingly urgent due to its detrimental effects on agriculture. Salinity, particularly in arid and semi-arid climates, stands out as a significant problem reducing soil fertility, thus threatening agricultural productivity in regions with limited rainfall.

Traditional agricultural and engineering solutions have increasingly fallen short in mitigating the impacts of salinity. Consequently, hopes are now focused on biological and genetic studies aimed at enhancing the physiological resistance of plants to salt stress (Munns & Gilliam, 2015). Despite extensive research

utilizing traditional breeding, genetics, and molecular biology methods to develop salt-tolerant plant varieties, limited success has been achieved in creating practical and widely beneficial solutions suitable for large-scale use (Kolomeichuk et al., 2020; Altunlu et al., 2024).

EFFECT OF SALT STRESS ON PLANT DEVELOPMENT

Any environmental or agricultural factor that restricts plant development is defined as "stress," and such stress negatively affects plant growth, leading to reductions in yield (Dağüstü, 2003; Üzal et al., 2020; Yaşar & Üzal, 2021). These stress factors, originating from natural environmental conditions or agricultural practices, are common challenges plants face throughout their life cycle. For instance, stress caused by soil composition can persist for days, whereas factors like air temperature usually have shorter effects (Taiz & Zaiger, 2010). Abiotic stress factors (e.g., low/high temperature, drought, salinity, heavy metals, radiation) and biotic stress factors (e.g., viruses, bacteria, fungal diseases, pests) prompt the development of defense mechanisms in plants. Plants strive to maintain growth and development under stress conditions. However, the response of plants under stress depends on their genotypic traits; some species and varieties are less affected, while others suffer severe damage or may even die. Plants' mechanisms to cope with stress depend on various factors, including genetic characteristics, growth stages, type of stress, and its severity (Yaşar & Üzal, 2021; Yaşar & Yaşar, 2022).

Salinity poses a significant problem for agricultural production in arid and semi-arid regions, negatively impacting plant development and productivity in both open-field and greenhouse cultivation. In coastal regions, finding sufficient quality water for irrigation in greenhouse cultivation is becoming increasingly difficult, necessitating the use of groundwater with high dissolved salt levels (Fernandez-Garcia et al., 2004). In the Mediterranean zone, seawater intrusion into groundwater has been identified as a major environmental problem, limiting the cultivation of certain plant species (Aksoy et al., 1998).

Saline irrigation water and soils create high osmotic pressure, restricting water absorption by plant roots and impeding the uptake of essential nutrients such as K^+ , Ca^{2+} , Mn^{2+} , and NO_3^- . Excessive salt accumulation disrupts cell membrane integrity, damaging vital organelles such as chlorophyll, which adversely affects plant growth and product quality (Hasegawa et al., 2000; Yıldız et al., 2010).

To support plant development in saline environments, various approaches have been proposed. For example, using resilient plant varieties as rootstocks, supplementing with nutrients like K and Ca, or applying chemicals such as

proline, salicylic acid, and melatonin can effectively enhance plant tolerance (Kaya et al., 2007; Yıldırım et al., 2008; Li et al., 2012). Additionally, symbiotic microorganisms like arbuscular mycorrhizal fungi (AMF) can form mutualistic relationships with plants, enhancing tolerance to salinity stress and improving water and nutrient uptake (Evelin et al., 2009; Hajbagheri & Enteshari, 2011). Studies on crops like tomatoes, eggplants, peppers, cucumbers, lettuce, and beans have reported that mycorrhizal applications mitigate the adverse effects of salinity and positively support plant development (Balliu et al., 2015; Sharma et al., 2017; Altunlu, 2020).

CONCLUSION

Salinity is one of the most critical environmental issues threatening agricultural production worldwide. In particular, soil and water salinity in arid and semi-arid regions creates severe negative effects on plant growth and productivity. Increasing salinity causes osmotic stress, ion toxicity, nutrient imbalances, and metabolic disorders in plants, leading to declines in yield and quality. This situation threatens not only agricultural production but also global food security. The biochemical and physiological mechanisms developed by plants to counteract salt stress provide a crucial foundation for mitigating its effects. However, traditional agricultural methods and engineering solutions have proven inadequate in addressing the salinity problem. Therefore, developing salt-tolerant plant varieties, implementing biological applications that support plant defense mechanisms, and adopting environmentally friendly management strategies are of great importance.

REFERENCES

- Abbasi, G. H., Akhtar, J., Ahmad, R., Jamil, M., Anwar-ulHaque, M., Ali, S. & Ijaz, M. (2015). Potassium application mitigates salt stress differentially at different growth stages in tolerant and sensitive maize hybrids. *Plant growth regulation*, 76(1), 111- 125.
- Ağaoğlu, Y. S., Çelik, H., Çelik, M., Fidan, Y., Gülşen, Y., Günay, A., Halloran, N., Köksal, A. İ., & Yanmaz, R. (2001). Genel bahçe bitkileri. Ankara Üniversitesi Ziraat Fakültesi Eğitim, Araştırma ve Geliştirme Vakfı Yayınları No:5. Ankara
- Aksoy, U., S. Hepaksoy, H.Z. Can, D. Anaç, B. Okur, C.C. Kılıç, S. Anaç, M.A. Ul ve Y. Kukul. 1998. Akdeniz havzasında çölleşme ve tuzlanma problemine karşı yeni tekniklerin geliştirilmesi, Bitkilerde Stres Fizyolojisinin Moleküler Temelleri Sempozyumu Bildirileri. 126-137, İzmir.
- Alcázar, R., Bueno, M., & Tiburcio, A.F. (2020). Polyamines: Small amines with large effects on plant abiotic stress tolerance. *Cells*, 9(11), 2373.
- Altunlu, H. (2020). Tuz stresi altındaki biberde (*Capsicum annuum* L.) mikoriza ve rizobakteri uygulamasının bitki gelişimi ve bazı fizyolojik parametreler üzerine etkisi. *Ege Üniversitesi Ziraat Fakültesi Dergisi*, 57(4), 501-510.
- Altunlu, H., Acar, Y. S., Altan, F., Tuna, A. L., & Bürün, B. (2024). Tuz stresi altındaki pamukta (*Gossypium hirsutum* L.) 24-epibrassinolid'in etkinliği. *Journal of Agriculture Faculty of Ege University*, 61(3), 367-381.
- Balliu, A., G. Sallaku and B. Rewald. 2015. AMF inoculation enhances growth and improves the nutrient uptake rates of transplanted, salt-stressed tomato seedlings. *Sustainability*. 7(12): 15967-15981.
- Benjamin, J.G., & Nielsen, D.C. (2006). Water deficit effects on root distribution of soybean, field pea and chickpea. *Field Crops Res*, 97: 248–253.
- Bennett, S.J., Barrett-Lennard, E.G., & Colmer, T.D. (2009). Salinity and waterlogging as constraints to saltland pasture production: a review. *Agriculture, Ecosystems & Environment*, 129, 349–360.
- Bhatnagar-Mathur, P., Devi, M.J., Vadez, V., & Sharma, K.K. (2009). Differential anti-oxidative responses in transgenic peanut bear no relationship to their superior transpiration efficiency under drought stress. *J Plant Physiol* 166: 1207- 1217.
- Carter, J.L., Colmer, T.D., Veneklaas, E.J. (2006). Variable tolerance of wetland tree species to combined salinity and waterlogging is related to regulation of ion uptake and production of organic solutes. *New Phytologist*, 169, 123- 134.
- Dağüstü, N. 2003. Ekmeklik buğday (*Triticum aestivum* L.) çeşitlerinin fide döneminde in vivo koşullarda NaCl stresine dayanma performanslarının belirlenmesi. *Türkiye*, 5: 13-17.

- Doğan, Y. L., Altuntaş, Ö., Yaşar, F., Üzal, Ö., & Önder, S. (2024). Hidroponik Ortamda Yetiştirilen Tuz Stresi Altındaki Kabak Bitkilerine PGPR ve Deniz Yosunu Uygulamalarının Bitki Gelişimi Üzerine Etkileri. *Akademik Ziraat Dergisi*, 13(1), 77-86.
- Ekmekçi, E., Apan, M. & Kara, T. (2005). Tuzluluğun bitki gelişimine etkisi. *Anadolu tarım bilimleri dergisi*, 20(3), 118-125.
- Estaji, A., Roosta, H.R., Rezaei, S.A., Hosseini, S.S., & Niknam, F. (2018). Morphological, physiological and phytochemical response of different *Satureja hortensis* L. accessions to salinity in a greenhouse experiment. *Journal of Applied Research on Medicinal and Aromatic Plants*, 10, 25-33.
- Evelin, H., R. Kapoor and B. Giri. 2009. Arbuscular mycorrhizal fungi in alleviation of salt stress: a review. *Annals of Botany*. 104(7): 1263-1280.
- Fernandez-García, N., V. Martínez and M. Carvajal. 2004. Effect of salinity on growth mineral composition and water relations of grafted tomato plants. *J. Plant Nutr. Soil Sci.* 167: 616-622.
- Ghassemi F., Jakeman A.J., Nix H.A. (1995) Salinisation of land and water resources: human causes, extent, management and case studies. CAB international, Wallingford, UK
- Hajbagheri S and S. Enteshari. 2011. Effects of mycorrhizal fungi on photosynthetic pigments, root mycorrhizal colonization and morphological characteristics of salt stressed *Ocimum basilicum* L. *Iran J Plant Physiol*. 1(4):215–222.
- Hao, S., Wang, Y., Yan, Y., Liu, Y., Wang, J. & Chen, S. (2021). A review on plant responses to salt stress and their mechanisms of salt resistance. *Horticulturae*, 7(6), 132.
- Hasegawa, P.M., R. A. Bressan, J.K. Zhu and H.J. Bohnert. 2000. Plant cellular and molecular responses to high salinity. *Ann. Rev. Plant. Physiol.* 51:463–499
- Hirabayashi, Y., Mahendran, R., Koirala, S., Konoshima, L., Yamazaki, D., Watanabe, S., Kim, H., & Kanae, S. (2013). Global flood risk under climate change. *Nature climate change*, 3(9), 816-821.
- Kaya, C., A.L.Tuna, M. Ashraf And H. Altunlu. 2007. Improved salt tolerance of melon (*Cucumis melo* L.) by the addition of proline and potassium nitrate. *Environmental and Experimental Botany*. 60(3): 397-403.
- Kınay, A., & Erdem, H. (2022). Tuz stresi altındaki tütün bitkisine yapraktan silisyum (Si) uygulamalarının etkileri. *Harran Tarım ve Gıda Bilimleri Dergisi*, 26(3), 380-388.
- Kolomeichuk, L.V., M.V. Efimova & I.E. Zlobin, 2020. 24-Epibrassinolide alleviates the toxic effects of NaCl on photosynthetic processes in potato plants. *Photosynthetic Research*, 146: 151- 163. <https://doi.org/10.1007/s11120-020-00708-z>

- Kurt, C. H., M. Tunçtürk & R. Tunçtürk, 2023. Tuz stresi koşullarında yetiştirilen soya (*Glycine max* L.) bitkisinde bazı fizyolojik ve biyokimyasal değişimler üzerine salisilik asit uygulamalarının etkileri. *Ege Üniversitesi Ziraat Fakültesi Dergisi*, 60 (1): 91-101. <https://doi.org/10.20289/zfdergi.1053742>
- Li, C., P. Wang, Z. Wei, D. Liang, C. Liu, L. Yin and F. Ma. 2012. The mitigation effects of exogenous melatonin on salinityinduced stress in *Malus hupehensis*. *Journal of pineal research*, 53(3):298-306.
- Maathuis, F.J.M., Ahmad, I., & Patishtan, J. (2014) Regulation of Na⁺ fluxes in plants. *Front Plant Sci* 5:467–477. <https://doi.org/10.3389/fpls.2014.00467>.
- Martin J., Fackler P.L., Nichols J.D., Lubow B.C., Eaton M.J., Runge M.C., Stith B.M., & Langtimm C.A. (2011) Structured decision making as a proactive approach to dealing with sea level rise in Florida. *Climatic Change*, 107, 185– 202.
- Muneer, S. & Jeong, B. R. (2015). Proteomic analysis of saltstress responsive proteins in roots of tomato (*Lycopersicon esculentum* L.) plants towards silicon efficiency. *Plant growth regulation*, 77(2), 133-146.
- Munns, R. & M. Gilliham, 2015. Salinity tolerance of crops-what is the cost? *New Phytologist*, 208: 668- 673. <https://doi.org/10.1111/nph.13519>
- Munns, R. & Tester, M. (2008). Mechanisms of salinity tolerance. *Annu. Rev. Plant Biol.*, 59, 651-681.
- Nefissi Ouertani, R., Abid, G., Karmous, C., Ben Chikha, M., Boudaya, O., Mahmoudi, H., ... Ghorbel, A. (2021). Evaluating the contribution of osmotic and oxidative stress components on barley growth under salt stress. *AoB Plants*, 13(4), plab034.
- Parvin, S., Lee, O.R., Sathiyaraj, G., Khorolragchaa, A., Kim, Y. J., & Yang, D.C. (2014). Spermidine alleviates the growth of saline-stressed ginseng seedlings through antioxidative defense system. *Gene*, 537(1), 70-78.
- Shah, J. P. & Thivakaran, G. A. (2014). GIS study on chemical properties of salt affected soils of coastal kachchh, Gujarat, India. *Annual Research & Review in Biology*, 3492-3503
- Sharma, N., A. Aggarwal and K. Yadav. 2017. Arbuscular mycorrhizal fungi enhance growth, physiological parameters and yield of salt stressed *Phaseolus mungo* (L.) Hepper. *European Journal of Environmental Sciences*, 7(1):22-27.
- Şen, Ö. (2008). Tuz stresi altında yetiştirilen patlıcan fidelerinin gelişimi ve besin elementi içerikleri üzerine arbuscular mikorizal fungus uygulamalarının etkisi. (Yüksek Lisans Tezi). Selçuk Üniversitesi, Fen Bilimleri Enstitüsü, Bahçe Bitkileri Anabilim Dalı. Konya.
- Taiz, L., Zeiger, E. 2010. Photosynthesis: carbon reactions. *Plant physiology*. Sunderland, England

- Talaat, N. B., Ghoniem, A. E., Abdelhamid, M. T. & Shawky, B. T. (2015). Effective microorganisms improve growth performance, alter nutrients acquisition and induce compatible solutes accumulation in common bean (*Phaseolus vulgaris* L.) plants subjected to salinity stress. *Plant growth regulation*, 75(1), 281-295.
- Uras, S. & Sonmez, S. (2010). Tarım Alanlarında Tuzluluk Oluşumu ve Bitkiler ile Çevre Üzerine Etkileri. *Ege Üniversitesi Zir. Fak. Dergisi*, 574-579.
- Üzal, Ö., Yaşar, F., Yıldırım, Ö. 2020. Tuz stresi altındaki biber bitkisindeki kalsiyum uygulamalarının antioksidatif enzim aktivitelerine etkisinin araştırılması. *ISPEC Journal of Agr. Sciences* 4(2): 346- 357.
- Yasar, F., Üzal, Ö. 2021. Effect of applications of different potassium (K⁺) doses on antioxidant enzyme activities in pepper plants under salt stress, *Journal of Elementology* 26 (4): 905-912
- Yaşar, F., & Yaşar, Ö. (2022). Tuz Stresi Altındaki Çarliston Biber Çeşidinin Gelişim Performansı. *ISPEC Journal of Agricultural Sciences*, 6(4), 835-841.
- Yıldız, M., H. Terzi, S. Cenkçi, E.S.A. Terzi ve B. Urşak. 2010. Bitkilerde tuzluluğa toleransın fizyolojik ve biyokimyasal markörleri. *Anadolu Üniversitesi Bilim ve Teknoloji Dergisi - C Yaşam Bilimleri ve Biyoteknoloji*, 1(1):1-33.
- Yılmaz, A., & Çiftçi, V. (2021). Pütresin'in tuz stresi altında yetişen yer fıstığı (*Arachis hypogaea* L.)'na etkisi. *Avrupa Bilim ve Teknoloji Dergisi*, (31), 562-567.
- Zhang, J.L., & Shi, H. (2013) Physiological and molecular mechanisms of plant salt tolerance. *Photosynth Res* 115(1):1–22.
- Zhao, S., Zhang, Q., Liu, M., Zhou, H., Ma, C. & Wang, P. (2021). Regulation of plant responses to salt stress. *International Journal of Molecular Sciences*, 22(9), 4609.



CHAPTER 36

Smart Agriculture Systems

Gözde Hafize Yıldırım¹

¹ Research Assistant Dr., Recep Tayyip Erdoğan University, Faculty of Agriculture, Department of Field Crops, Rize/Turkey, 0000-0002-0557-6442

INTRODUCTION

The agricultural sector faces numerous challenges, and the use of digital technologies has become increasingly critical in overcoming these difficulties. Smart farming systems enable a more informed and precise management of agricultural processes, driving a significant transformation in the sector. These technologies enhance the competitiveness of farmers and enterprises, while also contributing to reducing environmental impacts and lowering costs. Operations such as yield prediction, plant health analysis, and the detection of diseases and stress can be performed more quickly and accurately with the support of digital technologies. This enhances production quality and ensures more efficient use of resources. Smart farming applications, encompassing a broad range of technologies from agricultural machinery to wireless sensors, drones to big data analytics, are reshaping the agricultural sector. These systems not only provide economic benefits but also play a crucial role in achieving environmental sustainability goals.

Today, "Smart Agriculture" or "Agriculture 4.0" represents innovative approaches aimed at ensuring the sustainable use of natural resources, rural development, and food security. This technological transformation incorporates various tools, from autonomous technologies to cloud computing and satellite systems, as well as sensors, robotics, and information and communication technologies. Additionally, decision support systems and IoT technologies enable the monitoring and optimization of all stages of the production chain (Duman and Özsoy, 2019; Ercan et al., 2019; Kılavuz and Erdem, 2019; Arıcıoğlu et al., 2020; Ertaş, 2020). Smart agriculture can also be defined as the effort of farmers to increase product quality and productivity by utilizing information technologies in agricultural processes. According to Mistry et al. (2020), this concept involves the use of artificial intelligence algorithms in farm management, while Rose and Chilvers (2018) describe Agriculture 4.0 as a system based on robotics, cloud computing, and IoT technologies. Klerkx et al. (2019) highlight that Agriculture 4.0 integrates various data sources through cloud systems, drones, and sensors to monitor plants, animals, soil, and environmental factors. Furthermore, Klerkx and Rose (2020) state that this system encompasses a wide range of innovative technologies, including robotics, nanotechnology, gene editing, artificial intelligence, blockchain, and machine learning.

In this context, "Smart Agriculture" or "Agriculture 4.0" aims to enhance productivity in agricultural production and develop solutions throughout the supply chain using digital tools (tablets, computers), IoT, GPS, sensors, satellites, and data analytics platforms. These technologies used in agriculture can be

categorized into three main groups: mechanical, biological, and organizational (Ağızan et al., 2022). The purpose of this review is to explain the positive impacts of smart farming technologies on agricultural production and why these systems have become indispensable in agricultural activities.

INTERNET OF THINGS IN AGRICULTURE

The agricultural sector is rapidly advancing towards efficiency and sustainability goals with the innovations provided by digital technologies. The Internet of Things (IoT) is revolutionizing agricultural activities, allowing farmers to manage their fields more effectively and monitor crops with ease (Kahraman, 2017). GPS-supported precision agriculture technologies simplify the monitoring and management of agricultural lands (CEMA, 2017), while sensor-equipped machinery integrates production processes (Ercan et al., 2019). These technologies improve process control, reduce costs, and provide significant convenience to farmers. The integration of IoT into agricultural applications is critical for both efficiency gains and environmental sustainability. For example, drones expedite pest control and pesticide applications, reducing costs and environmental impacts (Kern, 2015). In China, pesticide usage decreased by half, and water consumption was reduced by 90% through drone-based applications, showcasing the profound impact of this technology.

The innovations brought by digital agriculture are not limited to technological advantages alone. The adaptation of employees and managers to digital transformation maximizes the benefits enterprises gain from digitalization, directly influencing the success of this process (Ersöz and Özmen, 2020; Sağlam, 2021). Moreover, adapting technological tools to meet business needs enhances competitive advantages.

IoT emerges as a pivotal technology in the agricultural sector, enabling farmers to optimize crop production, adapt to climate change, and increase efficiency. An exemplary IoT-Agro system implemented on a farm in Colombia was designed to plan harvest times, reduce crop diseases based on historical data, and estimate annual production. This system operates on a three-layer architecture: Agricultural Sensing, Edge Computing, and Data Analytics. For predicting coffee production, various algorithms (Decision Trees, Artificial Neural Networks, XGBoost, Support Vector Machines, and Random Forest) were evaluated, with XGBoost demonstrating the best performance with the lowest error rate (0.032) (Rodríguez et al., 2021; Özer et al., 2022).

IoT-based systems leverage machine learning techniques for tasks such as crop yield prediction and reconstructing incomplete or faulty sensor data. For

instance, neural network models achieved a success rate of nearly 90% for predicting apple and pear yields. Additionally, studies on CNR scientific data revealed that polynomial regression and decision trees are effective in predicting missing data (Balducci et al., 2018). Early detection and prevention of crop diseases is another critical component of IoT-supported systems. Deep learning algorithms (Inception-v3, VGG-16, VGG) and data mining methods (Support Vector Machines, Random Forest) have been compared for classifying plant diseases. Results indicated that deep learning methods outperformed machine learning methods, with the VGG-16 algorithm achieving the highest accuracy in disease classification (Sujatha et al., 2021).

IoT-based systems also significantly contribute to pest control in agriculture. Smart pest monitoring models developed using deep learning techniques have utilized methods like Classic CNN networks, transfer learning, and few-shot learning for pest classification (Li et al., 2021). In IoT and smart image recognition-supported harvesting systems, crop maturity is determined through object detection, and mature products are harvested using robotic arms. The MobileNet-SSD model has proven successful in this field, with an average accuracy rate of 84% (Horng et al., 2019; Özer et al., 2022). The growth potential of the sector is also noteworthy, with a projected market value of \$29.8 billion by 2027, growing at a rate of 10.5% between 2022 and 2027 (Anonymous, 2022). IoT and digital farming technologies have become the cornerstone of modern agriculture, heralding a new era of efficiency, sustainability, and eco-friendly practices in the sector.

DATA-DRIVEN SUPPORT SYSTEMS

Digital farming technologies support precise, efficient, and informed management processes to enhance productivity and quality in agriculture. Innovative methods such as wireless sensor networks (WSN) and remote sensing (RS) accurately detect soil moisture, temperature, and nutrient deficiencies, enabling irrigation and fertilization tailored to plant needs. This ensures optimized resource usage while preventing yield losses. These technologies also provide effective solutions in areas like yield estimation, plant health management, and disease detection, facilitating the more efficient management of agricultural processes.

In modern agricultural practices, tools such as big data analytics, artificial intelligence (AI), deep learning (DL), and machine learning (ML) play a critical role in agricultural production. Agricultural machinery and autonomous robots reduce workloads by increasing accuracy in tasks ranging from weed control to

precision farming operations. For example, drones and automation systems are effectively used in tasks such as crop classification and quality analysis.

Precision agriculture, bolstered by big data technologies, represents a new direction for agricultural development. Many countries are investing in the use of big data in the agricultural sector. For instance, in 2015, the United States invested \$4.6 billion in research on the application of big data and software in agriculture. Similarly, the Chinese government has developed policies to unlock the potential of big data for rural development. Big data, often used alongside technologies under the scope of Agriculture 4.0, enables farmers to manage agricultural production processes more precisely in spatial and temporal contexts. Robotics, sensors, IoT, blockchain, drones, and automated agricultural machinery are prominent tools for leveraging big data in this regard (Wolfert, 2017; Aydın, 2022).

The power of big data is often defined by six fundamental characteristics, known as the six "Vs": velocity, volume, variety, veracity, value, and variability. Technological advancements have enabled the exploitation of these characteristics to revolutionize agriculture (Sonka, 2015; Aydın, 2022). Advanced computing capacities have made it possible to analyze large volumes of data, such as evaluating weather data.

In agricultural applications, big data provides farmers with in-depth insights into their crops and field conditions, improving their decision-making processes. For instance, measurements related to field conditions, such as soil moisture, nutrient levels, pH, temperature, and precipitation, can be compared with input and output prices to optimize profits. These analyses allow farmers to use labor more efficiently, improve input purchasing strategies, and optimize production processes (Aydın, 2022). With the adoption of digital farming technologies, the agricultural sector will evolve into a more effective, informed, and sustainable structure in the future. Digitalization has become an indispensable tool for optimizing agricultural processes and achieving goals of efficiency, quality, and environmental protection.

CONCLUSION

The agricultural sector is undergoing a significant transformation driven by the solutions offered by digital technologies in addressing its challenges. Smart farming systems and Agriculture 4.0 not only enable more efficient and informed management of production processes but also play a crucial role in achieving critical objectives such as environmental sustainability, cost optimization, and rural development. These technologies, supported by innovative tools such as GPS, IoT, sensors, artificial intelligence, robotics, satellite technologies, and big data analytics, are revolutionizing every stage of agriculture.

In conclusion, digital farming technologies have become indispensable tools for enhancing productivity, reducing costs, and supporting environmental sustainability goals in the agricultural sector. This transformation represents a transition to a more sustainable, efficient, and innovative structure for future agriculture. Smart farming systems and Agriculture 4.0 address the evolving needs of the agricultural sector while playing a critical role in conserving natural resources and leaving a more livable world for future generations.

REFERENCES

- Akyol, I. (2023). *Tarımda Dijital Dönüşüme Yönelik Uygulamalar ve Politikaların Türkiye İçin Değerlendirilmesi* (Yüksek Lisans Tezi). Ankara Üniversitesi, Fen Bilimleri Enstitüsü, Ankara.
- Anonymous. 2022. Web Sitesi: <https://www.marketsandmarkets.com/Market-Reports/digital-agriculture-market-235909745.html?gclid=CjwKCAjwx Oym BhAFE iwAnodBLLfLKC1vhwha286gt2MfPnZU-5dNDvtTmCkCaL6BFJ-Ll6OIMwj ORoC 5REQA vD BwE> Erişim Tarihi: 17.03.2022
- CEMA (2017). Digital Farming: What does it Really Mean. 2020 tarihinde http://ce-maagri. org/sites/default/files/CEMA_Digital%20Farming%20-%20Agriculture%204.0_%2013% 2002%202017.pdf. Erişim Tarihi: 17.04.2022
- Ercan, ğ., Öztep, R., Güler, D., Saner, G. (2019). Tarım 4.0 ve Türkiye’de Uygulanabilirliğin Değerlendirilmesi, Tarım Ekonomisi Dergisi, 25(2).
- Ersöz, B., & Özmen, M. (2020). Dijitalleşme ve Bilişim Teknolojilerinin Çalışanlar Üzerindeki Etkileri. AJIT-e: Academic Journal of Information Technology, 11 (42).
- Kahraman, H., (2017). Dijital Tarım’la Birlikte Gelen Akıllı Tarım. <http://www.endustri40.com/endustri-4-0la-birlikte-gelen-akillitarim/> (Erişim Tarihi: 15.03.2022).
- Kern, M. 2015. Digital agriculture. ISPSW Strategy Series: Focus on Defense and International Security, 331(8).
- Sağlam, M. (2021). İşletmelerde Geleceğin Vizyonu Olarak Dijital Dönüşümün Gerçekleştirilmesi ve Dijital Dönüşüm Ölçeğinin Türkçe Uyarlaması. İstanbul Ticaret Üniversitesi Sosyal Bilimler Dergisi, 20 (40), 395-420.
- Ağızan, K., Bayramoğlu, Z., & Ağızan, S. (2022). Akıllı Tarım Teknolojilerinin Tarımsal İşletme Yöneticiliğine Sunduğu Avantajlar. *Turkish Journal of Agriculture-Food Science and Technology*, 10(9), 1697-1706.
- Duman B, Özsoy K. 2019. Endüstri 4.0 Perspektifinden Akıllı Tarım, 4th International Congress On 3d Printing (Additive Manufacturing) Technologies and Digital Industry, Antalya, 540-555.
- Ercan Ş, Öztep R, Güler D, Saner G. 2019. Tarım 4.0 ve Türkiye’de uygulanabilirliğinin değerlendirilmesi, Tarım Ekonomisi Dergisi, 25 (2), 259-265.
- Kılavuz E, Erdem İ. 2019. Dünyada tarım 4.0 uygulamaları ve Türk tarımının dönüşümü, Social Sciences, 14 (4), 133-157.
- Arıcıoğlu MA, Yılmaz A, Gülnar N. 2020. 4.0 For Agriculture, European Journal of Business and Management Research, 5 (3), 1-8.
- Ertaş B. 2020. A Tarım 4.0 İle Sürdürülebilir Bir Gelecek, Icontech International Journal, 4 (1), 1-12.

- Mistry I, Tanwar S, Tyagi S, Kumar N. 2020. Blockchain for 5Genabled IoT for industrial automation: A systematic review, solutions, and challenges, *Mechanical Systems and Signal Processing*, 135, 1-20.
- Rose DC, Chilvers J. 2018. Agriculture 4.0: Broadening responsible innovation in an era of smart farming, *Frontiers in Sustainable Food Systems*, 2, 87.
- Klerkx L, Jakku E, Labarthe P. 2019. A review of social science on digital agriculture, smart farming and agriculture 4.0: New contributions and a future research agenda, *NJASWageningen Journal of Life Sciences*, 90, 100315.
- Özer, B., Kuş, S., & Yıldız, O. (2022). Veri Madenciliği Yöntemleri ile Tarımsal Veri Analizi: Bir Akıllı Tarım Sistemi Önerisi. *Mühendislik Bilimleri ve Tasarım Dergisi*, 10(4), 1417-1429.
- Rodríguez, J. P., Montoya-Munoz, A. I., Rodriguez-Pabon, C., Hoyos, J., & Corrales, J. C. (2021). IoT-Agro: A smart farming system to Colombian coffee farms. *Computers and Electronics in Agriculture*, 190, 1-18.
- Balducci, F., Impedovo, D., & Pirlo, G. (2018). Machine Learning Applications on Agricultural Datasets for Smart Farm Enhancement. *MDPI, machines*, 6(38), 1-22.
- Sujatha, R., Chatterjee, J. M., Jhanjhi, N., & Brohi, S. N. (2021). Performance of deep learning vs machine learning in plant leaf disease detection . *Microprocessors and Microsystems*, 80, 1-11.
- Li, W., Zheng, T., Yang, Z., Li, M., Sun, C., & Yang, X. (2021). Classification and detection of insects from field images using deep learning for smart pest management: A systematic review. *Ecological Informatics* , 66(101460), 1-18.
- Horng, G.-J., Liu, M.-X., & Chen, C.-C. (2019). The Smart Image Recognition Mechanism for Crop Harvesting System in Intelligent Agriculture. *IEEE Sensors Journal*, 1-16.
- Wolfert, S., Ge, L., Verdouw, C. and Bogaardt, M.J. (2017). Big Data in Smart Farming—A review. *Agricultural Systems*, 153, pp.69-80.
- Sonka, S. (2015). Big Data: From Hype to Agricultural Tool. *Farm Policy Journal* 12 (1): 1–9.
- Aydın, N. (2022). Tarım Sektöründe Bilgi Teknolojileri. *Balkan & Near Eastern Journal of Social Sciences (BNEJSS)*, 8.



CHAPTER 37

Load Frequency Control in A Two-Area Power System With Renewable Energy Integration Using Sliding Mode Controller

Asaf Sayıl¹ & Yağmur Arıkan Yıldız²

¹ Sivas University of Science and Technology, Department of Astronautical Engineering,
Orcid: 0000-0003-4148-4825, Corresponding author

² Dr, Sivas University of Science and Technology, Department of Electric-Electronic Engineering,
Orcid: 0000-0003-0947-2832

1. Introduction

The transition from fossil fuels to renewable energy sources (RES) such as wind, solar, and hydro power is driven by the urgent need to address environmental concerns and promote sustainable development. The International Energy Agency (IEA) emphasizes that integrating RES into existing power systems is crucial for reducing greenhouse gas emissions and ensuring a sustainable energy future (Jia et al., 2021). However, the inherent intermittent and stochastic nature of renewable energy generation presents significant challenges for the stability and reliability of power systems. One of the primary issues arising from high levels of RES integration is the difficulty in maintaining system frequency within acceptable limits, which is exacerbated by the imbalance between power supply and demand (Cucuzzella et al., 2017).

Load Frequency Control (LFC) is a critical mechanism in power system operation, designed to maintain the nominal system frequency and regulate tie-line power flows between interconnected areas. Traditionally, LFC has relied on conventional controllers such as Proportional-Integral-Derivative (PID) controllers, which are based on linear system models and assume predictable power generation and consumption patterns (Wu & Lu, 2019). These controllers have been effective in systems dominated by conventional thermal and hydroelectric power plants, which exhibit relatively slow and predictable dynamics. However, the increasing integration of RES challenges these assumptions, as renewable sources, particularly wind and solar, exhibit significant variability and uncertainty due to their dependence on weather conditions (Elhajji et al., 2014). This variability leads to rapid and substantial fluctuations in power generation, resulting in frequency deviations and potential instability within the power system (Khan et al., 2021). Furthermore, the displacement of conventional generation units reduces system inertia, further complicating frequency control efforts (Woźniak et al., 2021).

To address these challenges, advanced control strategies have been proposed, with robust and adaptive control techniques gaining prominence for their ability to manage system uncertainties and external disturbances. Among these, Sliding Mode Control (SMC) has emerged as a promising nonlinear control method characterized by its robustness to certain classes of uncertainties and disturbances once the system states reach a predefined sliding surface (Balali et al., 2017). SMC offers advantages such as fast dynamic response, good transient performance, and resilience against parameter variations, making it particularly suitable for LFC in modern power systems facing high levels of renewable energy penetration (Oladunjoye et al., 2022).

The application of SMC in power system frequency control has garnered significant attention due to its robustness against uncertainties and disturbances, particularly in systems integrating renewable energy sources. (Jia et al., 2021) introduced a low-order sliding mode repetitive controller for discrete-time systems under complex disturbance environments, demonstrating enhanced dynamic performance compared to traditional PID controllers. However, their study did not address the complexities introduced by renewable energy integration, which can lead to increased stochastic variability in power generation. This gap highlights the necessity for more comprehensive approaches that consider the unique challenges posed by renewable sources.

(Cucuzzella et al., 2017) advanced the field by developing a decentralized sliding mode control for islanded AC microgrids with arbitrary topology. Their work effectively reduced chattering and enhanced the system's responsiveness to disturbances. Nonetheless, their focus remained on isolated microgrids, lacking detailed modeling of interconnected power systems that include essential components such as governors and turbines. This limitation underscores the need for methodologies that can be applied to larger, interconnected systems where the dynamics are more complex.

Further investigations by (Wu & Lu, 2019) and (Elhajji et al., 2014) explored SMC techniques in the context of renewable energy integration. (Wu & Lu, 2019) proposed an adaptive backstepping sliding mode control for boost converters with constant power loads, modeling power fluctuations as bounded disturbances. However, their approach simplified the stochastic nature of renewable generation, which is critical for accurate frequency stability analysis. Similarly, (Elhajji et al., 2014) introduced discrete fast terminal and integral sliding mode controllers, addressing uncertainties but failing to incorporate detailed system component modeling or the stochastic characteristics of renewable generation. Their results indicated improved performance over traditional controllers, yet they lacked a thorough analysis under realistic operating conditions.

(Khan et al., 2021) also contributed to the discourse by presenting a neuro-adaptive backstepping integral sliding mode control design for nonlinear wind energy conversion systems. While their controller adapted to parameter variations and external disturbances, it relied on simplified models that did not adequately account for the stochastic variability of renewables. This trend of oversimplification in existing studies suggests a pressing need for comprehensive modeling that accurately reflects the dynamics of inter-connected power systems with significant renewable energy penetration.

This paper aims to fill this gap by developing a detailed mathematical model of a two-area interconnected power system with renewable energy integration and designing a Sliding Mode Controller tailored for load frequency control. By incorporating stochastic renewable generation and comprehensive system modeling, we provide a thorough evaluation of the SMC's performance under realistic operating conditions, including step load changes and random load fluctuations. Our work contributes to advancing the application of SMC in modern power systems facing the challenges of high renewable energy penetration.

This paper investigates the application of a Sliding Mode Controller for Load Frequency Control in a two-area interconnected power system with renewable energy integration. The main contributions of this work are:

- Development of a detailed mathematical model of a two-area power system incorporating stochastic renewable energy sources, suitable for control design and simulation purposes.
- Design of a Sliding Mode Controller tailored for LFC, emphasizing robustness against system uncertainties and disturbances introduced by renewable energy variability.
- Implementation of the system model and SMC in MATLAB using a fixed time step approach to accurately simulate the stochastic processes and ensure numerical stability.
- Comprehensive evaluation of the SMC's performance under various scenarios, including step load changes and random load fluctuations, demonstrating its effectiveness in maintaining frequency stability.

The remainder of this paper is organized as follows: Section 2 presents the detailed system modeling, including the dynamics of the governor, turbine, generator, tie-line power flow, and renewable energy integration. The design of the Sliding Mode Controller is also elaborated in this section. Section 3 describes the simulation setup and discusses the performance of the SMC under different scenarios. Finally, Section 4 summarizes the findings and suggests directions for future research.

Notation

Throughout this paper, Δ denotes a deviation from the nominal value. Subscripts i and j refer to Area 1 and Area 2, respectively. The variables and parameters used are defined as follows:

- Δf_i : Frequency deviation in Area i (Hz).
-
- ΔP_{mi} : Mechanical power output deviation of the turbine in Area i (pu MW).
- ΔP_{gi} : Governor output power deviation in Area i (pu MW).
- ΔP_{ci} : Control input (SMC output) in Area i (pu MW).
- ΔP_{Li} : Load disturbance in Area i (pu MW).
- ΔP_{RE} : Renewable power output deviation in Area 1 (pu MW).
-
- ΔP_{tie} : Tie-line power flow deviation between the two areas (pu MW).
- T_g : Governor time constant (seconds).
- T_t : Turbine time constant (seconds).
- H : Inertia constant (seconds).
- D : Damping coefficient (pu MW Hz⁻¹).
- R : Speed regulation parameter (Hz pu⁻¹ MW).
- B : Frequency bias constant (MW Hz⁻¹).
- T_{12} : Tie-line synchronizing coefficient (pu MW Hz⁻¹).
- s_i : Sliding surface in Area i .
- K_s : Proportional gain of the SMC.
- η : Switching gain of the SMC.
- ϕ : Boundary layer thickness to reduce chattering in SMC.

The system parameters are selected based on typical values found in the literature (Bevrani, 2009; Kundur, 1994), and are provided in detail in Section 2.

2. Methodology

The two-area power system considered in this study consists of two interconnected areas, each comprising a synchronous generator, governor, turbine, load, and a control mechanism. The areas are connected via a tie-line that allows power exchange between them. A stochastic renewable energy source is integrated into Area 1 to represent the impact of renewable energy on system dynamics.

2.1 Governor Dynamics

The governor adjusts the input to the turbine based on frequency deviations to regulate the mechanical power output of the generator. The governor dynamics for each area are modeled as:

$$\frac{d\Delta P_{gi}}{dt} = \frac{1}{T_g} \left(-\Delta P_{gi} + \Delta P_{ci} - \frac{1}{R} \Delta f_i \right) \quad (1)$$

Where:

- ΔP_{gi} is the governor output power deviation in Area i (pu MW).
- T_g is the governor time constant (seconds).
- ΔP_{ci} is the control input from the controller in Area i (pu MW).
- R is the speed regulation parameter (Hz pu⁻¹ MW).
- Δf_i is the frequency deviation in Area i (Hz).

Parameter Values:

- $T_g = 0.08$ seconds.
- $R = 2.4$ Hz/pu MW.

2.2 Turbine Dynamics

The turbine converts the mechanical input from the governor into mechanical power driving the generator. The turbine dynamics are given by:

$$\frac{d\Delta P_{mi}}{dt} = \frac{1}{T_t} \left(-\Delta P_{mi} + \Delta P_{gi} \right) \quad (2)$$

Where:

- ΔP_{mi} is the mechanical power output deviation in Area i (pu MW).
- T_t is the turbine time constant (seconds).

Parameter Values:

- $T_t = 0.3$ seconds.

2.3 Generator Dynamics (Swing Equation)

The swing equation models the rotational dynamics of the synchronous generator, accounting for the balance between mechanical and electrical power. The generator dynamics are expressed as:

For Area 1:

$$\frac{d\Delta P_{m_i}}{dt} = \frac{1}{T_t} (-\Delta P_{m_i} + \Delta P_{g_i}) \quad (3)$$

For Area 2:

$$\frac{d\Delta f_2}{dt} = \frac{1}{2H} (\Delta P_{m_2} - \Delta P_{L2} - D\Delta f_2 + \Delta P_{tie}) \quad (4)$$

Where:

- Δf_i is the frequency deviation in Area i (Hz).
- H is the inertia constant (seconds).
- ΔPRE is the renewable power output deviation in Area 1 (pu MW).
- ΔPL_i is the load disturbance in Area i (pu MW).
- D is the damping coefficient (pu MW/Hz).
- ΔP_{tie} is the tie-line power flow deviation (pu MW).

Parameter Values:

- $H = 5$ seconds.
- $D = 0.015$ pu MW/Hz.

2.4 Tie-Line Power Flow

The tie-line allows power exchange between the two areas, and its power flow deviation is given by:

$$\Delta P_{tie} = T_{12}(\Delta f_1 - \Delta f_2) \quad (5)$$

Where:

- T_{12} is the tie-line synchronizing coefficient (pu MW/Hz).
- Δf_1 and Δf_2 are the frequency deviations in Areas 1 and 2, respectively.

Parameter Value:

- $T_{12} = 0.545$ pu MW/Hz.

2.5 Area Control Error (ACE)

The ACE measures the imbalance in each area, considering both frequency deviation and tie-line power flow deviation. It is used by the controller to adjust the control inputs.

The ACE for each area is defined as:

For Area 1:

$$ACE_1 = B\Delta f_1 + \Delta P_{tie} \quad (6)$$

For Area 2:

$$ACE_2 = B\Delta f_2 - \Delta P_{tie} \quad (7)$$

Parameter Value

- $B = 0.425$ MW/Hz.

2.6 Renewable Energy Integration

A stochastic renewable energy source is integrated into Area 1, modeled as a Wiener process to represent the variability and unpredictability of renewable power generation:

$$\Delta P_{RE} = \sigma_{RE} W(t) \quad (8)$$

where:

- σ_{RE} is the standard deviation of renewable power fluctuations (pu MW).

- $W(t)$ is a standard Wiener process representing white Gaussian noise.

Parameter Value:

- $\sigma_{RE} = 0.02$ pu MW.

2.7 Load Disturbances

Load disturbances are introduced as step changes and random fluctuations. At $t = 10$ seconds, a step load change occurs:

- $\Delta PL1 = 0.01$ pu MW in Area 1 (increase).

• $\Delta PL2 = -0.005$ pu MW in Area 2 (decrease). Random load fluctuations are modeled as:

$$\Delta P_{L_i} = \Delta P_{L_i}^{\text{step}} + \sigma_L \xi(t) \quad (9)$$

where:

- σ_L is the standard deviation of load fluctuations (pu MW).
- $\xi(t)$ is a white Gaussian noise process.

Parameter Value:

- $\sigma_L = 0.005$ pu MW.

3. Sliding Mode Controller Design

The Sliding Mode Controller is designed to enhance robustness against system uncertainties and external disturbances. The controller aims to drive the system states to a predefined sliding surface and maintain them there. The control law for the SMC is based on the sliding surface s_i defined as the Area Control Error (ACE):

$$s_i = ACE_i \quad (10)$$

The control input ΔP_{ci} for each area is given by:

$$\Delta P_{c_i} = -K_s s_i - \eta \text{sat}\left(\frac{s_i}{\phi}\right) \quad (11)$$

where:

- K_s is the proportional gain.
- η is the switching gain.
- ϕ is the boundary layer thickness (to reduce chattering).

$\text{sat}(\cdot)$ is the saturation function defined as:

$$\text{sat}(x) = \begin{cases} 1, & x > 1 \\ x, & |x| \leq 1 \\ -1, & x < -1 \end{cases} \quad (12)$$

- $K_s = 10.0$
- $\eta = 0.1$
- $\phi = 0.001$

3.1 Design Considerations

The proportional gain K_s is selected to ensure adequate responsiveness of the controller, while the switching gain η enhances robustness against disturbances. The boundary layer thickness ϕ is introduced to reduce chattering by smoothing the control action near the sliding surface. A smaller ϕ improves tracking accuracy but may increase chattering; hence, a balance is required.

3.2 Simulation Implementation

The system equations and the SMC are implemented in MATLAB using a fixed time step approach to accurately model the stochastic processes and ensure numerical stability.

3.2.1 Simulation Parameters

- Simulation Time: $t = 0$ to $t = 300$ seconds.
- Fixed Time Step: $\Delta t = 0.01$ seconds.
- Number of Time Steps: $n = \frac{300}{0.01} + 1 = 30,001$

3.2.2 Initialization

All state variables are initialized to zero at $t = 0$:

- $\Delta fi(0) = 0$
- $\Delta Pmi(0) = 0$
- $\Delta Pgi(0) = 0$
- $\Delta Pci(0) = 0$
- $\Delta PRE(0) = 0$
- $\Delta PLi(0) = 0$

3.2.3 Simulation Steps

At each time step i :

1. Update Renewable Power Output:

The renewable power output $\Delta PRE(t)$ is updated using the stochastic process:

$$\Delta P_{RE}(t + \Delta t) = \Delta P_{RE}(t) + \sigma_{RE} \sqrt{\Delta t} \epsilon(t)$$

Where $\epsilon(t)$ is a standard normal random variable generated using MATLAB's randn function.

2. Load Disturbance:

If $t \geq 10$ seconds, apply the step load change and add random fluctuations:

$$\Delta P_{L_i}(t) = \Delta P_{L_i}^{\text{step}} + \sigma_L \xi(t) \quad (12)$$

Otherwise, only random fluctuations are considered:

$$\Delta P_{L_i}(t) = \sigma_L \xi(t) \quad (13)$$

3. Calculate ACE:

Compute the ACE for each area:

$$\text{ACE}_1(t) = B\Delta f_1(t) + \Delta P_{tie}(t) \quad (14)$$

$$\text{ACE}_2(t) = B\Delta f_2(t) - \Delta P_{tie}(t) \quad (15)$$

4. Compute Control Inputs:

Apply the SMC control law:

$$\Delta P_{c_i}(t) = -K_s s_i(t) - \eta \text{sat}\left(\frac{s_i(t)}{\phi}\right) \quad (16)$$

Where $s_i(t) = \text{ACE}_i(t)$.

5. Update Governor and Turbine States:

Use the Euler method to update the governor and turbine outputs:

$$\Delta P_{g_i}(t + \Delta t) = \Delta P_{g_i}(t) + \frac{d\Delta P_{g_i}}{dt} \Delta t \quad (17)$$

$$\Delta P_{m_i}(t + \Delta t) = \Delta P_{m_i}(t) + \frac{d\Delta P_{m_i}}{dt} \Delta t \quad (18)$$

6. Update Frequency Deviations:

Update the frequency deviations using the swing equation:

$$\Delta f_i(t + \Delta t) = \Delta f_i(t) + \frac{d\Delta f_i}{dt} \Delta t \quad (19)$$

7. Update Tie-Line Power Flow:

Calculate the tie-line power flow deviation:

$$\Delta P_{tie}(t + \Delta t) = T_{12}(\Delta f_1(t + \Delta t) - \Delta f_2(t + \Delta t)) \quad (20)$$

A fixed random seed is set using MATLAB's *rng* function to ensure reproducibility of the stochastic processes.

4. Simulation and Results

The performance of the Sliding Mode Controller is evaluated under three scenarios. The simulation results, including figures generated from the MATLAB code, are presented in this section.

4.1 Scenario 1: Step Load Change without Renewable Integration

In this scenario, the renewable energy source is not integrated ($\sigma RE = 0$), and only the step load changes are applied at $t = 10$ seconds. The SMC effectively reduces the frequency deviations in both areas. The frequencies settle back to zero within approximately 3 seconds after the disturbance.

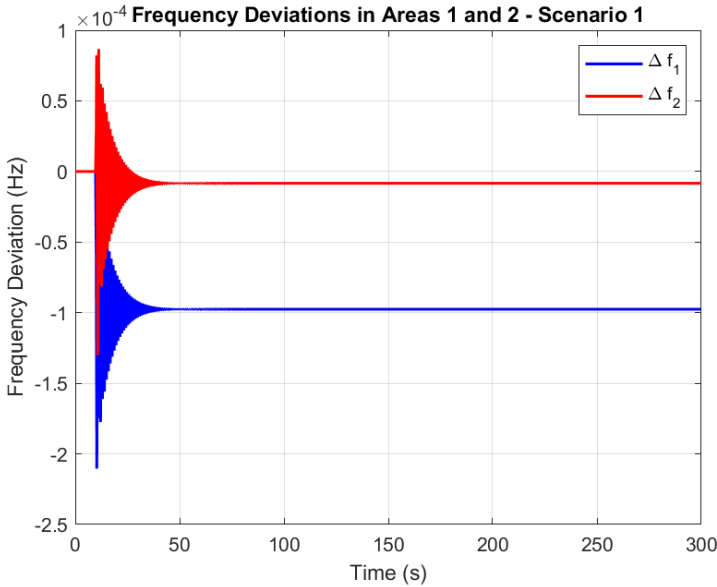


Figure 1: Frequency deviations in Areas 1 and 2 under Scenario 1.

Figure 1 shows the frequency deviations in both areas. The maximum overshoot in frequency deviation is about 0.0001 Hz in Area 1 and 0.00001 Hz in Area 2. The tie-line power flow deviation stabilizes quickly, as shown in Figure 2.

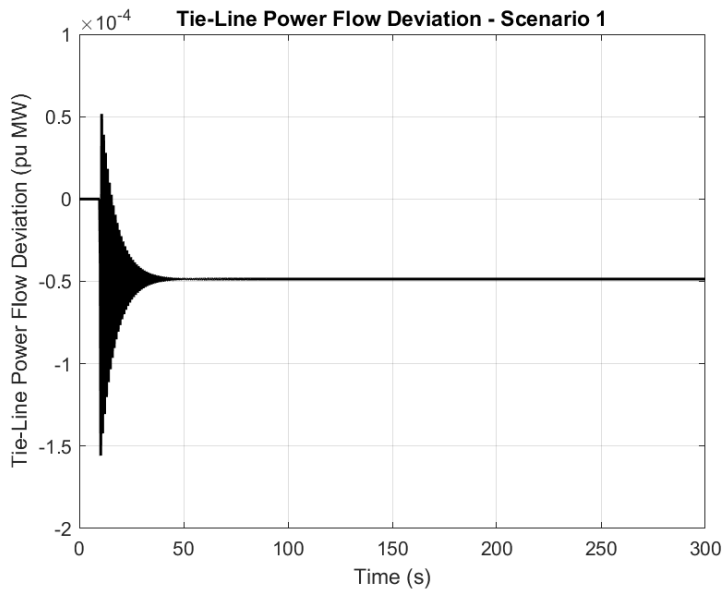


Figure 2: Tie-line power flow deviation under Scenario 1.

The control inputs from the SMC are depicted in Figure 3, exhibiting minor chattering which is mitigated by the saturation function.

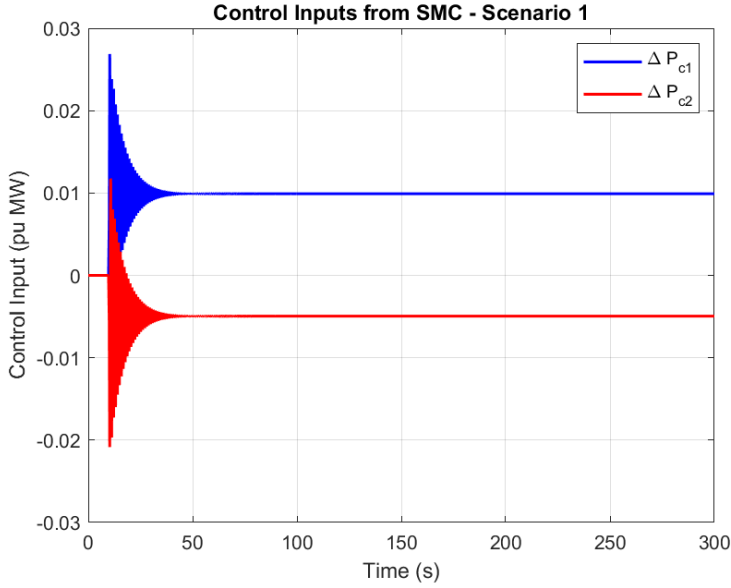


Figure 3: Control inputs from the SMC under Scenario 1.

The sliding surfaces converge to zero, confirming the effectiveness of the SMC in driving the system states to the desired values, as illustrated in Figure 4.

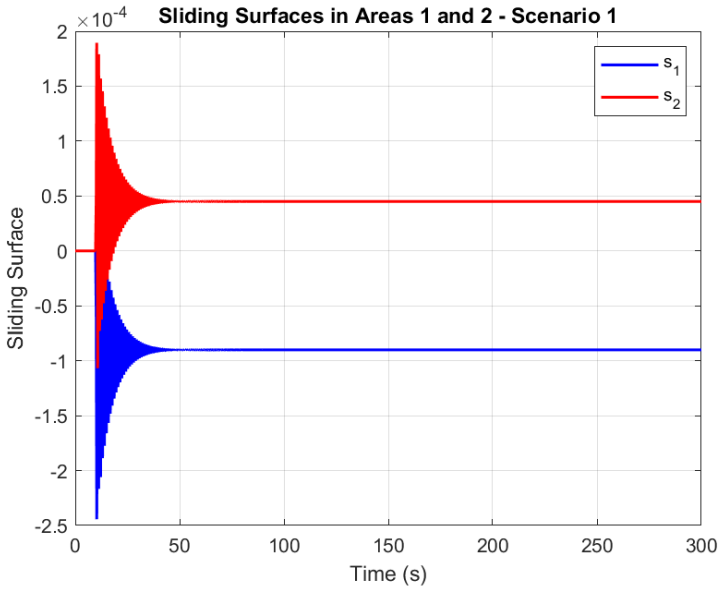


Figure 4: Sliding surfaces in Areas 1 and 2 under Scenario 1.

4.2 Scenario 2: Step Load Change with Renewable Integration

With the integration of the renewable energy source ($\sigma_{RE} = 0.02$), stochastic fluctuations are introduced into the system. The SMC maintains frequency deviations within a narrow band around zero despite the variability introduced by the renewable energy source.

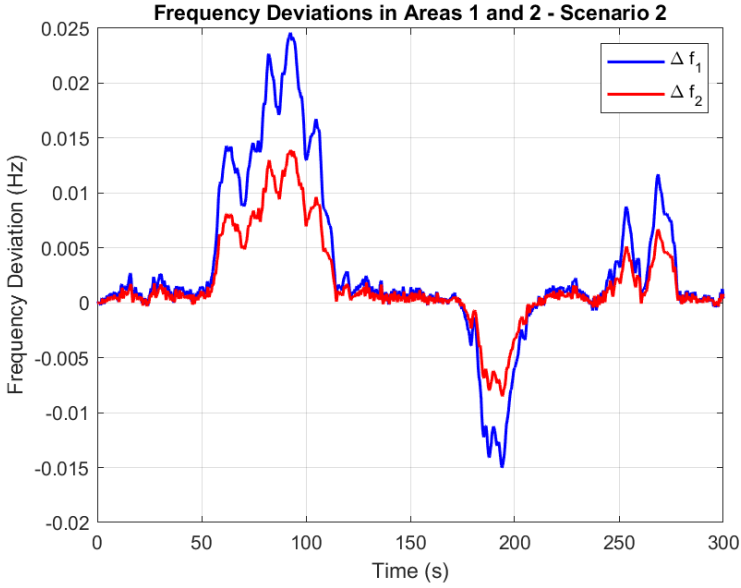


Figure 5: Frequency deviations in Areas 1 and 2 under Scenario 2.

Figure 5 shows that the frequency deviations settle back to zero values within approximately 60 seconds after the disturbance. The maximum overshoot in frequency deviation increases slightly but remains within acceptable limits.

The tie-line power flow deviation is shown in Figure 6, and the control inputs adapt effectively to the stochastic variations, as seen in Figure 7.

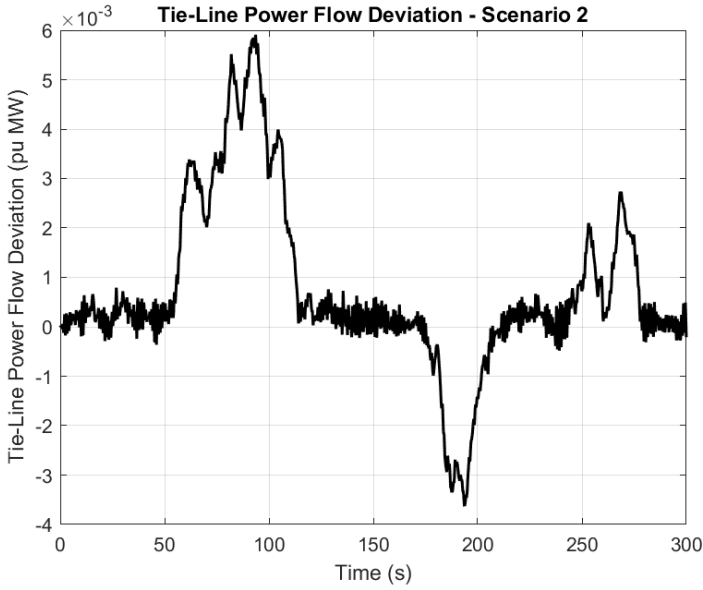


Figure 6: Tie-line power flow deviation under Scenario 2.

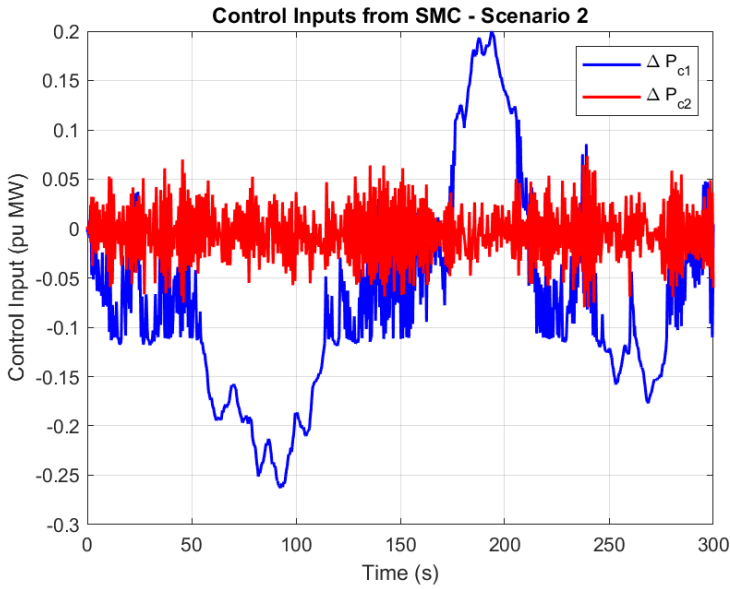


Figure 7: Control inputs from the SMC under Scenario 2.

The sliding surfaces remain close to zero, as illustrated in Figure 8, demonstrating the SMC's robustness.

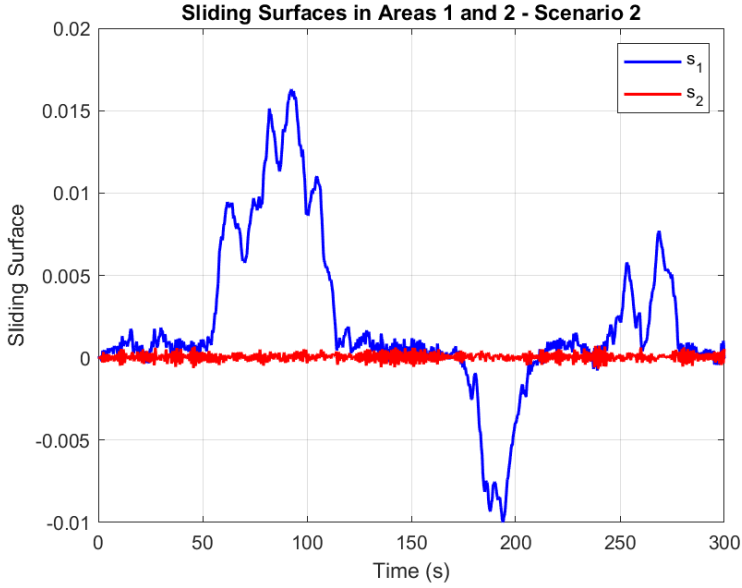


Figure 8: Sliding surfaces in Areas 1 and 2 under Scenario 2.

The stochastic renewable power output in Area 1 is depicted in Figure 9, illustrating the variability introduced by renewable energy integration.

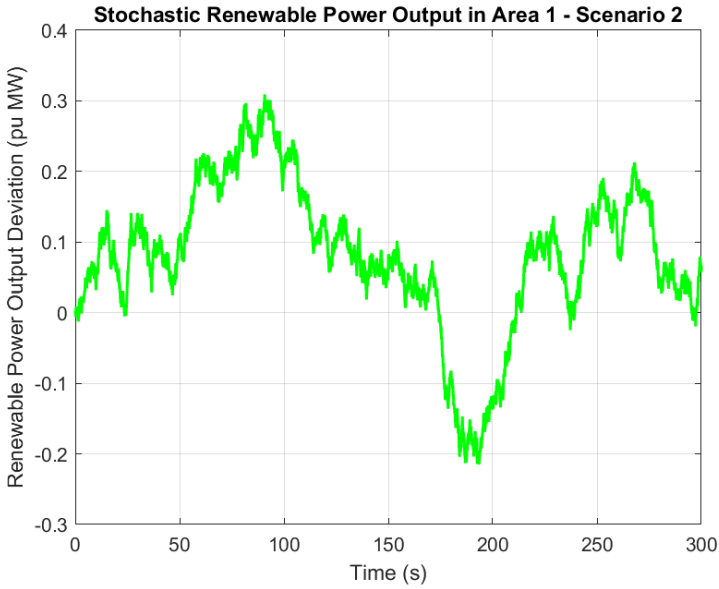


Figure 9: Stochastic renewable power output in Area 1 under Scenario 2.

4.3 Scenario 3: Random Load Fluctuations with Renewable Integration

In the most challenging scenario, random load fluctuations ($\sigma_L = 0.005$) are introduced alongside the renewable energy integration. The SMC effectively maintains frequency stability despite the increased disturbances.

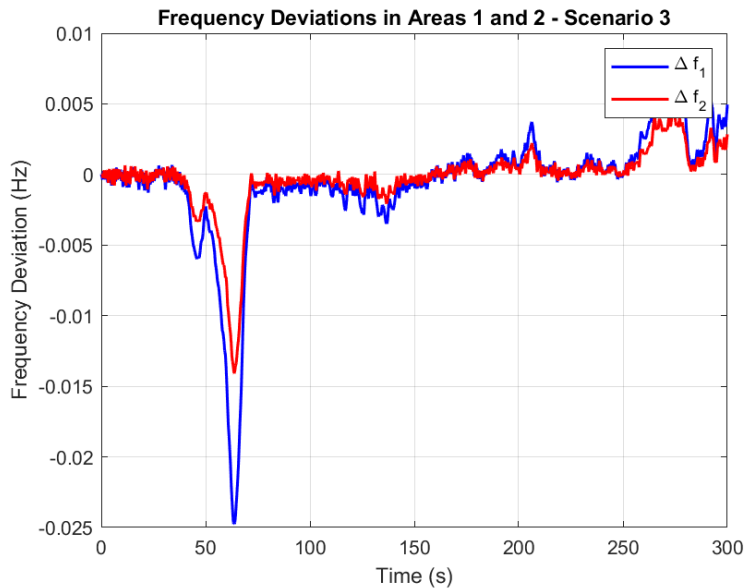


Figure 10: Frequency deviations in Areas 1 and 2 under Scenario 3.

Figure 10 shows that frequency deviations are kept within acceptable limits. The control inputs and sliding surfaces, shown in Figures 11 and 12, exhibit more activity due to the combined disturbances but remain stable.

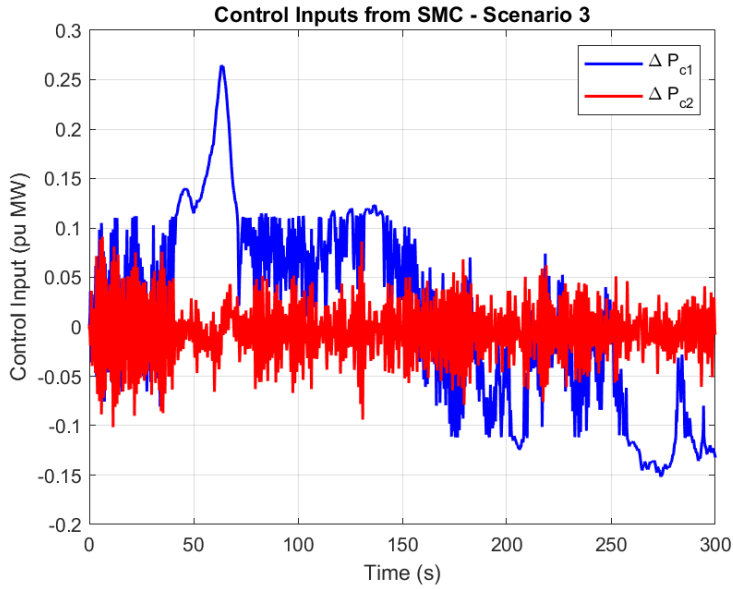


Figure 11: Control inputs from the SMC under Scenario 3.

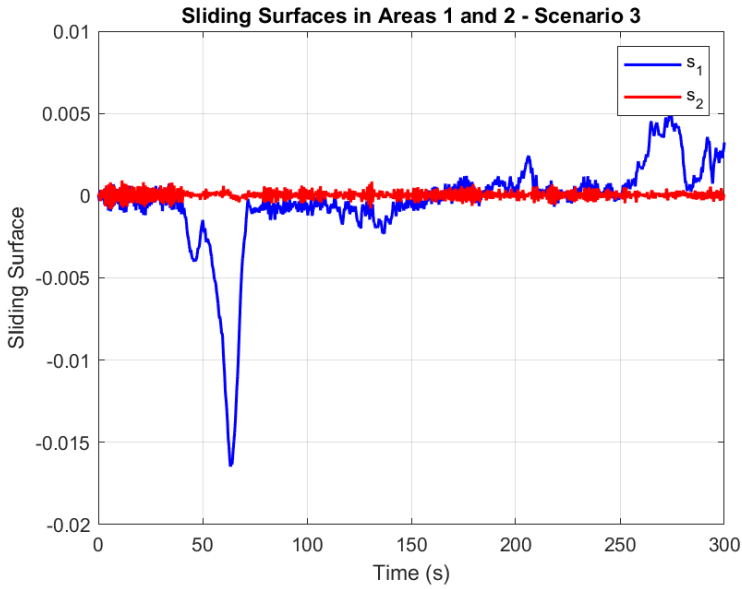


Figure 12: Sliding surfaces in Areas 1 and 2 under Scenario 3.

The stochastic renewable power output in Area 1 and the random load fluctuations are depicted in Figures 13 and 14.

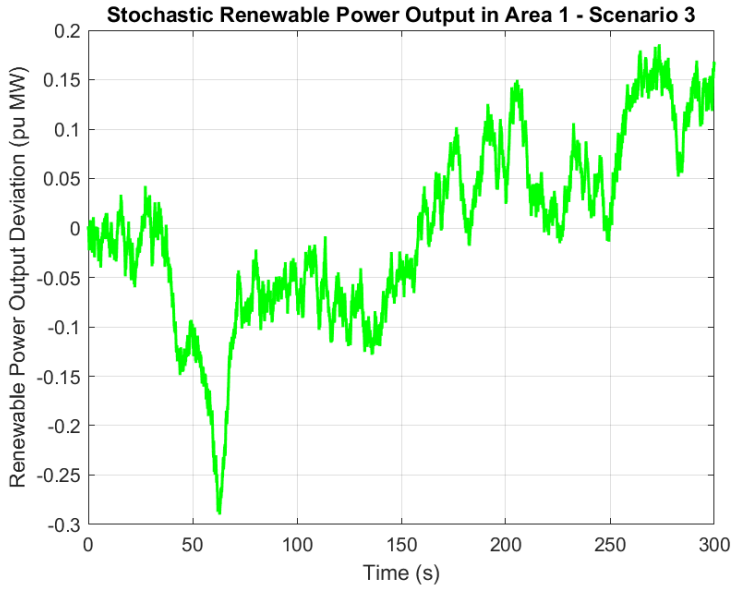


Figure 13: Stochastic renewable power output in Area 1 under Scenario 3.

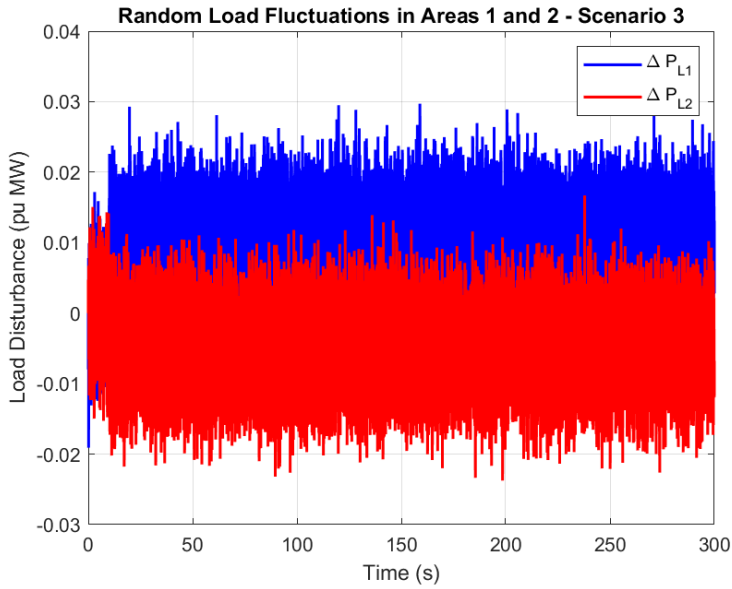


Figure 14: Random load fluctuations in Areas 1 and 2 under Scenario 3.

4.4 Discussion

The simulation results demonstrate that the Sliding Mode Controller effectively maintains frequency stability in the two-area power system under various operating conditions, including the integration of renewable energy sources and random load fluctuations. The SMC's robustness against system uncertainties and external disturbances is evident from its ability to keep frequency deviations within acceptable limits and ensure quick convergence to zero.

The use of a saturation function in the control law effectively reduces chattering, resulting in smoother control actions. The sliding surfaces converge to zero or fluctuate around zero, confirming that the system states are being driven to and maintained on the sliding surface despite the disturbances.

The SMC's performance in Scenario 3, which presents significant challenges due to combined renewable energy fluctuations and random load disturbances, highlights its suitability for modern power systems with high levels of uncertainty.

5. Conclusion

This paper investigated the application of a Sliding Mode Controller for Load Frequency Control in a two-area power system with renewable energy integration. A comprehensive mathematical model of the system was developed, and the SMC was designed to enhance robustness against system uncertainties and external disturbances. Simulations conducted using a fixed time step approach in MATLAB demonstrated that the SMC effectively maintains frequency stability under various scenarios, including step load changes and random load fluctuations.

The results showed that the SMC provides quick convergence to nominal frequency values, keeps frequency deviations within acceptable limits, and adapts effectively to stochastic variations introduced by renewable energy sources. The controller's robustness and adaptability make it a promising solution for modern power systems facing the challenges of renewable energy integration.

Future work could focus on refining the SMC design by incorporating adaptive or higher-order sliding mode control techniques to further improve performance and reduce chattering. Additionally, practical implementation aspects, such as measurement noise and actuator limitations, could be addressed to facilitate real-world applications.

References

- Balali, F., Nouri, N., Omrani, E., Nasiri, A., & Otieno, W. (2017). An overview of the environmental, economic, and material developments of the solar and wind sources coupled with the energy storage systems. *International Journal of Energy Research*, 41 (14), 1953–1971. <https://doi.org/10.1002/er.3755>
- Bevrani, H. (2009). *Robust power system frequency control*. Springer.
- Cucuzzella, M., Incremona, G. P., & Ferrara, A. (2017). Decentralized sliding mode control of islanded ac microgrids with arbitrary topology. *IEEE Transactions on Industrial Electronics*, 64 (5), 4038–4047. <https://doi.org/10.1109/TIE.2017.2694346>
- Elhajji, Z., Dehri, K., & Nouri, A. S. (2014). Discrete fast terminal and integral sliding mode controllers. 2014 5th International Conference on Sciences of Electronics, Technologies of Information and Telecommunications (SETIT), 528–534. <https://doi.org/10.1109/STA.2014.7086766>
- Jia, C., Longman, R. W., & Dong, E. (2021). Low-order sliding mode repetitive control for discrete-time systems under complex disturbance environment. *International Journal of Robust and Nonlinear Control*, 31 (14), 6505–6528. <https://doi.org/10.1002/rnc.5539>
- Khan, I., Khan, L., Khan, Q., Ullah, S., Khan, U., & Ahmad, S. (2021). Neuro-adaptive backstepping integral sliding mode control design for nonlinear wind energy conversion system. *Turkish Journal of Electrical Engineering & Computer Sciences*, 29 (4), 2069–2083. <https://doi.org/10.3906/elk-2001-113>
- Kundur, P. (1994). *Power system stability and control*. McGraw-Hill.
- Oladunjoye, O. O., Olasoji, Y. O., Adedeji, K. B., Oladunjoye, O. A., & Olebu, C. (2022). A solar energy control system for on-grid energy storage device. *European Journal of Electrical Engineering and Computer Science*, 6 (3), 72–79. [10.24018/ejece.2022.6.3.429](https://doi.org/10.24018/ejece.2022.6.3.429)
- Woźniak, M., Badora, A., Kud, K., & Woźniak, L. (2021). Renewable energy sources as the future of the energy sector and climate in poland—truth or myth in the opinion of the society. *Energies*, 15 (1), 45. <https://doi.org/10.3390/en15010045>
- Wu, J.-R., & Lu, Y. (2019). Adaptive backstepping sliding mode control for boost converter with constant power load. *IEEE Access*, 7, 49340–49348. <https://doi.org/10.1109/ACCESS.2019.2910936>